



Minnesota
Department of
Transportation

Acoustic Emission Monitoring of a Fracture-Critical Bridge

**RESEARCH
SERVICES
&
LIBRARY**

**Office of
Transportation
System
Management**

Arturo Schultz, Principal Investigator
Department of Civil Engineering
University of Minnesota

March 2014

Research Project
Final Report 2014-15



To request this document in an alternative format call [651-366-4718](tel:651-366-4718) or [1-800-657-3774](tel:1-800-657-3774) (Greater Minnesota) or email your request to ADArequest.dot@state.mn.us. Please request at least one week in advance.

Technical Report Documentation Page

1. Report No. MN/RC 2014-15	2.	3. Recipients Accession No.	
4. Title and Subtitle Acoustic Emission Monitoring of a Fracture-Critical Bridge		5. Report Date March 2014	
		6.	
7. Author(s) Arturo E. Schultz, Daniel L. Morton, Anton S. Tillmann, Javier E. Campos, David J. Thompson, Alexandria J. Lee-Norris, and Ryan M. Ballard		8. Performing Organization Report No.	
9. Performing Organization Name and Address University of Minnesota Department of Civil Engineering 500 Pillsbury Drive SE Minneapolis, MN 55455-0220		10. Project/Task/Work Unit No. CTS # 2011029	
		11. Contract (C) or Grant (G) No. (C) 89261 (WO) 183	
12. Sponsoring Organization Name and Address Minnesota Department of Transportation Research Services & Library 395 John Ireland Boulevard Mail Stop 330 St. Paul, MN 55155		13. Type of Report and Period Covered Final Report	
		14. Sponsoring Agency Code	
15. Supplementary Notes http://www.lrrb.org/PDF/201415.pdf			
16. Abstract (Limit: 250 words) With bridge infrastructure in Minnesota aging, advancing techniques for ensuring bridge safety is a fundamental goal of the Minnesota Department of Transportation (MnDOT). As such, developing health monitoring systems for fracture-critical bridges is an essential objective in meeting the stated goal. This report documents the acquisition, testing and installation of a 16-sensor acoustic emission monitoring system in the Cedar Avenue Bridge, which is a fracture-critical tied arch bridge in Burnsville, Minnesota. The overall goal of the project was to demonstrate that acoustic emission technology could be used for global monitoring of fracture-critical steel bridges. Project activities included the acquisition of the monitoring equipment, its testing to verify compliance with manufacturer specifications, installation of the equipment on the selected bridge, field testing to calibrate the system, development of data processing protocols for the acoustic emission (AE) data, and the collection of field data for a period of 22 months. Fracture tests of notched cantilever steel beams were conducted in the laboratory to provide characterization data for fracture events.			
17. Document Analysis/Descriptors Acoustic emission, Fatigue, Fracture-critical bridge, Steel bridges, Structural health monitoring		18. Availability Statement No restrictions. Document available from: National Technical Information Services, Alexandria, Virginia 22312	
19. Security Class (this report) Unclassified	20. Security Class (this page) Unclassified	21. No. of Pages 236	22. Price

Acoustic Emission Monitoring of a Fracture-Critical Bridge

Prepared by:

Arturo E. Schultz
Daniel L. Morton
Anton S. Tillmann
Javier E. Campos
David J. Thompson
Alexandria J. Lee-Norris
Ryan M. Ballard

University of Minnesota
Department of Civil Engineering
500 Pillsbury Drive S.E.
Minneapolis, MN 55455

March 2014

Published by:
Minnesota Department of Transportation
Research Services & Library
395 John Ireland Boulevard, MS 330
Saint Paul, MN 55155

This report represents the results of research conducted by the authors and does not necessarily represent the views or policies of the Minnesota Department of Transportation or the University of Minnesota. This report does not contain a standard or specified technique.

The authors, the Minnesota Department of Transportation, and the University of Minnesota do not endorse products or manufacturers. Any trade or manufacturers' names that may appear herein do so solely because they are considered essential to this report.

ACKNOWLEDGEMENTS

The authors offer their gratitude to Moises Dimaculangan, from the MnDOT Office of Bridge and Structures, who served as Technical Liaison, as well as the Nancy Daubenberger, Paul Kivisto, Jihshya Lin, Todd Niemann, Paul Rowekamp, Tom Styrbicki, also from the Bridge Office and Structures, who served as members of the Technical Advisory Panel. The authors also express their gratitude to Mark Pribula, from the MnDOT Metro Division, for the time he took to assist our activities at the bridge site, and to Duane Green, also from the MnDOT Metro Division, who served on the Technical Advisory Panel. The authors also appreciate the administrative assistance of Shirlee Sherkow, MnDOT Research Services Section, for her efforts to keep this project on schedule. The authors thank Paul Bergson and Rachel Gaulke of the T. V. Galambos Structures Laboratory of the Department of Civil Engineering at the University of Minnesota, as well as fellow graduate students Ben Dymond, Andrew Gastineau, Brock Hedegard, Krista Morris and Alireza Nojavan for their assistance in the installation and troubleshooting of the bridge monitoring equipment. Finally, the authors thank David Cook and David Stevens of Straen Inc., as well as Louis Crépeau and Jacques Bossé of Osmos Canada for making available the fiber optic monitoring equipment used in the fracture beam laboratory tests.

TABLE OF CONTENTS

CHAPTER 1 – INTRODUCTION	1
CHAPTER 2 –BACKGROUND, SCOPE AND OBJECTIVES	2
2.1 Background.....	2
2.2 Previous Research.....	2
2.2.1 Bridge Monitoring Systems.....	2
2.2.2 Acoustic Emission Monitoring.....	3
2.2.3 Fracture-Critical Steel Bridges.....	3
2.3 Scope.....	4
2.4 Objectives	4
CHAPTER 3 – EQUIPMENT ACQUISITION, INSTALLATION AND TESTING	5
3.1 Equipment Acquisition	5
3.2 Equipment Evaluation.....	7
3.2.1 Sensor Test Procedure	7
3.2.2 Sensor Test Results	8
3.2.3 Sensor Cable and SH-II Channel Tests	8
3.3 Field Installation	9
3.3.1 Installation Plan.....	9
3.3.2 Solar Panel Installation.....	10
3.3.3 Sensor Installation	12
3.3.4 Equipment Installation.....	13
3.4 Field Testing	14
3.4.1 Field Test Procedure.....	14
3.4.2 Field Test Results.....	15
3.4.2(a) Wave Velocity	15
3.4.2(b) Attenuation.....	19
3.5 Installation Schedule.....	21
CHAPTER 4 – DATA PROCESSING PROCEDURES	26
4.1 Setting Up AEwin TM SHSM Replay.....	26
4.1.1 Overview of Software Setup.....	26
4.1.2 AEwin TM Software Installation	26
4.1.3 AEwin TM Software Licensing	27
4.1.4 Constructing a Layout File.....	27
4.2 Maximum Sensor Spacing Considerations	27
4.2.1 Overview	27
4.2.2 AEwin TM Input for Sensor Spacing	28
4.2.3 Maximum Sensor Spacing.....	28
4.3 Signal Filtering.....	29
4.3.1 Overview of Signal Filtering.....	29

4.3.2	<i>Frequency Filtering</i>	29
4.3.3	<i>AE Front-End Filter</i>	29
4.3.4	<i>Waveform Front-End Filtering</i>	30
4.3.5	<i>Parametric Filtering</i>	30
4.3.6	<i>Discussion of Signal Filtering</i>	30
4.3.7	<i>AEwinTM Input for Signal Filtering</i>	30
4.4	Signal Characterization	31
4.4.1	<i>Overview of Signal Characterization</i>	31
4.4.2	<i>Notched Beam Test</i>	31
4.4.3	<i>AEwinTM Signal Clustering</i>	31
4.4.4	<i>Summary of Signal Characterization</i>	32
4.5	Signal Alarms	32
4.5.1	<i>Overview of Signal Alarms</i>	32
4.5.2	<i>Average Signal Level Alarm</i>	33
4.5.3	<i>Signal Cluster Alarm</i>	33
4.5.3(a)	<i>Trip Alarm</i>	33
4.5.3(b)	<i>Rate Alarm</i>	33
4.5.4	<i>Summary of Signal Alarms</i>	33
4.5.5	<i>AEwinTM Input for Signal Alarms</i>	34
CHAPTER 5 – NOTCHED BEAM FRACTURE TESTS		35
5.1	Overview	35
5.2	Beam Specimen Fabrication	35
5.3	Connection	36
5.4	Sensor Setup	37
5.5	Data Collection	37
5.6	First Notched Beam Test	37
5.7	Second Notched Beam Test	39
5.8	Third Notched Beam Test	40
5.9	Data Analysis	41
5.9.1	<i>Kaiser and Felicity Effects</i>	41
5.9.2	<i>Results from Data Analysis</i>	42
5.10	Noise Tests	43
5.11	Sensor Locations in the Notched Beam Tests	43
CHAPTER 6 – DATA ANALYSIS PROCEDURES		45
6.1	Overview	45
6.2	Hits vs. Time	45
6.3	Hits vs. Channel	46
6.4	Hits vs. Amplitude	47
6.5	Hits vs. Frequency Centroid	48
6.6	Counts, Energy, Amplitude and Rise Time vs. Duration	49
6.7	Duration vs. Amplitude	50
6.8	Peak Frequency vs. Frequency Centroid vs. Average Frequency	52
6.9	Hits vs. Peak Frequency	52
6.10	Counts vs. Frequency Centroid vs. Hits	53

6.11 Absolute Energy vs. Amplitude.....	54
6.12 Absolute Energy vs. Frequency Centroid.....	55
6.13 Conclusions.....	57
CHAPTER 7 – DATA COLLECTION AND EVALUATION.....	58
7.1 Overview.....	58
7.2 AE Data Sets and Timeline of Data Collection	58
7.3 Data Analysis.....	59
7.3.1 Hits vs. Time.....	60
7.3.2 Hits vs. Channel.....	61
7.3.3 Hits vs. Amplitude.....	63
7.3.4 Hits vs. Frequency Centroid.....	64
7.3.5 Other AE Parameters.....	65
7.4 Field Problems	65
7.4.1 Solar Panel Issues.....	65
7.4.2 Durability of Equipment and Materials.....	66
7.5 Discussion.....	66
CHAPTER 8 – SUMMARY, CONCLUSIONS AND RECOMMENDATIONS.....	67
8.1 Summary.....	67
8.2 Conclusions.....	67
8.3 Recommendations.....	68
REFERENCES.....	69

APPENDIX A: AEwin™ Software Procedures

APPENDIX B: Field Data Collected from 1/14/2011 to 10/30/2012

LIST OF TABLES

Table 3.1 Acoustic Emission Equipment from Mistras Group Inc.....	6
Table 3.2 Results for Signal Acquisition Test for all Sensors	8
Table 3.3 Material List.....	12
Table 3.4 Group 1 Wave Velocity Results	16
Table 3.5 Group 2 Wave Velocity Results	17
Table 3.6 Group 3 Wave Velocity Results	18
Table 3.7 Group 4 Wave Velocity Results	18
Table 3.8 Group 5 Wave Velocity Results	19
Table 3.9 Pencil Break Test Wave Velocity Results	19
Table 3.10 Signal Attenuation Results.....	20
Table 3.11 Average Attenuation Test Results	20
Table 3.12 Schedule for 1/10/2011	21
Table 3.13 Schedule for 1/11/2011	22
Table 3.14 Schedule for 1/12/2011	22
Table 3.15 Schedule for 1/13/2011	23
Table 3.16 Schedule for 1/14/2011	24
Table 3.17 Schedule for 2/22/2011	25
Table 3.18 Schedule for 2/24/2011	25
Table 4.1 Attenuation Plot Input for AEWin.....	28
Table 4.2 Low Pass and High Pass Frequency Filtering Thresholds.....	30
Table 7.1 AE Data Sets.....	59

LIST OF FIGURES

Figure 3.1	Sensor Highway II system.....	5
Figure 3.2	AE sensor locations along Cedar Avenue Bridge	9
Figure 3.3	Sensor locations in tie girder	10
Figure 3.4	Solar panel location in the Cedar Avenue Bridge	10
Figure 3.5	Optimum orientation of solar panels	11
Figure 3.6	Photograph of solar panel installation	11
Figure 3.7	Photograph of preparation for sensor installation	12
Figure 3.8	Wiring diagram for AE monitoring system.....	13
Figure 3.9	Pencil break test.....	14
Figure 3.10	Attenuation plot.....	20
Figure 5.1	Notched beam specimens	35
Figure 5.2	Test setup for the second notched beam test	36
Figure 5.3	Plot of hits vs. time for the first notched beam test	38
Figure 5.4	Plot of hits vs. time for the second notched beam test	39
Figure 5.5	Placement of fiber optic sensor on top flange	40
Figure 5.6	Plot of hits vs. time for the third notched beam test.....	41
Figure 5.7	Example of Kaiser and Felicity Effects.....	42
Figure 5.8	Acoustic emissions vs. fiber optic gauge deformation (inches) for third beam test..	42
Figure 5.9	First notched beam test sensor locations	43
Figure 5.10	Second notched beam test sensor locations.....	44
Figure 5.11	Third notched beam test sensor locations.....	44
Figure 6.1	Hits vs. time (sec).....	45
Figure 6.2	Hits vs. channel	47
Figure 6.3	Hits vs. amplitude (dB).....	48
Figure 6.4	Hits vs. frequency centroid (kHz)	49
Figure 6.5	Counts, energy, amplitude (dB) and rise time (μ s) vs. duration (μ s).....	50
Figure 6.6	Duration (μ s) vs. amplitude (dB)	51
Figure 6.7	Peak frequency (kHz) vs. frequency centroid (kHz) vs. average frequency (kHz)....	52
Figure 6.8	Hits vs. peak frequency (kHz).....	53
Figure 6.9	Counts vs. frequency centroid (kHz) vs. hits	54
Figure 6.10	Absolute energy (aJ) vs. amplitude (dB).....	55
Figure 6.11	Absolute energy (aJ) vs. frequency centroid (kHz).....	56
Figure 7.1	Hits vs. time (sec).....	61
Figure 7.2	Hits vs. channel	62
Figure 7.3	Hits vs. amplitude (dB).....	63
Figure 7.4	Hits vs. frequency centroid (kHz)	64

EXECUTIVE SUMMARY

In order for the Minnesota Department of Transportation to manage its bridge inventory, it is important to establish methods for monitoring fracture-critical steel bridges. This report provides a framework for selecting appropriate acoustic emission (AE) equipment and formulating effective data processing methods for assessing the formation and growth of cracks in steel bridges. The research includes thorough examination of AE parameters and their use for identifying fracture in AE signals from sensors on the bridge. A field-deployable notched cantilever beam test is also developed and tested in the laboratory for the purpose of characterizing fracture in AE signals recorded in steel bridge members.

The research conducted includes the acquisition of the AE equipment, its testing in the laboratory to verify compliance with manufacturer specifications, its installation on a selected bridge, and its calibration using ASTM procedures. The equipment was installed in the Cedar Avenue Bridge, a fracture-critical steel bridge with no history of cracking in its 34 years of service. AE signals consistent with fracture were generated using the notched cantilever beam tests. AE parameters and the software tools to analyze them are discussed and evaluated using a combination of AE signals from the fracture tests and AE signals from the Cedar Avenue Bridge.

Acoustic emission data from fracture tests on notched cantilever beams in the laboratory were used to systematically evaluate the AE parameters in terms of their ability to identify fracture from AE data. The data collected from the AE equipment in the Cedar Avenue Bridge during the 22-month monitoring period was evaluated. The conclusion based on this analysis was that the Cedar Avenue Bridge data does not contain evidence of fracture, as expected. Four types of plots were generated for each of the 289 AE files of significance generated at the bridge. The plots are included in an appendix.

It is recommended that the Cedar Avenue Bridge continue to be monitored and that further improvements on AE data analysis methods be investigated. It is also recommended that another steel bridge, but one with a history of cracking, be monitored with the AE equipment and data processing procedures investigated here. Lastly, it is recommended that bridge monitoring using AE equipment not be allowed to use solar panel systems. AE equipment has large electrical power demands necessitating the use of large and numerous solar panels. Additionally, the low durability and reliability of solar panel systems, relative to that of electrical power supplied by local utility companies, pose an unacceptable risk to the continuity of data collection and the integrity of the monitoring equipment.

CHAPTER 1 – INTRODUCTION

The project reported here implements an advanced health monitoring system in an in-service fracture-critical steel bridge to provide advance warning of bridge distress from fracture due to fatigue. Fracture-critical steel bridges, while non-redundant, are not inherently unsafe. However, they require increased frequency of inspections as they age. Bridge health monitoring offers the potential for identification of structural distress that can serve as an indicator of damage, or, in extreme cases, the distress may be a precursor to member failure or bridge collapse. The project combined evaluation criteria developed for the Minnesota Department of Transportation (MnDOT) to select a health monitoring system for the identification of distress in a fracture-critical bridge.

A tied-arch bridge was selected (Cedar Avenue Bridge), and a configuration of commercially available bridge health monitoring equipment and software was assembled and installed to provide warning of structural distress in the selected bridge. The selected bridge has not had any cracking distress since 1979 when it was completed and brought into service. Thus, the project was not intended as a measure to manage a problematic bridge. Rather, the Cedar Avenue Bridge served as a platform in which to develop, implement and test an acoustic emission system for fracture-critical steel bridges. This report documents the installation of the equipment, the development of data processing procedures, and the collection of data to ensure adequate operation of the system.

This report contains eight chapters and two appendices. Chapter 2 provides a background on fracture-critical steel bridges and acoustic emission monitoring, as well as the scope and objectives of the project. Chapter 3 describes the monitoring equipment that was acquired, as well as the installation plan and the testing needed to verify that the equipment was operating according to manufacturer specifications. Chapter 4 summarizes processing procedures for acoustic emission data according to the software tools provided by the equipment manufacturer. Chapter 5 documents a series of three laboratory-based fracture tests of steel beams and the data analysis needed to characterize fracture signals using acoustic emission monitoring equipment. Chapter 6 describes the use of the software tools from Chapter 4 and the fracture data from Chapter 5 to evaluate AE data from the Cedar Avenue Bridge. Chapter 7 presents analysis results for typical AE signals collected at the bridge, and it describes other issues pertinent to the collection of field data. Chapter 8 contains conclusions and recommendations drawn from the project. Appendix A is a brief summary of basic procedures for the software (AEwinTM) supplied by the manufacturer for the analysis of AE data. Appendix B contains plots illustrating the salient feature of all data files collected during the 22-month monitoring period.

CHAPTER 2 – BACKGROUND, SCOPE AND OBJECTIVES

2.1 Background

Current technologies for collapse warning of bridges are triggered by the collapse (FHWA 2012, Practical 2006), and, as such, they do not provide advance warning of structural distress at early stages that would allow inspection and repair, or even closing a bridge to prevent collapse in extreme cases. Yet, advanced warning is essential to avoid casualties to the driving public, as well as to reduce property loss to both bridge users and bridge owners. These and other related issues were studied in a recently completed research project funded by MnDOT (Gastineau et al. 2009). However, that project was limited to developing the criteria and a procedure for selecting the most appropriate monitoring system for a particular bridge application. The project documented in this report describes the implementation such equipment for bridge health assessment.

In a previous project (Schultz and Thompson, 2010), evaluation criteria developed for MnDOT by Gastineau et al. (2009) were used to select a health monitoring system for the identification of distress in a fracture-critical bridge, and a framework for the system was developed. A tied-arch bridge (MnDOT Bridge No. 9600, also known as the Cedar Avenue Bridge) was selected for instrumentation, and a basic configuration of commercially available bridge monitoring equipment was developed to provide indications of structural distress in the selected bridge. The research documented in the present report refines the plan for such equipment, including the configuration and placement, as well as the development of data processing protocols. The report also documents the installation procedure, and discusses other aspects of acoustic emission monitoring of a fracture-critical bridge.

2.2 Previous Research

2.2.1 Bridge Monitoring Systems

In 1995, Fish et al. identified non-destructive testing technologies that could be used for the inspection of fracture-critical bridges. This study was triggered by discovery of major cracking in the tie girder flanges of a two-girder, fracture-critical tied-arch bridge.

A recent noteworthy study commissioned by the Wisconsin Department of Transportation and conducted by the Center for Transportation Research and Education at Iowa State University synthesizes information on structural health monitoring technologies with a specific interest in those having smart-structure attributes (Phares et al. 2005). Phares et al. (2005) define a “smart system” within the context of bridge monitoring as one that can detect anomalies in bridge response and automatically determine whether further intervention is needed. Of all the sources investigated, this study approaches most closely the goal of the proposed project. However, it falls short of identifying monitoring systems that will detect impending bridge collapse with sufficient warning to allow bridge closure.

The finding by Thompson and Schultz (2010) that acoustic emission monitoring is the most appropriate of current commercial technologies for monitoring of fracture-critical steel bridges is later corroborated by Gastineau et al. (2011).

2.2.2. Acoustic Emission Monitoring

Pollock (2003) and Ono (2011) provide summaries of the principles, uses, benefits and shortcomings of acoustic emission monitoring. Ono further discusses the application of acoustic emission to the monitoring of steel bridges and notes that most efforts have focused on monitoring the growth of existing cracks. He also notes that for large steel bridges electrical grounding poses a problem with noise and lightning.

Yu et al. (2011) conducted a field study on the use of acoustic emission monitoring systems for evaluating crack growth in steel bridges. They found several parameters of the AE signal to be useful in assessing crack length and growth including the hits, absolute energy and signal strength (i.e., amplitude). Yu et al. also determined that filtering the AE signal, with filters based on friction tests, improved the effectiveness of the method.

Nair and Cai (2010) studied the use of acoustic emission technology for monitoring steel and prestressed concrete bridges. They determined that two indices previously proposed by Blessing et al. (1992) were able to provide an indication of cracking potential. One of these, the historic index, is a function of stress history of the AE signal, while the other, the severity index, is related to strength of the signal.

2.2.3 Fracture-Critical Steel Bridges

Problems with cracking in steel tied-arch bridges have a long history. In 1994, Koob et al. reported the discovery of cracks in welds in the junction of the tie girders and arch ribs, as well as in the connections between wide flange stiffeners and the side plates of the tie girders, in the Fremont Bridge (Portland, Oregon). This tied-arch suffered a major brittle fracture in one of the box-shaped tie girders near the end of the bridge at the beginning of the arch rib during construction in 1973.

Stallings et al. (1996) reported on the cracking of filler plate welds in numerous double angle tension and compression members of the floor trusses of twin tied-arch bridges on Interstate 1-65 in Alabama.

Miller and Amadi (2007) report on the design, fabrication, and construction of retrofits for a variety of brittle fracture and fatigue-prone details in the Neville Island Bridge (Pittsburgh, Pennsylvania). Instances of cracking were not reported in this tied-arch bridge with steel welded box tie-girders, but being a fracture-critical bridge, an extensive and expensive inspection program had been used in the previous 15 years due to the concerns with possible cracking and its consequences.

While the Cedar Avenue Bridge has not suffered any instances of cracking since it was opened to traffic in 1979, Thompson and Schultz (2010) identified stress concentrations in the tie

girder box sections at the locations where the girders are attached to the hangers. It is noted here that fracture-critical bridges, while non-redundant, are not inherently unsafe. However, they often require increased frequency of inspections as they age. Bridge health monitoring offers the potential for identification of structural distress that can serve as an indicator of damage, or, in extreme cases, the distress may be a precursor to member failure or bridge collapse.

2.3 Scope

The project documented in this report takes the monitoring technologies identified utilizing the evaluation criteria and the implementation program developed by Gastineau et al. (2007) and applying them in a fracture-critical steel bridge (Cedar Avenue Bridge) for sensing and warning of structural distress. A monitoring system was previously selected and configured by Thompson and Schultz (2010) for use in the Cedar Avenue Bridge, and the MnDOT Office of Bridges and Structures purchased the monitoring equipment separately. The project activities described in this report include the equipment installation, the development of data processing procedures, the collection of data to ensure that the monitoring system is operating properly, and the evaluation of the data processing procedures to ensure that they are working as intended.

2.4 Objectives

The project documented in this report encompasses the use of a reduced version of the final ‘acoustic emission’ monitoring system that was recommended by Thompson and Schultz (2010) in a previous project for monitoring the Cedar Avenue Bridge. The objectives of the study were (1) to study the characteristics of the Cedar Avenue Bridge, (2) to optimize the final system and sensor configuration, (3) to develop the necessary protocols for data processing, and (4) to collect sufficient data to ensure adequate operation of the system.

CHAPTER 3 – EQUIPMENT ACQUISITION, INSTALLATION AND TESTING

This chapter documents the acquisition of the acoustic emission monitoring equipment and its evaluation in the laboratory to ensure compliance with equipment specifications. The chapter also discusses the installation of the monitoring equipment in the Cedar Avenue Bridge, and the subsequent field testing to determine the characteristics needed for calibrating the layout file that is used to acquire and process the acoustic emission data. A detailed schedule for the field installation activities is included.

3.1 Equipment Acquisition

The acoustic emission monitoring system used in the present project is a reduced version (i.e., fewer sensors) of a system that was configured in a previous project (Thompson and Schultz 2010). The system was procured by the MnDOT Office of Bridges and Structures, and the equipment shipment was subsequently transferred to the Department of Civil Engineering at the University of Minnesota. The system is a Sensor Highway II Smart Remote Monitoring (SH-II-SRM) system manufactured and sold by Mistras Group, Inc. It was designed for monitoring of various types of bridges and other civil infrastructure assets.



Figure 3.1: Sensor Highway II system
(courtesy of Mistras Group, Inc.)

The Sensor Highway II system for bridge testing is an acoustic emission (AE) system with up to 16 high-speed AE monitoring channels, and it can handle 16 additional low-speed, parametric inputs (± 10 volts). The overall system utilizes industrial grade, low power components and has been developed for unattended use in condition monitoring applications. The system is housed in a rugged outdoor case (Figure 3.1), and is capable of operating in extreme weather conditions. A key feature of the SH-II system is its flexible sensor interface for

input and processing of a variety of sensors. The system was purchased with 16 AE sensors. A list of the components of the system is included in Table 3.1

Table 3.1: Acoustic Emission Equipment from Mistras Group Inc.

Item	Mistras Part No.	Description
1	SH-II SRM	SH-II SRM Smart Remote, Sensor Highway system. Includes outdoor case, Sensor Highway 16 channel motherboard, Atom N270 wide temperature range CPU, 2GB internal SSD, 64GB SATA SSD, Windows XP operating system, AEwin ready, and Ethernet connectivity to a factory network or Internet. Time synchronization capability between units up to 12 feet. 110/220VAC or 9-28 VDC power at 30 watts.
2	9380-2054	SH-4 AE, four 4 channel AE plug-in module for Sensor Highway with 1 MHz AE bandwidth.
3	9380-7003	AEwin-SH-16 software for automated AE data collection, file link, signal and alarm processing and remote communication software.
4	9380-5165	Solar Panel Kit, stand-alone 520-watt solar power kit with 4 days of battery backup. Includes four 130-watt Solar Panels, four 110Ah batteries with enclosure, 45A charge controller, 400-watt AC inverter with enclosure, and mounting pole and hardware.
5	9380-5035	Cellular wireless 3G modem with remote CPU reset capability.
6		NEMA enclosure for externally mounted modem.
7		8-50m and 8-100m BNC-BNC cables
8	9800-7110-setup	RMA (Remote Monitoring Application) setup charges, includes AE system preparation for remote access, phone/email support, and "standard" web hosting account setup charges.
9	R15I-LP-AST	16 low-power, pre-amplified sensor, 150kHz, with 26 dB gain, AST, coated for outdoor use, 5 meter coaxial RG-58A/U cable, and BNC connectors.
10		On-Site support by one MISTRAS employee for two days (includes travel & expenses).

The SH-II remote monitoring system was purchased with a solar panel kit that includes an array of four solar panels, an AC inverter, a charge controller, a battery backup and mounting hardware. The kit was purchased because MnDOT was unable to provide AC (alternating current) at the bridge site. This decision went against manufacture recommendations which were strongly in favor of AC power, as well as the recommendations made by Thompson and Schultz (2010) that the monitoring system at the Cedar Avenue Bridge be operated using AC power. This decision eventually led to field problems that threatened the successful completion of the project from damage due to vandalism and exposure of the solar panel array.

3.2 Equipment Evaluation

The equipment delivered to the Department of Civil Engineering of the University of Minnesota was checked to verify that it was operational within manufacturer specifications. In order to check the sensors, cables, and SH-II system a series of tests were conducted. The tests followed procedures of ASTM E976 (2010) to determine if the sensors fall within the tolerance range designated by ASTM.

3.2.1 Sensor Test Procedure

The first step for testing all acoustic emission (AE) sensors was labeling the sensors and sensor cables according to their eventual location on the bridge. This helped to ensure that all sensors were properly tested. Each sensor was assigned a designation according to its eventual installation location on the Cedar Avenue Bridge. The first letter designation in sensor labeling indicated the traffic direction of the bridge, i.e. “N” for northbound bridge. The second letter designation indicated which side of the bridge the instrument was located, i.e. “E” for the east girder. The third letter indicates whether the sensor was located north or south of the system module. Finally, the single numerical digit indicated its location in relation to the system module (i.e., the SH-II field computer). As an example, a sensor labeled “NEN1” is located on the northbound (N) bridge on the east (E) girder on the north (N) side of the system module. Once all sensors were labeled in this manner, all sensor cables were labeled in a similar manner.

After labeling the equipment, the other test equipment was prepared. A test block was needed where the sensors were placed and signals generated. For these tests, a 41-inch long wide-flange steel section was selected and cleaned to serve as the test block. The sensors were attached to the test block using a predetermined force. For these tests, a downward force of 25 lbs. was applied to all sensors to hold the sensor to the test block. The location of where the sensors were installed on the test block was used for all sensor tests, and the sensors had to be a minimum of four inches from the source of the signal. In these tests, the sensors were installed twelve inches from the end of the block, and the signal was generated twelve inches from the sensor location. The sensors were installed on the top flange of the block for all tests.

The signal was produced by breaking a 0.5-mm diameter pencil lead at the signal source location. The pencil is placed against the surface to which the sensors are attached at one of the predetermined distances (4, 8 and 12 in.) at a 45-degree angle. Before recording the final measurement, several initial measurements were taken in order to ensure reproducibility of the signal. This procedure was repeated for each sensor tested. The measurements taken for this reproducibility test were the peak signal amplitudes. Deviations in the peak amplitude recorded during these tests cannot exceed 4 dB. If the amplitude recorded by a specific sensor during the pencil break test deviates more than 4 dB from the mean peak amplitude, then the sensor has to be retested. If upon retesting the sensor the amplitude recorded is again outside the allowable variation on signal amplitude, then the sensor is deemed unacceptable for installation and will be returned the manufacturer.

3.2.2 Sensor Test Results

The test procedure described above was used to test all sensors delivered to the University of Minnesota by the Mistras Group. The results of the tests are shown in Table 3.2. The mean peak signal amplitude for all of the pencil-break tests was 60.75 dB. Moreover, all sensors fall within the acceptable range of deviation in signal amplitude. Therefore, they were all considered acceptable for installation in the Cedar Avenue Bridge.

Table 3.2: Results for Signal Acquisition Test for all Sensors

Bridge Sensor Code	Manufacturer Sensor Number	Peak Amplitude (dB)	Deviation from Mean (dB)	Acceptable
NEN1	F154	61	0.25	YES
NEN2	F153	62	1.25	YES
NEN3	F152	62	1.25	YES
NEN4	F151	60	0.75	YES
NEN5	F150	63	2.25	YES
NEN6	F146	61	0.25	YES
NEN7	F145	58	2.75	YES
NEN8	F144	63	2.25	YES
NES1	F143	62	1.25	YES
NES2	F141	62	1.25	YES
NES3	F138	58	2.75	YES
NES4	F137	58	2.75	YES
NES5	F136	58	2.75	YES
NES6	F135	62	1.25	YES
NES7	F134	63	2.25	YES
NES8	F129	59	1.75	YES
<i>Mean</i>		<i>60.75</i>		

3.2.3 Sensor Cable and SH-II Channel Tests

The final check of the equipment delivered to the University of Minnesota by the Mistras Group included the sensor cables and the SH-II channels (i.e. the data ports in the SH-II system module). In order to ensure that all cables were properly delivering the signal from the sensor to the system module, and that each channel in the system module was properly reading the sensor signal, the following method was employed. Each cable and system channel was tested during the sensor signal test in accordance with the sensor and location of eventual installation in the Cedar Avenue Bridge. This means that when sensor NEN1 was tested, the shortest cable (also labeled “NEN1”) was used and plugged into the first channel. The channel ordering is as follows: channels one through eight are designated to all sensors north of the system module, channels nine through sixteen are assigned to all sensors south of the system module, and the sensors nearest the system module are assigned their respective lowest channel number. In this manner, all sensor cables and all system channels were checked. The results, presented above,

demonstrate that all sensors, sensor cables, and system channels were in good working order upon delivery of the SH-II system.

3.3 Field Installation

Upon installing the SH-II monitoring system in the Cedar Avenue Bridge in Burnsville, Minnesota, field tests were conducted for the purpose of initial calibration of the system. Installation and field testing are described in the following sections.

3.3.1 Installation Plan

The installation of the SH-II monitoring system began on January 10, 2011, and was completed on February 24, 2011. The plan was developed taking into account climate conditions (i.e., mid-winter), material considerations (e.g., curing of epoxy in temperatures well below freezing), and site restrictions (e.g., restricted access).

The sensors were installed inside the tie girder on the east side of the northbound bridge according to the configuration shown on the elevation of the Cedar Avenue Bridge in Fig. 3.2. The sensors were placed on the interior web of the box girder (i.e., the web closest to the roadway) as shown in Fig. 3.3. The SH-II module, the backup batteries, the charge controller and the power inverter were all placed inside the tie girder as well. This equipment was placed on the tie girder floor at a location approximately at mid-span, as shown in Fig. 3.2.

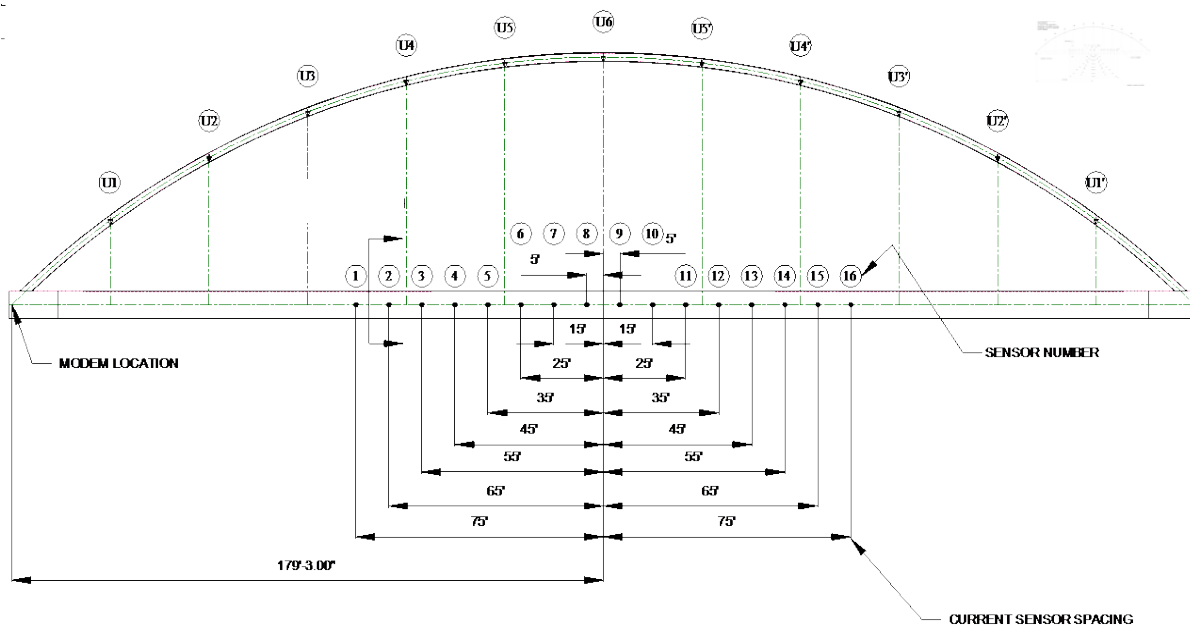


Fig. 3.2: AE sensor locations along Cedar Avenue Bridge

The cellular modem was also placed inside the tie girder, but at a location close to the south end of the tie girder. This location was controlled by access to the modem antenna. Modem signals cannot penetrate the steel plates forming the tie girder, thus the antenna had to be placed outside of the tie girder. The modem antenna was placed outside of the tie girder at the same location as the solar panel array, and a coaxial cable was used to connect it to the modem.

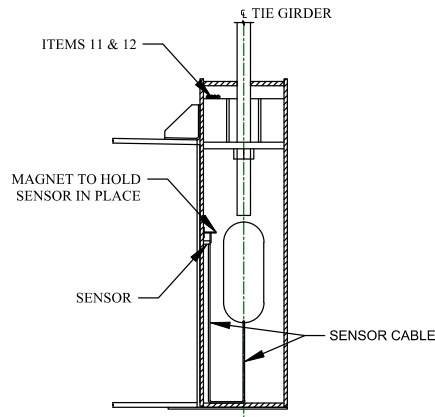


Fig. 3.3 Sensor locations in tie girder

3.3.2 Solar Panel Installation

The four solar panels were mounted as an array on a single Unirac® mount. The four-panel array was erected on the pedestrian walkway, cantilevered off the east side of the northbound lanes of the Cedar Avenue Bridge (Fig. 3.4). The array was installed at the L1 location (see Fig. 3.2), which is the southernmost point of the arch span. The four-panels array and Unirac® mount were connected to a steel post that was attached to an existing HSS tube that forms part of the framing for the pedestrian walkway (Fig. 3.4).

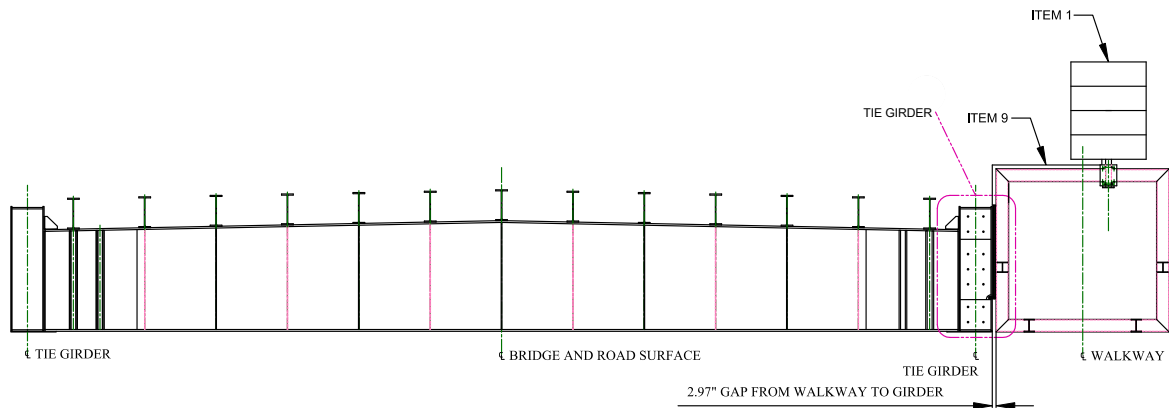


Fig. 3.4 Solar panel location in the Cedar Avenue Bridge

The solar panel mount allows rotation about a horizontal axis parallel to the top and bottom edges of the solar panel array. Additionally, the U-clamps that were used to secure the panel mount to the steel pipe allow rotation about a vertical axis. The ability to rotate the panels about these axes allows precise orientation, as per manufacturer specifications, of the panels to maximize power generation. The solar panels were installed at an angle of 45 degrees to the horizon and oriented due south for optimal energy production (Fig. 3.5).

Each solar panel was wired independently with 10-gage electrical wire running down the post, along the walkway HSS frame, into the tie girder through a hole in the access panel. The

power cables extend to the mid-span of the bridge, where the battery charger is located. A material list for the components of the solar panel array is given in Table 3.3. A photo of the solar panel installation can be seen in Figure 3.6.

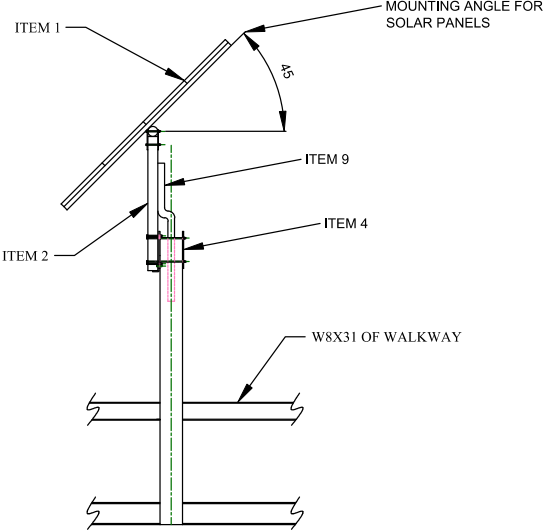


Fig. 3.5: Optimum orientation of solar panels



Figure 3.6: Photograph of solar panel installation

Table 3.3: Material List

Item No.	Description	Qty.
1	Solar panel	4
2	Mounting apparatus	4
3	16½ × 13 × ½ in. steel plate	1
4	16½ × 13 × ½ in. steel plate	1
5	½ in. diameter × 17 in. threaded steel bolt	4
6	½ in. diameter × 6½ in. steel U-bolt	2
7	½ in. diameter hexagonal nut	10
8	½ in. diameter steel washer	10
9	3 in. diameter × 20 ft UV-resistant PVC pipe	1
10	2½ × 2½ × 8 in. steel angle	1
11	200 ft. of 10 gage electrical wire	4
12	200 ft of CAT5 Ethernet cable	1

3.3.3 Sensor Installation

All sixteen acoustic emission sensors were mounted at a spacing of 10 ft. on center between sensors. The southernmost sensor was located 75ft. from mid-span, and the northernmost sensor is located 75ft. from mid-span (Fig. 3.2). All sensors were installed on the interior side of the interior web of the tie girder at the mid-height of the girder. A schematic of the sensor locations can be found in the installation plan drawings in Fig. 3.2 and 3.3.

The sensor installation required multiple steps, the first of which was to prepare the steel surface of the tie girder. This was achieved by lightly sanding the web of the girder where the sensor was to be installed in order to remove all the paint. Typically, about 1 in.² of paint was removed from the girder web. Next, an area around the sensor installation location, including the paint removal location, was cleaned using a degreaser. This ensured that impurities were not present at the sensor location because they may have impeded the curing of the epoxy used to fix the sensor, or they may have interfered with acoustic signal transmission. A photograph of the preparatory work required prior to sensor installation can be seen in Figure 3.7.



Figure 3.7: Photograph of preparation for sensor installation

Once all the preparation work on the girder web was completed, the sensor was ready for installation. First, the head of the sensor was covered in a low-temperature rated epoxy. Sufficient epoxy was applied to the head of the sensor to guarantee complete epoxy coverage between the sensor head and the steel surface of the girder web. The sensor was then pressed hard against the steel until some epoxy was visibly extruding from the sides of the sensor. Finally, a magnet was placed to ensure the sensor would remain in place while the epoxy cured. This magnet was left in place for the life of the sensor (or of its usage).

After application of the epoxy adhesive, the sensors were connected to the SH-II computer, which was placed at a location at mid-span (i.e., between L5 and L6 in Fig. 3.2). Each sensor was connected independently, using a dedicated sensor cable. In order to pass the sensor cable through each diaphragm and hanger location, the sensor cable was placed through access holes in the tie girder diaphragms, provided for inspection.

3.3.4 Equipment Installation

There were five pieces of monitoring equipment installed on the Cedar Avenue Bridge, excluding the solar panels and sensors. These items include: the SH-II computer, the four batteries (housed in a battery box), the battery charge controller, the power inverter and the cellular modem. All of these items were brought to the mid-span of the bridge between L5 and L6, except the cellular modem.

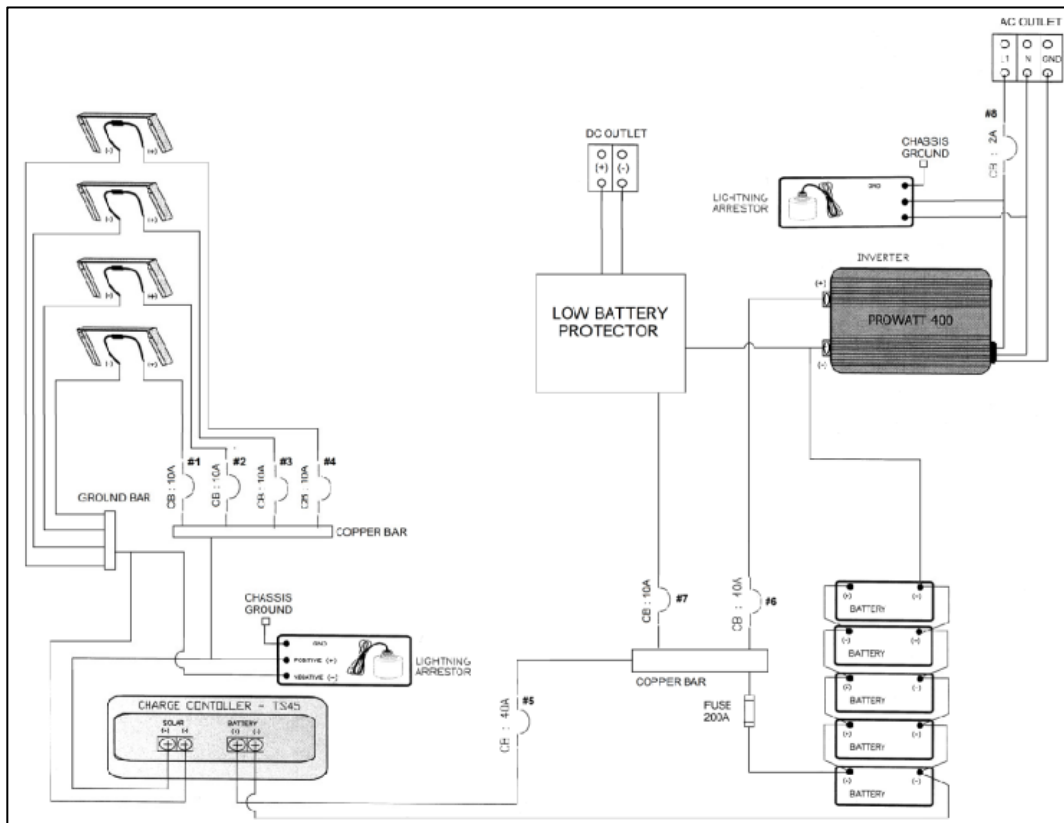


Fig. 3.8: Wiring diagram for AE monitoring system (Mistras Group 2010)

The cellular modem was installed directly inside the south side access panels of the bridge. The modem was installed at this location because cellular telephone signals cannot be sensed by the cellular modem inside of the tie girder. Installation of the modem at this location enabled the antenna to be installed outside of the tie girder, but at a close proximity to the modem. Additionally, modem installation in a secure location inside of the access panels was enabled by means of an Ethernet cable (phone signal) and electrical wire (power) that were extended to the SH-II computer at girder mid-span.

Once all of the wiring was extended, the system was wired according to the schematic provided in Figure 3.8. The electrical wiring of the monitoring system was completed by the team from Mistras Group.

3.4 Field Testing

Field tests were conducted once the AE monitoring system had been installed. The tests followed procedures given in ASTM E976 (2010) to determine data needed to calibrate the layout file defining the AE monitoring array.

3.4.1 Field Test Procedure

The field tests comprised pencil break tests conducted in accordance with the procedure described standardized in ASTM E976 (2010). The pencil break tests (Fig. 3.9) were conducted between sensors 6 and 7, whose location can be seen in the installation plan (Fig. 3.2).

Prior to conducting the tests, the pencil break locations were prepared in a method similar to that used for preparing the sensors locations. The paint was lightly sanded off the girder web at distances of 4 in., 8 in., and 12 in. north of sensor 6 on the interior girder, along a straight line from sensor 6 to sensor 7. Additionally, paint was sanded off the web girder 4 in., 8 in., and 12 in. south of sensor 7, along the same line. Cleaning the area at these locations using a degreaser was not necessary for the pencil break tests.

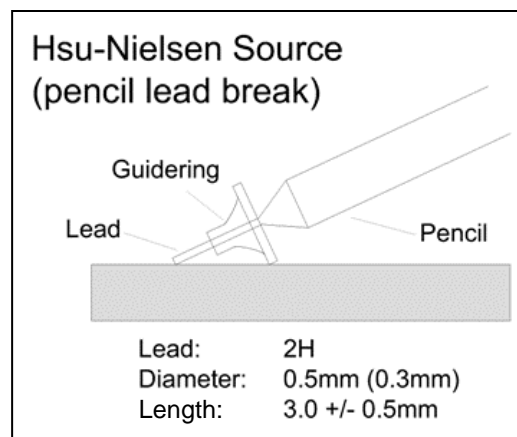


Fig. 3.9: Pencil break test (ndt.net 2013)

Once the pencil break sites were prepared, a minimum of 3 pencil breaks were conducted at each location. After each pencil break was completed, the resultant signal velocity was recorded by the monitoring system at sensors 6 and 7. After it was determined that the signal velocity from a given pencil break location was ‘regular,’ that is, the signal velocities from the three pencil break tests had repeatable magnitudes, the Mistras Group personnel who were conducting the tests recorded the average signal velocity. This procedure of producing AE signals by means of pencil breaks and recording their resultant signal velocity was repeated for all six pencil break locations. This information was used to develop a layout file for the monitoring system. The layout file defines the linear location of each sensor along the tie girder and the expected signal velocity of AE signals traveling through the steel tie girder in the bridge.

3.4.2 Field Test Results

The Mistras Group team conducted the pencil break tests, and used the recorded data from the field tests directly to develop the layout file for the monitoring system. The values for signal velocity in the layout file is used to determine the linear location of a signal source. The attenuation (i.e., decrease in signal strength with distance from the source) is used for determining sensor spacing.

3.4.2(a) Wave Velocity

Pencil break tests were conducted for the sensors organized in groups depending on the location in the bridge to determine the expected signal velocity for each group. The results for these tests are summarized in Tables 3.4 – 3.8.

Table 3.9 displays the calculated wave velocity for each sensor group for the Cedar Avenue Bridge. The results listed are the average of all test results for each group. These values were input directly into AEwin to create the layout file. The results of the tests indicate several trends. First, the signal wave velocity is greatest when not impeded by a splice plate or a floor beam to girder connection. Group 1 was tested across the diaphragm location at L3. Group 2 was tested across the splice plate. Group 3 was tested in a location with no diaphragm or splice plate impeding the signal. Group 4 was tested across the splice plate for the mid and north sections. Finally, group 5 was tested across the diaphragm at bridge node L4'. These test results suggest that for the layout file, groups be based upon whether or not the sensors cross a splice, a diaphragm, or are located on an uninterrupted span of the bridge.

Table 3.4: Group 1 Wave Velocity Results

Group	Test	d_i	Sensor No.		t_{s1}	t_{s2}	Δt	Δd	Velocity
		(in.)	S_1	S_2	(sec.)	(sec.)	(ms)	(in.)	(in/sec.)
1	1	4	2	3	42.35	42.35	2287	116	50,721
1	2	4	2	3	44.27	44.28	1744	116	66,514
1	3	4	2	3	46.11	46.11	1820	116	63,736
1	4	4	2	3	47.97	47.97	1624	116	71,429
1	5	4	2	3	49.82	49.82	1233	116	94,079
1	1	8	2	3	3.91	3.91	2423	112	46,224
1	2	8	2	3	5.42	5.42	2433	112	46,034
1	3	8	2	3	6.83	6.83	1944	112	57,613
1	1	12	2	3	25.56	25.57	1887	108	57,234
1	2	12	2	3	26.79	26.79	1290	108	83,721
1	3	12	2	3	28.04	28.04	1048	108	103,053
1	4	12	2	3	29.91	29.91	1024	108	105,469
1	5	12	2	3	31.87	31.87	1787	108	60,436
1	6	12	2	3	33.90	33.90	1224	108	88,235
1	1	4	3	2	16.50	16.50	2806	116	41,340
1	2	4	3	2	18.49	18.50	2508	116	46,252
1	3	4	3	2	20.89	20.89	2514	116	46,142
1	4	4	3	2	23.30	23.30	1395	116	83,154
1	5	4	3	2	26.09	26.09	1228	116	94,463
1	1	8	3	2	8.64	8.65	2734	112	40,966
1	2	8	3	2	45.33	45.33	2601	112	43,060
1	3	8	3	2	47.67	47.67	2608	112	42,945
1	4	8	3	2	50.03	50.03	3094	112	36,199
1	5	8	3	2	52.34	52.34	1307	112	85,692
1	6	8	3	2	54.57	54.57	3842	112	29,151
1	1	12	3	2	9.51	9.51	2664	108	40,541
1	2	12	3	2	11.40	11.40	1558	108	69,320
1	3	12	3	2	13.45	13.45	2207	108	48,935

Table 3.5: Group 2 Wave Velocity Results

Group	Test	d_i	Sensor No.		t_{s1}	t_{s2}	Δt	Δd	Velocity
		(in.)	S_1	S_2	(sec.)	(sec.)	(ms)	(in.)	(in/sec.)
2	1	4	3	4	8.74	8.74	1602	116	72,409
2	2	4	3	4	10.30	10.30	1559	116	74,407
2	3	4	3	4	11.95	11.95	1296	116	89,507
2	4	4	3	4	13.58	13.58	1545	116	75,081
2	5	4	3	4	15.30	15.30	787	116	147,395
2	1	8	3	4	3.24	3.24	1522	112	73,587
2	2	8	3	4	4.79	4.79	1564	112	71,611
2	3	8	3	4	6.43	6.43	1095	112	102,283
2	4	8	3	4	8.13	8.13	1400	112	80,000
2	5	8	3	4	9.88	9.88	1106	112	101,266
2	6	8	3	4	11.57	11.57	1345	112	83,271
2	1	12	3	4	10.81	10.81	1379	108	78,318
2	2	12	3	4	12.38	12.38	1324	108	81,571
2	3	12	3	4	13.98	13.98	1344	108	80,357
2	4	12	3	4	15.70	15.71	995	108	108,543
2	5	12	3	4	17.40	17.40	1223	108	88,307
2	6	12	3	4	19.14	19.15	961	108	112,383
2	1	4	4	3	10.77	10.77	1521	116	76,266
2	2	4	4	3	12.56	12.56	1323	116	87,680
2	3	4	4	3	14.45	14.45	1605	116	72,274
2	4	4	4	3	16.35	16.36	1456	116	79,670
2	1	8	4	3	4.50	4.50	1314.3	112	85,216
2	2	8	4	3	6.02	6.02	1515.3	112	73,913
2	3	8	4	3	7.93	7.93	1330.3	112	84,192
2	4	8	4	3	10.13	10.13	1261.3	112	88,797
2	5	8	4	3	12.44	12.45	1313.3	112	85,281
2	1	12	4	3	10.65	10.65	1289	108	83,786
2	2	12	4	3	13.21	13.22	1256	108	85,987
2	3	12	4	3	15.82	15.82	1226	108	88,091
2	4	12	4	3	18.37	18.37	1373	108	78,660
2	5	12	4	3	20.87	20.88	1243	108	86,887

Table 3.6: Group 3 Wave Velocity Results

Group	Test	d_t	Sensor No.		t_{s1}	t_{s2}	Δt	Δd	Velocity
		(in.)	S_1	S_2	(sec.)	(sec.)	(ms)	(in.)	(in/sec.)
3	1	4	7	8	2.64	2.64	832.7	116	139,306
3	2	4	7	8	5.73	5.73	833.7	116	139,139
3	3	4	7	8	12.2	12.2	833.7	116	139,139
3	1	8	7	8	2.1	2.1	780.7	112	143,461
3	2	8	7	8	6.13	6.13	780.7	112	143,461
3	3	8	7	8	11.1	11.1	781.7	112	143,277
3	1	12	7	8	2.84	2.84	728.7	108	148,209
3	2	12	7	8	6.48	6.48	728.7	108	148,209
3	3	12	7	8	9.72	9.73	725.7	108	148,822
3	1	4	8	7	8.57	8.58	836	116	138,756
3	2	4	8	7	12.2	12.2	833	116	139,256
3	3	4	8	7	16	16.1	832	116	139,423
3	1	8	8	7	2.21	2.21	781.3	112	143,351
3	2	8	8	7	6.39	6.39	784.3	112	142,803
3	3	8	8	7	11	11	784.3	112	142,803
3	1	12	8	7	2.24	2.24	712.3	108	151,621
3	2	12	8	7	5.68	5.68	710.3	108	152,048
3	3	12	8	7	9.42	9.42	723.3	108	149,316

Table 3.7: Group 4 Wave Velocity Results

Group	Test	d_t	Sensor No.		t_{s1}	t_{s2}	Δt	Δd	Velocity
		(in.)	S_1	S_2	(sec.)	(sec.)	(ms)	(in.)	(in/sec.)
4	1	4	14	13	30.44	30.44	2301.7	116	50,398
4	2	4	14	13	55.66	55.66	1244.7	116	93,195
4	3	4	14	13	57.55	57.55	1278.7	116	90,717
4	4	4	14	13	21.51	21.51	1281.7	116	90,505
4	5	4	14	13	23.65	23.65	1246.7	116	93,046
4	6	4	14	13	25.98	25.98	1526.7	116	75,981
4	7	4	14	13	28.15	28.16	1278.7	116	90,717
4	8	4	14	13	30.46	30.47	1271.7	116	91,216
4	1	12	14	13	4.17	4.17	1026.7	108	105,191

Table 3.8: Group 5 Wave Velocity Results

Group	Test	d_t	Sensor No.		t_{s1}	t_{s2}	Δt	Δd	Velocity
		(in.)	S_1	S_2	(sec.)	(sec.)	(ms)	(in.)	(in/sec.)
5	1	4	14	15	48.82	48.82	1746	116	66,438
5	2	4	14	15	34.10	34.10	1935	116	59,948
5	3	4	14	15	40.54	40.54	1448	116	80,111
5	1	8	14	15	15.05	15.06	8064	112	13,889
5	1	12	14	15	59.17	59.17	1847	108	58,473
5	2	12	14	15	2.89	2.89	1720	108	62,791
5	3	12	14	15	6.44	6.45	3118	108	34,638
5	1	4	15	14	19.74	19.75	1719	116	67,481
5	2	4	15	14	22.05	22.05	2008	116	57,769
5	3	4	15	14	24.24	24.24	1721	116	67,403
5	4	4	15	14	26.52	26.52	2040	116	56,863
5	1	8	15	14	8.95	8.95	1501	112	74,617
5	2	8	15	14	11.41	11.41	1613	112	69,436
5	3	8	15	14	13.65	13.65	1164	112	96,220
5	4	8	15	14	15.87	15.87	1115	112	100,448
5	1	12	15	14	4.74	4.74	3779	108	28,579
5	2	12	15	14	8.50	8.50	1202	108	89,850
5	3	12	15	14	13.02	13.02	1361	108	79,353

Table 3.9: Pencil Break Test Wave Velocity Results

Group No.	Wave Velocity (in/s)
1	62,238
2	86,355
3	144,022
4	86,774
5	64,684

3.4.2(b) Attenuation

The second valuable piece of information gathered from the pencil break tests are data pertaining to the maximum sensor spacing on the Cedar Avenue Bridge. Table 3.10 displays the results of the individual tests for each sensor group. Table 3.11 lists the signals, normalized to a maximum of 90 dB, at three different distance intervals for each sensor group. These results demonstrate again that signal strength is greater when no diaphragms or splice plates are present between any two sensors. However, the limitations of the AEwin software require that only one signal attenuation plot be used for all sensor groups. Therefore, the average attenuation given in Table 3.1 is suggested for input into the AEwin software. Since the data results only contain three points, a second order polynomial best-fit line equation has been provided in the figure below. This equation is used to generate points on the attenuation plot for the AEwin software. The polynomial best-fit equation and the average test data are illustrated in Fig. 3.10.

Table 3.10: Signal Attenuation Results

Group No.	Sensor No.				d_1	d_2	d_3	d_4	A_1	A_2	A_3	A_4
	S_1	S_2	S_3	S_4	(in.)	(in.)	(in.)	(in.)	(dB)	(dB)	(dB)	(dB)
1	2	3	4	N/A	4	116	236	N/A	92	80	66	N/A
1	2	3	4	N/A	8	112	232	N/A	84	80	66	N/A
1	2	3	4	N/A	12	108	228	N/A	85	82	68	N/A
1	3	2	4	N/A	4	116	124	N/A	93	68	70	N/A
1	3	2	4	N/A	8	112	128	N/A	96	66	72	N/A
1	3	2	4	N/A	12	108	132	N/A	88	65	67	N/A
2	3	4	2	5	4	116	124	236	94	71	68	67
2	3	4	2	5	8	112	128	232	97	74	68	66
2	3	4	2	5	12	108	132	228	96	74	68	65
2	4	3	5	2	4	116	124	236	90	72	68	67
2	4	3	5	2	8	112	128	232	95	75	77	66
2	4	3	5	2	12	108	132	228	90	79	74	67
4	13	14	12	11	4	116	124	244	97	71	87	69
4	13	14	12	11	12	108	132	252	92	65	76	65
4	14	13	12	N/A	4	116	236	N/A	96	79	65	N/A
4	14	13	12	N/A	8	112	232	N/A	91	71	65	N/A
5	15	14	16	13	4	116	124	236	84	70	72	69

Table 3.11: Average Attenuation Test Results

d (in)	A (dB)
0	90
120	71
240	65

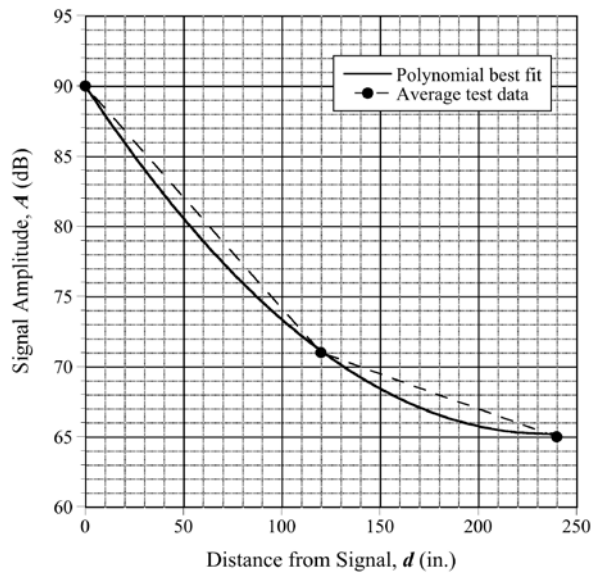


Figure 3.10: Attenuation Plot

3.5 Installation Schedule

This section contains tables, which indicate when each task was completed, how long it took to complete each task, and the number of people required to complete each installation task. The schedule follows all the work laid on in the installation plan. To ensure the safety of all people working on the system installation, one safety officer was available outside the girder, on the pedestrian walkway, at all times as well as one safety officer on the ground, below the bridge, at all times. The schedule accounts for all time expended in the installation effort. The pre-installation effort began on January 10, 2011 and ended on January 14, 2011, and Tables 3.12 - 3.16 summarize the time spent on these activities in preparation for the installation of the sensors by Mistras Group personnel. Activities summarized in Tables 3.17 and 3.18 correspond to the installation of the sensors, completion of the wiring (which had been laid out but not connected in the pre-installation phase), pencil break testing, development of the layout file. The installation phase took place on February 22 and 24, 2010. In total, the installation required fifty hours of work each from a minimum of four people on site at all times.

Table 3.12: Schedule for 1/10/2011

Task/Time	1:00 PM	1:30 PM	2:00 PM	2:30 PM	3:00 PM	3:30 PM	4:00 PM
Check Access	4	-	-	-	-	-	-
Safety Check	-	4	-	-	-	-	-
Conf. Space Trm.	-	-	4	-	-	-	-
Plate Machining	-	-	-	2	2	2	2

Table 3.13: Schedule for 1/11/2011

Task/Time	9:00 AM	9:30 AM	10:00 AM	10:30 AM	11:00 AM	11:30 AM	12:00 PM	12:30 PM	1:00 PM	1:30 PM	2:00 PM	2:30 PM	3:00 PM	3:30 PM
Unloading	4	4	-	-	-	-	-	-	-	-	-	-	-	-
Access	-	-	2	-	-	-	-	-	-	-	-	-	-	-
Equipment into Bridge	-	-	-	2	2	2	2	-	2	2	2	2	-	-
Close Access	-	-	-	-	-	-	-	-	-	-	-	-	2	-
Pack	-	-	-	-	-	-	-	-	-	-	-	-	-	4
On bridge safety	-	-	1	1	1	1	1	-	1	1	1	1	1	-
In parking safety	-	-	1	1	1	1	1	-	1	1	1	1	1	-

Table 3.14: Schedule for 1/12/2011

Task/Time	9:00 AM	9:30 AM	10:00 AM	10:30 AM	11:00 AM	11:30 AM	12:00 PM	12:30 PM	1:00 PM	1:30 PM	2:00 PM	2:30 PM	3:00 PM	3:30 PM
Unloading	4	4	-	-	-	-	-	-	-	-	-	-	-	-
Access	-	-	2	-	-	-	-	-	-	-	-	-	-	-
Equipment into Bridge	-	-	-	2	2	2	2	-	-	-	-	-	-	-
Install S.P. Post	-	-	-	-	-	-	-	-	2	2	2	2	-	-
Close Access	-	-	-	-	-	-	-	-	-	-	-	-	2	-
Pack	-	-	-	-	-	-	-	-	-	-	-	-	-	4
On bridge safety	-	-	1	1	1	1	1	-	1	1	1	1	1	-
In parking safety	-	-	1	1	1	1	1	-	1	1	1	1	1	-

Table 3.15: Schedule for 1/13/2011

Task/Time	9:00 AM	9:30 AM	10:00 AM	10:30 AM	11:00 AM	11:30 AM	12:00 PM	12:30 PM	1:00 PM	1:30 PM	2:00 PM	2:30 PM	3:00 PM	3:30 PM
Unloading	4	4	-	-	-	-	-	-	-	-	-	-	-	-
Access	-	-	2	-	-	-	-	-	-	-	-	-	-	-
Equipment into Bridge	-	-	-	2	-	-	-	-	-	-	-	-	-	-
Install S.P. Rail	-	-	-	-	2	2	2	-	-	-	-	-	-	-
Install S.P.	-	-	-	-	-	-	-	-	2	2	2	2	2	-
Wire SH	-	-	1	1	1	1	1	-	1	1	1	1	-	-
Mark Sensory Array	-	-	2	2	2	2	-	-	-	-	-	-	-	-
Prep Sensor Locations	-	-	-	-	-	-	1	-	1	1	-	-	-	-
Run Sensor Cable	-	-	-	-	-	-	1	-	1	1	-	-	-	-
Install Sensors	-	-	-	-	-	-	-	-	-	-	2	2	-	-
Close Access	-	-	-	-	-	-	-	-	-	-	-	-	2	-
Pack	-	-	-	-	-	-	-	-	-	-	-	-	-	4
On bridge safety	-	-	1	1	1	1	1	-	1	1	1	1	1	-
In parking safety	-	-	1	1	1	1	1	-	1	1	1	1	1	-

Table 3.16: Schedule for 1/14/2011

Task/Time	9:00 AM	9:30 AM	10:00 AM	10:30 AM	11:00 AM	11:30 AM	12:00 PM	12:30 PM	1:00 PM	1:30 PM	2:00 PM	2:30 PM	3:00 PM	3:30 PM
Unloading	4	-	-	-	-	-	-	-	-	-	-	-	-	-
Access	-	2	-	-	-	-	-	-	-	-	-	-	-	-
Install S.P.	-	-	2	2	2	2	-	-	-	-	-	-	-	-
Run Power Cable	-	-	-	-	-	-	2	-	-	-	-	-	-	-
Prep Sensor Locations	-	-	2	2	-	-	-	-	-	-	-	-	-	-
Run Sensor Cable	-	-	-	-	2	2	-	-	-	-	-	-	-	-
Install Sensors	-	-	-	-	-	-	2	-	2	2	-	-	-	-
Initial Tests	-	-	-	-	-	-	-	-	-	-	2	2	-	-
Close access	-	-	-	-	-	-	-	-	-	-	-	-	2	-
Pack	-	-	-	-	-	-	-	-	-	-	-	-	-	4
On bridge safety	-	1	1	1	1	1	1	-	1	1	1	1	1	-
In parking safety	-	1	1	1	1	1	1	-	1	1	1	1	1	-

Table 3.17: Schedule for 2/22/2011

Task/Time	9:00 AM	9:30 AM	10:00 AM	10:30 AM	11:00 AM	11:30 AM	12:00 PM	12:30 PM
Unloading	4	-	-	-	-	-	-	-
Access	-	2	-	-	-	-	-	-
Sensor Cable	-	-	2	2	2	2	-	-
Run Ethernet	-	-	-	-	-	-	-	-
Run Power Cable	-	-	-	-	-	-	-	-
Close access	-	-	-	-	-	-	2	-
Pack	-	-	-	-	-	-	-	4
On bridge safety	-	1	1	1	1	1	1	-
In parking safety	-	1	1	1	1	1	1	-

Table 3.18: Schedule for 2/24/2011

Task/Time	9:00 AM	9:30 AM	10:00 AM	10:30 AM	11:00 AM	11:30 AM	12:00 PM	12:30 PM
Unloading	4	-	-	-	-	-	-	-
Access	-	2	-	-	-	-	-	-
Run Ethernet	-	-	1	1	-	-	-	-
Run Power Cable	-	-	1	1	-	-	-	-
Re-wire SH	-	-	-	-	1	-	-	-
Re-wire Modem	-	-	-	-	1	-	-	-
Obtain signal	-	-	-	-	-	1	-	-
Execute layout file	-	-	-	-	-	1	-	-
Close access	-	-	-	-	-	-	2	-
Pack	-	-	-	-	-	-	-	4
On bridge safety	-	1	1	1	1	1	1	-
In parking safety	-	1	1	1	1	1	1	-

CHAPTER 4 – DATA PROCESSING PROCEDURES

This chapter discusses procedures, using vendor provided software, to collect and process bridge monitoring data. The procedures allow correlation of monitoring data with bridge health. Basic information on how to set up a layout file (monitoring file specific to each monitoring application), establish sensor spacing, and begin monitoring is described. This chapter also describes the procedure and methodology for setting high and low pass filters to eliminate unwanted signals, as well as those for all additional signal filtering capabilities of the monitoring software. Step-by-step procedures for the execution of all software options are presented in the Appendix A, including screen images of the vendor provided software.

This report also describes the optional test procedure for final calibration of the bridge monitoring software. This calibration can be used to correlate directly recorded signals with crack initiation and propagation in the members attached to the bridge superstructure. The report also describes how to set monitoring alarms based on the results of final calibration tests. The software used to monitor the Cedar Avenue Bridge is Mistras Group's AEwin™. The procedures and methods described in the following are specifically for use on the AEwin™ software running on the Cedar Avenue Bridge system, but they can also be applied to copies of the AEwin™ software installed locally in remote computers.

4.1 Setting Up AEwin™ SHSM Replay

4.1.1 Overview of Software Setup

This section of the report describes how to install, license, and begin using AEwin™ SHSM Replay, which is the software provided by Mistras Group to install on a computer other than the dedicated field computer that forms part of the Cedar Avenue Bridge monitoring system. The SHSM Replay software may be accessed by the user to analyze bridge monitoring data after it is transferred from the bridge monitoring system to an online data storage location provided by Mistras Group and finally to the user's computer. This software does not allow for real-time monitoring capabilities, since only segments of the monitoring history can be analyzed at any given time and the user must wait for data transfer (from monitoring system to online storage and then to user's computer) to be completed prior to analysis. The SHSM Replay is most applicable for post-event analysis, where the user is interested in analyzing the time history of data taken at the time when an alarm event occurred. The procedures for utilizing monitoring software described in this report are applicable to both the AEwin™ installed on the Cedar Avenue Bridge and the AEwin™ SHSM Replay installed on the user's computer. Note that any changes to AEwin™ SHSM Replay on the user's computer will not affect the AEwin™ software installed on the Cedar Avenue Bridge monitoring system.

4.1.2 AEwin™ Software Installation

The installation of AEwin™ SHSM Replay (AEwin) on the user's machine follows similar procedures to the installation of any computer software. The user should exit all running applications. The SETUP.EXE file found on the AEwin installation CD is executed to begin the

process. A Windows® installer leads the user through the definition of a file path where the software is to reside, as well as additional information which is explained clearly in the setup process. Once the AEwin software is installed, the user must license the software.

4.1.3 AEwin™ Software Licensing

A single license file was provided to The University of Minnesota by Mistras Group. This license file and software may be transferred to an alternate machine at any time. Since only one license file was provided, the software may be used on only one machine at a time. To license the AEwin software title, AEwin must be running. When a dialog box pops up, the “More Options” button should be selected. A second dialog box will then pop up, and the “Mistras License File” button in the dialog box should be selected to install the License File provided. Once the software is licensed, it may be used at any time for analysis of data from the Cedar Avenue Bridge acoustic emission data.

4.1.4 Constructing a Layout File

A ‘layout file’ is a setup file, which contains all the user defined information about the monitoring application including: AE sensor locations, signal filtering, wave velocities, signal attenuation, source localization, signal characterization, and signal alarms. This report does not describe all capabilities of AEwin or how to adjust the layout file accordingly. However, this report does describe adjustments to a layout file for the purpose of the Cedar Avenue Bridge monitoring. For a list of complete capabilities of AEwin, the reader is referred to the user’s manual (Mistras Group 2010).

The following sections explain how to adjust the layout file for establishing sensor spacing, sensor layout, signal filtering, signal clustering, and signal alarms. When the AEwin licensed software operating the Cedar Avenue Bridge monitoring system is opened remotely, the current layout file will be in use. Anytime a sensor location is changed or the user decides to change the signal alarms, the layout file must be adjusted accordingly. In order to adjust the layout file operating the Cedar Avenue Bridge monitoring system, acquisition of data must be terminated until all changes are made and the new version of the layout file is saved. If a separate license of AEwin is being operated to analyze AE data after it is recorded, a new layout file must be constructed with all sensor locations and data analysis specifications.

4.2 Maximum Sensor Spacing Considerations

4.2.1 Overview

This section of the report describes the procedure and methodology for determining the maximum allowable sensor spacing for the Cedar Avenue Bridge. In addition, a definition of maximum allowable sensor spacing is provided in the following section. In general, this procedure can be applied to any acoustic emission monitoring of a steel bridge. This section refers to the results from University of Minnesota field tests to determine the maximum allowable sensor spacing for the Cedar Avenue Bridge that was reported in Chapter 3 (section 3.4). A step-by-step procedure on how to input the results of the tests for determining maximum sensor spacing using AEwin is given in Appendix A.

The procedure for determining the maximum sensor spacing allowable on the Cedar Avenue Bridge requires pencil break tests at multiple bridge locations. Since the bridge was erected in three pieces, signal attenuation is assumed to be non-similar for each section of the bridge or across the section splices. Therefore, pencil break tests were conducted at a total of five locations: along the length of the first box girder section of the bridge, on the splice plate between the first and second sections of the box girder, along the length of the second box girder section, on the splice plate between the second and third sections of the bridge, and finally along the length of third section of the box girder. These five pencil break test locations are referred to as Group 1, Group 2, Group 3, Group 4, and Group 5 respectively. Each sensor located within the boundaries of each group is associated with its specific group when developing the layout file for the Cedar Avenue Bridge. The pencil break tests reported in section 3.4 were used to determine the expected signal velocity for each group.

4.2.2 *AEwin™ Input for Sensor Spacing*

The input values for establishing the wave velocities and signal attenuation plot can be found in the section 3.4. For the signal attenuation plot, the best-fit curve equation is applied at two-foot intervals to define the relation listed in Table 4.1. These values are used to populate AEwin’s signal attenuation function. Once input into AEwin, the system automatically increases or decreases signal amplitudes based upon the source distance from a sensor. The wave speed or wave velocity of the signal should remain approximately constant for the pencil break locations of each sensor group. Therefore, the wave velocity input into AEwin differs for each sensor group, but not for each sensor.

Table 4.1: Attenuation Plot Input for AEwin

<i>d</i> (in)	<i>A</i> (dB)
0	90
24	85
48	81
72	77
96	74
120	72
144	70
168	69
192	68
216	68
240	68

4.2.3 *Maximum Sensor Spacing*

The results of the pencil break tests, specifically signal attenuation, were used in establishing the suggested maximum sensor spacing for the Cedar Avenue Bridge. As the test results indicate, signals appear to have smaller loss per unit distance when they do not cross a splice or diaphragm. For the purpose of conservatism, it is suggested to use the most severe (largest loss) results when defining the maximum sensor spacing. This is especially true since diaphragms are located at an average separation distance of fifteen feet. However, the results of

the test indicate that signals recorded at or near twenty feet remain unchanged regardless of where the signal crosses a splice plate or diaphragm. Therefore, it is suggested that the sensors on the Cedar Avenue Bridge be spaced at a maximum of twenty feet on center. Sensor spacing greater than 20 feet is not suggested, because this may lead to a signal crossing multiple discontinuities (splice plate, diaphragm) before being recorded by the nearest sensor.

4.3 Signal Filtering

4.3.1 Overview of Signal Filtering

This section discusses the signal filtering options available when using the vendor provided software, AEwin. Signal filtering provides the user with the ability to remove certain signals (i.e., high-frequency and/or low-frequency) prior to recording and storage. The main advantage of signal filtering is that it saves memory space on the user's hard drive and it removes signals that are known not to contain useful data. Available options for signal filter include: frequency filtering, AE front end filtering, waveform front end filtering, and/or parametric filtering. All filtering methods are presented as alternatives, but multiple signal filters may be applied simultaneously. A step-by-step procedure on how to apply the filtering methods in AEwin is presented in Appendix B.

4.3.2 Frequency Filtering

Frequency filtering allows the user to eliminate signals, prior to their being recorded and stored, by discarding any signals not within a user defined frequency range. The AEwin software allows the user to define low pass and high pass filter thresholds. All signals below the low pass threshold are accepted, as are all signals above the high pass threshold. Table 3.4 lists typical high pass and low pass threshold frequencies provided by Mistras Group. The sensors purchased and installed on the Cedar Avenue Bridge are R151-LP-AST, which have a sample rate of 10MSPS (i.e., 10^6 samples/sec.). Appendix B of this report provides details on how to adjust the threshold frequency in AEwin. The implementation of frequency filters is common practice and should be used in the application of monitoring on the Cedar Avenue Bridge.

4.3.3 AE Front-End Filter

AE front-end filters provide the user with the ability to determine which signals to accept or reject based upon signal features. Signal features the user may select include: amplitude, energy, counts, duration, rise time, counts to peak, average frequency, absolute energy, and average signal level, among others. After selecting a specific signal feature, the user establishes a low level and high level of acceptance and the channels for which to apply the filter. Unlike the frequency filters, AE front-end filters are inclusive. The use of AE front-end filters rejects all hits and associated waveform data, preventing it from being stored. A total of four AE front-end filters can be applied simultaneously. Although the capability of AE front-end filter is provided, and it facilitates saving memory space through the reduction of recorded data, the use of AE front-end filters is not recommended. With the price of memory space being relatively inexpensive, the University of Minnesota research team believes it is in the best to record all data that passes through the frequency filters. Unwanted signals can just as easily be eliminated in a post-processing application. This practice will prevent the unintentional elimination of bridge distress signals prior to their being recorded.

4.3.4 Waveform Front-End Filtering

Waveform front-end filtering is identical to AE front-end filtering in application and purpose, except waveform front-end filtering only rejects waveform data, while retaining information on the number of hits. For the same reasons as those described in the AE front end filtering section, the University of Minnesota research team does not recommend the use of waveform front end filters. Post acquisition analysis is recommended for differentiating between background noise and distress signals. A detailed explanation of how to differentiate between multiple signal types is described in the section 4.4 of this report.

4.3.5 Parametric Filtering

Similar to the AE and waveform filtering, parametric filtering prevents the recording of data unless parametric readings are within a user-defined tolerance. The parameters are defined by the user and become features of an AE signal. Therefore, this application of signal filtering is an expansion on AE filtering, except it applies to user-defined AE features. For the same reasons as those described in the AE and waveform sections above, the University of Minnesota research team does not recommend the use of parametric filtering.

4.3.6 Discussion of Signal Filtering

As stated in the preceding, the safest form of front-end signal filtering is frequency filtering. The sensors are constructed with a certain range of acceptable signal frequencies, as noted in Table 4.2. The sensor based frequency filters are built into the AEwin software and should not need adjustment. However, the user may adjust the range of acceptable signal frequencies if desired. In regards to additional front end filtering, it is beneficial for the purpose of data reduction if memory space is a driving factor, but is not necessary otherwise. The amount of data produced by one SH-II system, which is the system in place on the Cedar Avenue Bridge, is low (well below 1 MB per day). AE feature, waveform and parametric front-end filtering will reduce the amount of data produced each day, but the gain in memory space may not be worth the risk of losing valuable information. Post processing filters achieve the same ends as these three front-end filters, but without the risk of missing potential distress signals of unknown forms. Thus, the University of Minnesota research team currently recommends implementing frequency front-end filters but not AE feature, waveform, or parametric front-end filters.

4.3.7 AEwin™ Input for Signal Filtering

Table 4.2 lists typical frequency filters for acoustic emission monitoring (Mistras Group 2010). The sensors installed on the Cedar Avenue Bridge have a sample rate of 10MSPS.

Table 4.2: Low Pass and High Pass Frequency Filtering Thresholds

HP Filters (Analog)	LP Filters (Analog)	LP Filters (Digital)	Sample Rate
1, 5, 20, 100 kHz	1 MHz	8, 12, 16, 20 kHz	100kSPS
1, 5, 20, 100 kHz	1 MHz	20, 30, 40, 50 kHz	250kSPS, 500kSPS
1, 5, 20, 100 kHz	1 MHz	40, 60, 80, 100 kHz	1MSPS
1, 5, 20, 100 kHz	1 MHz	100, 150, 200, 250 kHz	2.5MSPS
1, 5, 20, 100 kHz	1 MHz	200, 300, 400, 500 kHz	5MSPS
1, 5, 20, 100 kHz	1 MHz	Not Available	10MSPS, 20MSPS

4.4 Signal Characterization

4.4.1 Overview of Signal Characterization

This section references a test described in Chapter 5, the notched beam test, developed specifically for the purpose of characterizing acoustic emission signals. This section discusses the procedure for using the results from signal characterization tests to adjust settings in AEWin to provide the user with automated signal characterization capabilities. Appendix A contains procedures on how to use notched cantilever beam test results to establish signal clustering (characterization) techniques, using AEWin.

4.4.2 Notched Beam Test

The notched beam test was developed to provide physical data for characterizing acoustic emission signals so that signals produced by fracture can be discriminated from those generated by non-AE events (e.g., traffic, bolt fretting). In general, a steel cantilever beam with a notch is loaded monotonically until a crack initiates at the notch, and the crack propagates into the web of the beam. The acoustic emission system was used to record the signals due to crack initiation and propagation. The AE features (parameters) of interest include: amplitude, energy, counts, duration, rise time, counts to peak, average frequency, absolute energy, average signal level and frequency centroid. With these AE parameters recorded for each crack event, the monitoring system user is in a better position to differentiate between a crack event and non-AE signals.

A series of notched beam tests were conducted in the laboratory in order to perfect the beam configuration and to facilitate the recording of signals in a relatively noise-free environment. Details of these tests are described in Chapter 5.

4.4.3 AEWin™ Signal Clustering

Signal clustering allows for the user to define limits for differentiating between different signal types recorded. The clustering capability analyzes different patterns in AE features (amplitude, energy, counts, duration, rise time, counts to peak, average frequency, absolute energy, and average signal level) to define the signal clusters. In a new AE monitoring application, determining what features demonstrate discernable pattern differences in signal types requires trial and error of different AE features. After conducting signal characterization tests, such as the notched beam tests, the two AE features displaying the most significant pattern features (signal characterization) relative to observed background noise are defined.

In general, the user must define the type and size of anticipated signal clusters. This means the user must decide if the signal clusters should be at or near a fixed location on a XY scatter plot or have a floating location. After the signal characterization test, it can be determined what crack initiation and crack propagation warrant a fixed value signal cluster with two features at their respective fixed values. Any signals recorded outside of this cluster zone are then defined as background noise.

In addition to defining the cluster type and size, the user needs to define the number of signals within the cluster necessary to correctly accept a cracking event as occurring. In the AEWin software, this is called the point threshold. Since background noise signal data does have occasional outliers, it is recommended that the point threshold be set to 10 points before the AE

event is characterized as a crack event. This means that 10 signals within the defined range must occur before it is defined as being due to a specific event.

The next important step in developing signal clustering capabilities for the monitoring application on the Cedar Avenue Bridge are defining the grading levels for each cluster. Cluster grading is based upon the percent of hits associated with a given signal. For example if a total of 10 hits were recorded, 8 of the hits inside the range of the crack cluster and 2 hits outside the crack cluster range, then the crack cluster would contain 80% of the signals and background noise would contain 20% of the signals. The user can select to use no cluster grading, which would prevent the use of a trip alarm system, described below, automatic cluster grading, which defines percentages of < 20%, < 40%, < 60%, < 80%, ≤100%, or user defined cluster grading. Since the ultimate goal of signal clustering is to identify crack signals and trigger the alarm, the use of cluster grading is recommended. Additionally, if no front-end filters are used in the monitoring application, a large percentage of the signals recorded will be due to background noise and therefore it is not recommended to use the automatic cluster grading. Using cluster grading if no front-end filters are used, would assign a more severe grading for background noise than crack signals. To avoid this problem, signal clustering filters can be applied which allow the user to define filter levels in the exact way as the front end filters only specifically for signal clustering. This will reduce the amount of background noise analyzed during signal clustering, and allow the user to use automatic cluster grading, which is then used for establishing cluster alarms.

Signal clustering or signal characterization has two alarm system options built into it: trip alarm and rate alarm. The alarm capabilities of signal clustering are described in section 4.5 of this report. Additional customization of signal clustering is available, but pertains to output formatting (not analysis).

4.4.4 Summary of Signal Characterization

The purpose of conducting a signal characterization test (e.g., the notched beam test) is to produce AE signals for crack initiation and crack propagation. The goal of the test is to use the AE signals recorded from crack initiation and crack propagation, compare the signals during the time of cracking to the time period prior to the crack events, and ultimately differentiate between crack initiation, crack propagation, and background noise. The knowledge of the qualitative AE feature values to expect during crack initiation and crack propagation will give the user the ability to alert bridge inspection, bridge maintenance, and if necessary the general public. If a clear and reliable distinction between signal types is established, the system can be automated to monitor the health of the Cedar Avenue Bridge.

4.5 Signal Alarms

4.5.1 Overview of Signal Alarms

This section of the report explains how to set various signal alarm capabilities for acoustic emission monitoring, using the AEwin software. There are several options for signal alarms provided in AEwin including: average signal level alarms and signal cluster alarms, which include trip alarm and rate alarm. This section defines each alarm capability, as well as

pros and cons for each option. Multiple signal alarms may be set simultaneously, and the decision of which to use is at the discretion of the user.

4.5.2 Average Signal Level Alarm

The average signal level (ASL) alarm allows the user to define a low level and high level signal amplitude average at which alarm data will be produced. If the ASL is below the user defined low level amplitude, then alarm data is recorded, and similarly for high level. The range produced by the low level and high level thresholds defines the non-alarm range. An acceptable input for low level ASL is 0 dB, while the high level ASL should be defined just below the ASL corresponding to crack initiation and/or crack propagation, or above previously recorded background noise levels. This method for establishing an alarm system for the Cedar Avenue Bridge is the most simplistic and straightforward method. Its application should be used on all sensors on the bridge, and it is suggested that MnDOT treat a high-level exceedance alarm as bridge distress.

4.5.3 Signal Cluster Alarm

The two signal cluster alarms available with the AEwin software are trip alarm and rate alarm. The following two sections explain how to use each cluster alarm respectively.

4.5.3(a) Trip Alarm

As described in section 4.4.3, in order to use the trip alarm capabilities of the software, the user must use either automatic or user defined cluster grading. The trip alarm system will notify the user, via an alarm message, when the cluster analysis enters a user defined grading level. For example, if the user selects to be notified when 50% of the signals being recorded are associated with bridge distress, then the trip alarm level must be set to the grading level associated with 50% exceedance. The user can choose to be notified of a trip alarm occurring via text message if the line display is enabled. Otherwise, the user will be notified of a trip alarm when accessing the AEwin program after the alarm has been triggered.

4.5.3(b) Rate Alarm

The rate alarm is a user defined alarm for signal clustering based on the rate of signals recorded that are associated with a user defined cluster. This alarm will notify the user when a specified amount of signals occur during a user defined time interval. For example, for the Cedar Avenue Bridge, this alarm should be triggered to sound when many signals falling within the previously defined range for a crack cluster are recorded during a certain time interval. The AEwin software is programmed to notify the user with one rate alarm until the rate drops below the rate alarm threshold. This setting is to prevent receiving multiple rate alarms over a short period of time.

4.5.4 Summary of Signal Alarms

All three signal alarms (i.e., average signal level alarm, signal cluster trip alarm, and signal cluster rate alarm) are beneficial for application to the monitoring of the Cedar Avenue Bridge. Although all three alarms are relatable, since they all relate to AE signal features, the implementation of all three signal alarms independently is advisable when needed. There is no

additional computational cost in using all three alarms. However, the University recommends the implementation of the ASL alarm. The use of trip alarm and the rate alarm should be implemented once a signal characterization test (e.g., notched beam test) has demonstrated clear and reliable differences in the AE characteristics for cracking and no-AE events.

4.5.5 AWin™ Input for Signal Alarms

Based upon the results of multiple months of recording data on the Cedar Avenue Bridge, it has been determined that background noise has an ASL of between 55 dB and 80 dB. Therefore, the authors suggest that an ASL alarm be set with an upper threshold of at least 90 dB. A threshold at this level will prevent background noise signals producing alarms, but also trigger an alarm if a more severe event occurs. When results of the signal characterization test (i.e., notched beam test) become available, the value of the upper threshold can be adjusted to represent more accurately the processes of crack initiation and propagation.

CHAPTER 5 – NOTCHED BEAM FRACTURE TESTS

5.1 Overview

A series of notched beam tests was performed at the University of Minnesota Theodore V. Galambos Structures Laboratory. The purpose of these tests was to generate, capture, and record the acoustic emissions of fracture in mild structural steel using the same monitoring system as currently being used at the Cedar Avenue Bridge. Data associated with the waveforms of these fracture emissions was analyzed in Chapters 6 and 7 to identify characteristics that differentiate them from non-AE events. Such differentiation enable the formulation of data analysis procedures for the AE monitoring system at the Cedar Avenue Bridge that discriminates between fracture and non-AE events, thus enabling the system to provide an advanced warning of cracking distress. Information from this analysis was subsequently used to determine what parameter, or set of parameters, best indicate fracture, allowing for the definition of successful alarming protocols to be used at the Cedar Avenue Bridge.

5.2 Beam Specimen Fabrication

An S4x9.5 structural steel beam of length 24 in. was used to fabricate the specimens for all three notched cantilever beam tests. Disregarding the notch and hole, the beam was fabricated in a nearly identical manner for all tests. The bottom flange was cut with a band saw except for a 6" portion at one end where the beam was to be fixed to a support, as well as a 2-3" portion at the other end where the jacking force was to be applied. Two schematic diagrams showing the dimensions and specifications of the notched beams can be seen in Figure 5.1.

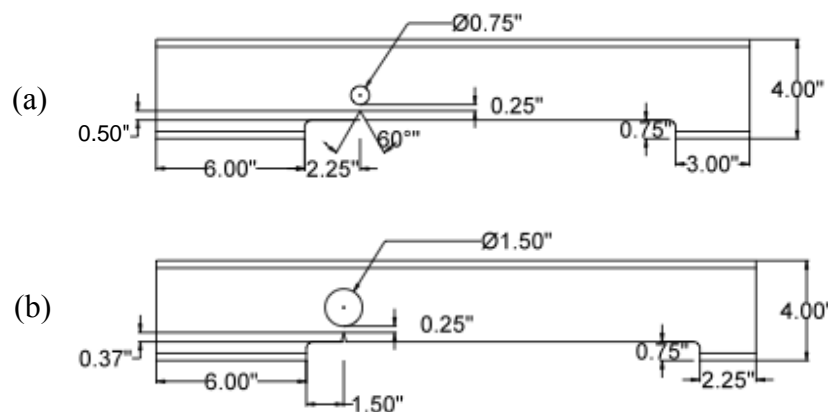


Figure 5.1: Notched beam specimens. (a) Dimensions for first notched beam test. (b) Dimensions for second and third notched beam tests

A sharp notch tip was required for each beam in order to maximize the stress concentration and induce a fracture. Given that the purpose of the notched beam test was to capture fracture using acoustic emission measurement technology, it was important that the notched beam did not exhibit significant yielding prior to ultimate failure. Creating a sharp crack

tip near the point of maximum moment successfully produced fracture, as well as the audible emissions that go along with it.

For the first test, a 1/2" deep notch with a 60° opening angle was saw-cut into the beam. A small rectangular notch had previously been placed at the same location for an earlier preliminary test, however, this new 60° notch completely enveloped it. The second and third tests utilized electric discharge machining (EDM) wire-cutting equipment to create the notch. This fabrication method produced a similarly sharp crack tip as the first test, but also exhibited a more consistent finish. Also, the height of the notch was reduced to 3/8" in order to increase the stress at the notch tip, and the opening angle was lowered to 30° in an effort to further increase the stress concentration at the notch tip.

A hole was drilled above the notch tip in all three tests. The first test used a 3/4" diameter hole while the other two used a 1 1/2" diameter hole. These holes served multiple purposes. For one, it reduced the area and thus moment of inertia of the cross section at the failure plane. This forced the section to fail at a smaller moment and, therefore, a smaller nominal stress. The hole also raised the neutral axis at the failure plane, thereby increasing the stress at the notch tip (i.e., hot spot stress) for a given nominal stress (i.e., away from notch) or displacement. And finally, it provided a stopping point for the crack, so that the AE sensors would be able to pick up the loud noise associated with the ultimate failure of the steel between the notch tip and the bottom of the hole.

5.3 Connection

The notched beam specimens were fixed to the top flange of a large steel I-beam (representing the girders in the bridge superstructure) using both large clamps and epoxy. The I-beam was used to model the much larger steel girders at the Cedar Avenue Bridge. The steel I-beam was bolted and tensioned to the laboratory floor. The epoxy was applied to the 6" portion of the bottom flange (Fig. 5.1) on the notched beam and clamped to the superstructure. A small hydraulic loading jack was placed in the center of the 2-3" bottom flange portion at the other end of the beam, directly beneath the web. This setup is shown in Figure 5.2 for the second notched beam, and it shows the epoxy, the clamps, the jack, and the AE sensors.



Figure 5.2: Test setup for the second notched beam test

The notched beam was connected to the superstructure using a combination of clamps and epoxy. Epoxy was applied to the interface, the beam was placed in position, and the clamps were tightened to hold the pieces in close contact while the epoxy cured. The epoxy alone would not be enough to prevent the notched beam from detaching from the superstructure, thus the clamps were left in place. However, the epoxy was necessary in order to act as a couplant to facilitate the transfer of acoustic waves between the two beams. The epoxy also helped reduce friction stress releases associated with the interface, and thereby reduced the noise picked up by the AE system.

5.4 Sensor Setup

Sensors on the notched beam were used primarily as guard sensors. The function of guard sensors is to enable the use of hit arrival times to determine the source location of an event. These are crucial to the notched beam tests in order to isolate the events originating from fracture at the notch. In each test, a guard sensor was attached near the jacking surface in order to filter out the noise related to friction between the jack and notched beam. Two more guard sensors were placed on the web at equal distances on either side of the notch tip in order to isolate the hits that result from activity around the notch and filter out hits originating from sources outside the region. Finally, a guard sensor was placed near the interface between the two beams in each test in an effort to filter the noise associated with friction at this interface.

Other sensors were placed on the superstructure in order to examine the way acoustic waves travel, not only through a large steel structure, but also through the notched beam interface. Sensors were applied to both the superstructure flange and stiffeners. Only one sensor was placed on the web of the superstructure due to placement issues, but the stiffener sensors should behave in a similar manner. The complete sensor location setup for each test can be found in section 5.11 of this chapter.

5.5 Data Collection

Data was collected using the Sensor Highway II Remote Monitoring System and eight acoustic emission sensors, all purchased from the MISTRAS Group, and identical to the system at the Cedar Avenue bridge. Acoustic waveforms were detected and recorded for each hit over a threshold defined at 50 dB.

In addition to the waveforms for each acoustic emission being measured and recorded, a number of waveform parameters were recorded for each hit. These parameters are arrival time, rise time, counts, energy, duration, peak amplitude, average frequency, counts to peak, initiation frequency, reverberation frequency, signal strength, absolute energy, frequency centroid, and peak frequency. The latter two are properties of the power spectrum of the waveform.

5.6 First Notched Beam Test

The first test in which fracture was achieved, of which specimen is shown in Fig. 5.1(a), was actually the second test performed on a notched beam. The initial preliminary test was unsuccessful in producing a fracture at the notch. It was determined that the stress concentration generated around the notch tip was not large enough to produce fracture prior to significant yielding. The beam in the preliminary test experienced significant yielding near the notch plane.

The bottom flange where the notched beam connected to the superstructure also was subjected to yielding due to the epoxy cracking during the test.

The notch and the cross-section at its plane were modified (Fig. 5.1(a)), and the beam was retested and is reported here as the first test. As previously described, a 60° notch of ½" height was sawed over the existing rectangular notch, and a ¾" diameter hole was drilled such that the bottom of the hole was about ¼" above the notch tip.

Five AE sensors were attached to the notched beam and three were placed on the superstructure. Four were placed on the web of the notched beam, in the horizontal plane in which the notch tip lay. Two were placed 4" on either side of the notch, another was placed 8" from the notch towards the jack end, and the last 12" from the notch. One more was placed on the top flange of the notched beam, a distance 3" from the notch towards the jacking end. The final three sensors were placed on the top flange of the superstructure, at distances of 6", 18", and 42" from the centerline of the notched beam.

At the connection between the notched beam and the superstructure, both epoxy and clamps were used. However, the epoxy was only useful around the edges of the interface, as previous damage had distorted the bottom surface, preventing the region from bonding reliably. Because of this condition, the three sensors on the superstructure received a lower percentage of hits compared to the second and third tests.

During testing, load was applied at a fast rate in order to ensure fracture would occur prior to any significant amount of new yielding, as shown in Figure 5.3. While there was an absence of audible fracturing during the loading, the steel did eventually fracture. A large energy release at ultimate failure was recorded by the SH-II system. Overall, more than 12,000 hits were detected by the AE system.

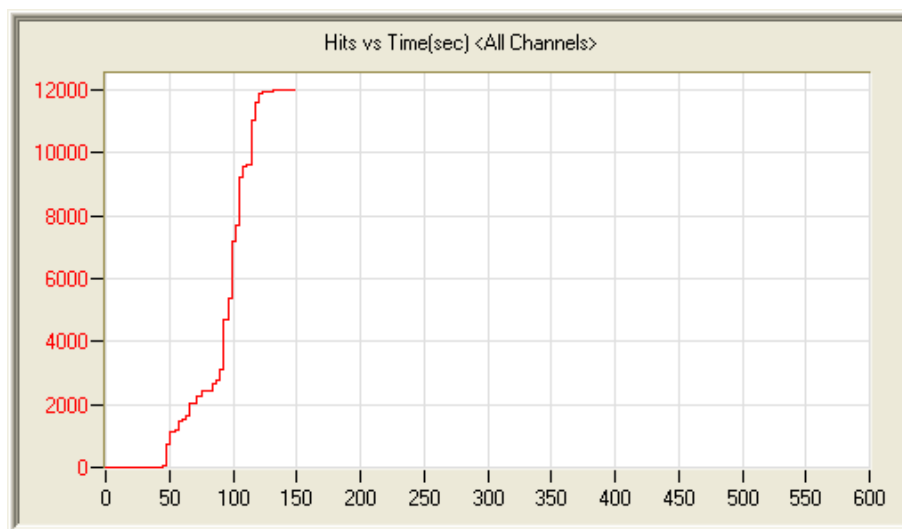


Figure 5.3: Plot of hits vs. time for the first notched beam test

5.7 Second Notched Beam Test

The sensor locations for the second notched beam test differed from the previous test substantially (see section 5.11). Only three sensors were installed on the notched beam and thus the other five were placed on the superstructure. On the notched beam, two sensors were placed on the web 3" to either side of the notch, and one was placed on the web near the loading end. On the superstructure, two sensors were placed 12" down from the top flange on stiffeners that were equidistant from the centerline of the notched beam. Another was placed on a different stiffener, 8" offset horizontally from one of the aforementioned stiffeners. Another was placed on the web of the superstructure, near the end. And, finally, the last sensor was installed on the top flange of the superstructure, 6" from the centerline of the notched beam.

There were a few reasons for the change in sensor alignment for the second test. First, as previously mentioned, the first notched beam test failed to provide a large number of hits to the sensors on the superstructure. Placing additional sensors on the superstructure provides a better understanding of how fracture waves propagate through a large steel specimen. Secondly, using sensors on the superstructure to determine fracture better illustrates field conditions. At the Cedar Avenue Bridge, the sensors are spaced 10 ft. apart, meaning a crack may occur up to 5 ft. from the closest sensor. Therefore, it is imperative a predictive alarm system be developed on the basis of data from sensors both close to and far from the source location.

Loading during the recording was done at a very slow, but steady, rate relative to the first notched beam test, in order to space out the arrival times of hits for a clearer analysis of the data after the test. This change in load rate is demonstrated by the slopes of the hits vs. time plots of Figures 5.3 and 5.4, as load rate and hit rate tend to be correlated. Fracture events were audible throughout the course of the loading, culminating in a very large energy release as ultimate fracture was achieved. No evident yielding of the section occurred during the test. Times at which audible cracking was heard were recorded for analysis purposes. Over 12,000 hits were recorded, although many of the hits were simply due to noise (i.e., non-fracture events).

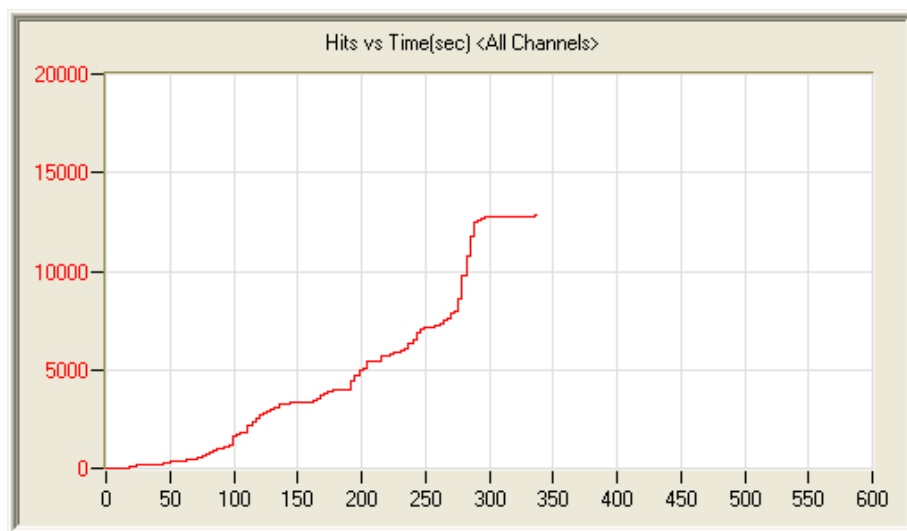


Figure 5.4: Plot of hits vs. time for the second notched beam test

5.8 Third Notched Beam Test

The third notched beam test was instrumented similar to the second test, and eight AE sensors were used. Three sensors were placed on the notched beam. One was placed on the web a few inches from the jacking end of the beam. The other two were placed on the web, 5" in each direction of the notch tip. The five remaining sensors were placed on the superstructure. One was placed on the top flange near the notched beam interface, 6" from the web center of the notched beam. Two others were placed on the top flange at distances 16" and 24.5" away from the web center (directly above web stiffeners). The final two sensors were placed on the stiffeners, approximately 12" below the top of the flange.

An OSMOS fiber optic strain gage was attached to the top flange of the notched beam in the third notched beam test. Figure 5.5 shows the placement of the fiber optic gage on the top flange of the beam, even though this picture was taken from the preliminary test. The setup for the fiber optic gauge, however, remained the same. Holes were drilled in the top flange of the notched beam, and brass end-clamps were used for securing the fiber optic gauge onto the beam. The fiber optic gage was stressed slightly in tension prior to its placement, so that when compressed during the test, an accurate measurement would be obtained.



Figure 5.5: Placement of fiber optic sensor on top flange

During the test, load was applied to the beam at a rate similar to that of the second notched beam test in order to slow the rate of emissions received by the system, which would allow for ease in analysis later. Initially, the load was brought up to 1000 pounds, and then released. Then, the load was brought up to 1500 pounds. At this point, the load was held constant for about 60 seconds while audible cracking took place around the notch. After noise ceased, the load was released. Finally, the load was applied until ultimate failure, when the portion of steel between the notch tip and the drilled hole suffered a complete fracture. This loading protocol can be seen in the color-coded hits vs. time plot shown in Figure 5.6. In this plot, the blue region was the loading to 1000 pounds, the orange region was loading to 1500 pounds, the purple region was loading to ultimate failure, the green region indicated the unloading periods, and the black and red regions indicate pauses during the loading.

Overall, over 12,000 hits were recorded by the AE system using a 50 dB threshold. Unlike the previous tests, this event experienced a period of fracturing under constant load. This period should prove valuable in determining wave properties that are associated with fracture emission. Also, unlike previous tests, the load applied to the end of the beam was monitored better, permitting a better description between loading and acoustic emission during fracture.

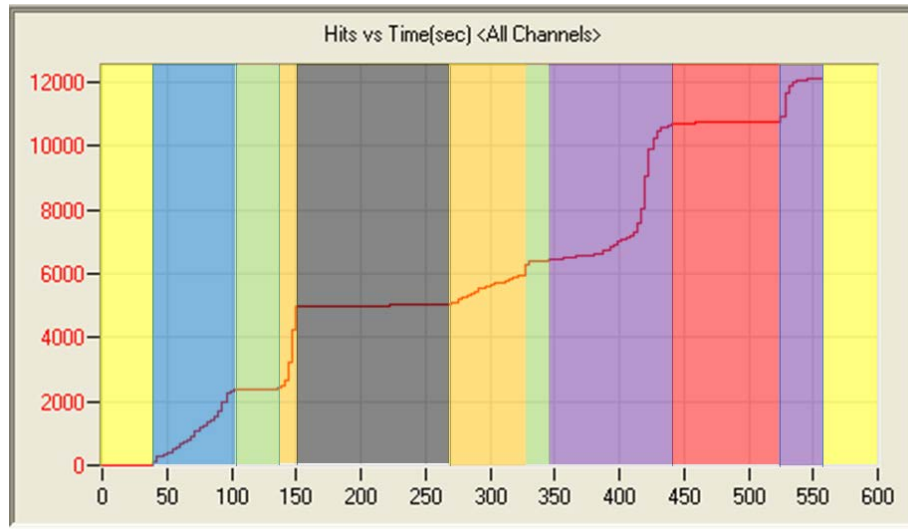


Figure 5.6: Plot of hits vs. time for the third notched beam test

5.9 Data Analysis

The acoustic emission data collected during the three notched beam tests are used in subsequent chapters to evaluate data analysis procedures for the Cedar Avenue Bridge. Besides the hits vs. time relations given in Figures 5.3, 5.4 and 5.6, no additional data is presented in this chapter except for the third test. The acoustic emission sensors and the fiber optic gage proved to be a powerful combination and it enabled the construction of the cumulative hits vs. deformation plot with interesting and useful features. These features are associated with the Kaiser and Felicity effects.

5.9.1 Kaiser and Felicity Effects

The Kaiser effect states that, in metals or other fracture-prone materials, acoustic emission activity is not observed during the unloading and reloading of a material specimen until the current stress surpasses the highest previously experienced stress (path A-B-C-B in Fig. 5.7). This phenomenon can be understood in relation to discontinuities created in the material, and which do not mobilize until the previous peak stress is exceeded. However, when a material begins to show signs of failure, the stress at which acoustic emission activity starts up again upon reloading will be smaller than the previous peak stress prior to unloading (path D-E-F-G in Fig. 5.7). The ratio of the stress (or load) at F to that at D (in Fig. 5.7) is known as the Felicity ratio.

The Felicity ratio is determined when both the load (or stress) history and the cumulative acoustic emission activity (as shown in Fig. 5.7) are measured. Felicity ratios equal to 0.90-0.95 are often used as the threshold of failure initiation. However, the value of the Felicity ratio at

failure may vary with the structure being tested, but it is often assumed to be approximately equal to 0.5.

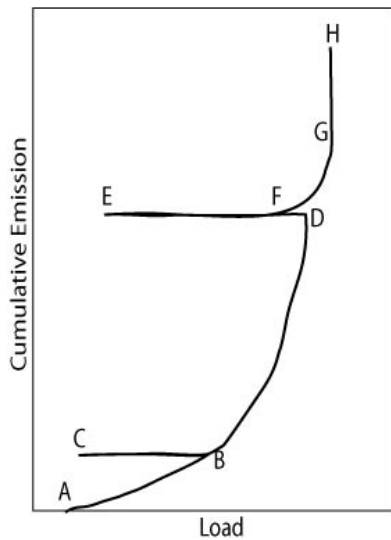


Figure 5.7: Example of Kaiser and Felicity Effects
(www.ndt-ed.org)

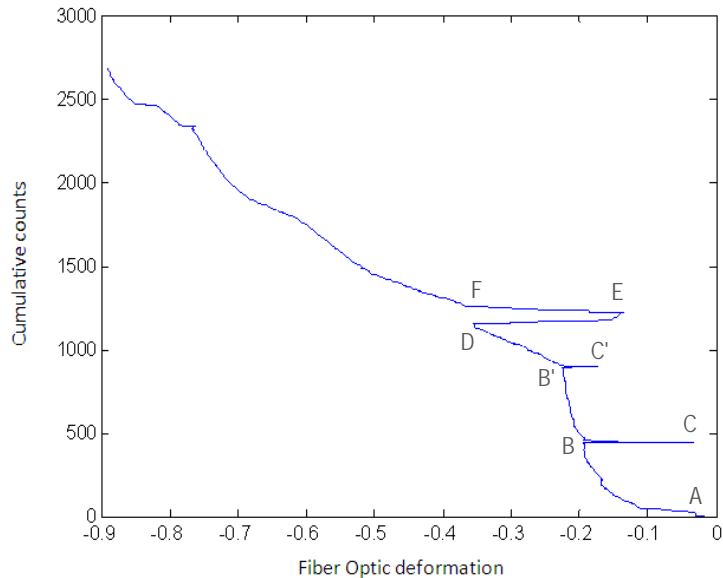


Figure 5.8: Acoustic emissions vs. fiber optic gauge deformation (inches) for third beam test

5.9.2 Results from Data Analysis

Figure 5.8 shows the cumulative acoustic emission activity vs. the total shortening of the fiber optic gauge (in inches). The total deformation of the fiber optic gauge installed on a member that is loaded in the linear, elastic range, is proportional to strain, therefore stress and load. Thus, the fiber optic gauge reading can be used to construct a plot that is analogous to the cumulative (acoustic) emission vs. load plot in Fig. 5.7.

The first unloading and reloading (A-B-C-B in Fig. 5.8) occurred at approximately 500 acoustic emission counts, and the beam behaved as expected. That is, further acoustic emission activity did not begin until the previous deformation was reached (point B in Fig. 5.8). However, the epoxy seal between notched and support beams broke after the second reloading (B'-C'-B' in Fig. 5.8). The loss of contact along the epoxied surfaces resulted in fewer acoustic emission sensors being effective, and, therefore, a reduction in cumulative acoustic emission activity. The reduced acoustic emission activity (at approximately 1,000 counts) produced a flatter rather than a steeper slope beyond B' in Fig. 5.8. Nevertheless, there is a clear example of the Felicity effect in the third unloading (D-E-F in Fig. 5.8).

Use of the Felicity ratio in purely acoustic emission applications may be difficult, if not impossible, since it is seldom possible to measure the loads or stresses that the member experiences. However, the Felicity ratio can be used as a successful analysis tool if fiber optic gauges are also included in the monitoring system. The use of the felicity ratio in a program to monitor steel bridges for fracture is promising, but further testing and research is needed to assess its viability as a global bridge monitoring technique.

5.10 Noise Tests

For each setup, prior to performing the fracture test, a series of “noise” tests were conducted on the specimens. These included both impact tests and friction tests. Impact tests included striking the beam and superstructure with a hammer at various locations, dropping pebbles on the beam, and pencil break tests. Friction tests included rubbing sandpaper, a metal wrench, and fingers against the specimens. These “noise tests” were recorded using the AE equipment, and were used in subsequent analysis for testing filtering techniques. Since the goal of the analysis is to be able isolate fracture incidents, a successful filter, when applied to the noise tests, should remove all hits due to noise.

5.11 Sensor Locations in the Notched Beam Tests

Figures 5.9 – 5.11 provide diagrams of the sensor locations in the three notched beam specimen tests.

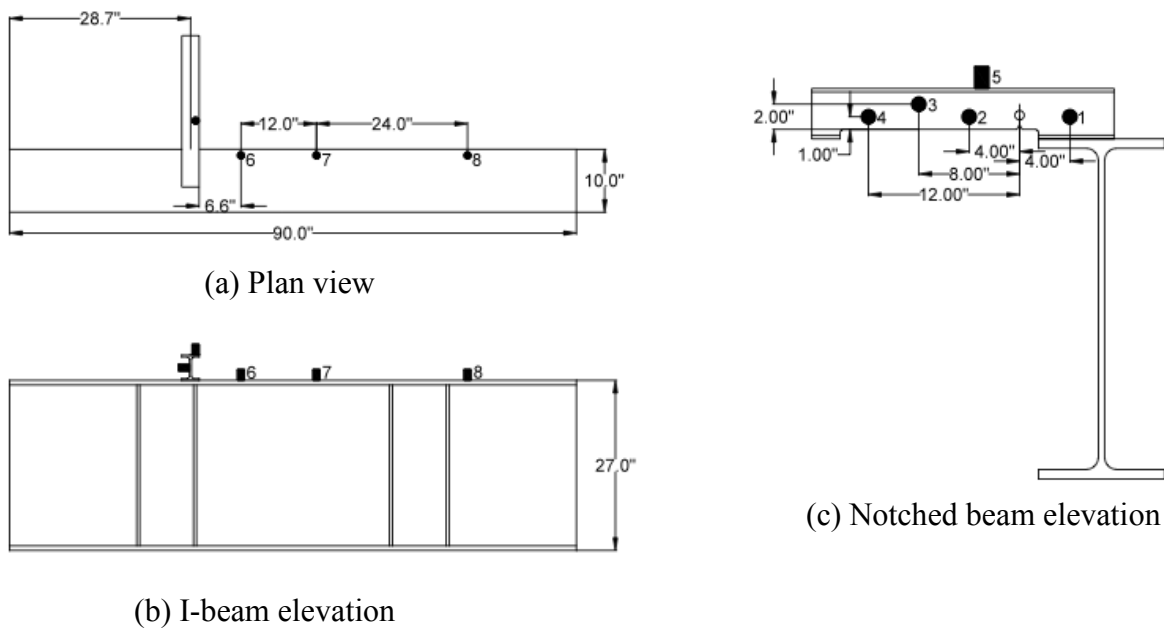


Figure 5.9: First notched beam test sensor locations

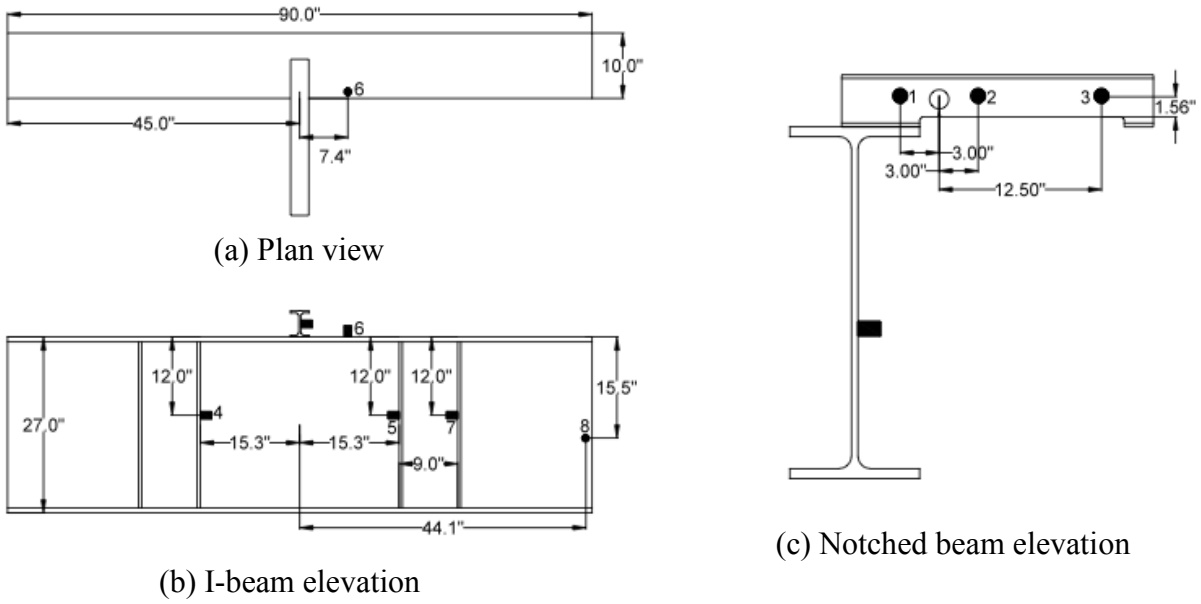


Figure 5.10: Second notched beam test sensor locations

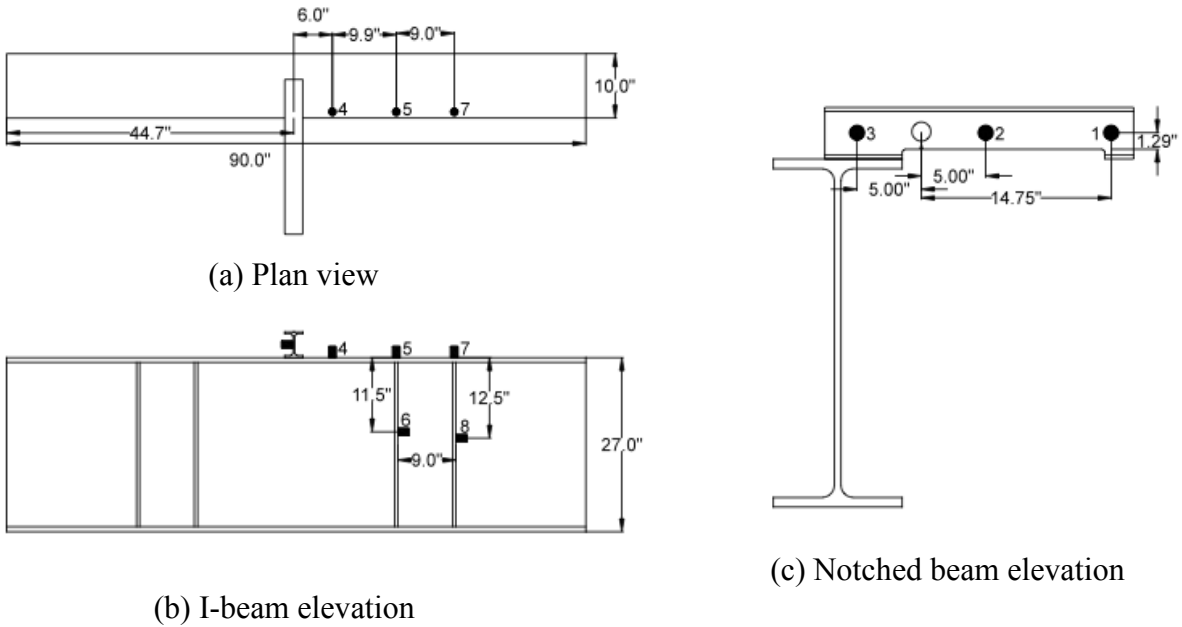


Figure 5.11: Third notched beam test sensor locations

CHAPTER 6 - DATA ANALYSIS PROCEDURES

6.1 Overview

This chapter summarizes an effort to evaluate the data analysis tools in the AEwin software with the goal of developing procedures for use with the Cedar Avenue Bridge data. The AEwin software evaluates a series of acoustic emission parameters, and the analysis documented here comprises the evaluation of a number of these parameters. To evaluate and select analysis tools, several datasets data were selected for comparison: the three fracture tests (Chapter 5), AE data from the Cedar Avenue Bridge comprising “normal” activity (dated August 13, 2013), and “anomalous” data recorded in the Cedar Avenue Bridge (dated June 7, 2013).

6.2 Hits vs. Time

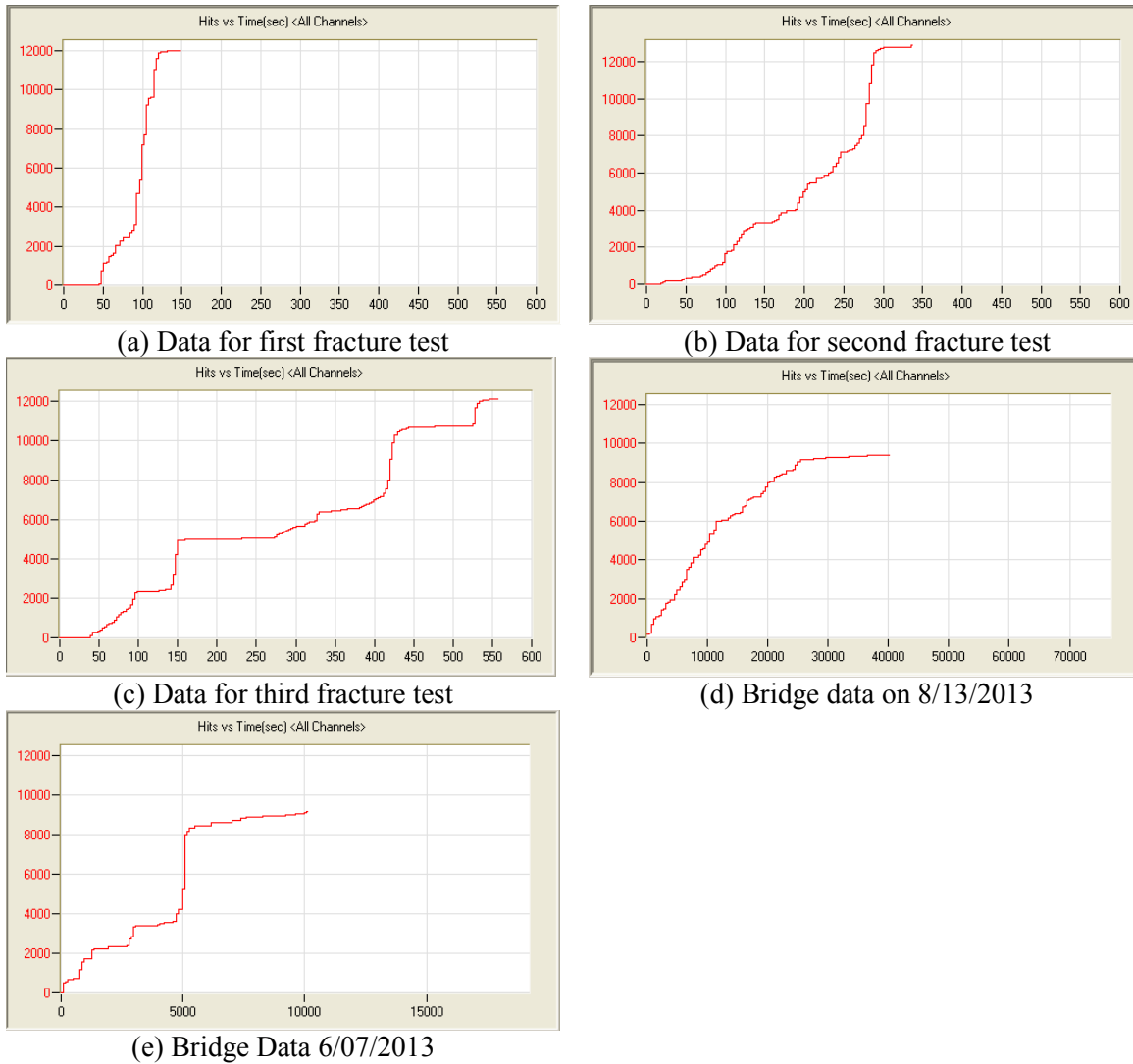


Figure 6.1: Hits vs. time (sec)

The first two parameters that were evaluated are number of cumulative number of hits and elapsed time (in seconds). The plot of hits vs. time is commonly used to demonstrate increased AE activity when a cracking event takes place.

One of the observations that is evident in the hits vs. time graphs can be seen by comparing Figures 6.1(a)-(c) for the fracture tests with Figures 6.1(d)-(e) for the bridge data. For example, the number of hits in Figure 6.1(a) rises from 0 to 12,000 hits in less than 2 minutes. The 2nd test shows a similar trend due to fracture, with a sudden rise from 8,000 to 12,000 hits in a short period of time. The fracture caused a sudden increase in the number of hits over time, a pattern previously observed during the first two tests.

When analyzing the bridge data in Figure 6.1(d), the typical pattern found in the graph of hits vs. time is a steady accumulation of hits during the day. The number of hits recorded did not reach the 12,000 hits in 11 hours, while the fracture tests exceeded that amount in a few minutes. Moreover, there are none of the sudden increases, marked by large increases in slope, in the hits vs. time relation that were observed for the fracture tests. Therefore, the behavior on the August 13th data does not resemble that of the fracture tests.

Figure 6.1(e) shows that on June 7, an unusual type of event caused a sudden increase in the number of hits over time. This type of behavior is very similar to what is observed from the fracture tests. However, as a result of these measurements, the authors accompanied a bridge inspector from MnDOT's Metro Division to inspect the Cedar Avenue Bridge, and no evidence of any cracking distress was found. Thus, further evidence is required before a hits vs. time relation alone is used to conclude that a cracking event has occurred in the bridge.

In general, when assessing hits vs. time plots, normal behavior (i.e., when cracking is not occurring) is consistent with (1) a steady increase of hits vs. time, and (2) no sudden increases occurring in short periods of time.

6.3 Hits vs. Channel

The plots shown in Figure 6.2 illustrate the number of hits recorded by each sensor. Figures 6.2(a) – 6.2(c) show that sensors closest to the fracture in the tests reached 2000 hits in less than 5 minutes, while the bridge data sensors in August 13, 2013 (Fig. 6.2(d)) did not reach this mark in more than 11 hours. A different situation occurs by observing Figure 6.2(e), which shows that all relevant acoustic hits were captured by a single sensor (No. 14). This figure provides clear evidence of unusual or anomalous behavior occurred during June 7, 2013. Typical activity in the bridge would show graphs similar to Figure 6.2(d), which have AE hits spread over several different sensors. This observation was noticeable enough to distinguish it from all the different data files that have been analyzed during July and August. It appears that an unusual AE event occurred, but it is still unclear its source. Possible effects include abnormal electrical activity, as AE monitoring systems are subject to disruption from electrical grounding in steel bridges (Ono 2011), or a temporarily malfunctioning AE sensor.

In general, when assessing hits vs. channel plots, normal behavior is consistent with (1) the hits being distributed over several sensors, and (2) the number of hits per sensor not exceeding some threshold value, say 200 hits per hour.

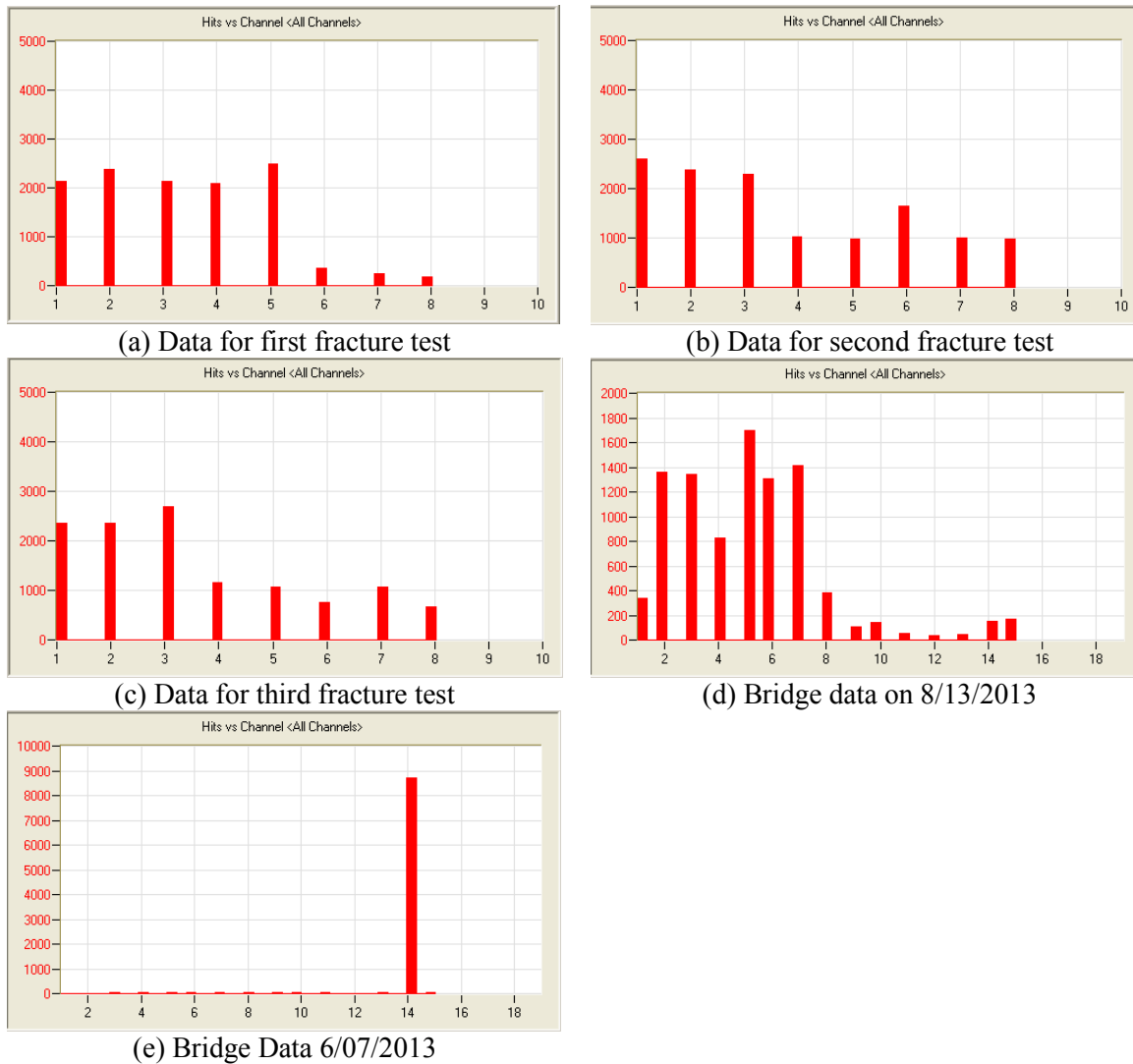


Figure 6.2: Hits vs. channel

6.4 Hits vs. Amplitude

The typical behavior for hits vs. amplitude during a normal bridge operation is similar to the one shown in figure 6.3(d). The range of amplitudes with many hits is narrow, and the average value is close to 60 dB. Moreover, there is a rapid decay in hits with increasing amplitude, there are few hits reaching 70 dB, and rarely are there hits reaching 80 dB. When comparing this pattern with that for the fracture tests, Figures 6.3(a) – 6.3(c), there is a broader range of amplitudes with numerous hits, starting with 50 dB and with a relatively large amount of hits reaching amplitudes of 90 dB or more. All fracture tests have a similar shape to the hits vs. amplitude distribution.

The anomalous bridge data obtained in June 7, 2013 (Fig. 6.3(e)) shows an uncommon trend to what is typically observed, with a large amount of hits with amplitudes in excess of 70 dB. Additionally, the shape of the distribution is surprisingly different to that observed for normal bridge behavior (Fig. 6.3(d)) and for fracture (Fig. 6.3(a) – (c)).

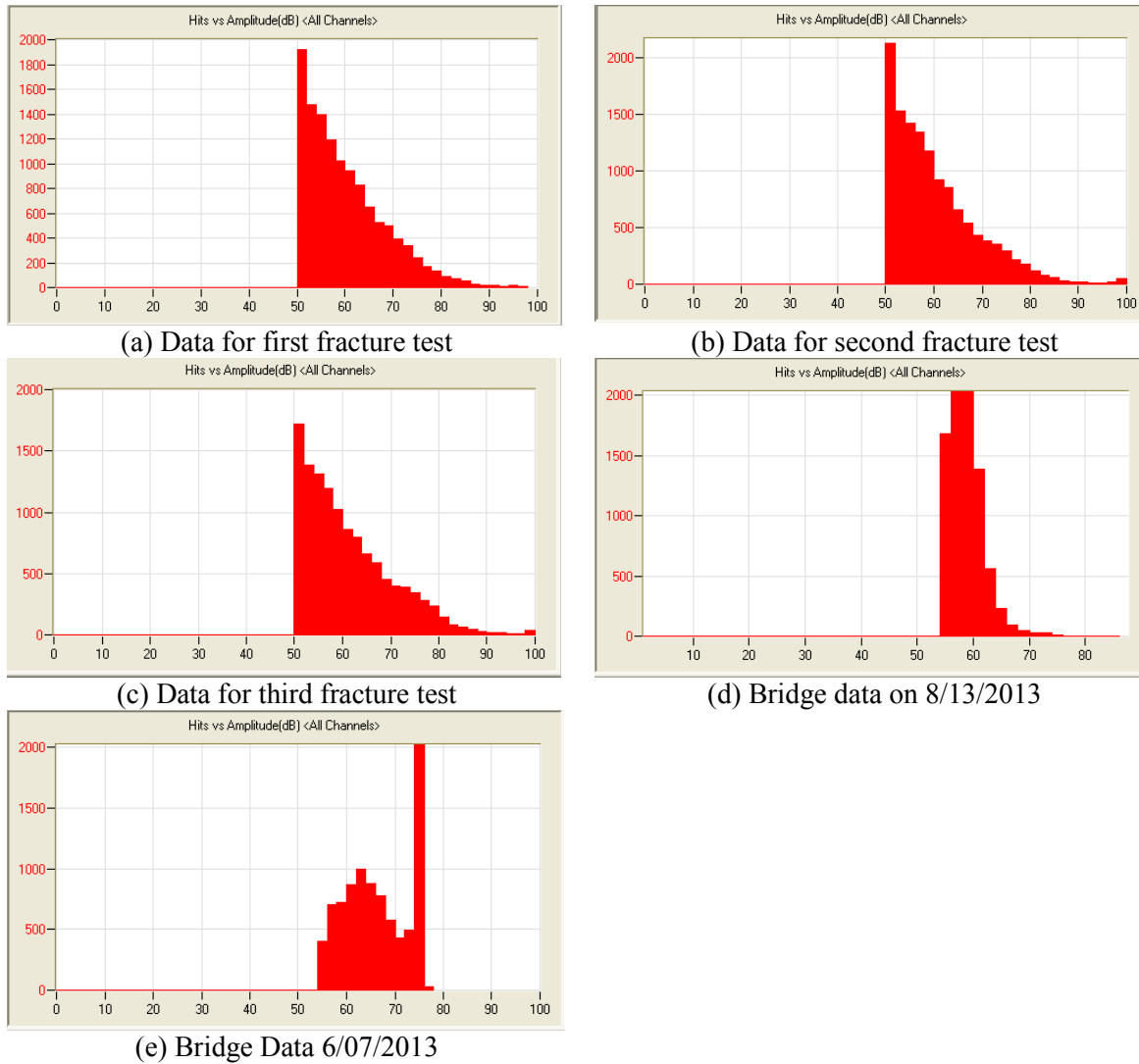


Figure 6.3: Hits vs. amplitude (dB)

Normal bridge behavior features hits vs. amplitude plots that exhibit a common shape (Fig. 6.3(d)). Most of the hits should have amplitudes that do not exceed 50 and 60 dB, and with a rapid decay for amplitudes in excess of 70 dB. Fracture will cause an increase in the measured amplitudes.

6.5 Hits vs. Frequency Centroid

The frequency centroid data observed in the “normal” sample of bridge data (Fig. 6.4(d)) is in the range of 100 to 130 kHz, with a peak value of approximately 110 kHz. During the fracture tests, the frequency centroids shifted dramatically to the right, with the majority of hits between in excess of 130 kHz, and the peak values in excess of 140 kHz. These observations suggest that when fracture occurs, the average frequency of the acoustic wave tends to increase in magnitude. The anomalous bridge data recorded on June 7, 2013 does not exhibit the characteristics of either the fracture tests or the “normal” bridge data. In fact, the number of hits is very low since only one sensor is collecting large numbers of hits (Fig. 6.3(e)).

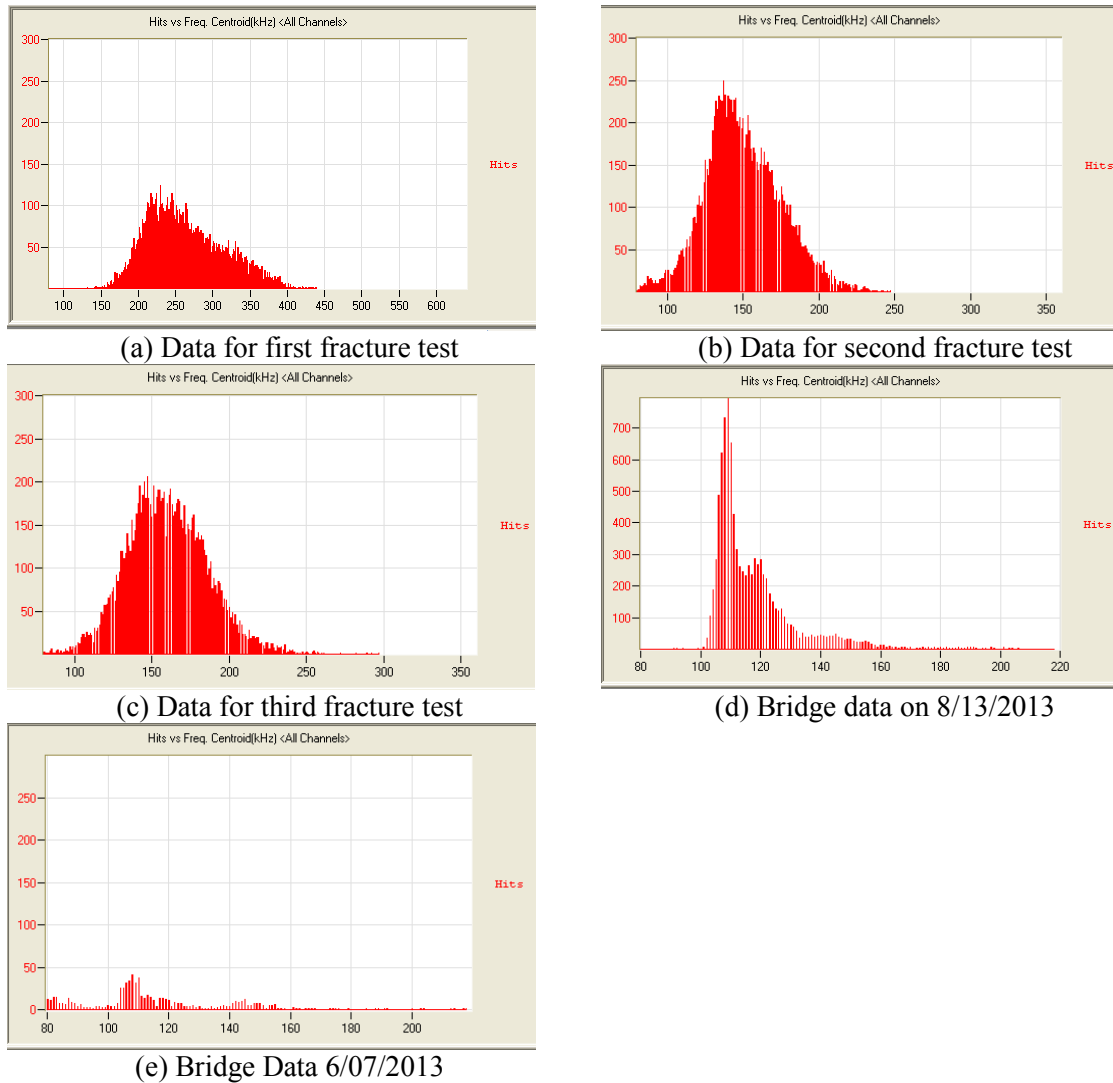
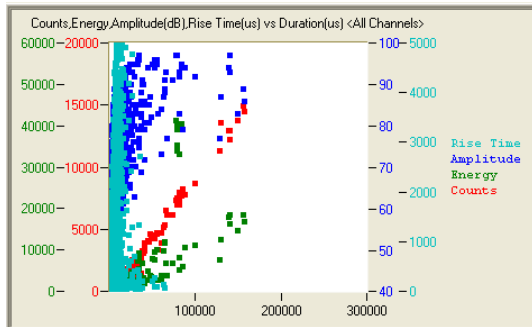


Figure 6.4: Hits vs. frequency centroid (kHz)

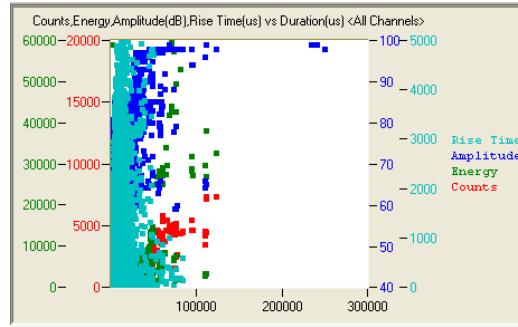
Normal bridge behavior should feature hits with frequency centroids that are within the range of 100 and 130 kHz, and with the peak value on the order of 120 kHz. Peak frequency centroids in excess of 140 kHz are suggestive of fracture.

6.6 Counts, Energy, Amplitude and Rise Time vs. Duration

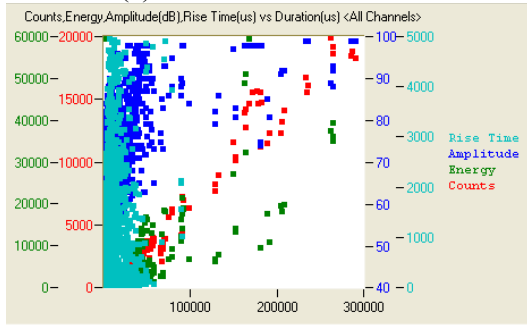
When fracture occurs, durations increase in relation to amplitude (dB), energy and counts (Fig. 6.5(a) – (c)). The difference between fracture and ‘normal’ bridge behavior is dramatic (Fig. 6.5(d)). For the latter, the four parameters are clustered to the left of the duration (μs) axis. The independent variable, duration, is defined as the elapsed time from the 1st threshold crossing of the AE to the last. This variable depends on the magnitude of the AE event, and it is valuable to recognize that crack formation and propagation lengthens duration. On a normal day (Fig. 6.5(d)), the number of acoustic emissions crossing the threshold should be low and thus explains why the data is clustered to the left. During fracture, the number of acoustic emissions crossing the threshold extends over a longer period of time.



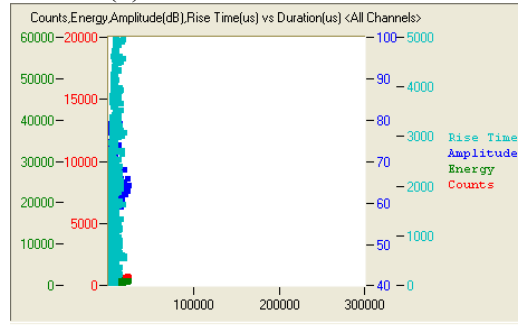
(a) Data for first fracture test



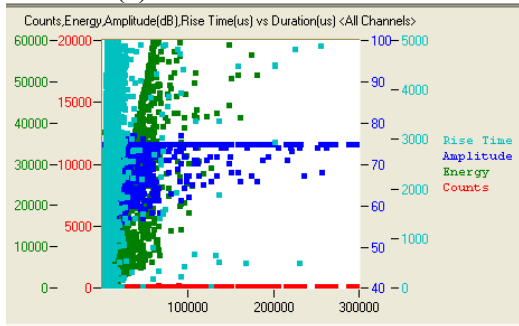
(b) Data for second fracture test



(c) Data for third fracture test



(d) Bridge data on 8/13/2013



(e) Bridge Data 6/07/2013

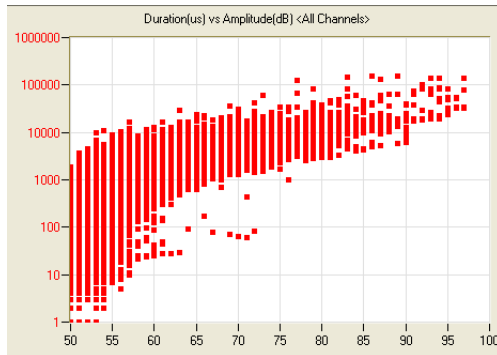
Figure 6.5: Counts, energy, amplitude (dB) and rise time (μs) vs. duration (μs)

In evaluating AE data, it is worthwhile to observe if the data is clustered. If the data is not clustered, the data should be evaluated to determine if there is a spread of the data towards the right, and if the energy and amplitude increase significantly. These would be suggestive of fracture. There is also a maximum duration threshold, on the order of 50,000 μs , that can be used to distinguish between cracking and non-cracking events.

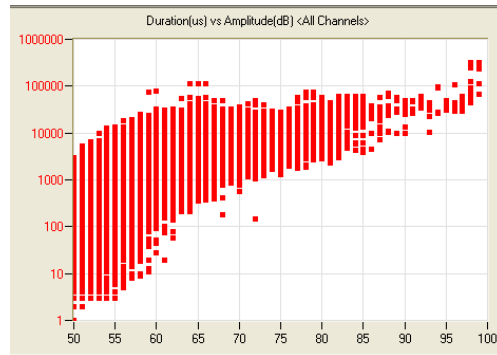
6.7 Duration vs. Amplitude

Figure 6.6 shows the relationship between duration and amplitude for the five AE data sets. During normal activity, the amplitude rarely reaches values above 80 dB, and most of the activity occurs in the 50 to 70 dB range. The duration appears to fall within 0 to 10,000 μs , and it remains high for larger amplitudes. Duration is the elapsed time from the first threshold crossing to the last. The fracture tests, as well as the anomalous data recorded on June 7, 2013, reveal that as the amplitude increases, the duration of threshold crossing increases. More importantly, the durations increase to values exceeding 100,000 μs , which is ten times as large as the maximum

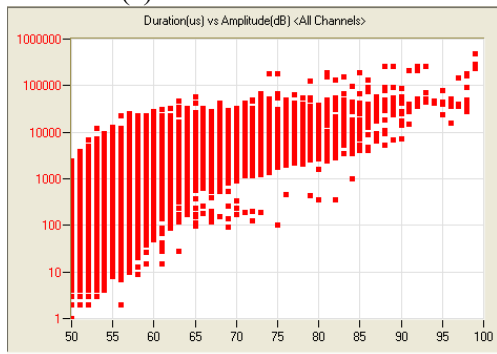
duration for ‘normal’ activity. The amplitude also increases to at least 95 dB, which is considerably larger than the largest values observed during ‘normal’ activity.



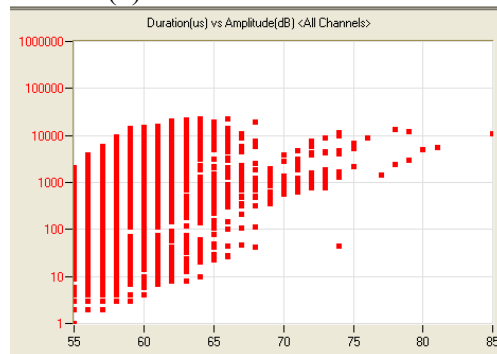
(a) Data for first fracture test



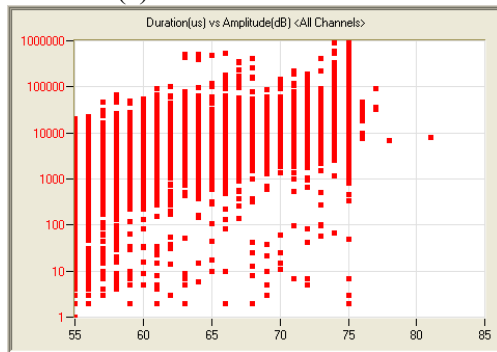
(b) Data for second fracture test



(c) Data for third fracture test



(d) Bridge data on 8/13/2013



(e) Bridge Data 6/07/2013

Figure 6.6: Duration (μs) vs. amplitude (dB)

In evaluating AE data from the Cedar Avenue Bridge, the amplitude spectrum should be checked. Of interest is activity for which duration exceeds 10,000 μs (say a 50,000 μs limit), and if there are a significant number of data points above 80 or 85 dB.

6.8 Peak Frequency vs. Frequency Centroid vs. Average Frequency

Figures (32-26) show the peak frequency (kHz) and frequency centroid (kHz) vs. the average frequency (kHz). The color scale shows frequency centroid magnitude, while the values on the x and y axes show average and peak frequencies. These plots provide only one clear trend: Normal and anomalous data (Fig. 6.7(d) and (e)) exhibit few peak frequencies in excess of 200 kHz, whereas the fracture data (Fig. 6.7(a) – (c)) have ample data between 200 and 400 kHz.

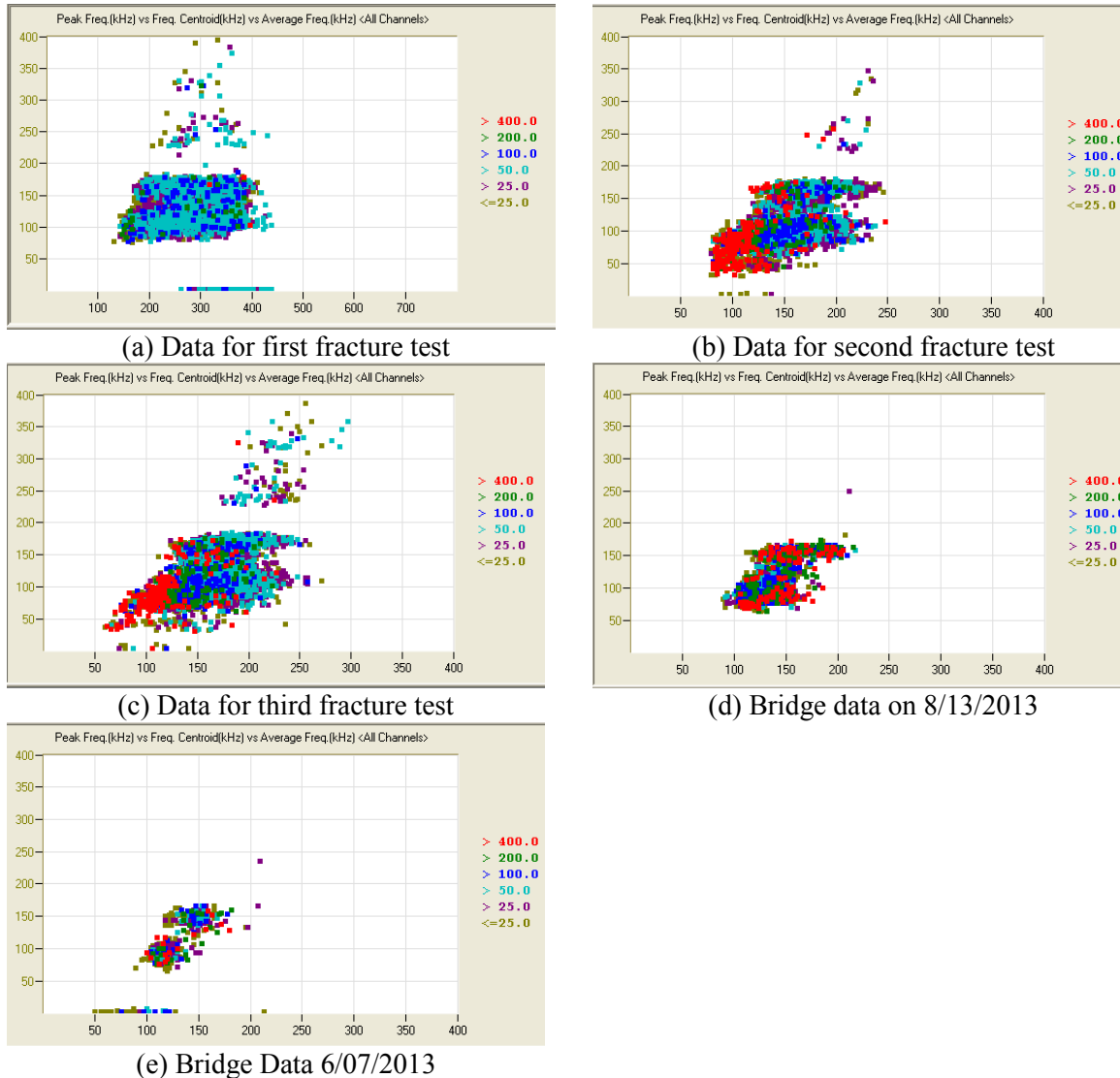


Figure 6.7: Peak frequency (kHz) vs. frequency centroid (kHz) vs. average frequency (kHz)

6.9 Hits vs. Peak Frequency

Figure 6.8(d) shows the shape of the spectrum of hits vs. peak frequency observed during ‘normal’ bridge activity. Most of the hits are seen to fall within peak frequencies of 80 and 110 kHz, with relatively low hits greater than 120 kHz. The fracture tests (Fig. 6.8(a) – (c)), on the other hand, show that the number of hits increases for peak frequencies greater than 100 kHz because the spectrum has a ‘bi-modal’ distribution with a second large peak at high frequencies

(i.e., in excess of 150 kHz). Figure 6.8(e) for the anomalous data set shares the same characteristic, with a secondary peak between 140 and 160 kHz.

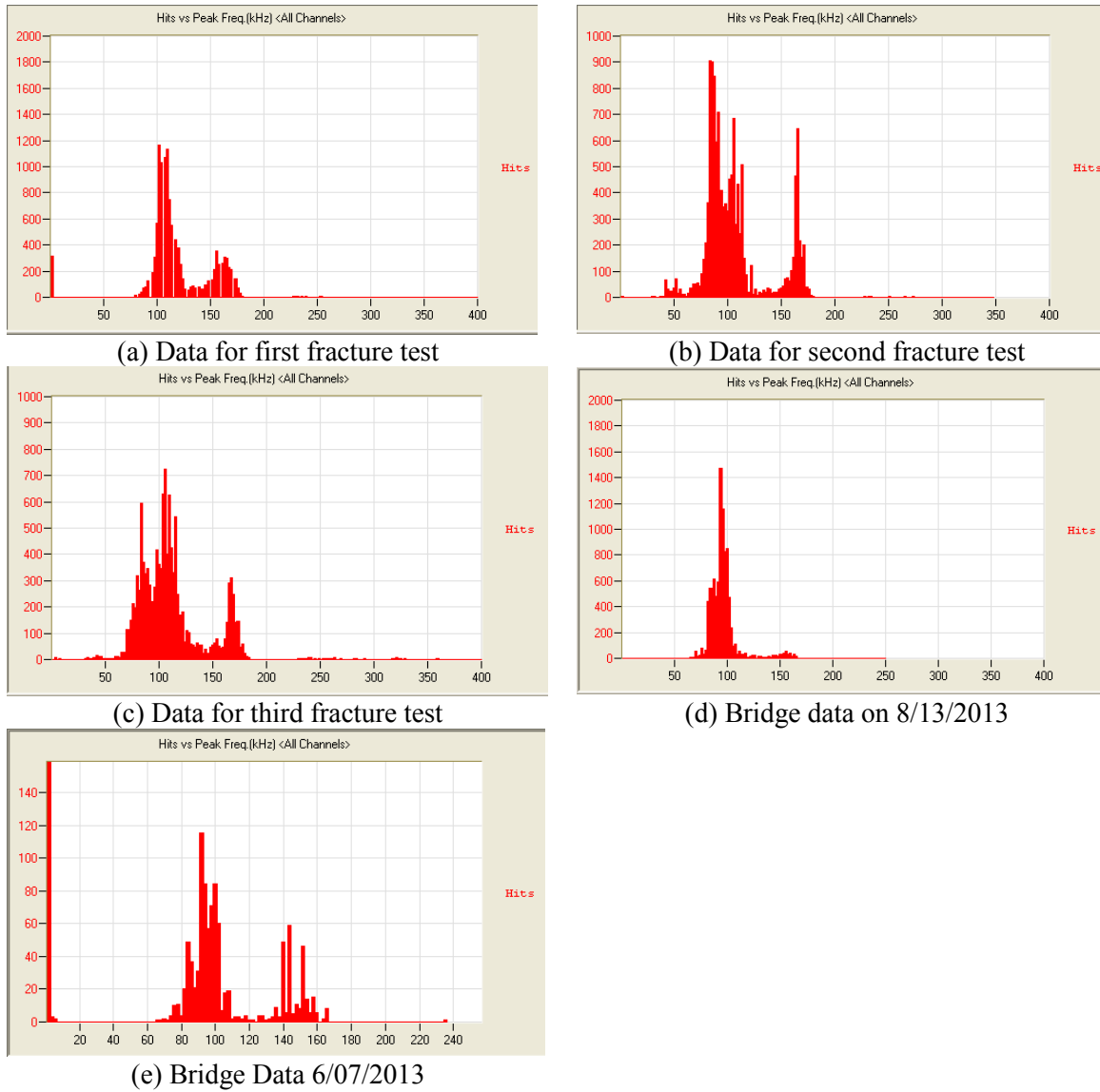


Figure 6.8: Hits vs. peak frequency (kHz)

In evaluating AE data, it is worthwhile checking to see if the peak frequency does not exceed the 80-110 kHz range. If there are significant numbers of hits with peak frequencies exceeding the 120 kHz, it is possible that the data corresponds to fracture or to some anomalous event. A bi-modal distribution with a second large peak would also be suggestive of fracture.

6.10 Counts vs. Frequency Centroid vs. Hits

Figure 6.9 shows the plots for counts vs. frequency centroid (kHz) vs. hits. The count axis is located at the left side of the graph, while frequency centroid is defined by a color scale. Counts are defined when there is a threshold crossing pulse and depend on the magnitude of the AE event. The number of hits is the independent variable. The graphs for all fracture tests look

very similar, but they differ from what is observed for the bridge data under ‘normal’ conditions. Aside from number of counts, both bridge data sets show little differences in Fig. 6.9, and thus these parameters are not strong indicators to discriminate anomalous activity from fracture.

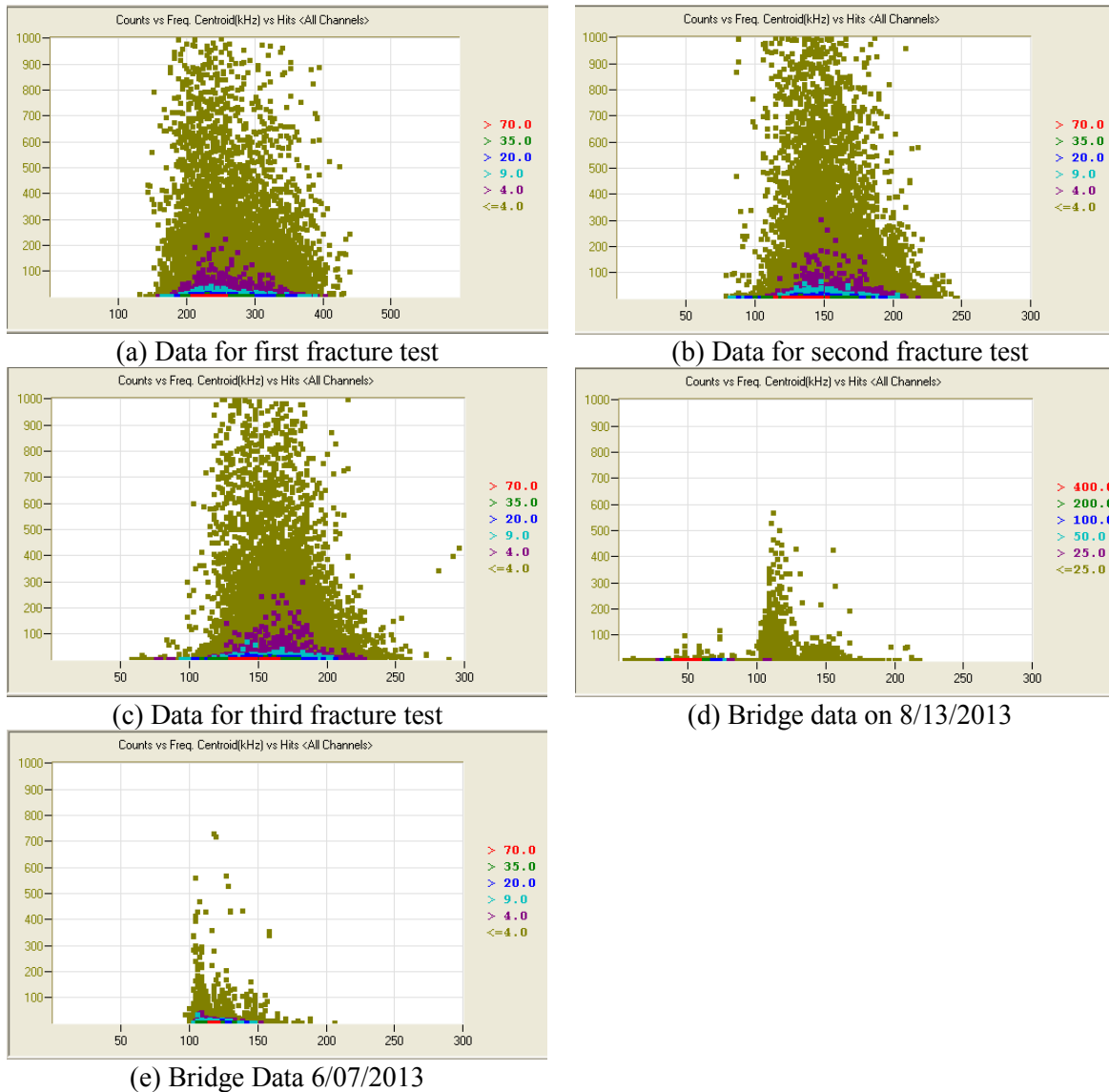


Figure 6.9: Counts vs. frequency centroid (kHz) vs. hits

6.11 Absolute Energy vs. Amplitude

Figure 6.10 shows plots of absolute energy (aJ) vs. amplitude (dB) for all sensors. The fracture tests (Fig. 6.10(a) – (c)) show that the absolute energy increases very quickly as amplitude increases. The energy, in aJ, ranges from 10^7 to 10^9 , and the amplitude exceeds 95 dB in all three cases. Normal bridge activity is seen in Figure 6.10(d), with energy reaching a maximum range of 10^6 aJ, so it is at least one order of magnitude smaller than that for the fracture tests. There are a few hits that exceed 80 dB, but none exceed the 95 dB limit of the fracture tests. More importantly, except for the anomalous data (Fig. 6.10(e)), the largest value of absolute energy coincides with the largest amplitude for a given dataset. Moreover, the

anomalous data recorded in June 2013 is clearly different from that for fracture. Thus, such anomalous behavior could be separated from fracture events using the plots shown in Fig. 6.10.

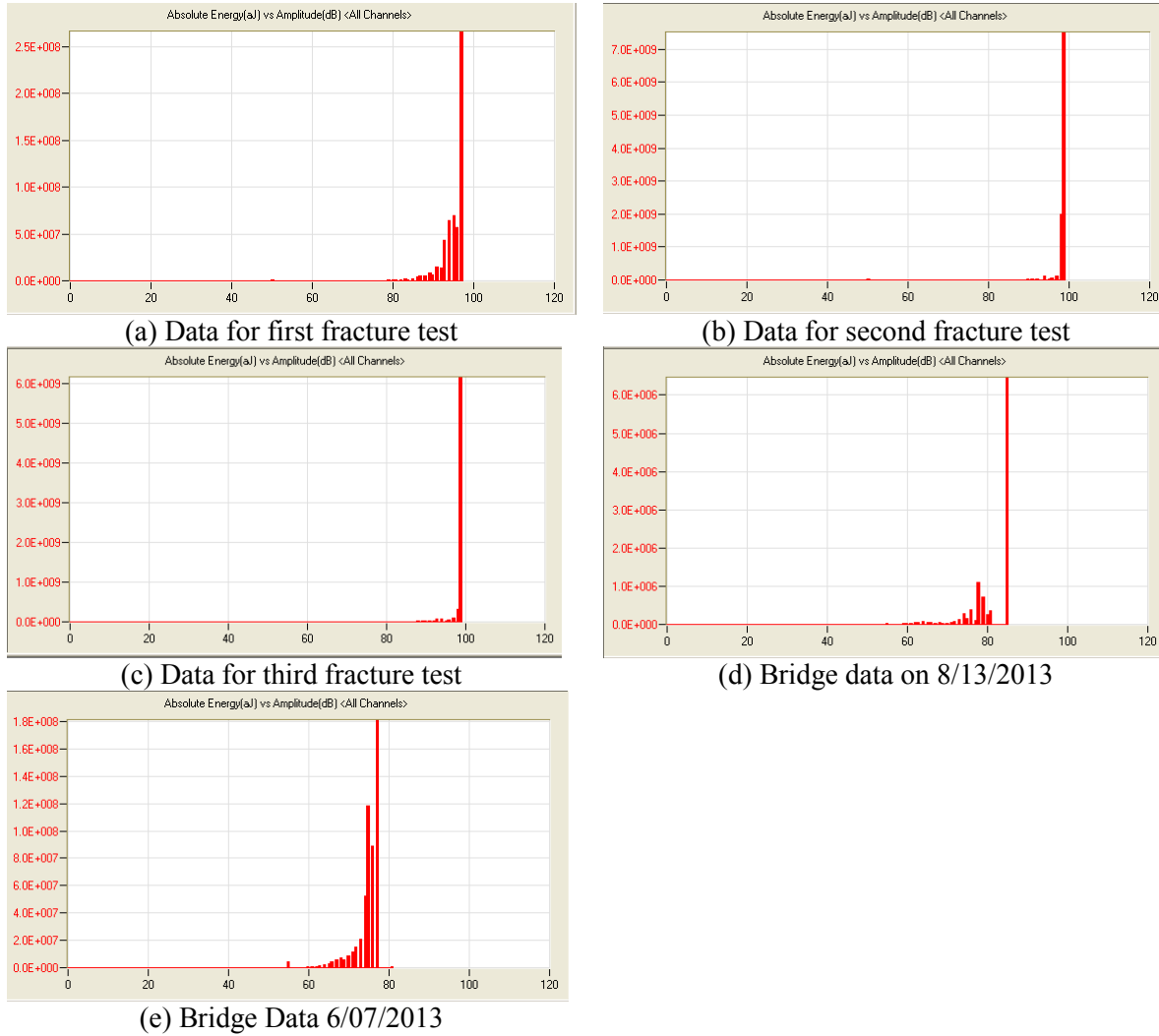


Figure 6.10: Absolute energy (aJ) vs. amplitude (dB)

In the analysis of AE data, amplitudes exceeding the 85 or 90 dB can be taken as indications of fracture. Similarly, absolute energy, in aJ, exceeding 10^7 or even 10^8 can be used to identify fracture. Normal activity would exhibit low amplitudes, in the range of 40 to 85 (or 90) dB, and absolute energy not exceeding 10^6 , or even 10^7 aJ.

6.12 Absolute Energy vs. Frequency Centroid

Figure 6.11 shows plots of absolute energy (aJ) vs. frequency centroid (kHz). The fracture tests (Fig. 6.11(a) – (c)) show frequency centroids greater than 100 kHz, and reaching 150 kHz. The absolute energy seen in the fracture tests ranged from 10^6 to 10^8 aJ. ‘Normal’ activity on the bridge shows frequency centroid values close to 100 kHz, with a few points reaching frequency centroids greater than that. The absolute energy during normal activity ranges typically can reach up to 10^6 aJ, while the anomalous recorded in June 2013 shows

absolute energy values that range from 10^7 up to 10^9 aJ. The anomalous data also shows frequency centroids that are significantly smaller and larger than 100 kHz, with a large amount of energy.

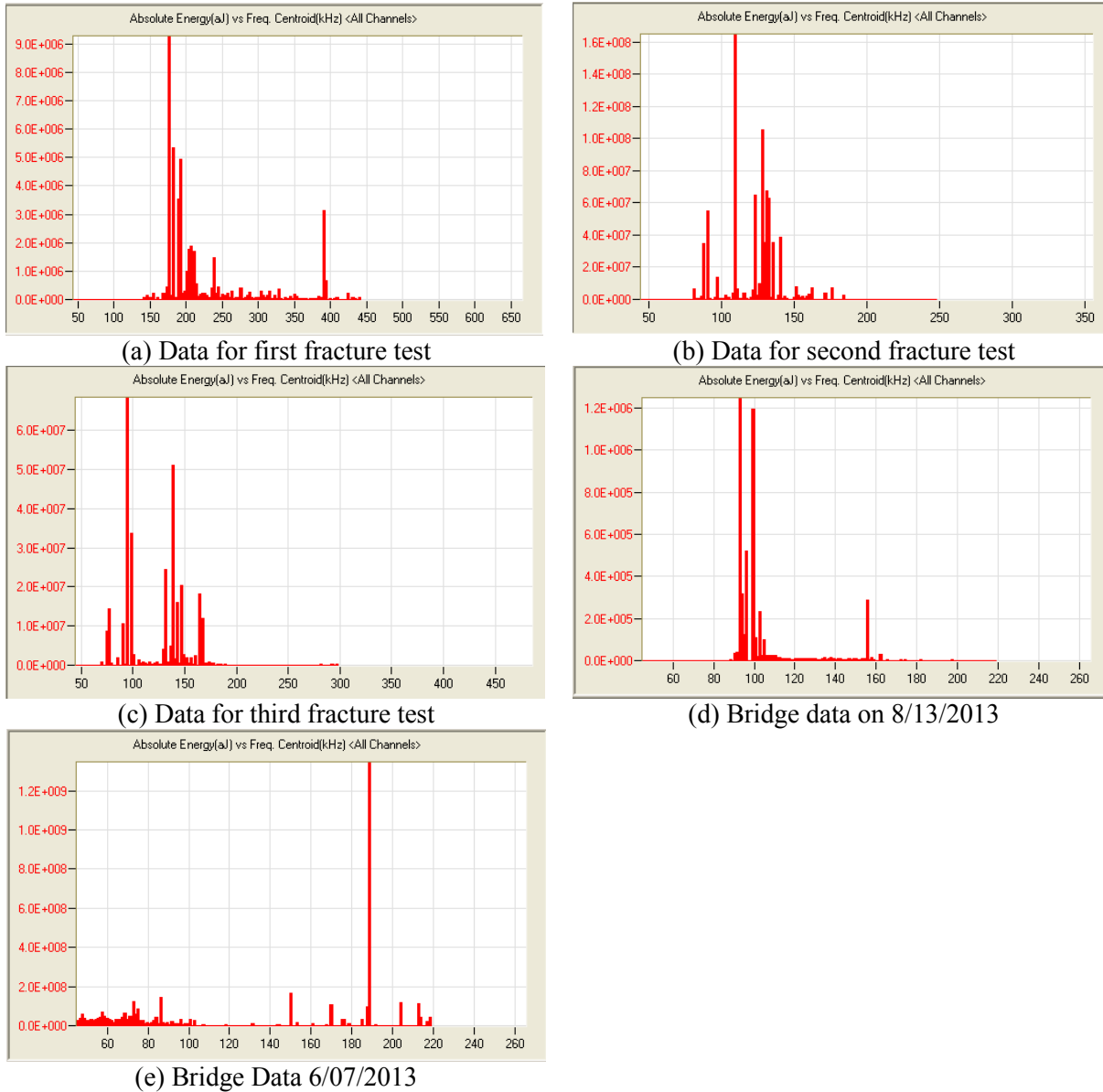


Figure 6.11: Absolute energy (aJ) vs. frequency centroid (kHz)

While there may be some trends present in the data shown in Fig. 6.11 for absolute energy vs. frequency centroid, it is difficult to translate such trends into criteria for separating fracture data from ‘normal activity’ and fracture data from anomalous activity of the type recorded in June 2013.

6.13 Conclusions

Systematic analysis of the parameters computed by the AEwin software was conducted comparing common patterns in the AE data sets that were obtained in the Cedar Avenue Bridge as well as the fracture tests conducted in the laboratory. Data throughout the months of June – August 2013, have been analyzed to detect any events that are out of the ordinary. With the help of laboratory experiments, it was possible to identify a baseline in the trends that affect the AE parameters during fracture. In addition, the anomalous data pattern observed during June 2013 shares some of the characteristics seen in the fracture tests, but it also deviates from the fracture data with regard to other parameters. This exercise helped identify approaches to discriminate between similar anomalous events and real AE events.

Eleven different plots with distinct variables were sampled and analyzed to determine their usefulness during the evaluation of the AE data. The most relevant relations for the purpose of discriminating between AE data from the fracture tests and AE data from ‘normal’ bridge activity were found to be: Hits vs. Time (s), Hits vs. Channel, Hits vs. Amplitude (dB), Hits vs. Frequency Centroid (kHz), Duration (μ s) vs. Amplitude (dB), and Absolute Energy (aJ) vs. Amplitude (dB). Equally important is the fact that these plots also discriminate between fracture and the anomalous data recorded in June 7, 2013. Some of the other plots complement the information found in these suggested graphs, and can provide further insight in detecting fracture.

CHAPTER 7 – DATA COLLECTION AND EVALUATION

7.1 Overview

This chapter documents the collection of acoustic emission (AE) data from the Cedar Avenue Bridge for a 22-month period, as well as the evaluation of the data to provide an assessment of the Cedar Avenue Bridge. In this application, the condition of the bridge is limited specifically to the formation and propagation of cracks in the east tie girder of the northbound bridge. The 22-month period of data collection began on January 14, 2011, when the equipment was installed, and ended in October 30, 2012. During this time, a Mistras Groups SH-II monitoring system collected the data from the acoustic emission sensors, and the AEwin™ software uploaded the data by wireless modem to an FTP website operated by Mistras Group (<ftp://ftp.mistrasholdings.com>). If the collected data falls within a reasonable range for the various AE parameters being investigated, then bridge condition can be considered satisfactory.

7.2 AE Data Sets and Timeline of Data Collection

Between the dates of January 10, 2011 and January 14, 2011, the 16 acoustic emission sensors with lead wires, SH-II computer, four batteries (housed in a battery box), DC power management module, and cellular modem were installed on the bridge. As part of the installation process, a layout file based on the spatial location of each of the 16 sensors was executed in AEwin™. Although data files were collected by the system during the installation time period, they are disregarded. They correspond to the initial pencil break tests used to calibrate the system following the placement of the sensors. The signals during the installation time period are assumed to be artificially induced by the persons installing the equipment and will not be analyzed for this reason.

During the subsequent month of data collection, issues with the internet connection were detected which produced several interruptions in the data record. However, multiple AE data files were collected and uploaded to the FTP website. In the following, the AE data from January 14, 2011 to February 24, 2011 (Data Set I) are analyzed as part of the entire set.

Based on the internet connection problems, the modem was relocated between the dates of February 22, 2011 and February 24, 2011. After this date, all 16 sensors collected data which was transferred to the FTP website by means of a reliable internet connection. The data collected between February 24, 2011 and March 21, 2011 (Data Set II) will serve as another source of information for the structural health assessment.

Between the dates of March 21, 2011 and March 25, 2011, the notched cantilever beam was installed at the L6 diaphragm location inside the tie girder. The effort to test the notched cantilever specimen was eventually discontinued. However, during this process, sensors 7 and 10 were relocated from the inside wall of the tie girder (i.e., closest to the roadway) to the sides of the notched cantilever beam which was, in turn, clamped and adhered with epoxy to a horizontal stiffener plate next to a diaphragm. Figure 3.2 shows the AE sensor layout before the relocation of sensors 7 and 10 for the attempted notched beam test of the Cedar Avenue Bridge. Sensors 7

and 10 were relocated for the notched beam test and a new layout file in AEwin™ was executed after the notch beam installation. Due to the relocation of sensors 7 and 10, the AE data collected by sensors 7 and 10 cannot readily assist in the characterization of fracture in the bridge.

Excluding the data collected by sensors 7 and 10 between the dates of March 25, 2011 and May 25, 2011 (Data Set III), additional acoustic emission data was collected and transferred to the FTP website. This data serves as yet another source of information for analyzing the structural health of the bridge.

On May 25, 2011 and May 26, 2011 maximum sensor spacing tests were performed. These tests were performed in order to calculate a theoretical maximum spacing of the sensors. Conducting pencil break tests at multiple locations required the manufacture of signals with amplitudes as high as 95 dB. For this reason, data files collected during this period have abnormally large signal amplitudes, which are attributed to pencil breaks used in these tests.

Acoustic emissions data was collected between May 26, 2011 and July 11, 2011 (Data Set IV). Excluding sensors 7 and 10 (which were still located on the notched cantilever beam), the data collected during this time period serves as another source of information for analysis.

On July 7, 2011, the solar panel array was vandalized and two of the four panels were damaged to the point that they were not producing any power. This event coincided with the Minnesota state government shutdown (July 1 - July 20, 2011). Thus, the authors were not allowed to service the solar panel array. In the meantime, the remaining two panels would recharge the backup batteries, but the power requirements are such that the charge was drawn down very quickly after the system restarted. The repeated restart and shutdowns of the SH-II module eventually burned out part of the circuitry. When the authors were allowed to return to the bridge, the SH-II had to be removed and was sent to the manufacturer for repair. The system was not operational again until Nov. 22, 2011.

Table 7.1: AE Data Sets

Data Set	Collection Dates	Description
I	Jan. 14 – Feb. 24, 2011	internet connection interruptions
II	Feb. 24 – Mar. 21, 2011	after modem relocation
III	Mar. 25 – May 25, 2011	after sensor 7 and 10 relocation
IV	May 26 – Jul. 11, 2011	after sensor 7 and 10 relocation
V	Mar. 21 – Mar. 25, 2011	notched beam test installation
VI	May 25 – May 26, 2011	maximum sensor spacing tests
VII	Nov. 22, 2011 – Oct. 30, 2012	post-vandalism & shutdown

7.3 Data Analysis

The data collected in data sets I - IV, and VII will serve as the principal source of information to be analyzed. Aside from the data collected by sensors 7 and 10 in data sets III and IV, the graphs included in this section from each data set show uniform values over the duration of monitoring. Data set VI, which was collected for the purpose of determining maximum sensor spacing, was discussed in Chapter 3.

The software AEwin™ provides various graphing and data display options of which several were discussed and evaluated in Chapter 6. Moreover, in Chapter 6, a group of 6 different graphs were found to provide information that allows the discrimination between fracture and non-AE events. The graphs included (1) Hits vs. Time, (2) Hits vs. Channel, (3) Hits vs. Amplitude, (4) Hits vs. Frequency Centroid, (5) Duration vs. Amplitude, and (6) Absolute Energy vs. Amplitude. Of these, the first four types were selected here for analysis of the data sets during the 22-month monitoring period, excluding data sets V and VI.

Appendix B contains a cluster of four plots for each significant file that was uploaded to the Mistras Group ftp site for all data sets. The date and time when the file was recorded is shown below the lower left plot (Hits vs. Amplitude), and there are two clusters per page. Plots for files from all data sets are provided in Appendix B, so care must be exercised when reviewing these files, and the reader should consult Table 7.1 when reviewing Appendix B.

The SH-II system does not record continuously, it records only when sensor signals exceed an amplitude threshold. Even when the monitoring system records and uploads data, the resulting files may be insignificant, that is, they contain very few hits (less than 100) with low amplitudes (less than 60 dB). Review of the data indicates that significant files utilize at least 200 kB of computer storage space. Only these files, or any file smaller than 200 kB but which contained more than 100 hits, were evaluated. In the following, sample plots of each type are given for data sets I – IV, and VII.

7.3.1 Hits vs. Time

The hits vs. time graph provides a chronological view of the acoustic emission activity on all sensors. The number of hits is displayed on the vertical axis on the left with the time in seconds displayed along the x -axis. A linear display of increasing hits with time is considered normal, and sharp increases in the cumulative number of hits could indicate a fracture event. However, fracture events occur over very short periods of time, i.e., a few seconds or even fractions of a second, and increases in the number of hits, when they occur over longer period, say minutes or hours, are usually due to non-AE events. By investigating the time period over which a large number of hits occur in conjunction with the amplitude of the hits, a more complete picture of the event can be obtained which is able to better assess a potential issue.

Figure 7.1 displays typical results from data sets I-IV and VII. Although some plots (e.g., Fig. 7.1(c) for data set III and Fig. 7.1(d) for data set IV) display sharp increases, the time axis indicates that these increases were actually occurring over periods that are too long for these events to be associated with fracture. Moreover, as discussed in section 7.3.3, the amplitude of these hits (less than 70 dB in most cases) in combination with the small quantity of hits marks this data set as unremarkable acoustic emission activity (i.e., non-AE events).

The hits vs. time plots in display behavior that is common for the Cedar Avenue Bridge, namely a linearly increasing number of hits with increasing time. Knowing the amplitudes of these hits, the data sets display behavior that can most likely be attributed to traffic loading.

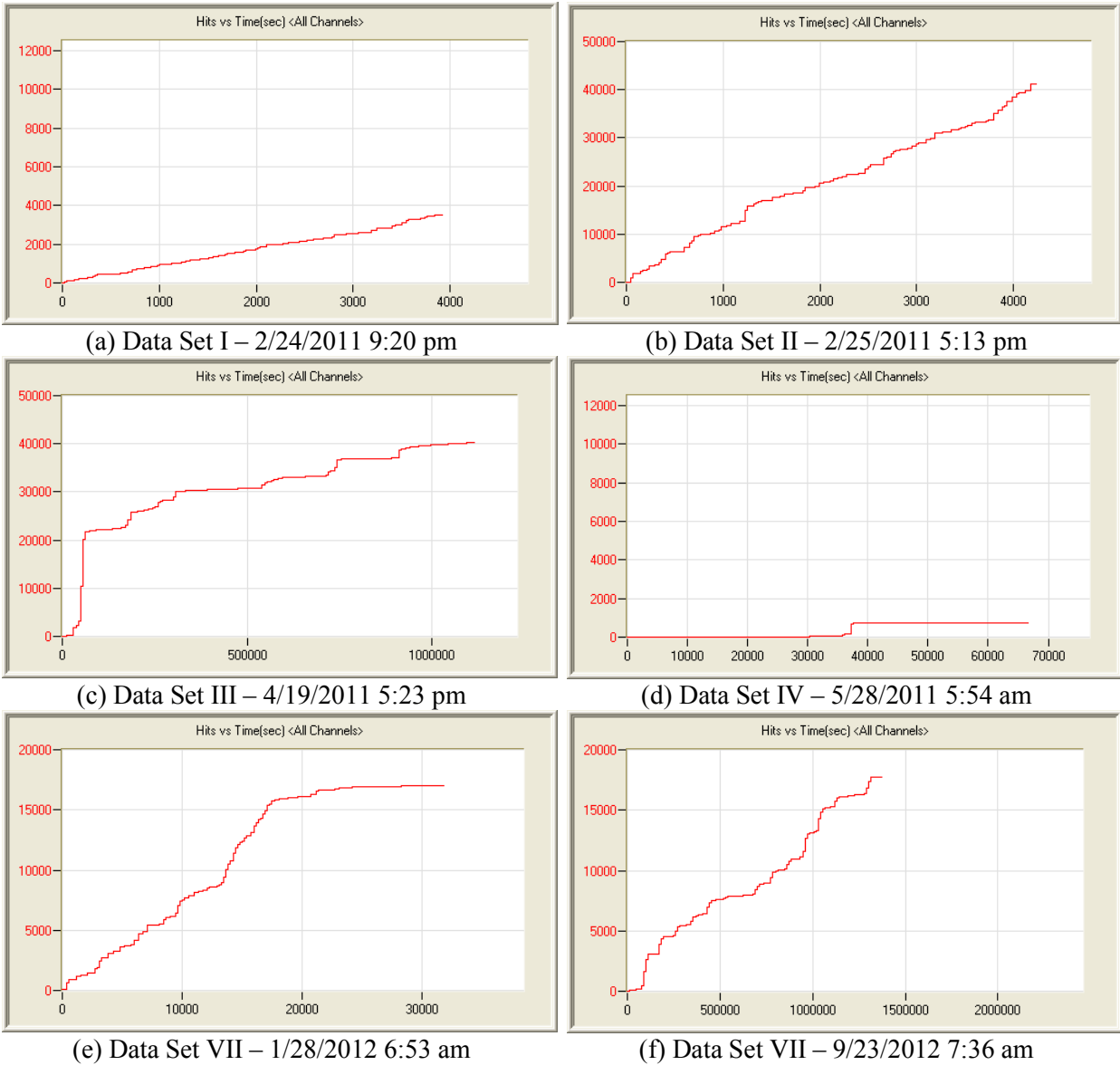


Figure 7.1: Hits vs. time (sec)

7.3.2 Hits vs. Channel

The graphing option entitled hits vs. channel displays the number of hits against each of the 16 channels that recorded them, with each channel corresponding to one of the 16 AE sensors installed in the bridge. During the 22-month period of data collection, millions of hits were recorded. Of these, some are attributed to the hits produced from initial pencil break tests to determine wave velocities, as well as the second set of pencil break tests to determine maximum spacing. However, even given these manufactured hits, the actual number of hits is even larger than those recorded because there are events that do not exceed the amplitude threshold to trigger the SH-II system to record them.

The magnitude of overall hits is important, but its distribution over the network of sensors is also important. This graphing option allows the user to identify exactly which sensor

recorded the events. In the fracture tests (Chapters 5 and 6) all of the sensors that were used registered signals. However, in these tests the sensors were installed relatively close to the source. Nonetheless, if a number of high amplitude hits were recorded, the location of the hits could be quickly determined.

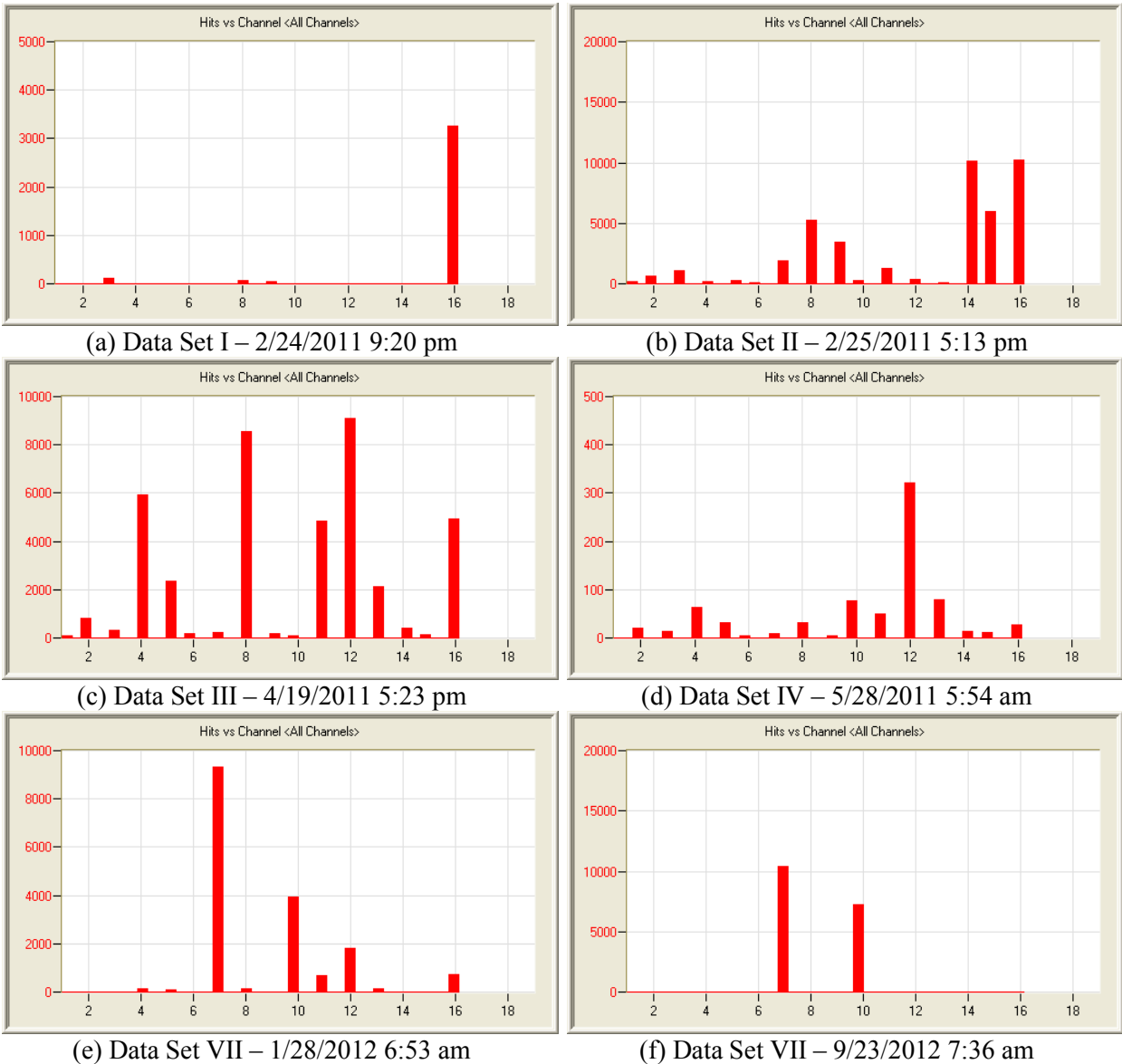


Figure 7.2: Hits vs. channel

Figure 7.2 shows that most recorded events were distributed over many sensors (Fig. 7.2(b) – 7.2(e)). But, in a few cases like Fig. 7.2(a) and 7.2(f), the hits were concentrated over a few sensors. The latter are often associated with small files i.e., files with a relatively low number of hits (less than 2000). Furthermore, section 7.3.3 indicates that cases like Fig. 7.2(a) and 7.2(f) are typical for files with for low amplitudes (i.e., less than 70 dB) and are, therefore, considered to be unimportant non-AE events.

7.3.3 Hits vs. Amplitude

Some of the most important information collected and displayed by the software concerns the amplitude in decibels (dB) of the AE signals received by the AE sensors. Based on the information available from Mistras Group, hits with amplitudes below approximately 80 dB are considered nonthreatening to the condition of the Cedar Avenue Bridge. Hits with amplitudes much above 80 dB, say 90 dB or higher, are considered concerning if they occur in large numbers relative to the quantity of other hits. Moreover, in the fracture tests reported in Chapters 5 and 6, fracture events produced a particular distribution of hits vs. amplitude, where the hits did not decay as quickly as is shown in Fig. 7.3. For the fracture events, the decay of hits with amplitude was approximately linear, whereas it is highly nonlinear in Fig 7.3. Moreover, the fracture tests indicated a significant number of hits in excess of 80 dB, and even some non-trivial content in the 90 to 100 dB range.

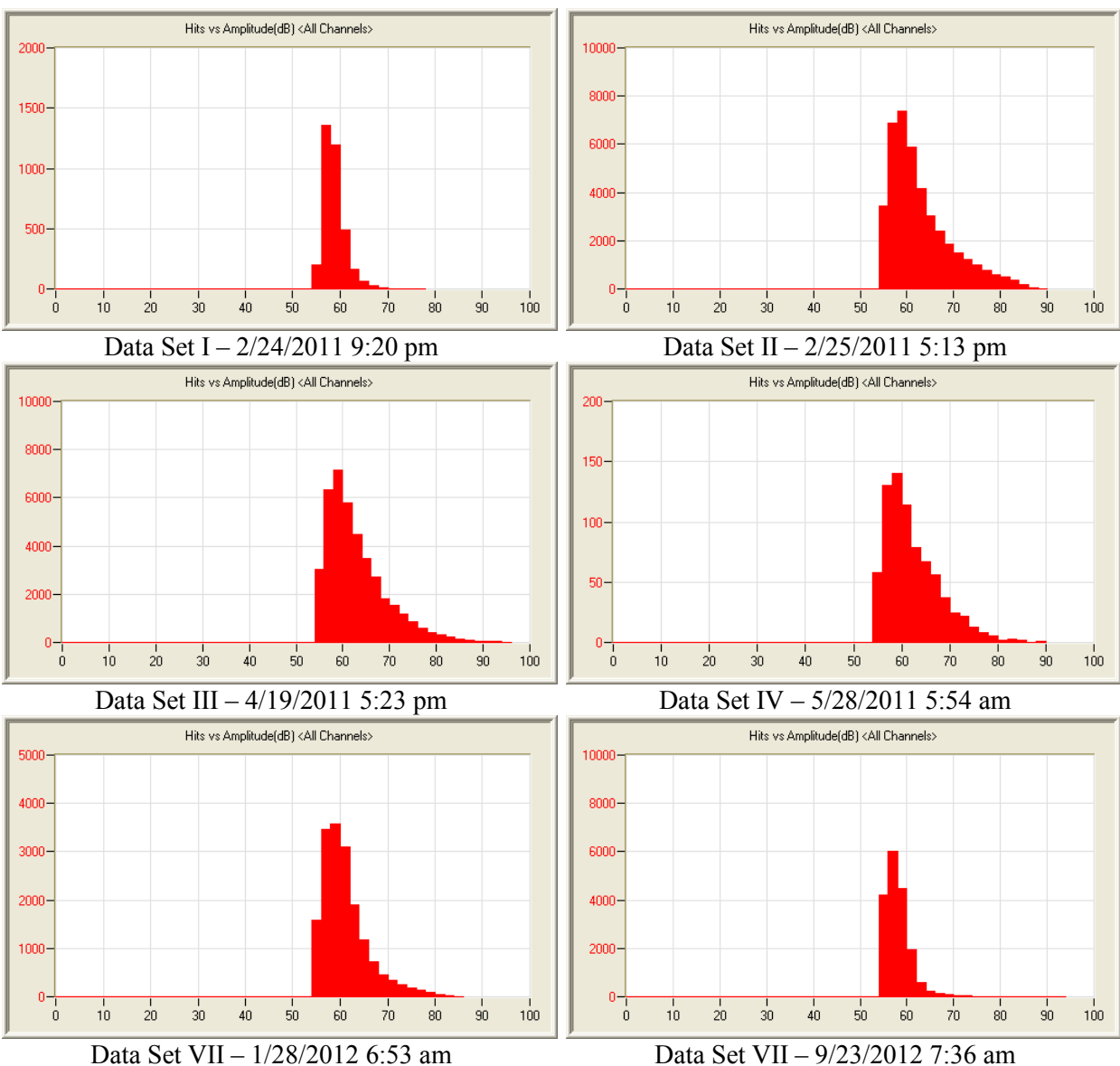


Figure 7.3: Hits vs. amplitude (dB)

Examining the typical hits vs. amplitude graphs for each data set, it is clear that the signature pattern for the Cedar Avenue Bridge is a narrow distribution with a sharp peak shape, with a range of values from approximately 55 to 80 dB, and a rapid and highly nonlinear decay after 70 dB. The data displays a mode (i.e., mean value) between 60 and 70 dB, and that is considered a safe range of values for the majority of hits.

7.3.4 Hits vs. Frequency Centroid

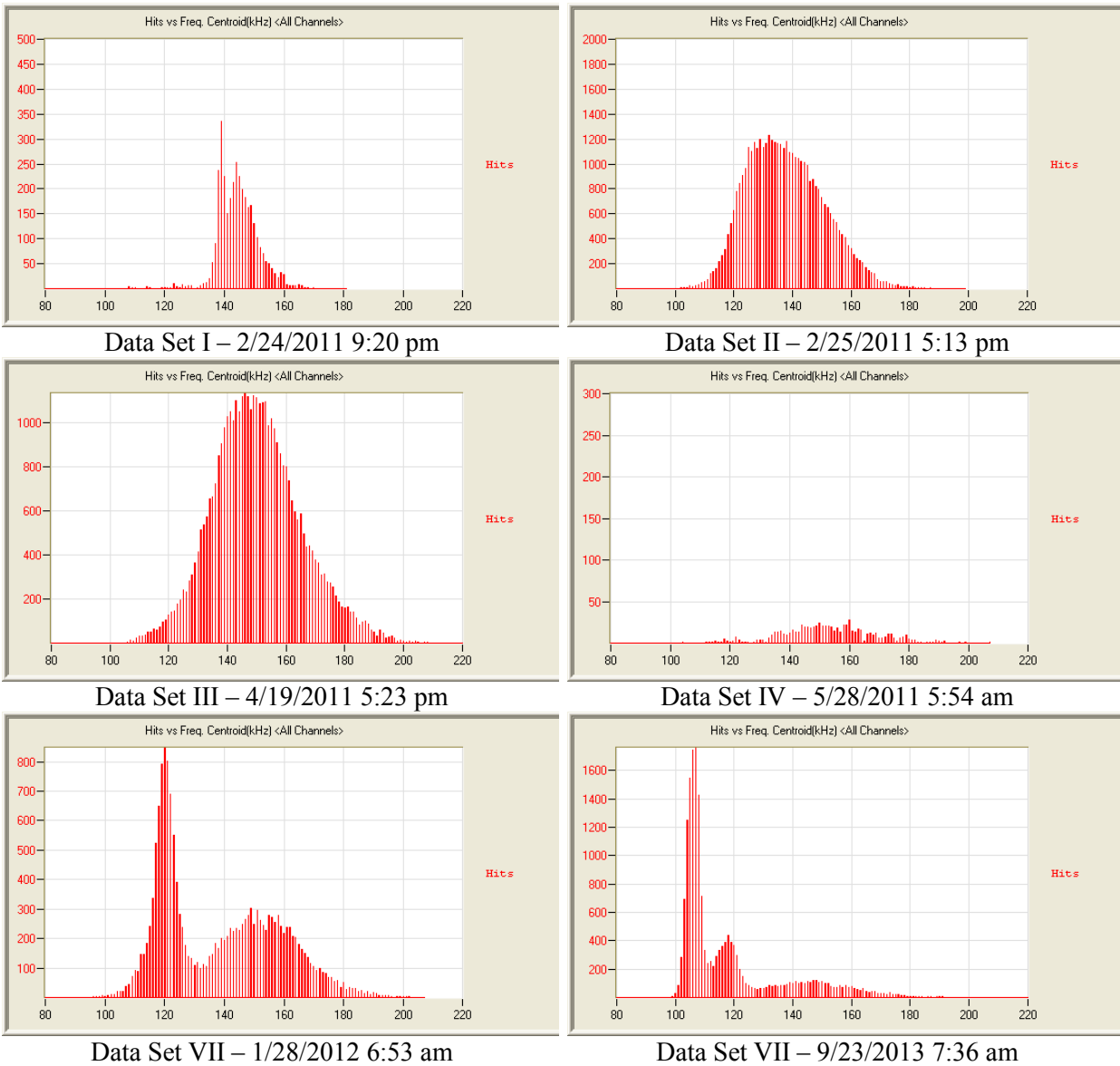


Figure 7.4: Hits vs. frequency centroid (kHz)

The frequency centroid is the centroid (i.e., similar to center of “mass”) of the power spectrum for an AE signal, and the higher the frequency centroid, the faster the energy delivery rate. Large frequency centroids are often associated with fracture events, and for the first fracture test described in Chapters 5 and 6, the peak frequency centroid (i.e., the frequency centroid

associated with the largest number of hits) was 240 kHz. However, for the other two fracture tests, the peak frequency centroids were on the order of 160 kHz. Generally, the AE files recorded for the Cedar Avenue Bridge feature peak frequency centroids approximately equal to 140 kHz.

7.3.5 Other AE Parameters

Other AE parameters were evaluated but are not shown here for brevity. These parameters provide further evidence that none of the recorded AE activity in the Cedar Avenue Bridge during the 22-month monitoring period is associated with fracture events. One such measure is duration, which is defined as the elapsed time from the first threshold crossing to the last. Generally, as the amplitude of an event increases, the duration also increases. For the fracture tests, maximum durations larger than 100,000 μ s were recorded in all three cases. However, AE files recorded for the bridge feature durations that seldom, if ever, exceed 20,000 μ s. So there is nearly a five-fold increase in this parameter when fracture test data is compared with field data.

Another useful parameter is the absolute energy associated with a measured signal, and this parameter increases with both amplitude and duration of the signal. The maximum values for absolute energy measured during the fracture tests are typically one order of magnitude larger than the maxima for the signals measured in the bridge. Thus, this parameter further corroborates the notion that none of the measured AE activity in the Cedar Avenue Bridge is indicative of fracture.

7.4 Field Problems

Problems with the deployment and use of the monitoring equipment in the field affected the progress of the project. The most troubling problem was due to the use of a solar panel array with backup batteries to power the SH-II monitoring system. Others are related to durability of equipment and materials, and to occasional undefined events that generate ‘anomalous’ AE data that is difficult to process.

7.4.1 Solar Panel Issues

At the time that the monitoring equipment was being purchased by the MnDOT Office of Bridges and Structures, the equipment manufacturer strongly recommended that AC electrical service be made available at the bridge site to power the SH-II module and the modem. However, MnDOT was unable to provide AC electrical service, and the decision was made to use a solar panel array to provide electrical power. This decision, in retrospect, was extremely unwise as the solar panel kit has been the source of numerous problems, costly delays, and unanticipated repair and maintenance costs. The solar panel kit includes four solar panels, four power cables, four backup batteries, a charge controller, a power inverter, and a mounting rack for the panels. All of the equipment except the solar panels, the mounting rack, and portions of the power cables, are secured inside the tie girder. The solar panel array (4 panels and mounting rack) was installed above a pedestrian walkway on the east side of the Cedar Avenue Bridge.

In June 2011, two of the four solar panels were vandalized, and a replacement set of four new panels was purchased and installed. However, during the time that the damaged solar panels

were in place (which coincided with the Minnesota state government shut down in 2011), the SH-II module was damaged as the system tried to restart repeatedly when the weakened solar panel array was generating insufficient current for continuous usage. The SH-II module had to be removed from the bridge, packaged and sent to the manufacturer for repair. By the time the repaired unit arrived, was inspected, installed and reconnected, several months had transpired. No data was collected from July 11 to November 22, 2011.

In order to safeguard the solar panels, a protective cage comprising galvanized steel tubes and welded wire mesh was installed around the panels and secured to the mounting rack. In spite of these measures, the solar panel array was vandalized a second time after the reporting period for this project. The damaged panels have been replaced, and the protective cage strengthened. However, it is impossible to prevent all vandalism to equipment that is installed in a visible manner in a public place. The protective cage cannot be strengthened further because such measures would block some of the sunlight incident on the panels.

Another complication with the use of solar panel kit to power the AE system, is that the solar panels, even when new, were insufficient to provide the necessary current to operate the monitoring system. This problem is especially acute during winter months when the sky is overcast, the days are short, and the air temperatures are low. The authors have consulted with the equipment manufacturer to identify potential improvements, but none have been identified.

7.4.2 Durability of Equipment and Materials

Other performance problems have been encountered in relation to the durability and reliability of the equipment and materials. The first of these was described in the preceding section concerning the burnt out circuitry in the SH-II module. As part of the repair, the Mistras Group installed protective circuitry to prevent this problem from reoccurring. Additionally, the modem sometimes operates in an intermittent manner. The reasons for this problem are unclear. Optimal placement of the antenna has been investigated, but these efforts have not eliminated the problem altogether. During intermittent operation, data is not collected.

The AE sensors were initially installed during a very cold period in mid-January 2011. Installation of the AE sensors was particularly difficult under such conditions. The authors noted in March 2013, roughly 2 years after installation, that the signal strength for all sensors appeared to have dropped noticeably over signal strengths shortly after installation. Inspection of the sensors revealed evidence of debonding between the epoxy and the steel web of the tie girder. The AE sensors were subsequently removed and reinstalled in warm weather. However, it is unclear if the installation will last longer than 2 years before reinstallation is needed again.

7.5 Discussion

In spite of the field problems, the data collected over the 22-month period, from January 14, 2011 to October 30, 2012, was analyzed in detail using the AEwin™ software provided by the Mistras Group. Six samples of the data collected during various time periods were presented and evaluated using parameters computed by AEwin™. These samples were taken from the data that is reported graphically in Appendix B. The data indicates that no events have been recorded that exhibit characteristics consistent with the formation and propagation of cracks.

CHAPTER 8 – SUMMARY, CONCLUSIONS AND RECOMMENDATIONS

8.1 Summary

The objective of the project summarized in this report was to develop an acoustic emission (AE) monitoring system to sense cracking in fracture-critical steel bridges. Unlike previous applications of acoustic emission technology to steel bridges where the sensors are concentrated in areas where fracture is expected, the system developed here utilizes distributed sensors at large spacing to provide global monitoring of an entire tie girder in a tied-arch steel bridge. The northbound portion of the Cedar Avenue Bridge (MnDOT Bridge No. 9600) was selected for monitoring. However, the project was not designed for the purpose of determining the condition of the bridge, because the bridge has not exhibited cracking during its 34 years of service, and it is not expected to do so in the immediate future. Rather, the goal of the project was to demonstrate that acoustic emission technology could be used for global monitoring of fracture-critical steel bridges.

Project activities included the acquisition of the monitoring equipment, its testing to verify compliance with manufacturer specifications, installation of the equipment on the selected bridge, field testing to calibrate the system, development of data processing protocols for the AE data, and the collection of field data for a period of 22 months. Fracture tests of notched cantilever steel beams were conducted in the laboratory to provide characterization data for fracture events.

8.2 Conclusions

The project demonstrated that commercially available acoustic emission technology could be used for global monitoring of a steel bridge to identify crack formation and propagation. However, to accomplish the task, it was found necessary to generate AE data for fracture events in steel bridge members. This data was needed to characterize the fracture process given the large amount of non-AE events that are generated in a steel bridge that is in-service.

The project also demonstrated that a simple test could be used to generate the AE data necessary to characterize fracture events. A simple cantilever beam specimen with a notch was configured and optimized by means of laboratory tests. The fracture test procedure requires only a hydraulic jack and a manual pump to operate, and it was also designed to be deployable to the field for in-situ tests in steel bridges.

The project developed data processing procedures, using the software provided by the manufacturer of the AE equipment, to evaluate the AE data that was generated in the Cedar Avenue Bridge. The procedures rely on peak amplitude (i.e., the amplitude of the AE signal corresponding to the largest number of hits), peak frequency centroid (i.e., the frequency centroid corresponding to the largest number of hits), and rapid increases in the number of hits (defined from a plot of hits vs. time). Other parameters that were found to hold promise for improving the data processing scheme include maximum duration and absolute energy.

The AE data collected at the Cedar Avenue Bridge and processed using the procedures developed in this project indicated there was no indication of cracking during the 22-month monitoring period. This observation coincides with past performance of the Cedar Avenue Bridge as well as the long-term outlook for its condition.

8.3 Recommendations

Fracture tests utilizing notched cantilever beam specimens should be conducted in the east tie girder of the northbound lanes of the Cedar Avenue Bridge. All of the notched beam fracture tests conducted as part of the project reported in this document were conducted in the laboratory.

Data should continue to be collected from the Cedar Avenue Bridge so that the data processing procedures can be further improved. Furthermore, data processing outside of the limitations of the manufacturer specified software should be investigated.

The MnDOT Office of Bridges and Structures should commission another project to use AE monitoring equipment and the data processing procedures developed here on a steel bridge with a history of cracking.

The documented problems with power generation using solar panels are strongly suggestive that a more robust and reliable power source be used for bridge monitoring. Future projects on the monitoring of fracture-critical bridges should rely on AC power exclusively. Solar panels are not sufficiently durable and reliable to be the sole power supply for a bridge monitoring system. Besides increasing the risk of losing valuable monitoring data when solar panel-based power systems are not operational, they also increase the risk of damage to the monitoring equipment during repeated instances of powering up and shutting down.

It is further recommended that the MnDOT Office of Bridges and Structures provide AC power to the monitoring equipment in the Cedar Avenue Bridge if the monitoring system is to continue being operational for much longer.

REFERENCES

ASTM (2010). *Standard Guide for Determining the Reproducibility of Acoustic Emission Sensor Response*, E976-05, American Society for Testing and Materials, West Conshohocken, PA.

AEwin™ User's Manual, Physical Acoustics Corp., Princeton Junction, NJ.

Barsom, J.M. (1971). "Fatigue-Crack Propagation in Steels of Various Yield Strengths." *Journal of Engineering for Industry*. pp. 1190-1196, Nov.

Blessing, J.A., Fowler, T.J., Strauser, F.E. (1992). "Intensity analysis." *Proc., 4th International Symposium on Acoustic Emission from Composite Materials*. Columbus, OH, American Society for Nondestructive Testing.

Chen, G. et al. (2005). *Failure Investigation of the Steel Strut on the Paseo Suspension Bridge*. Final Report RDT 05-008, Missouri Department of Transportation, Jefferson City, MO.

Choi, J.H. (2000). *The Fracture Analysis and Remaining Life Estimation of the AVL B Sub-Components*. College of Engineering and Mineral Resources at West Virginia University.

Chopra, Anil. (2007). *Dynamics of Structures: Theory and Applications to Earthquake Engineering*. Upper Saddle River, N.J.: Pearson Prentice Hall.

Chung, H.-Y., Manuel, L., and Frank, K.H. (2003). "Reliability-Based Optimal Inspection for Fracture-Critical Steel Bridge Members," *Transportation Research Record*, No. 1845, Paper No. 03-4296, p. 39-47.

Craig, Roy R. and Andrew Kurdila. (2006). *Fundamentals of Structural Dynamics*. Hoboken, N.J.: John Wiley.

Dalder, E.N.C. (1997). *Effect of Decreased Static Fracture Toughness on Fracture Mechanics Analyses of the Ederer Cranes in the Device Assembly Facility*. Final Report UCRL 125068, Lawrence Livermore National Laboratory, United States Department of Energy, Livermore, CA.

eFatigue LLC. Material Property Finder. <www.efatigue.com> Accessed February 2011.

Fleck, N.A. and Smith, R.A. (1984). "Fatigue Life Prediction of a Structural Steel Under Service Loading." *International Journal of Fatigue*. 6(4): 203-210.

FHWA (2012). "Showcasing an Advanced Motorist Warning System in Texas," *FOCUS Accelerating Infrastructure Innovations*, FHWA-HRT-13-008, <http://www.fhwa.dot.gov/publications/focus/12nov/12nov04.cfm>, accessed Nov. 17, 2013.

Fish, P. E. (1995). "NDT applications in a successful fracture critical bridge inspection program and anchor bolt inspection program," *Proceedings of SPIE – The International Society for Optical Engineering*. 2456: 149-165.

Gastineau, A., Johnson, T., and Schultz, A. (2009). *Bridge Health Monitoring and Inspection – A Survey of Methods*, Final Report 2009-29, Minnesota Department of Transportation, St. Paul, MN.

Gastineau, A., Schultz, A. and Wojtkiewicz, S. (2011). *Response Modification for Enhanced Operation and Safety of Bridges*, Final Report CTS 11-14, Center for Transportation Studies, University of Minnesota, Minneapolis.

Gdoutos, E. E., C. A. Rodopoulos, and J. R. Yates. (2003). *Problems of Fracture Mechanics and Fatigue: a Solution Guide*. Boston: Kluwer Academic.

Kaiser, S. (1983). "On the Relation Between Stable Crack Growth and Fatigue." *Fatigue of Engineering Materials and Structures*. 6(1): 33-49.

Koob, M. J., Hanson, J. M. and Fisher, J. W. (1984). "Post-construction evaluation of the Fremont Bridge." *Transportation Research Record*. 2:131-140.

Lindberg, A.Y., and Schultz, A.E. (2007). *Incorporation of Fatigue Detail Classification of Steel Bridge into the Minnesota Department of Transportation Database*, Report No. 2007-22, Minnesota Department of Transportation, St. Paul, MN.

Miller, D.A. Ahmadi, A.K. (2007). "Design and construction of fatigue-prone detail retrofits for interstate 79 Neville Island interchange bridges." *Bridge Structures*, 3(1):35-50.

Mistras Group (2010). *Sensor Highway II – Smart Monitor User's Manual*, Part No. 9380-1001, Mistras Group Inc., Princeton Junction, New Jersey.

Nair, A., Cai, C.S. (2010). "Acoustic emission monitoring of bridges: Review and case studies", *Engineering Structures*, 32:1704-1714.

NDT.net, "Acoustic emission Hsu-Nielsen source," <http://www.ndt.net/ndtaz/>, accessed Nov. 22, 2013.

NDT Resources Center, <http://www.ndt-ed.org/>, accessed 18 Oct. 2013.

Ono, K. (2011). "Application of Acoustic Emission for Structure Diagnosis," *Diagnostyka - Diagnostics and Structural Health Monitoring*. 2(58):3-18.

Phares, B. M., Wipf, T., Greimann, L. F., and Lee, Y.-S. (2005). *Health Monitoring of Bridge Structures and Components Using Smart Structure Technology*, Wisconsin Highway Research Program Report No. WHRP 05-03.

Pollock, A.A. (2003). *Acoustic Emission Inspection*. Technical Report TR-103-96-12/89. Physical Acoustics Corp., Princeton Junction, NJ.

Practical Technology (2006). "Bridge Operation Warning System," <http://www.practical-technology.com/>, accessed Nov. 17, 2013.

Schilling, C.G., Klippstein, K.H., Barsom, J.M. and Blake, G.T. (1978). *NCHRP Report 188: Fatigue of Welded Steel Bridge Members Under Variable-Amplitude Loadings*. Transportation Research Board, National Research Council, Washington, D.C.

Stallings, J. M., Cousins, T. E. and Christopher, B. P. (1996). "Fatigue life of double angle tension members," *Engineering Journal*, AISC, 33(2):55-64.

Tanaka, T. et al. (1985). "On the Impact of Fatigue Crack Growth Behavior of Metallic Materials." *Fatigue of Engineering Materials and Structures*. 8(1):13-22.

Thompson, D.J. and Schultz, A.E. (2010). *Development of an Advanced Structural Monitoring System*, Final Report 2010-39, Minnesota Department of Transportation, St. Paul, MN.

Yu, J., Ziehl, P., Pollock, A. (2011). "Remote Monitoring and Prognosis of Fatigue Cracking in Steel Bridges with Acoustic Emission," *Proc. of SPIE, Nondestructive Characterization for Composite Materials, Aerospace Engineering, Civil Infrastructure, and Homeland Security 2011*, Wu, H.F., ed., Vol. 7983.

APPENDIX A: AEWIN™ SOFTWARE PROCEDURES

A.1 Adjusting the Sensor Layout in AEWin™

1. In the File menu select → Acquisition Setup → Location

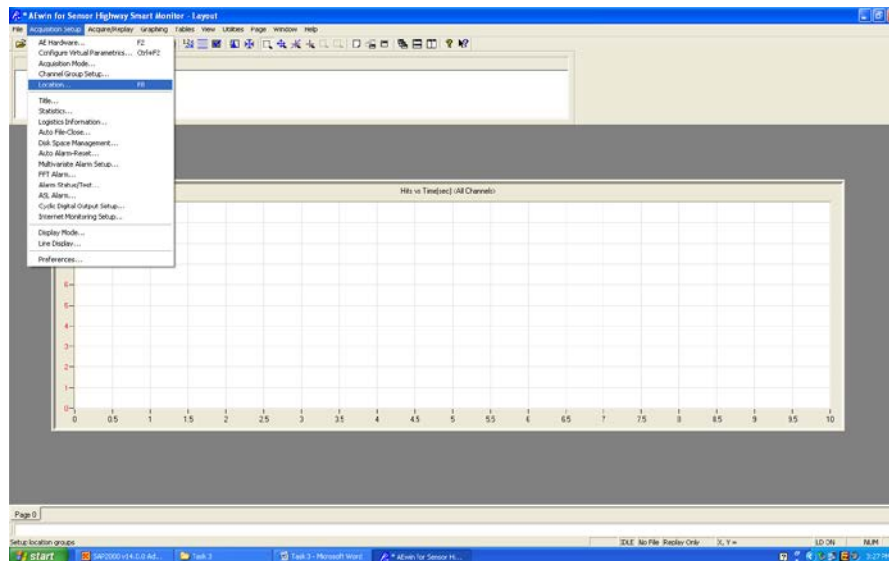


Figure A.1: Access to Sensor Location Information

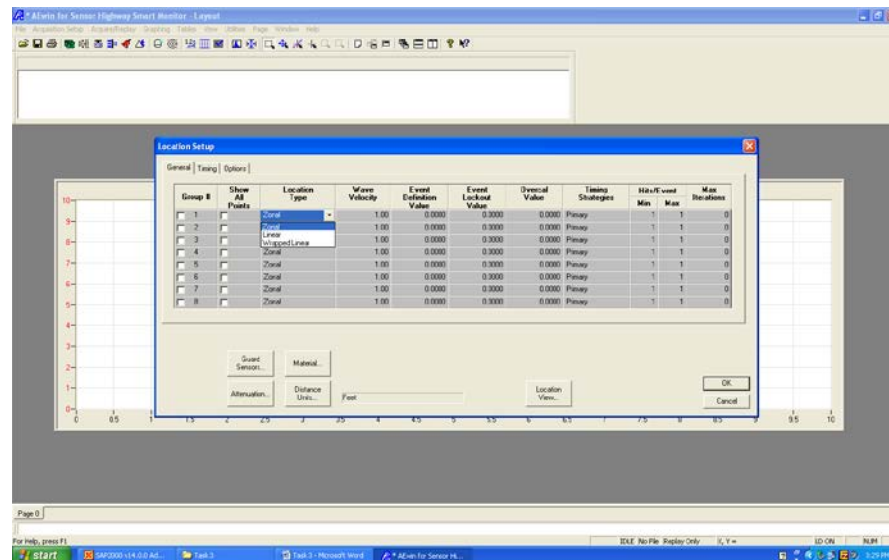


Figure A.2: Location Setup Window

2. In the Location Setup window adjust the Location Type to “Linear”
3. Input the Average Wave Velocity from the pencil break tests into the Wave Velocity column
4. Select the Location View button to produce the Placement Window

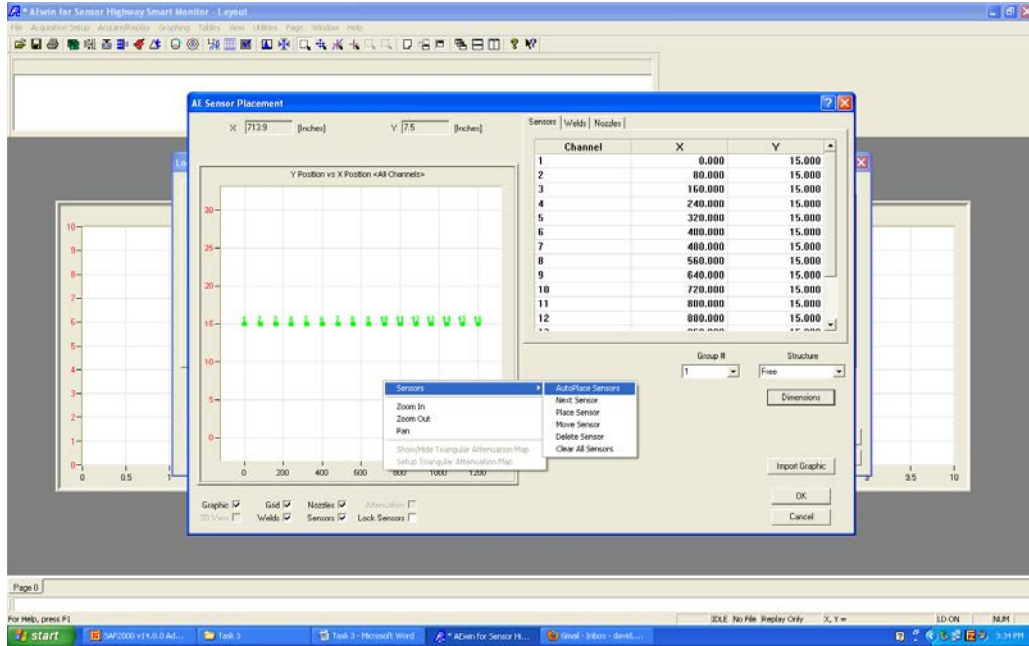


Figure A.3: Sensor Placement Window

5. Click the Dimensions button → change dimensions to Inches
6. Right-click inside the Y Position vs. X Position plot
7. Click the Sensors button → and select AutoPlace Sensors
8. Input first sensor location, sensor spacing, and height of sensors on girder web
9. If necessary adjust X and Y values in sensor location table using current locations
10. Close the Sensor Placement window

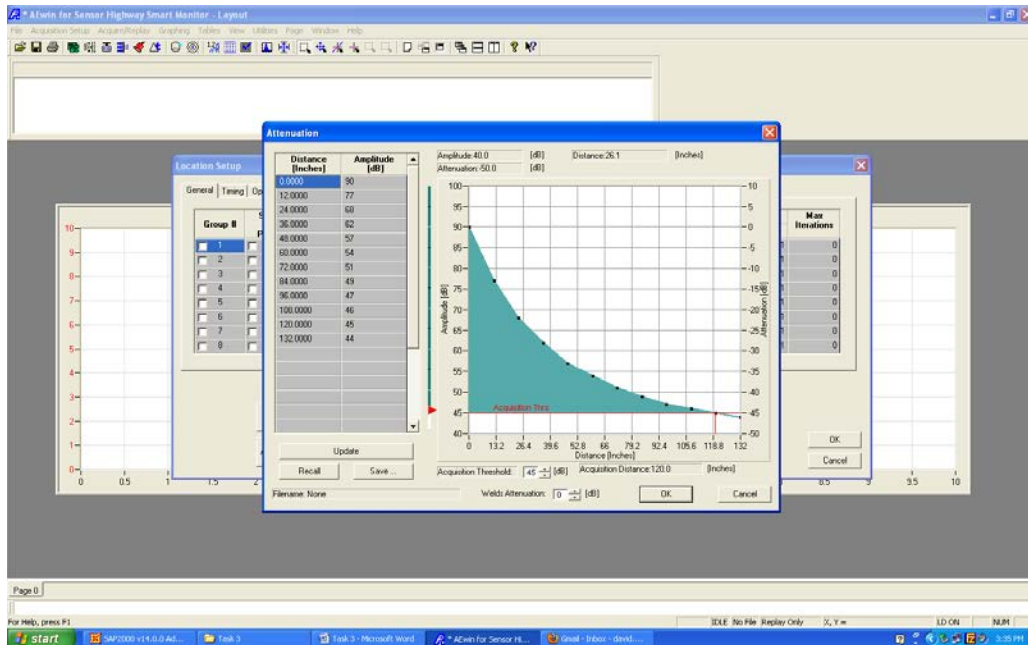


Figure A.4: Attenuation Window

11. From Location Setup Window select Attenuation button
12. Input attenuation data from the pencil break tests, on average amplitude and distance into corresponding column
13. Click OK button in bottom right
14. Close Location Setup Window

A.2: Signal Filtering using AEWin™

1. In the File menu select → Acquisition Setup → AE Hardware...

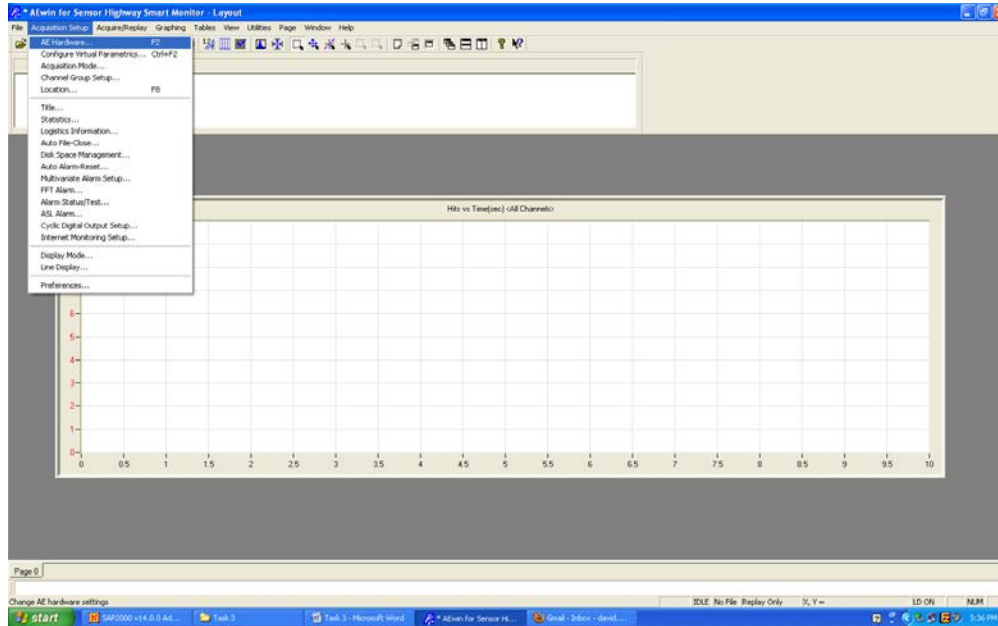


Figure A.5: Access to Signal Filtering Capabilities

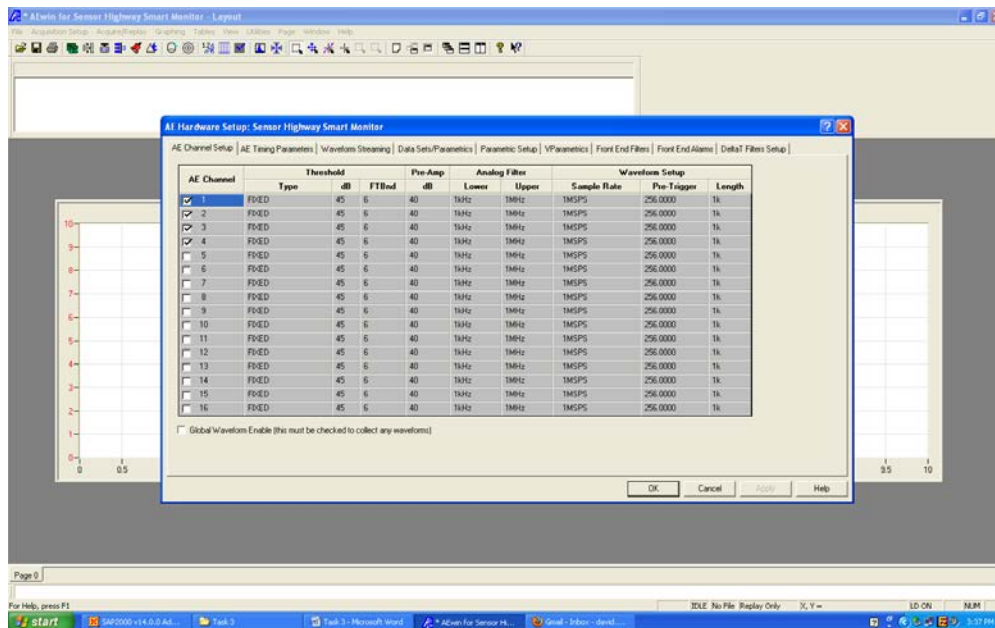


Figure A.6: Frequency Filter Setup

2. Adjust Analog Filter columns for lower/upper bounds
3. Select Front End Filters tab

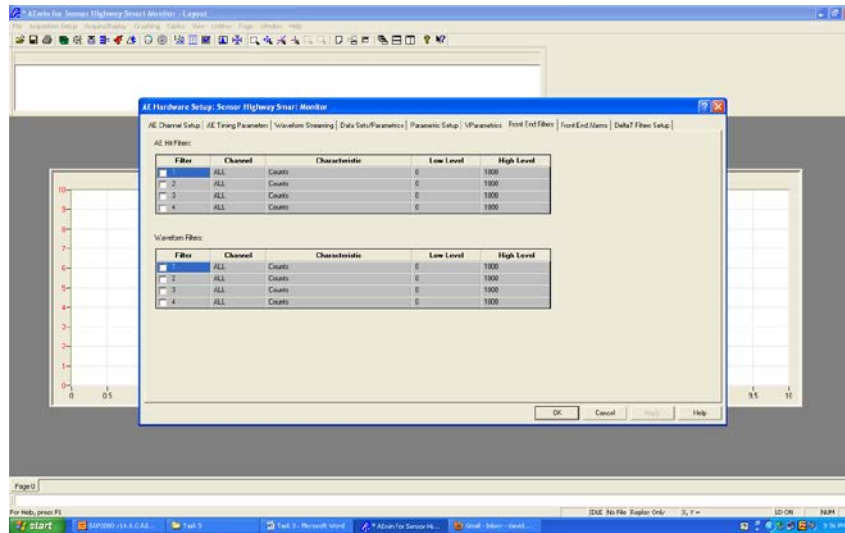


Figure A.7: Front End Filters

4. Select number of filters to turn on
5. Select what sensors (Channel) to apply filter
6. Select AE feature to use as filter (Characteristic)
7. Input Low Level filter threshold
8. Input High Level filter threshold
9. Repeat as needed
10. Close AE Hardware Window

A.3 Signal Clustering using AEWIn™

1. In the File menu select → Graphing → New Graph

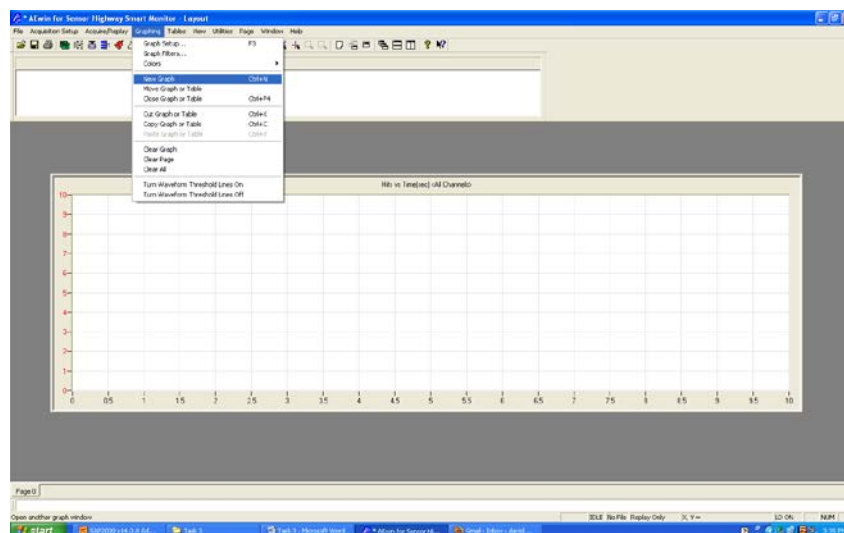


Figure A.8: Access Signal Clustering

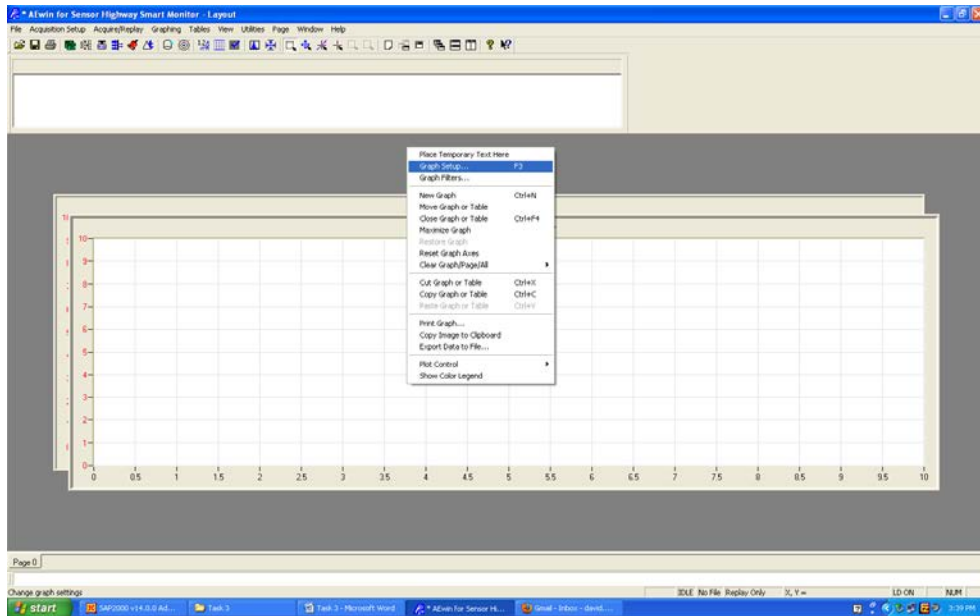


Figure A.9: Graph Setup

2. Right-click on the new graph and select → Graph Setup
3. Select Clustering tab

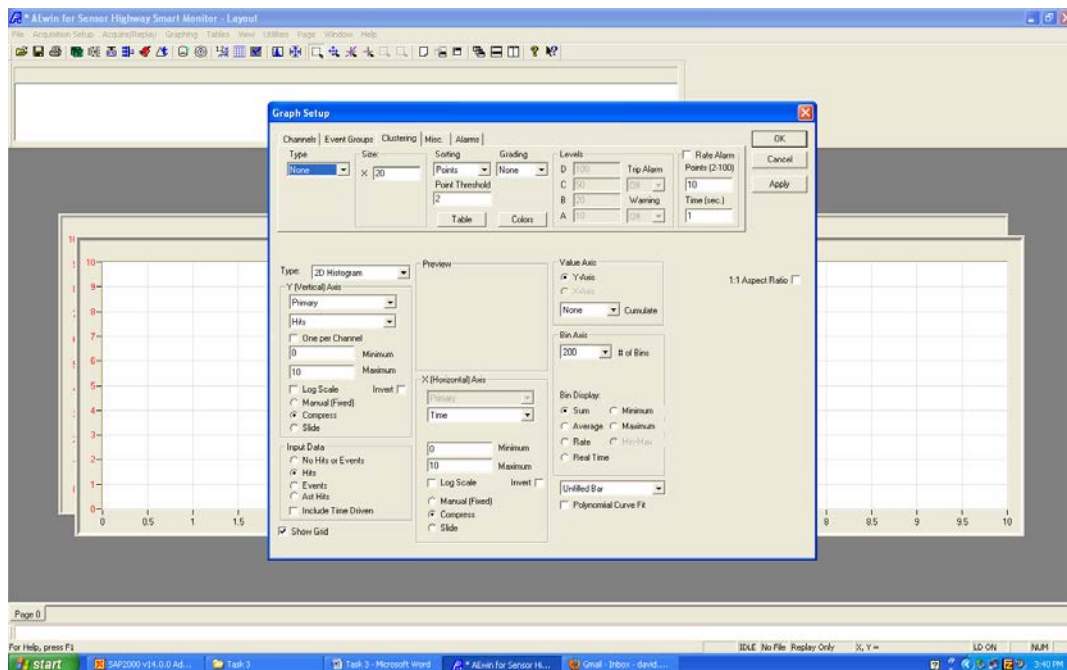


Figure A.10: Graph Setup - Clustering

4. Input information for Type, Size, Y (Feature), X (Feature), and Sorting
5. Click OK box
6. Repeat as needed

A.4: Setting Signal Alarms using AEWin™

1. In the file Menu select → Graphing → New Graph

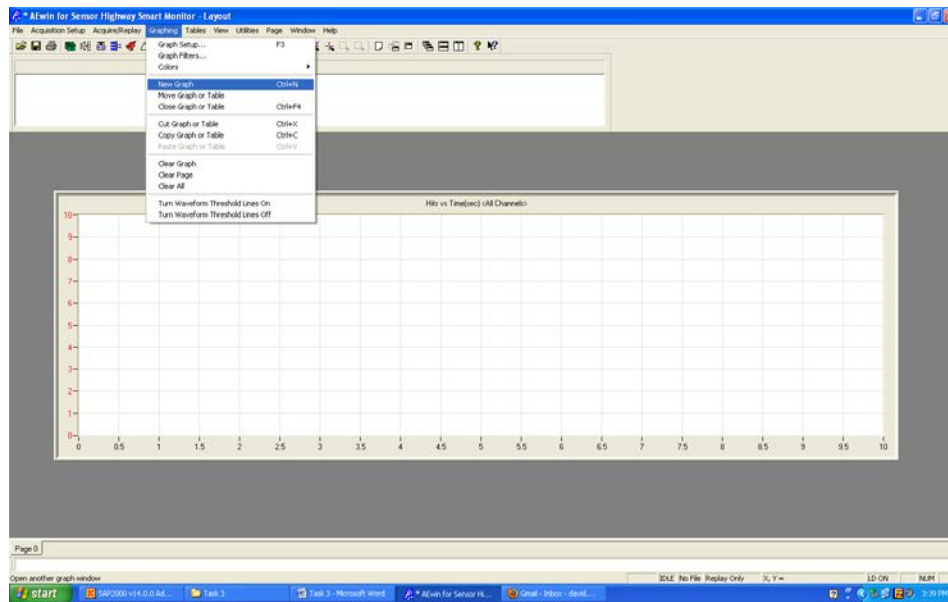


Figure A.11: Access to Signal Cluster Alarms

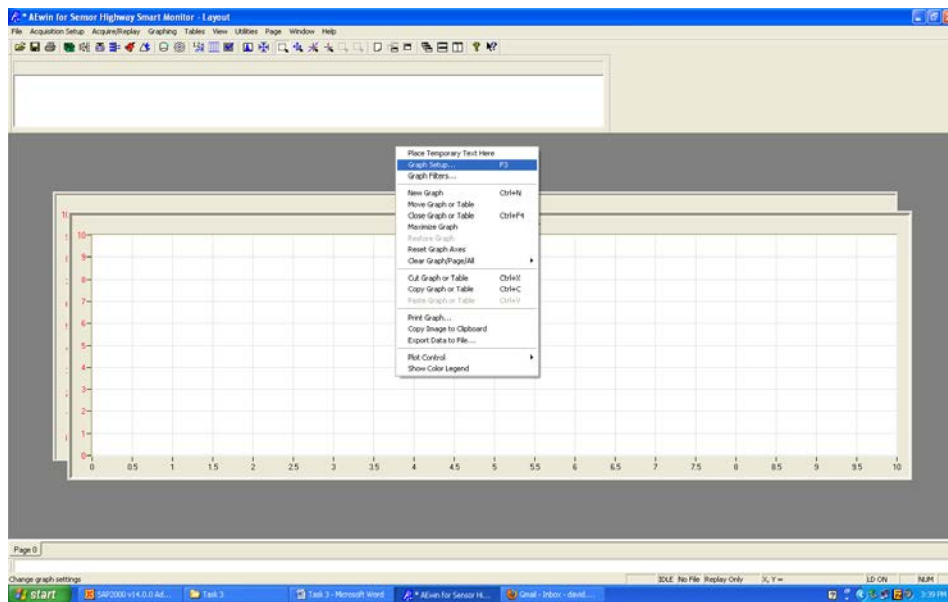


Figure A.12: Cluster Alarm Setup

2. Right click on new or on existing cluster graph and select → Graph Setup
3. Input information for Grading, Levels, Trip Alarms, and Rate Alarms

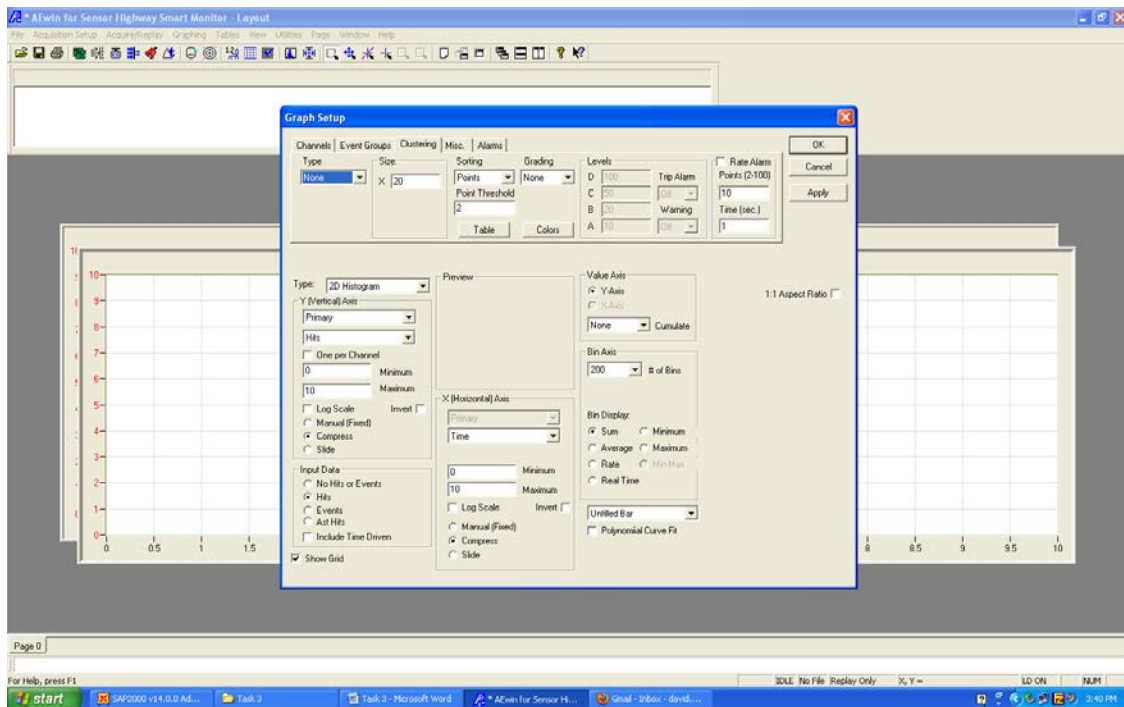
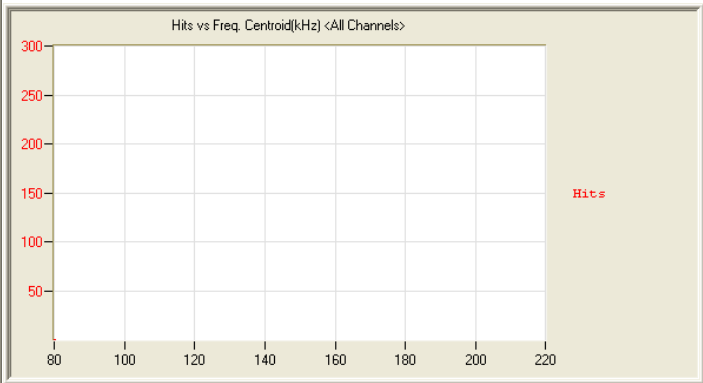
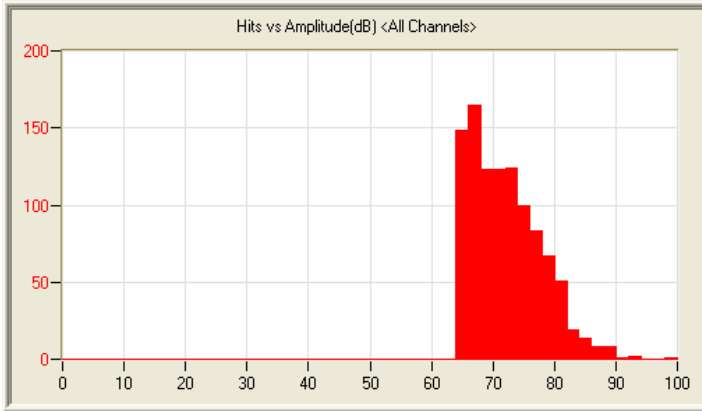
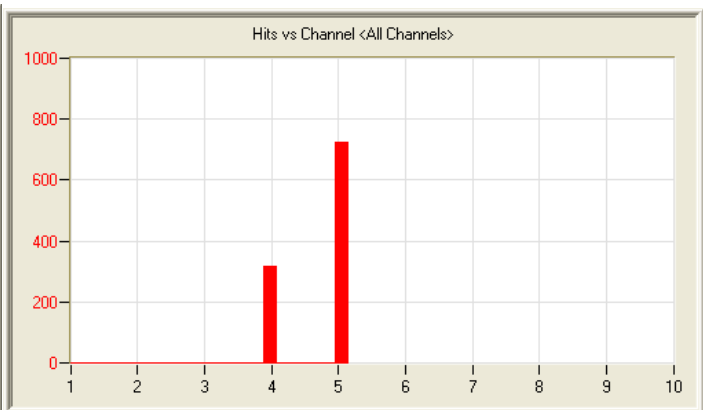
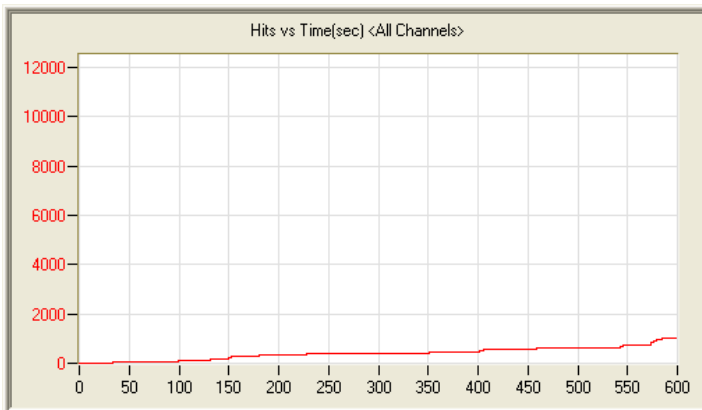


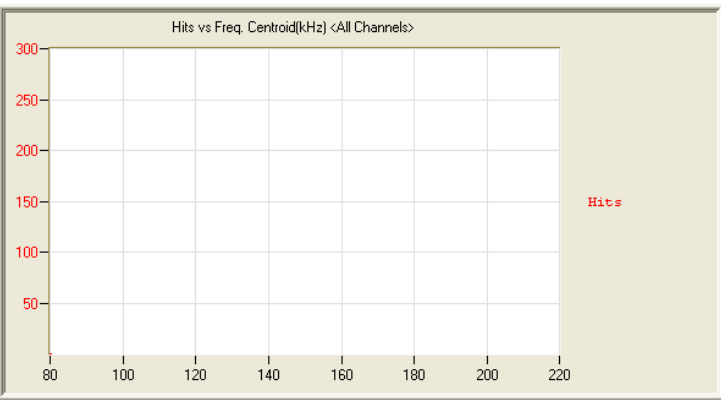
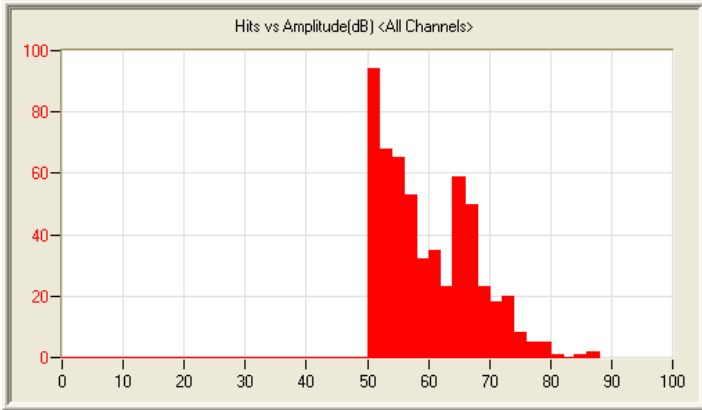
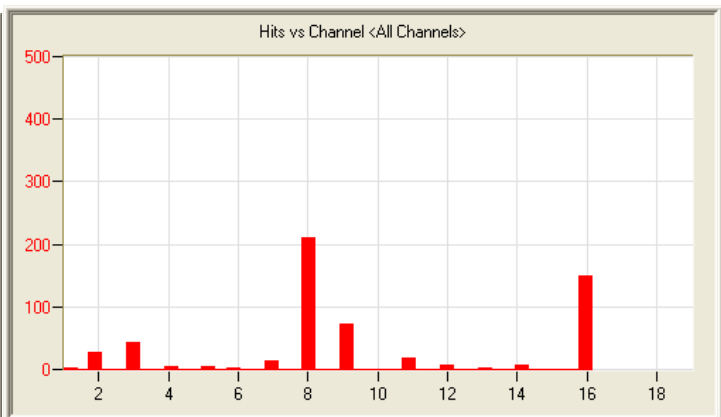
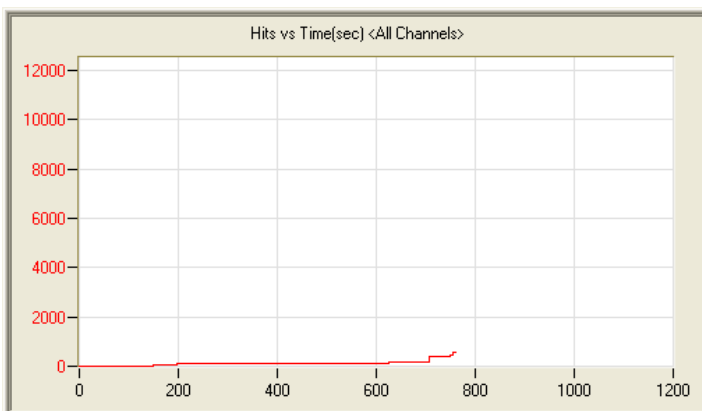
Figure A.13: Alarm Setup - Clustering

4. Click OK
5. Repeat as needed

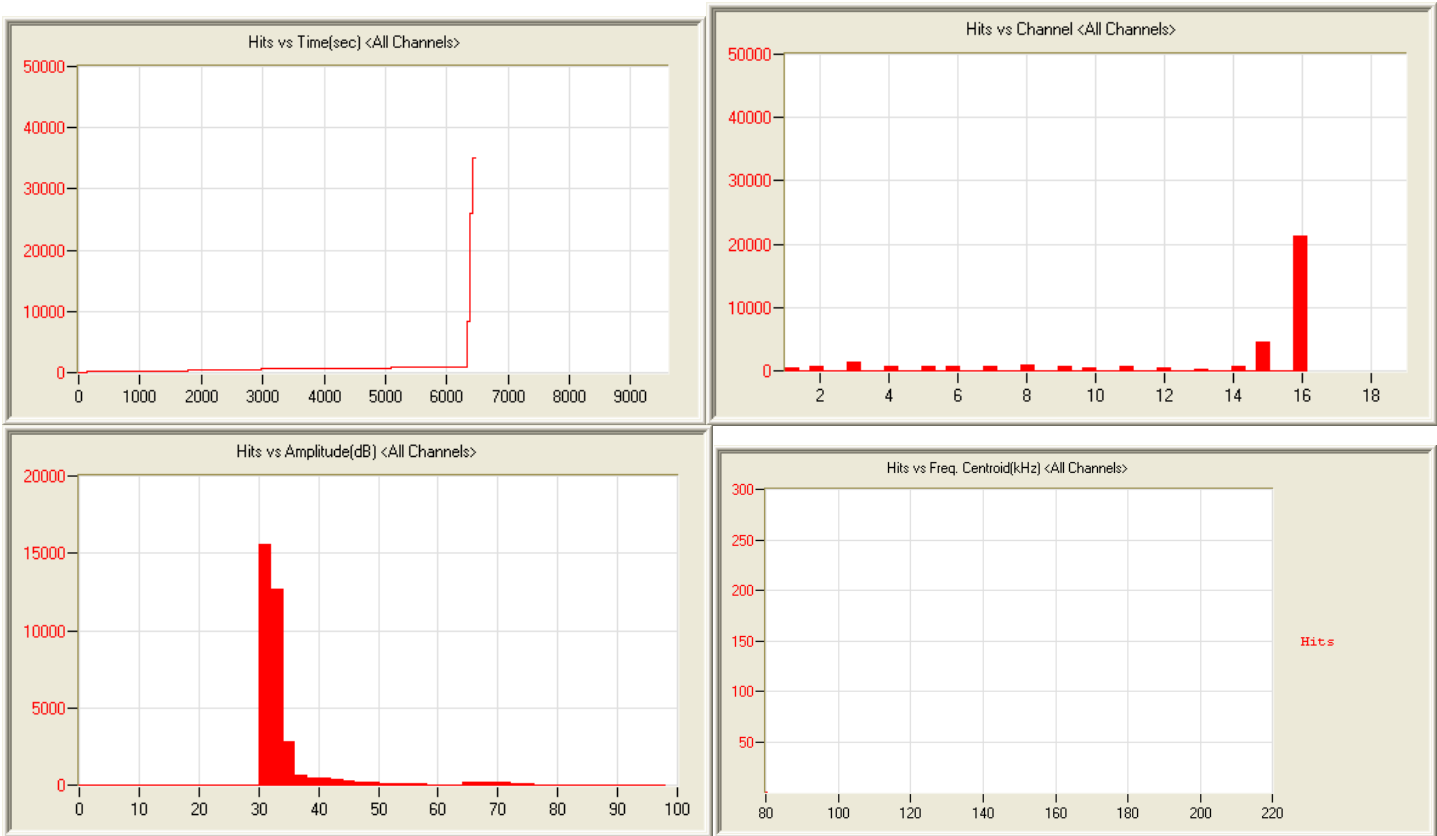
APPENDIX B: FIELD DATA COLLECTED FROM 1/14/2011 TO 10/30/2012



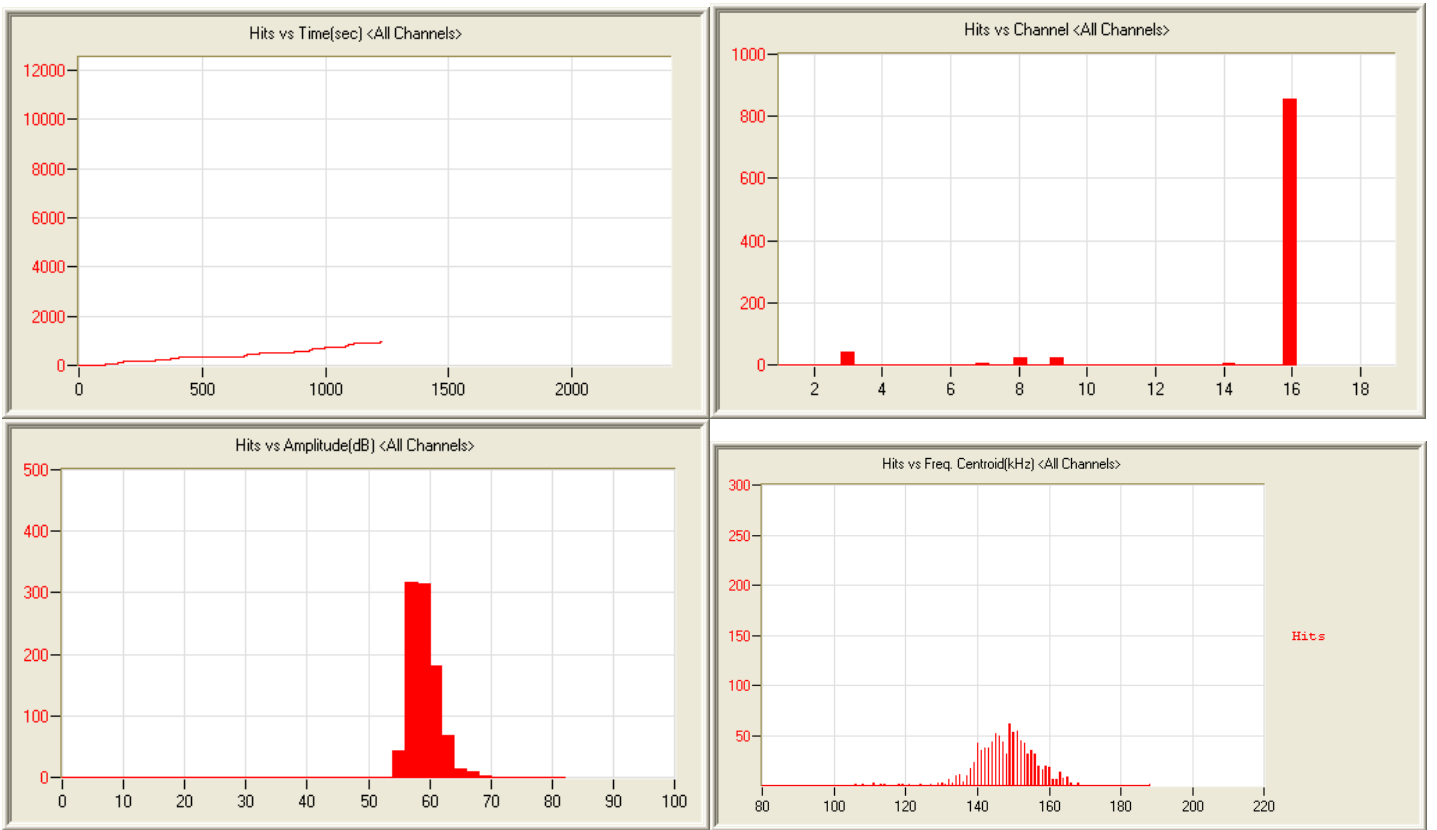
1/14/11 11:08am 0:10:00 1037 110114110837_0 106kb



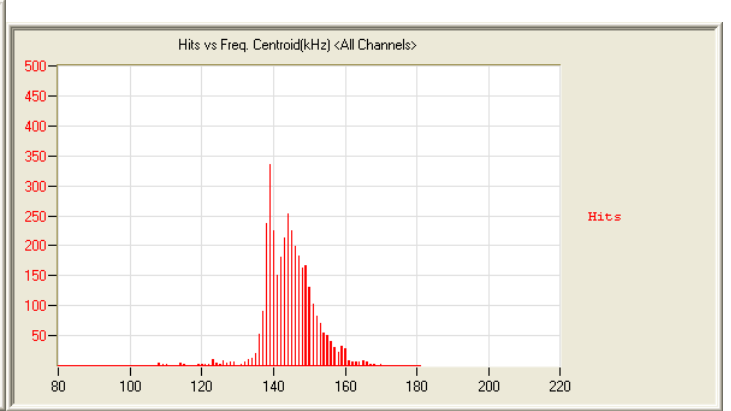
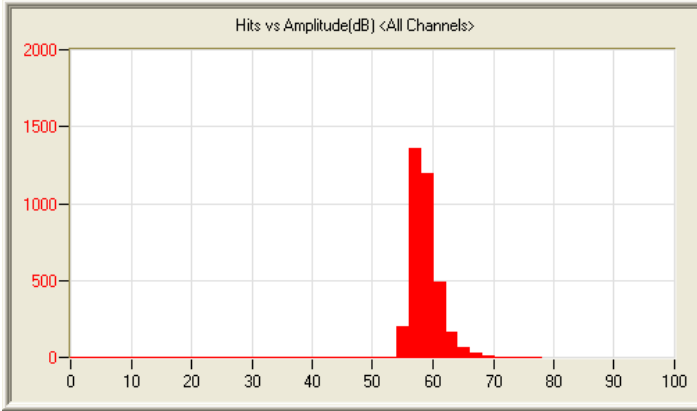
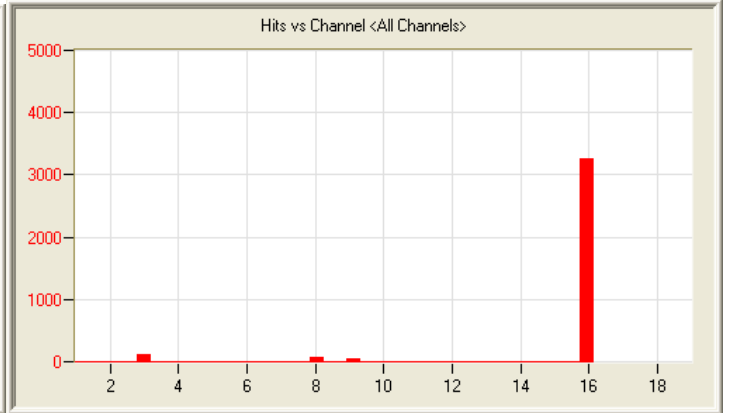
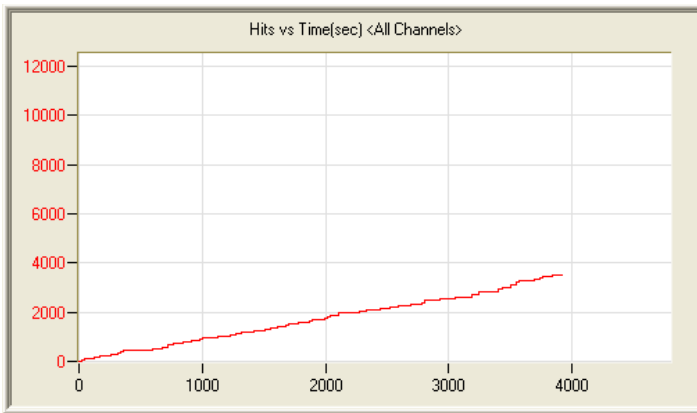
2/24/11 8:14am 0:12:39 562 110224081418_0 103kb



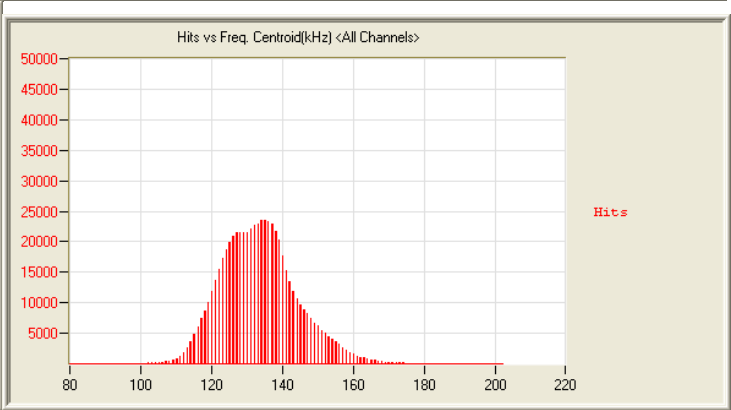
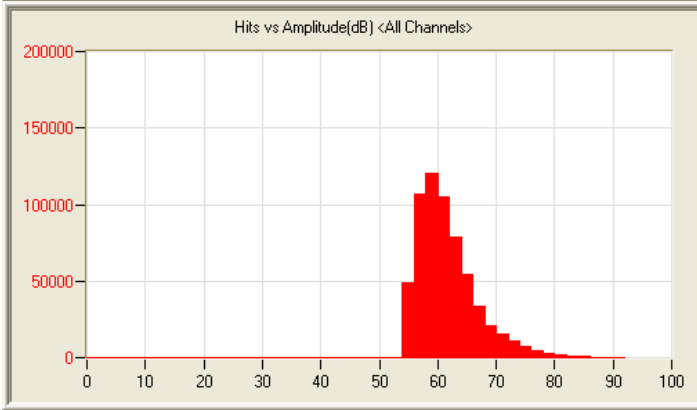
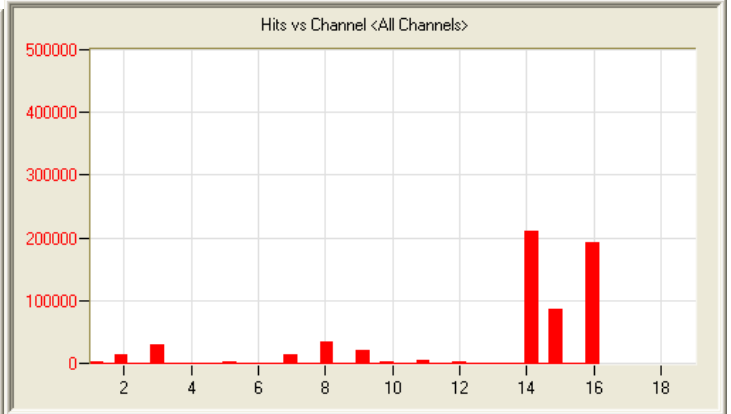
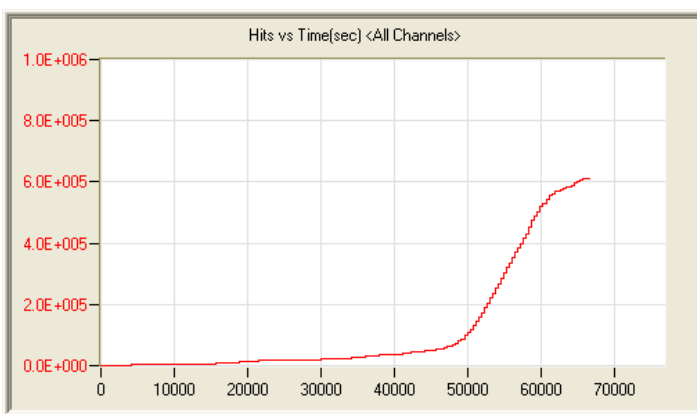
2/24/11 4:39pm 1:47:46 35083 110224163949_0 1.0mb



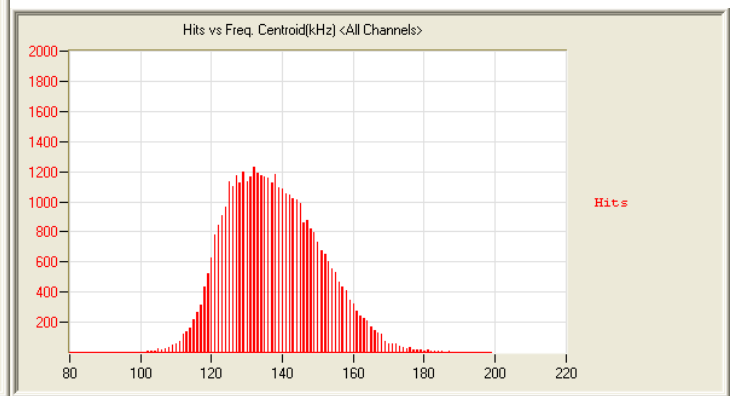
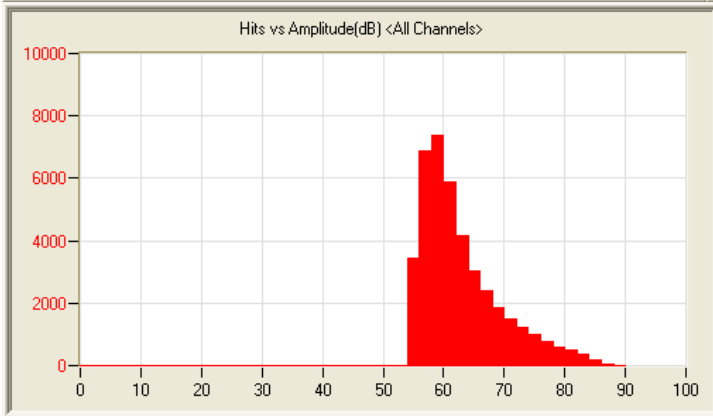
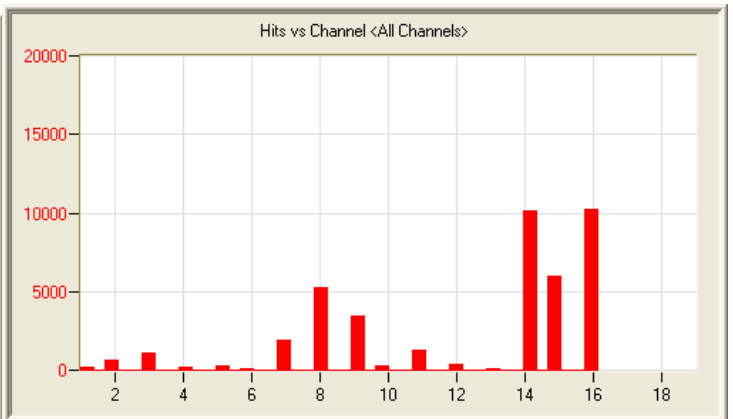
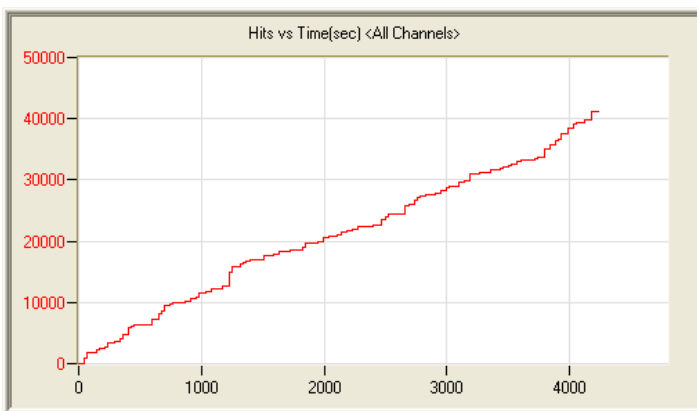
2/24/11 8:56pm 0:20:35 952 110224205614_0 187kb



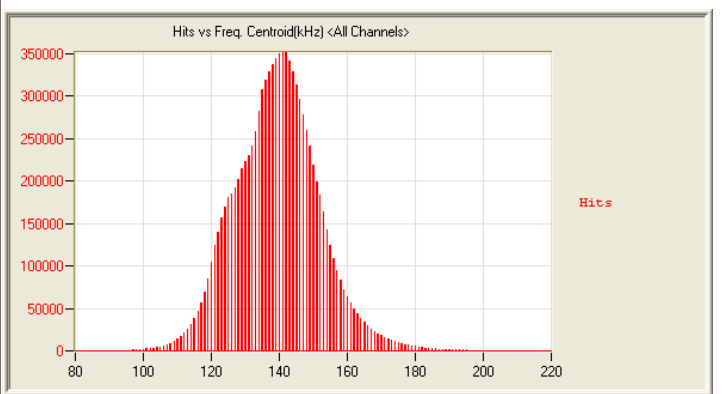
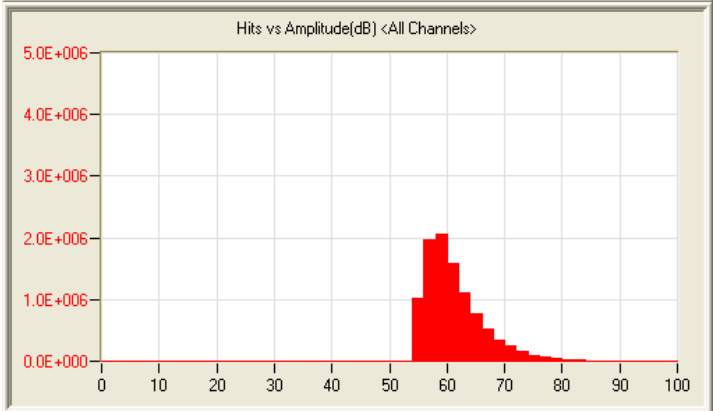
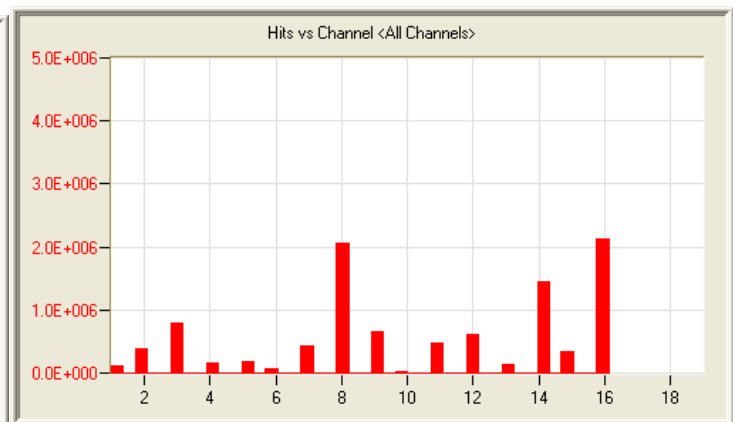
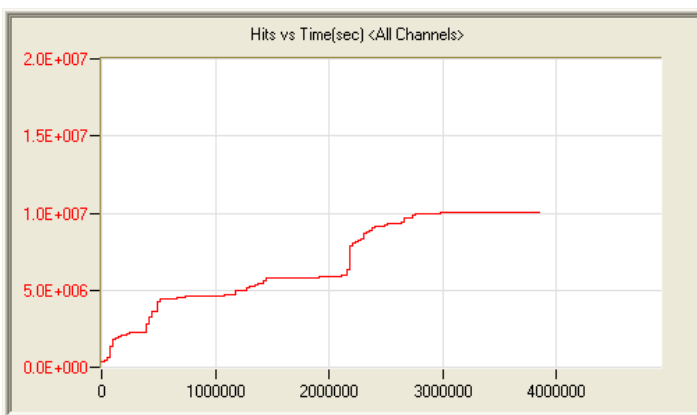
2/24/11 9:20pm 1:05:25 3497 110224212019_0 480kb



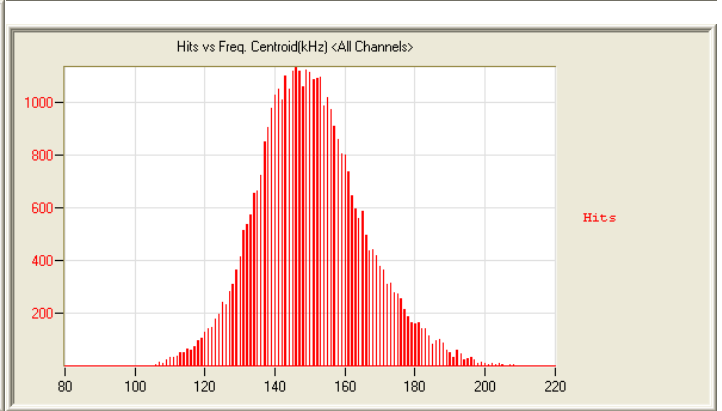
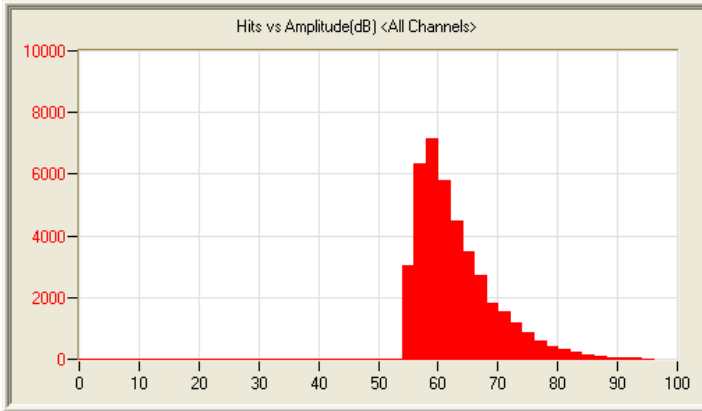
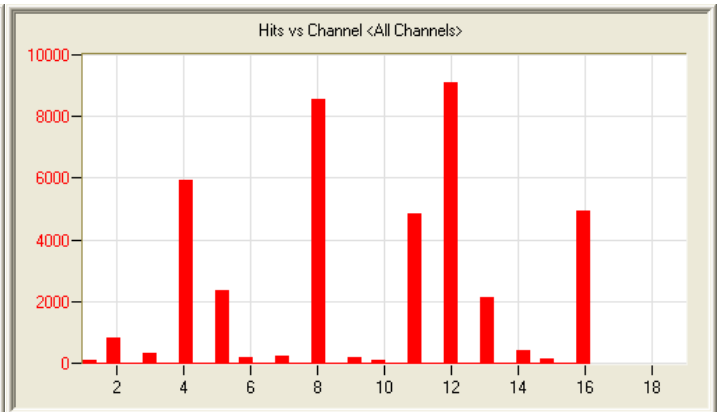
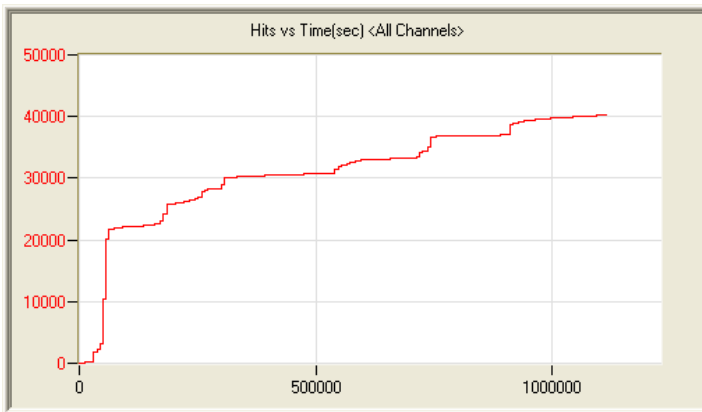
2/24/11 10:26pm 18:29:56 612974 110224222614_0 29.5mb



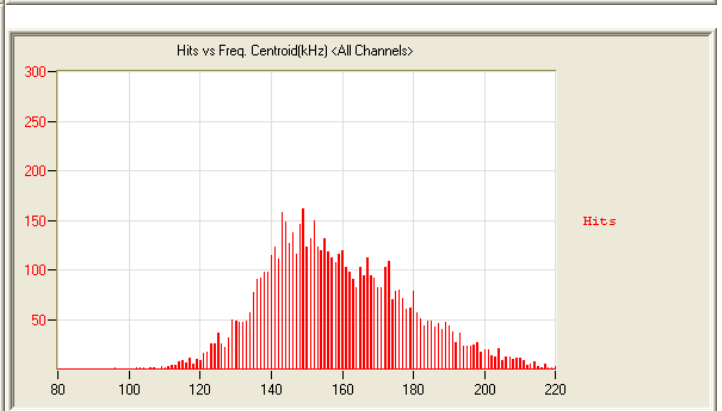
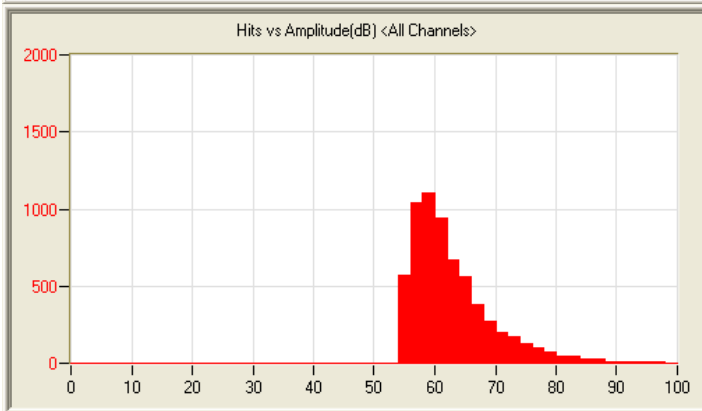
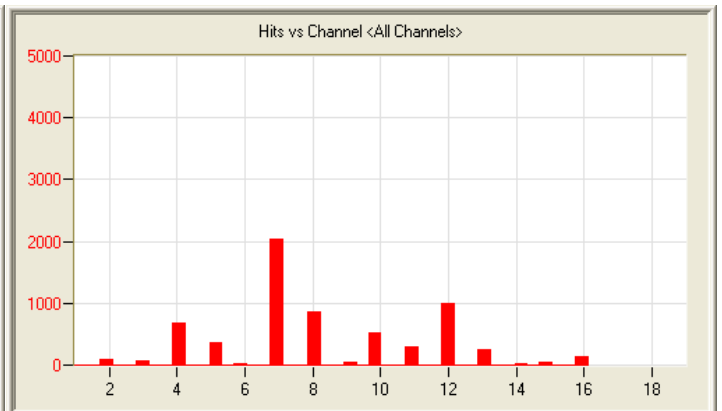
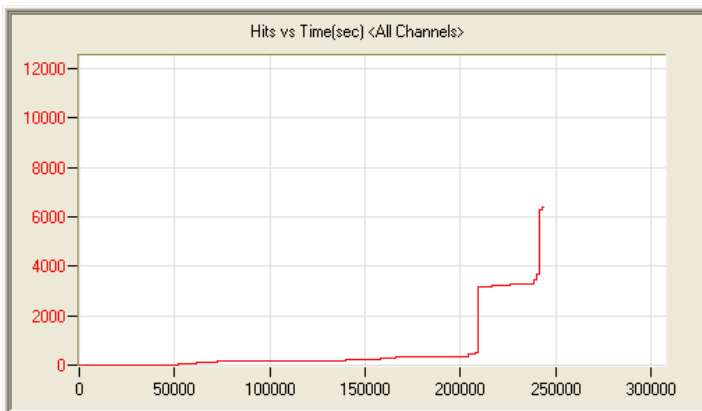
2/25/11 5:13pm 1:10:48 41239 110225171356_0 2.0mb



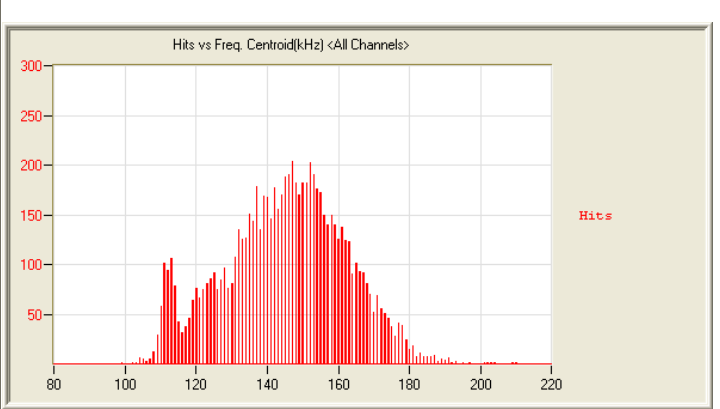
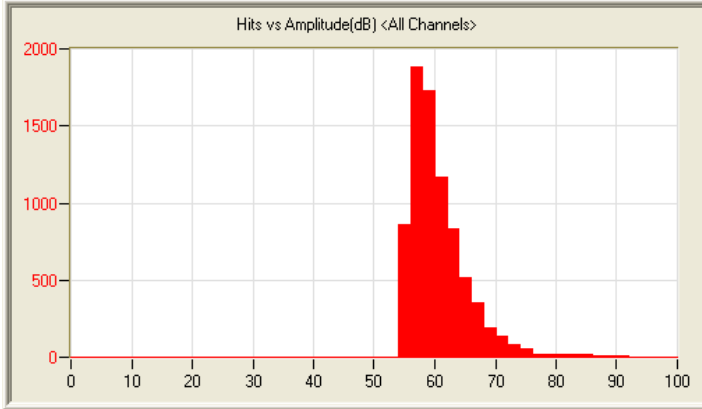
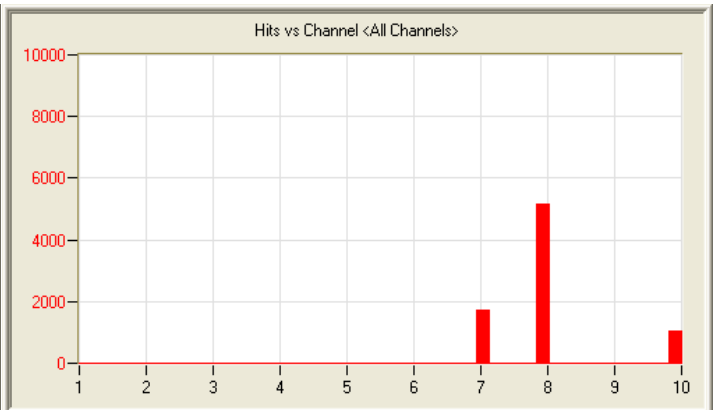
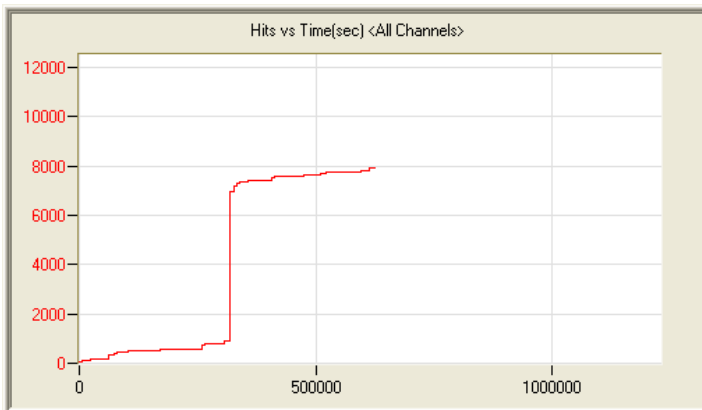
2/25/11 6:27pm 44:13:27:56 10011073 110225182659_0 678.7mb



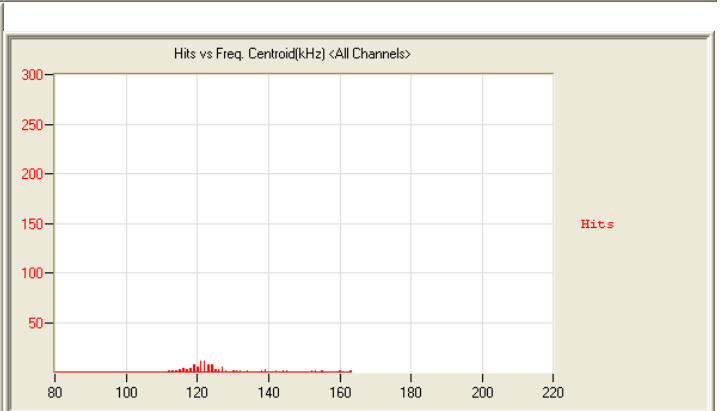
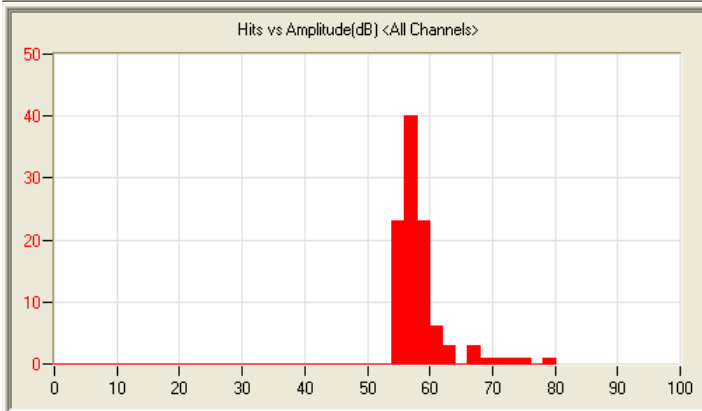
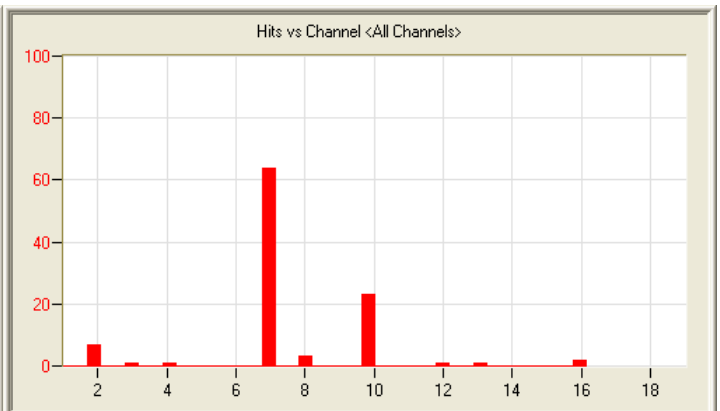
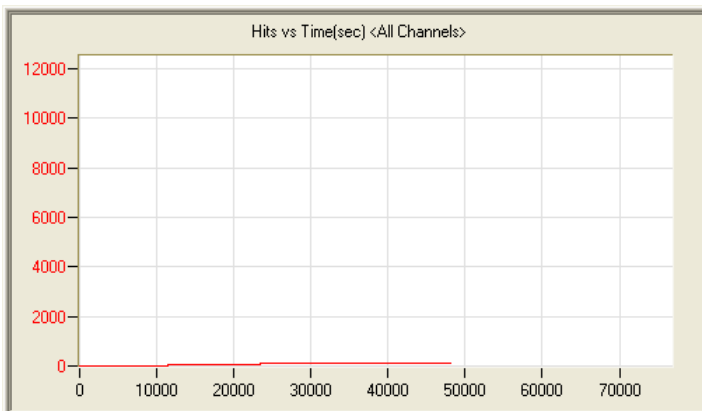
4/19/11 5:23pm 12:23:09:31 40320 110419172325_0 82.0mb



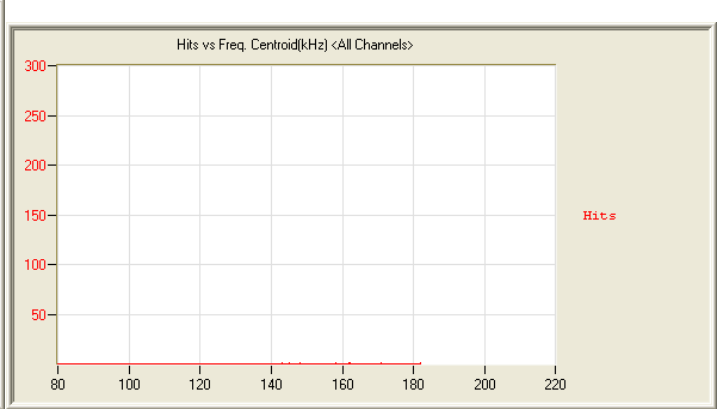
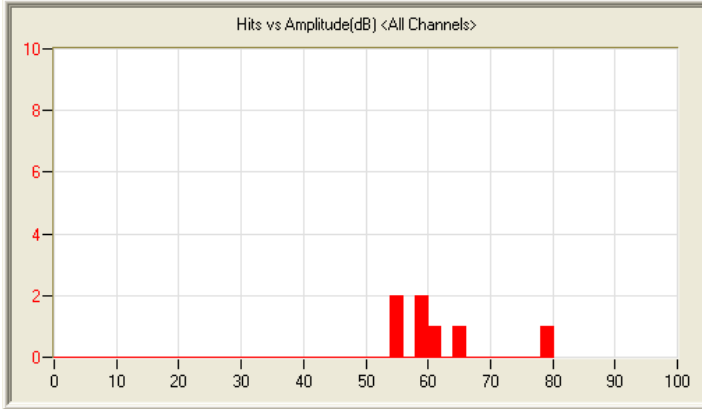
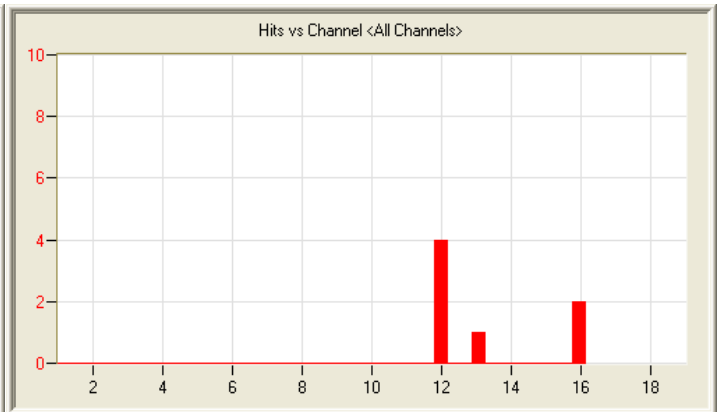
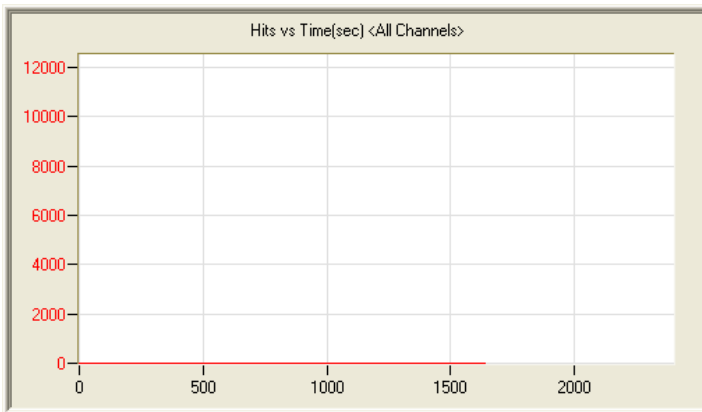
5/2/11 5:03pm 2:19:40:22 6393 110502170356_0 12.7mb



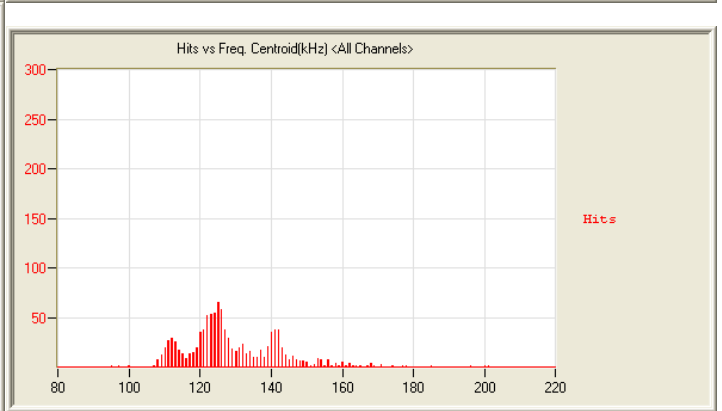
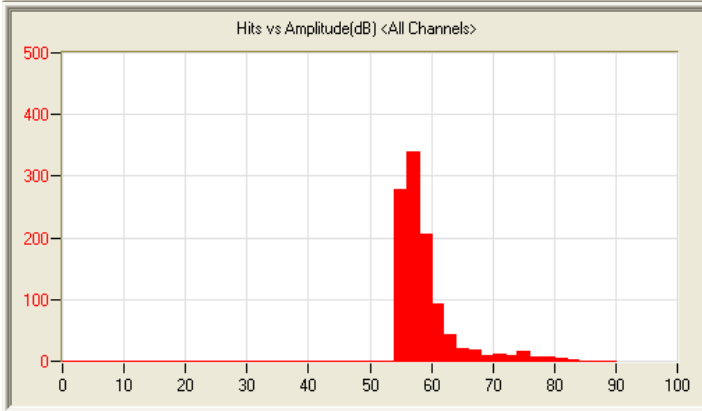
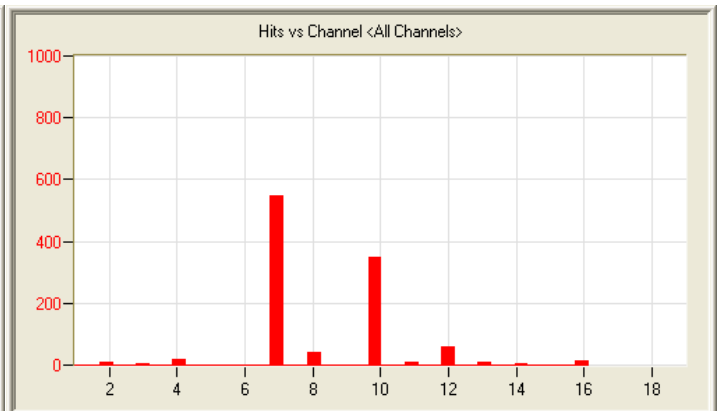
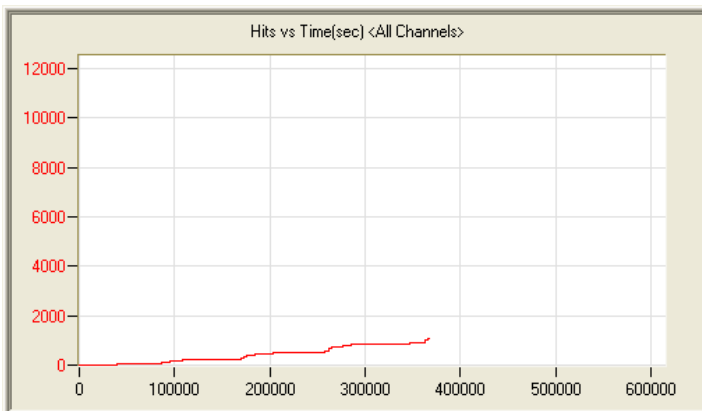
5/5/11 1:13pm 7:06:05:42 7919 110505131322_0 15.5mb



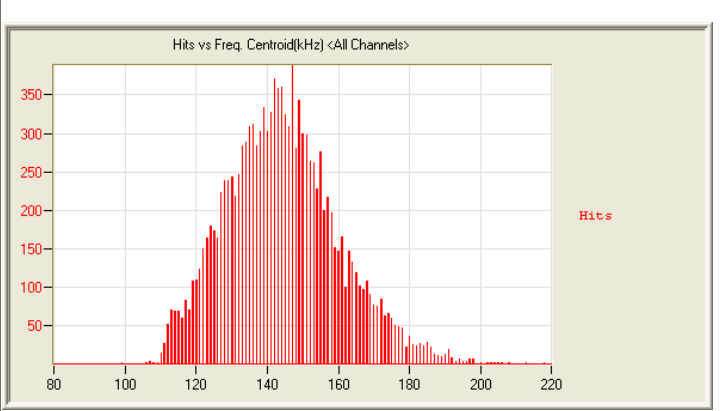
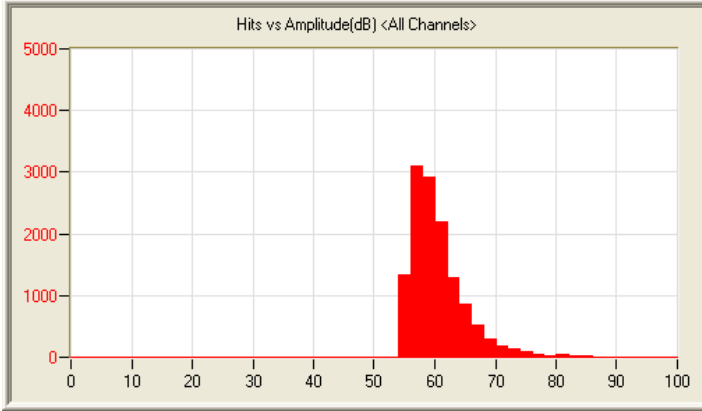
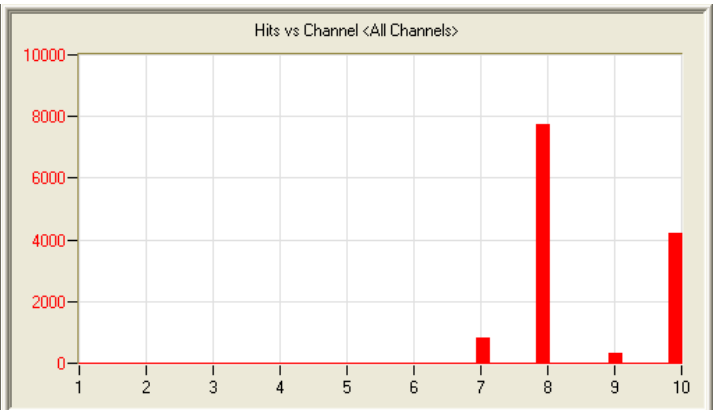
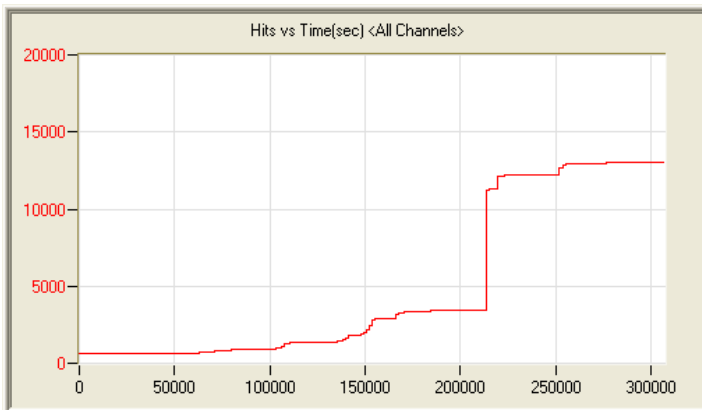
5/13/11 6:04am 13:27:24 103 110513060456_0 3.5mb



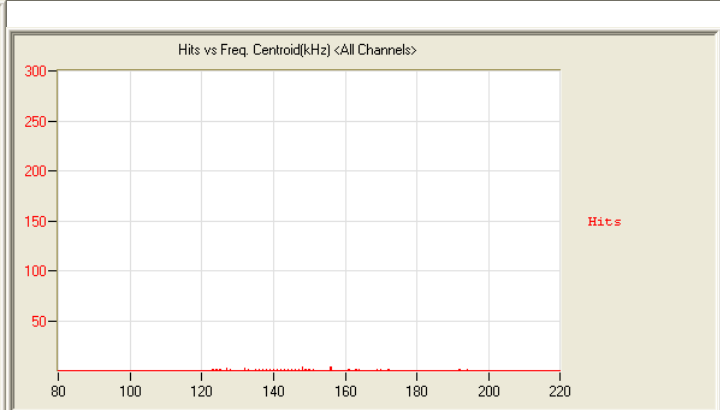
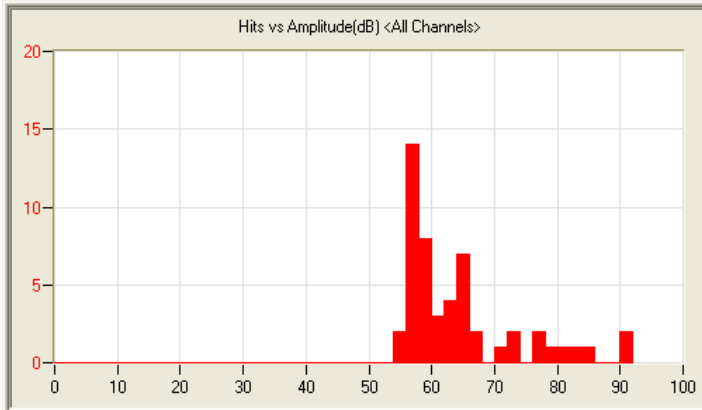
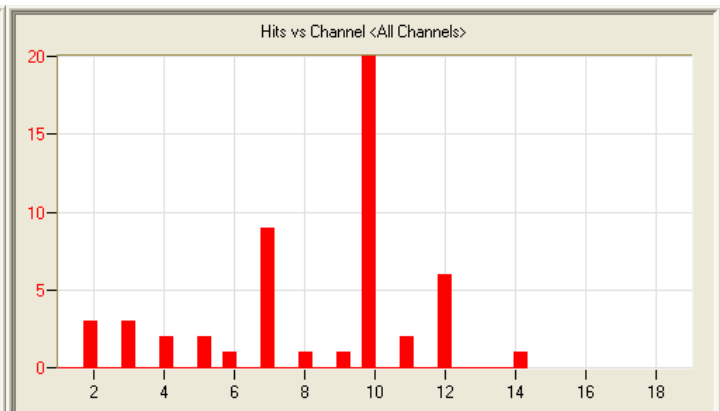
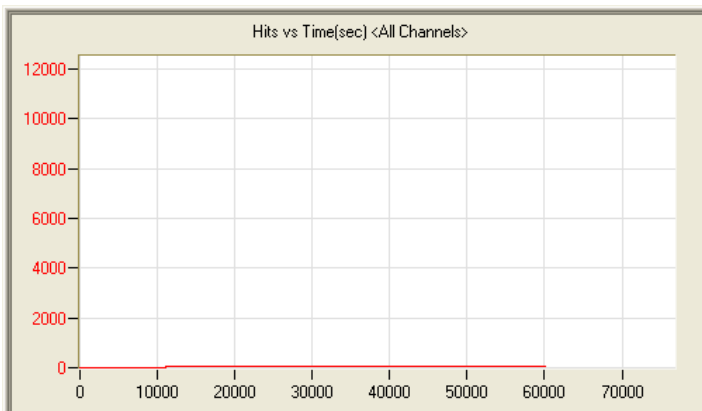
5/14/11 1:23pm 0:37:42 7 110514132347_0 222kb



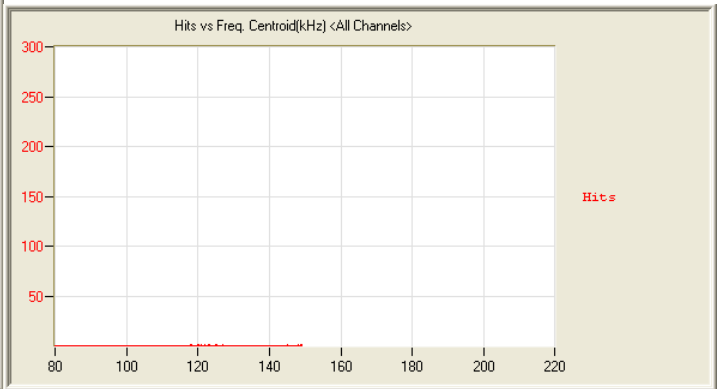
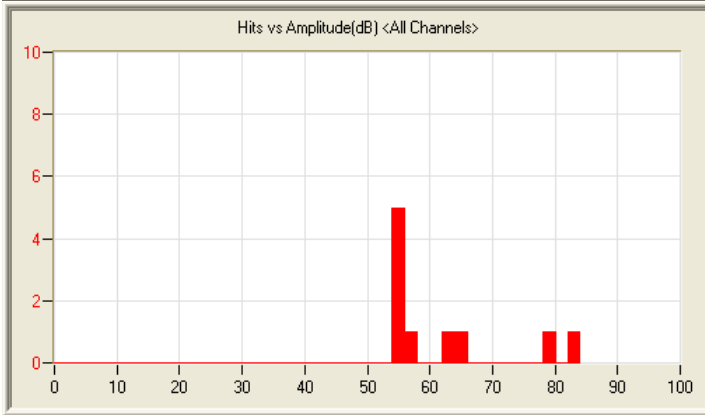
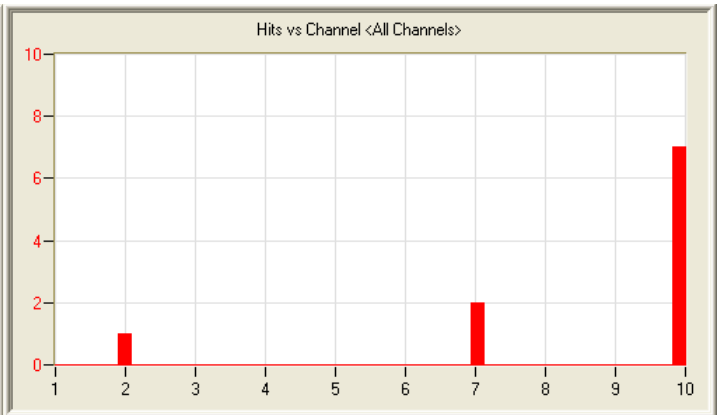
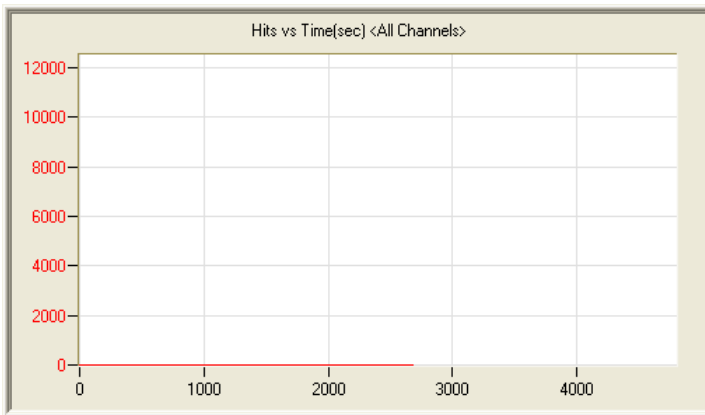
5/15/2011 6:54am 4:06:03:34 1065 110515065412_0 27mb



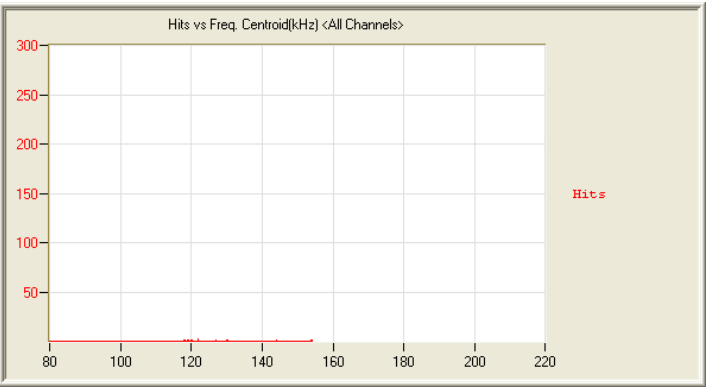
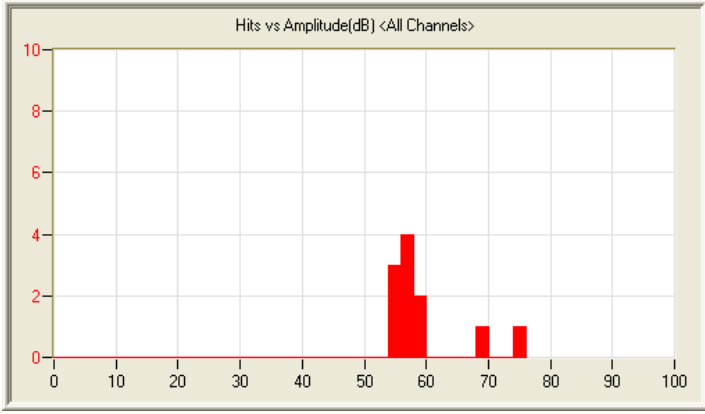
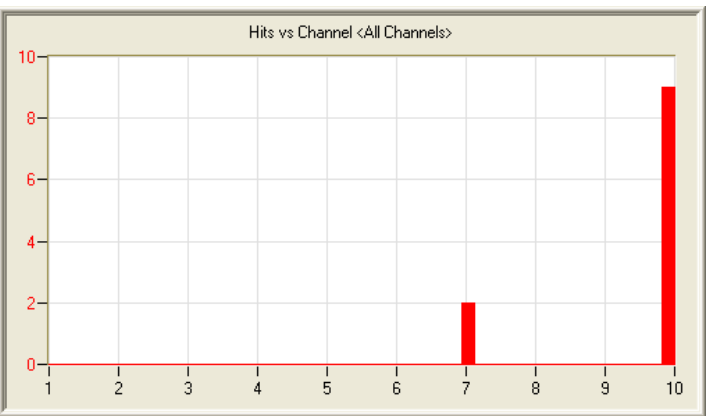
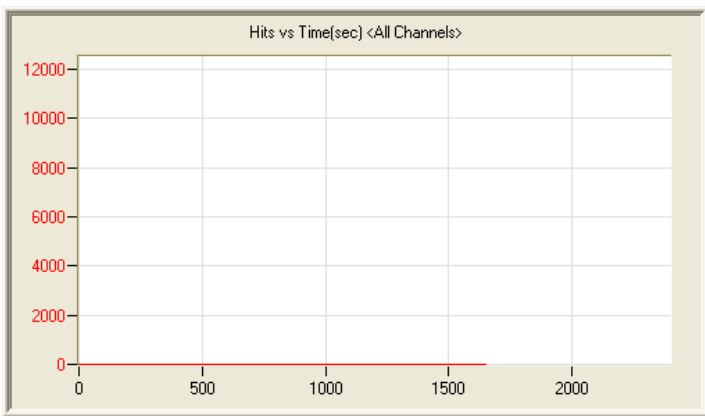
5/19/11 12:58pm 3:13:08:47 13062 110519125827_0 8.0mb



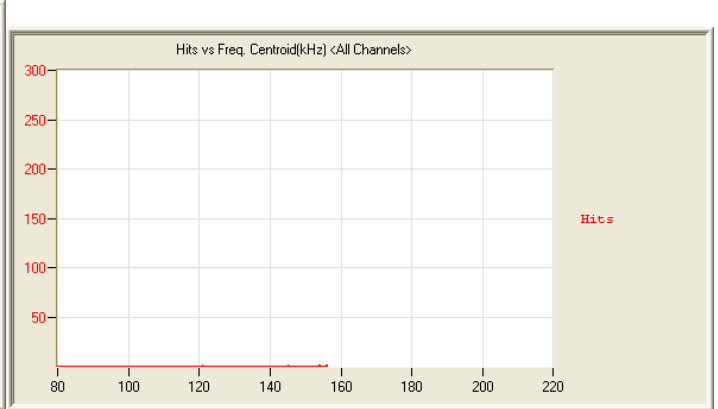
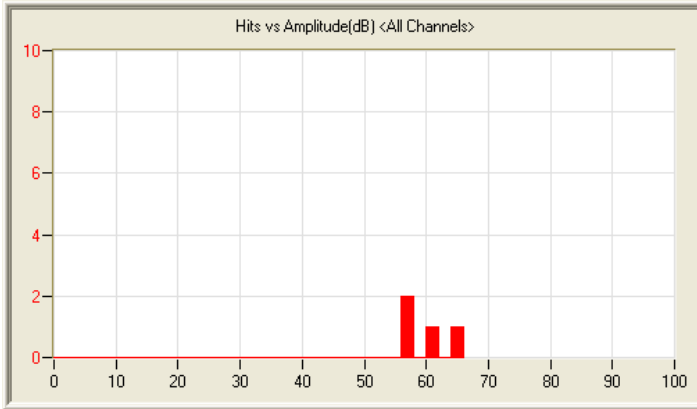
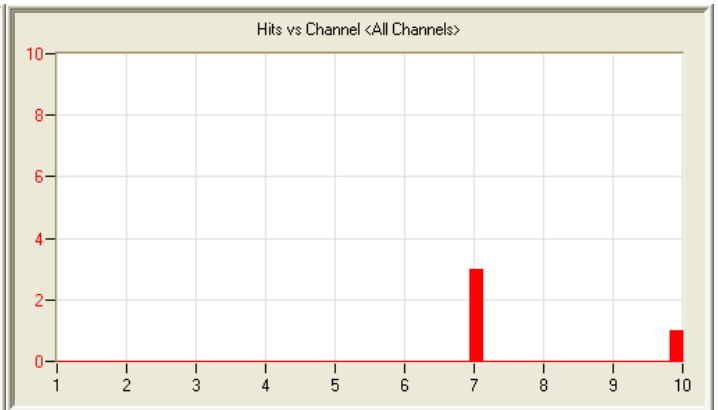
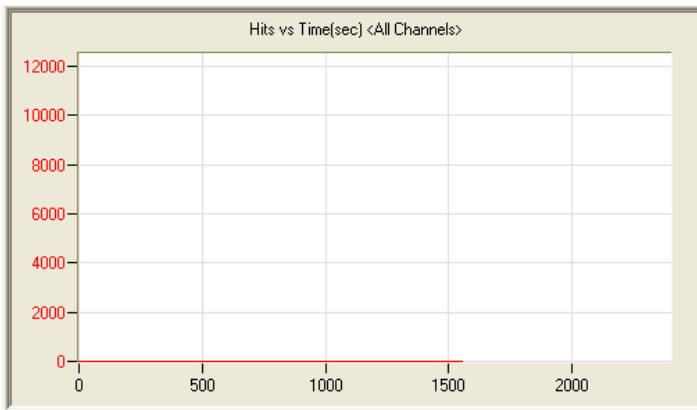
5/23/11 8:21am 16:51:47 51 110523082153_0 4.4mb



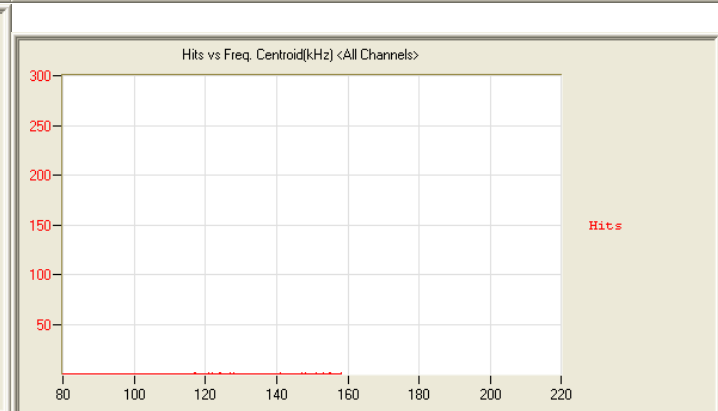
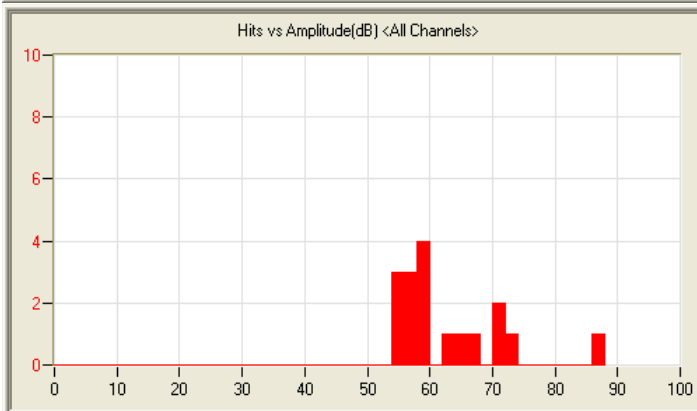
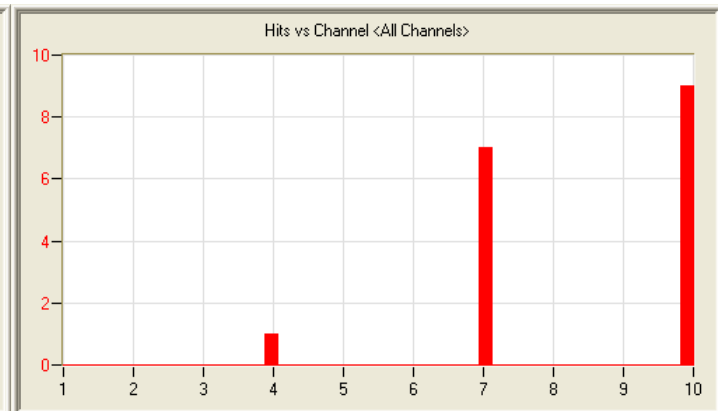
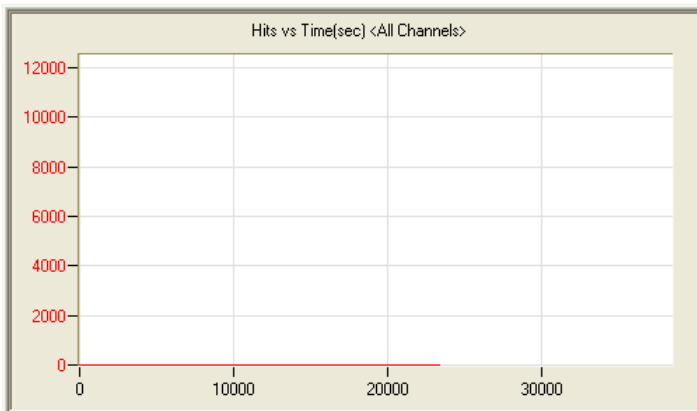
5/24/11 7:15am 1:07:24 10 110524071514_0 349kb



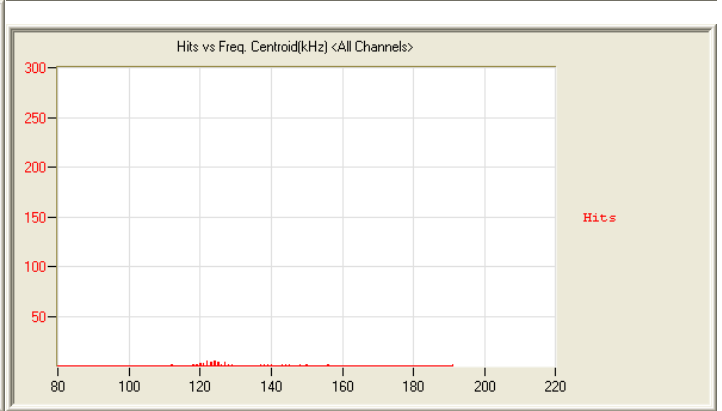
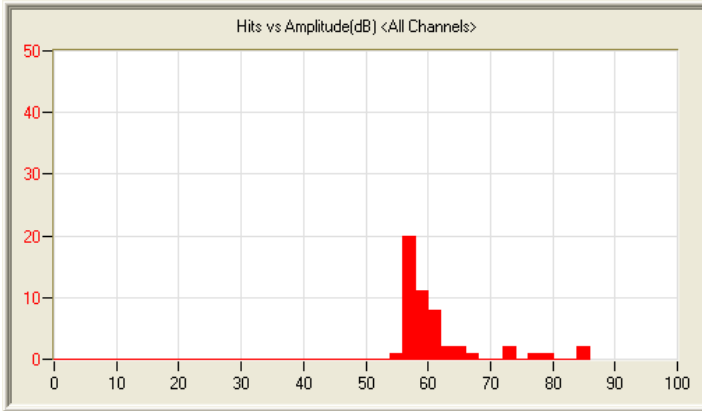
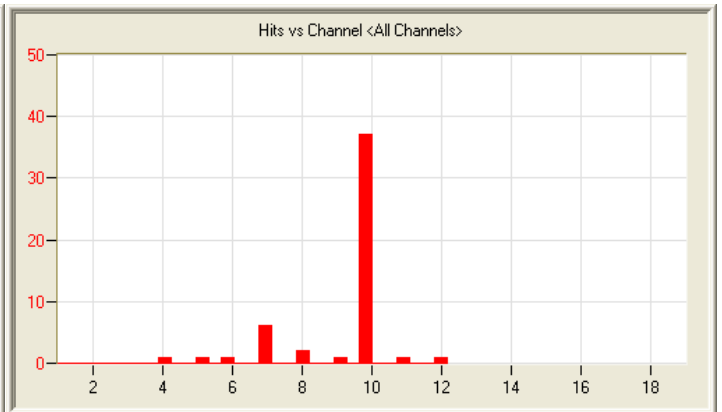
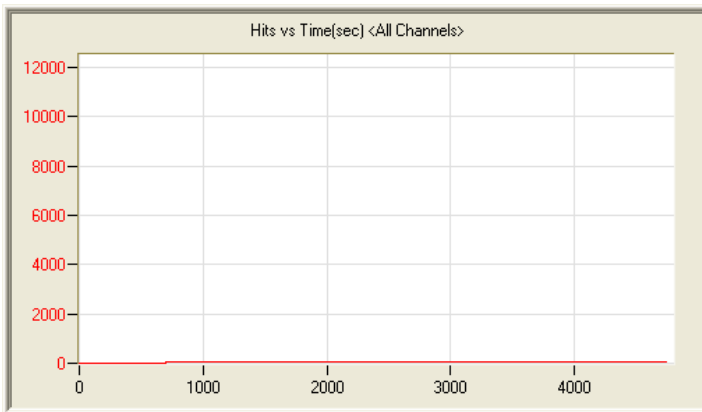
5/24/11 9:24am 0:48:30 11 110524092444_0 269kb



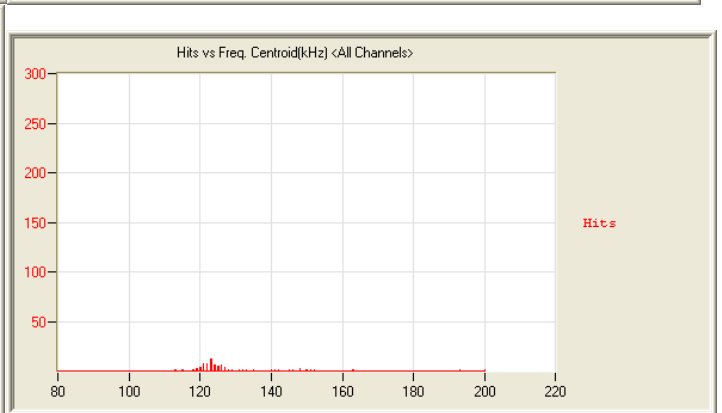
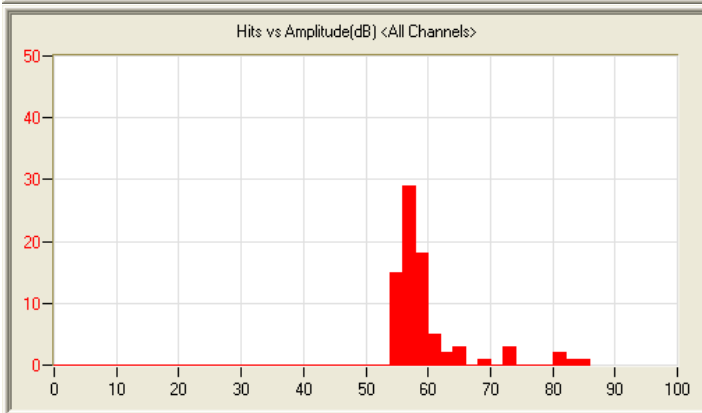
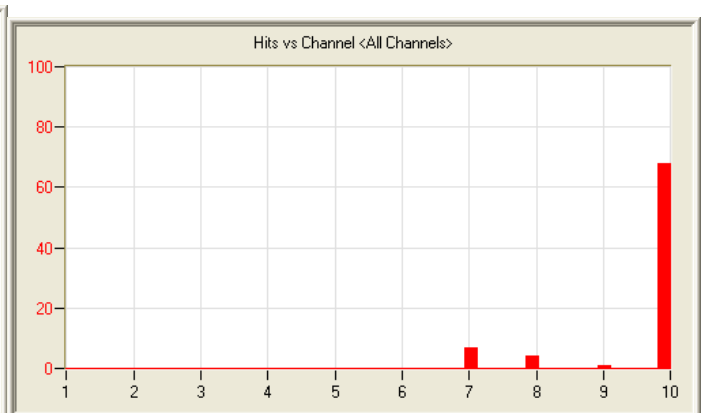
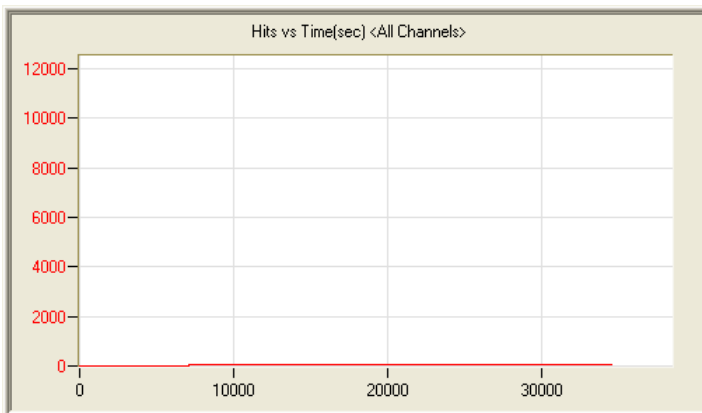
5/24/11 11:46am 0:32:31 110524114625_0 200kb



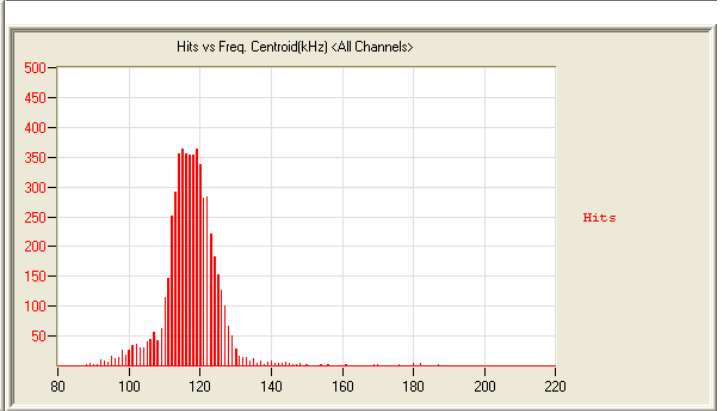
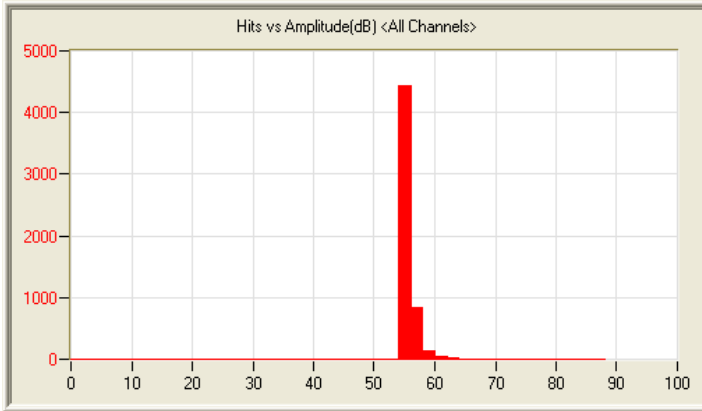
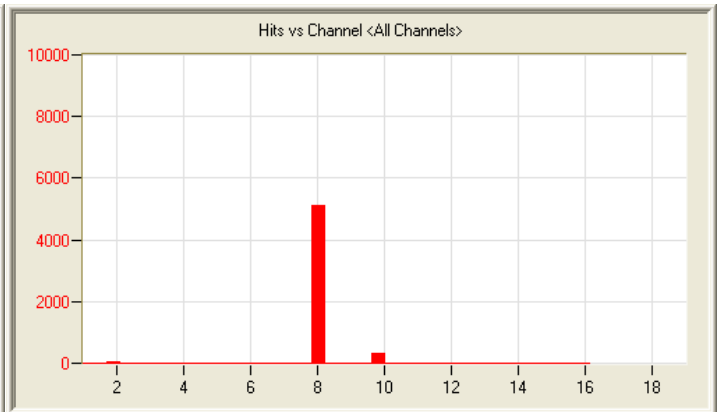
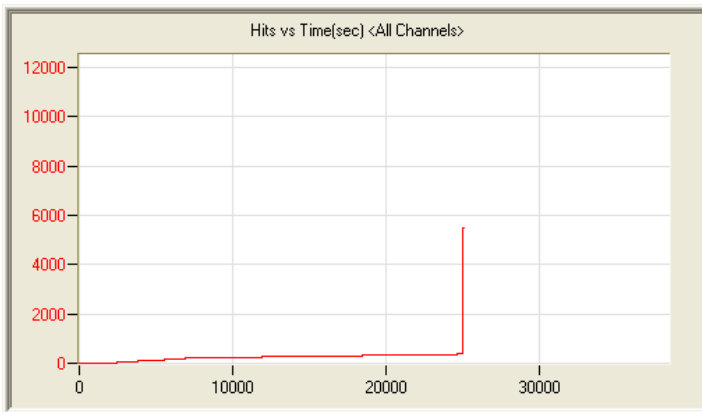
5/24/11 12:23pm 7:54:34 17 110524122338_0 2.1mb



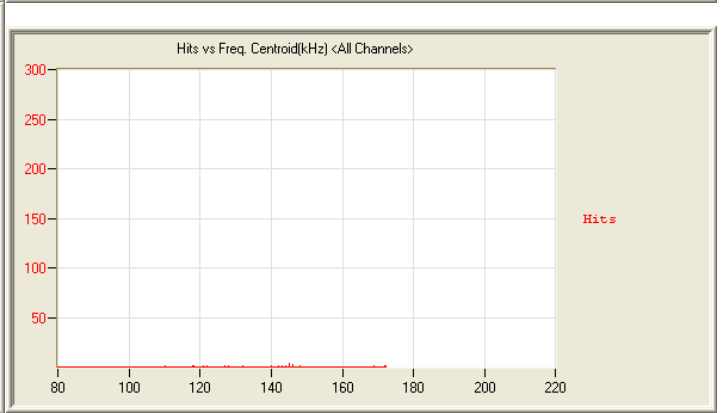
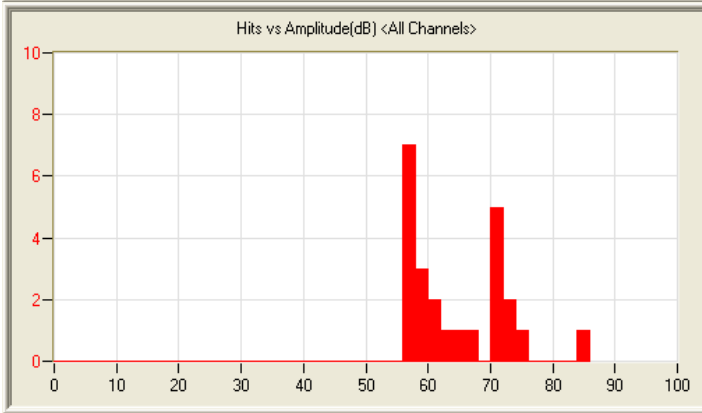
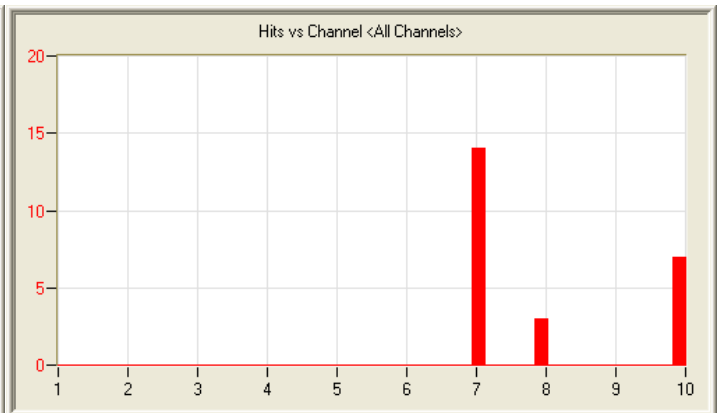
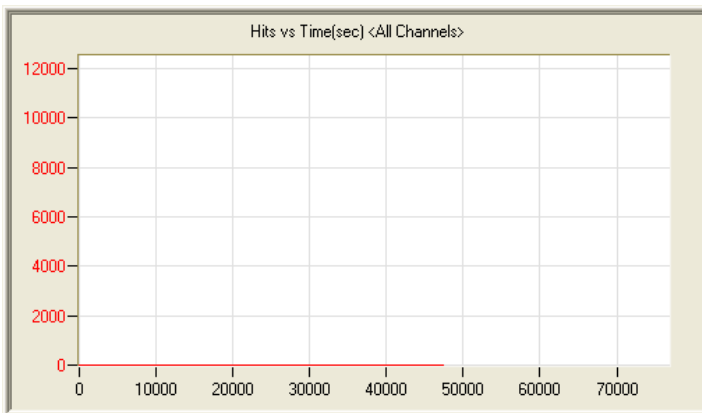
5/25/11 9:18am 1:22:23 51 110525091814_0 415kb



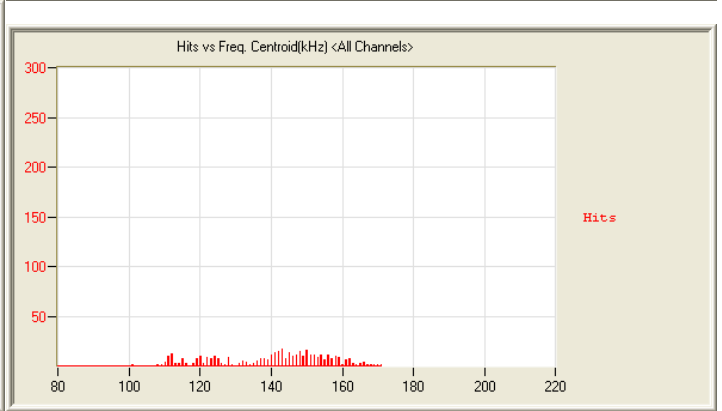
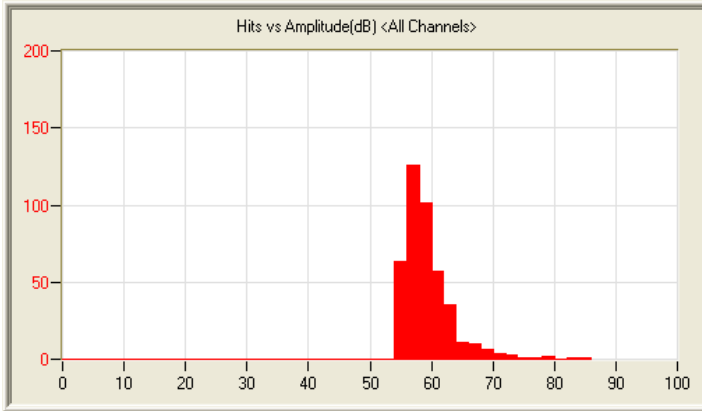
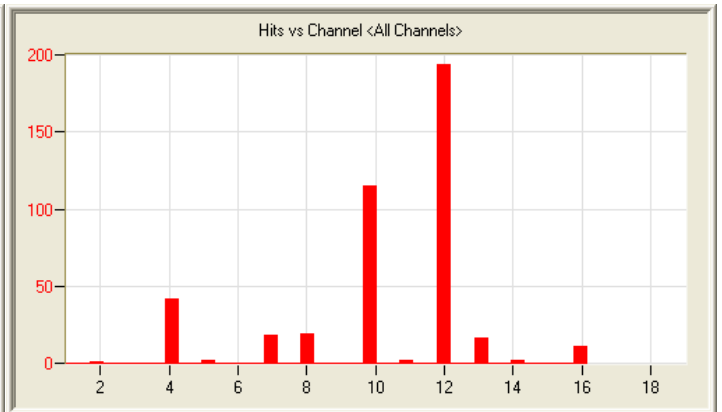
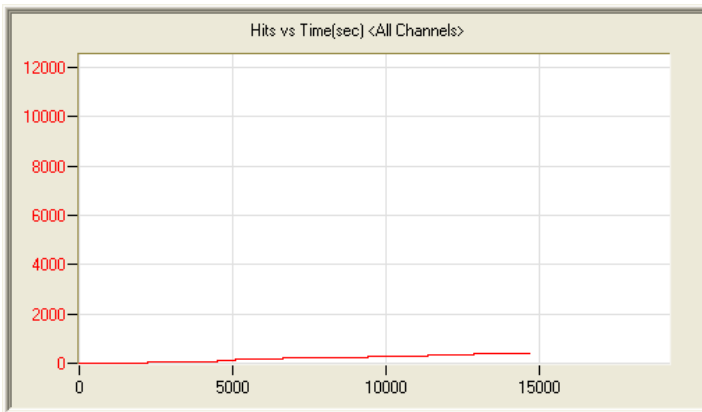
5/25/11 10:41am 10:19:38 110525104139_0 970kb



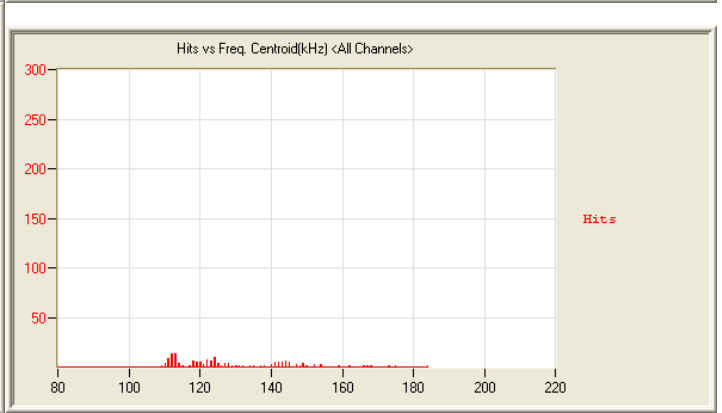
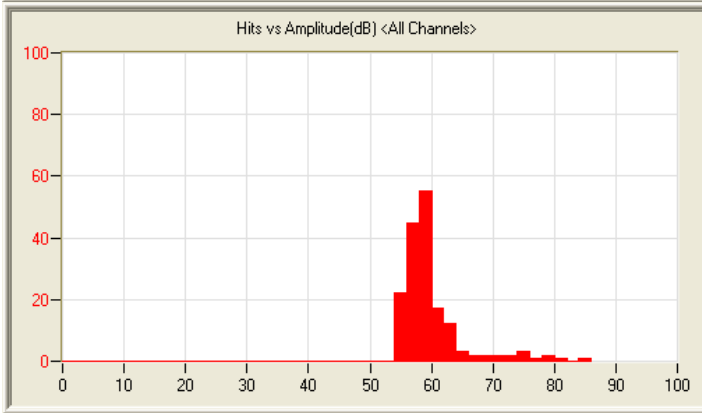
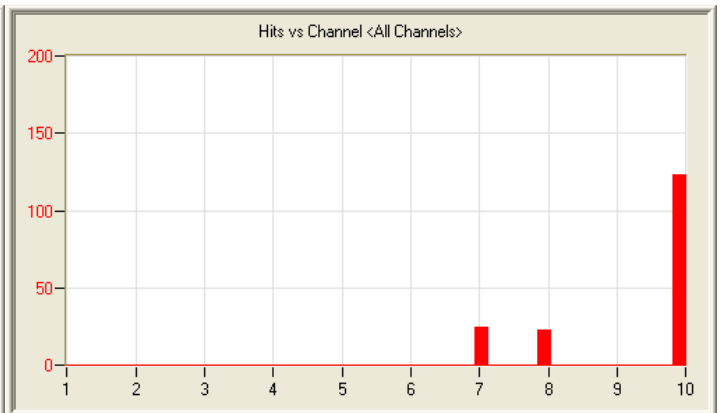
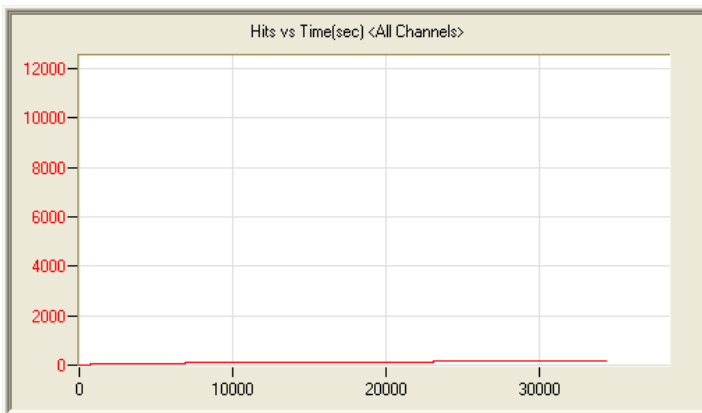
5/26/11 5:58am 6:59:03 5492 110526055809_0 2.1mb



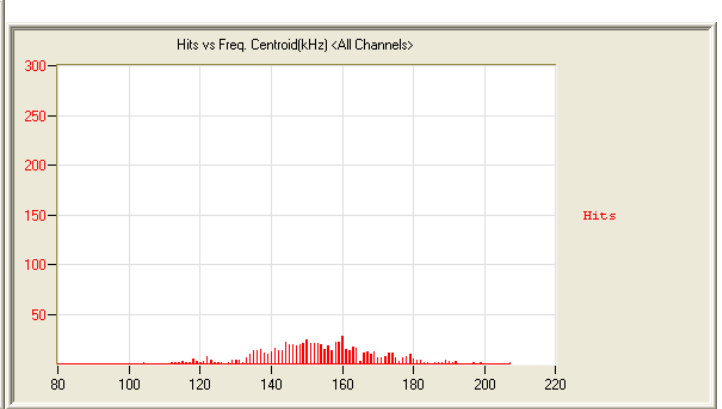
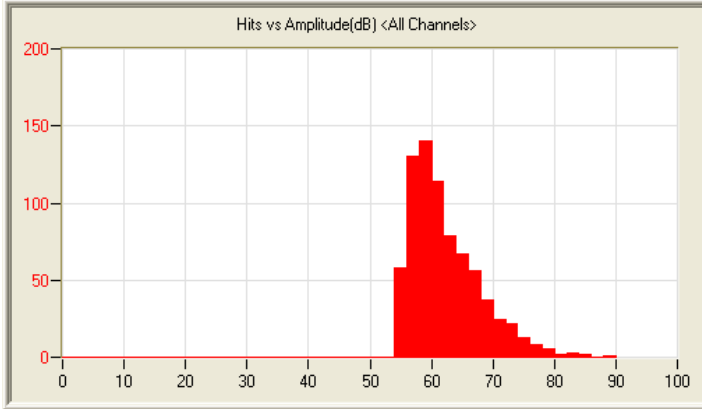
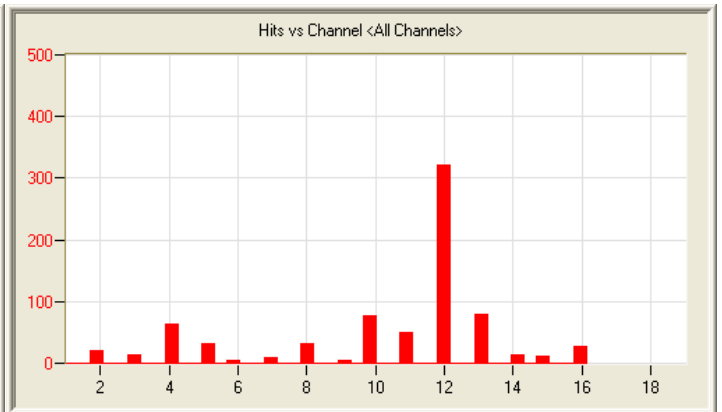
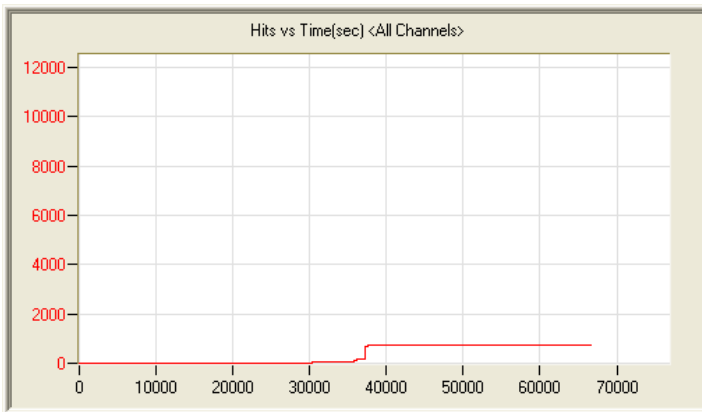
5/26/11 2:38pm 13:53:37 24 110526143853_0 1.3mb



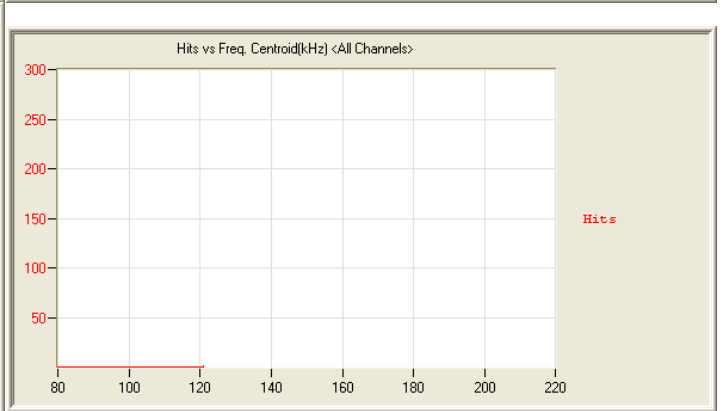
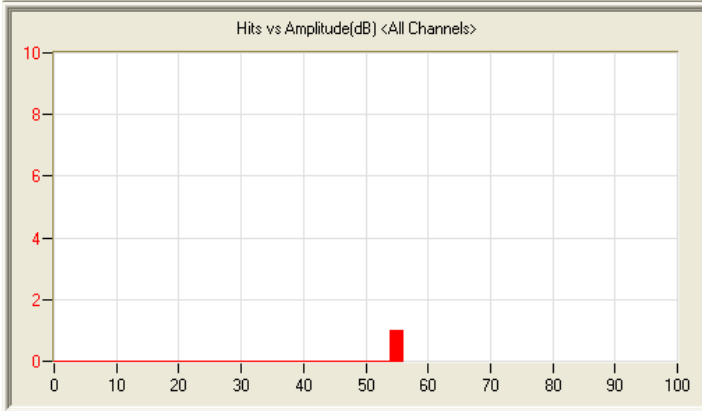
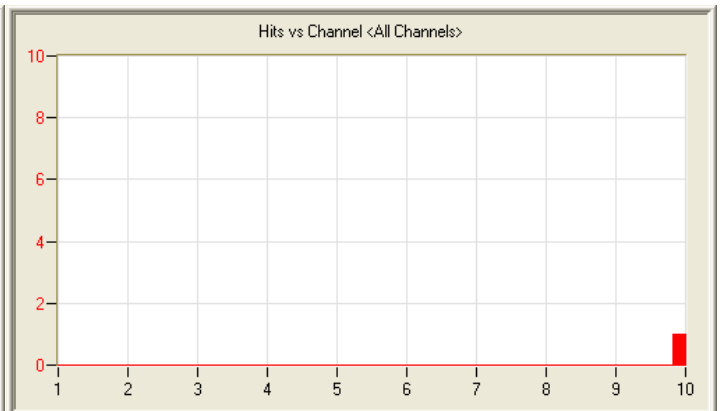
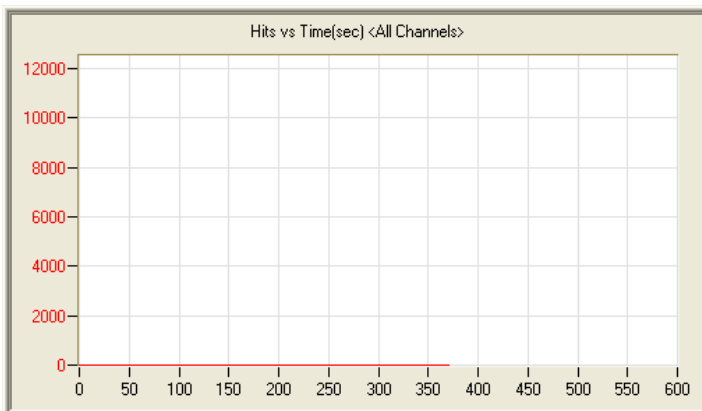
5/27/11 6:20am 4:08:18 422 110527062033_0 1.1mb



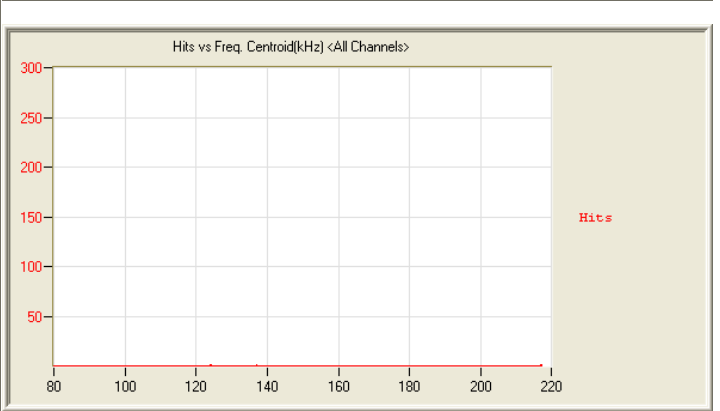
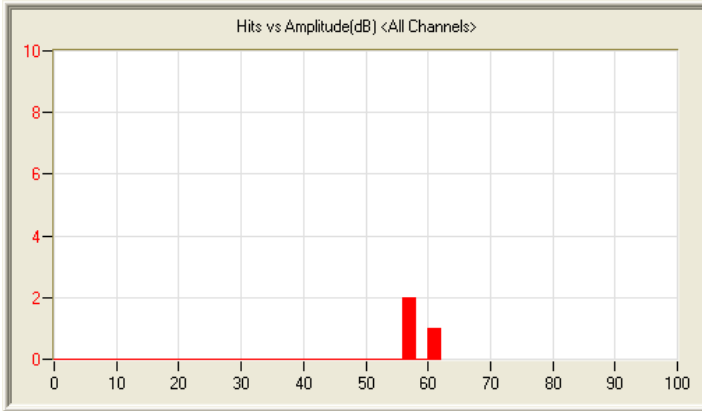
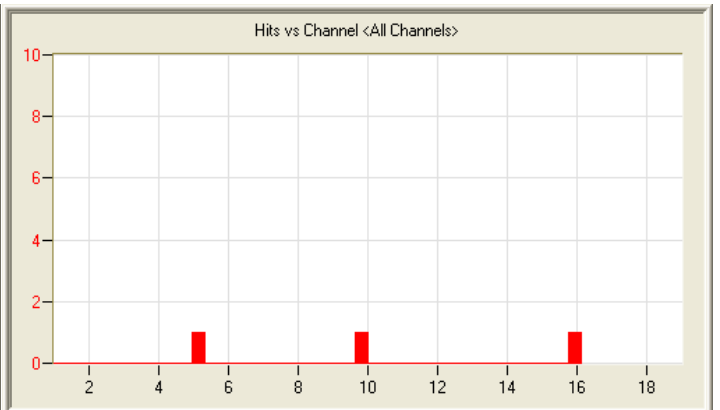
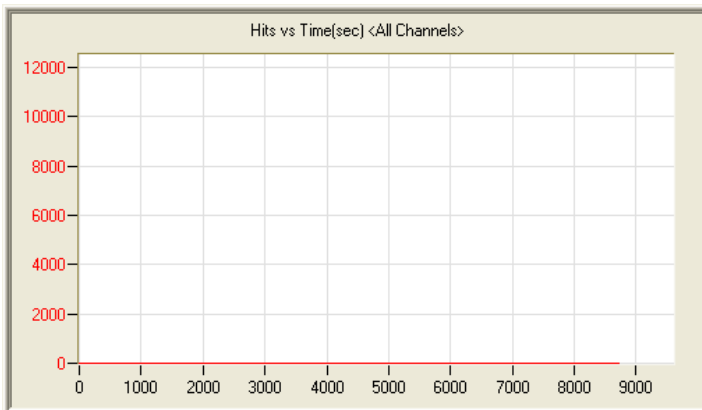
5/27/11 10:30am 10:13:28 170 110527103021_0 965kb



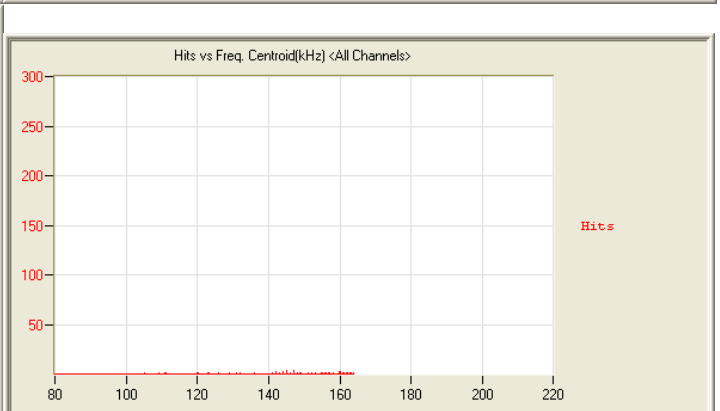
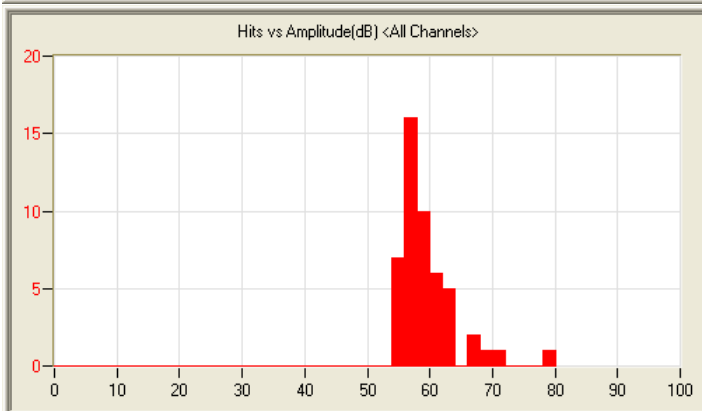
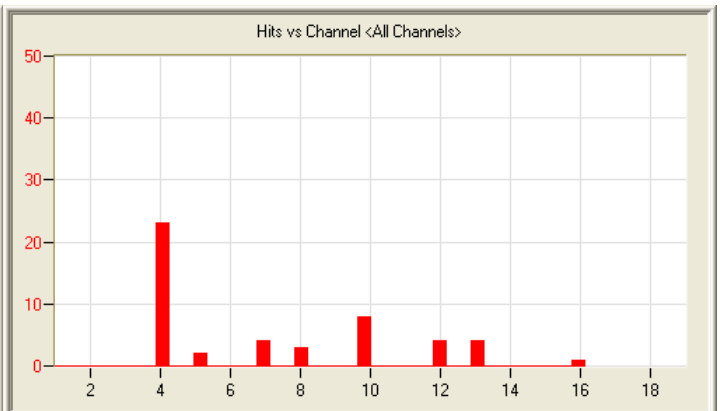
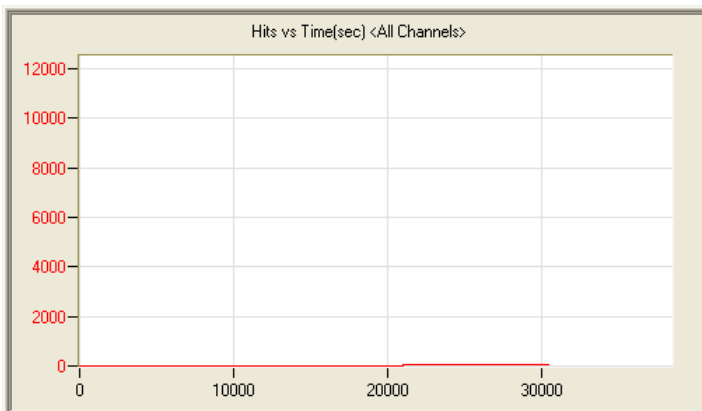
5/28/11 5:54am 18:51:10 761 110528055452_0 4.9mb



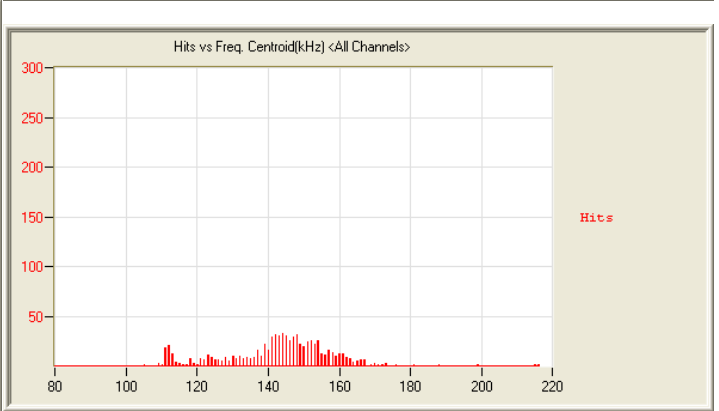
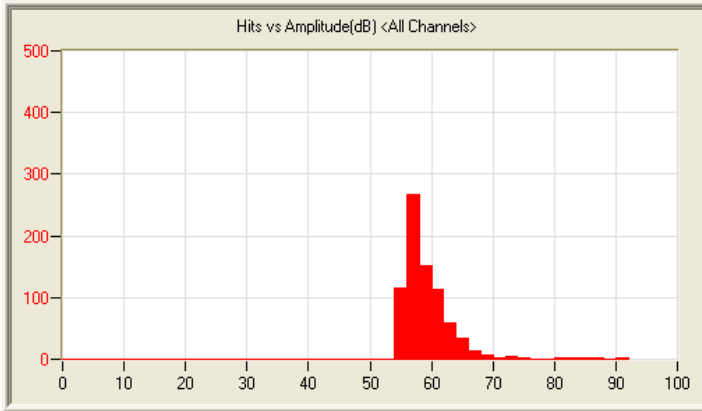
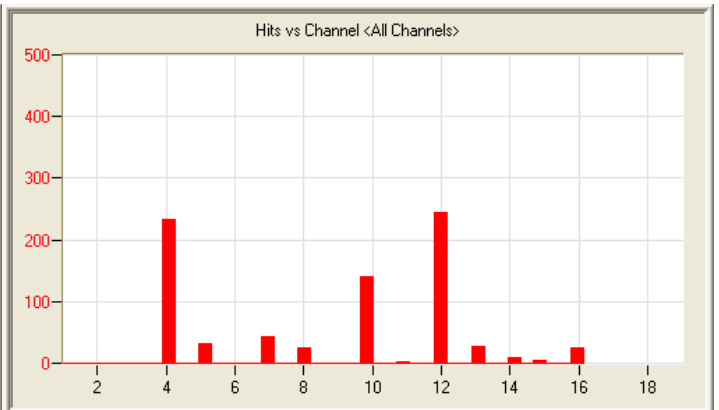
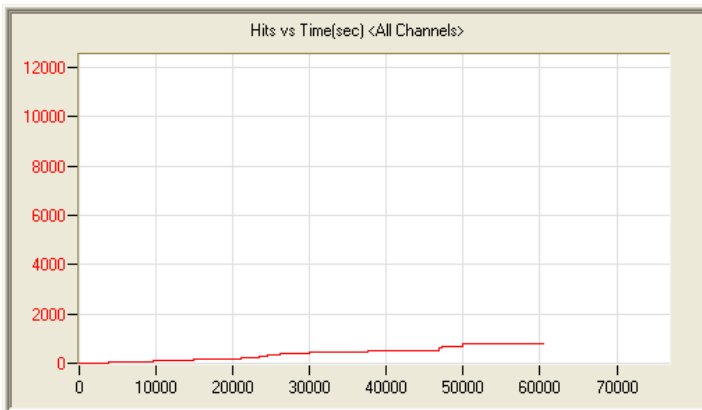
5/29/11 7:16am 0:33:53 1 110529071644_0 206kb



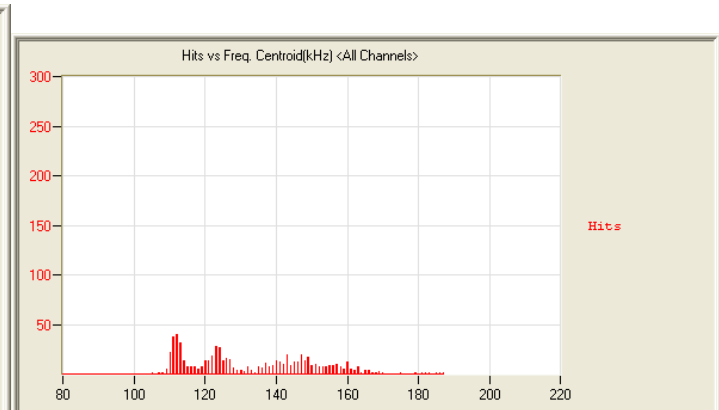
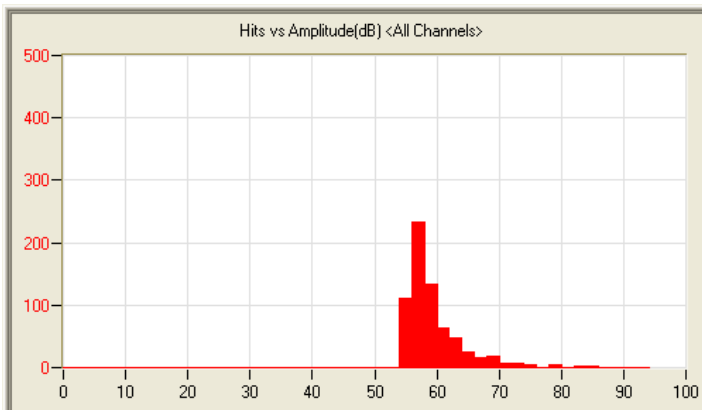
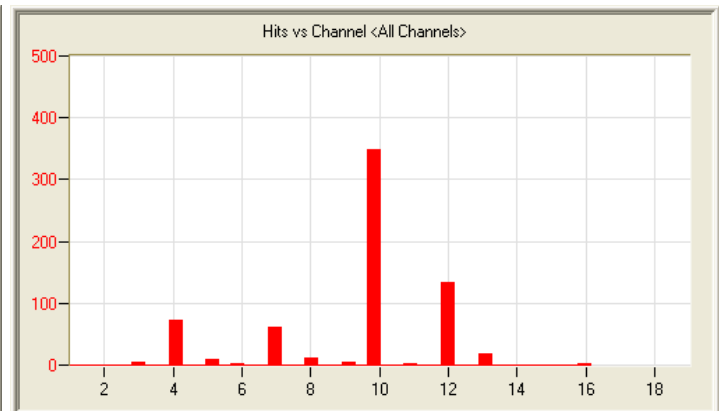
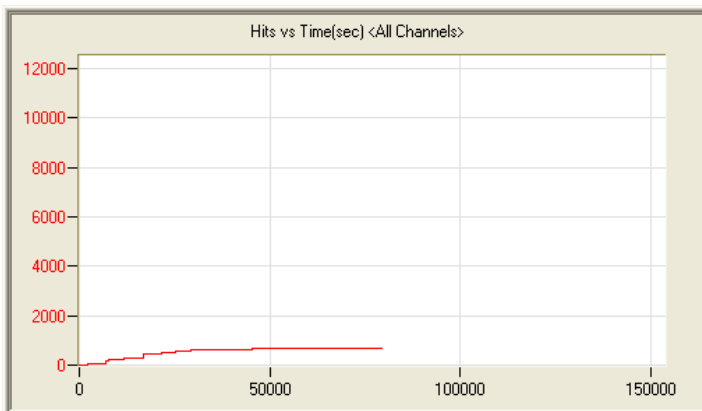
5/29/11 11:07am 4:01:54 3 110529110725_0 1.1mb



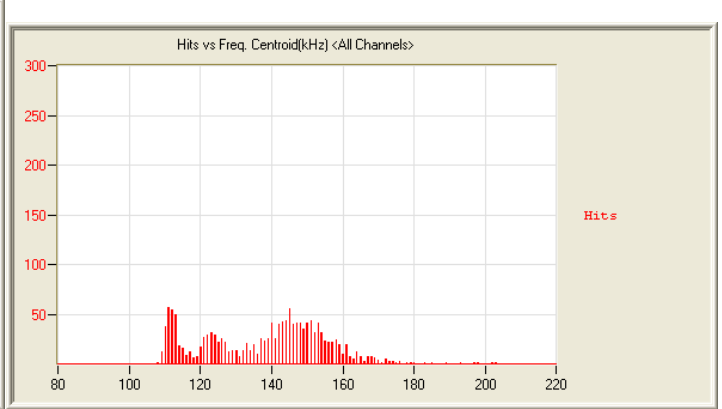
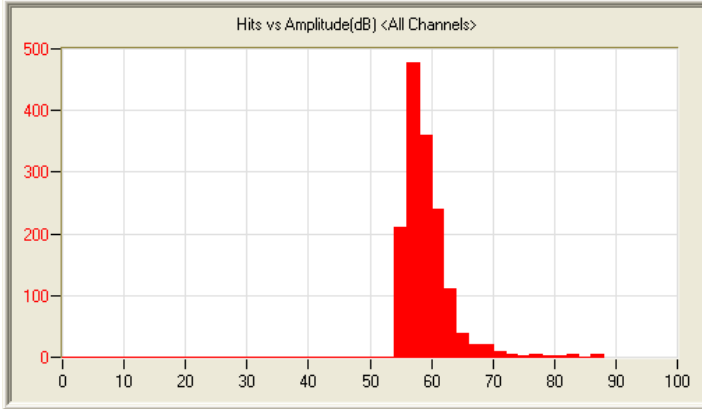
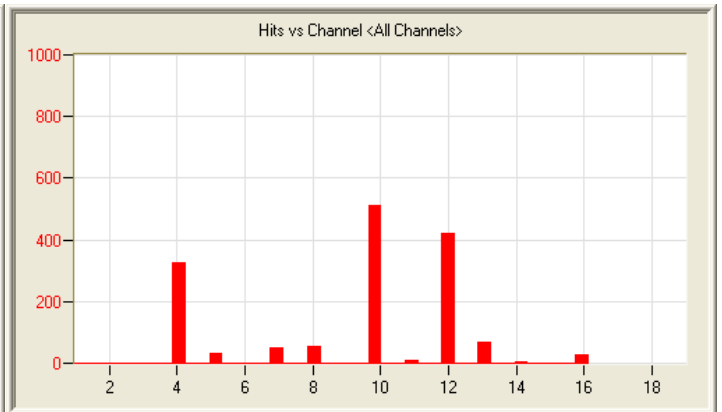
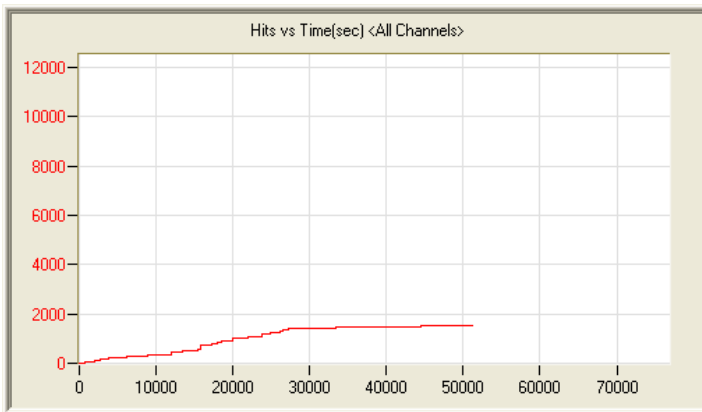
5/30/11 10:50am 8:52:20 49 110530105031_0 2.3mb



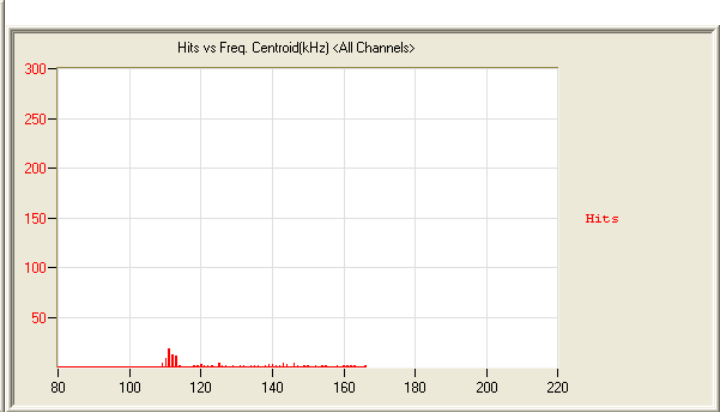
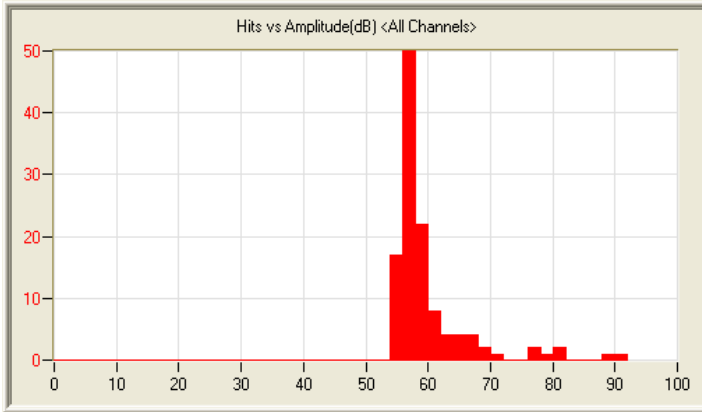
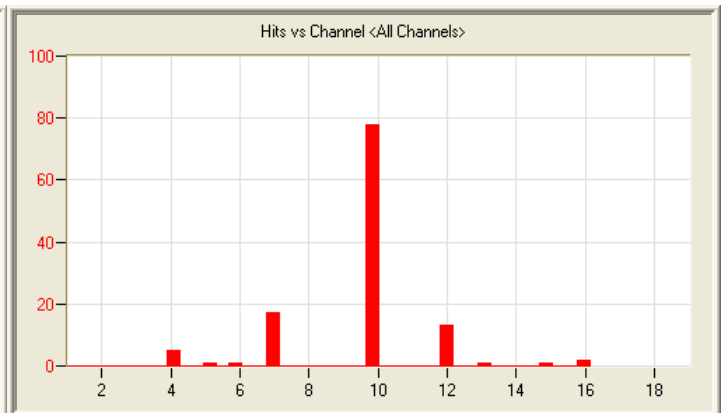
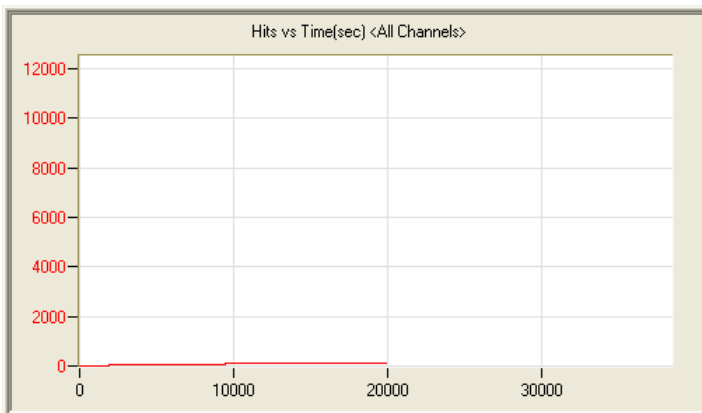
5/31/11 8:12am 16:51:49 786 110531081236_0 4.4mb



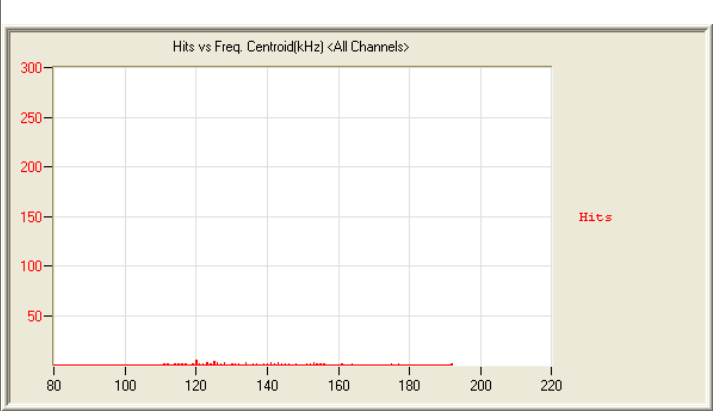
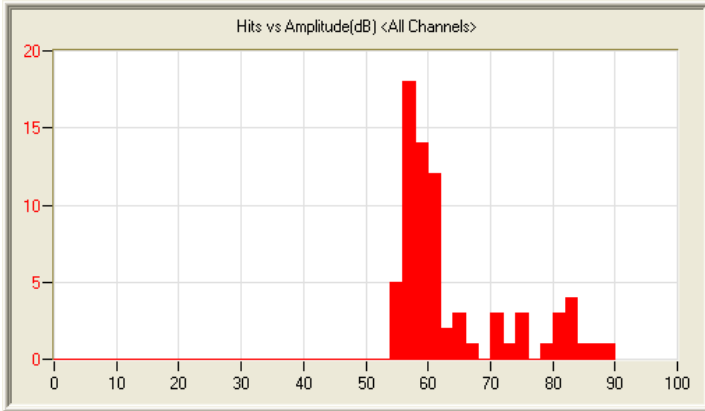
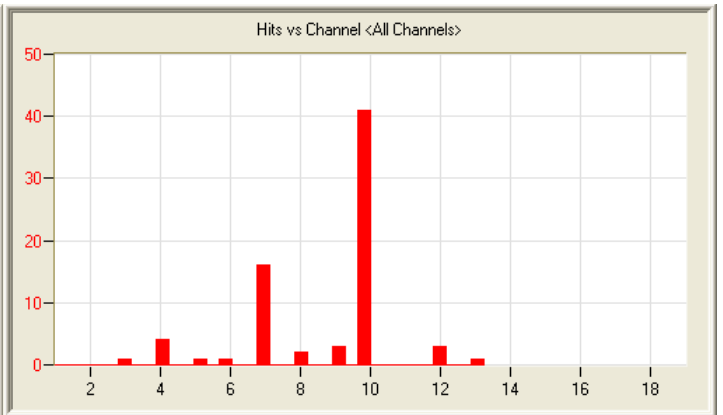
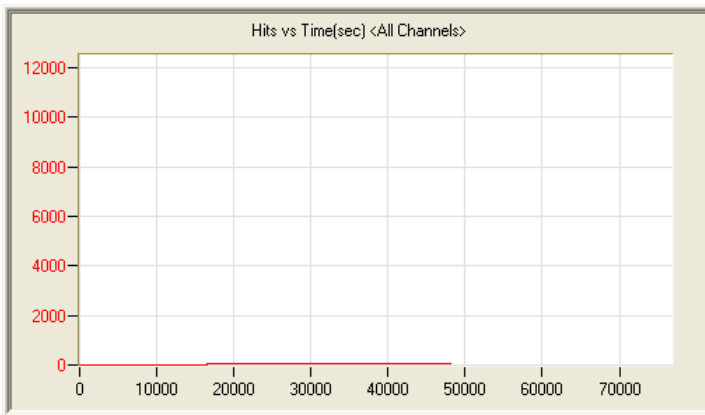
6/1/11 5:58am 22:55:44 678 110601055812_0 6.0mb



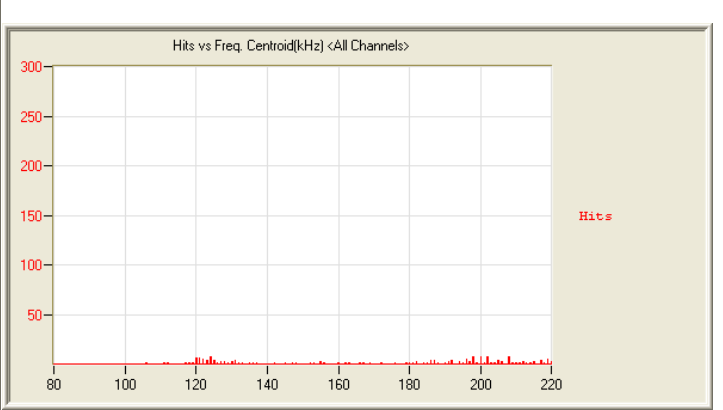
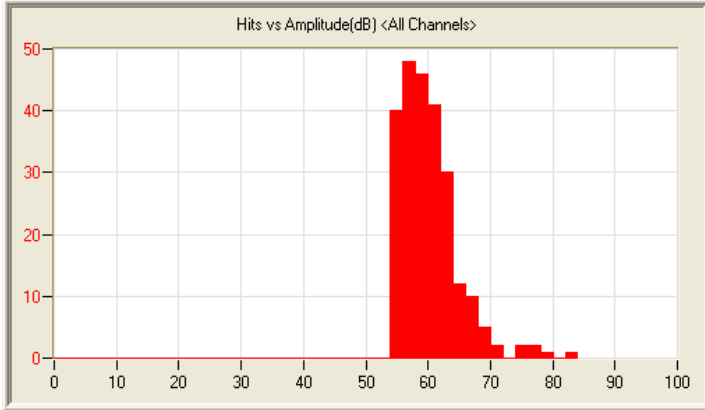
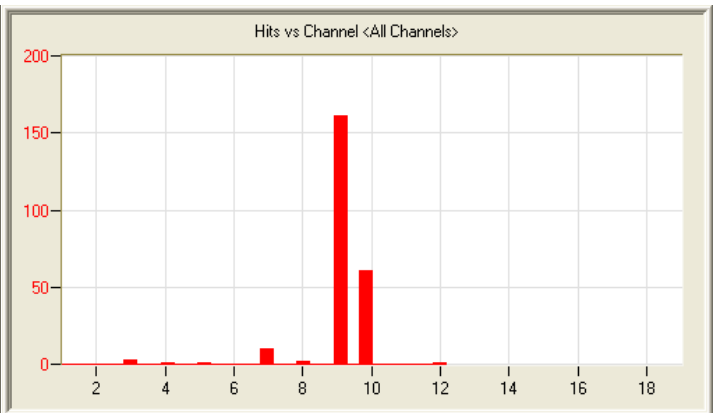
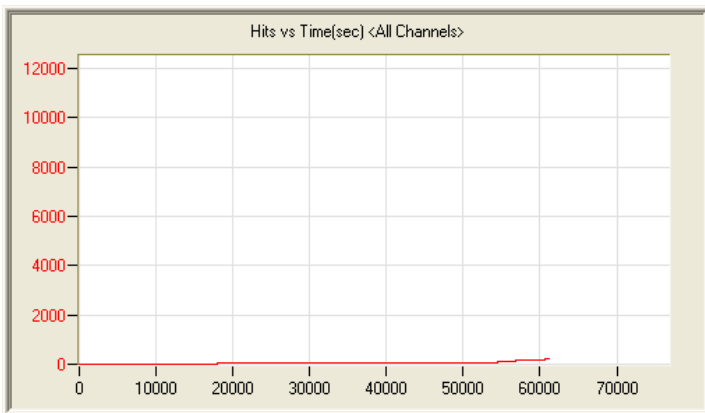
6/2/11 7:32am 14:21:25 1507 110602073239_0 3.8mb



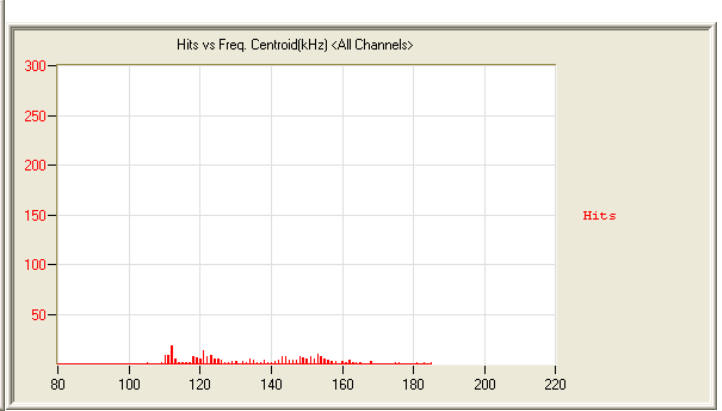
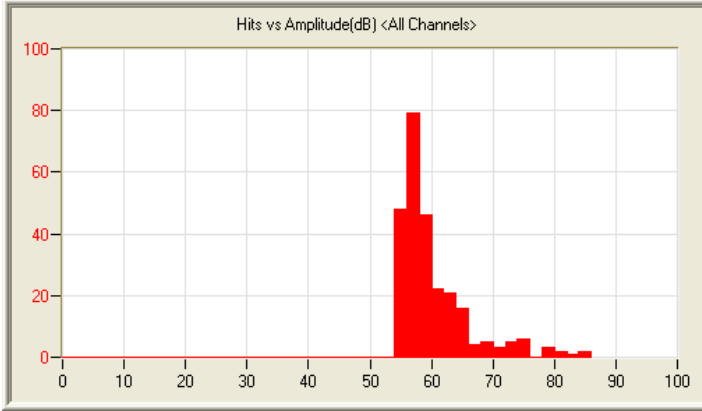
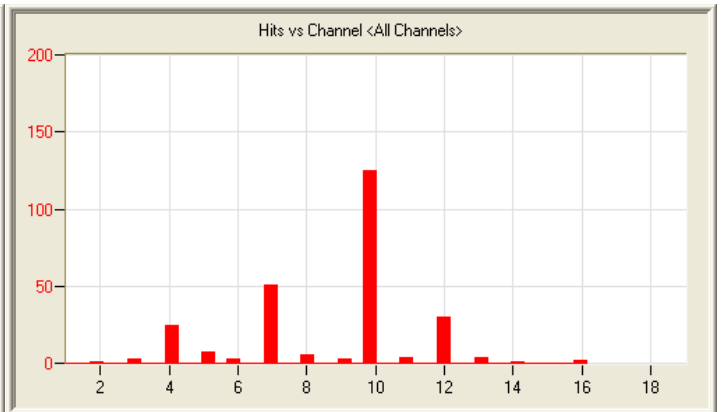
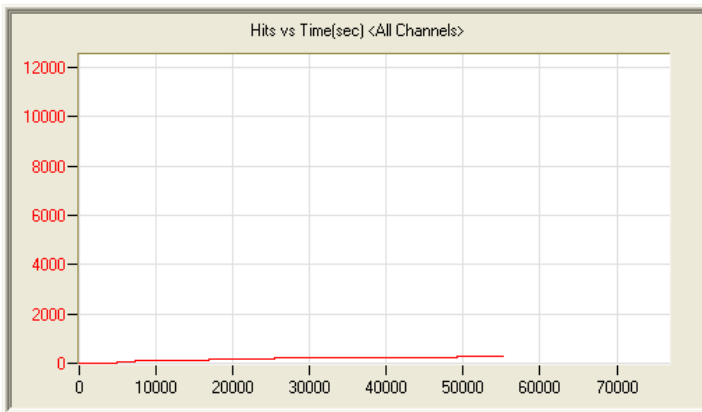
6/3/11 10:17am 5:32:44 119 110603101659_0 1.5mb



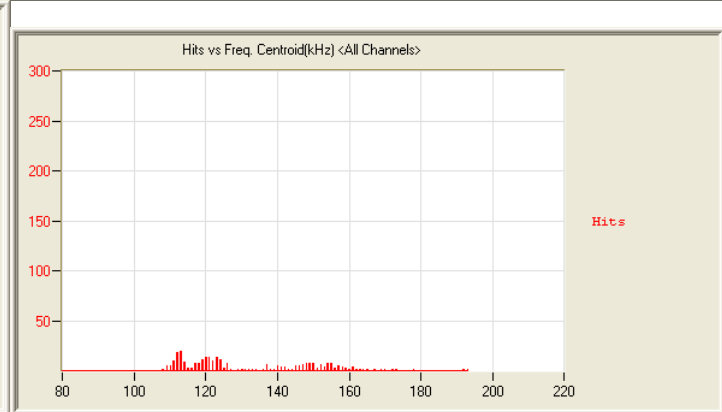
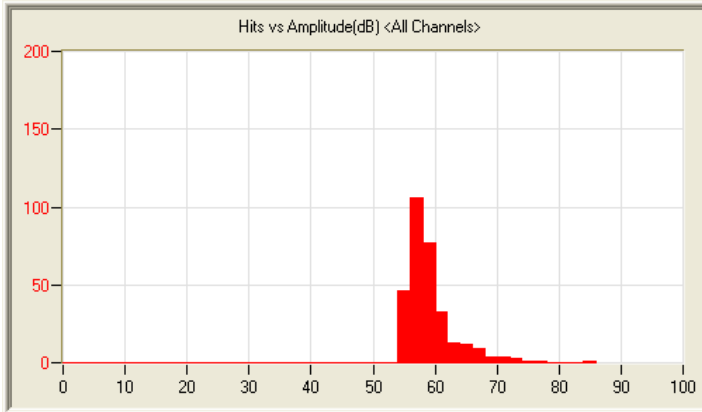
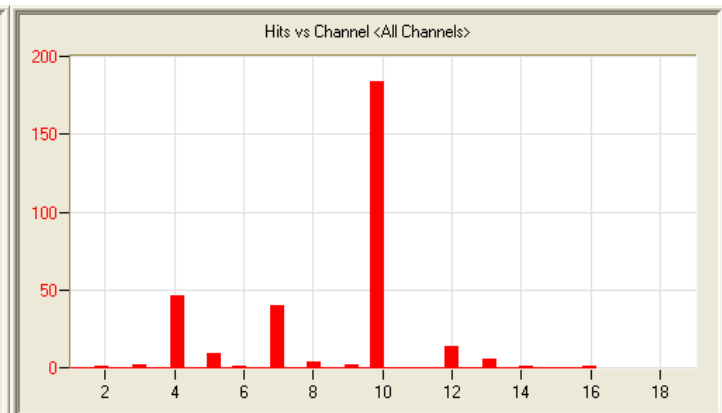
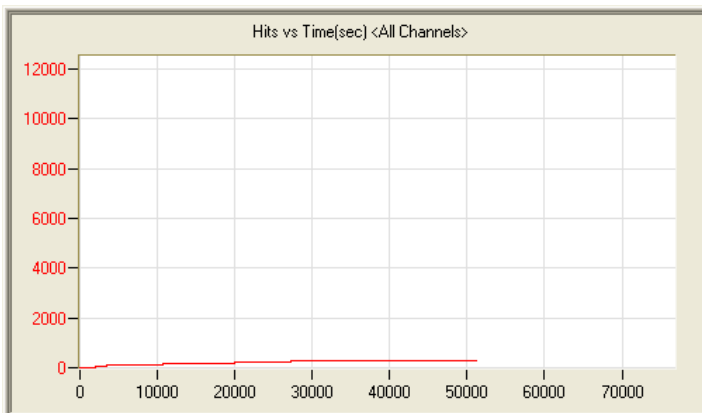
6/4/11 7:37am 13:33:41 73 110604073726_0 3.5mb



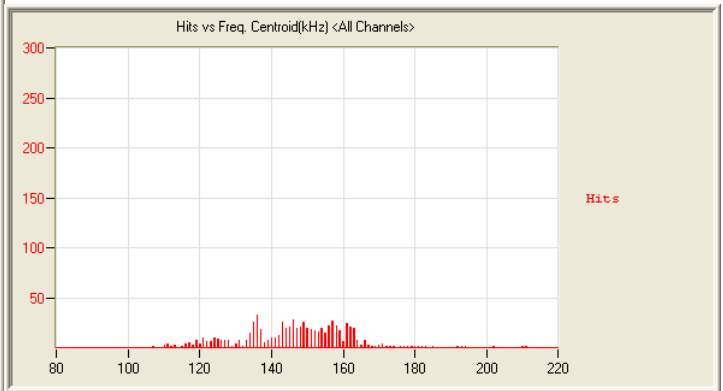
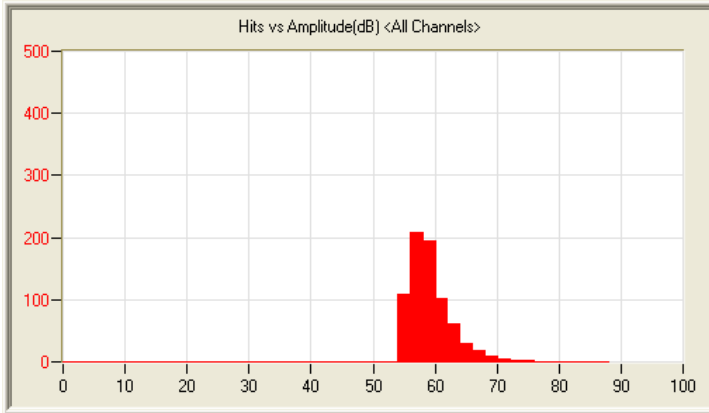
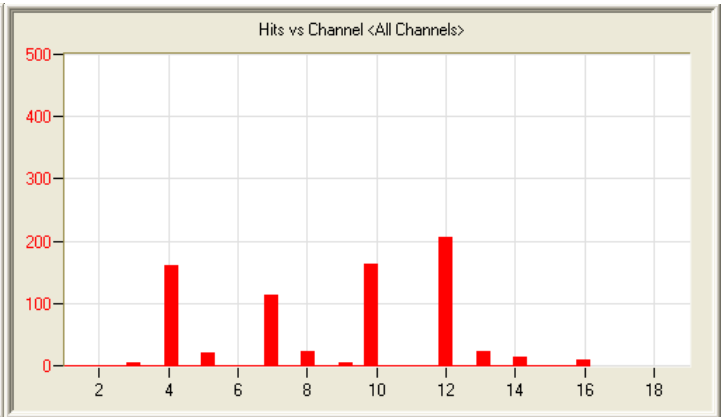
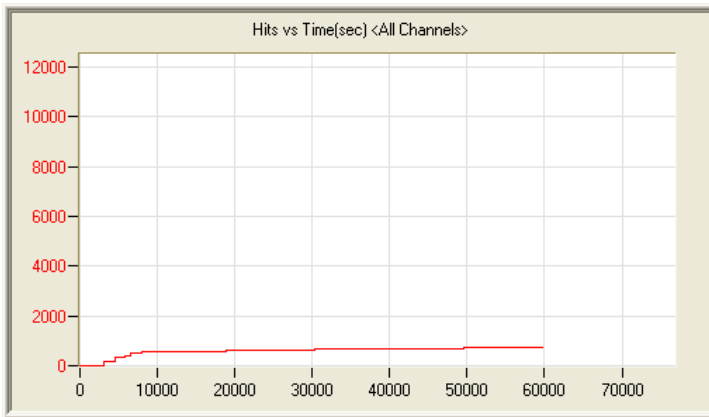
6/5/11 6:11am 17:07:10 240 110605061448_0 4.4mb



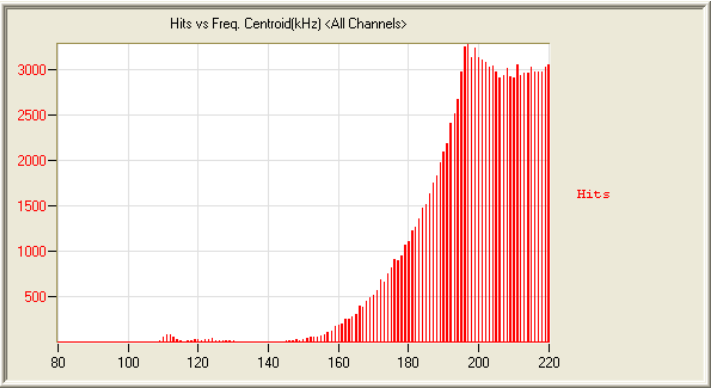
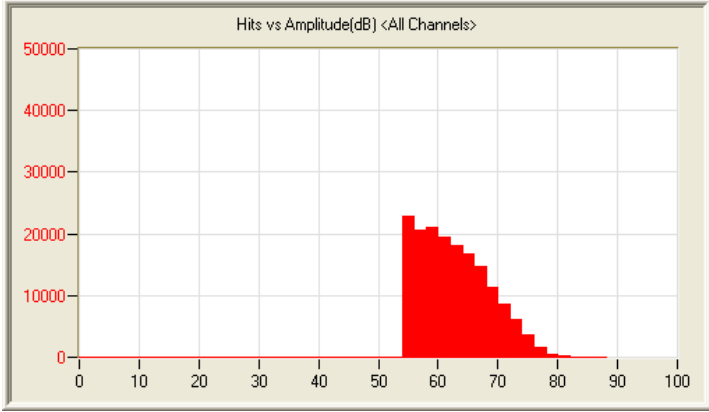
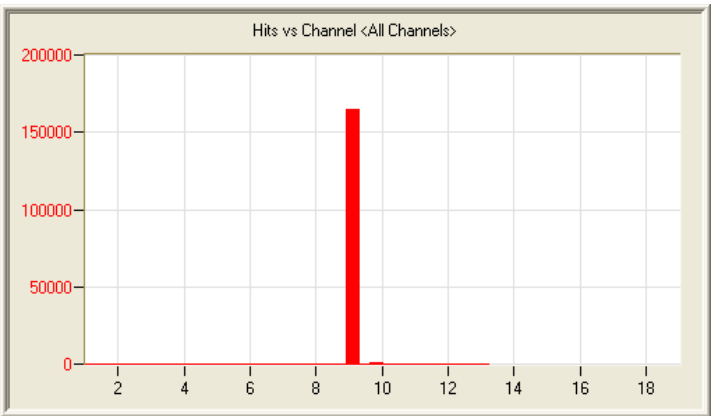
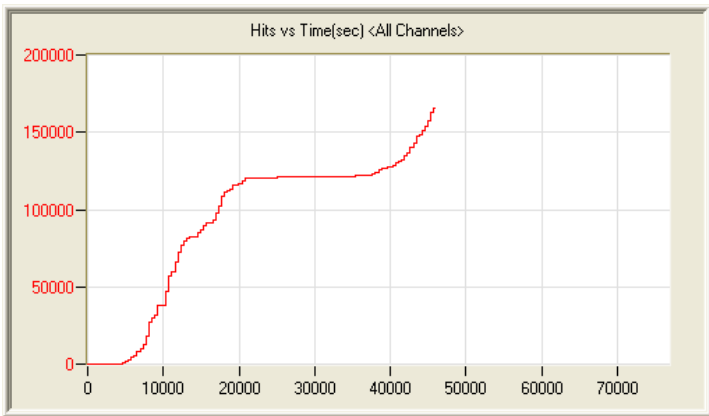
6/6/11 6:34am 16:06:56 263 110606063440_0 4.2mb



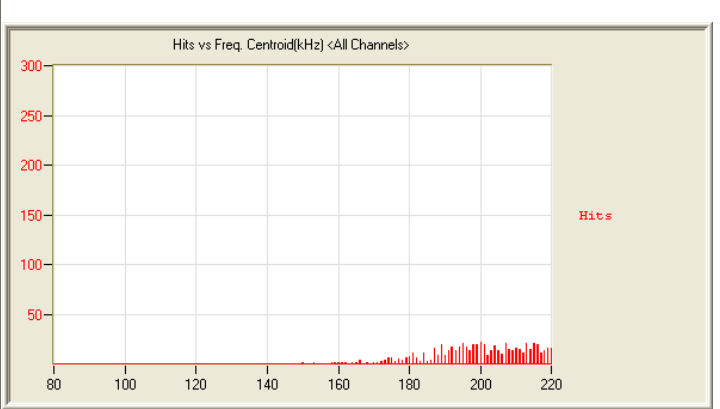
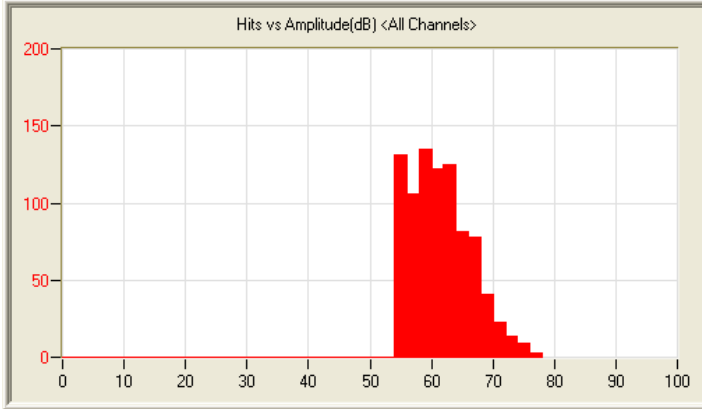
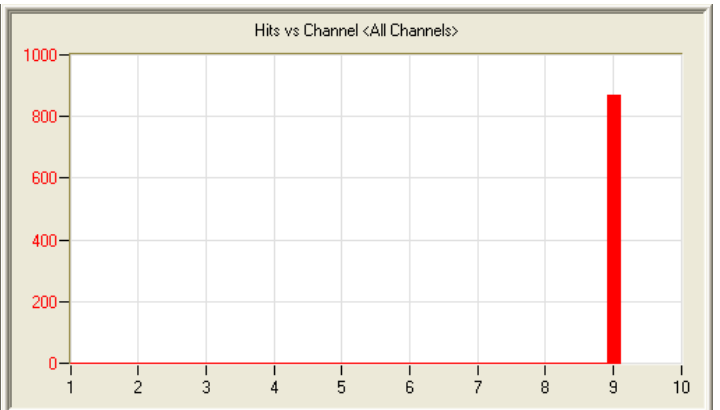
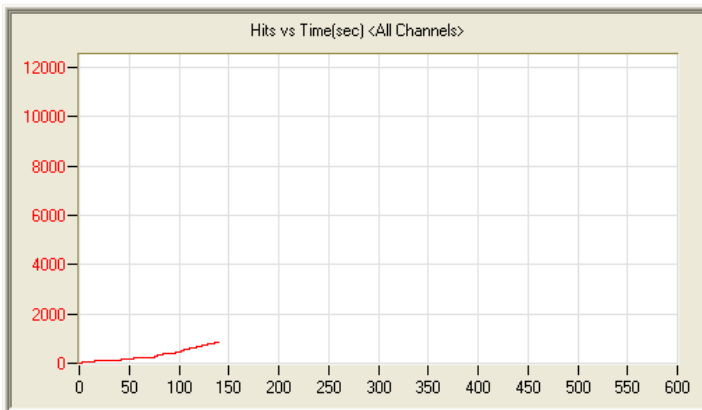
6/7/11 7:20am 14:43:34 310 110607072033_0 3.8mb



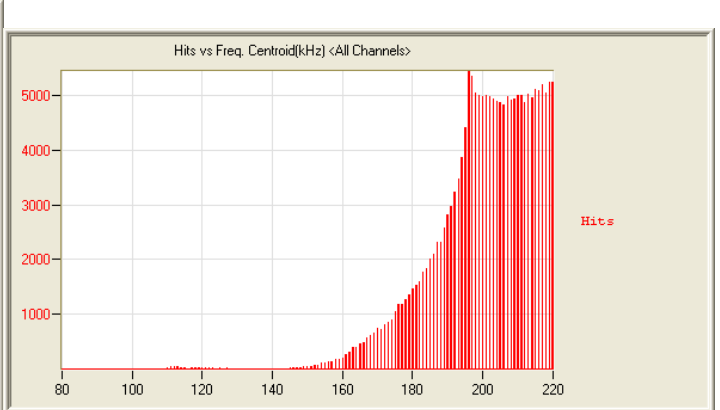
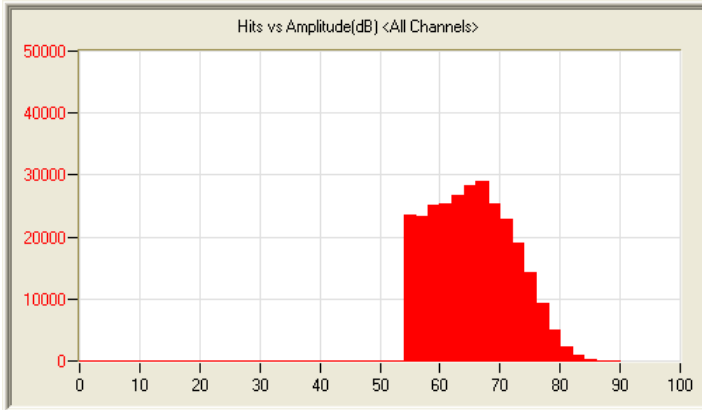
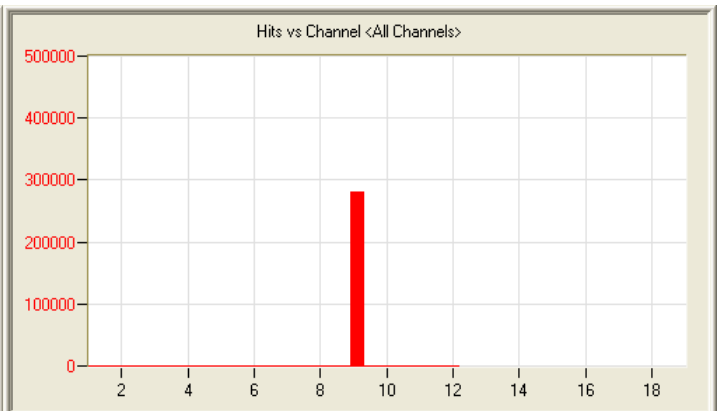
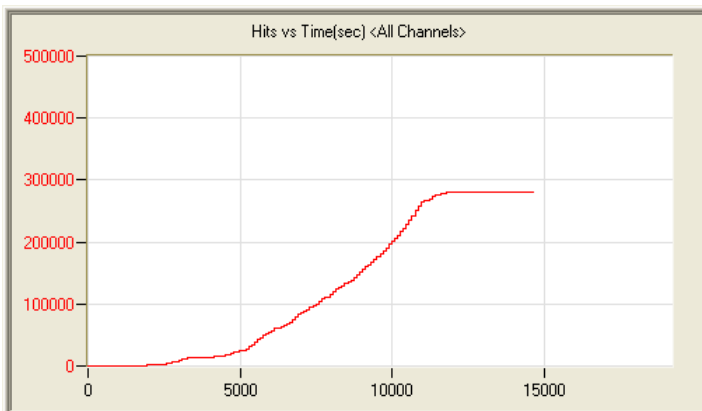
6/8/11 6:29am 16:50:01 742 110608062903_0 4.4mb



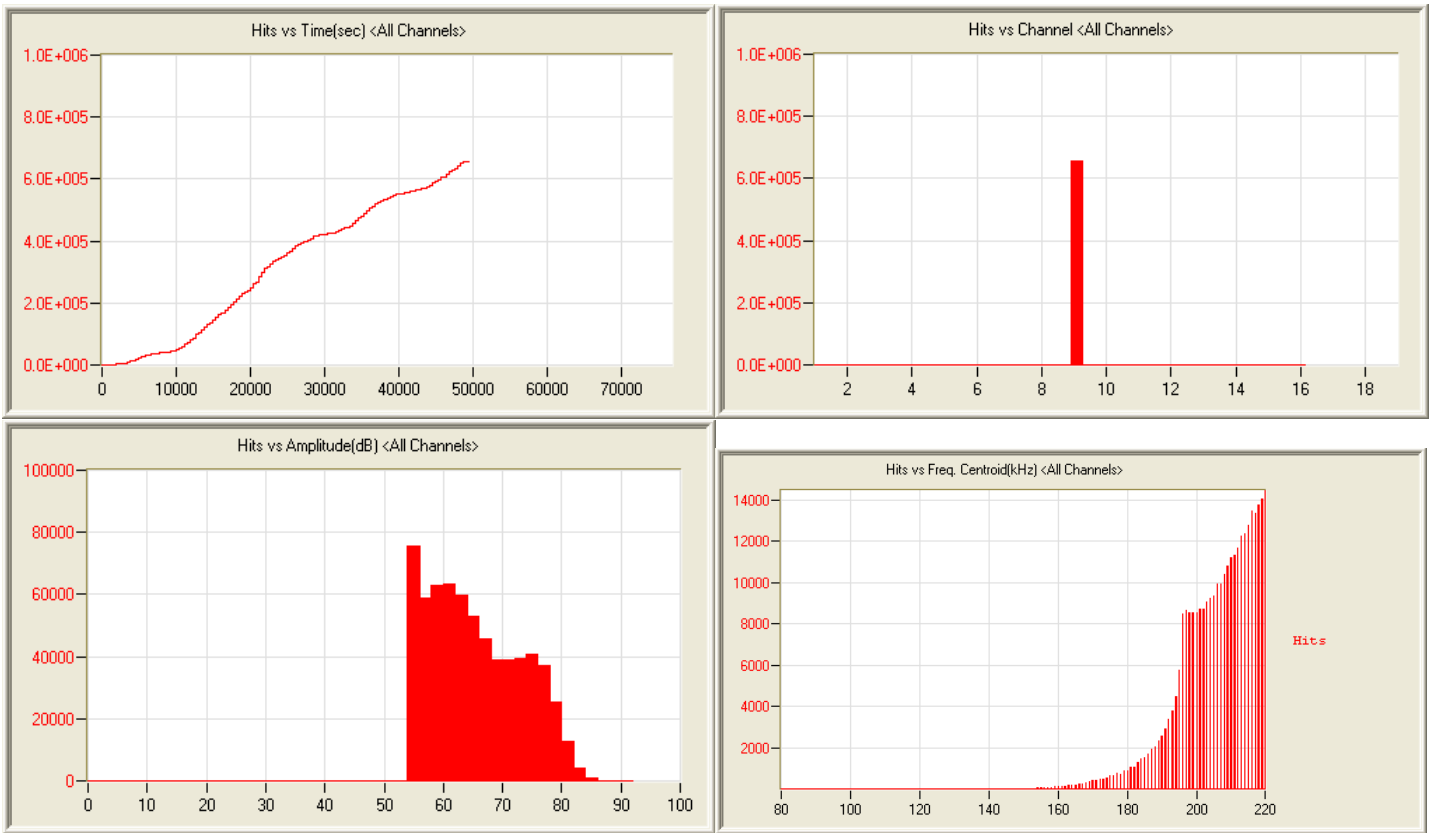
6/9/11 8:54am 12:44:43 165562 110609085434_0 9.9mb



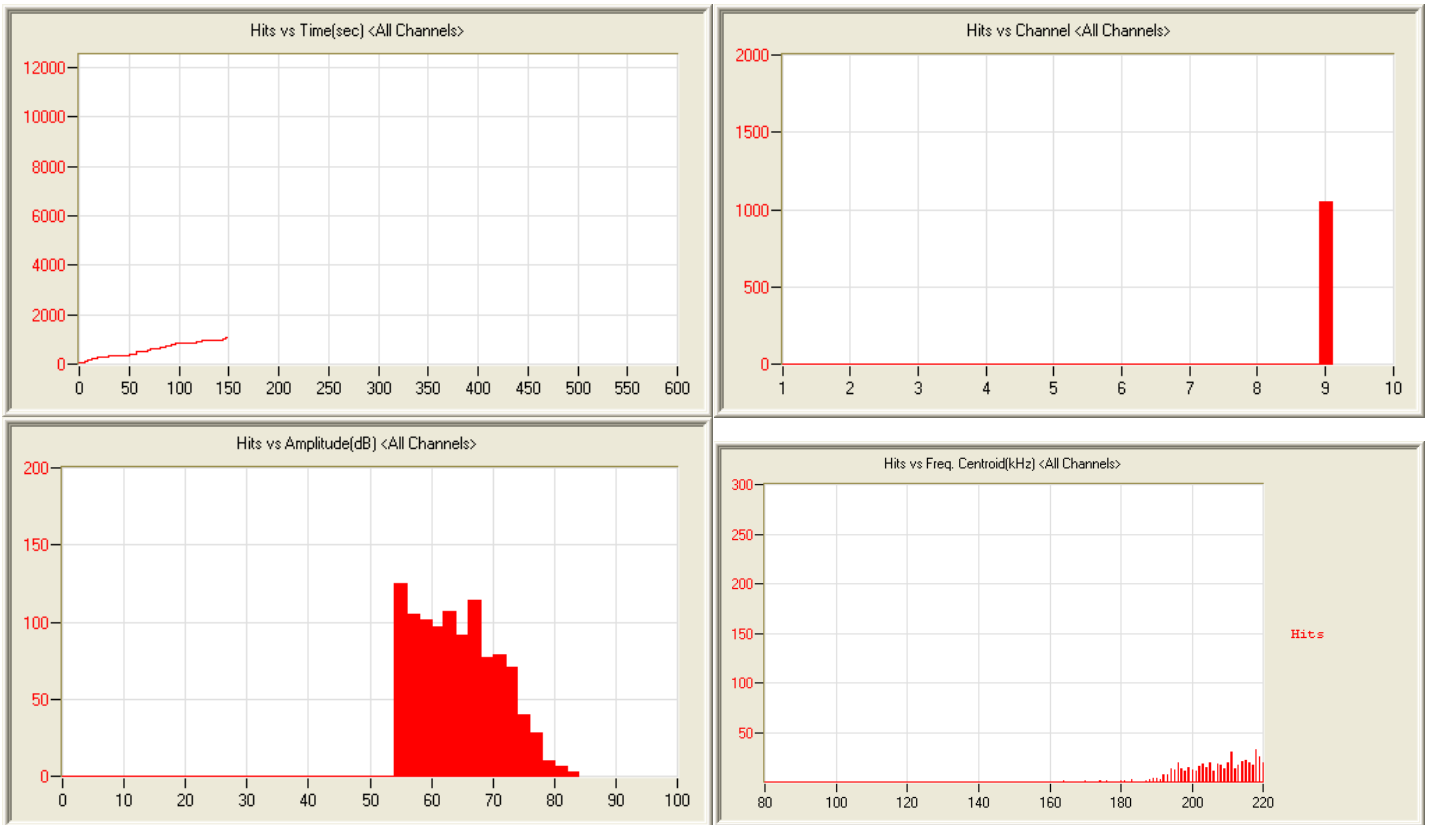
6/9/11 9:45pm 0:02:20 868 110609214549_0 105kb



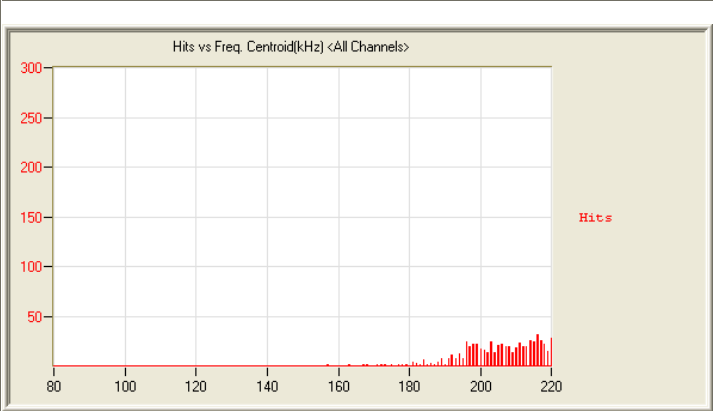
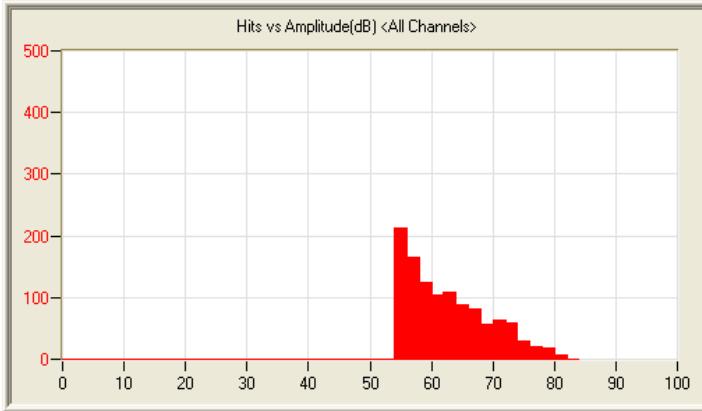
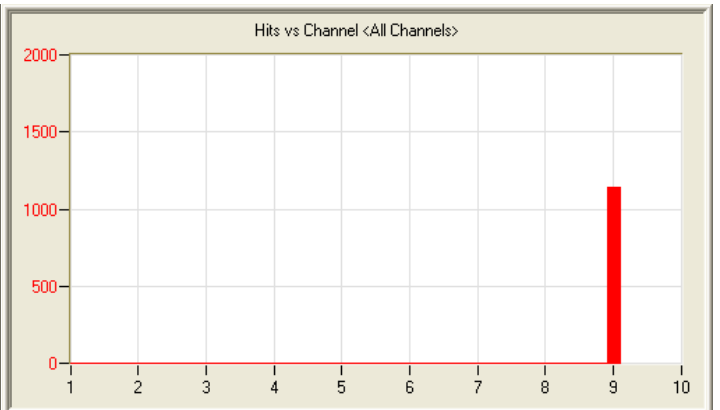
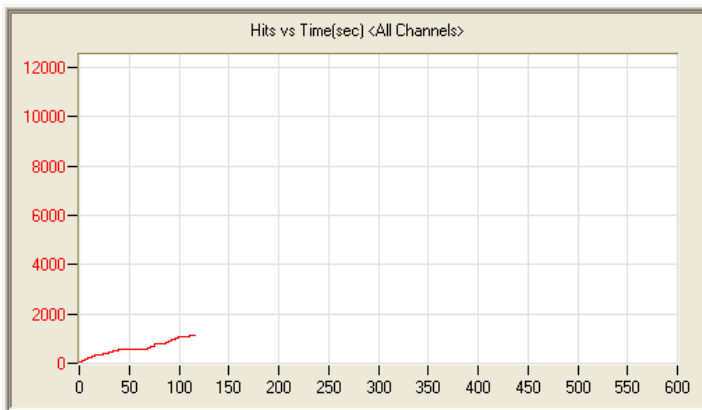
6/10/11 10:54am 4:04:50 281133 110610105450_0 12.2mb



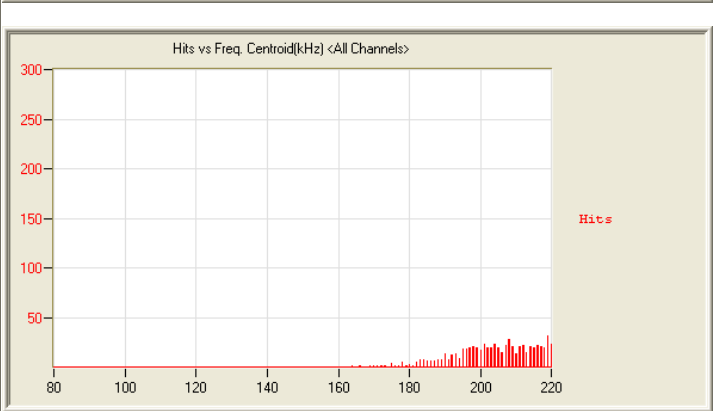
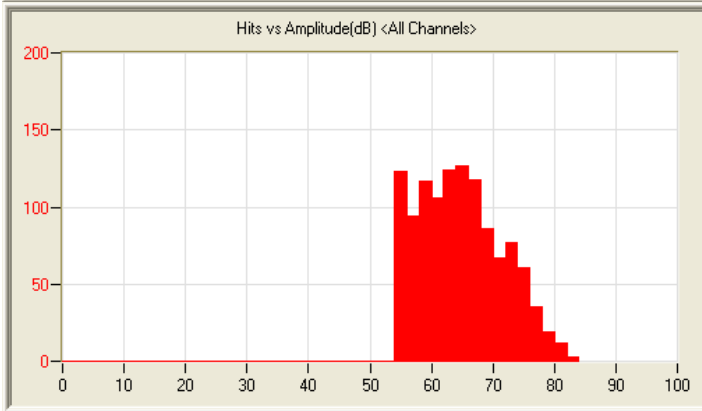
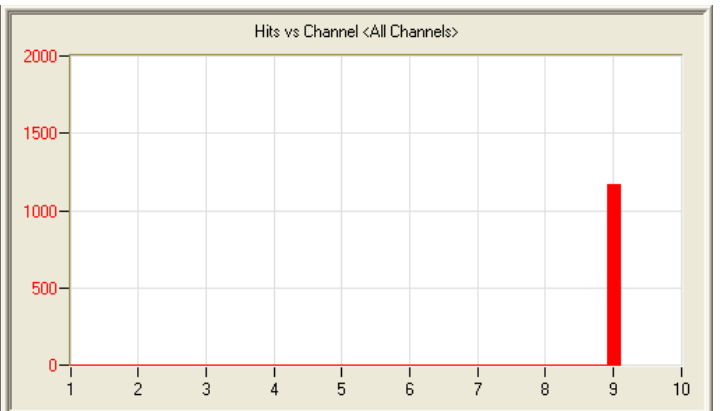
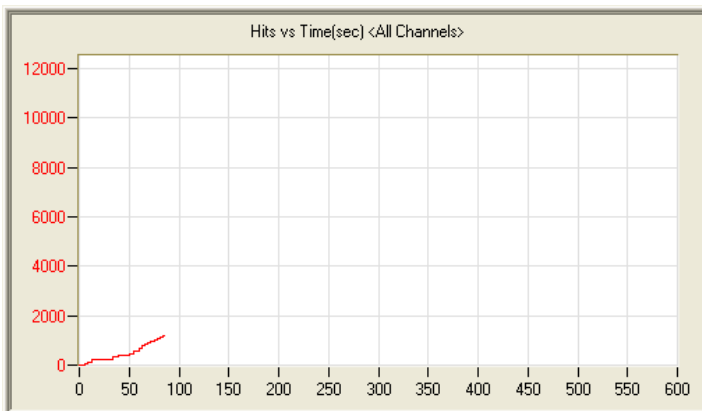
6/11/11 7:32am 13:41:27 656703 110611073221_0 29.5mb



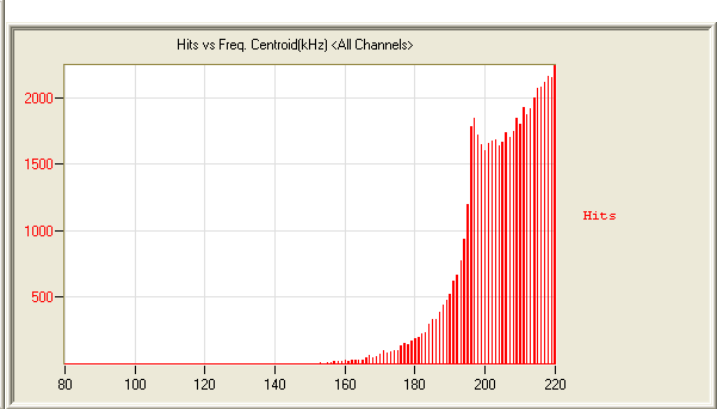
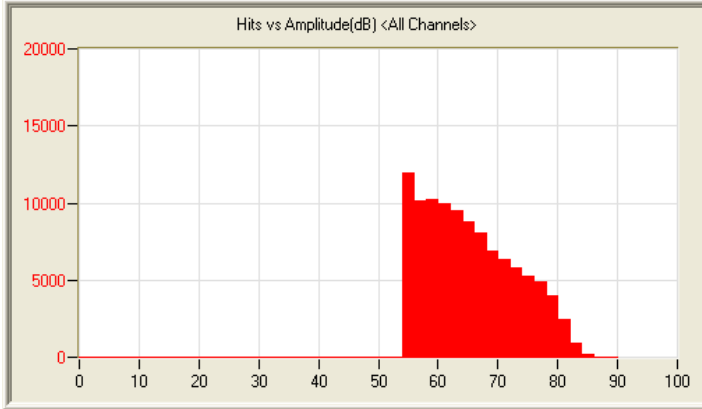
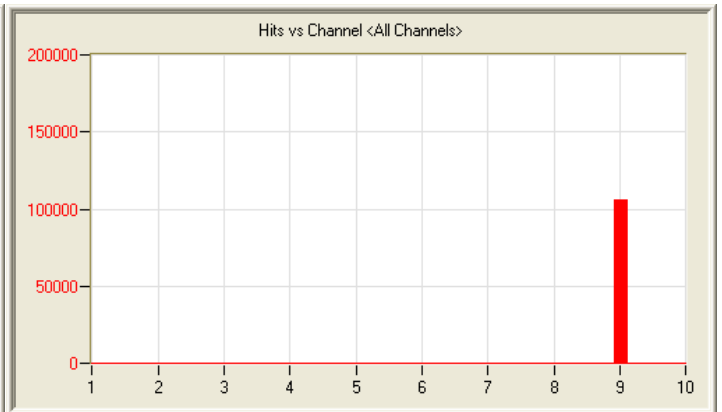
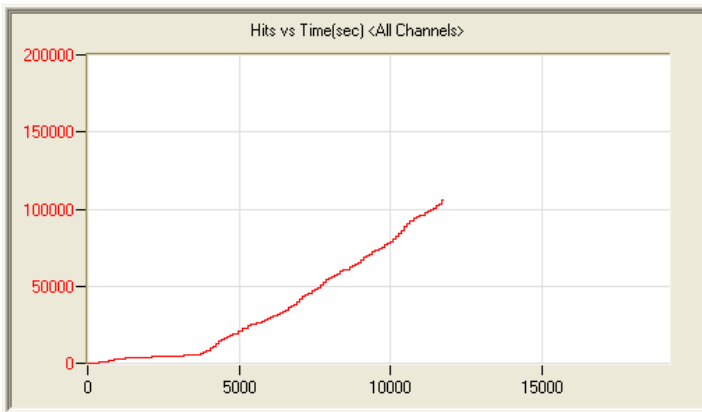
6/11/11 9:21pm 0:02:27 1054 110611212100_0 113kb



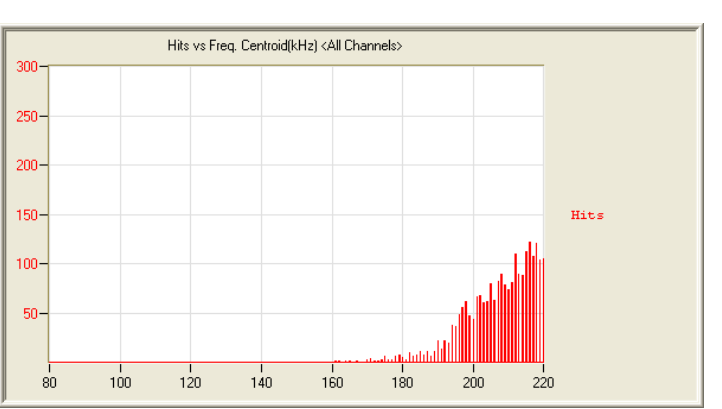
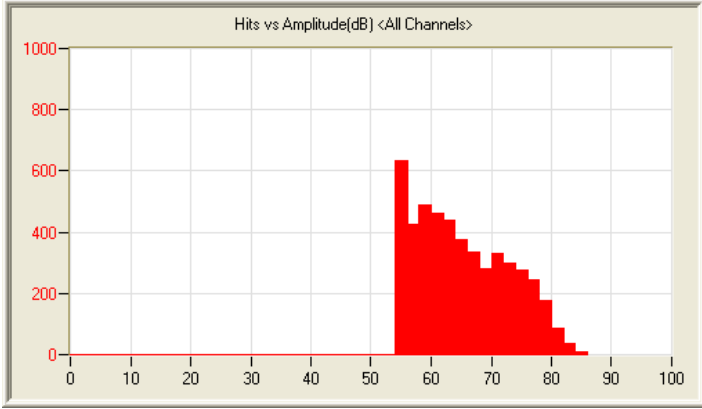
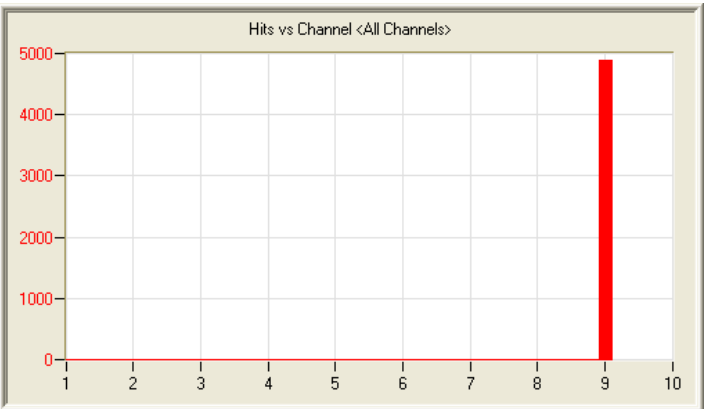
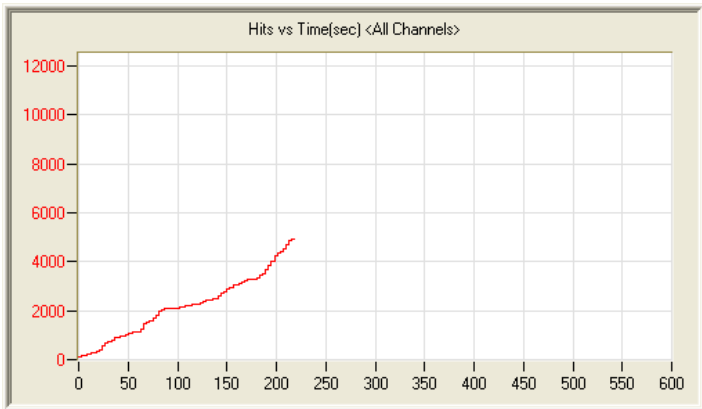
6/11/11 9:30pm 0:01:54 1142 110611213017_0 114kb



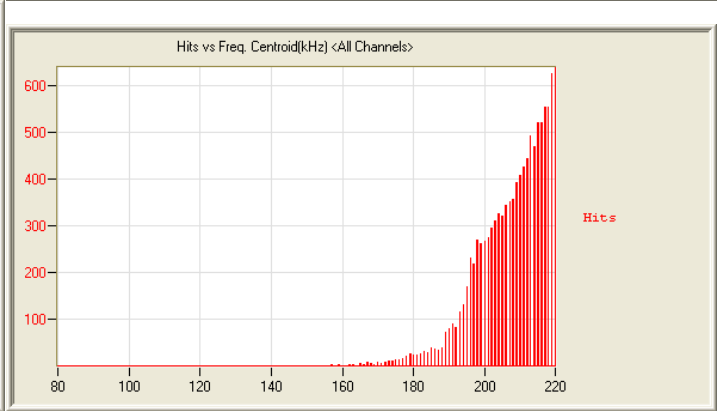
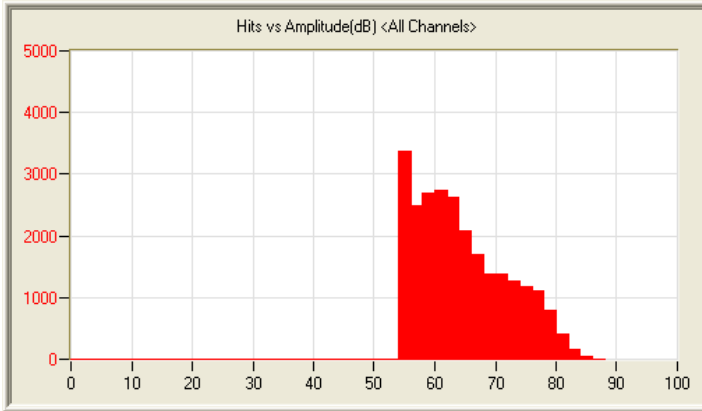
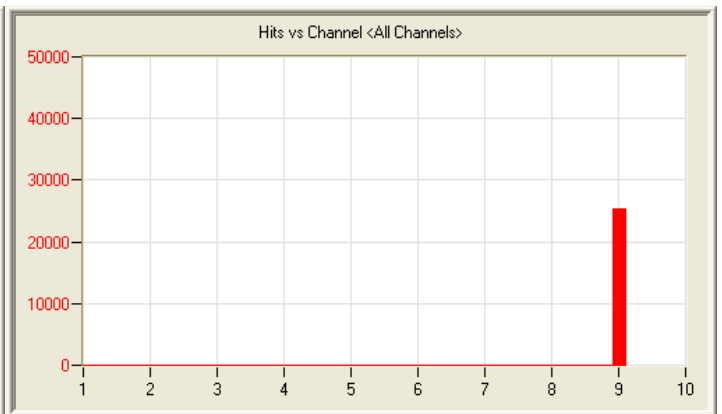
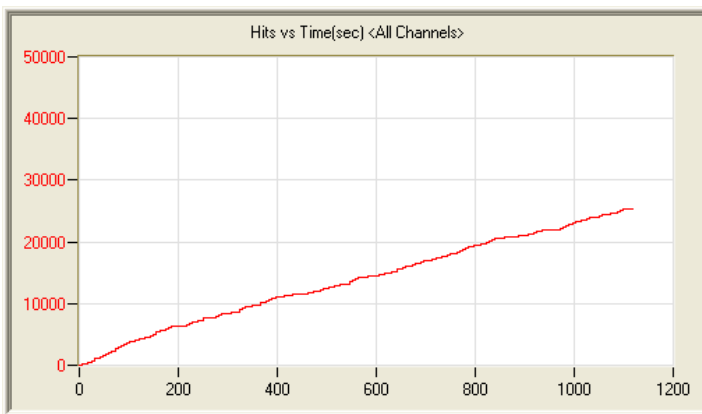
6/11/11 9:39pm 0:01:25 1169 110611213940_0 113kb



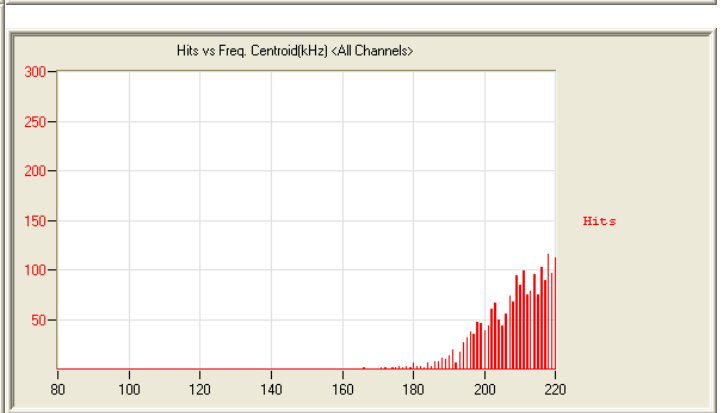
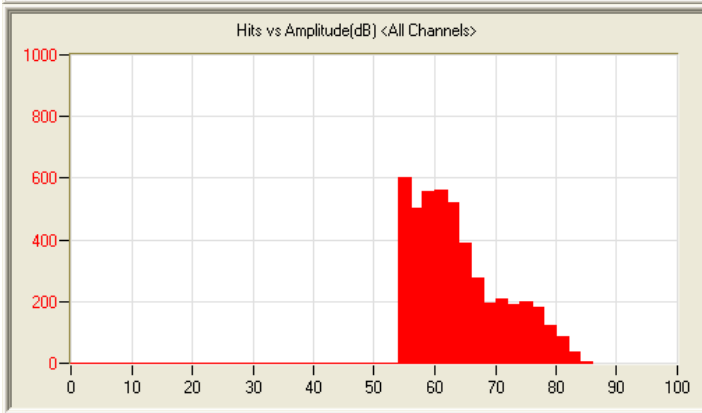
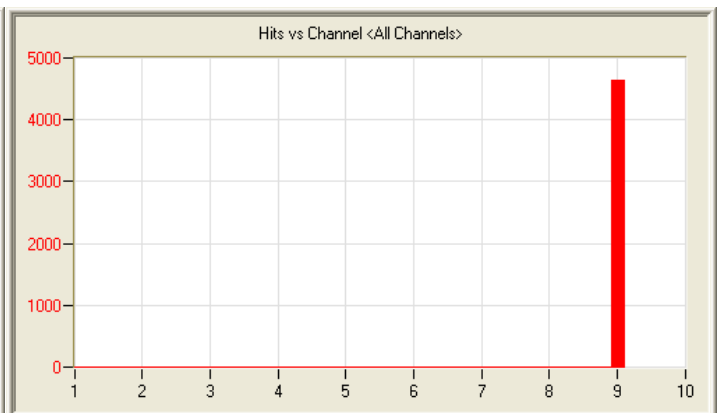
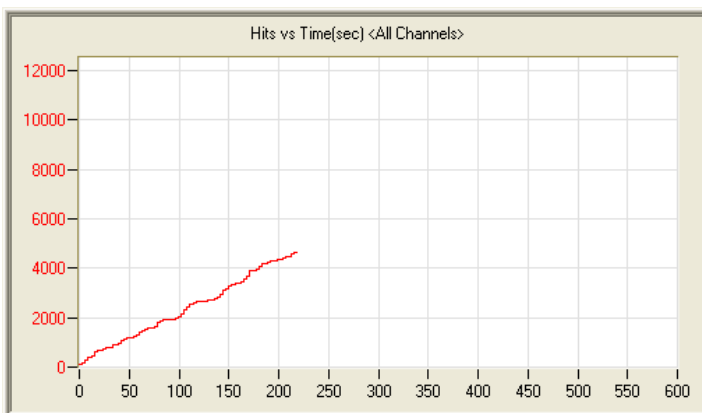
6/12/11 6:43am 3:16:44 105549 110612064312_0 5.2mb



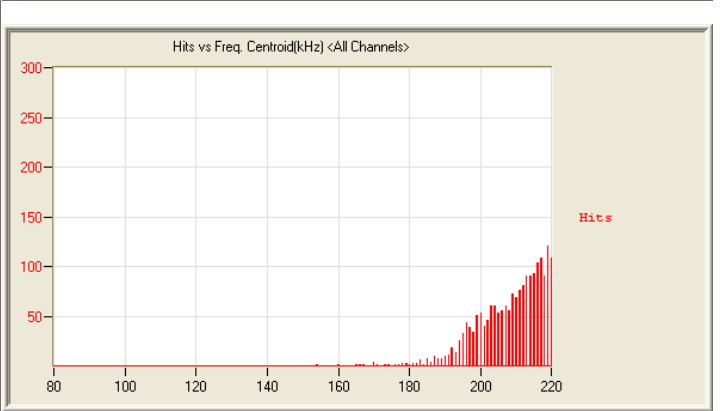
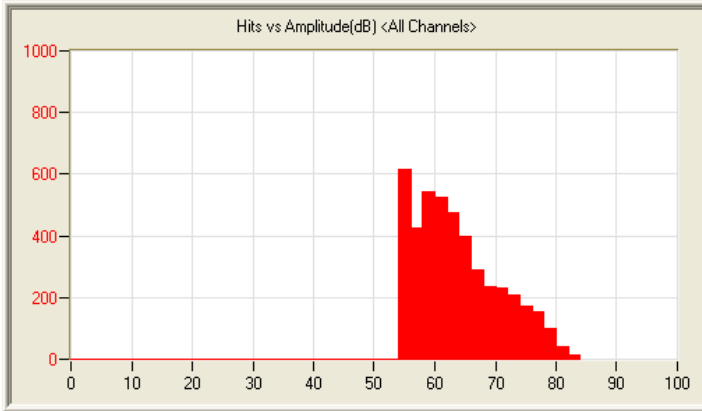
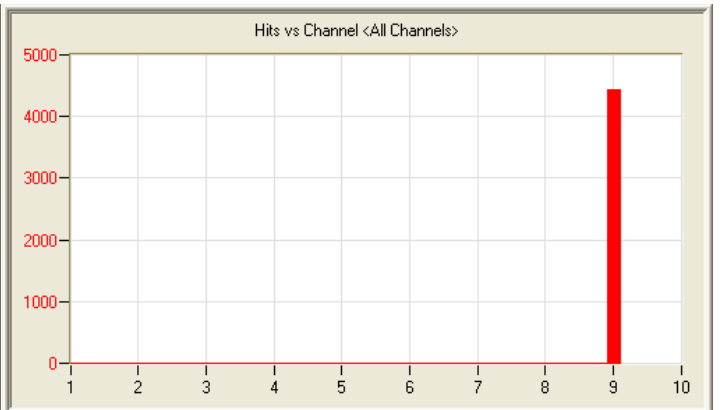
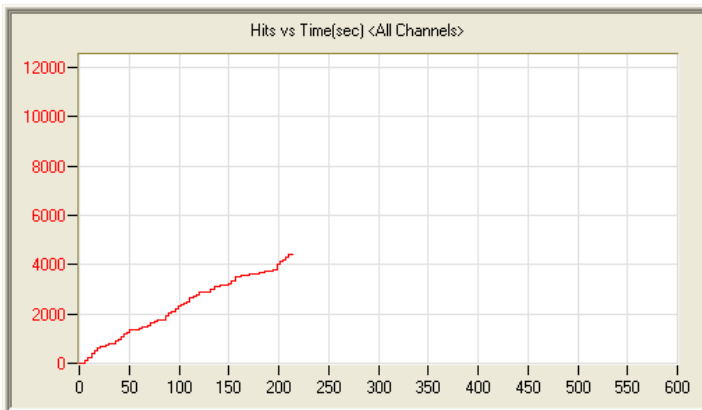
6/12/11 2:55pm 0:03:36 4893 110612145548_0 272kb



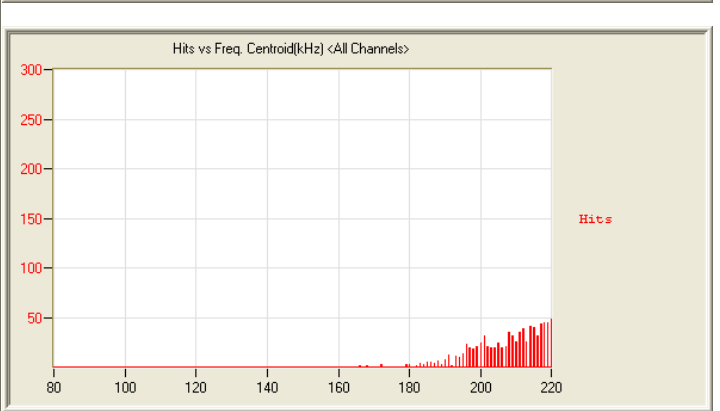
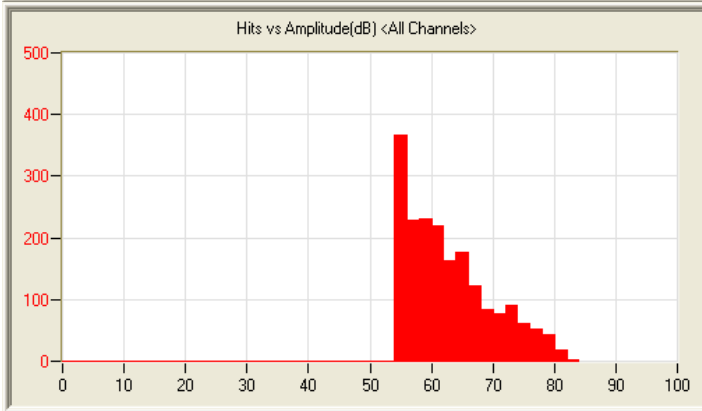
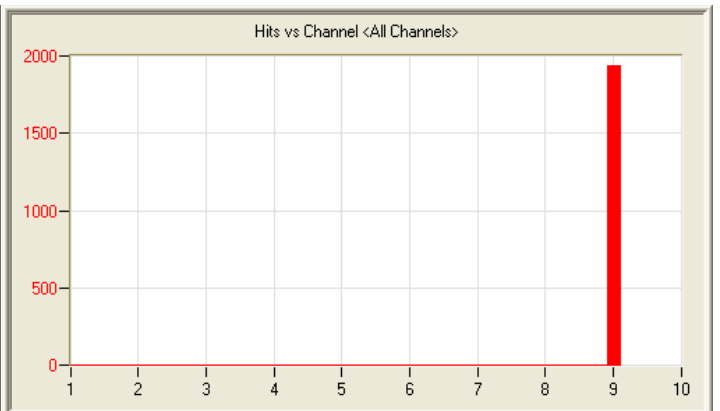
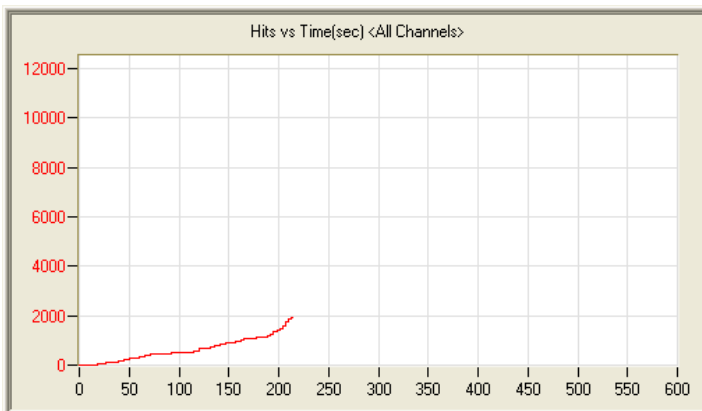
6/12/11 3:00pm 0:18:40 25417 110612150051_0 1.2mb



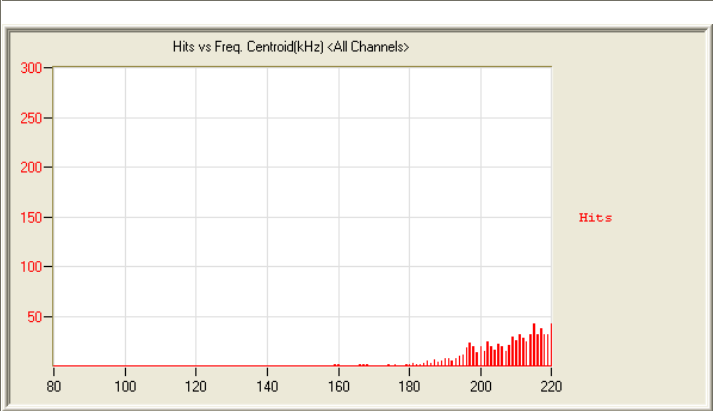
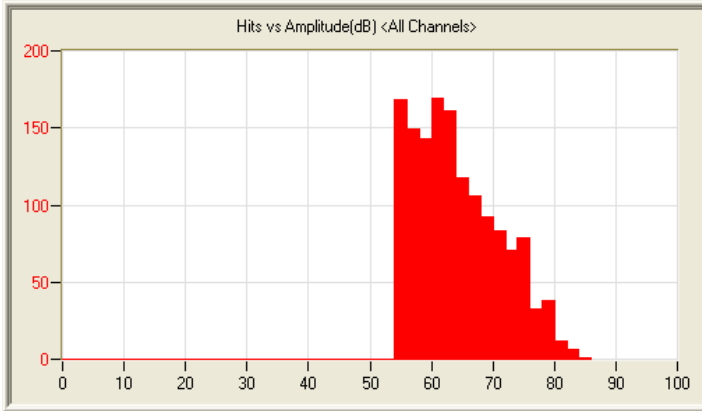
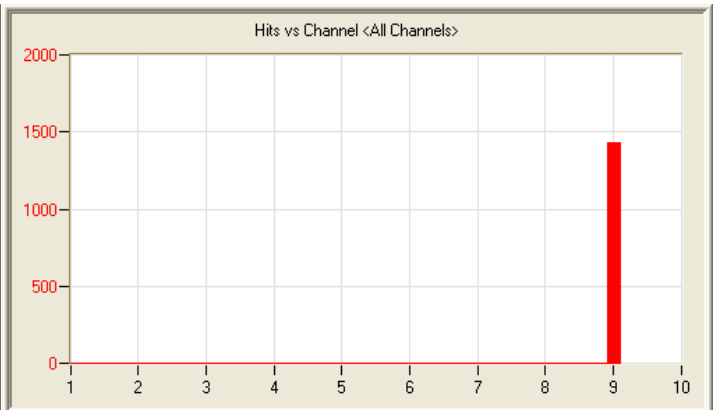
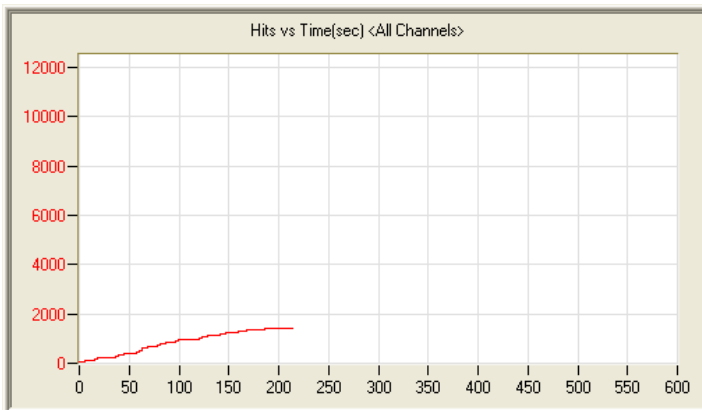
6/12/11 3:20pm 0:03:38 4640 110612152053_0 262kb



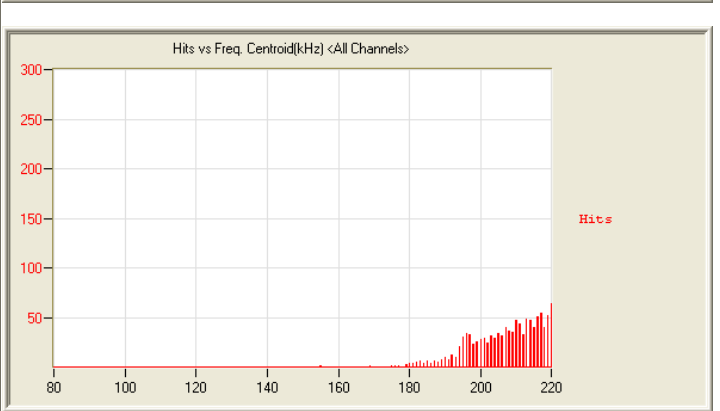
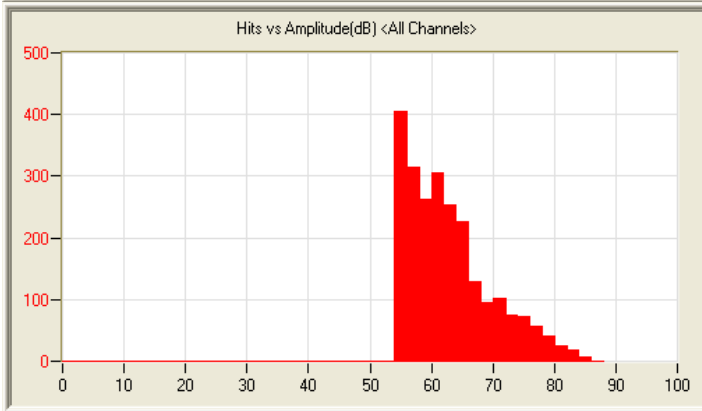
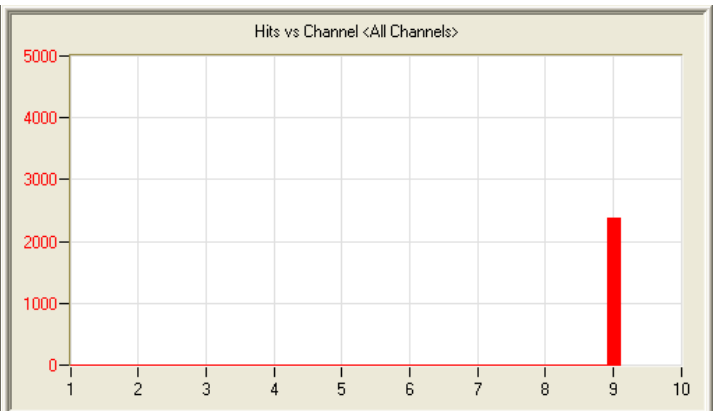
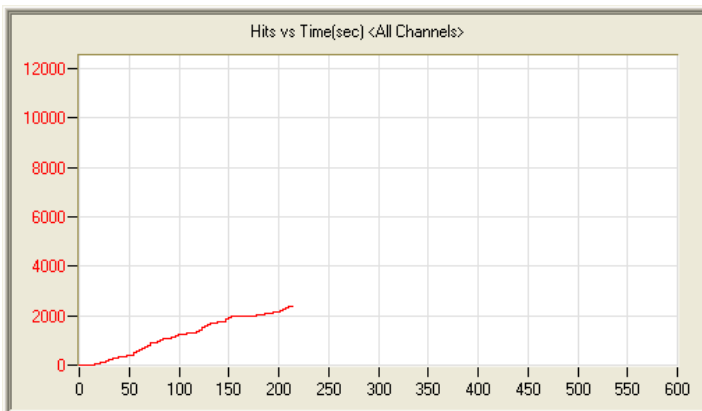
6/12/11 3:25pm 0:03:38 4431 110612152557_0 254kb



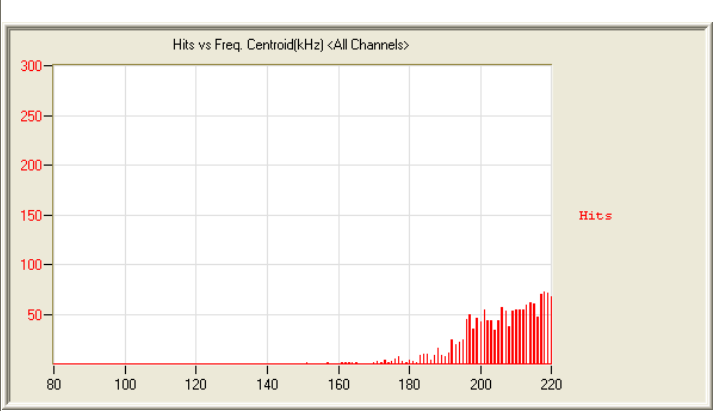
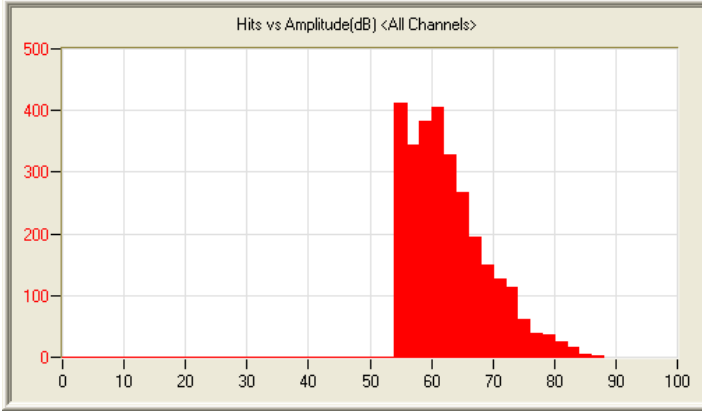
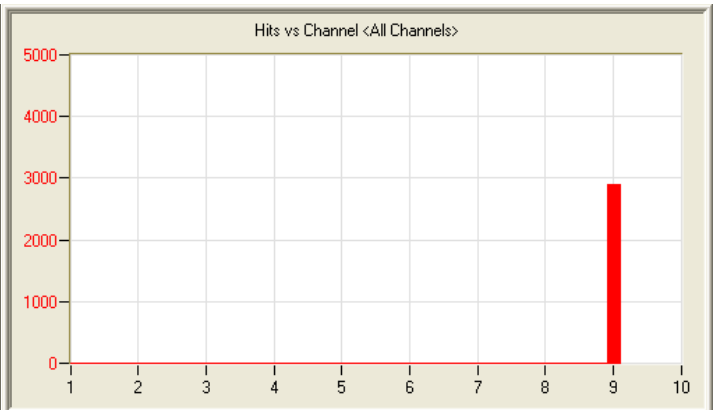
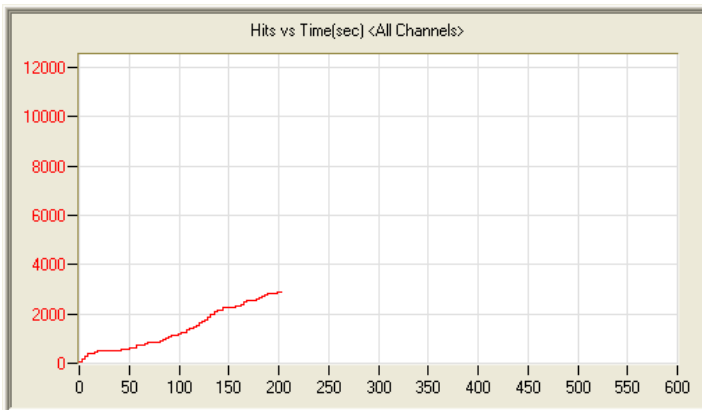
6/12/11 3:31pm 0:03:35 1937 110612153059_0 153kb



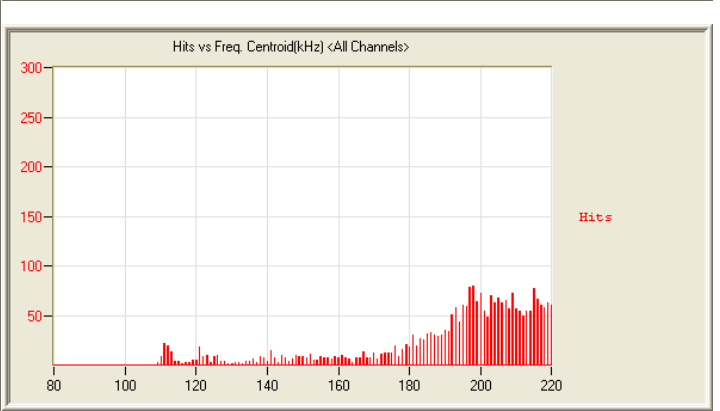
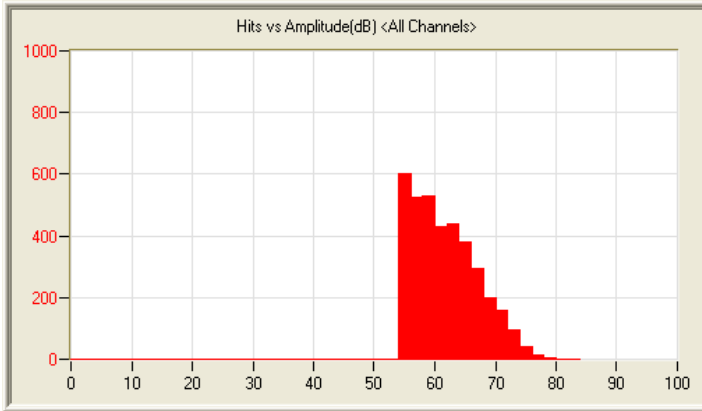
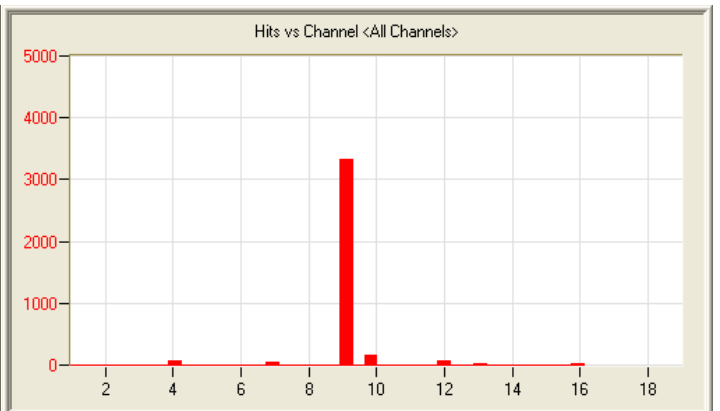
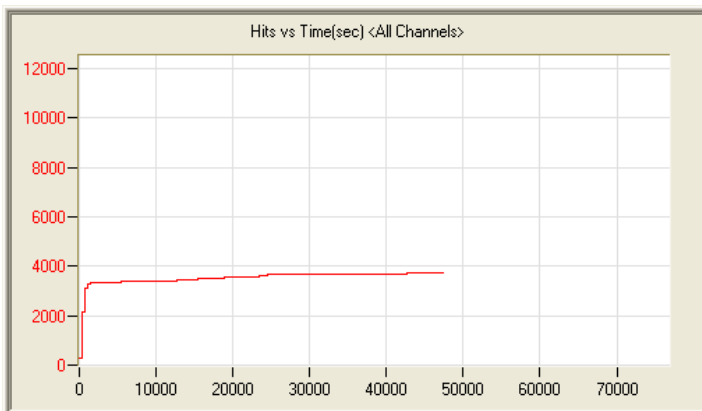
6/12/11 3:56pm 0:03:33 1429 110612155609_0 133kb



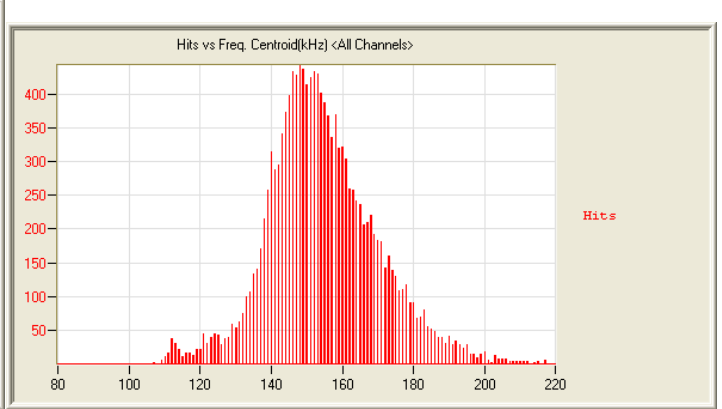
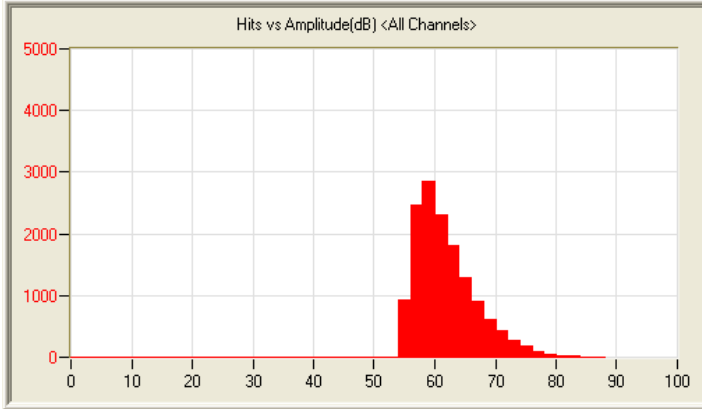
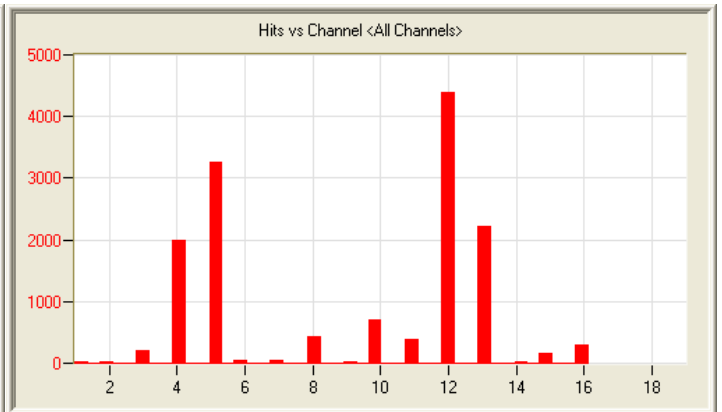
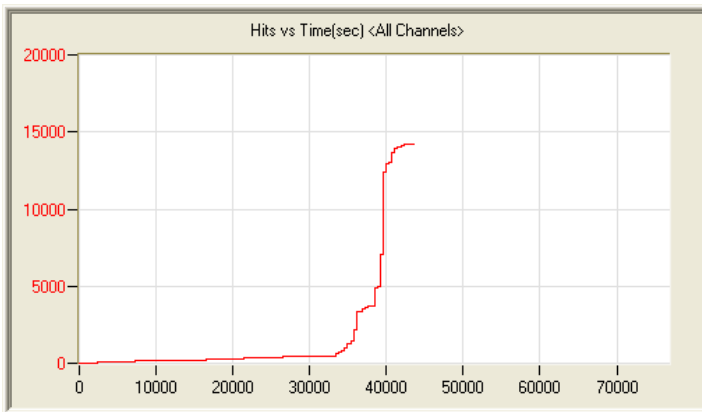
6/12/11 4:01pm 0:03:35 2385 110612160108_0 171kb



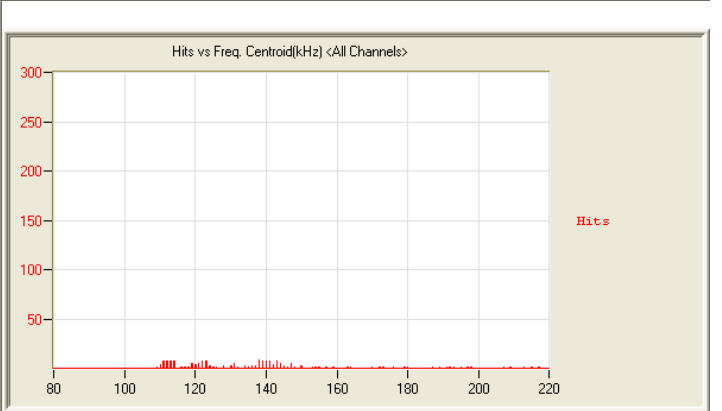
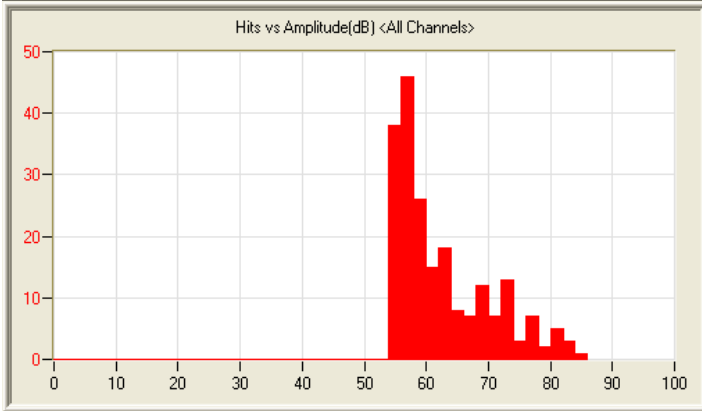
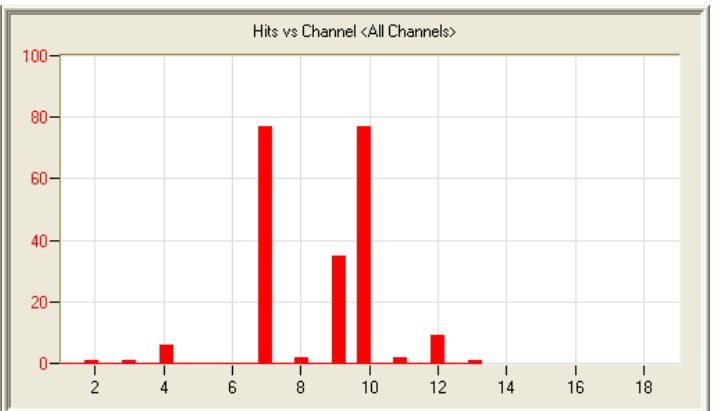
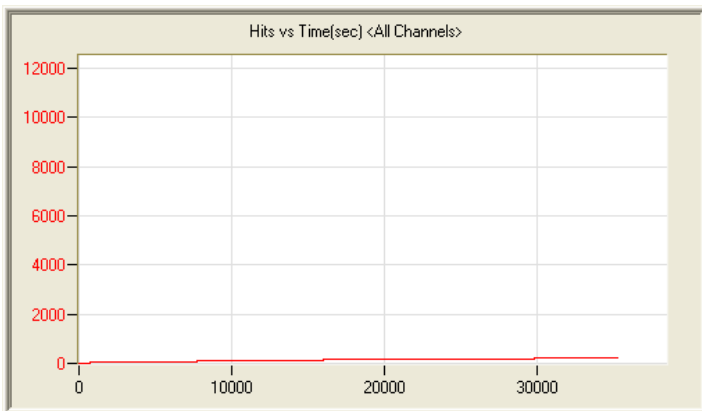
6/12/11 4:06pm 0:03:22 2903 110612160611_0 191kb



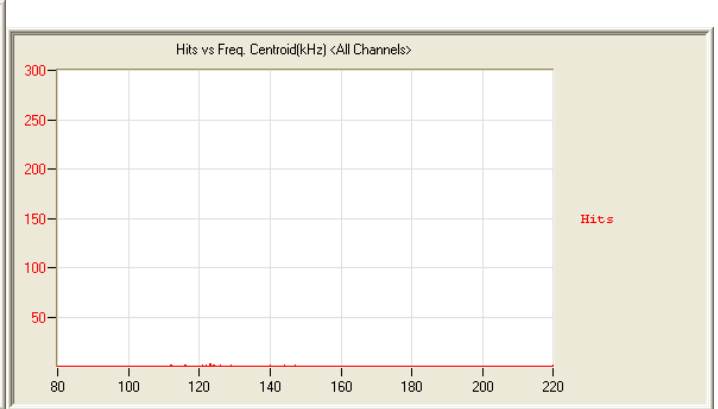
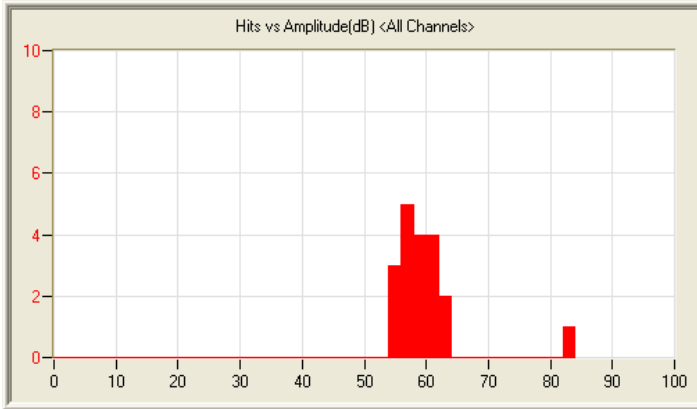
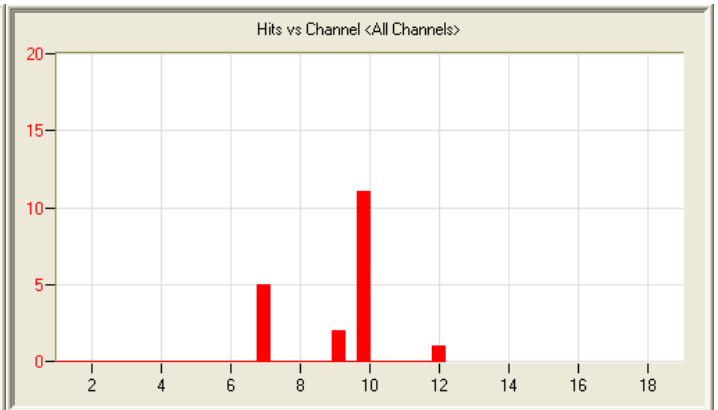
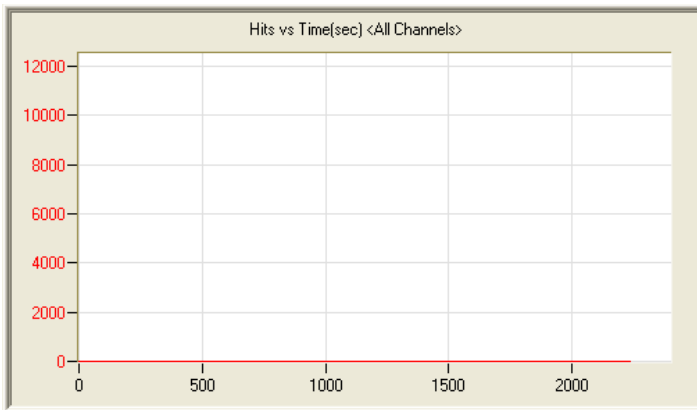
6/13/11 7:28am 13:54:14 3709 110613072844_0 3.8mb



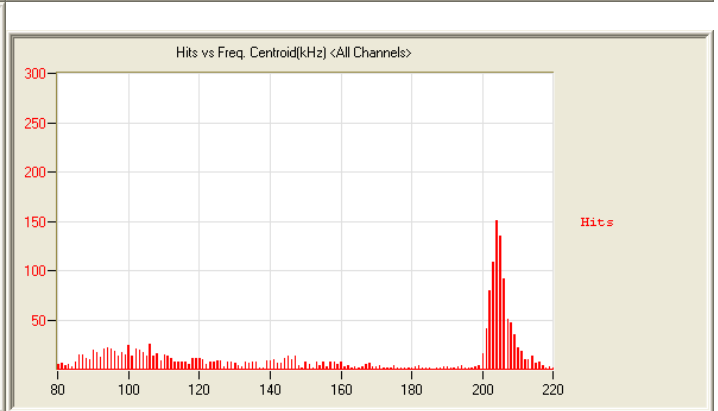
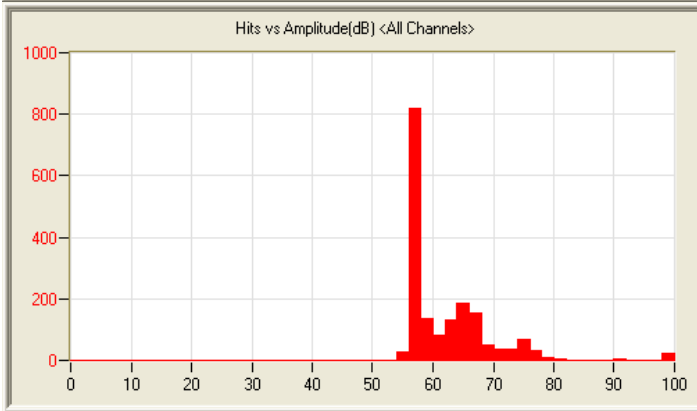
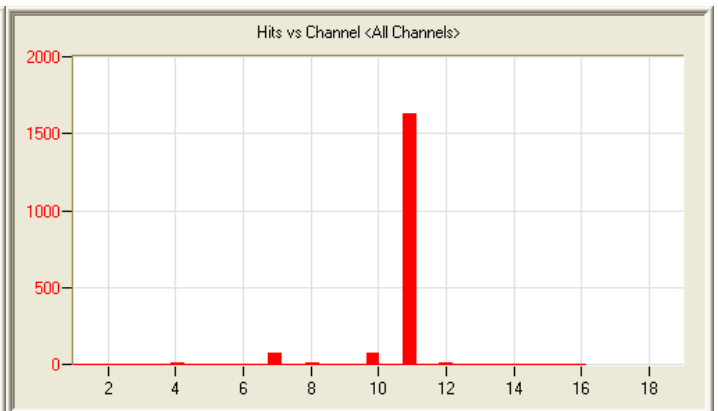
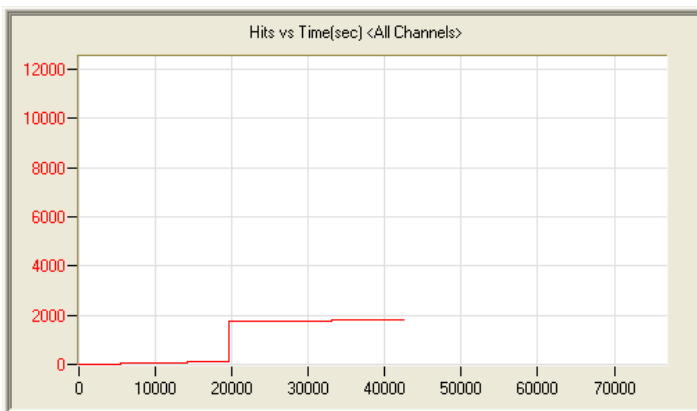
6/14/11 8:03am 12:06:50 14249 110614080312_0 3.7mb



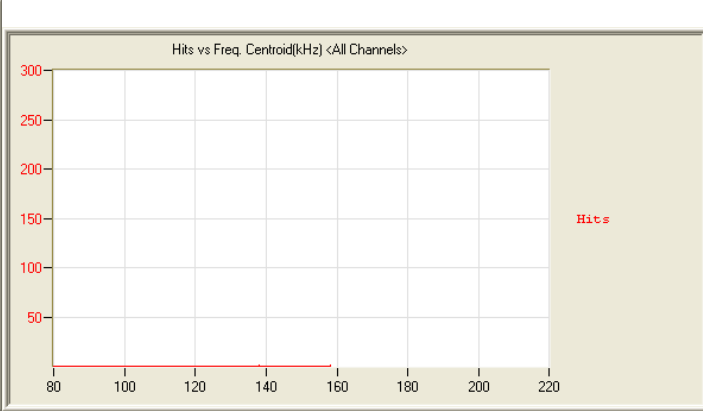
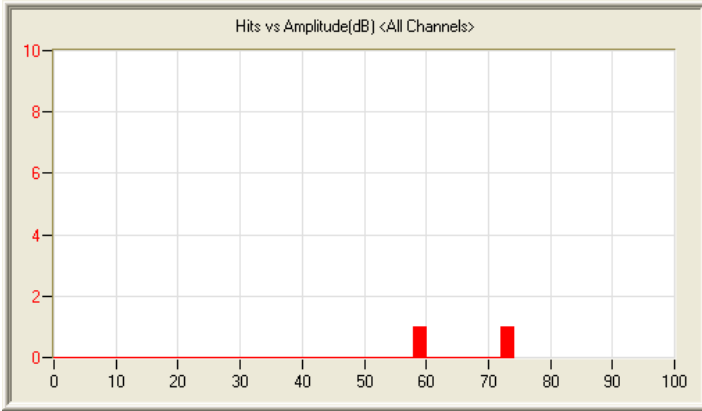
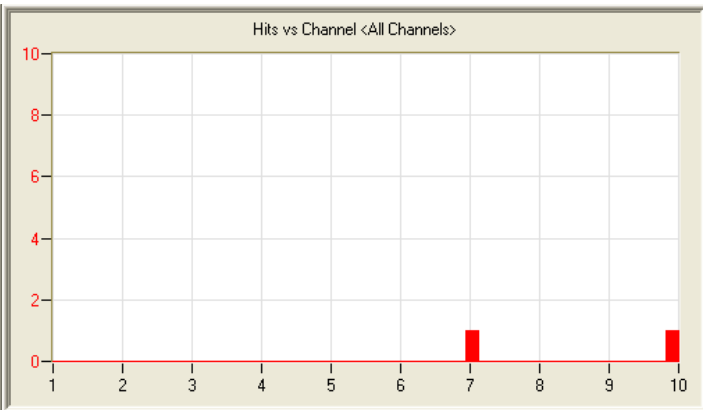
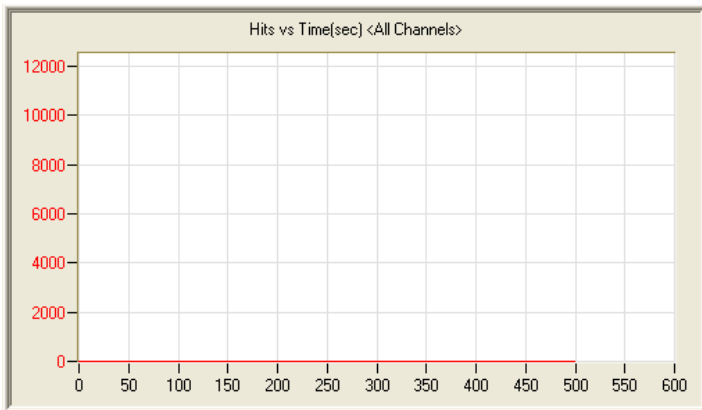
6/16/11 8:02am 10:04:31 211 110616080244_0 2.7mb



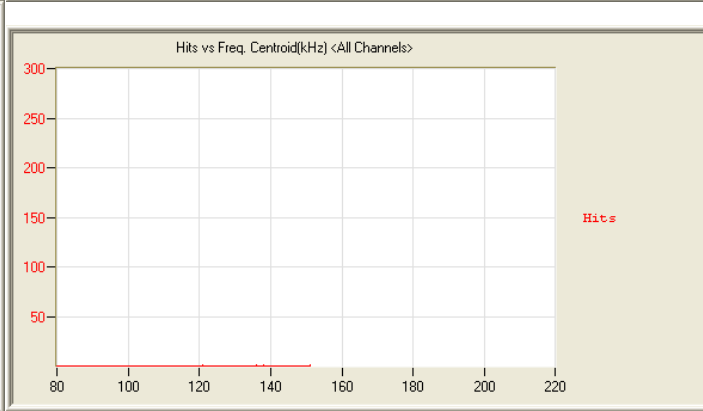
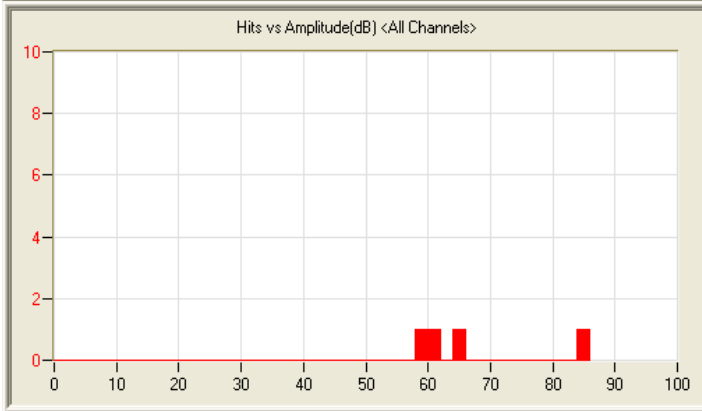
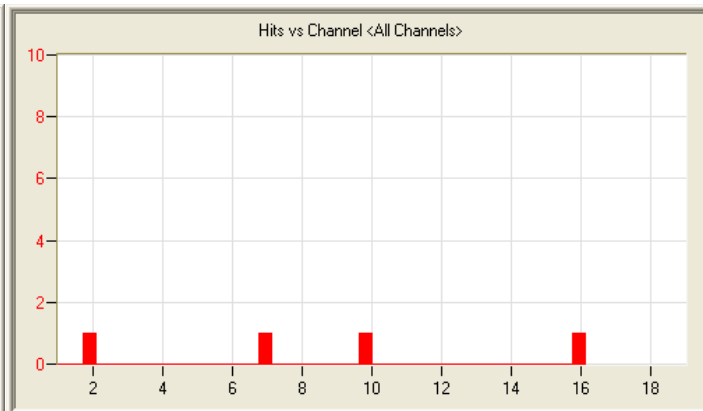
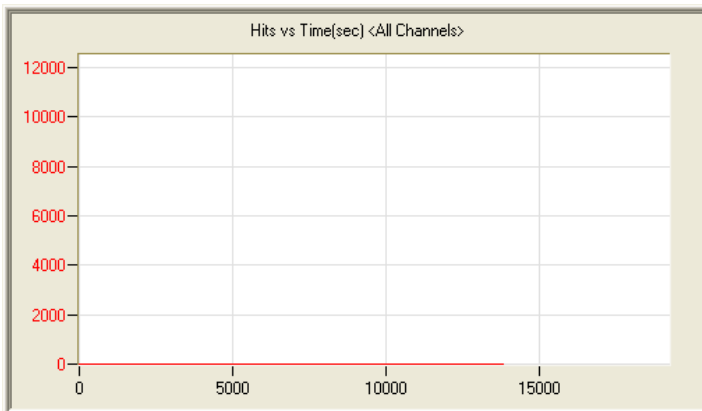
6/17/11 7:09am 0:41:48 19 110617070900_0 240kb



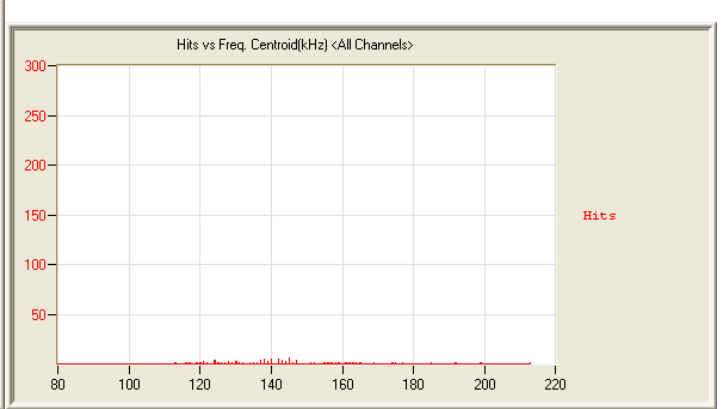
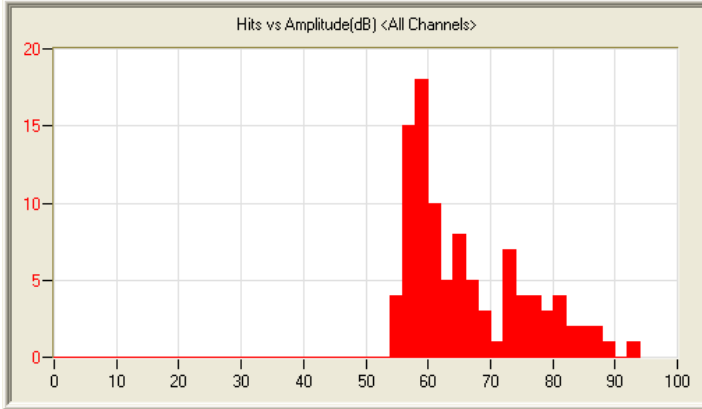
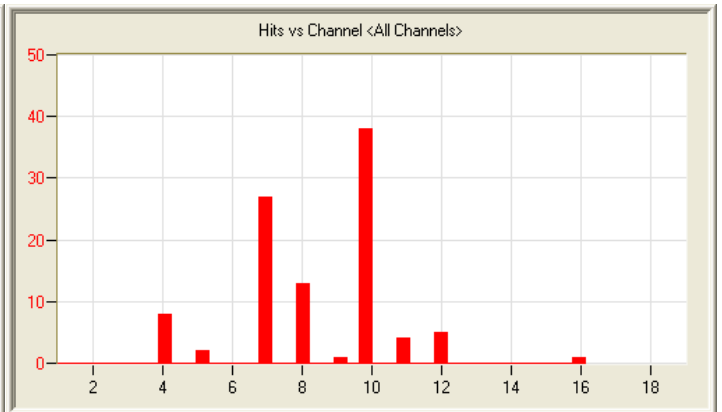
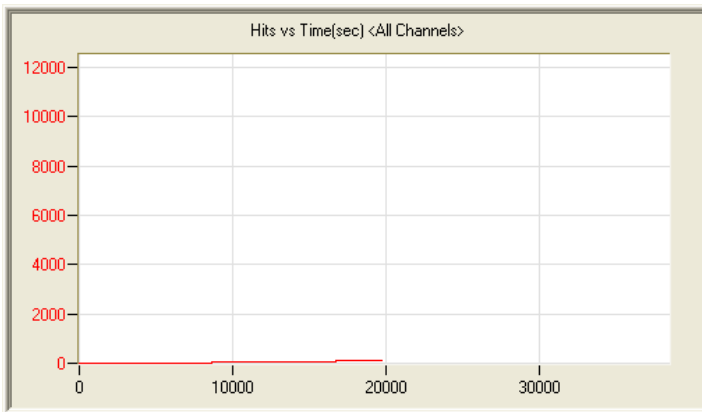
6/17/11 8:24am 11:49:45 1807 110617082424_0 3.2mb



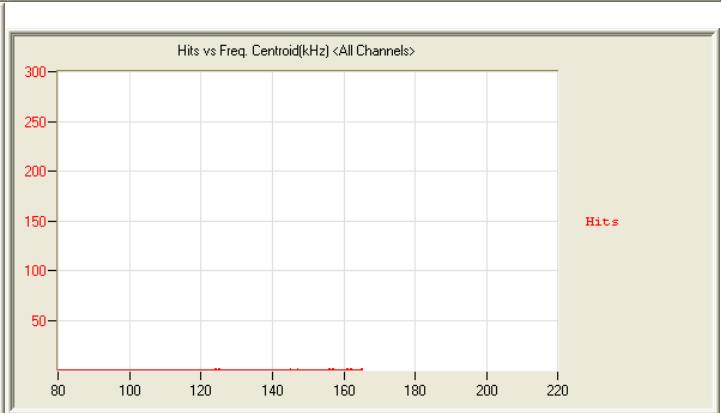
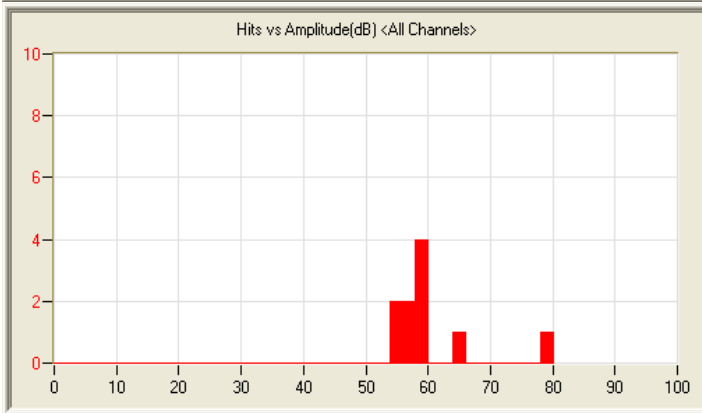
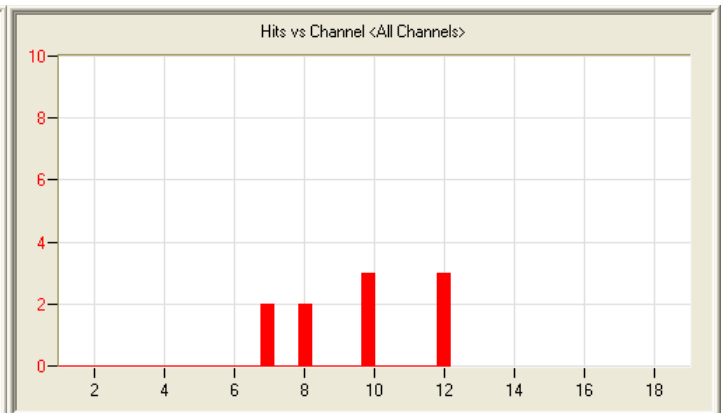
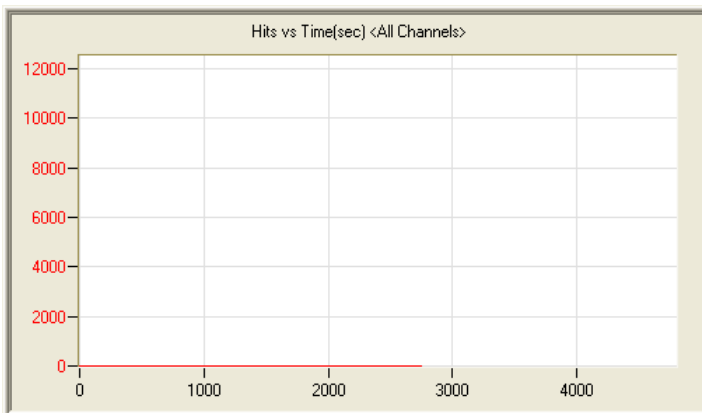
6/19/11 12:01pm 0:33:52 2 110619120143_0 206kb



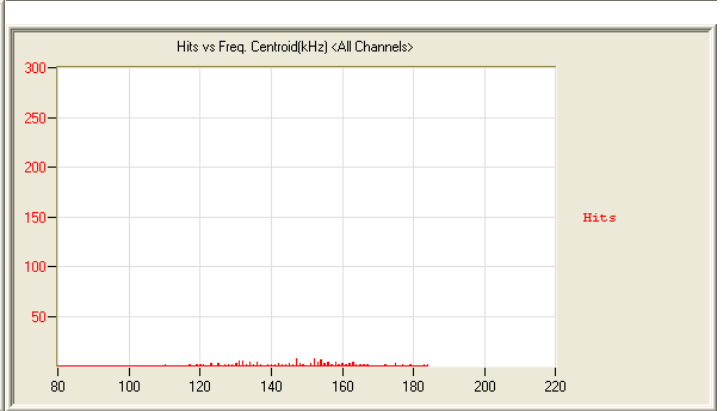
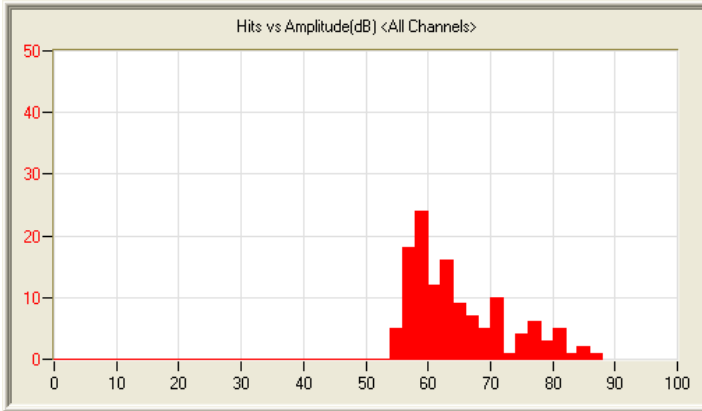
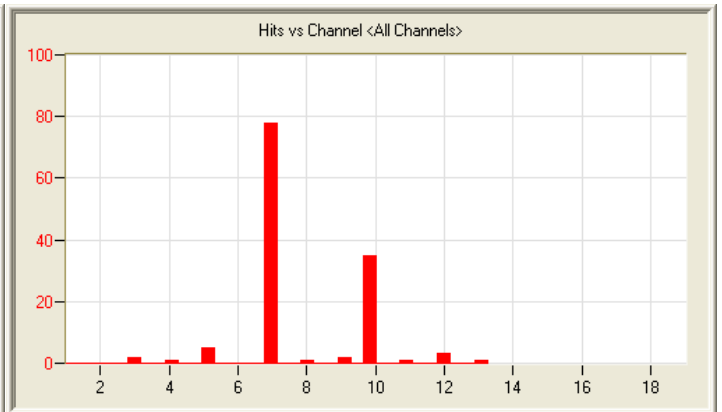
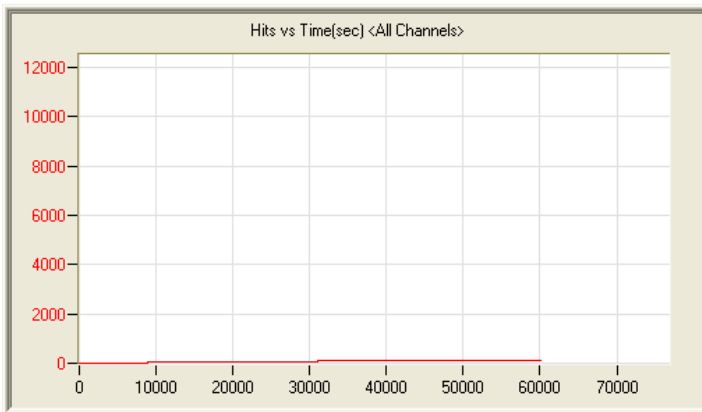
6/19/11 12:41pm 4:05:00 4 110619124157_0 1.1mb



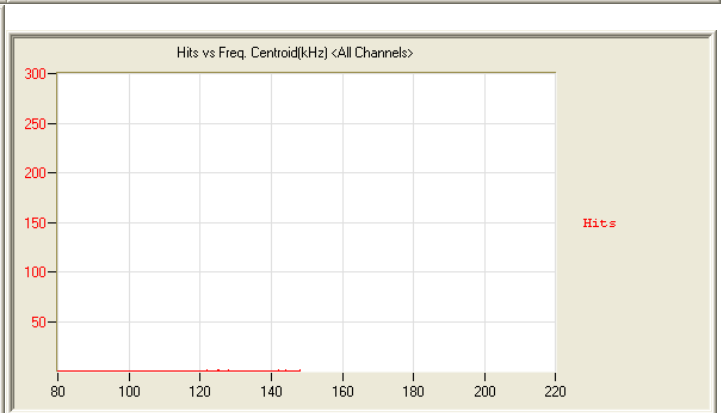
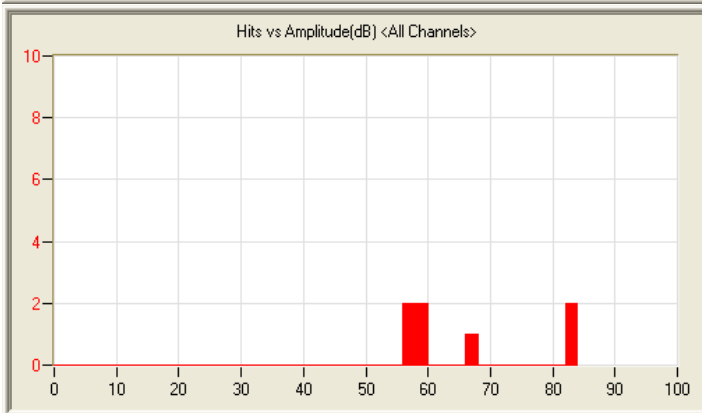
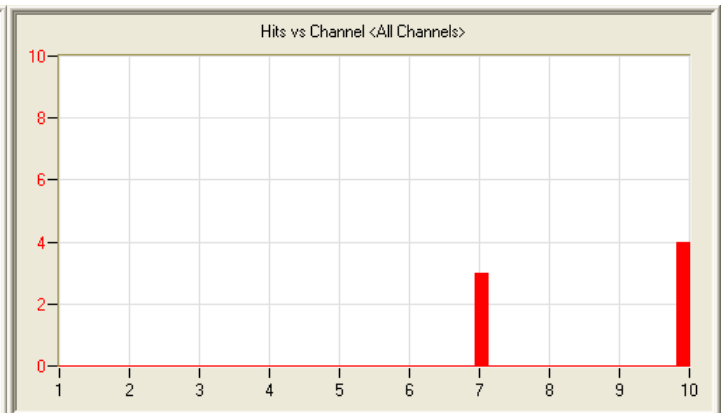
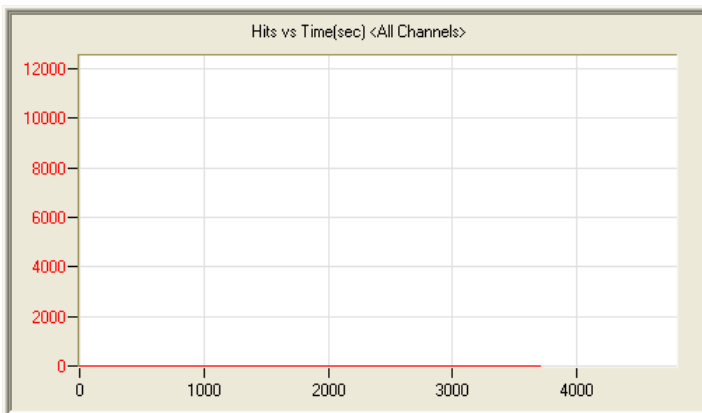
6/21/11 10:50am 5:38:15 99 110621105031_0 1.5mb



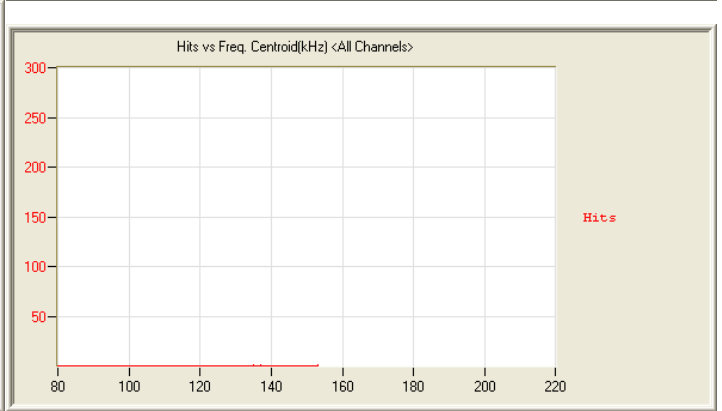
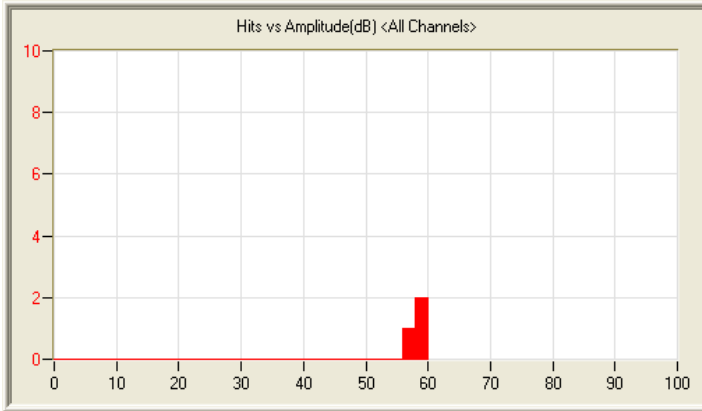
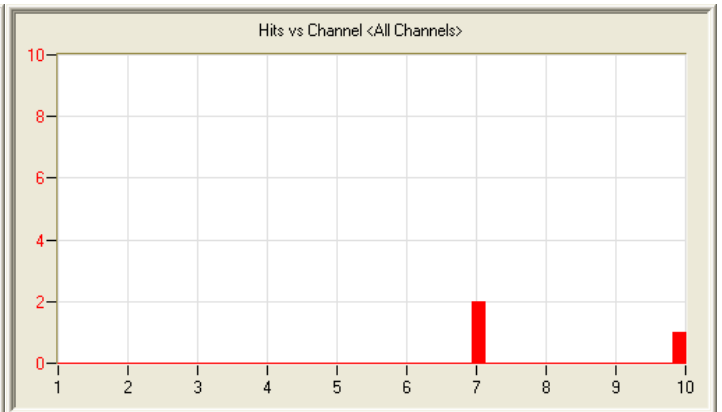
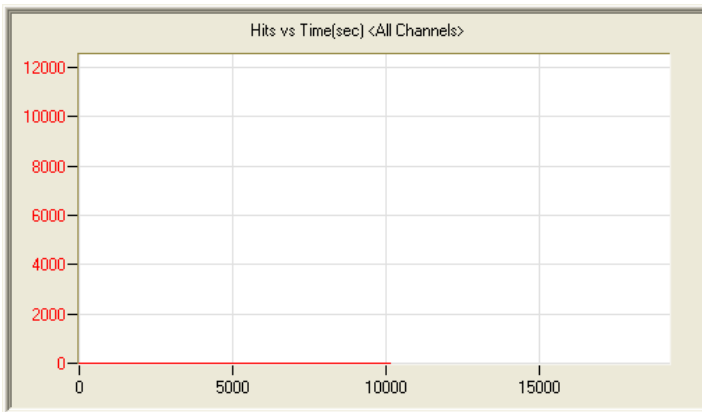
6/22/11 12:38pm 1:08:56 10 110622123856_0 356kb



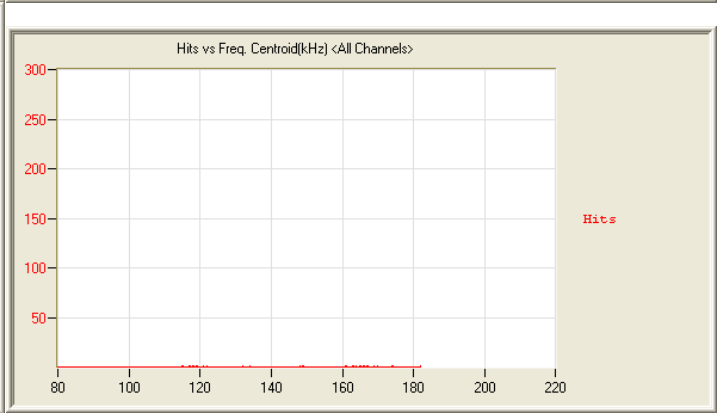
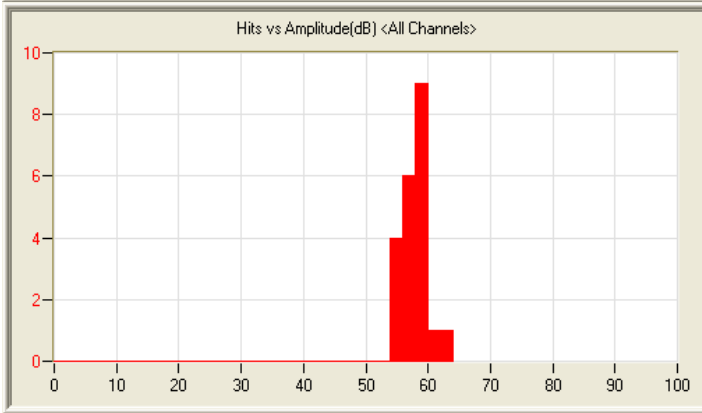
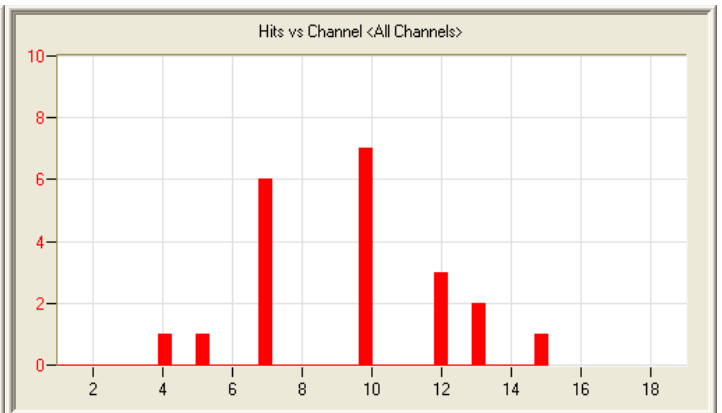
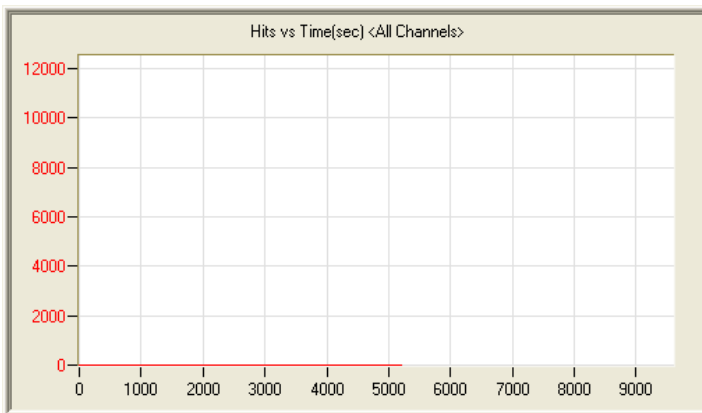
6/24/11 6:38am 17:45:00 129 110624063821_0 4.6mb



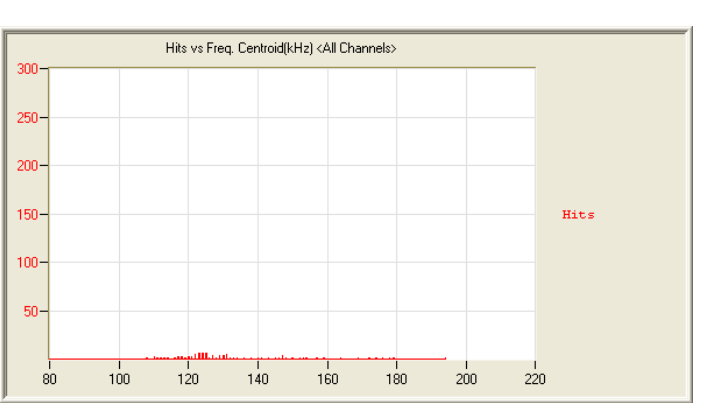
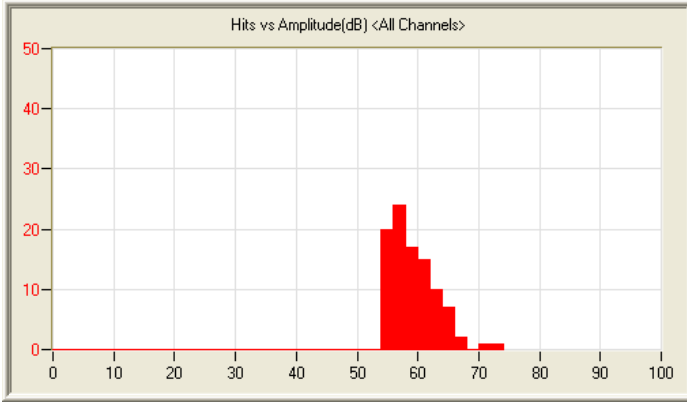
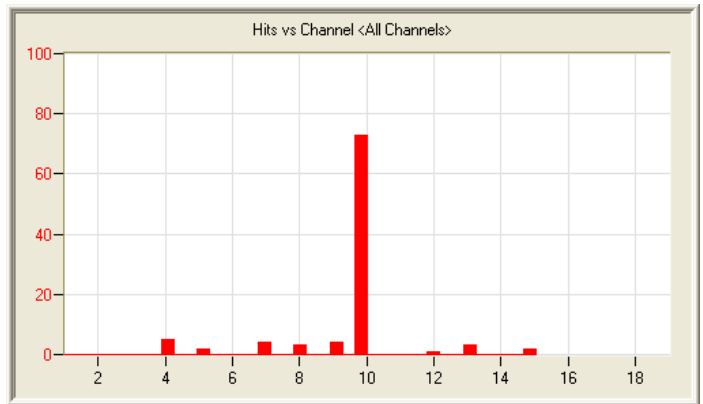
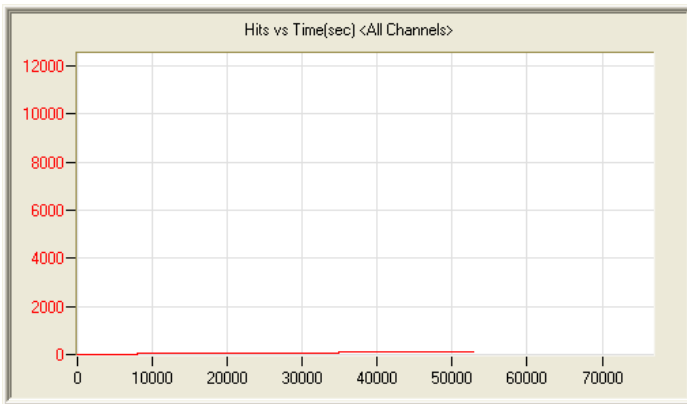
6/25/11 7:45am 1:27:24 7 110625074548_0 435kb



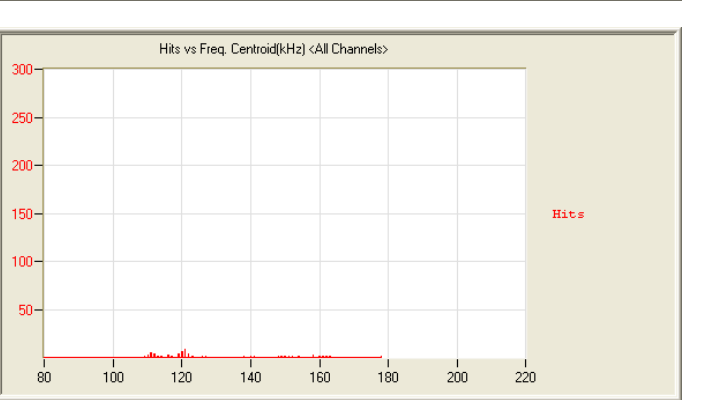
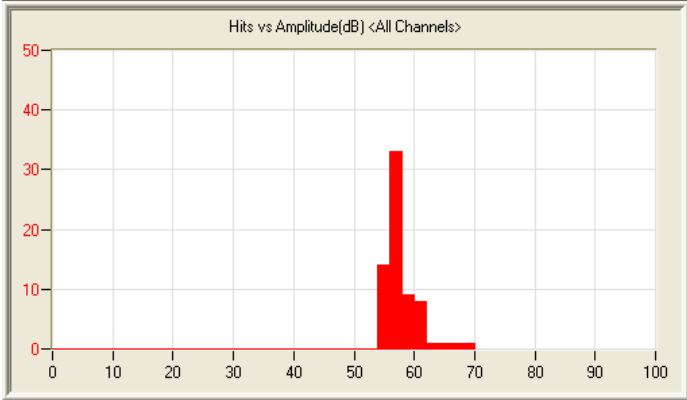
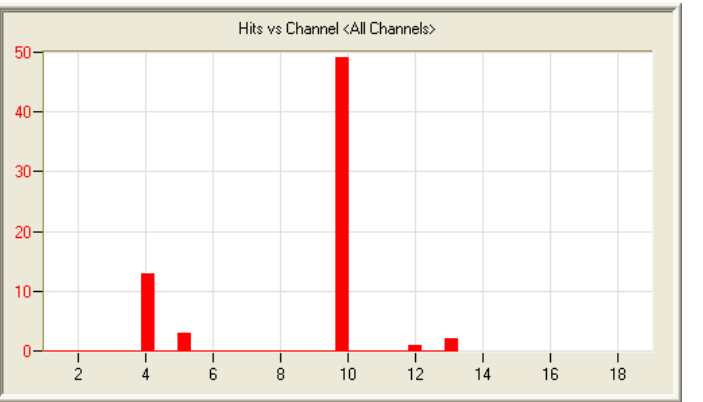
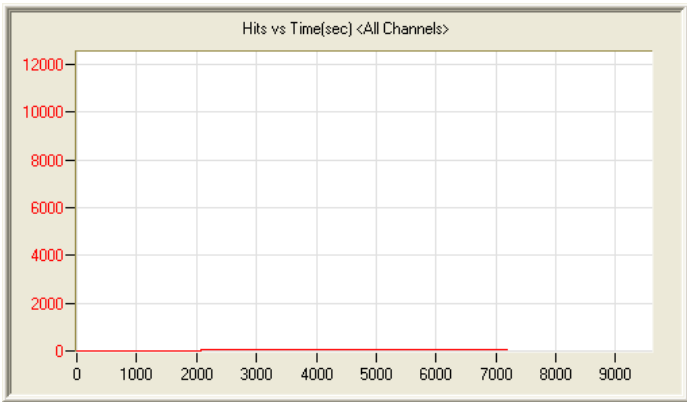
6/26/11 12:38pm 3:34:51 3 110626123813_0 980kb



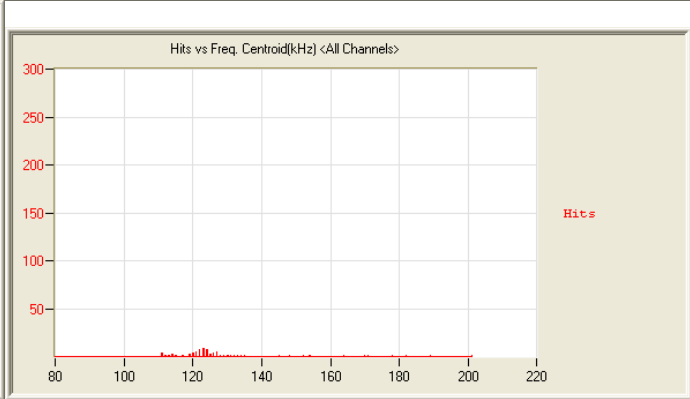
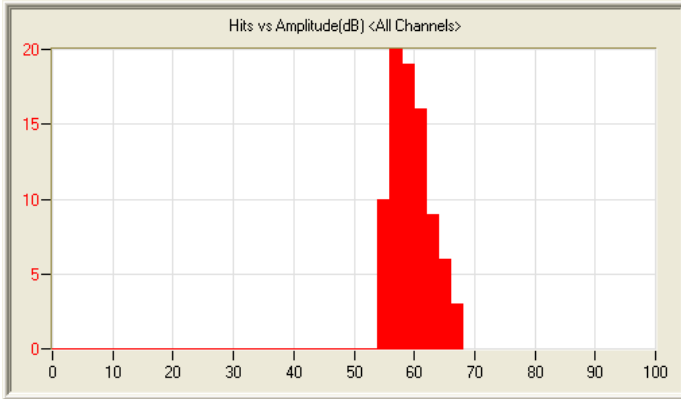
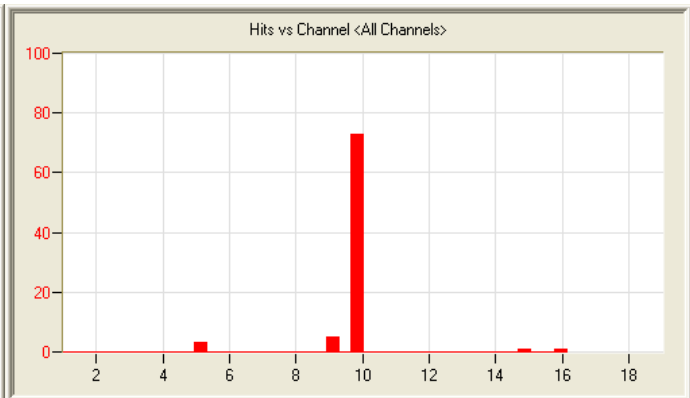
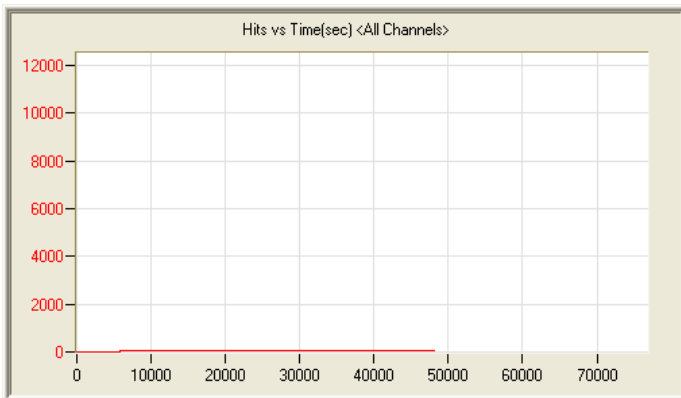
6/28/11 6:34am 1:27:09 21 110628063431_0 434kb



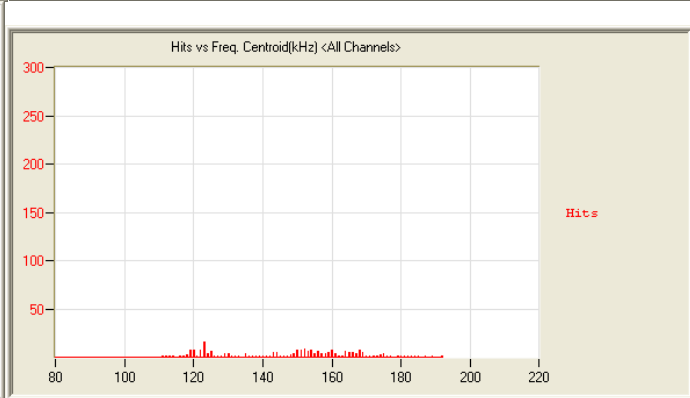
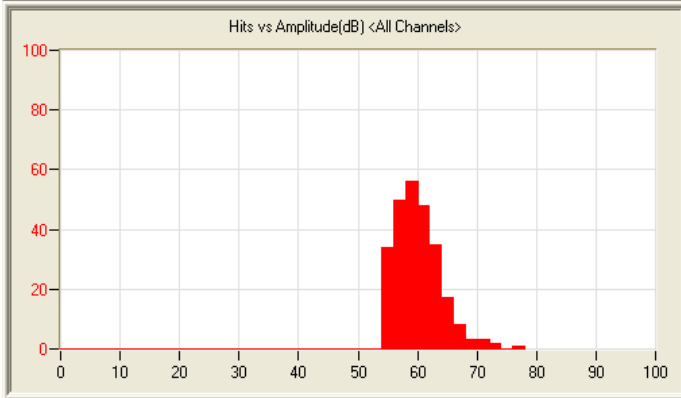
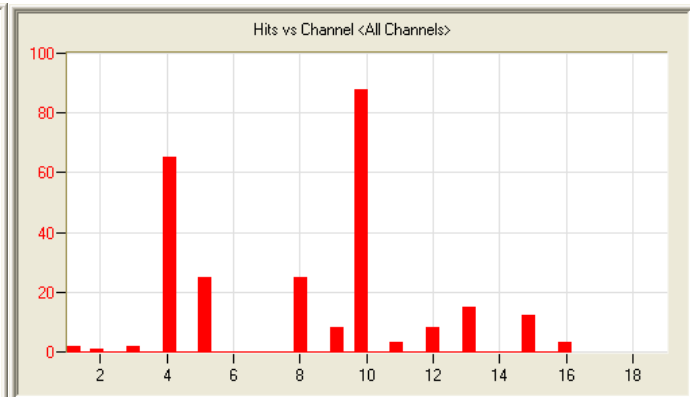
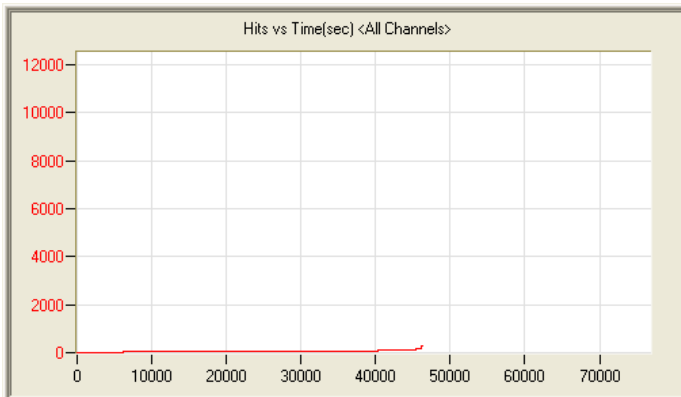
6/29/11 7:13am 15:12:47 97 110629071353_0 4.0mb



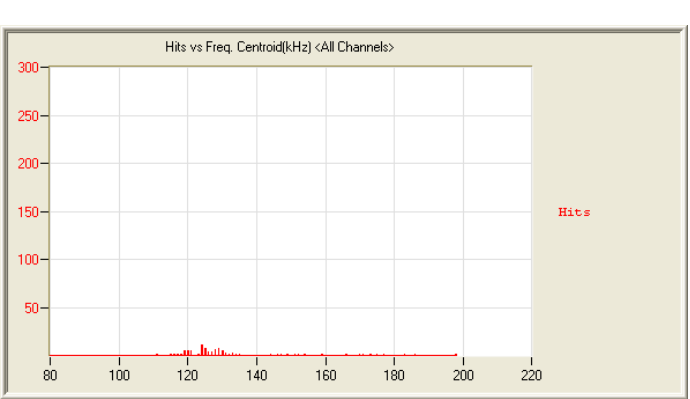
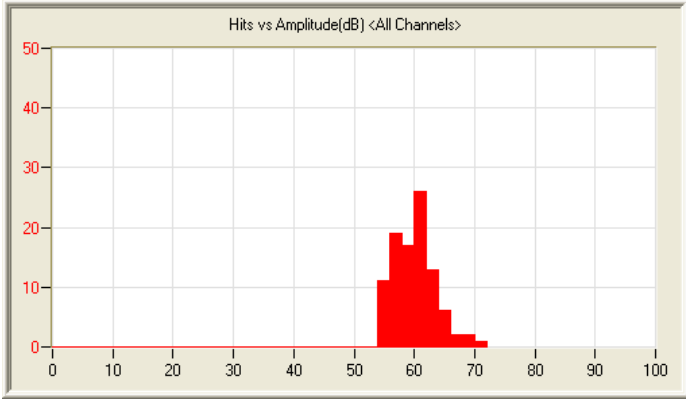
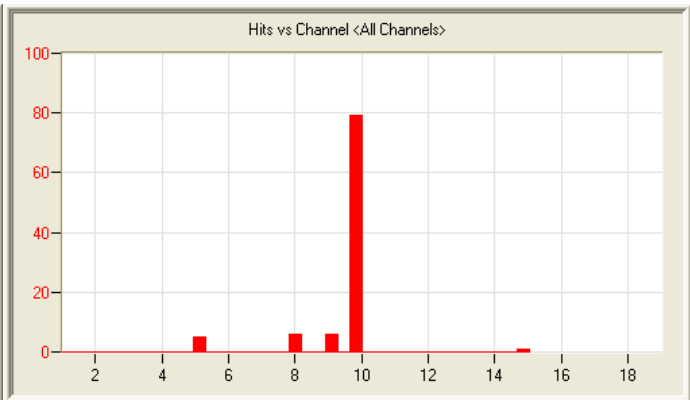
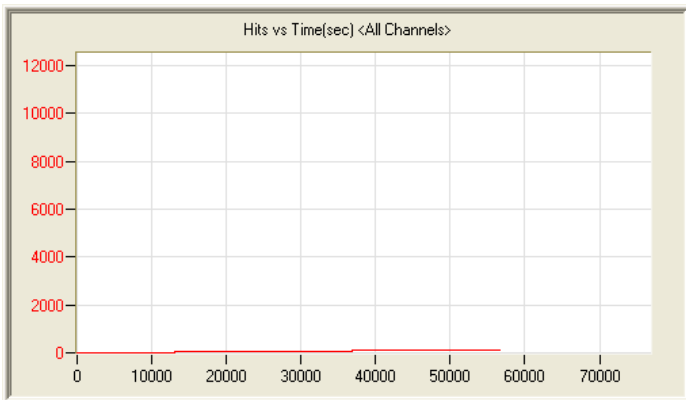
6/30/11 6:53am 2:01:30 68 110630065346_0 583kb



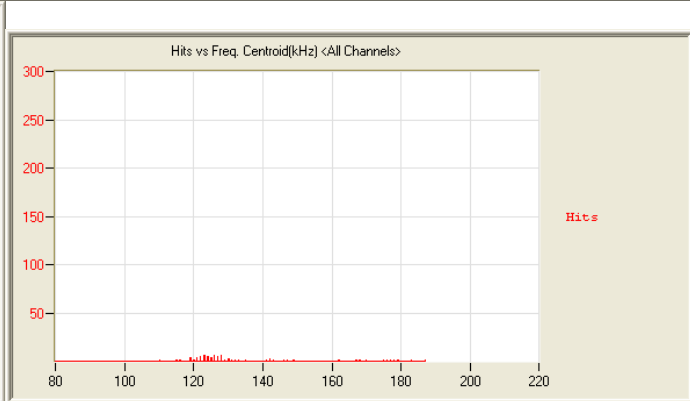
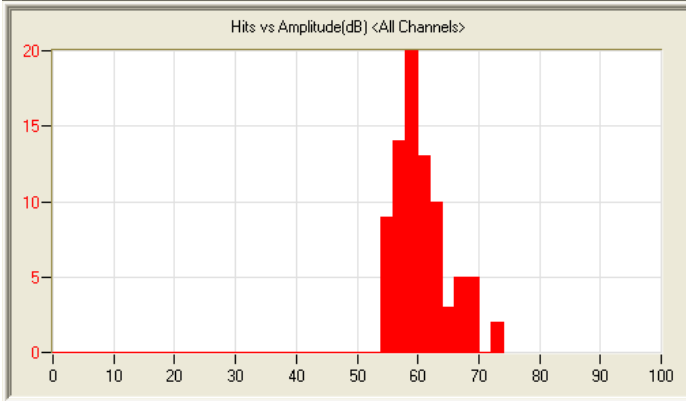
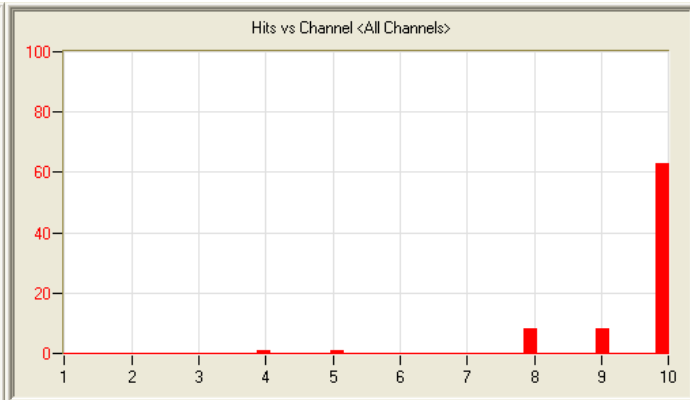
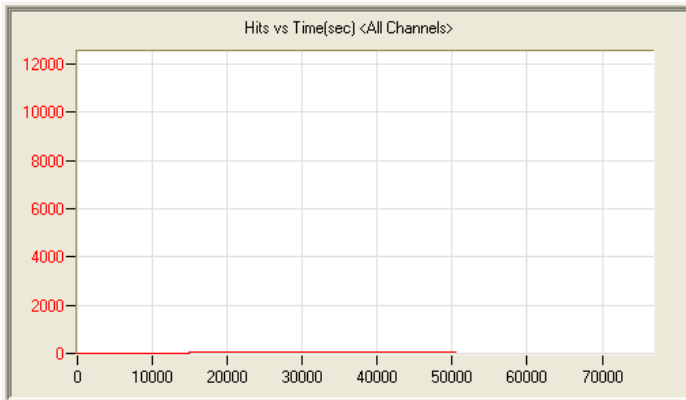
6/30/11 8:59am 13:22:15 83 110630085858_0 3.5mb



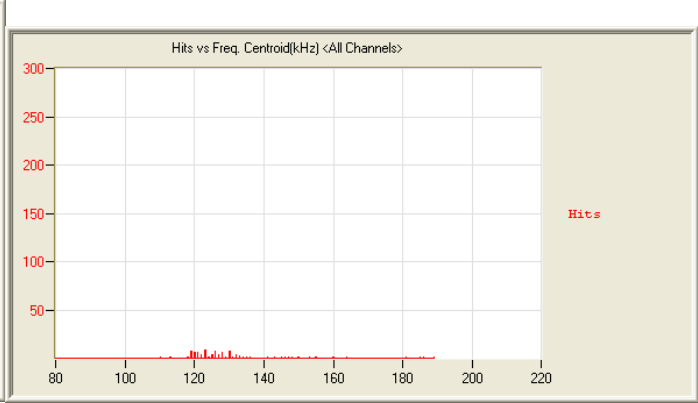
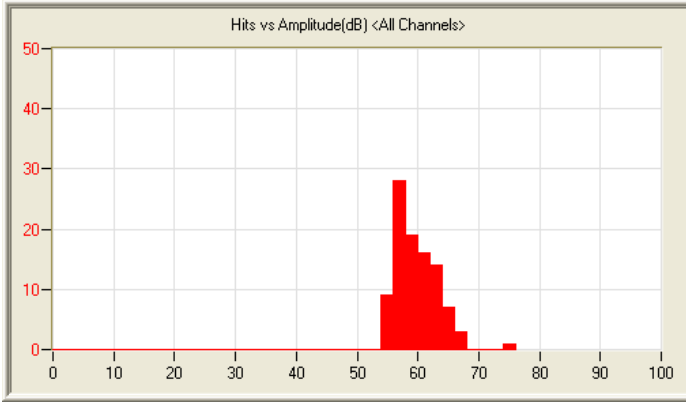
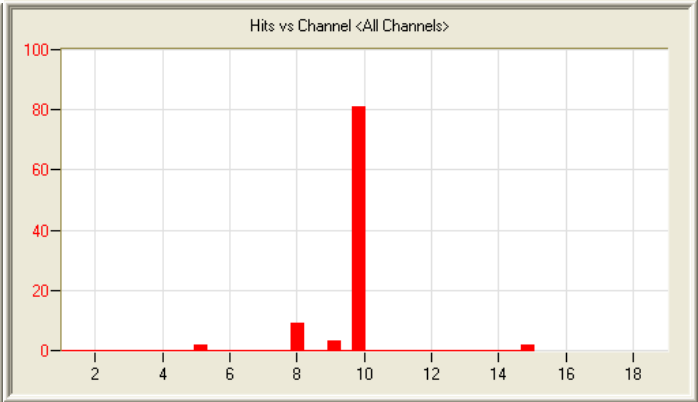
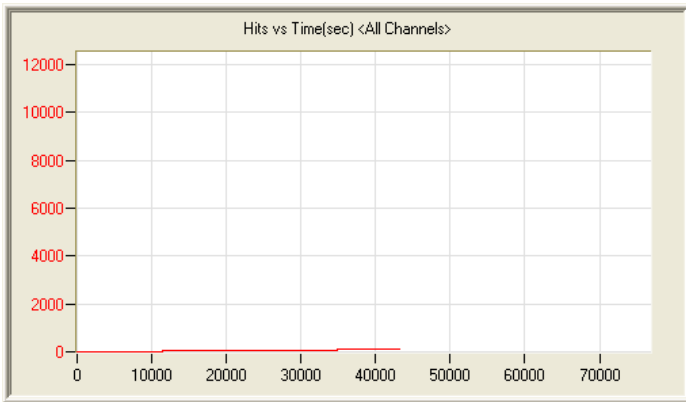
7/1/11 7:29am 12:54:04 257 110701072941_0 3.4mb



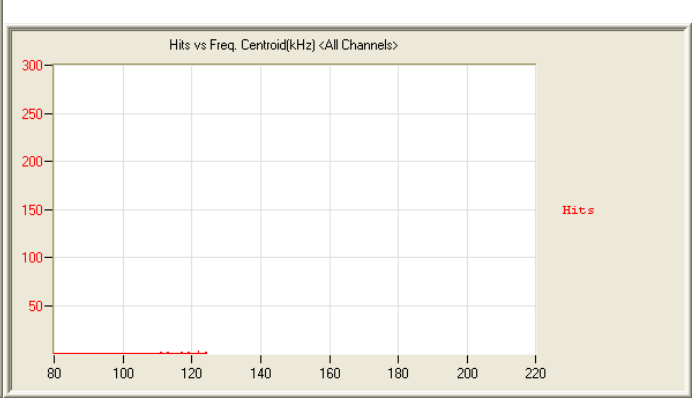
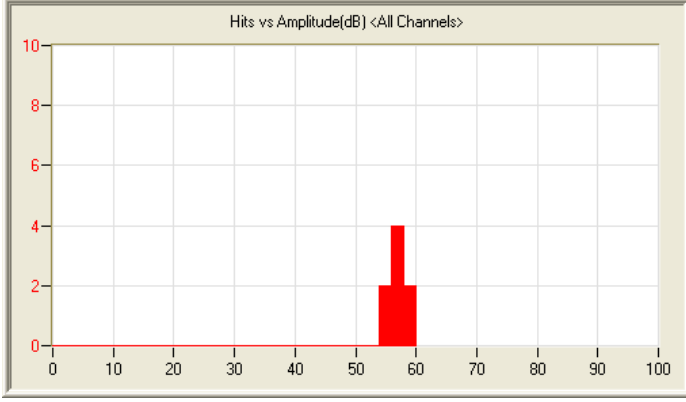
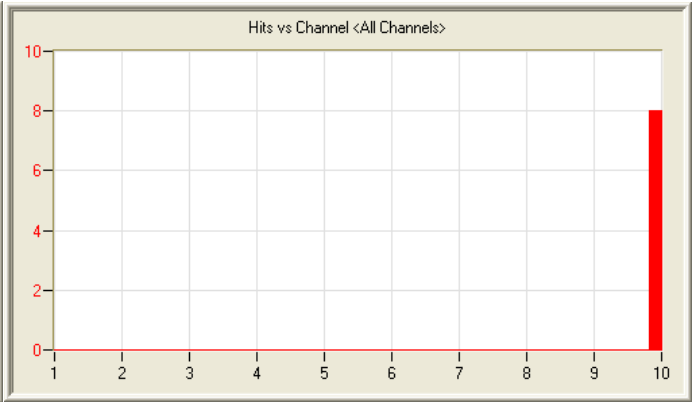
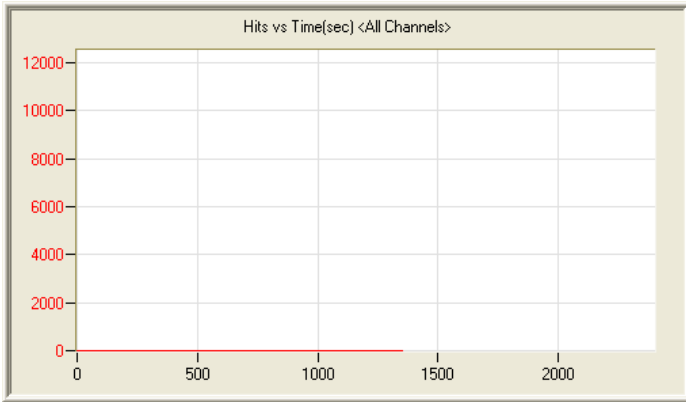
7/2/11 6:28am 16:08:32 97 110702062825_0 4.2mb



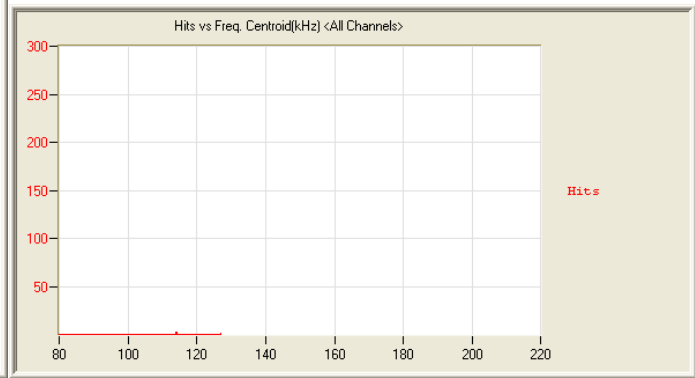
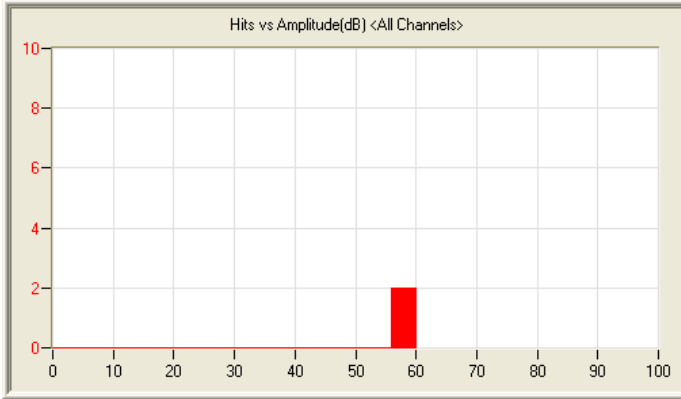
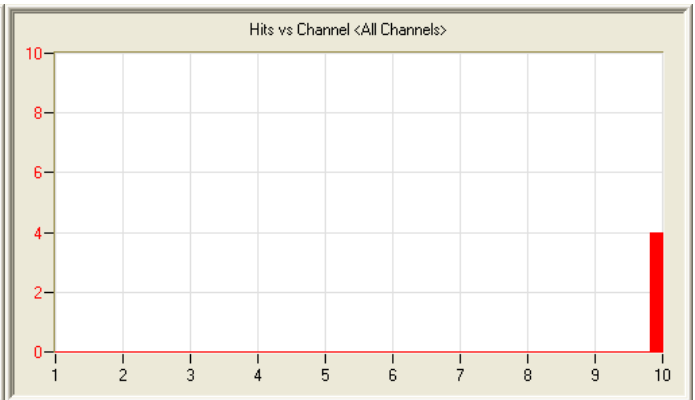
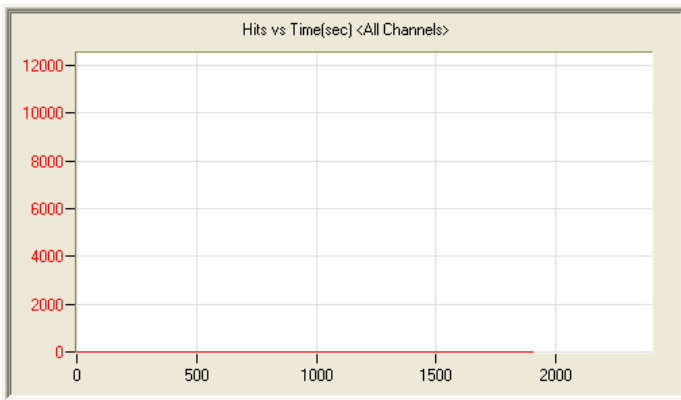
7/3/11 6:58am 13:35:49 81 110703065844_0 3.8mb



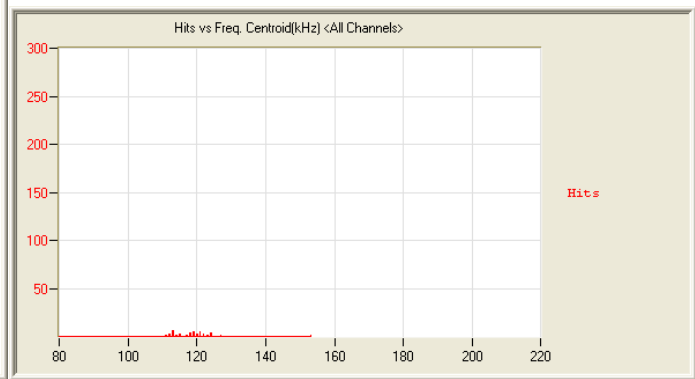
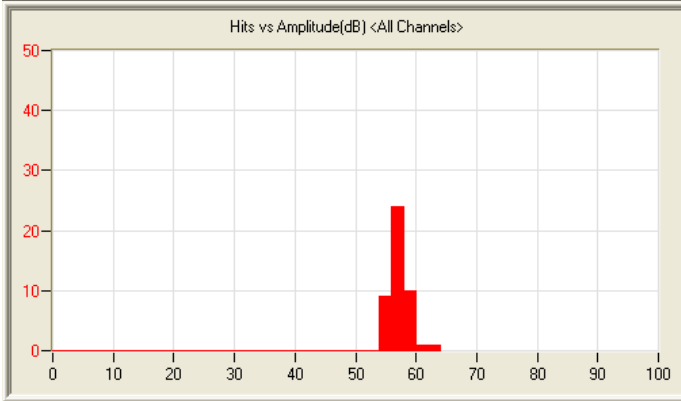
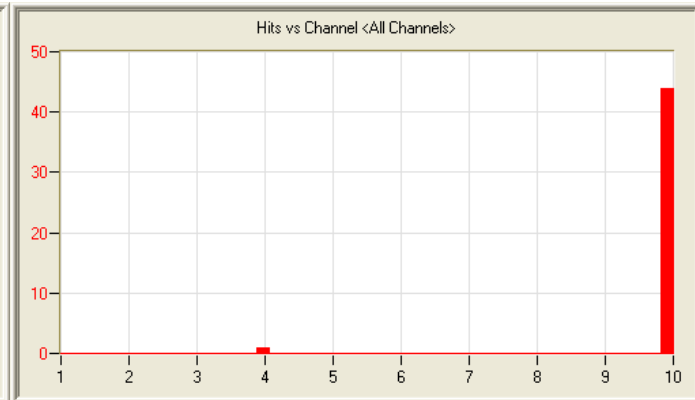
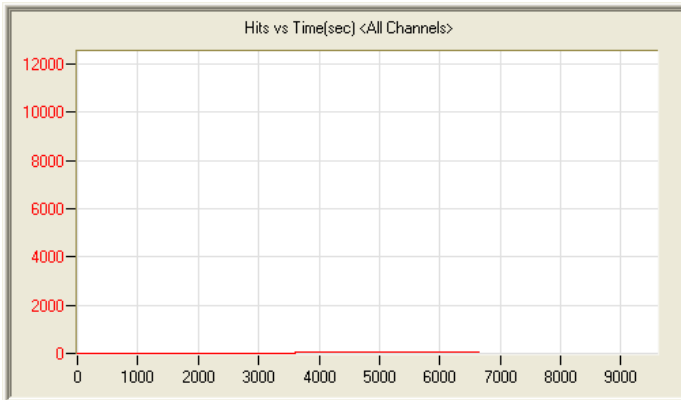
7/4/11 6:34am 15:44:04 97 110704063401_0 4.1mb



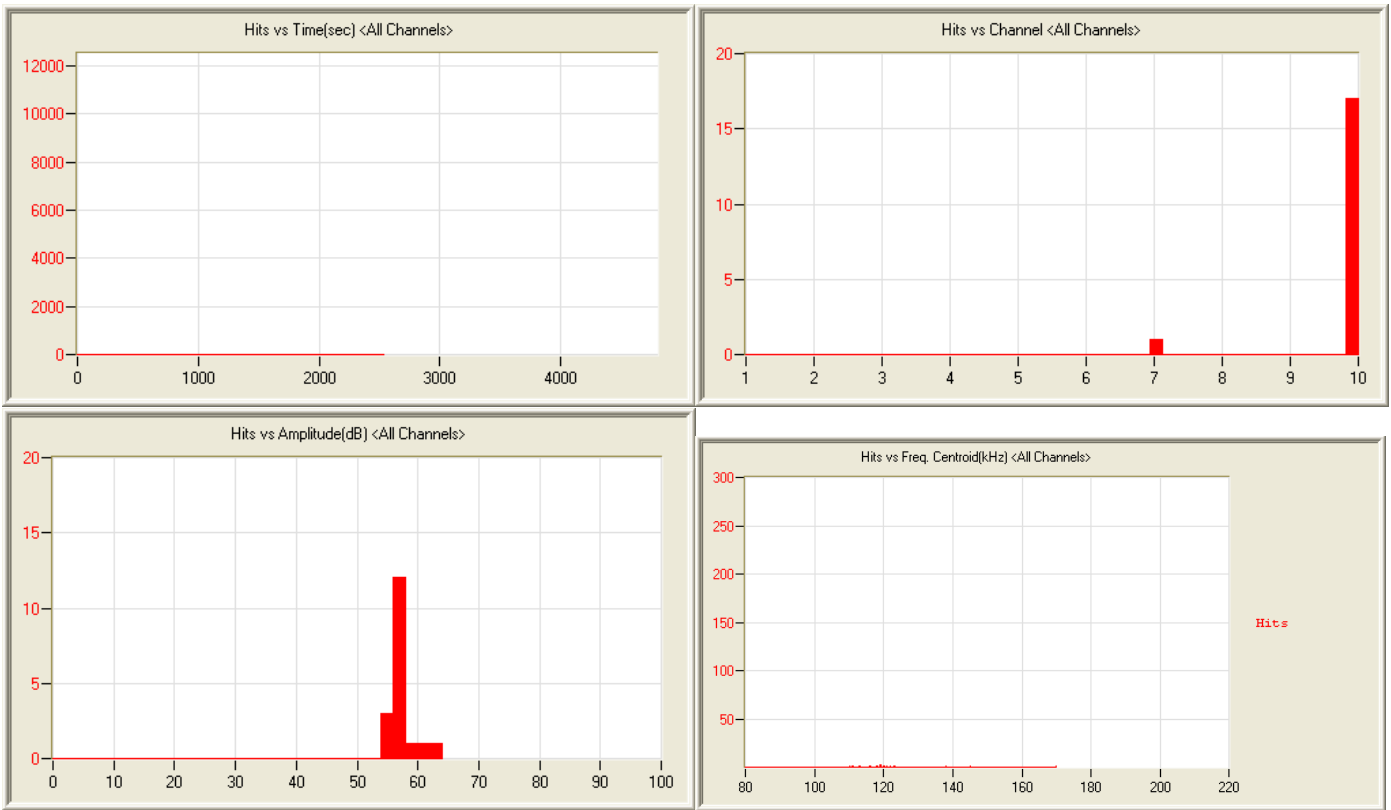
7/5/11 9:02am 0:43:55 8 110705090202_0 249kb



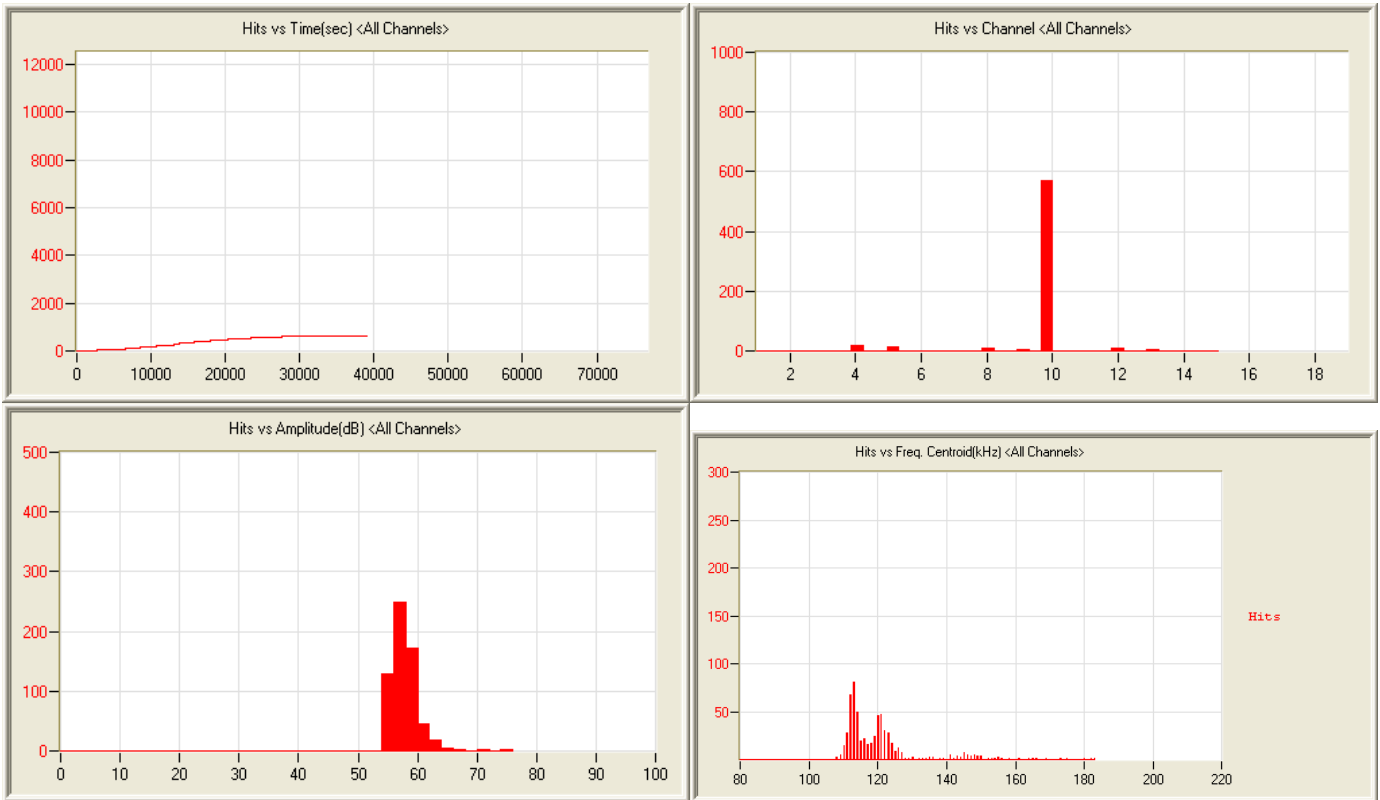
7/5/11 10:37am 0:38:54 4 110705103733_0 227kb



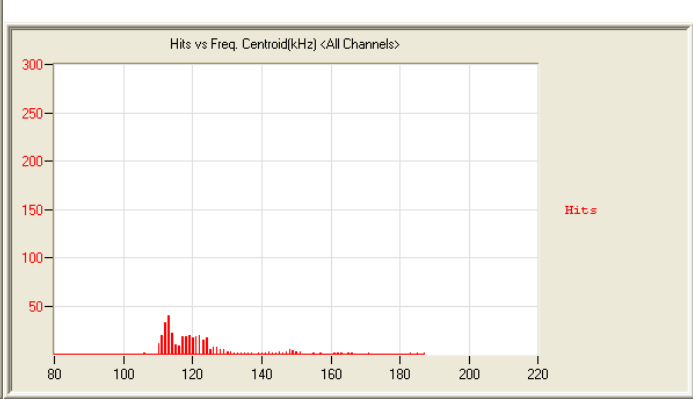
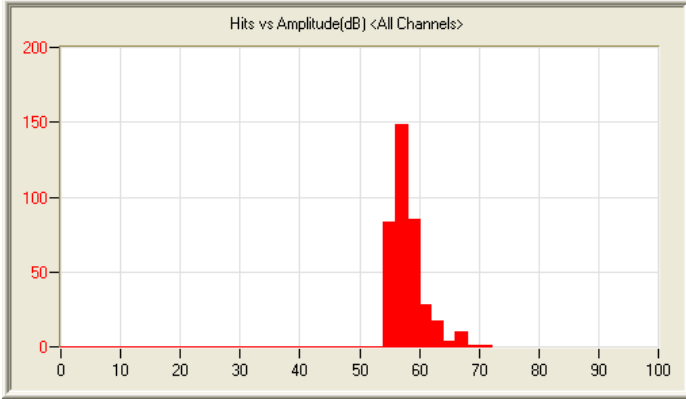
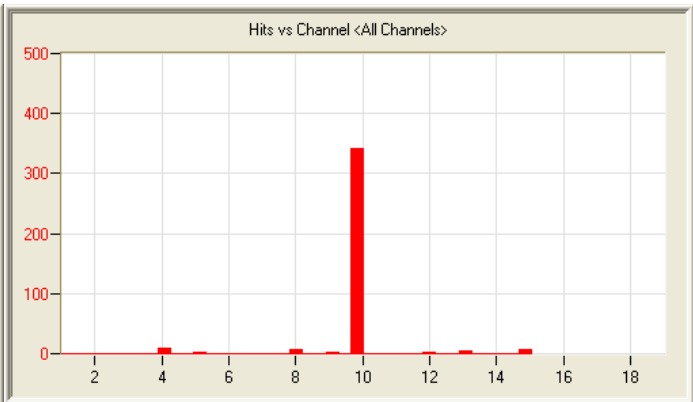
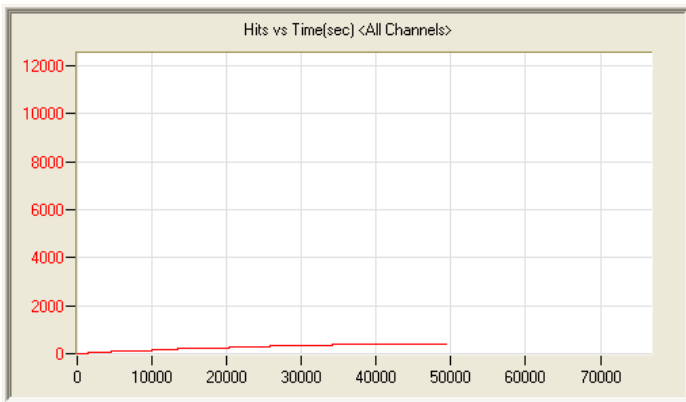
7/5/11 12:38pm 2:29:29 45 110705123811_0 702kb



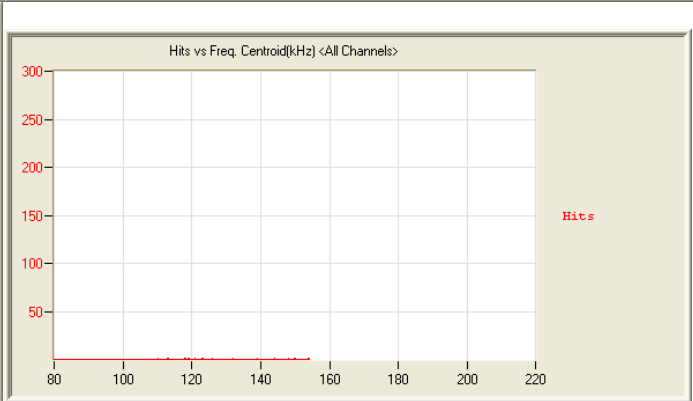
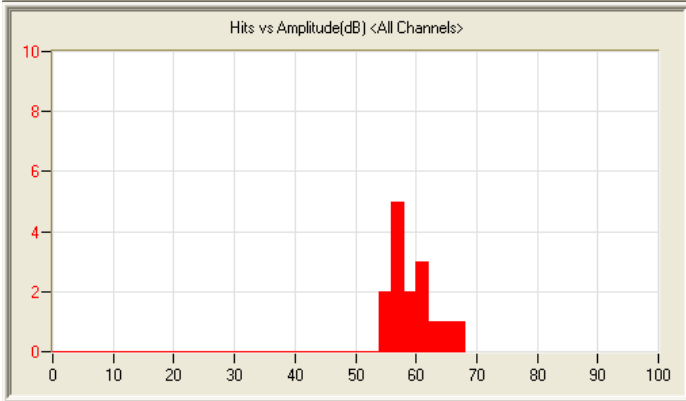
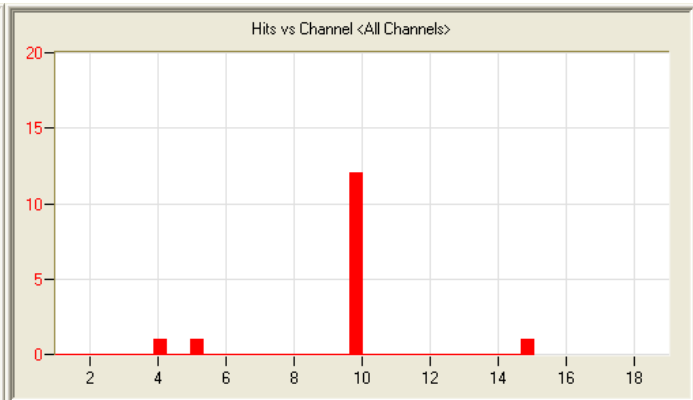
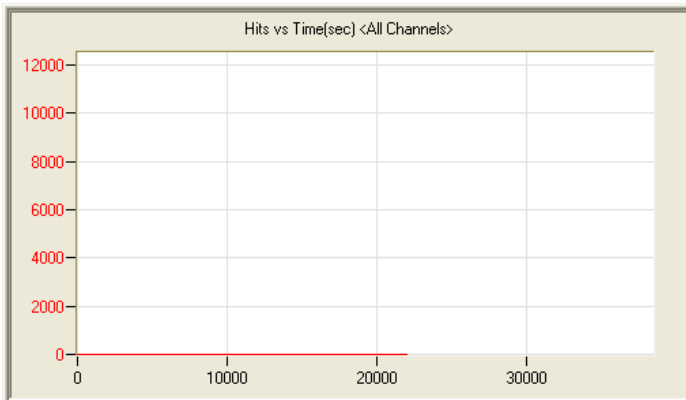
7/6/11 6:42am 0:49:51 18 110706064257_0 275kb



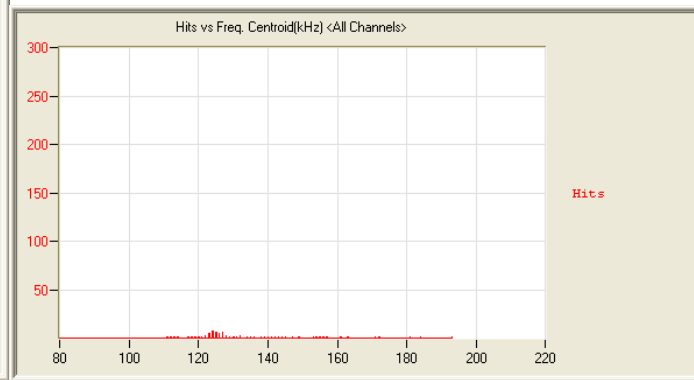
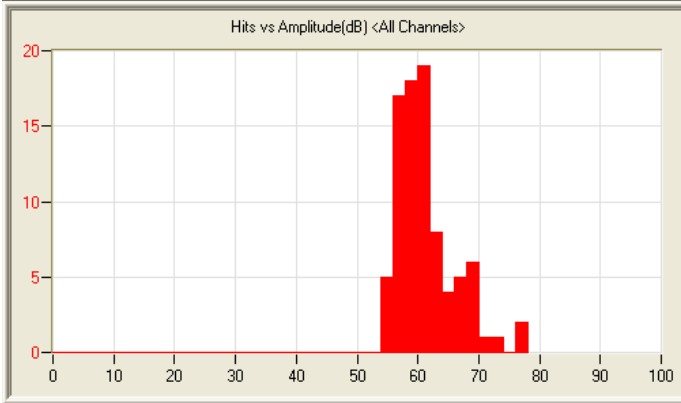
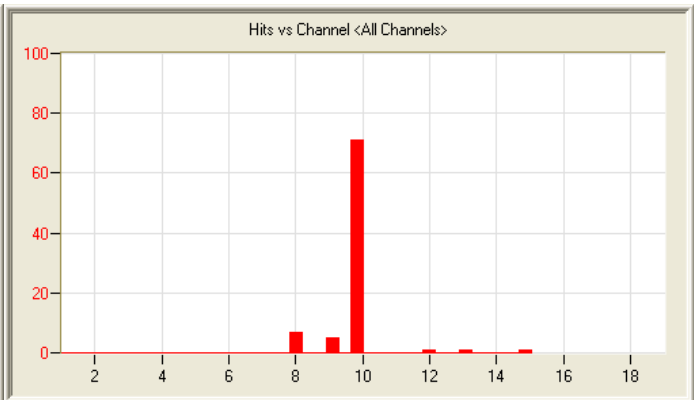
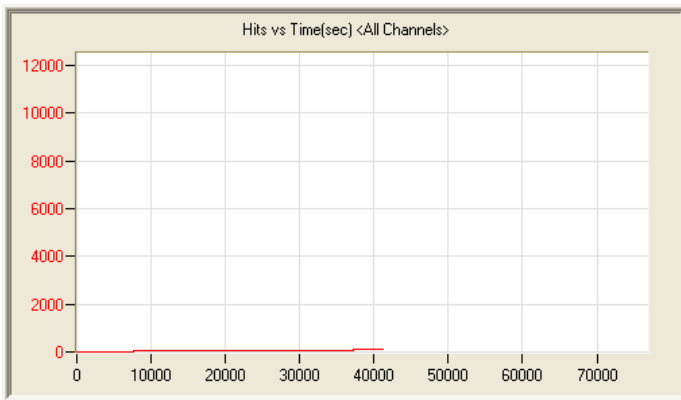
7/7/11 7:41am 11:05:37 627 110707074147_0 2.9mb



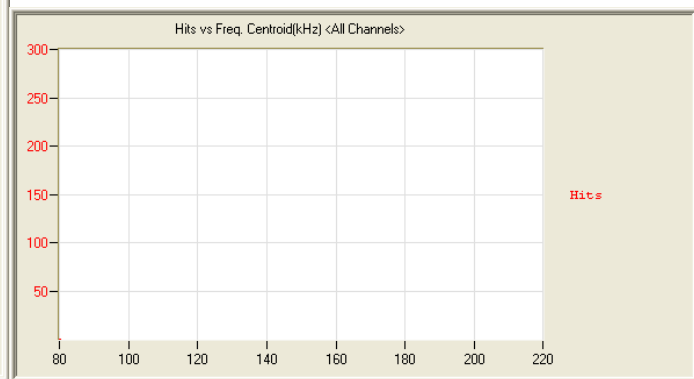
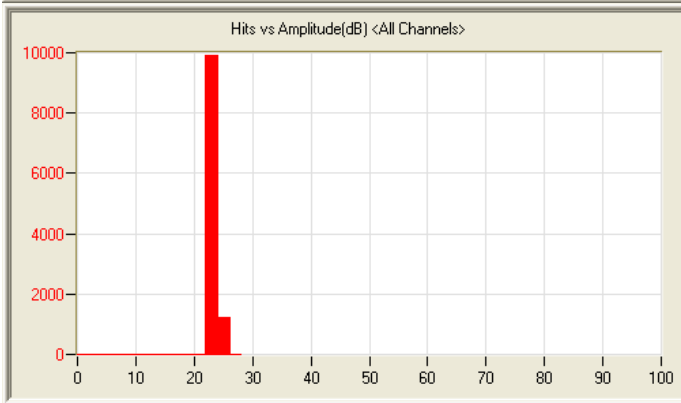
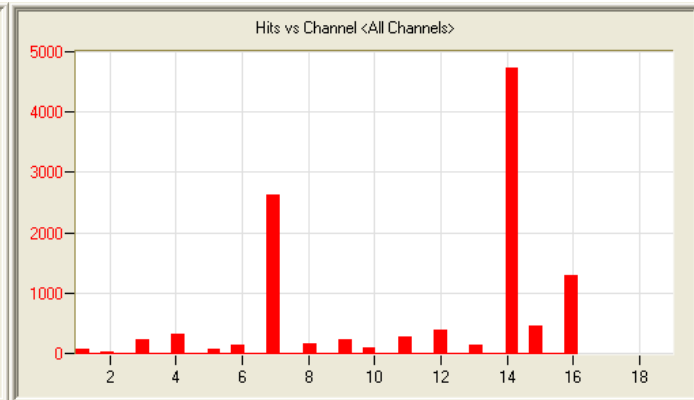
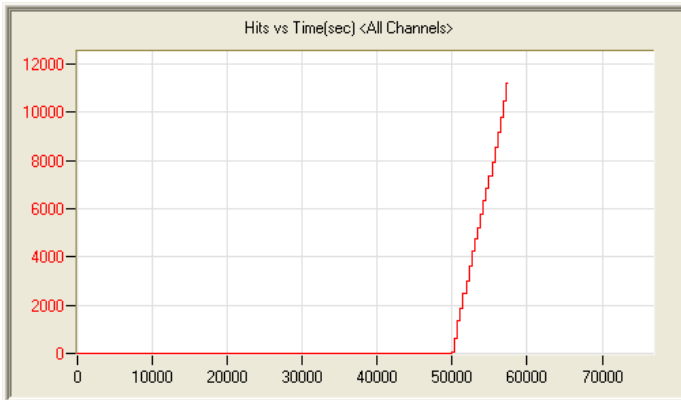
7/8/11 6:43am 15:39:23 377 110708064340_0 4.1mb



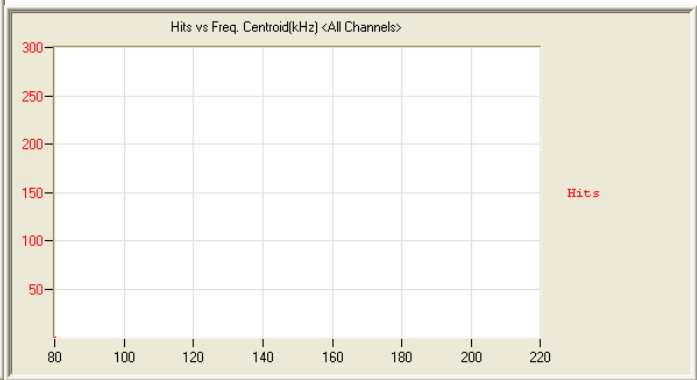
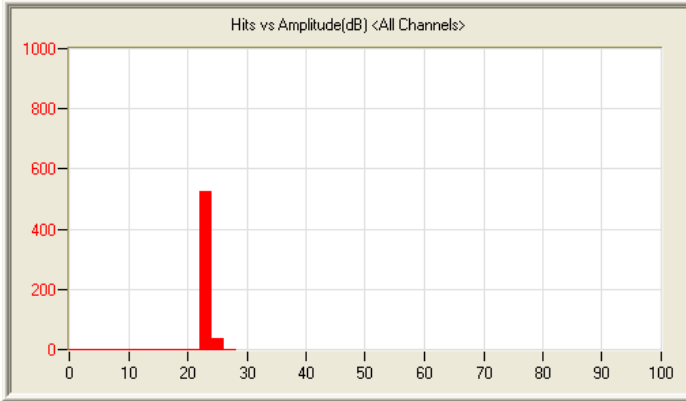
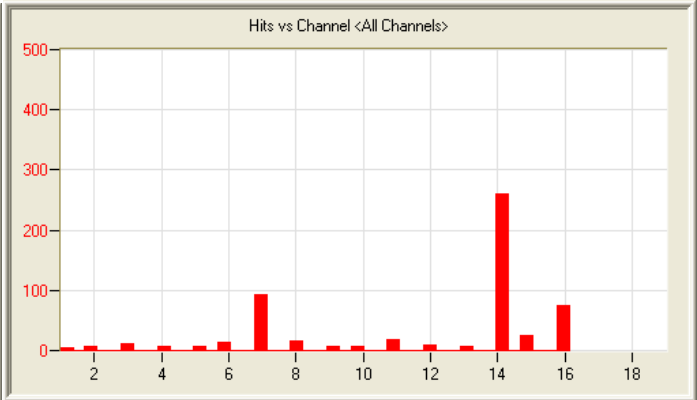
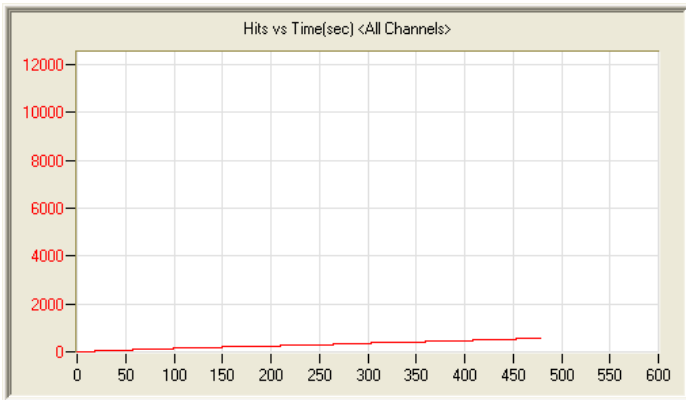
7/9/11 10:49am 7:06:02 15 110709104946_0 1.9mb



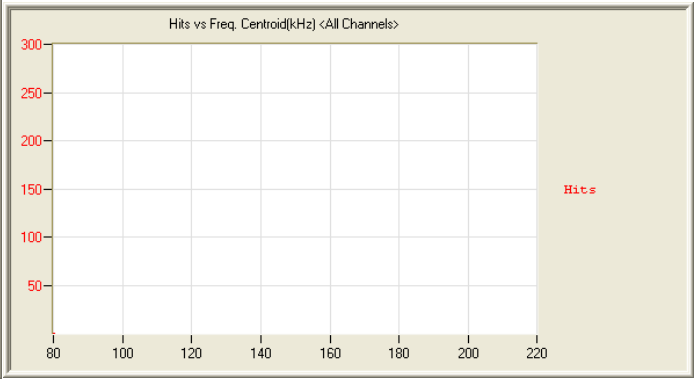
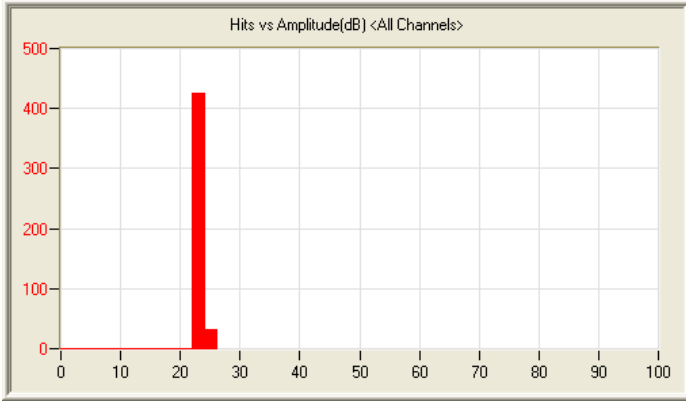
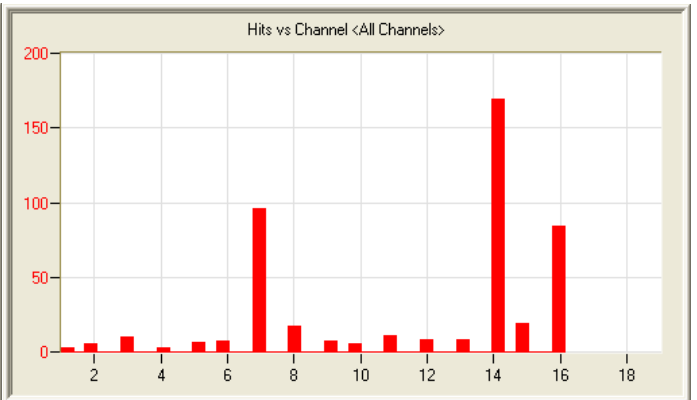
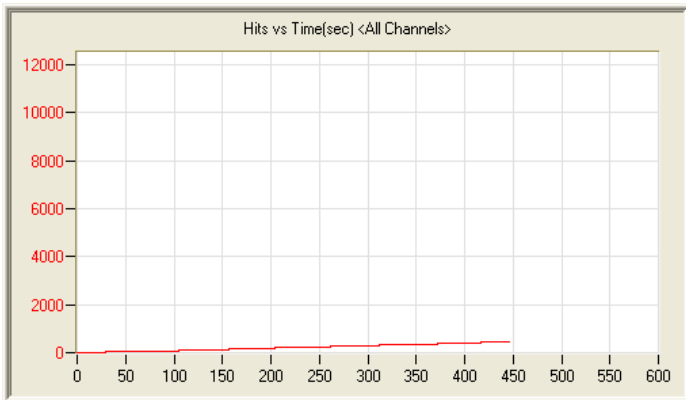
7/10/11 8:32am 11:41:10 86 110710083236_0 3.1mb



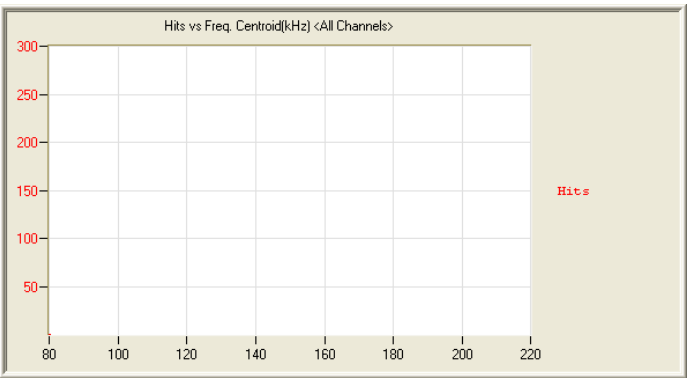
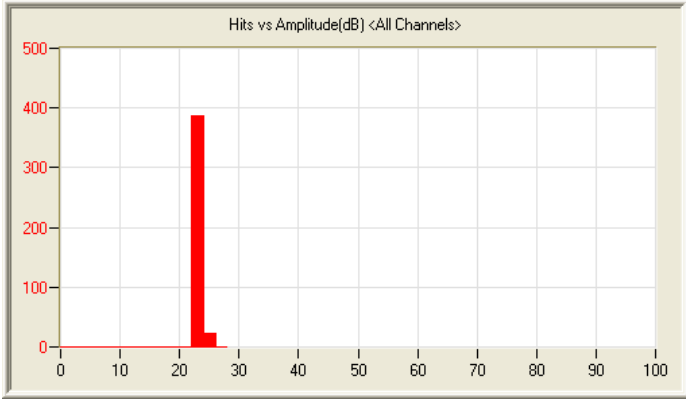
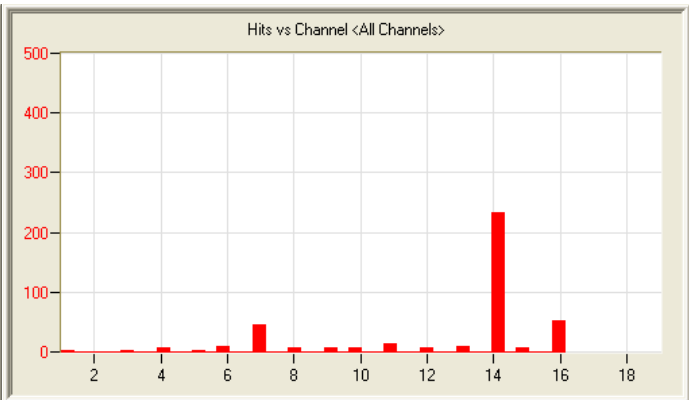
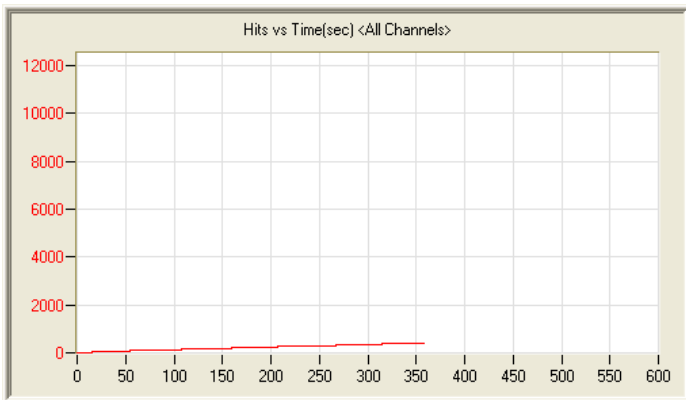
11/22/11 4:51pm 15:59:50 11171 111122165122_33 23mb



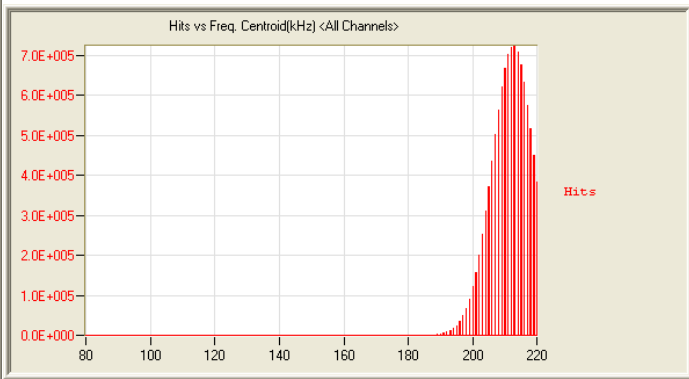
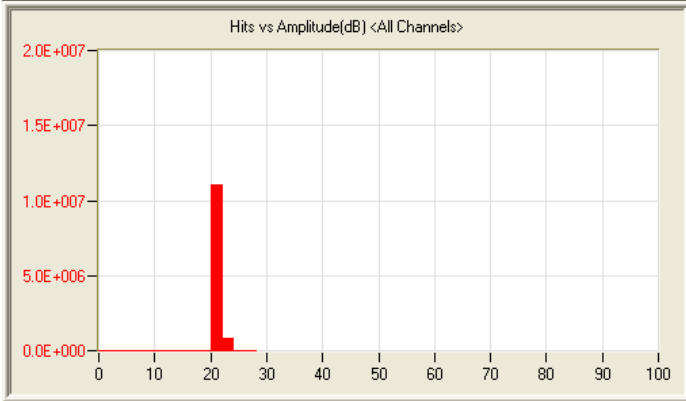
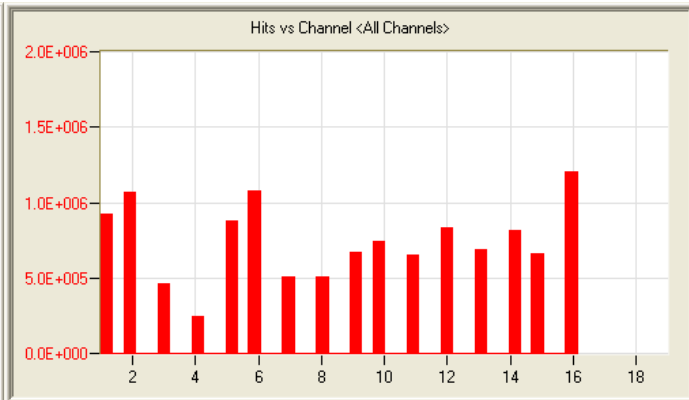
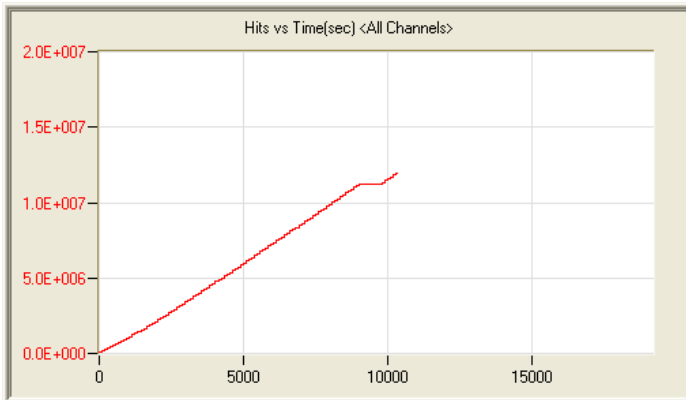
11/23/11 9:05am 0:07:57 566 111123090534_0 1.2mb



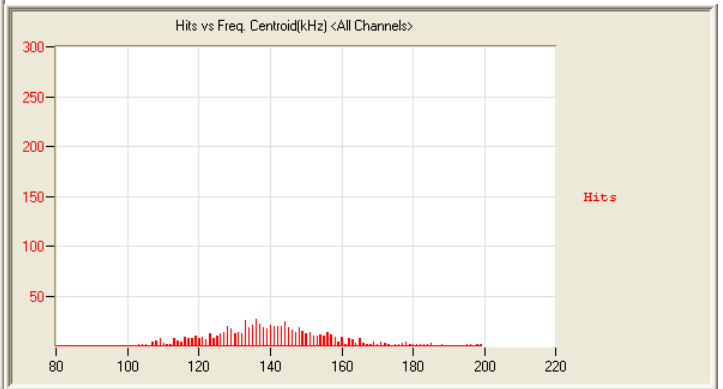
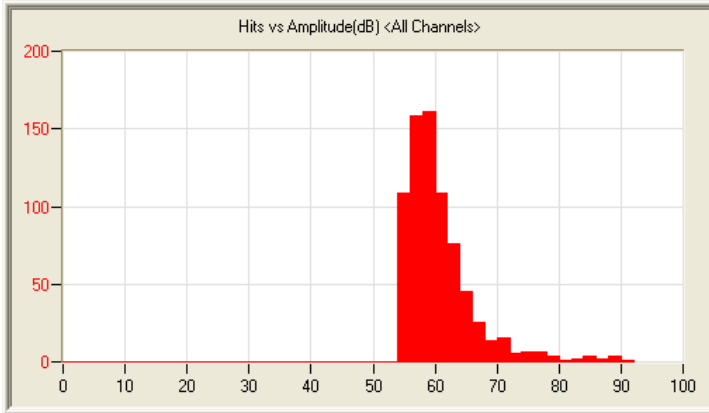
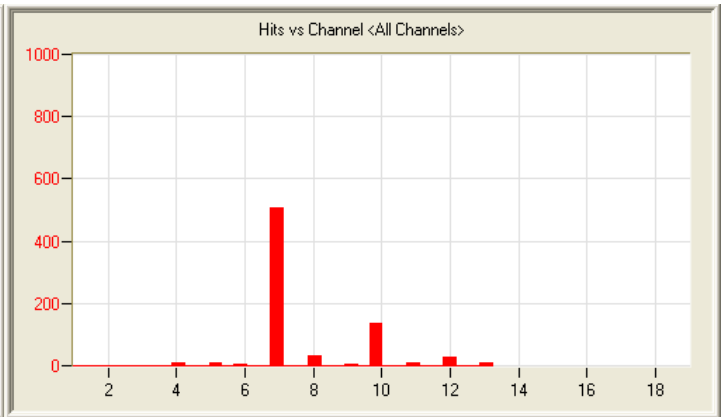
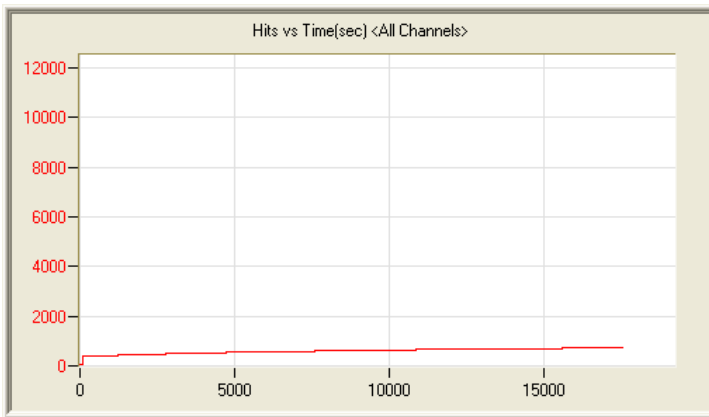
11/23/11 9:14am 0:07:25 458 111123091454_0 1.0mb



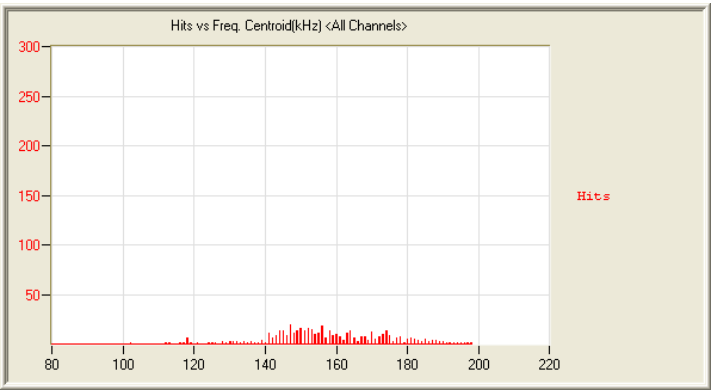
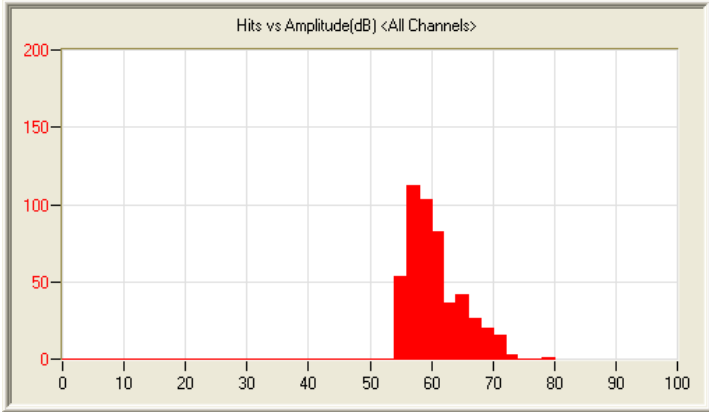
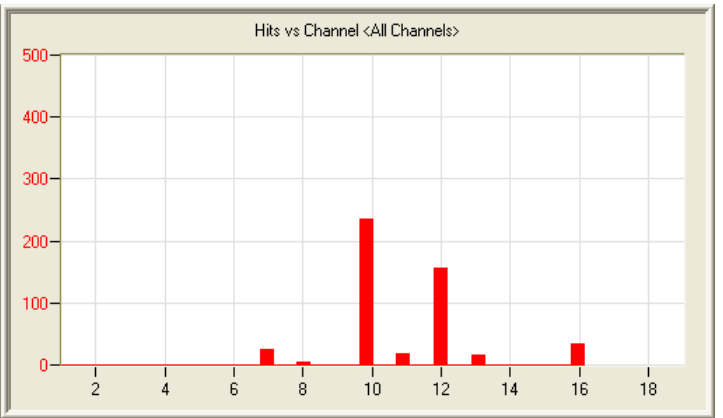
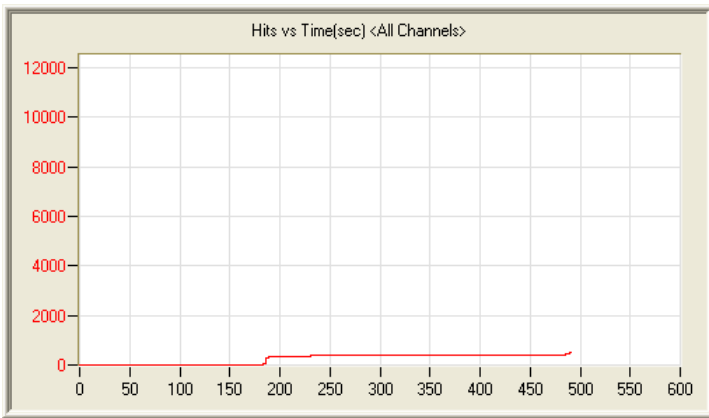
11/23/11 9:28am 0:05:57 411 111123092802_0 917kb



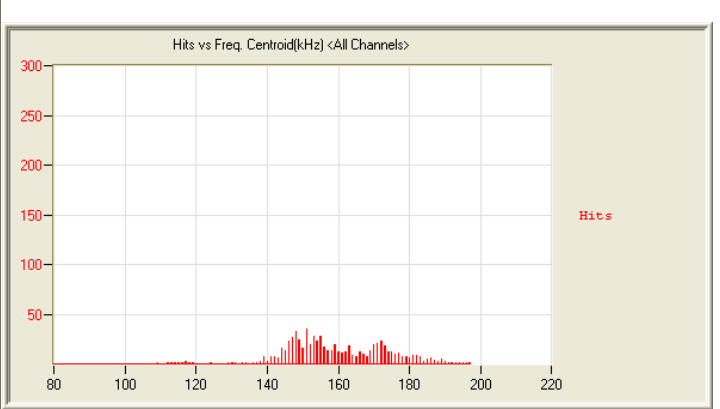
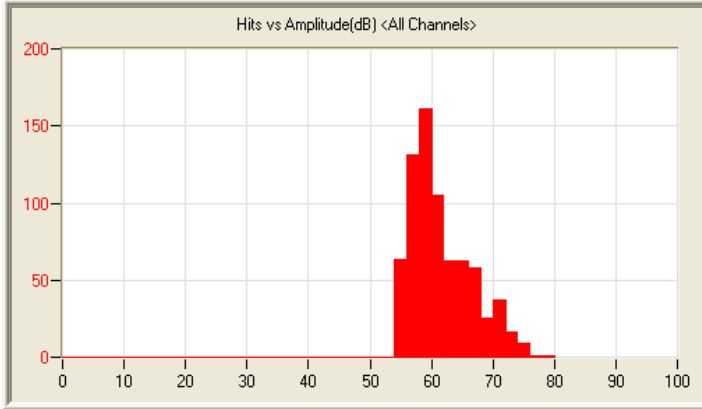
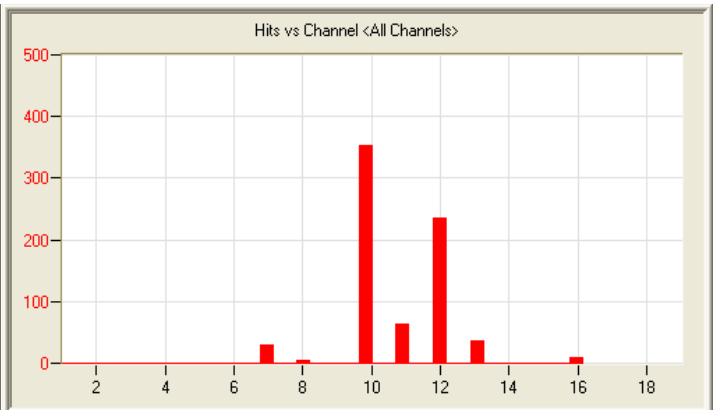
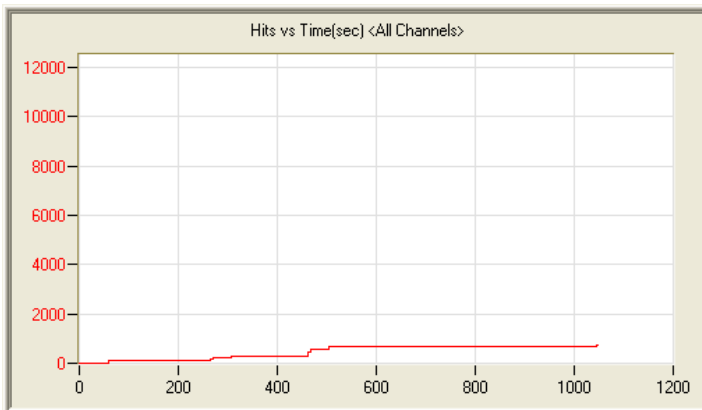
11/23/11 10:07am 2:52:13 11923537 111123100748_0 480.2mb



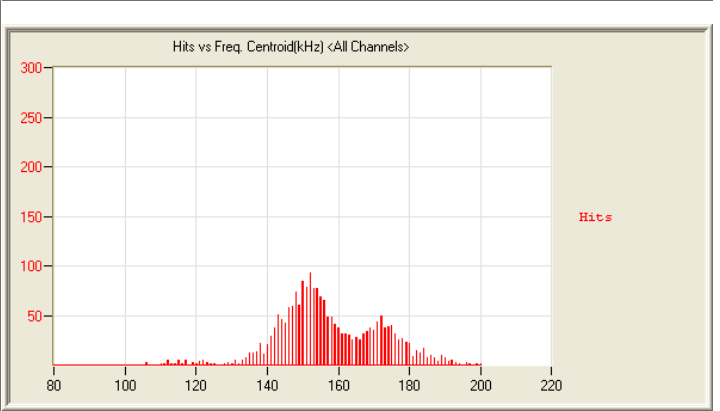
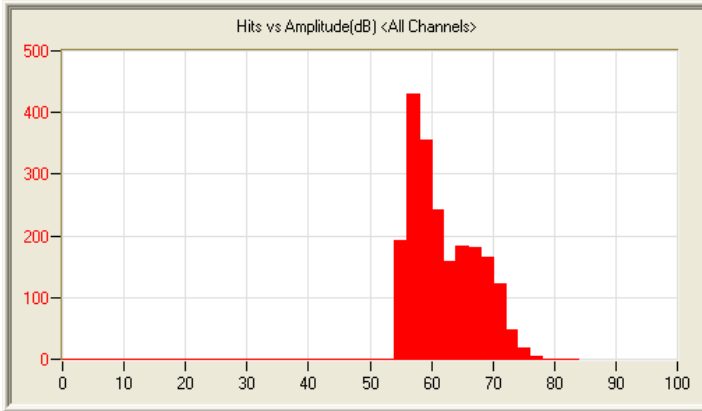
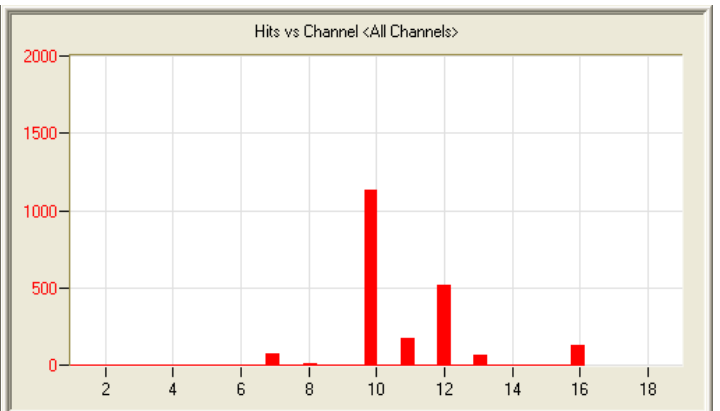
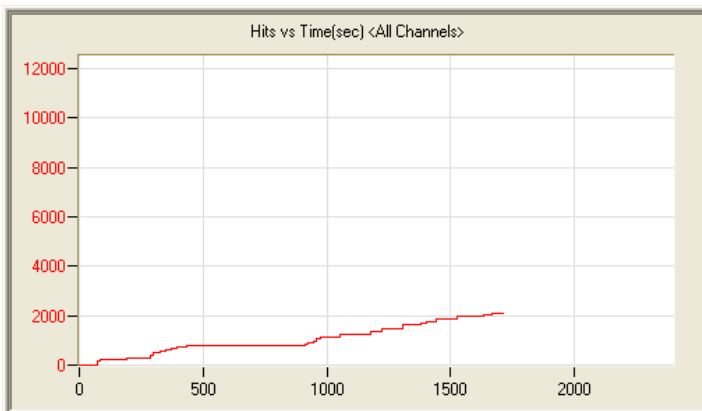
1/26/12 11:17am 4:53:20 747 120126111753_0 801kb



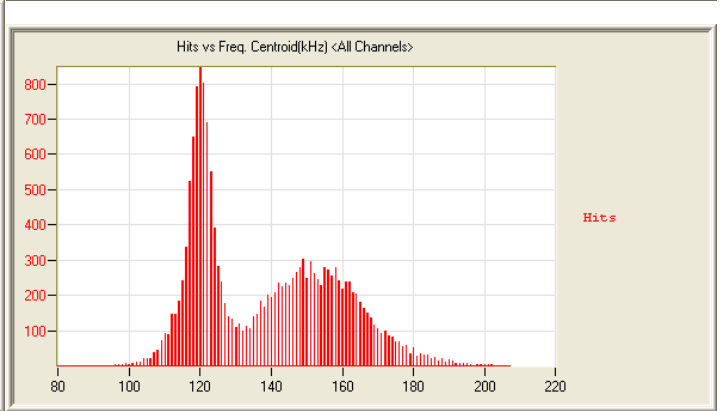
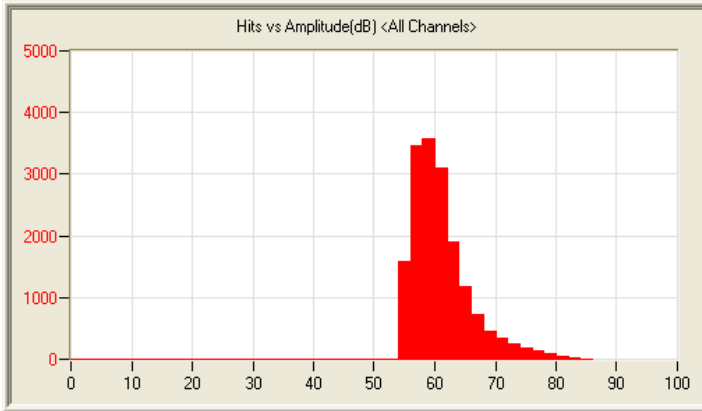
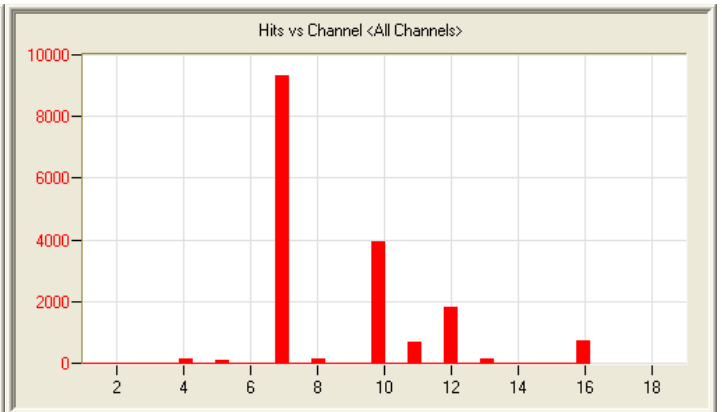
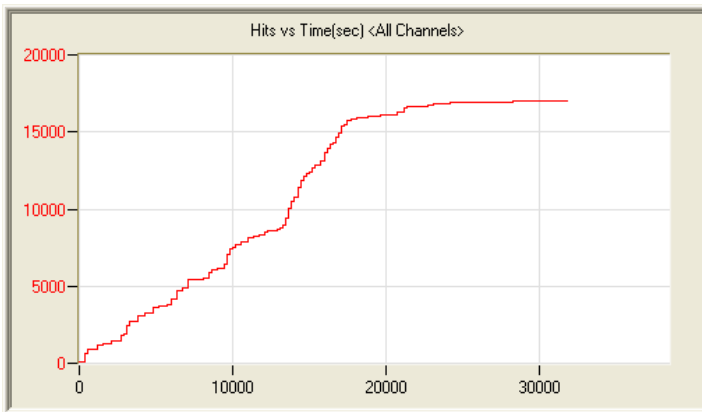
1/27/12 7:43am 0:08:10 493 120127074310_0 106kb



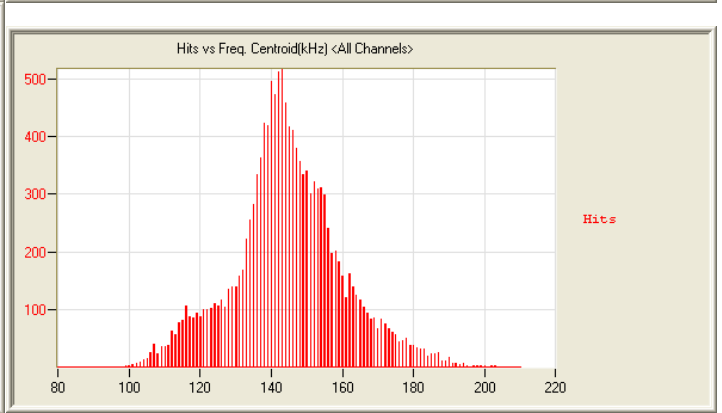
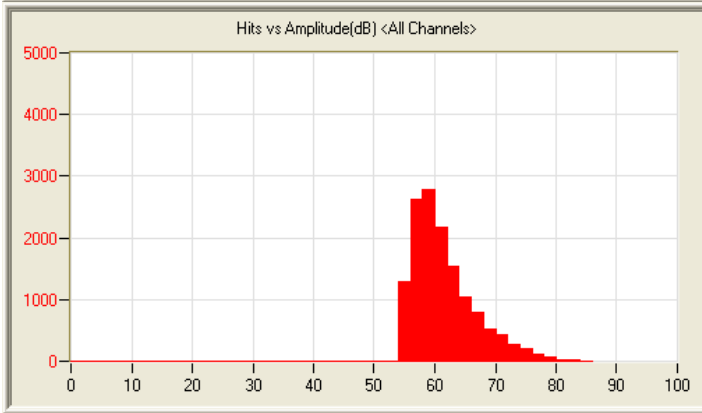
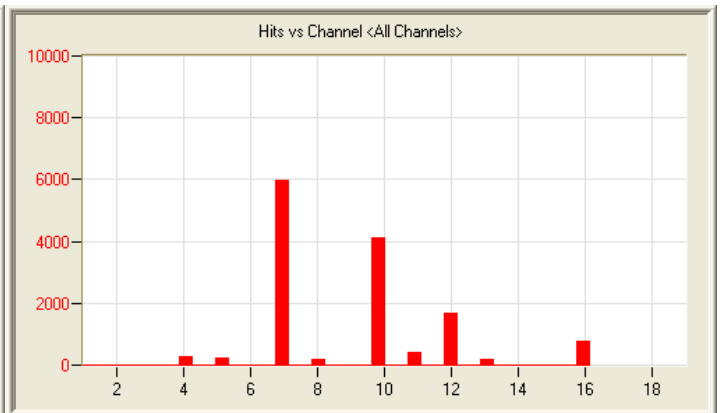
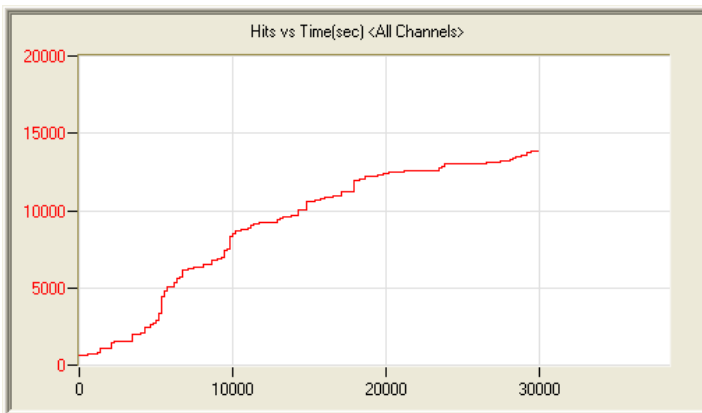
1/27/12 8:14am 0:18:40 731 120127081411_0 140kb



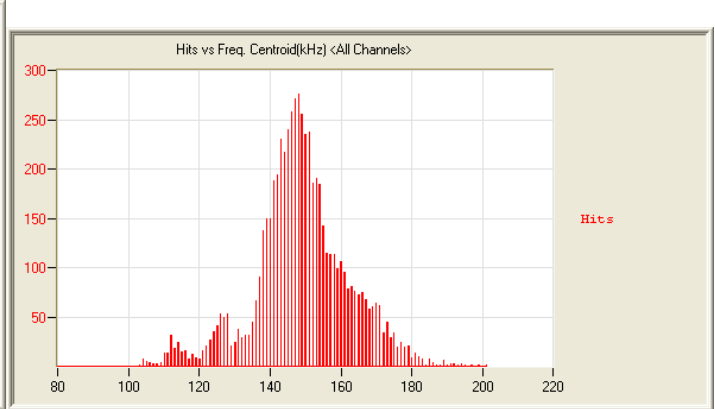
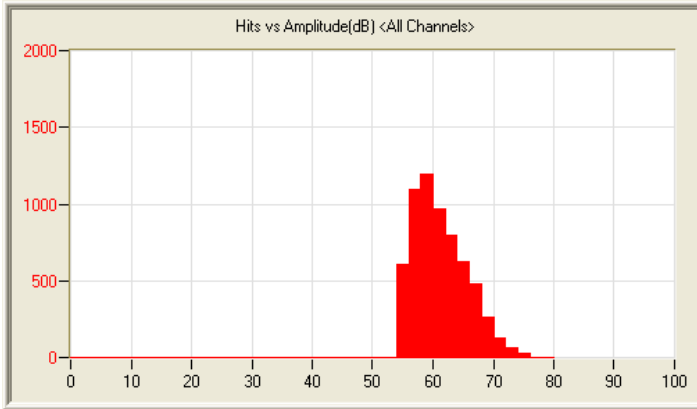
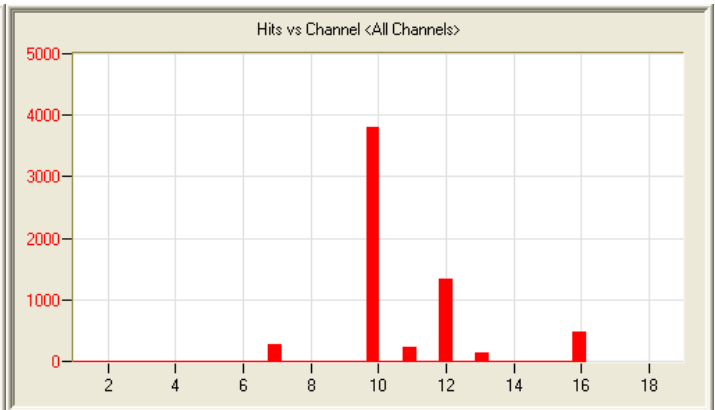
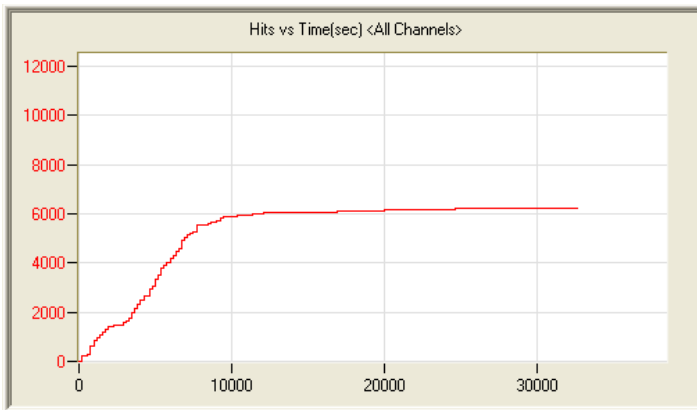
1/27/12 8:56am 0:31:00 2104 120127085617_0 225kb



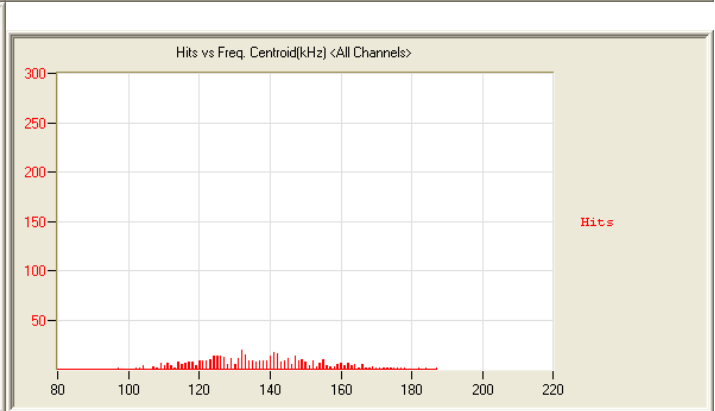
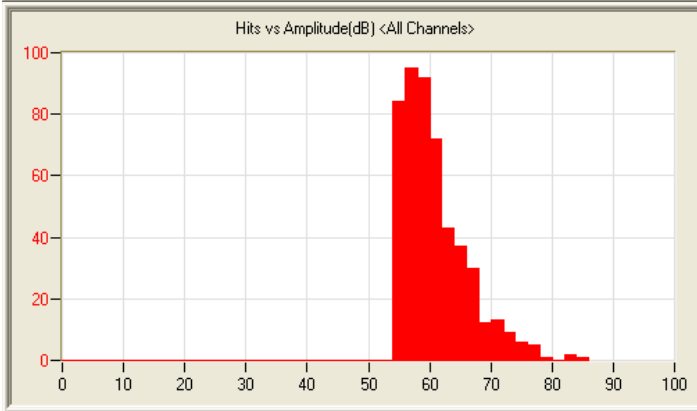
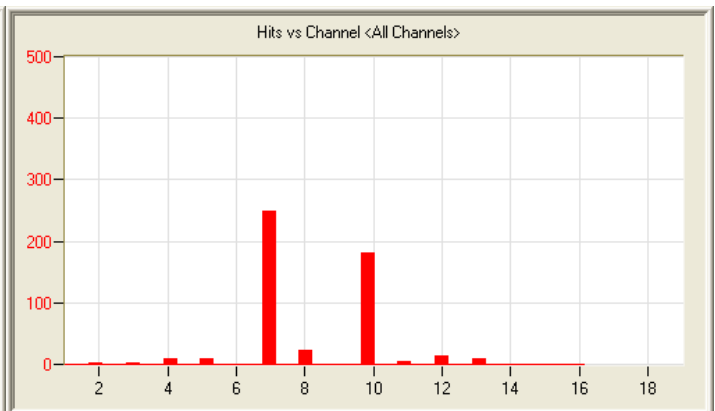
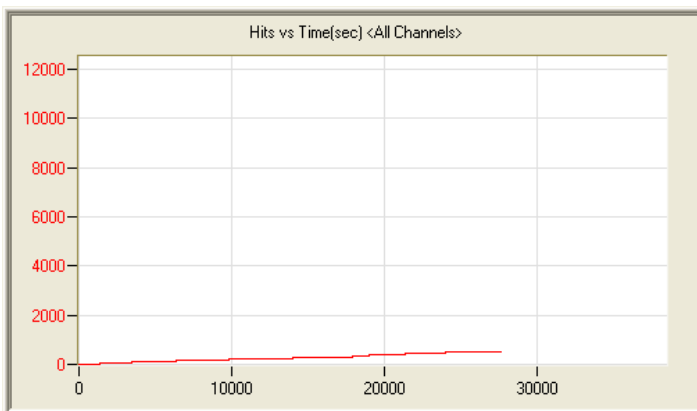
1/28/12 6:53am 9:07:56 17044 120128065307_0 2.1mb



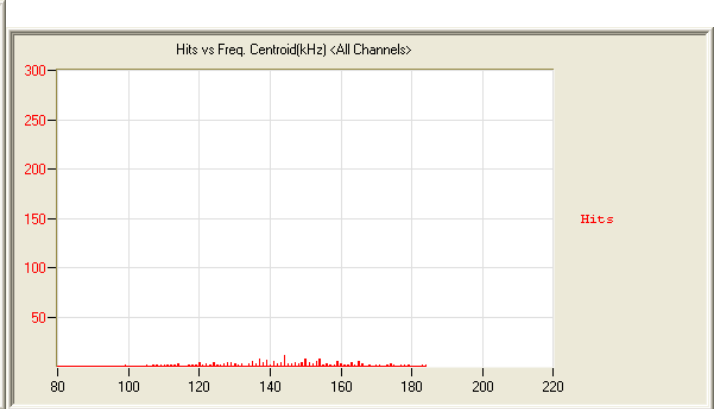
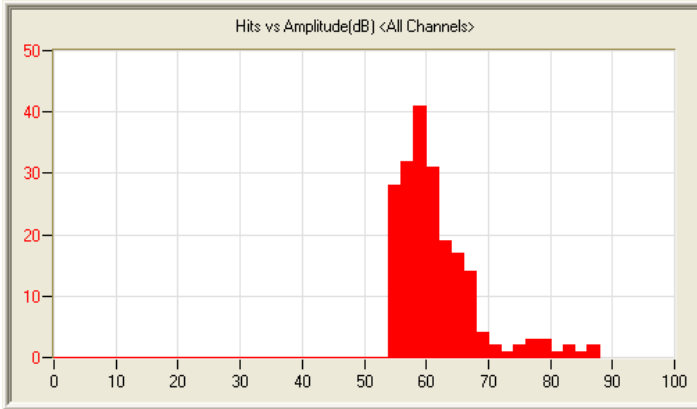
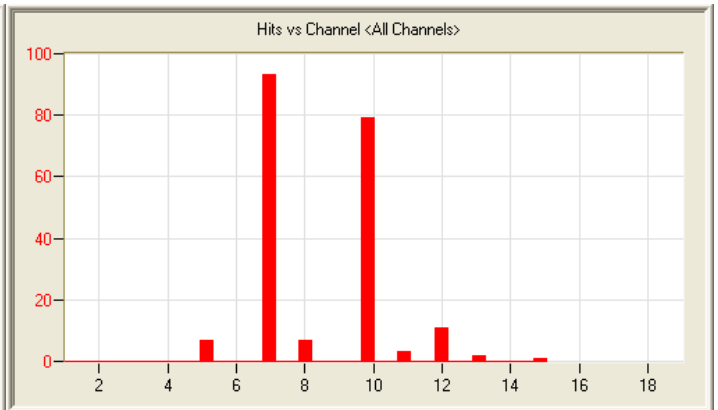
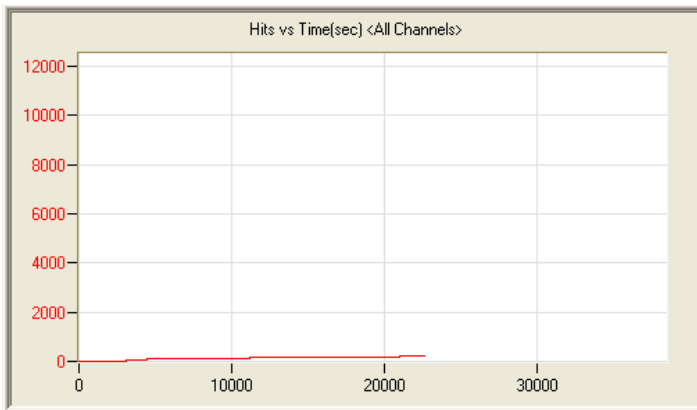
1/29/12 6:53am 8:16:29 13884 120129065321_0 1.8mb



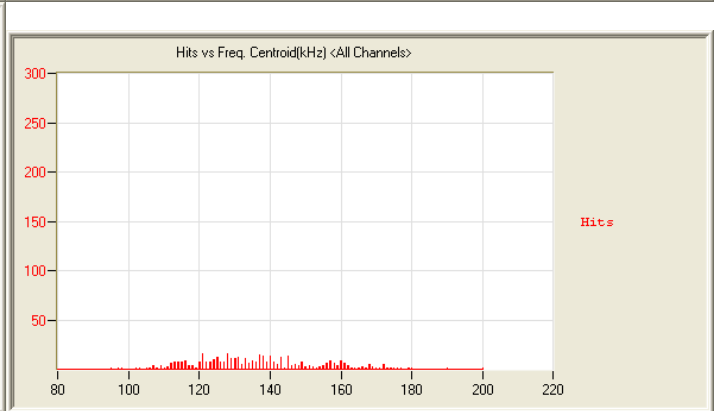
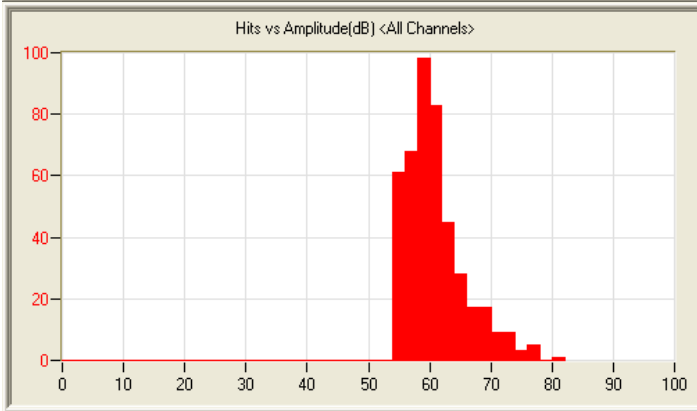
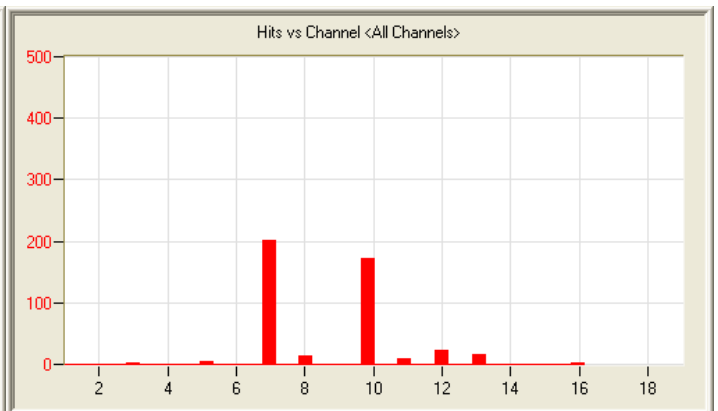
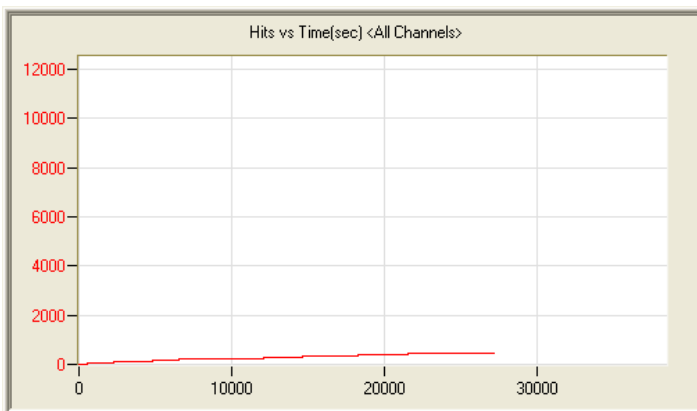
1/30/12 6:59am 9:02:56 6247 120130065927_0 1.6mb



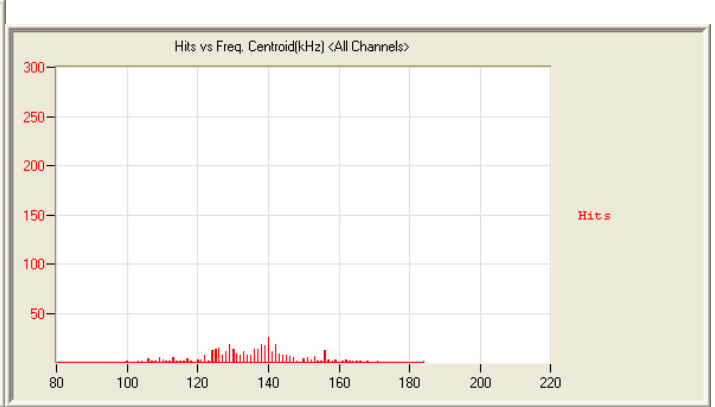
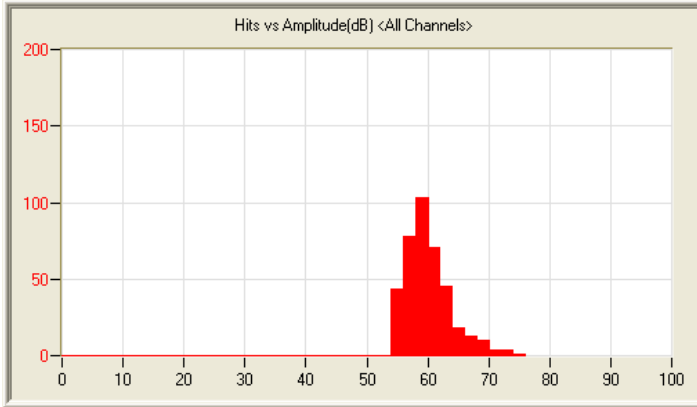
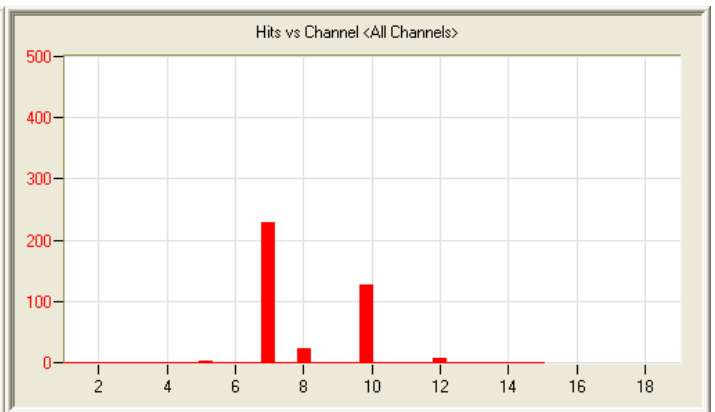
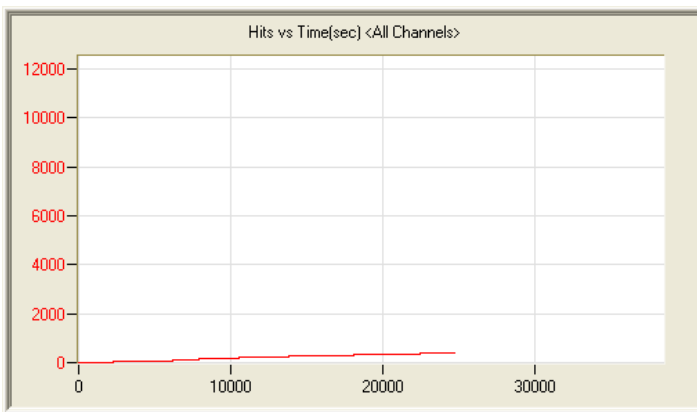
1/31/12 7:36am 7:44:22 502 120131073641_0 1.2mb



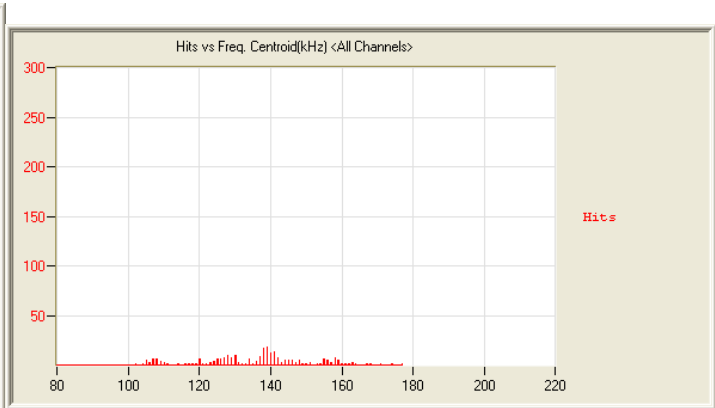
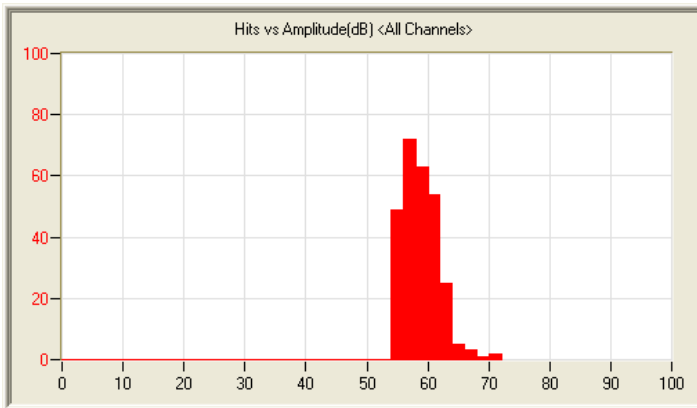
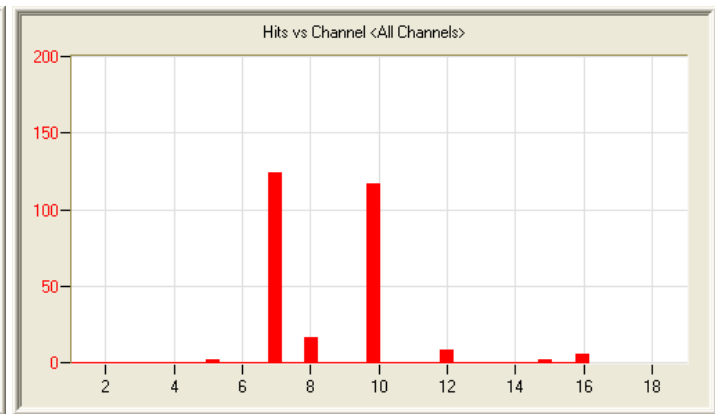
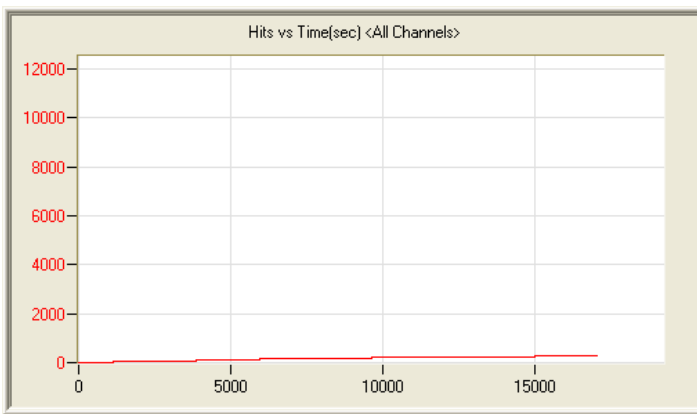
2/4/12 9:49am 6:17:34 203 120204094911_0 981kb



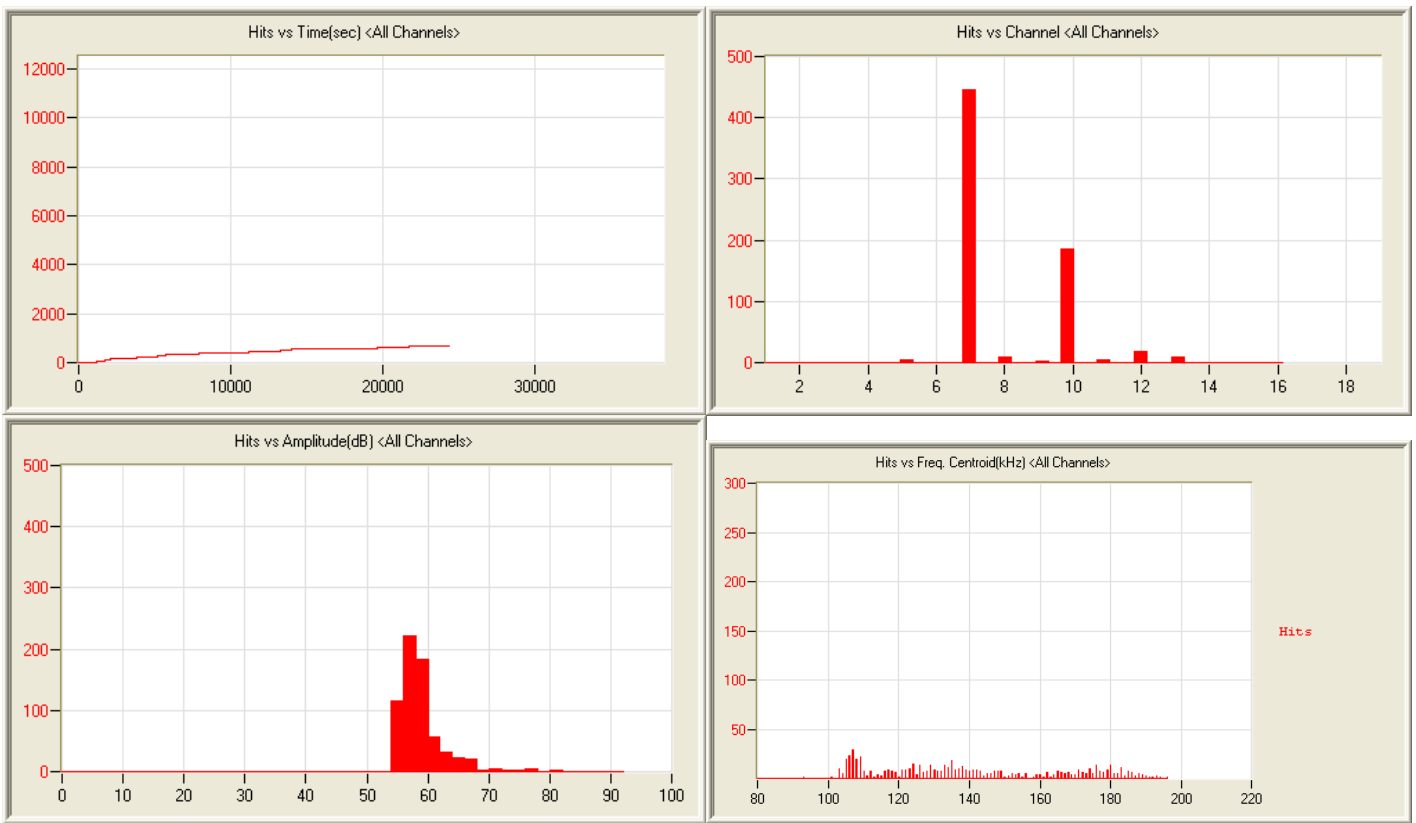
2/6/12 6:42am 7:35:35 444120206064223_0 1.2mb



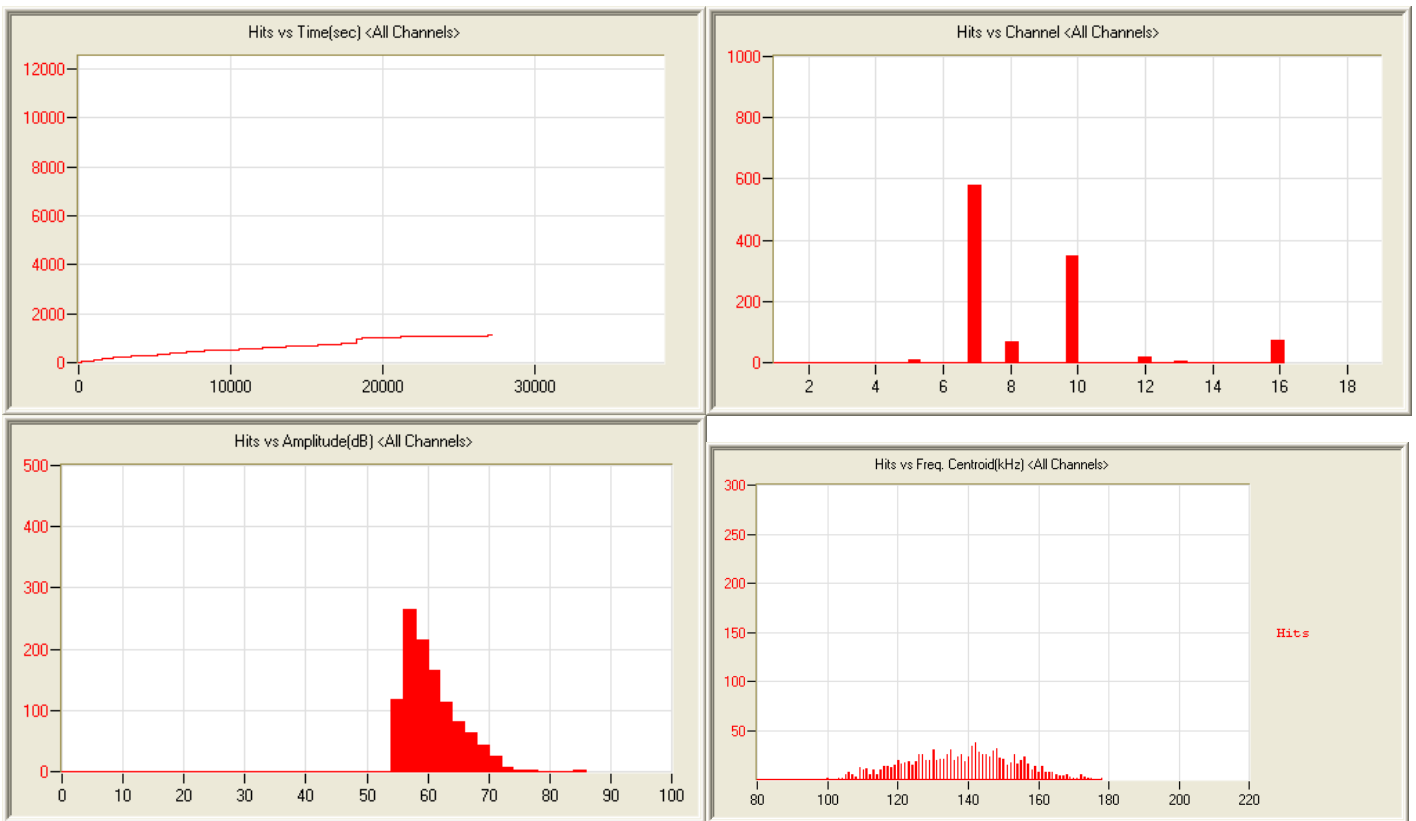
2/7/12 9:12am 6:55:26 390 120207091217_0 1.1mb



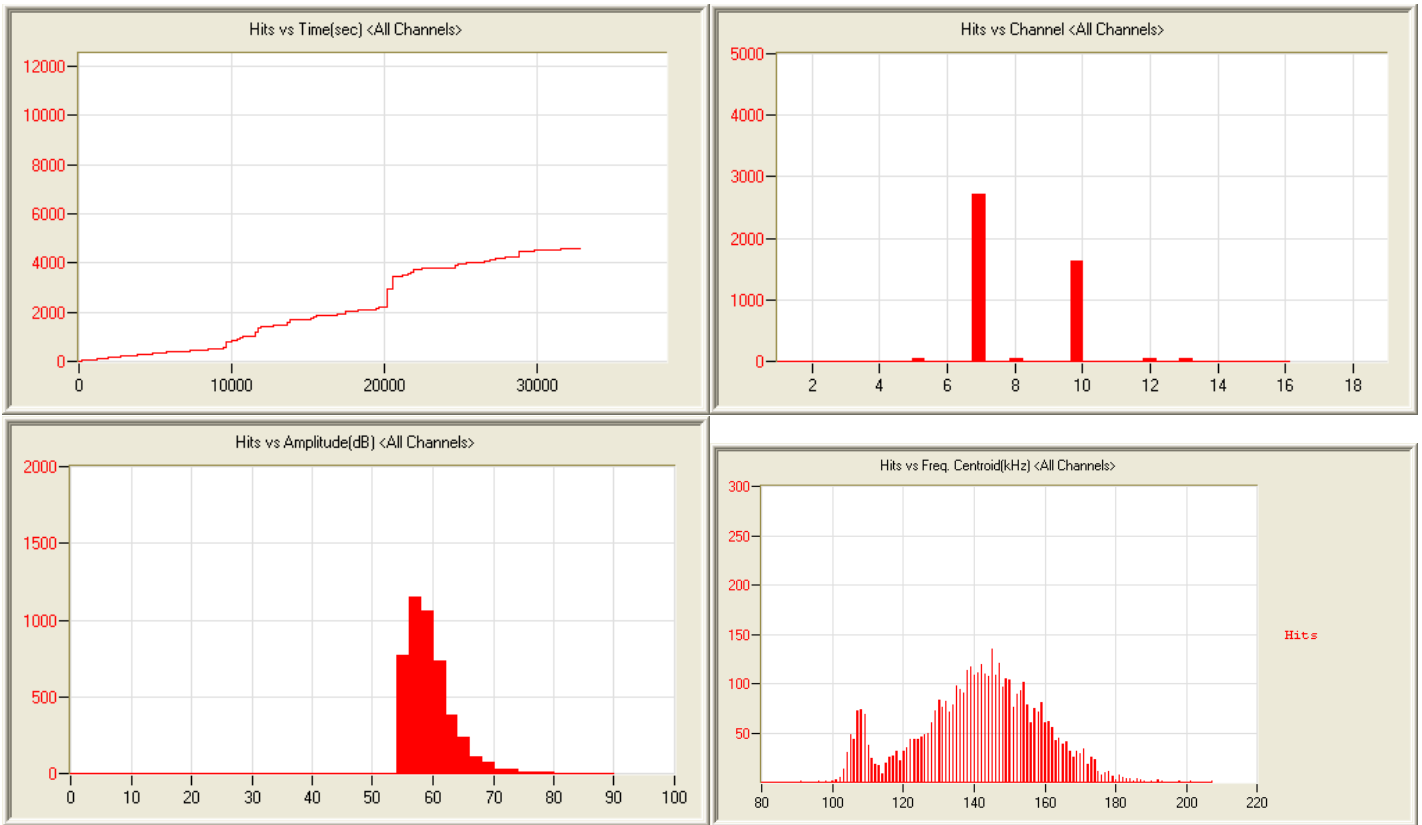
2/13/12 9:21am 4:44:21 274 120213092139_0 760kb



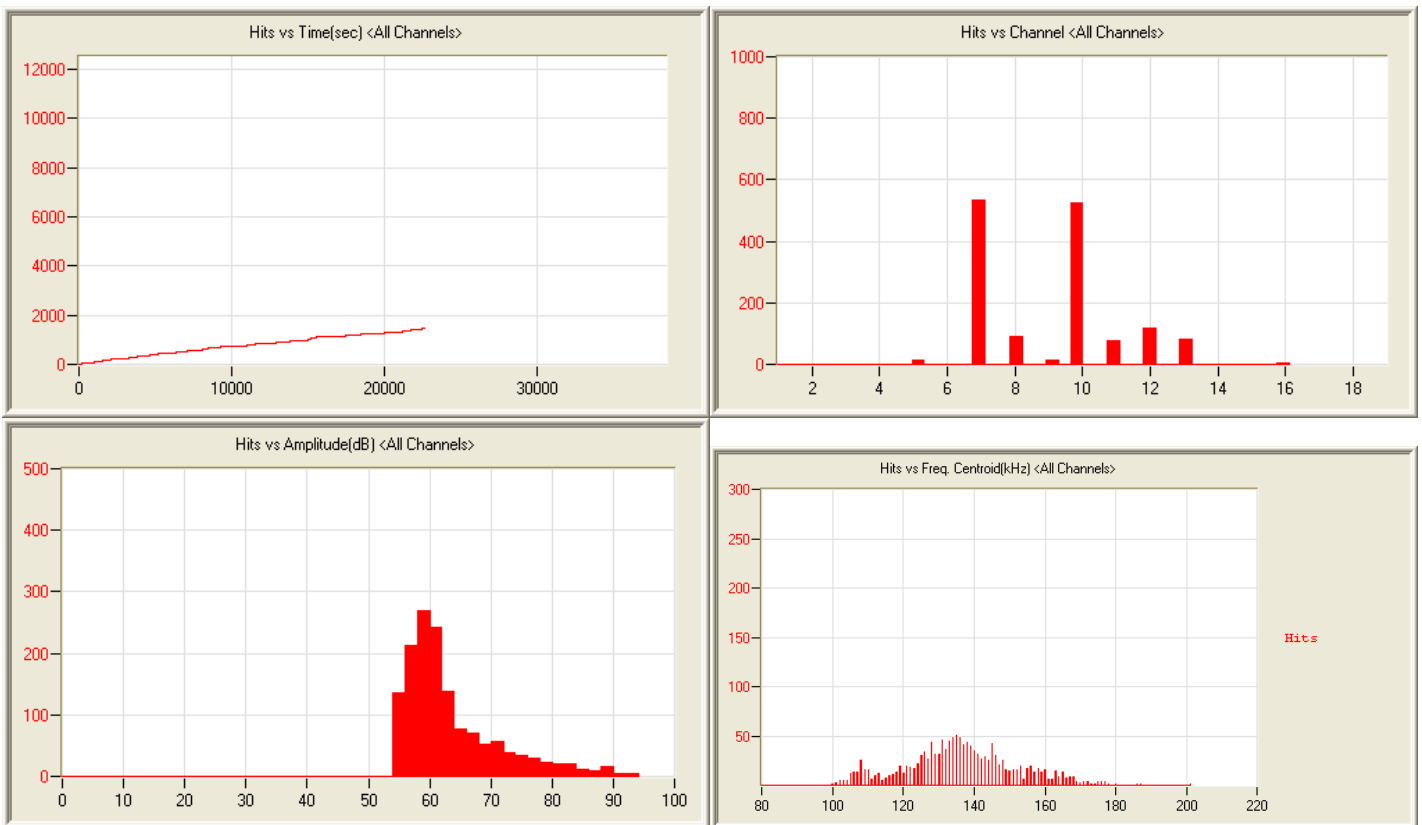
2/14/12 9:18 6:46:27 678 120214091830_0 1.1mb



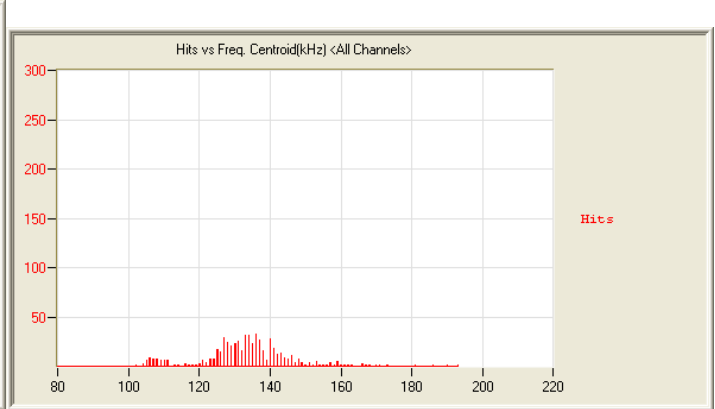
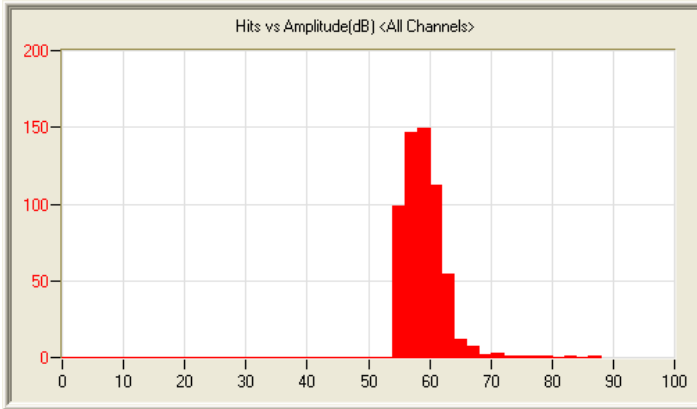
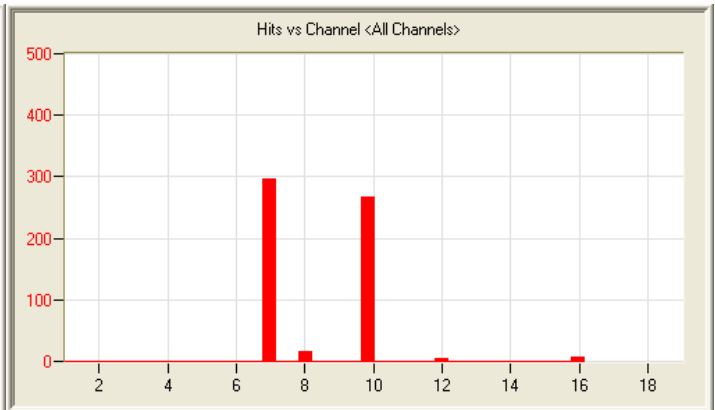
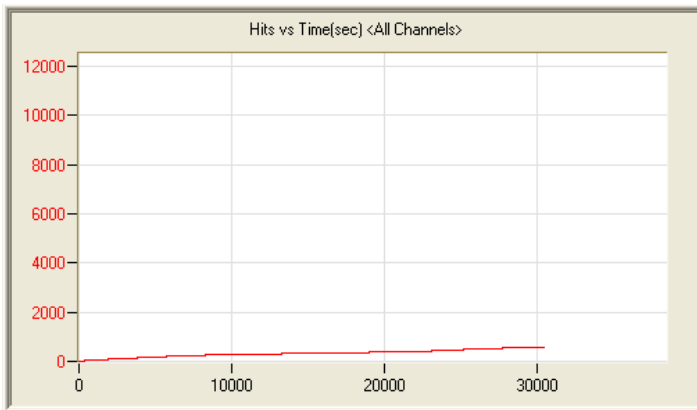
2/16/12 7:10am 7:40:24 1104 120216071004_0 1.2mb



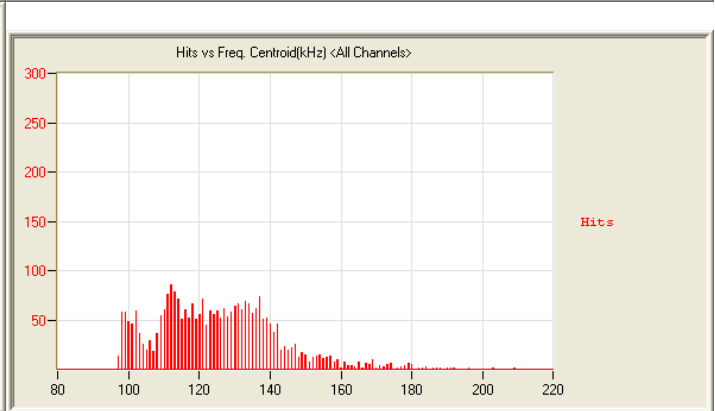
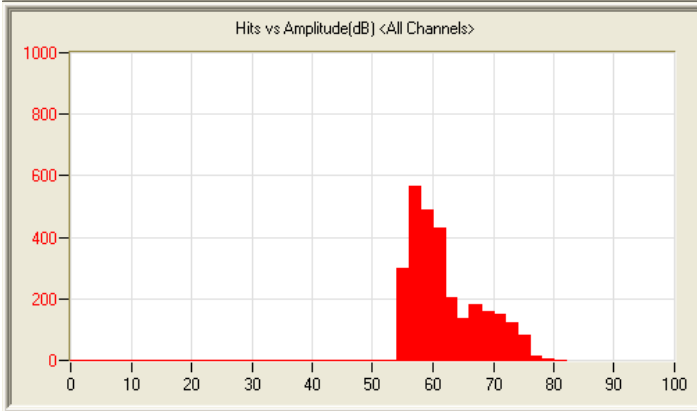
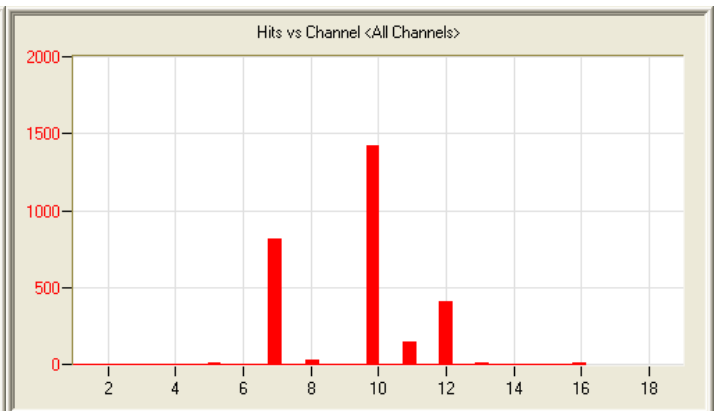
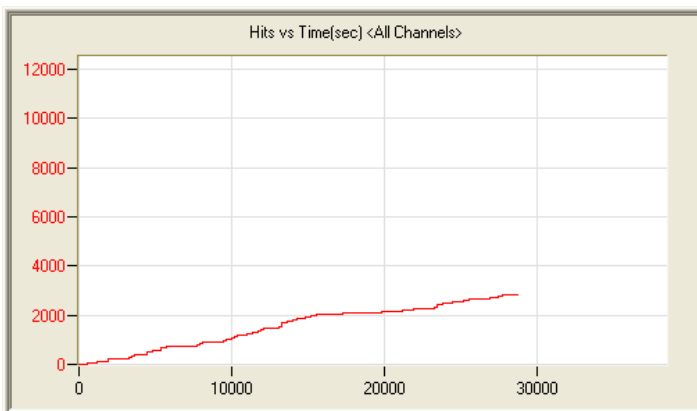
2/20/12 7:17am 9:09:15 4572 120220071719_0 1.6mb



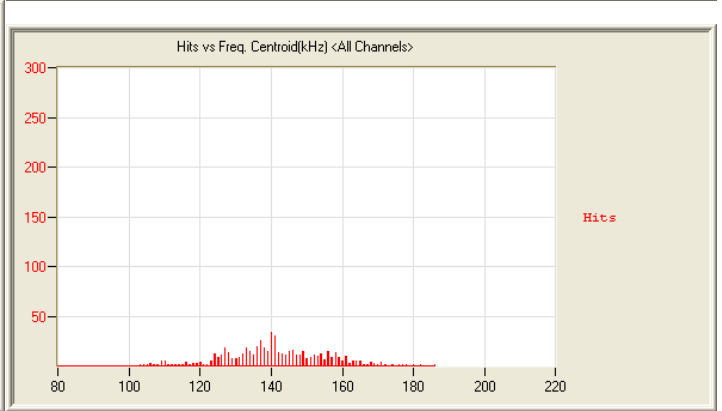
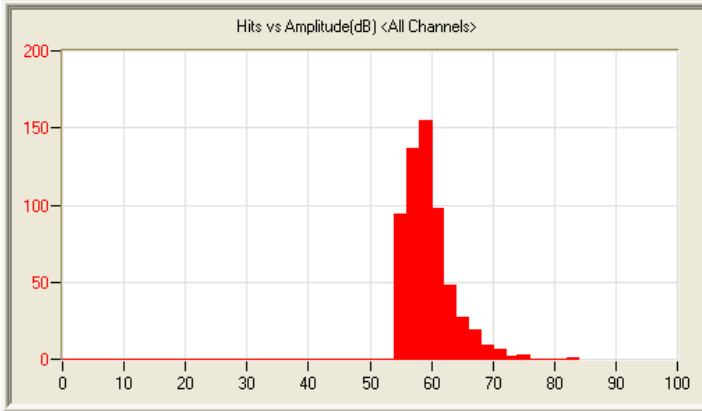
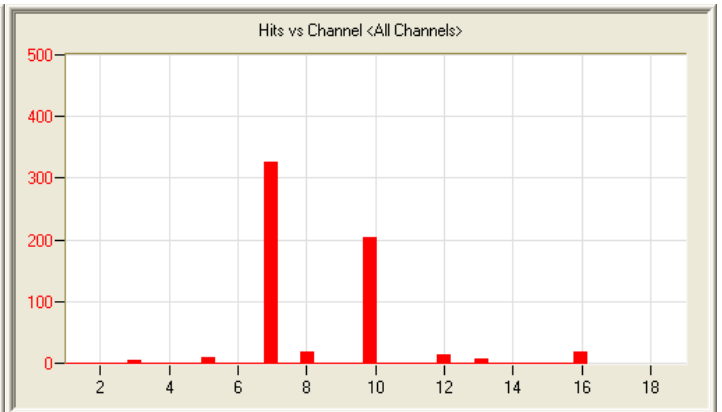
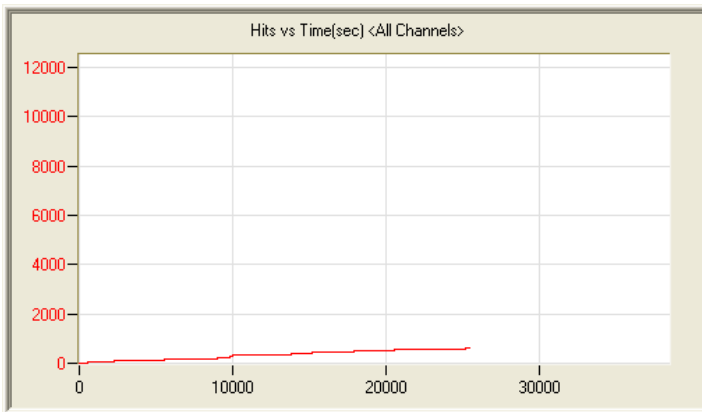
2/21/12 7:03am 6:17:11 1462 120221070324_0 1.0mb



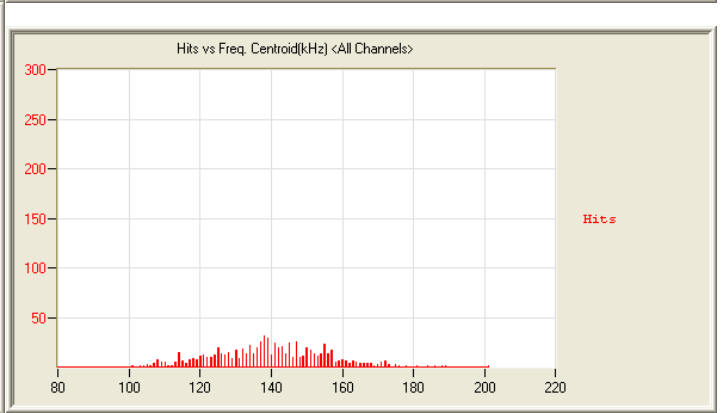
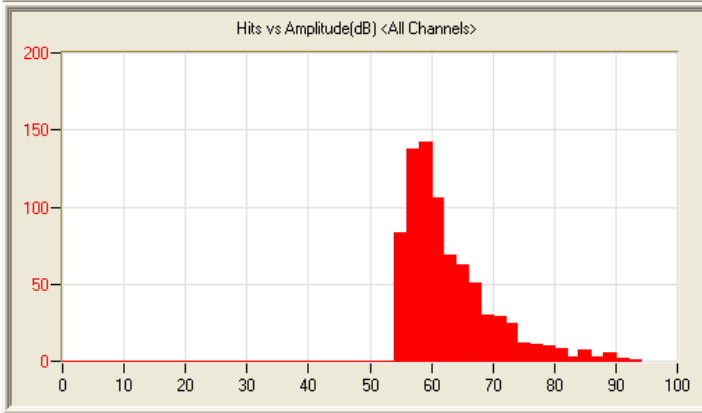
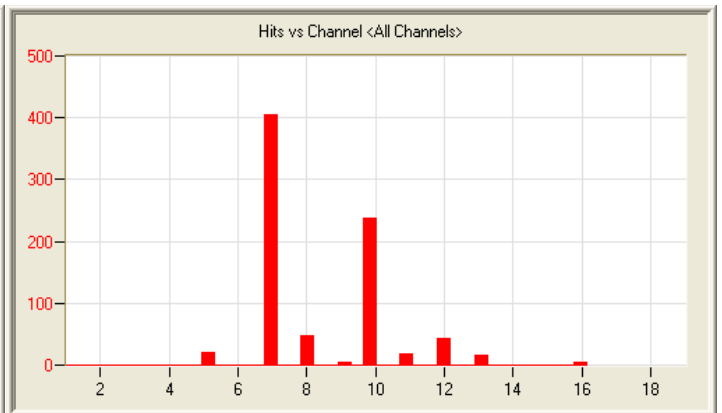
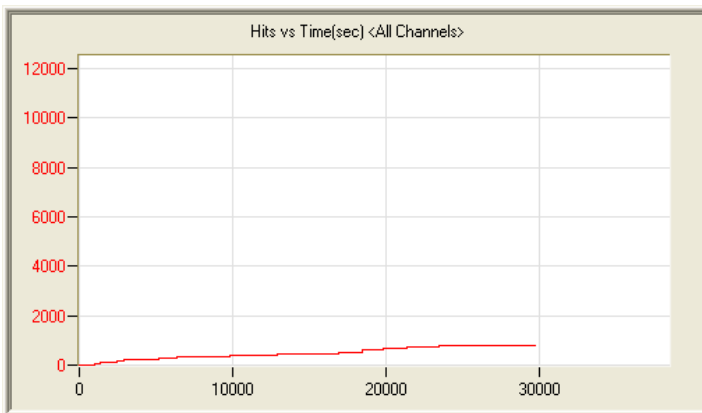
2/23/12 7:13am 8:28:48 591 120223071355_0 1.3mb



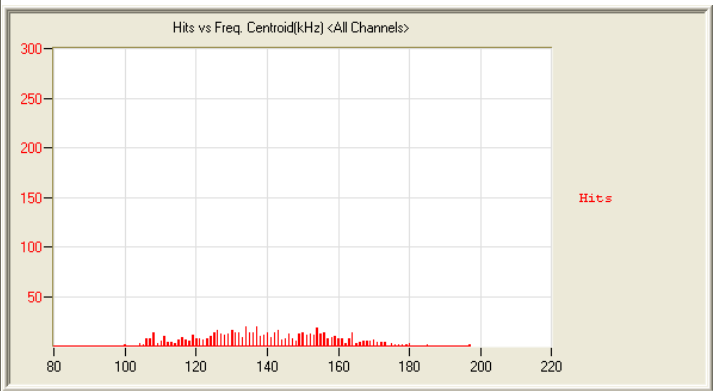
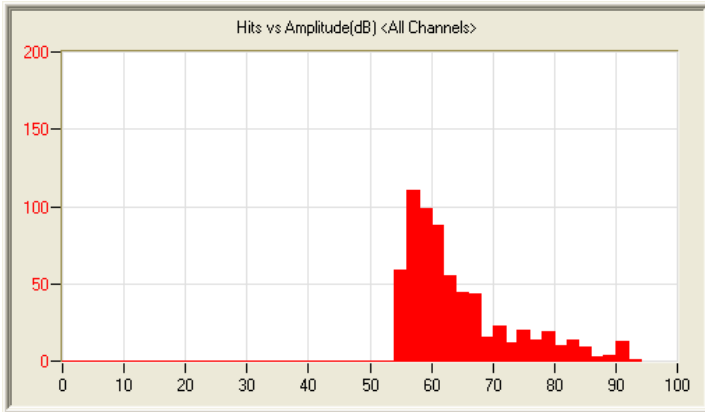
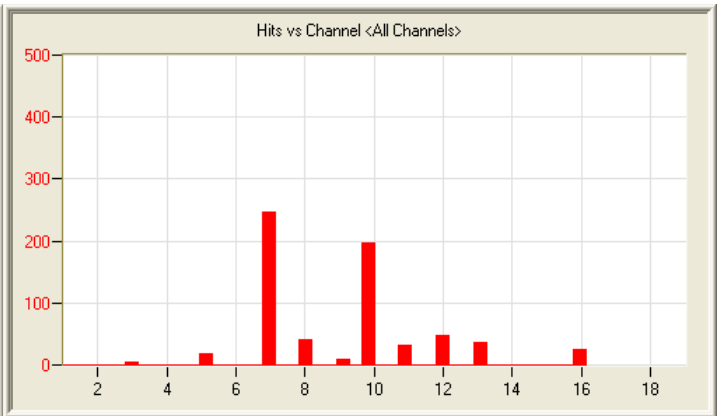
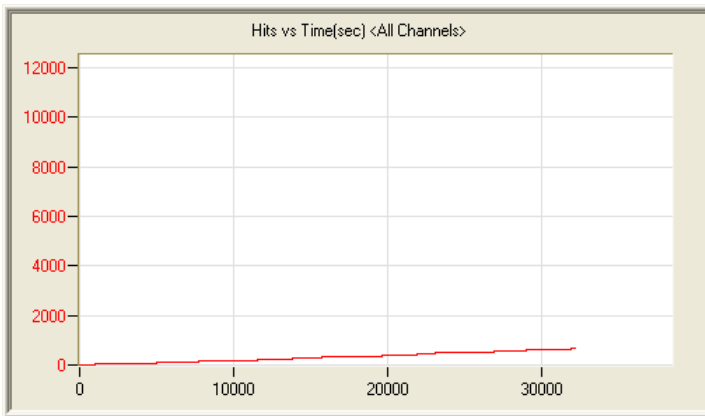
2/24/12 8:15am 8:00:04 2843 120224081507_0 1.3mb



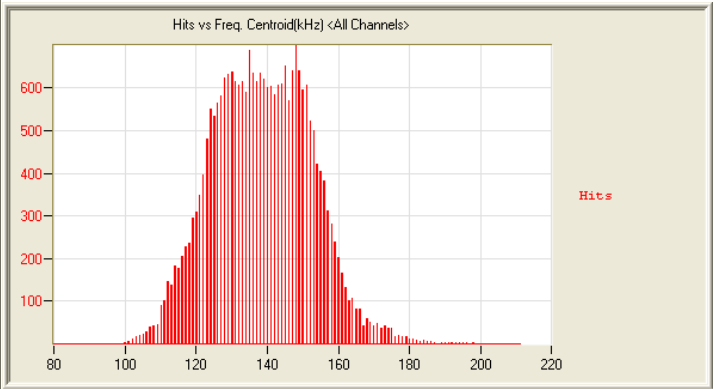
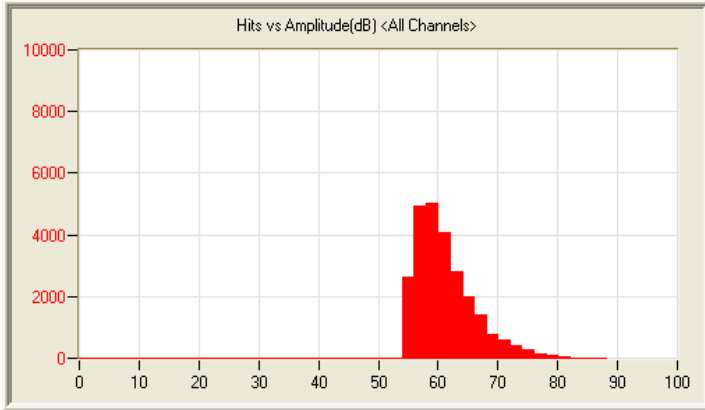
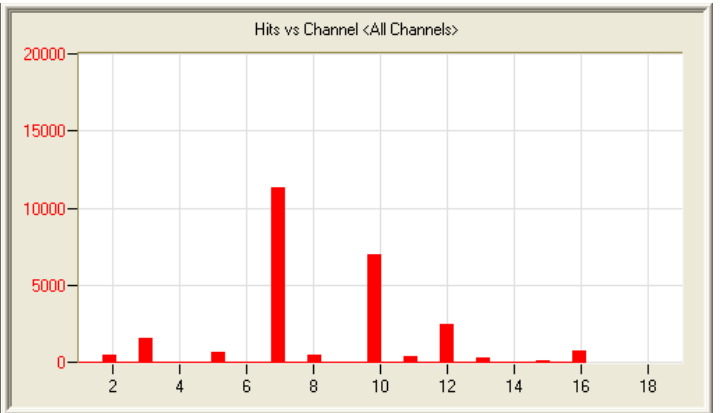
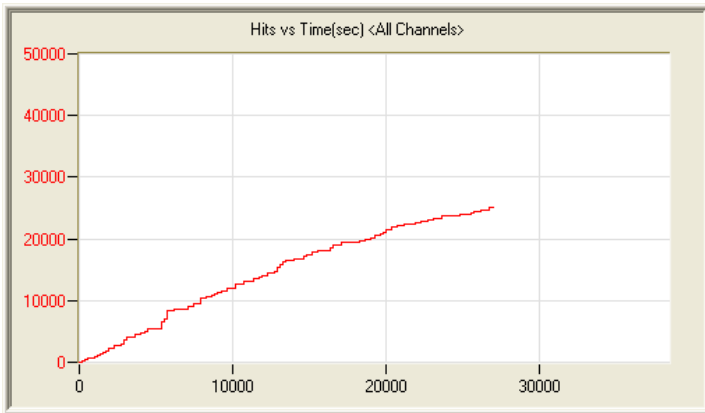
2/27/13 8:25am 7:11:45 599 120227082507_0 1.1mb



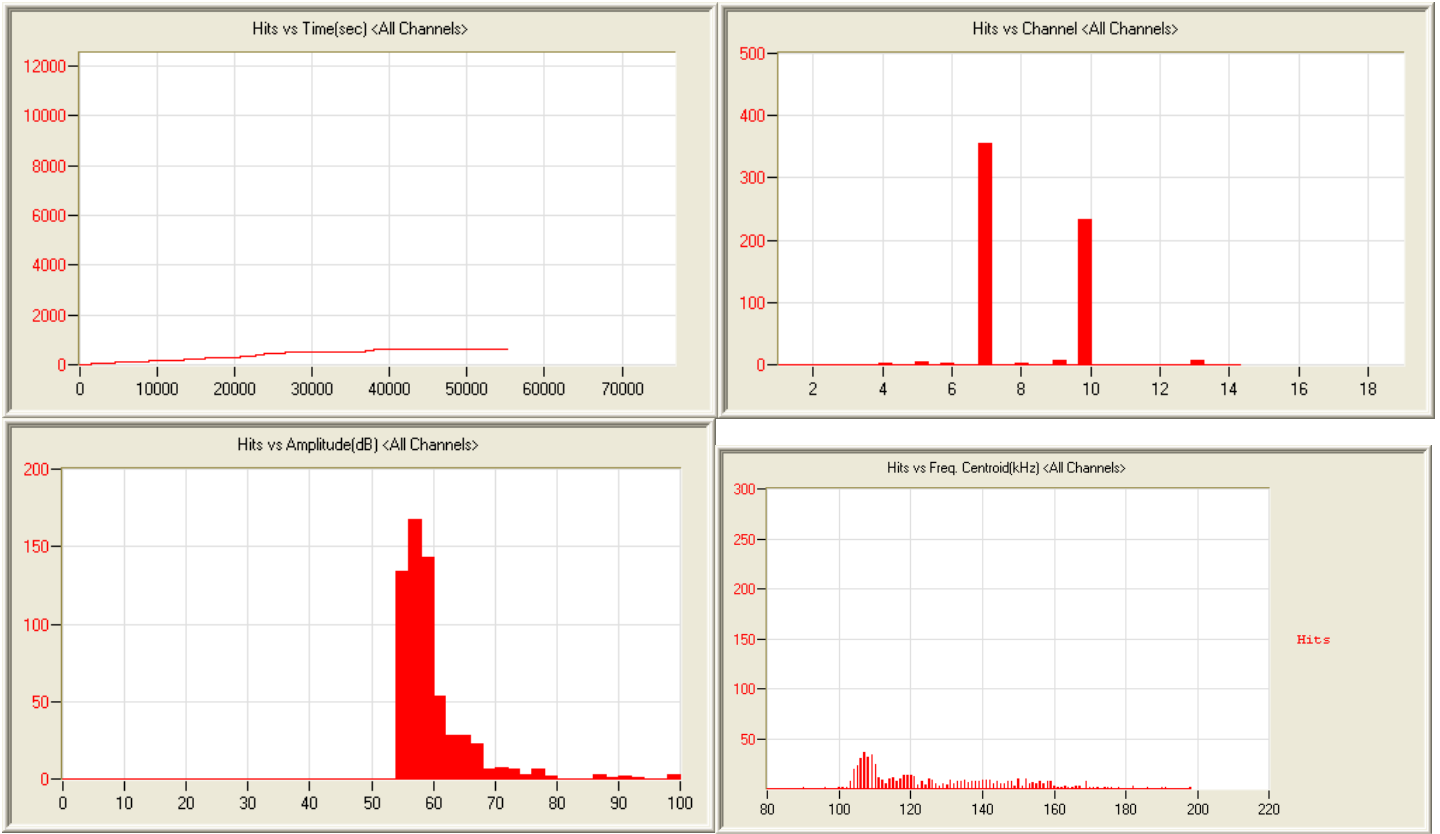
3/1/12 7:42am 8:16:35 796 120301074210_0 1.3mb



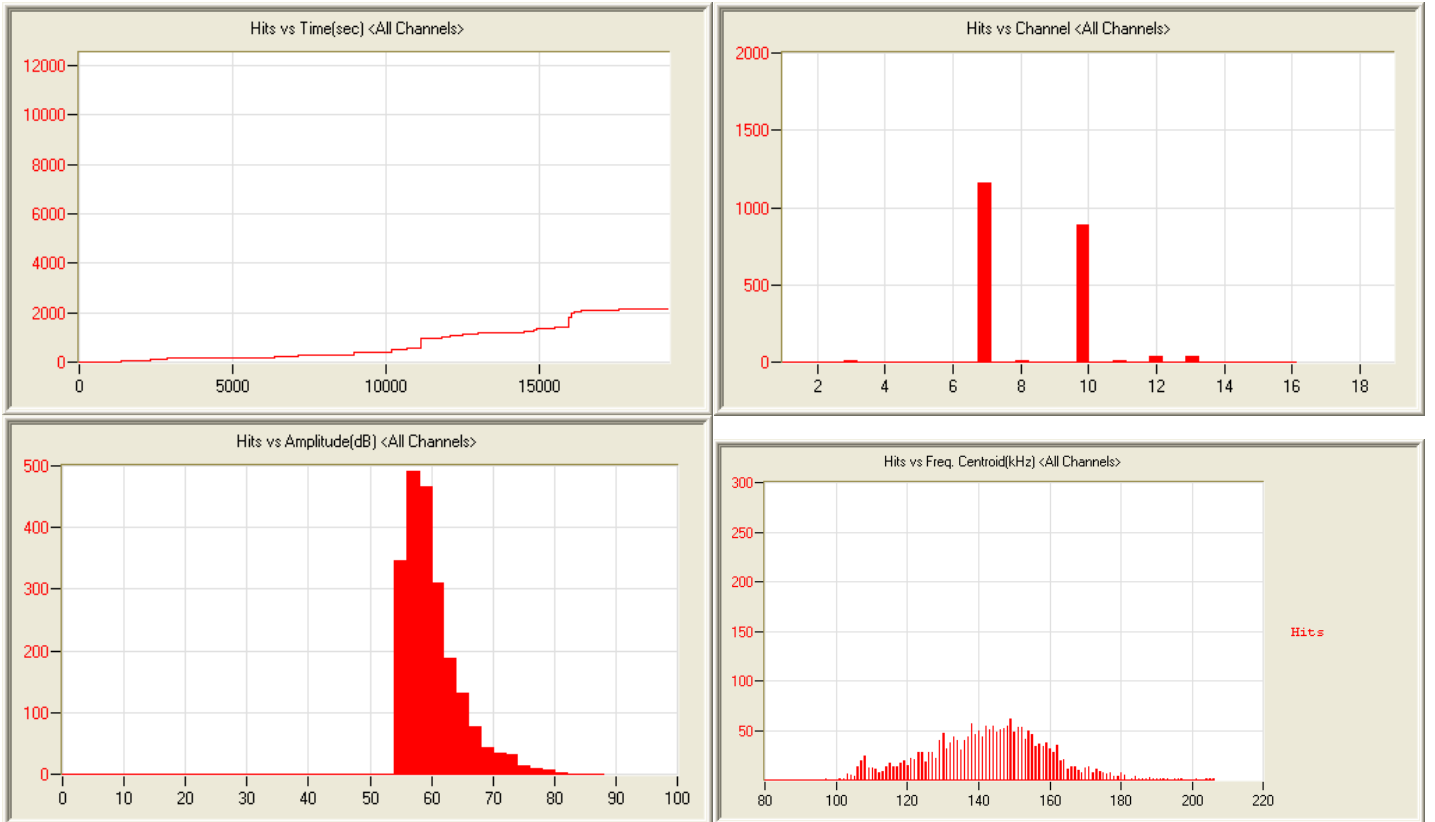
3/2/12 6:41am 8:59:05 655 120302064102_0 1.4mb



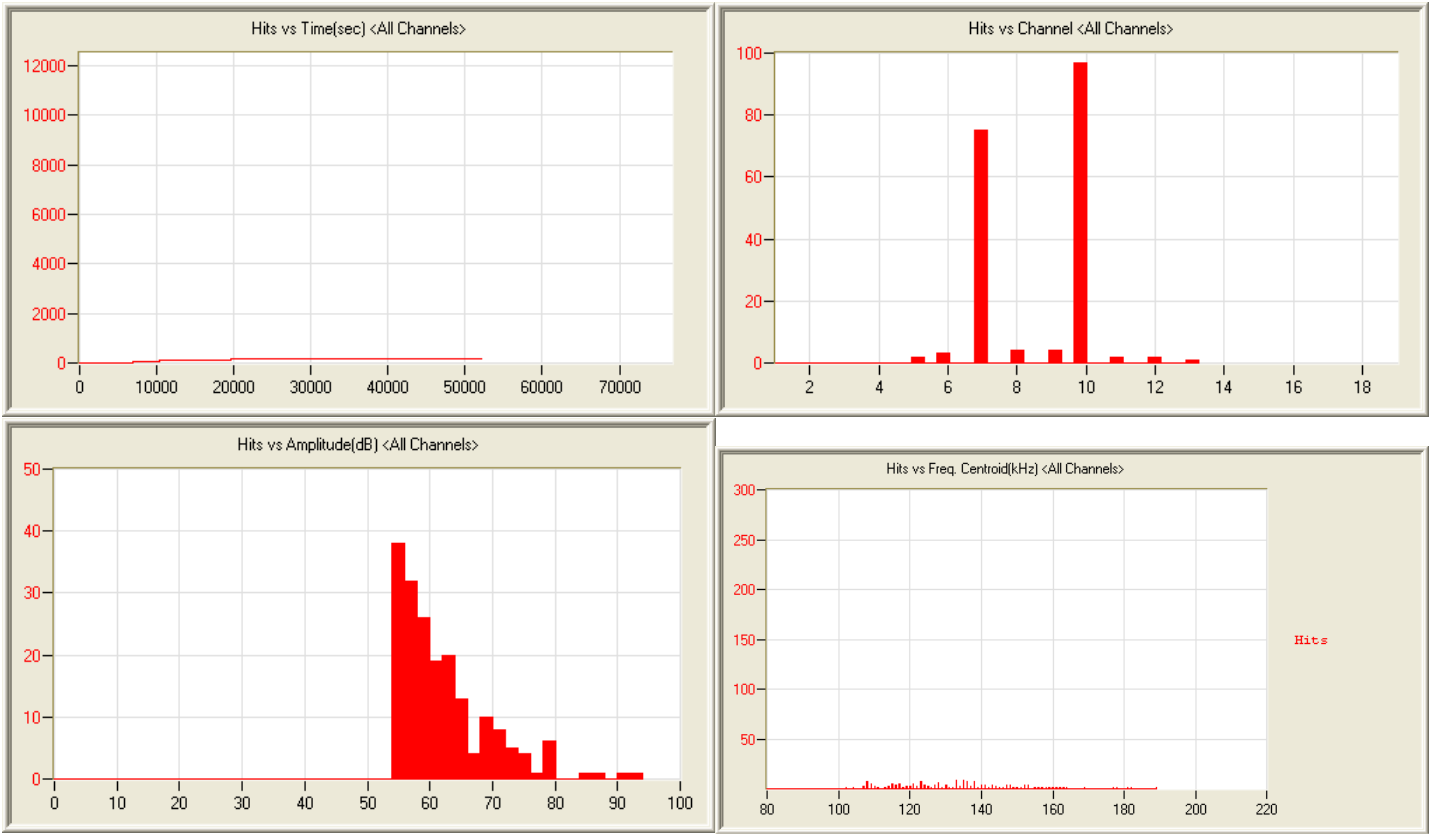
3/3/12 9:09am 7:28:44 25209 120303090920_0 2.2mb



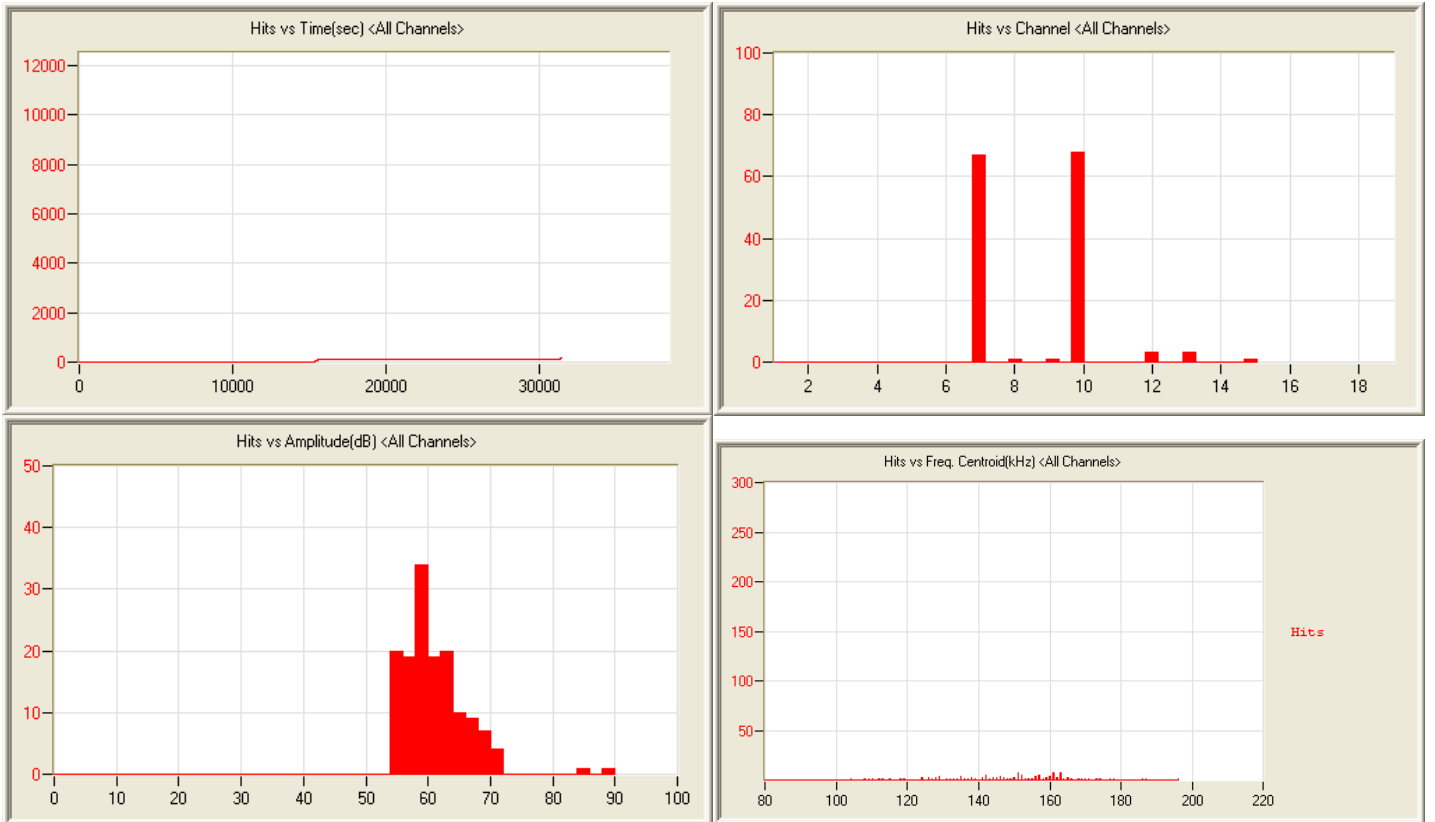
4/12/12 7:05am 15:59:12 616 120412070542_0 2.4mb



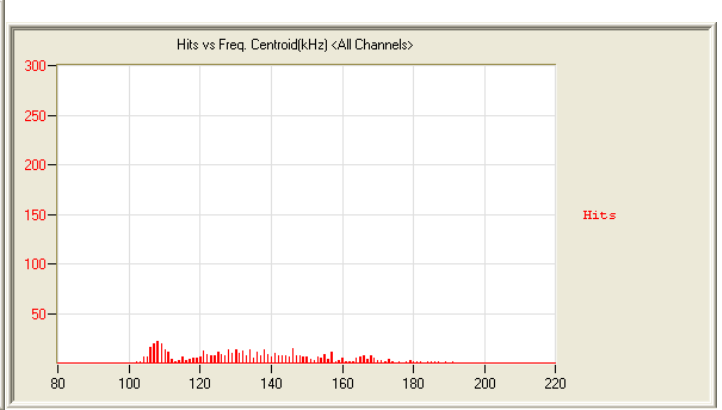
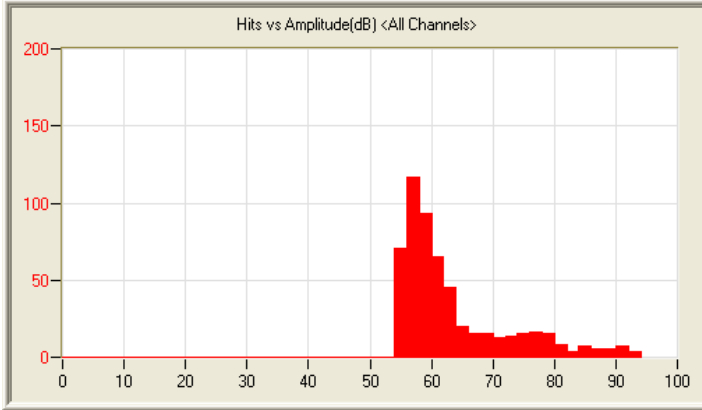
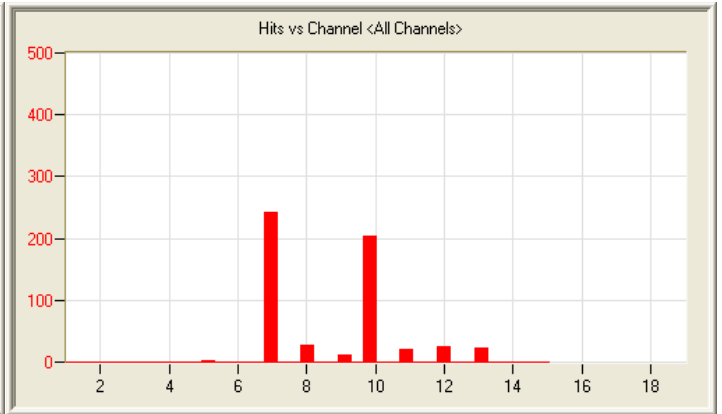
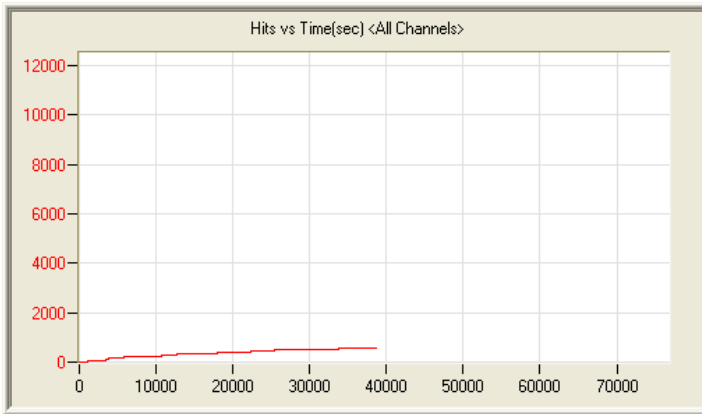
4/13/12 11:17am 5:27:10 2150 120413111752_0 938kb



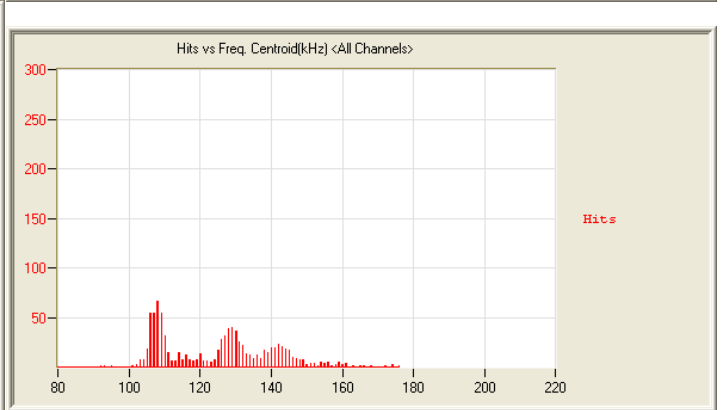
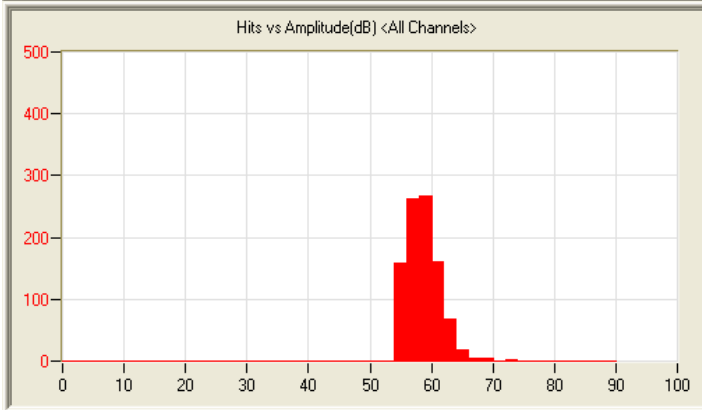
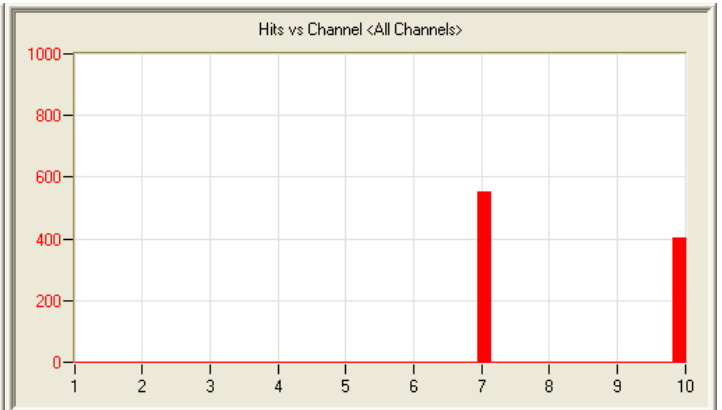
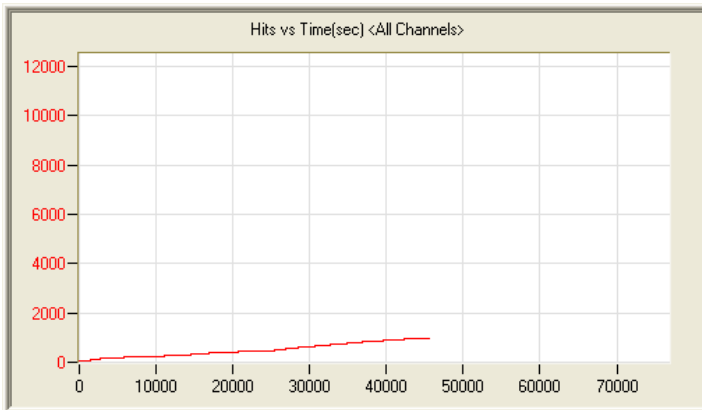
4/14/12 11:02am 15:17:43 190 120414110257_0 2.3mb



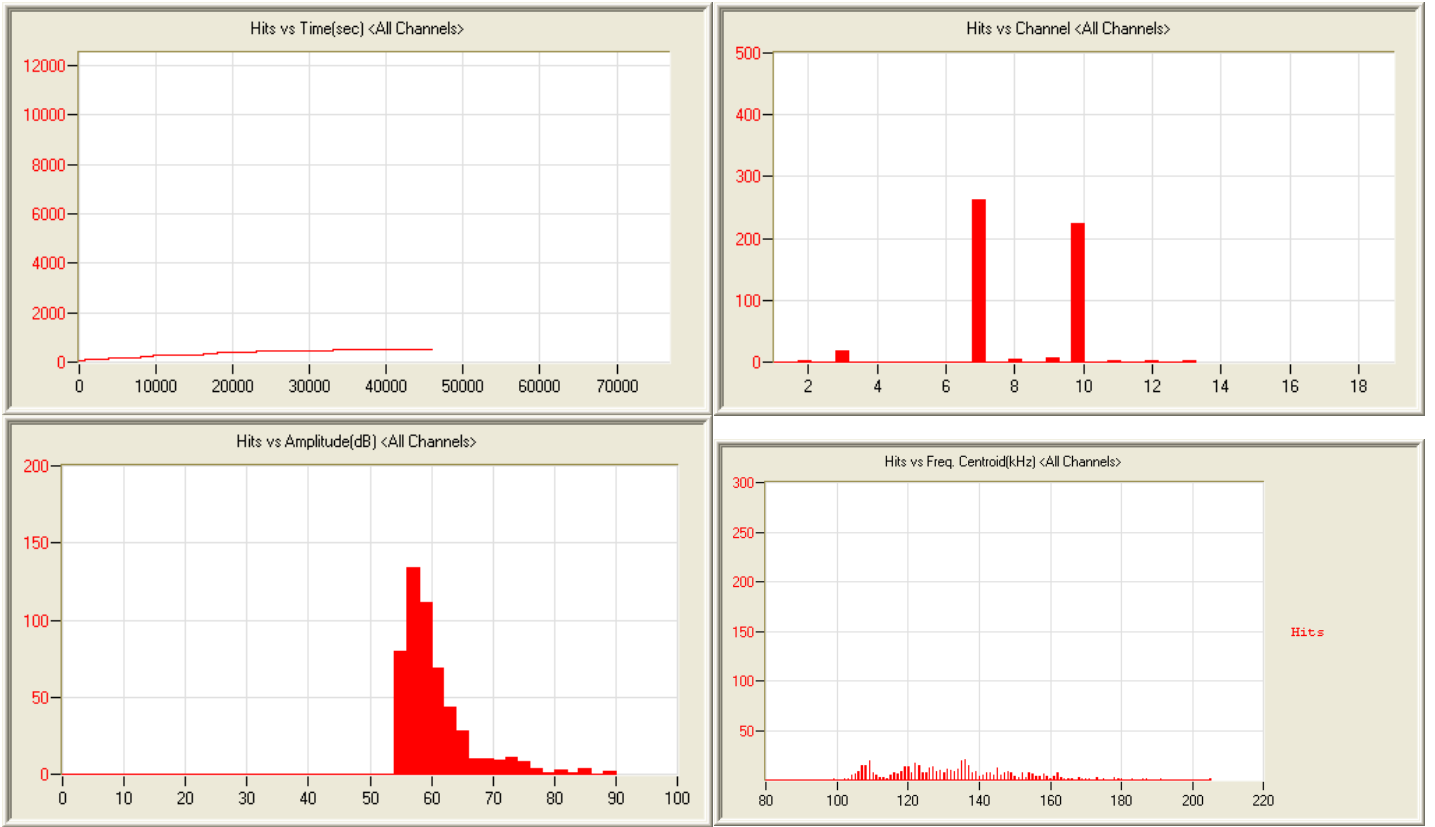
4/15/12 2:25pm 9:24:43 144 120415142536_0 1.4mb



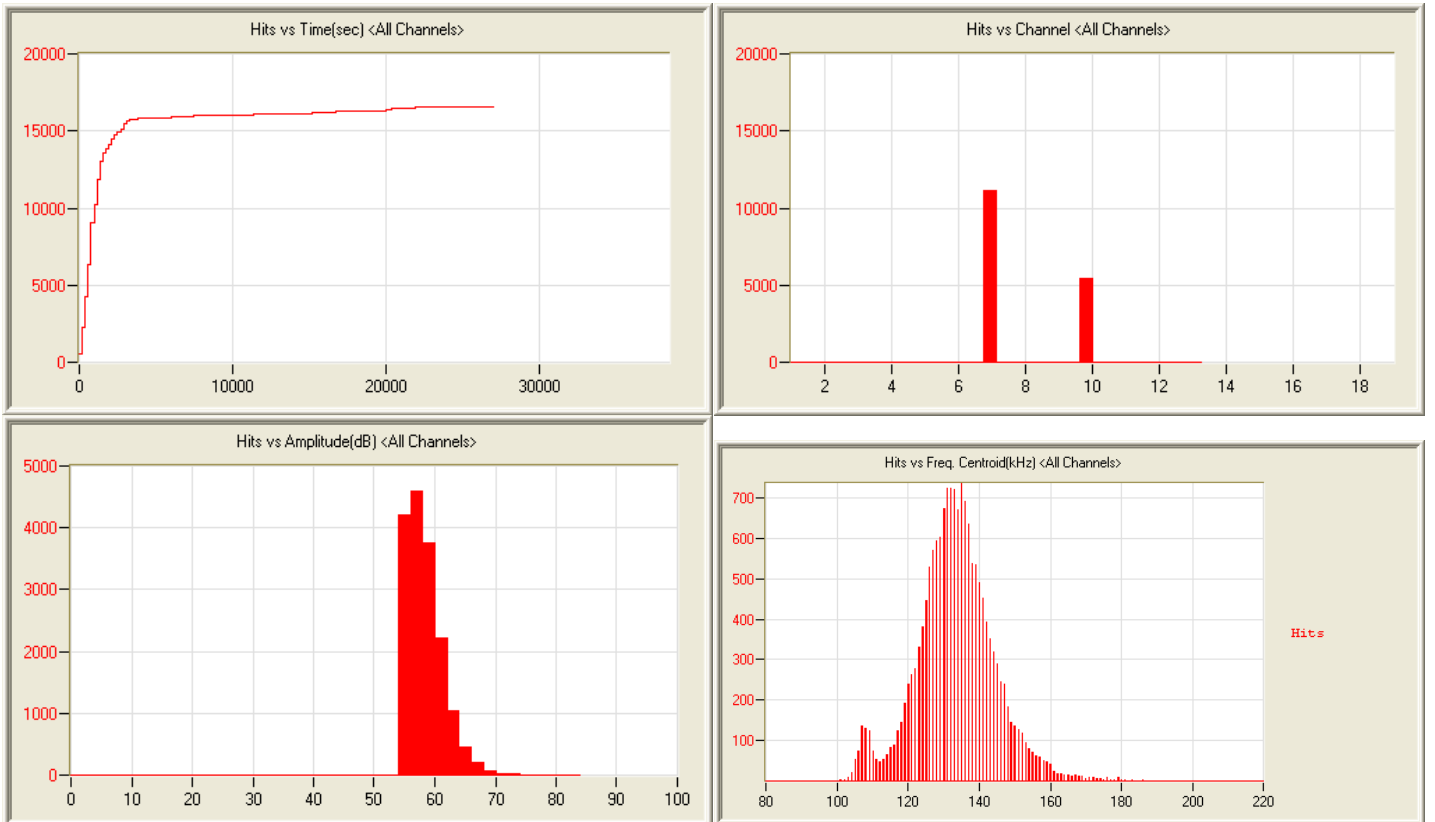
4/16/12 3:43pm 11:18:26 554 120416154326_0 1.7mb



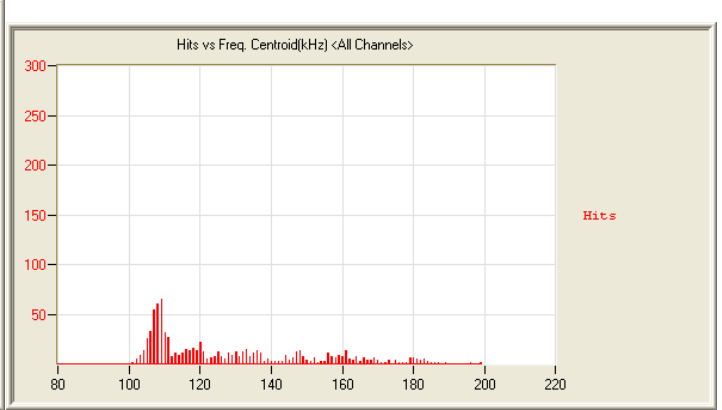
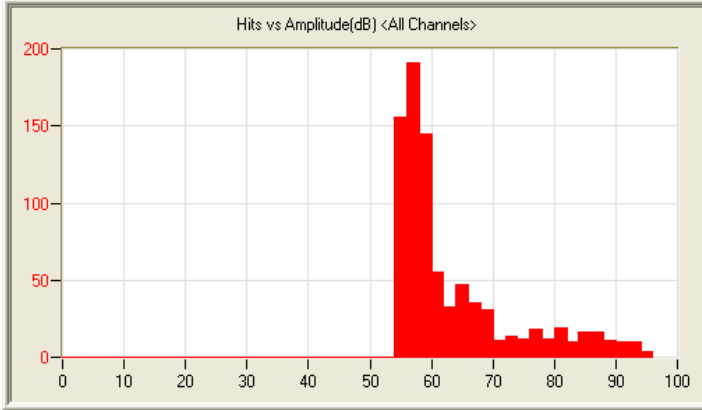
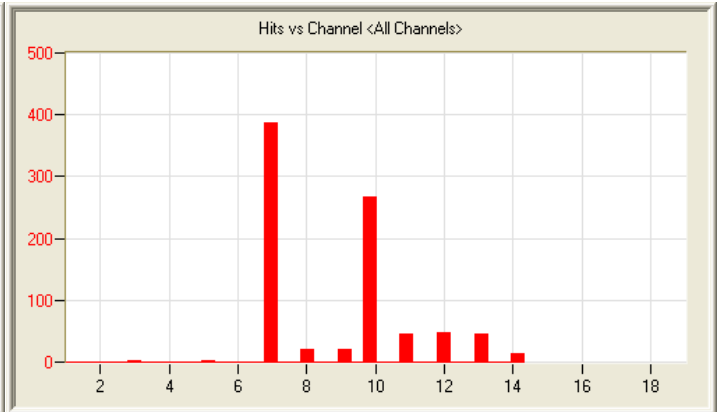
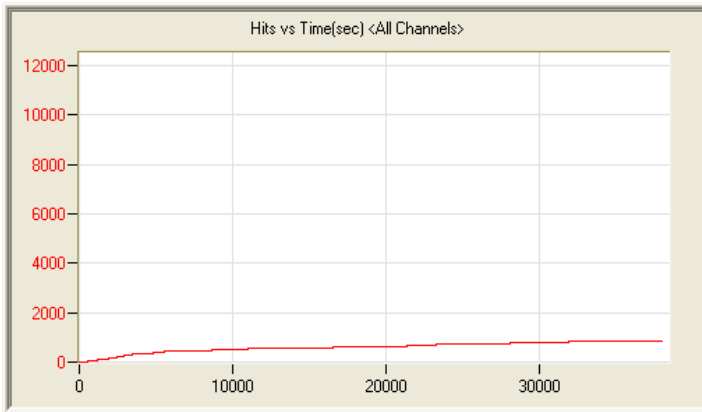
4/17/12 4:33pm 12:43:48 954 120417163304_0 1.9mb



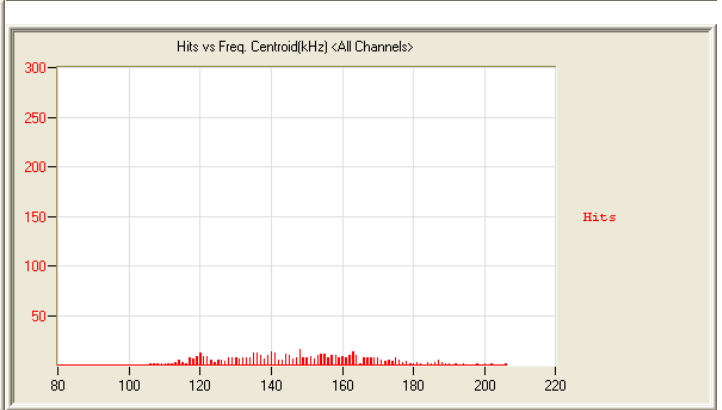
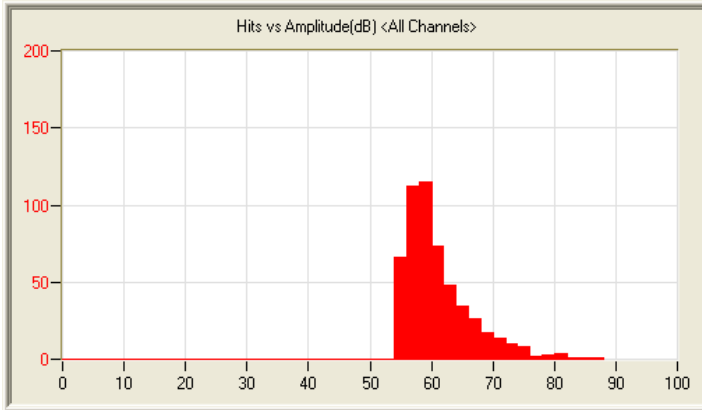
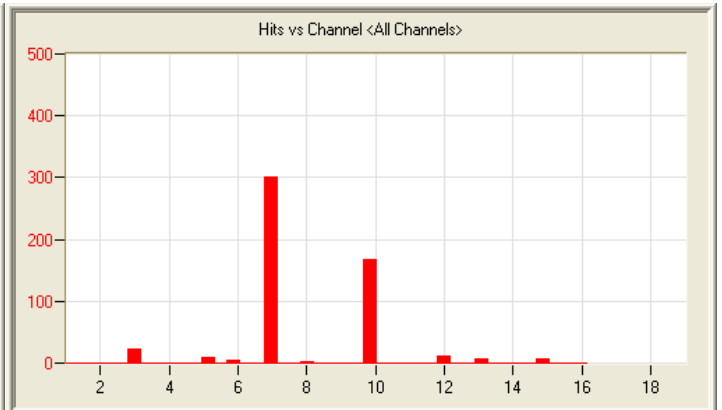
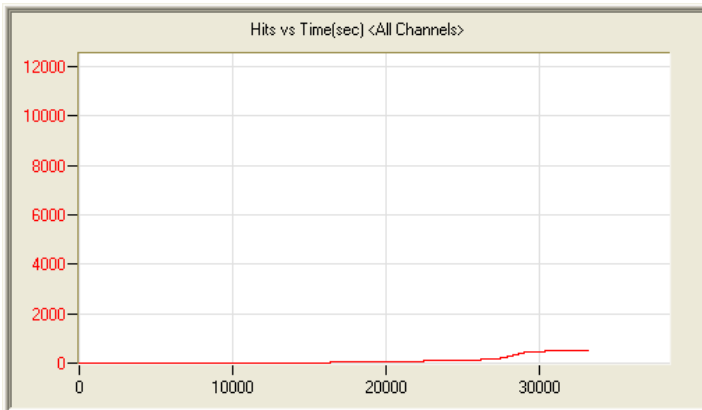
4/18/12 7:43pm 12:48:10 528 120418194335_0 1.9mb



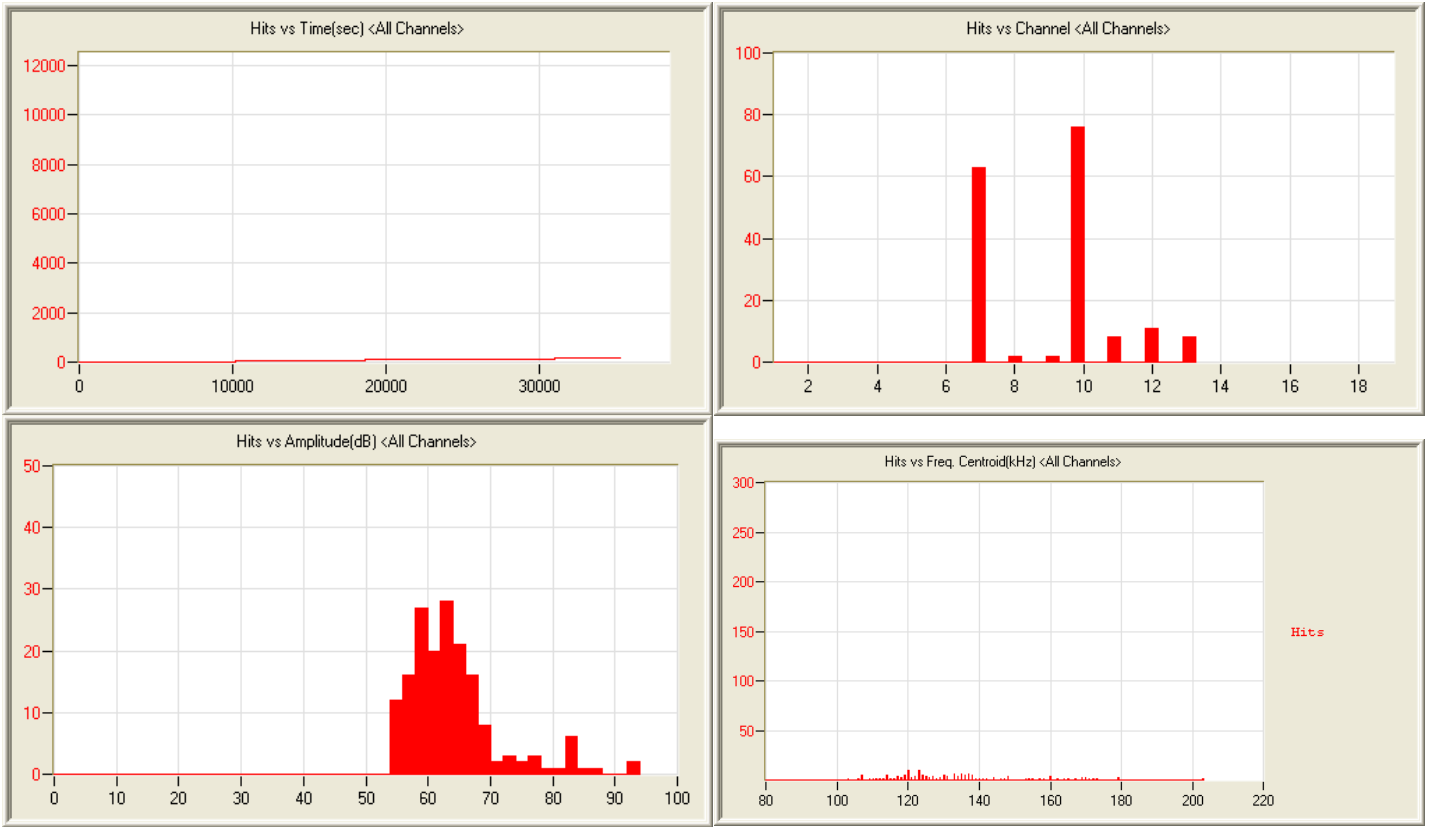
4/19/12 9:49pm 7:30:06 16564 120419214904_0 1.8mb



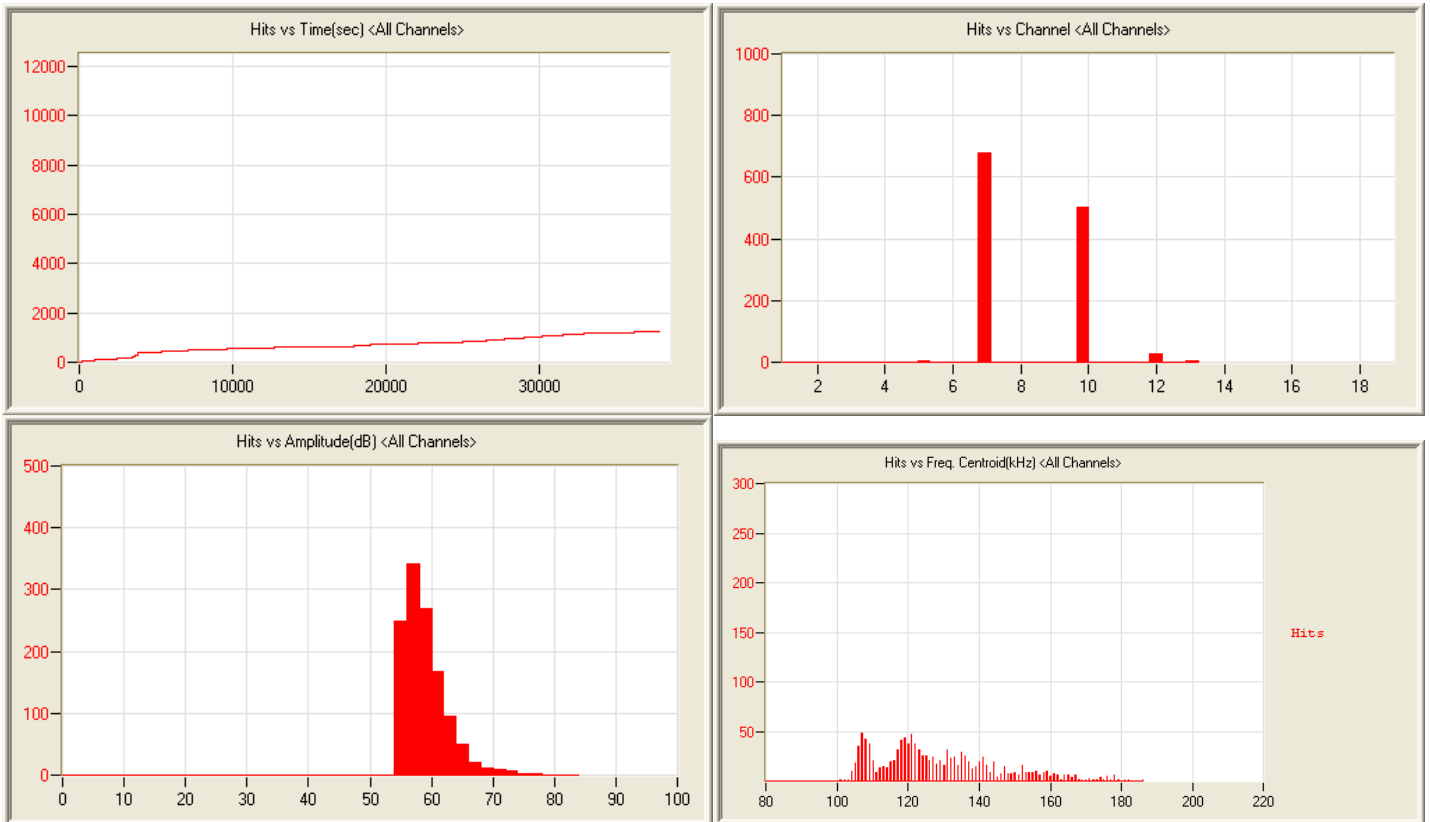
4/21/12 2:01am 10:37:01 856 120421020132_0 1.6mb



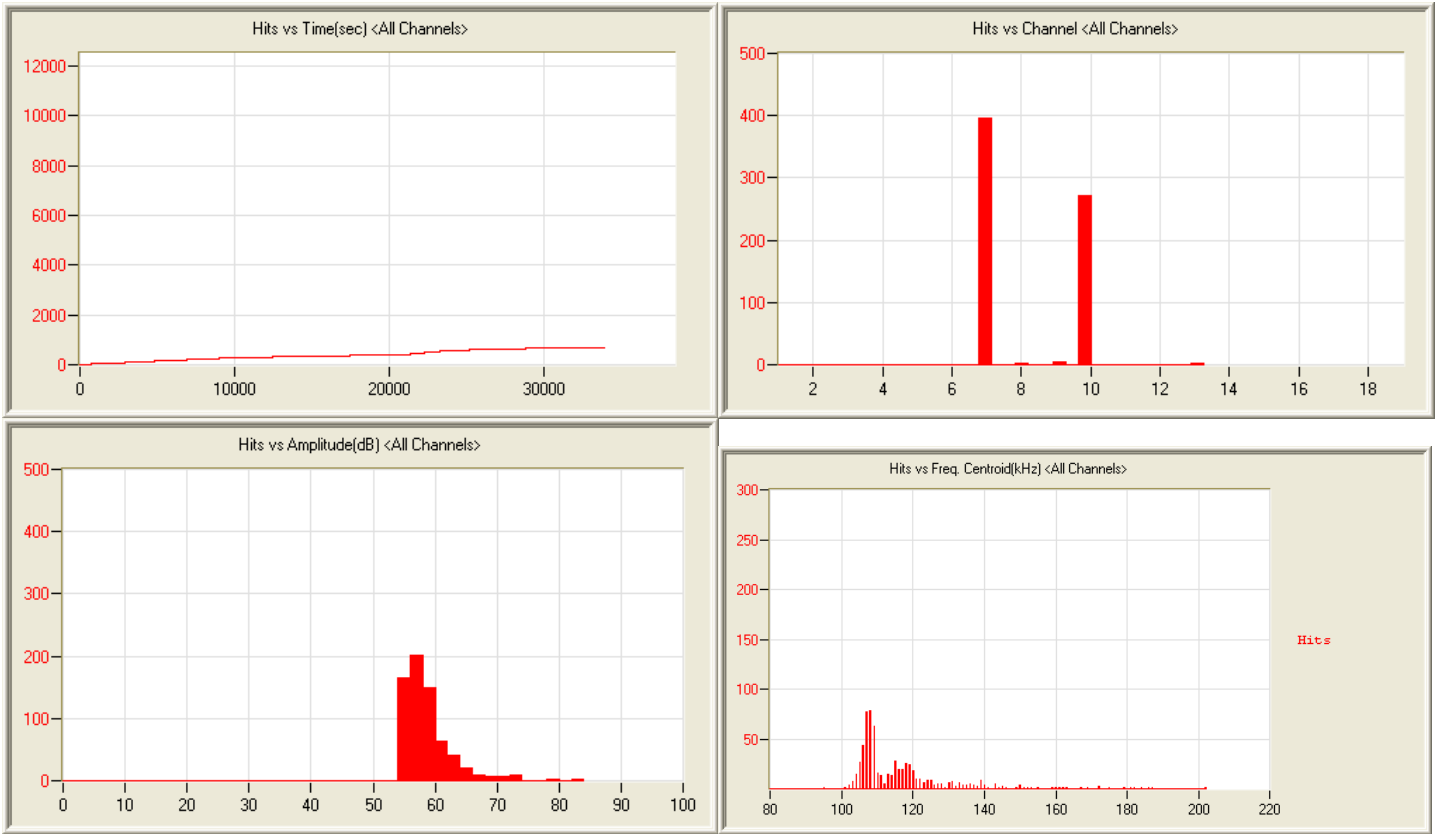
4/22/12 5:14am 9:15:13 535 120422051423_0 1.4mb



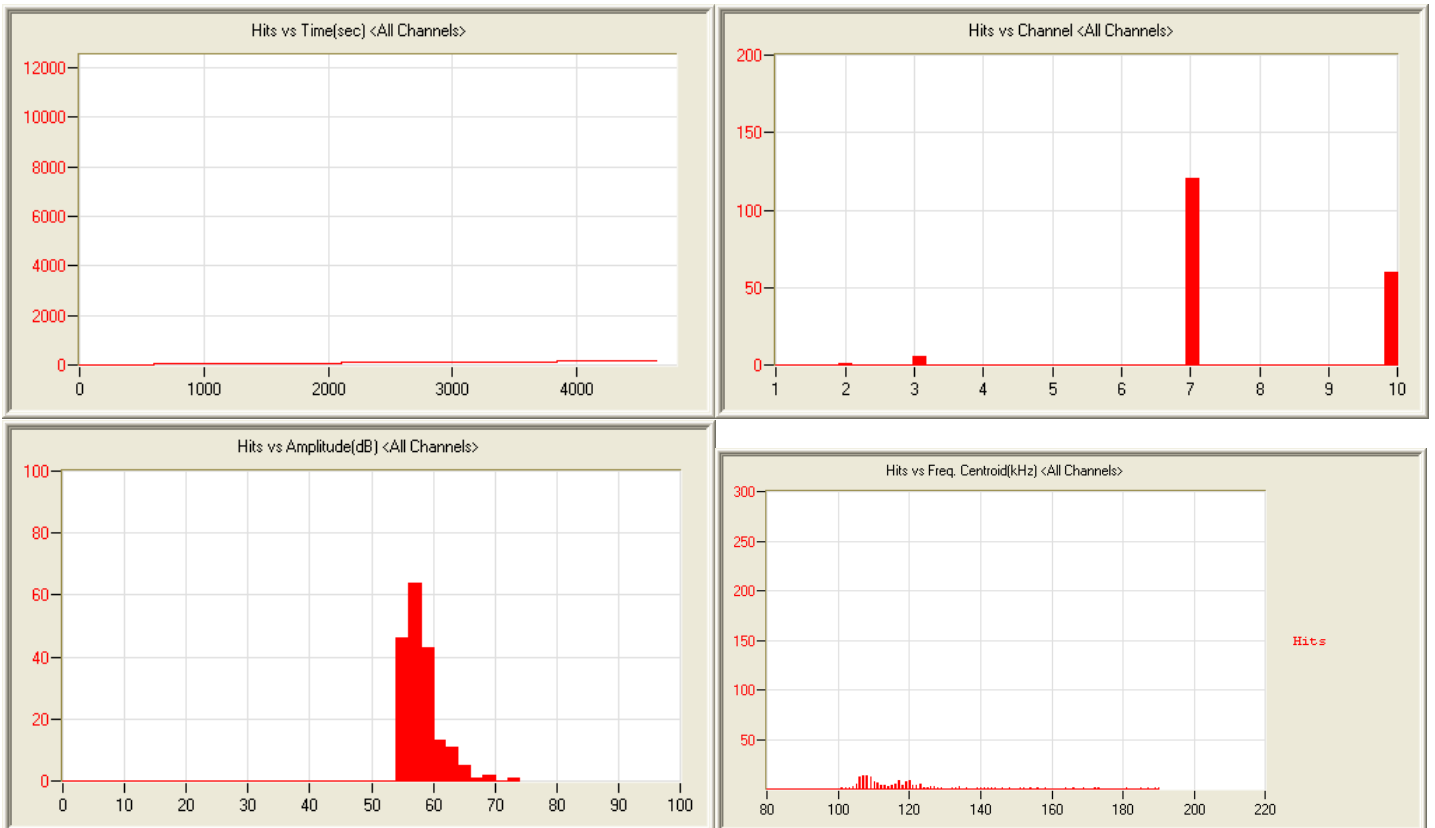
4/23/12 11:45am 9:57:00 120423114542_0 1.5mb



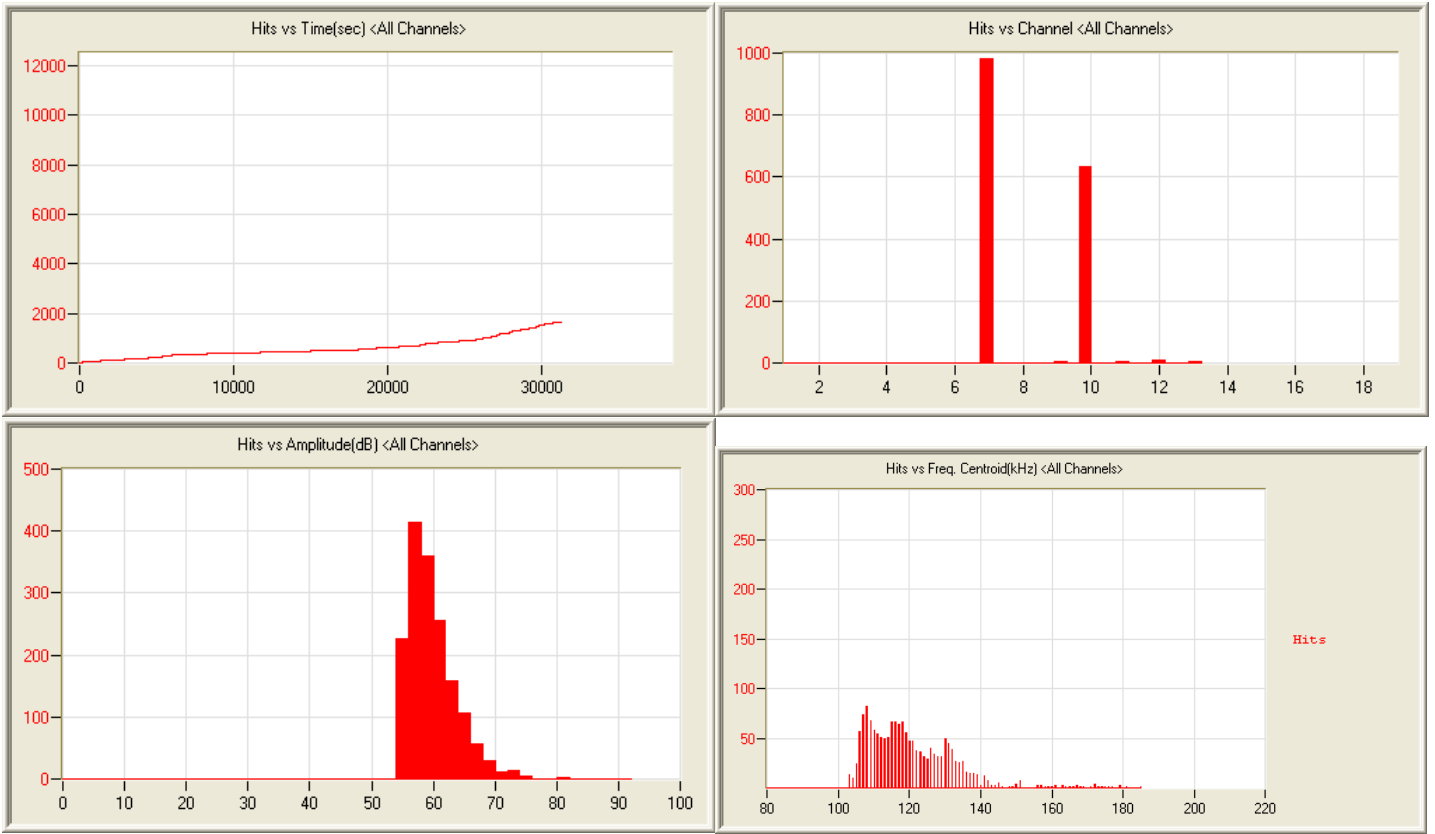
4/24/12 10:56am 10:33:22 120424105604_0 1.6mb



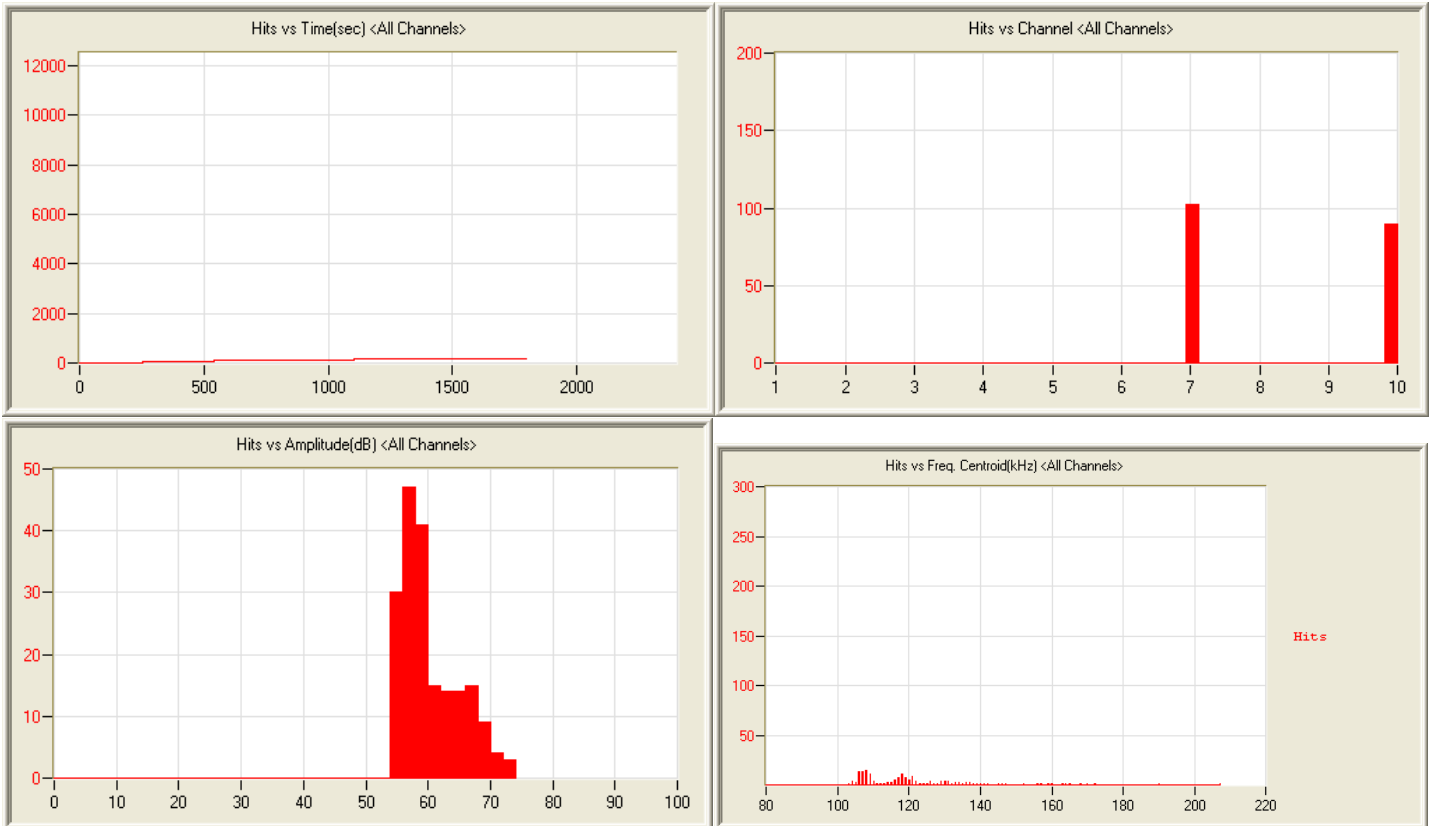
4/25/12 3:21pm 9:28:15 678 120425152115_0 1.5mb



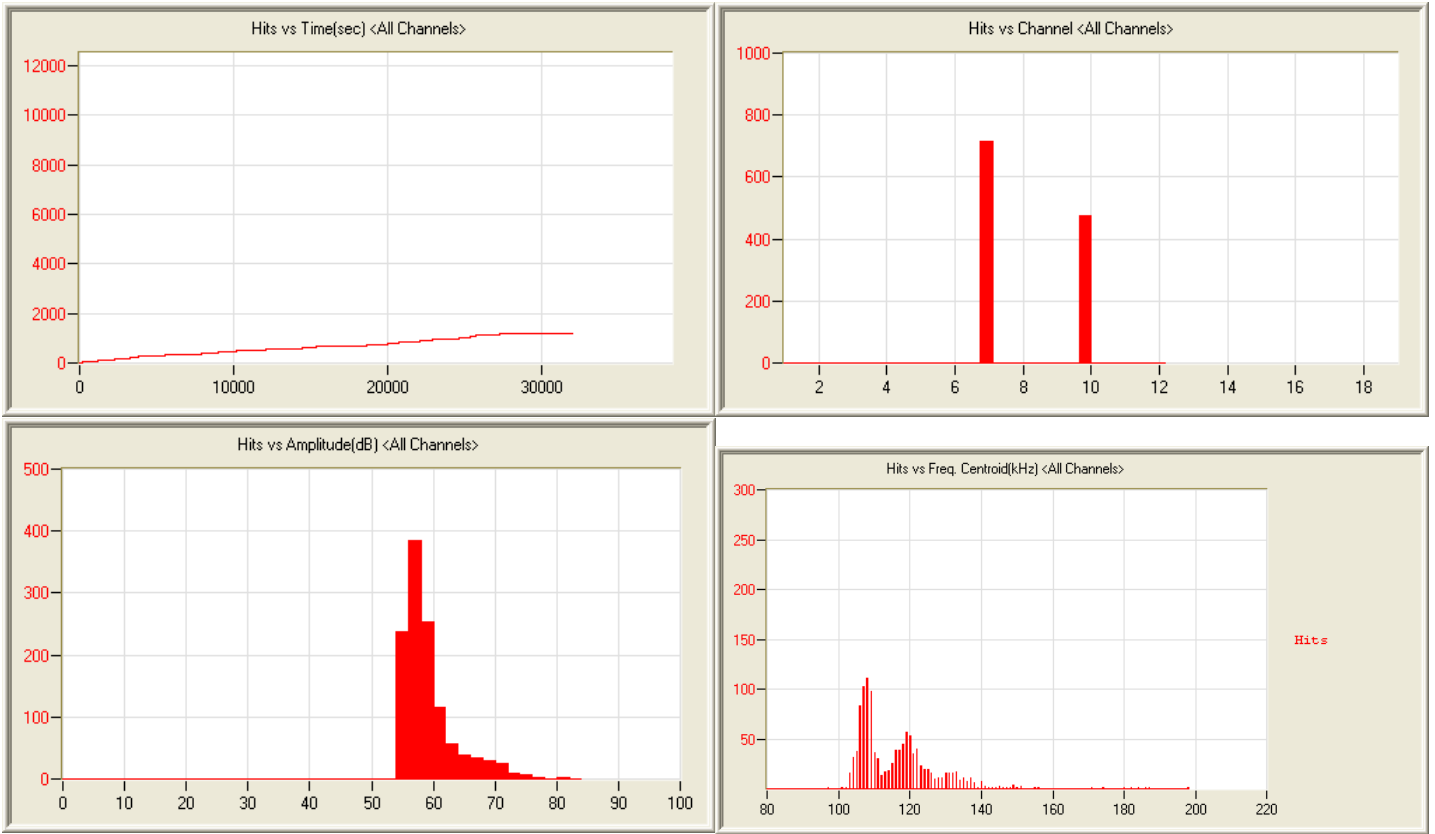
4/26/12 6:09pm 1:22:23 186 120426180947_0 272kb



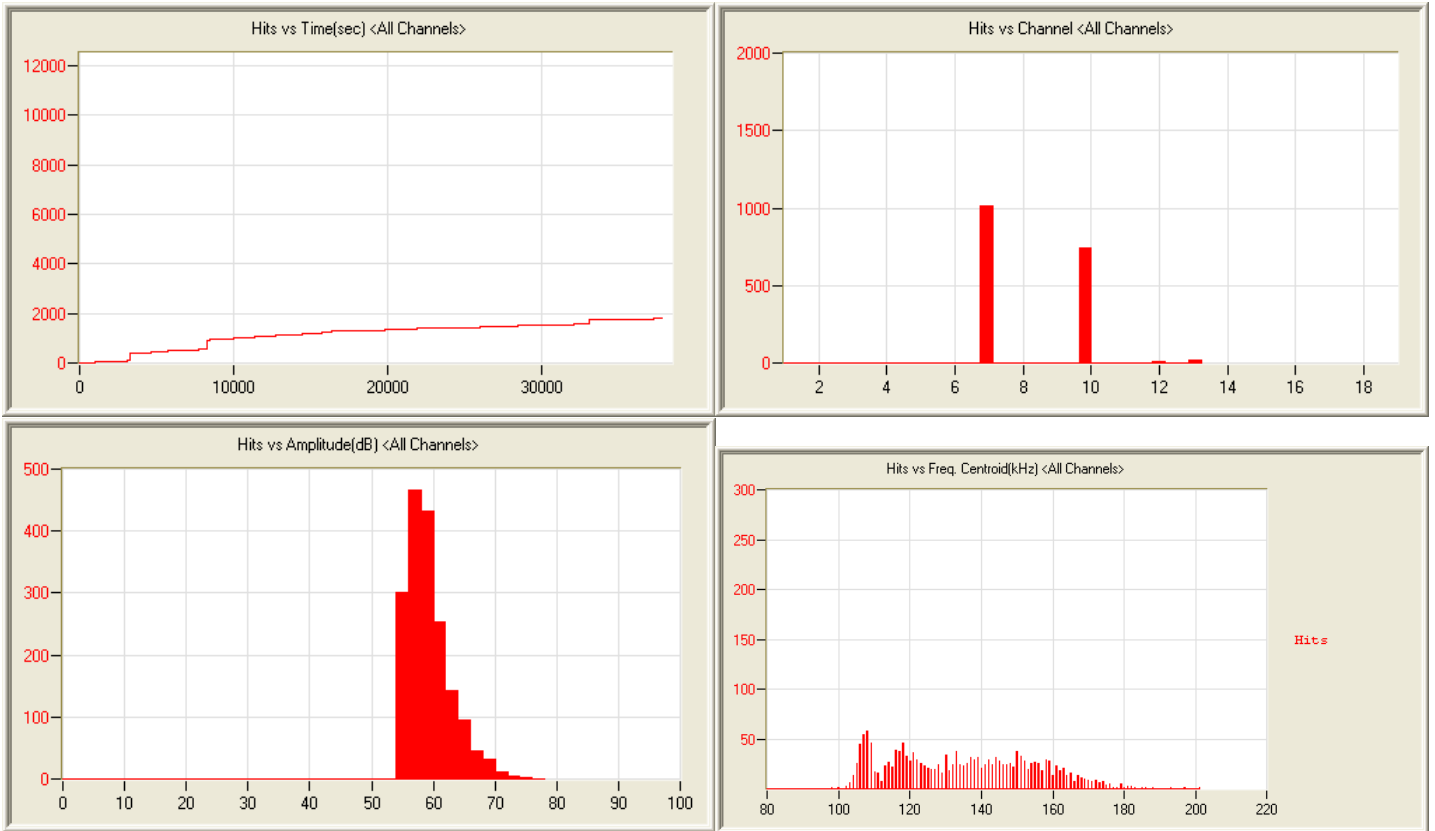
4/27/12 0:05am 08:40:11 1639 120427000508_0 1.4mb



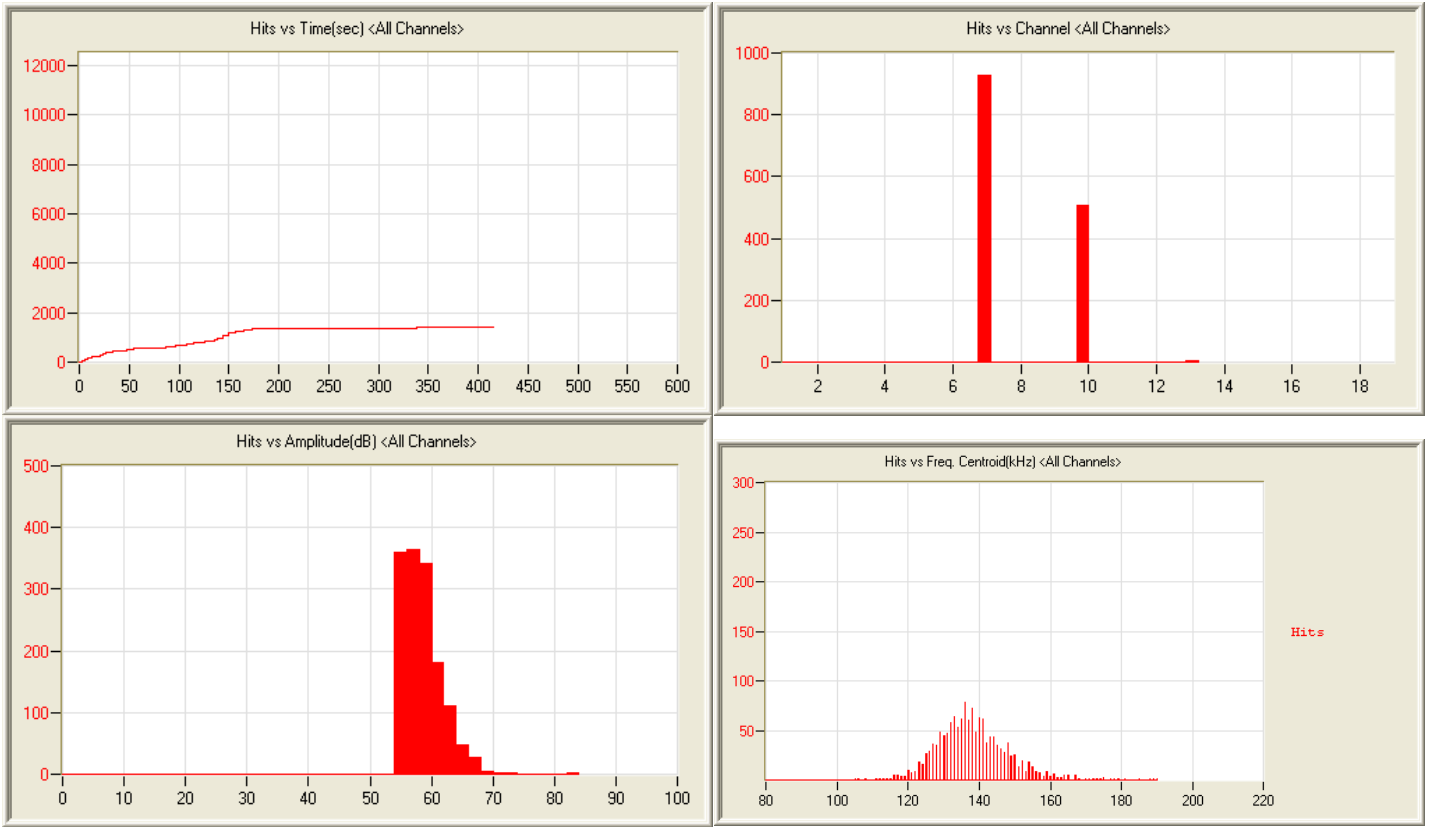
4/27/12 11:19pm 0:31:30 192 120427231932_0 150kb



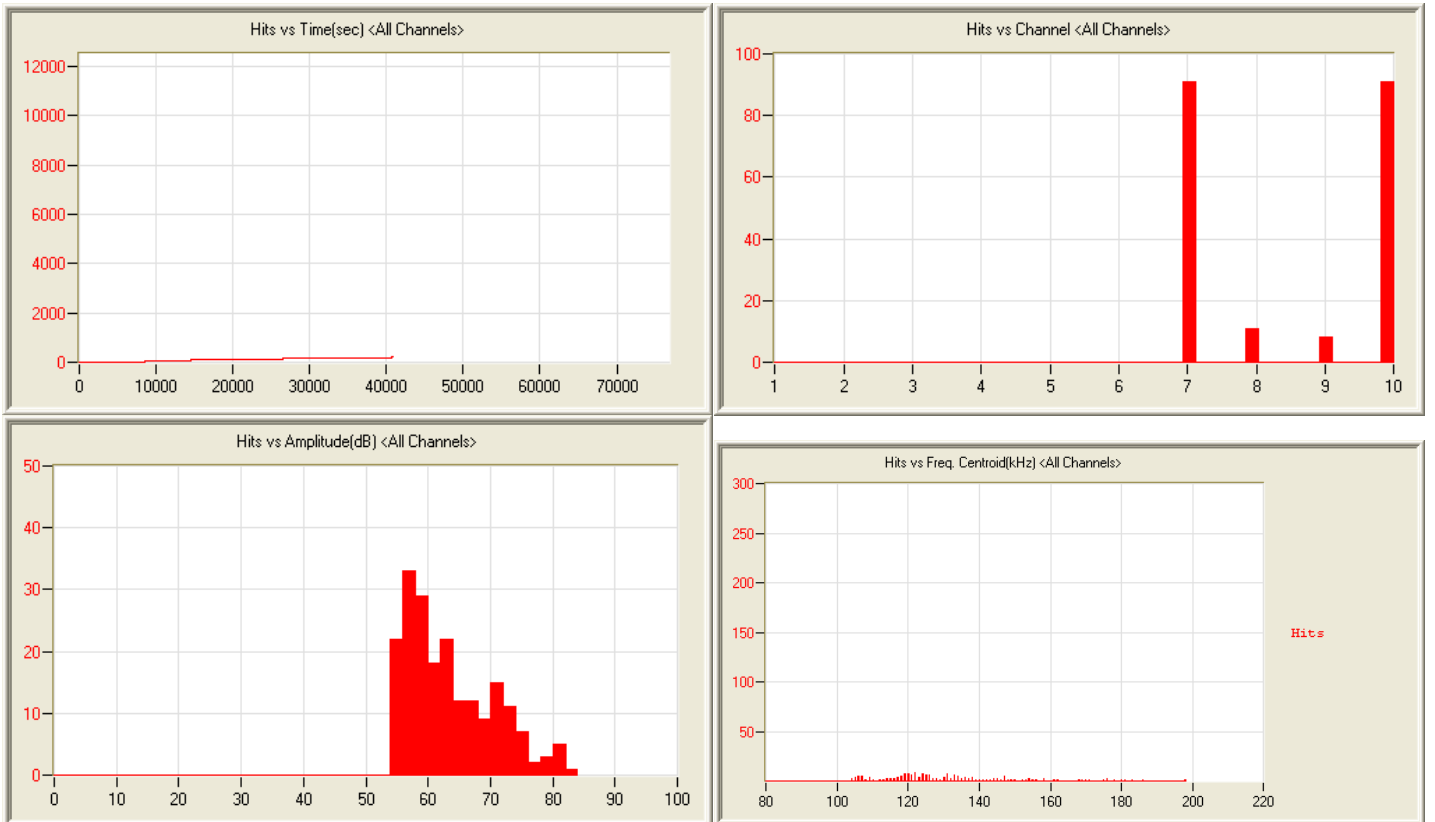
4/28/12 0:56am 8:58:28 1196 120428005621_0 1.4mb



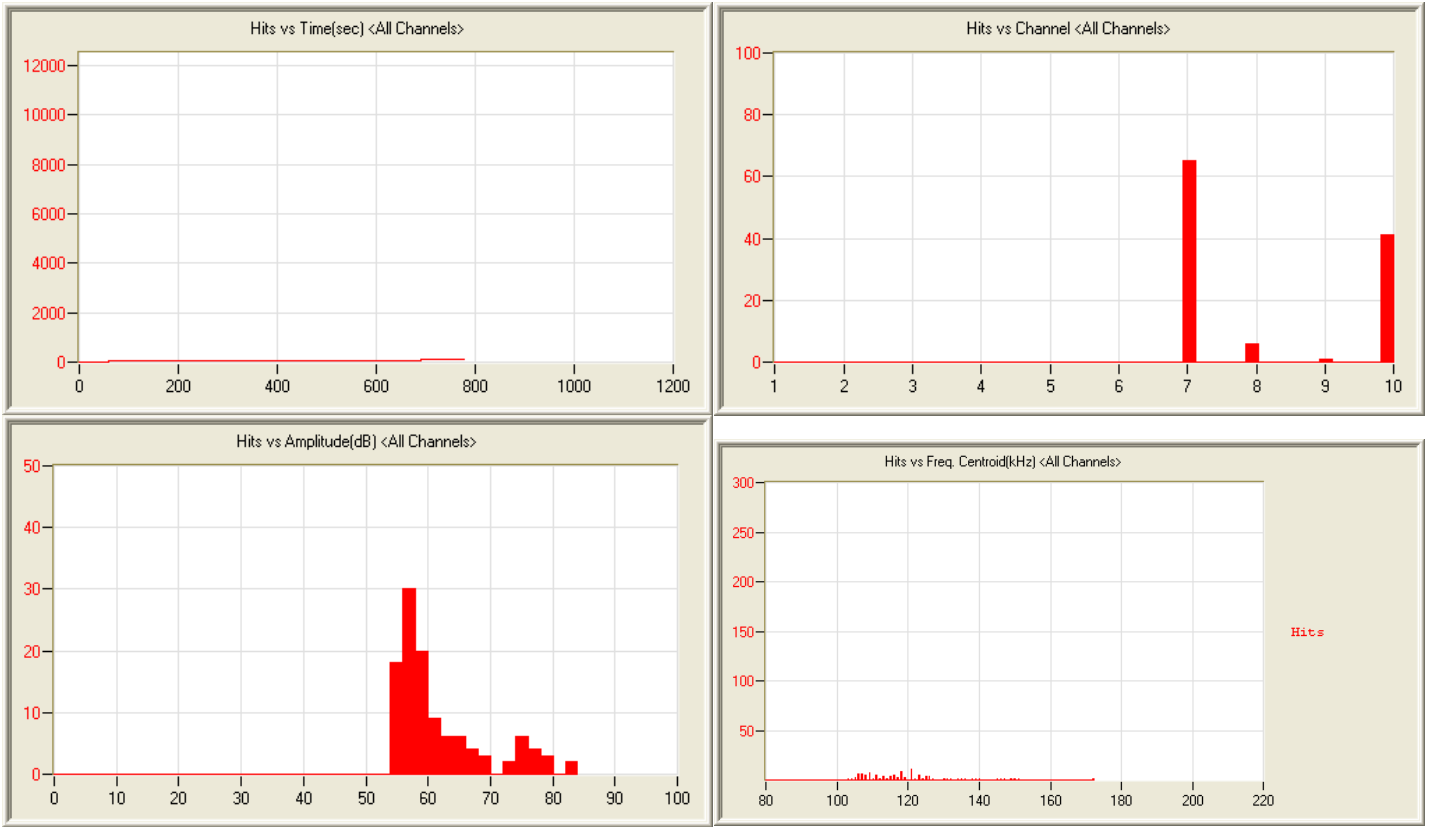
4/29/12 6:43am 10:31:48 1784 120429064311_0 1.7mb



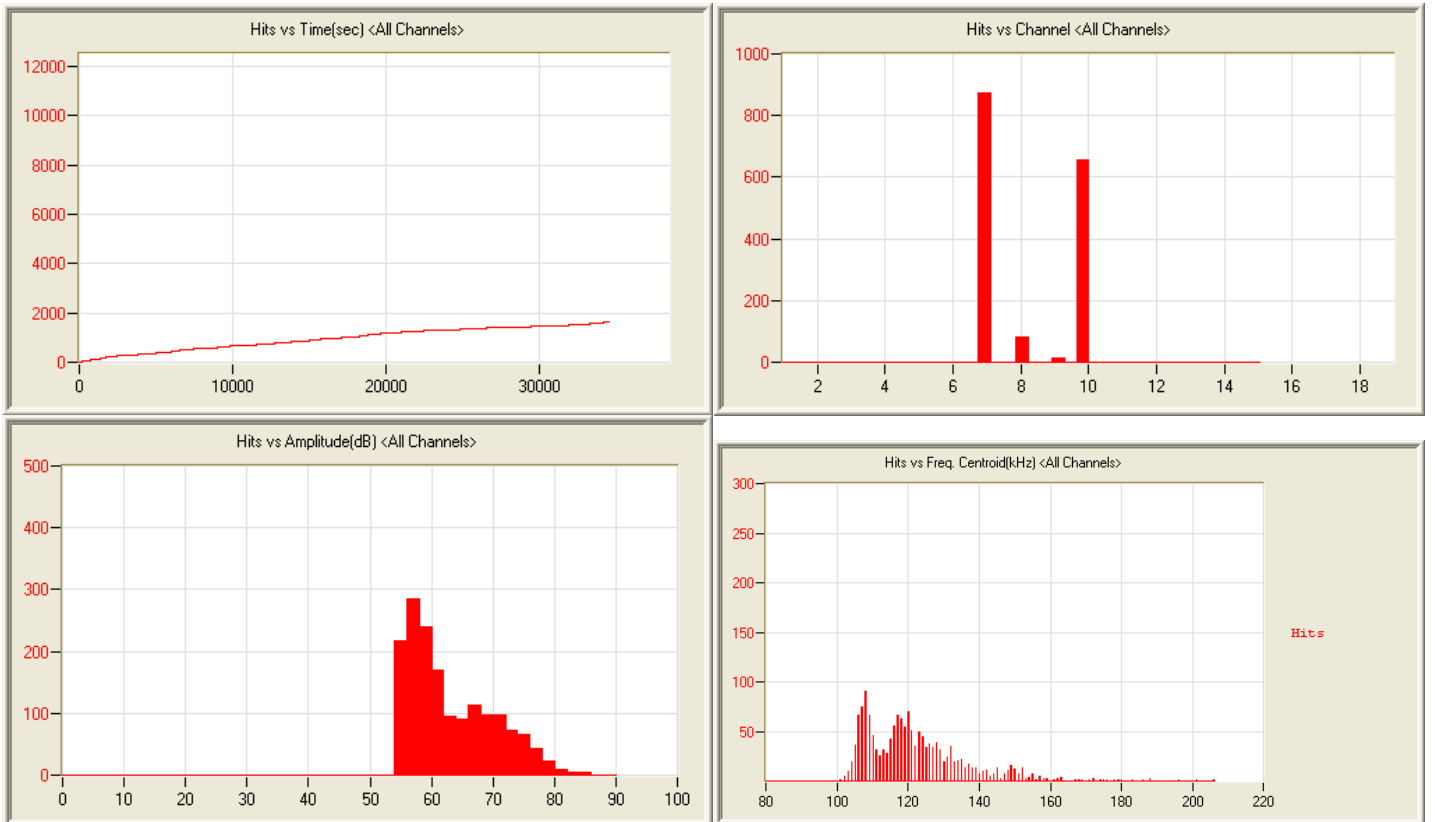
4/30/12 10:42am 0:06:56 1441 120430104254_0 141kb



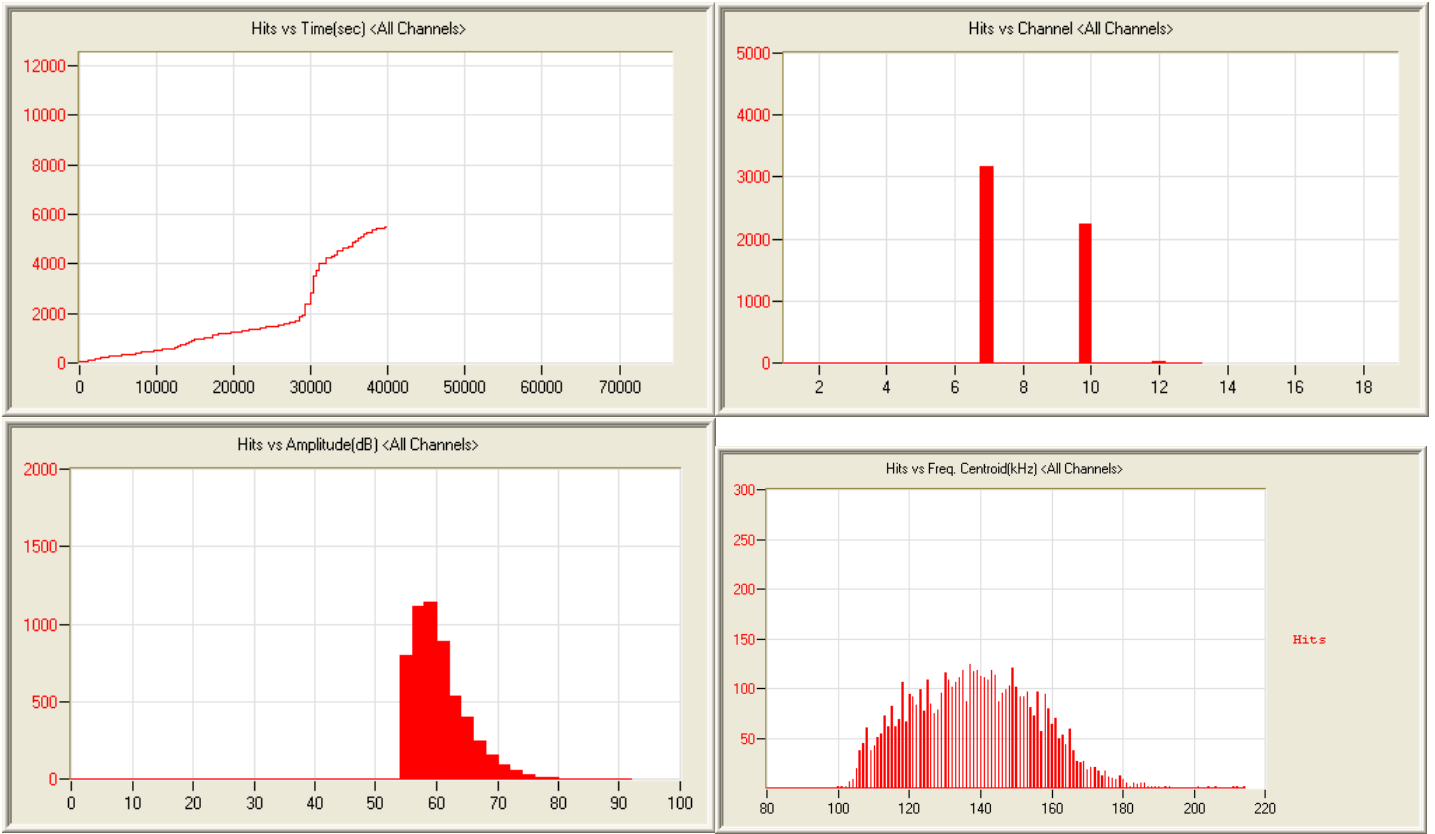
5/3/12 8:19am 11:29:24 201 120503081917_0 1.7mb



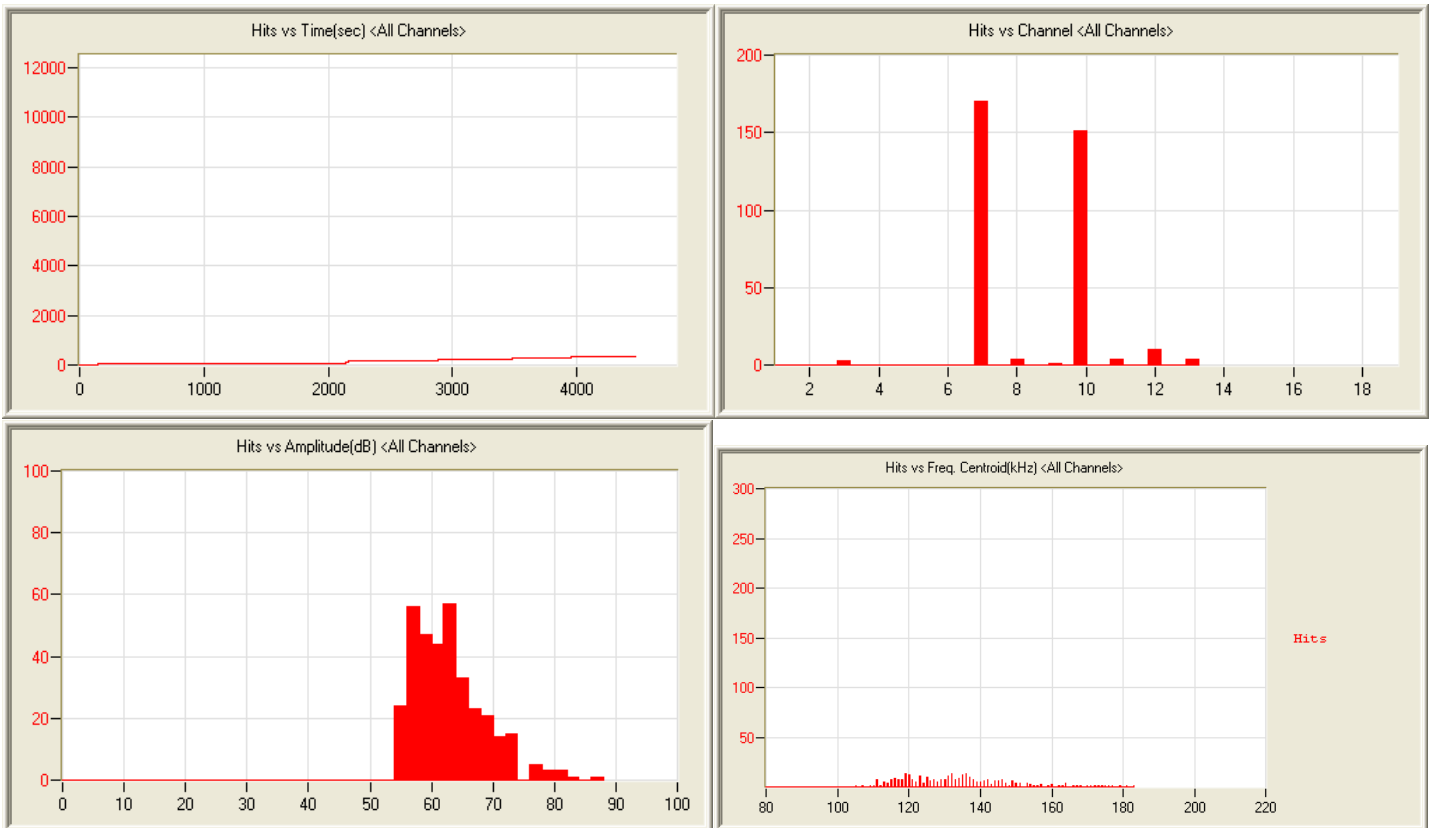
5/4/12 2:03pm 0:13:13 113 120504140324_0 103kb



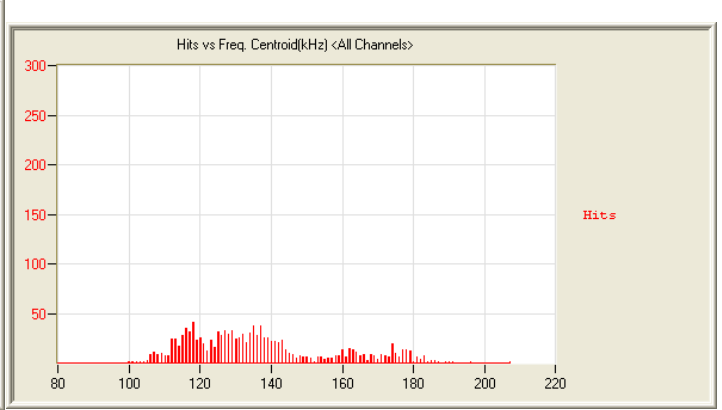
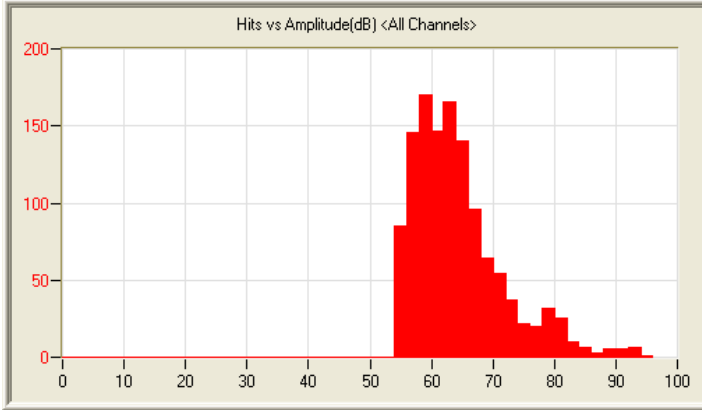
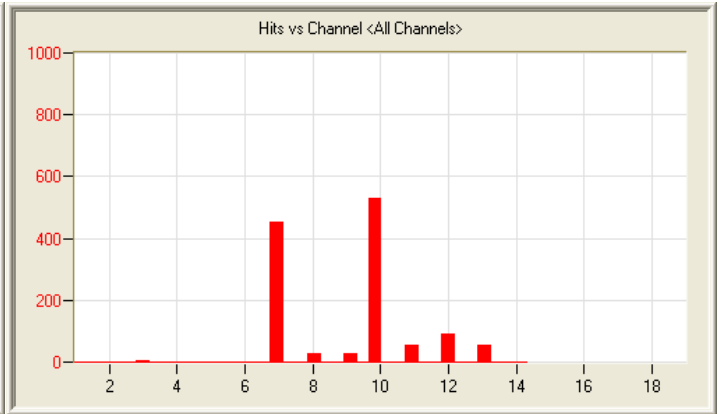
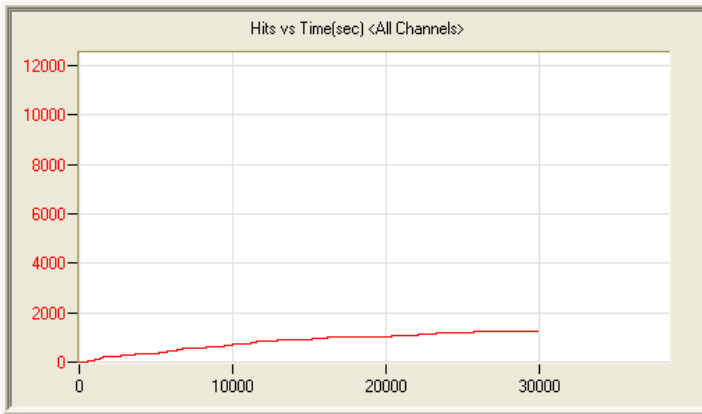
5/4/12 3:21pm 9:35:55 1627 120504152148_0 1.5mb



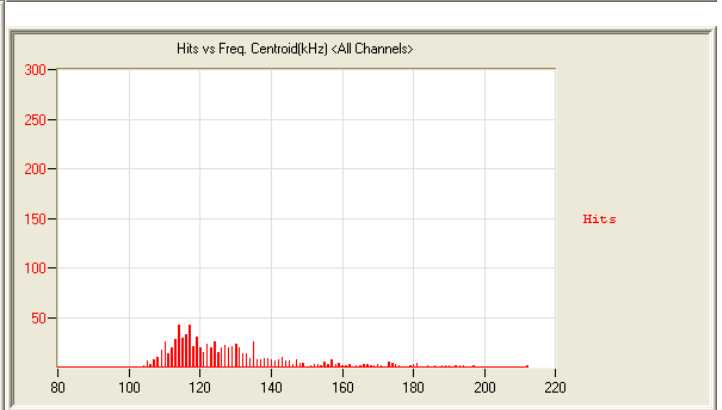
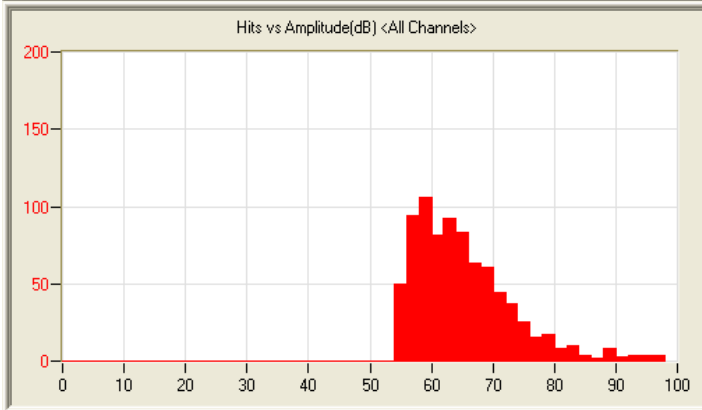
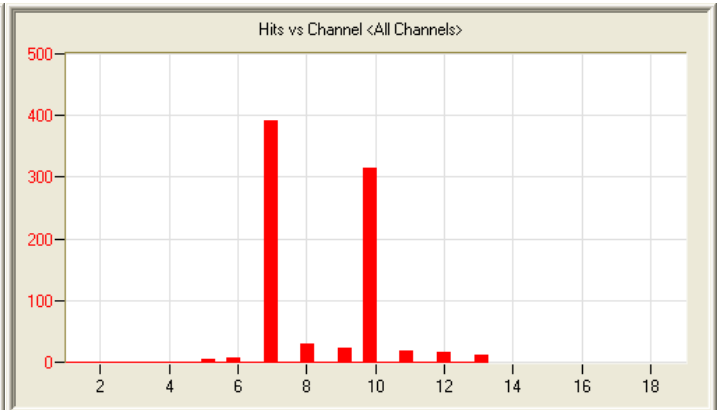
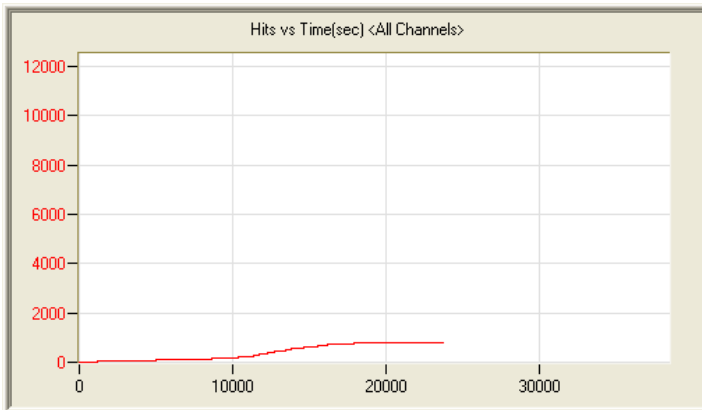
5/5/12 1:49pm 10:59:43 5464 120505134942_0 1.9mb



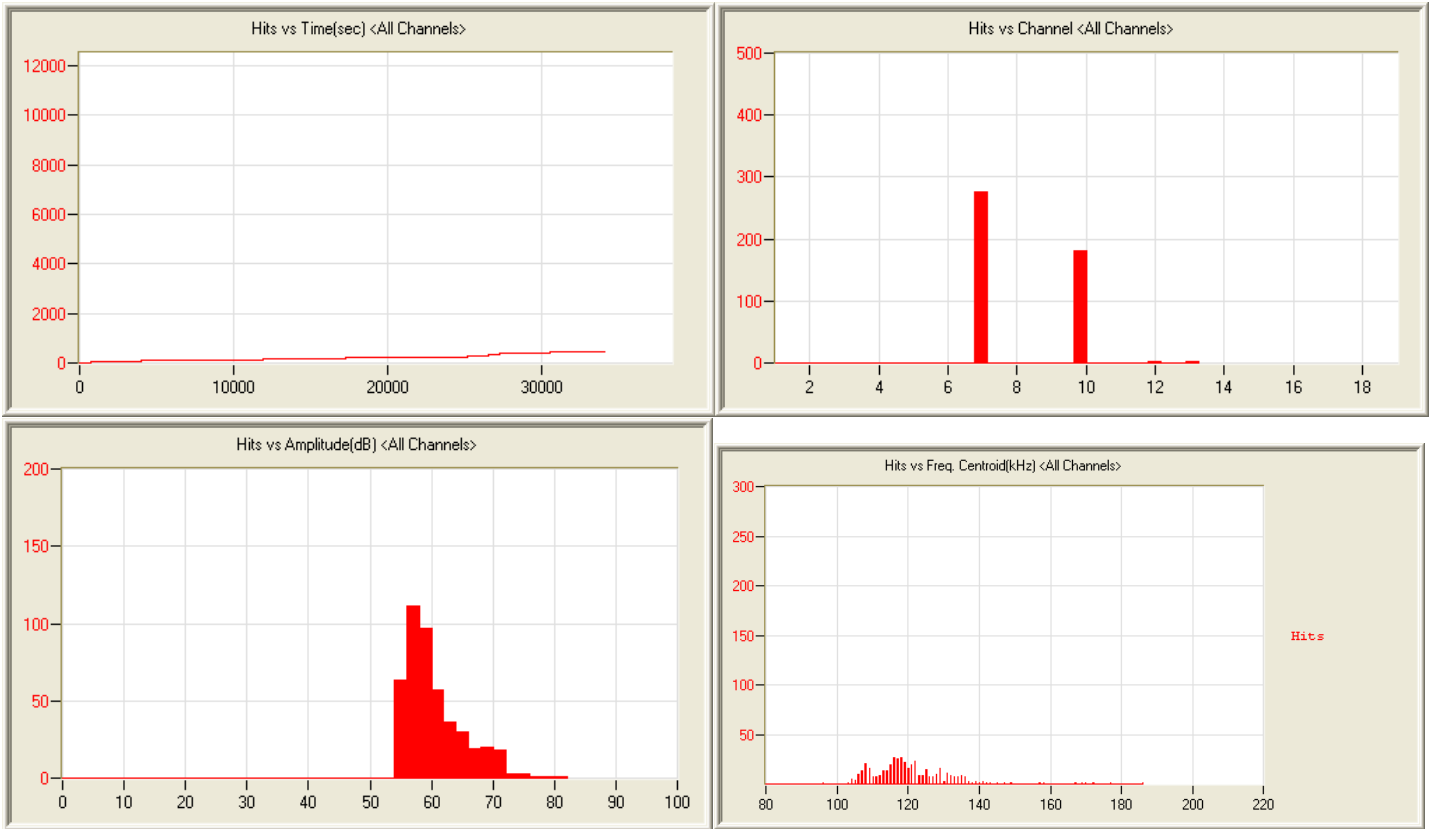
5/6/12 2:51pm 1:14:42 347 120506145058_0 260kb



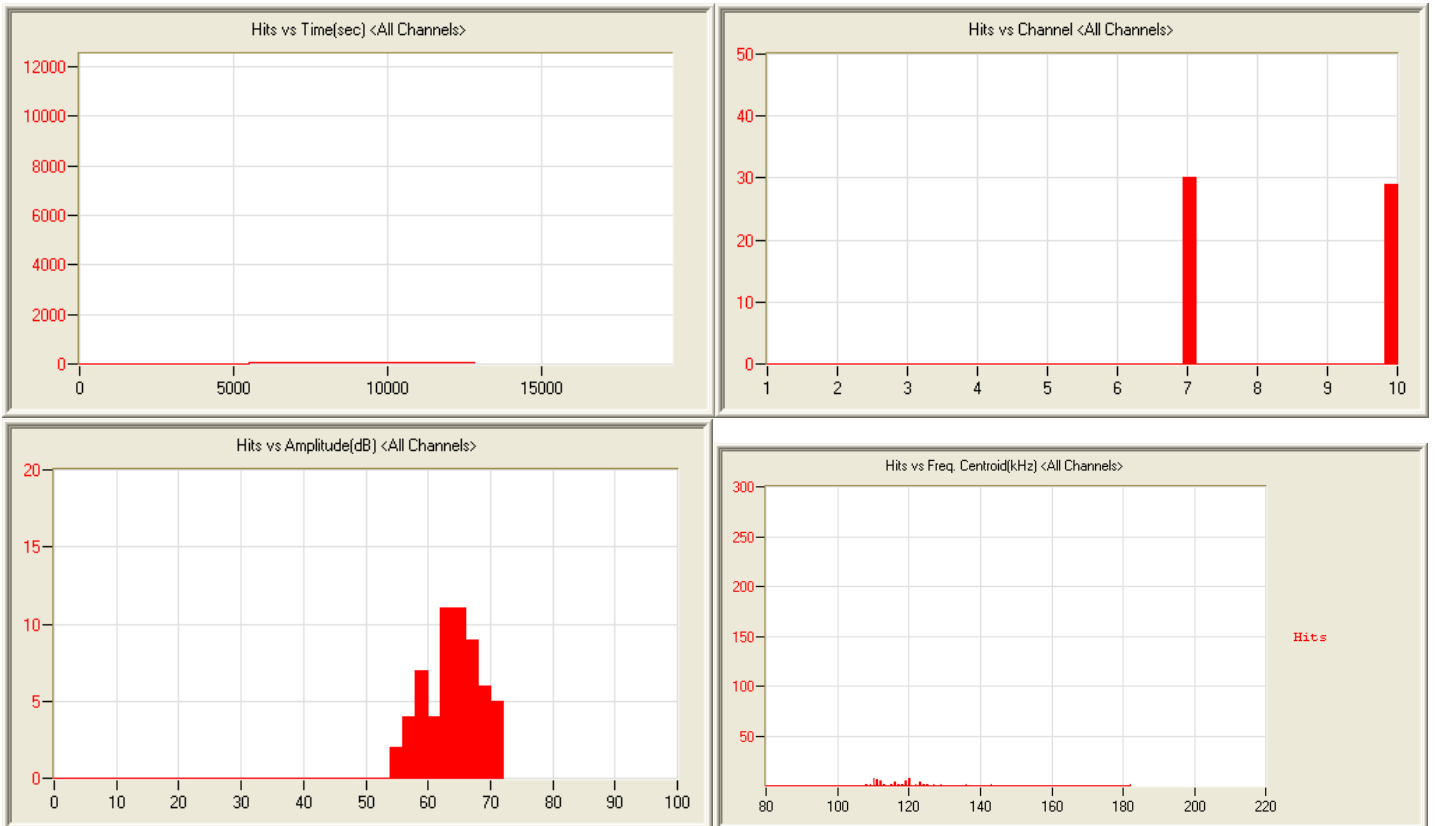
5/6/12 5:15pm 8:23:05 1240 120506171543_0 1.3mb



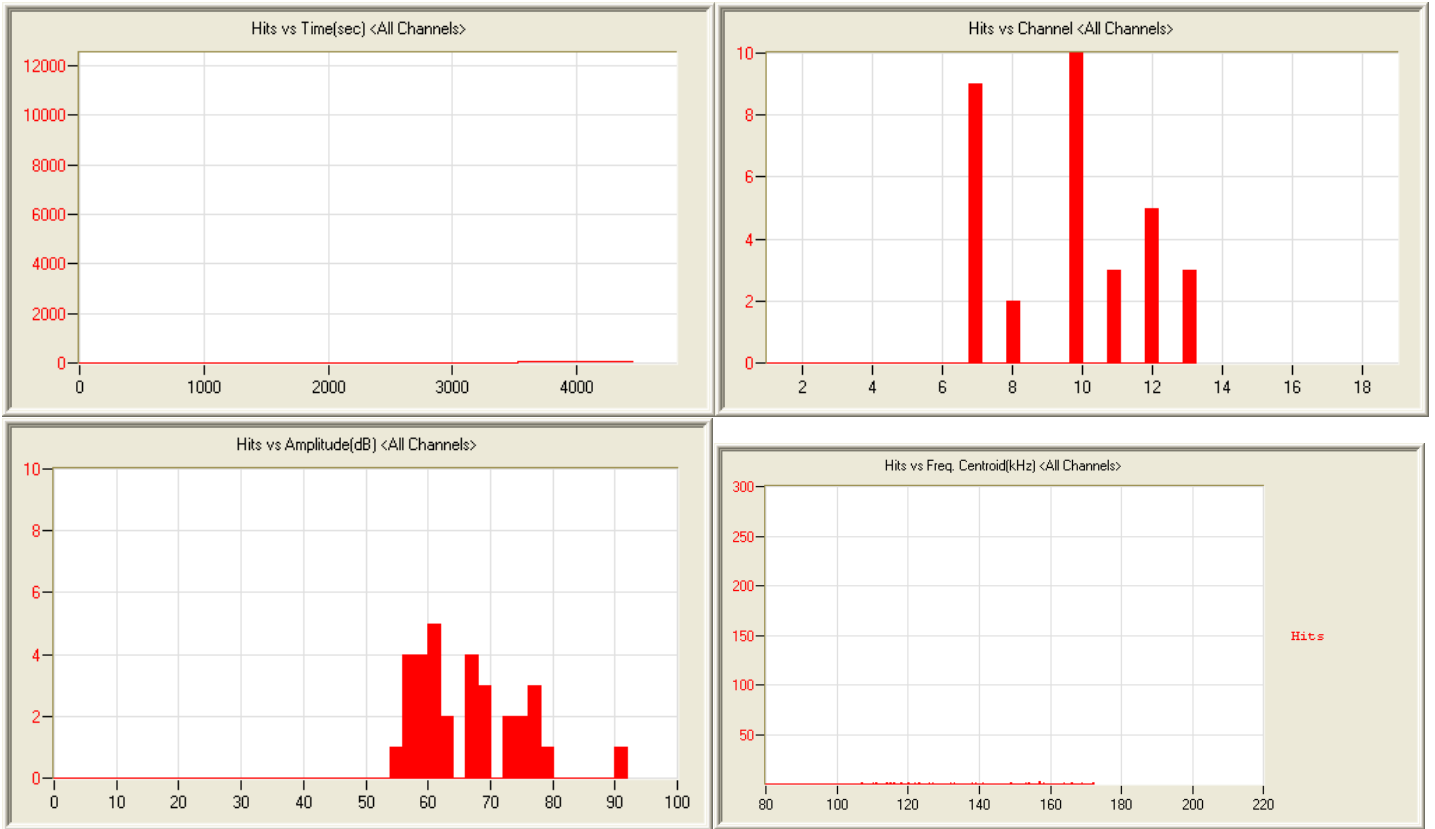
5/8/12 10:18am 6:42:29 815 120508101836_0 1.1mb



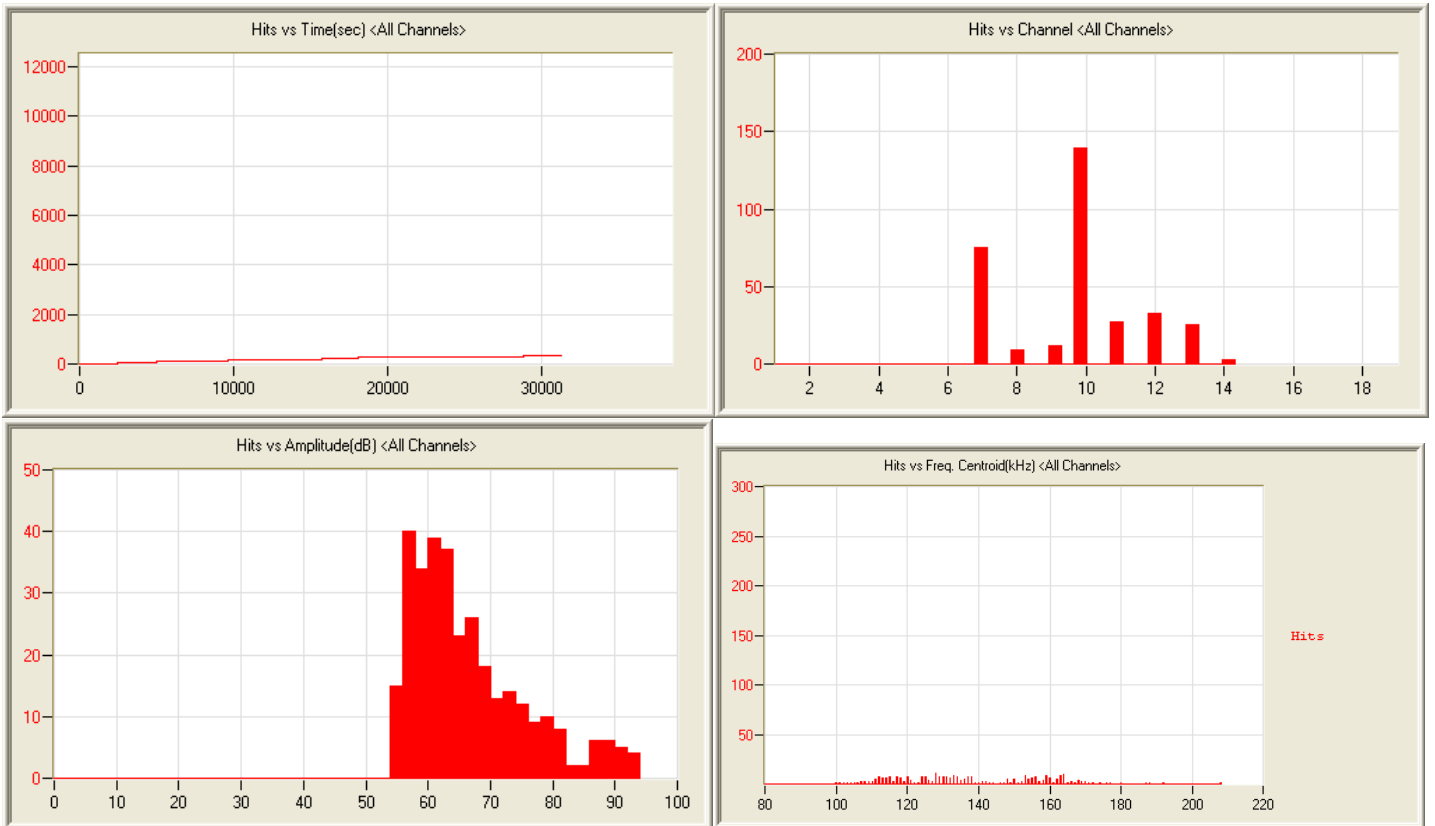
5/9/12 6:42am 9:31:04 460 120509064222_0 1.5mb



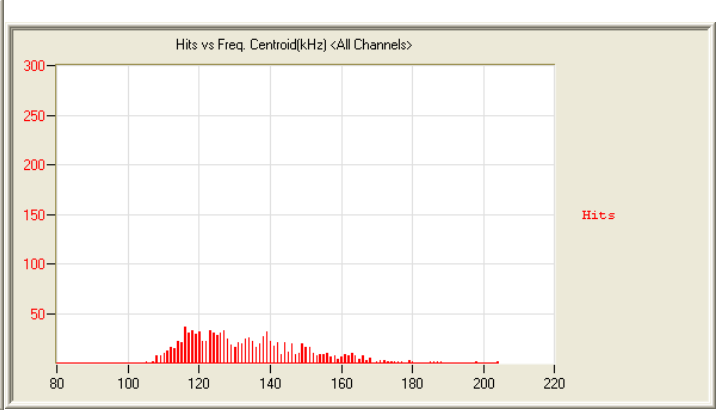
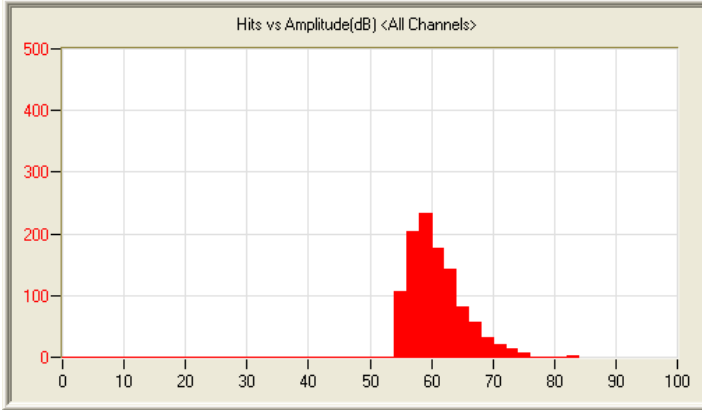
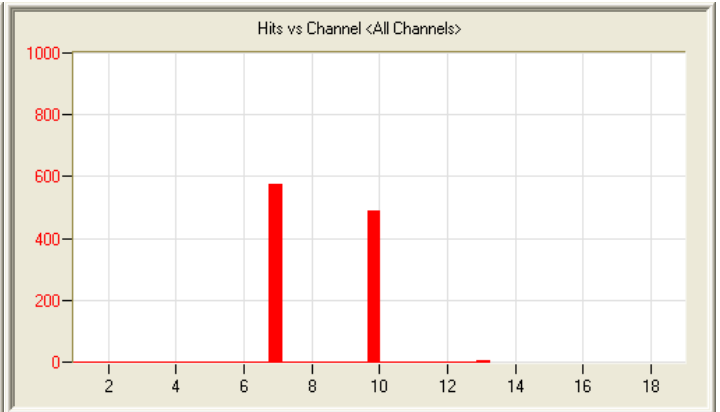
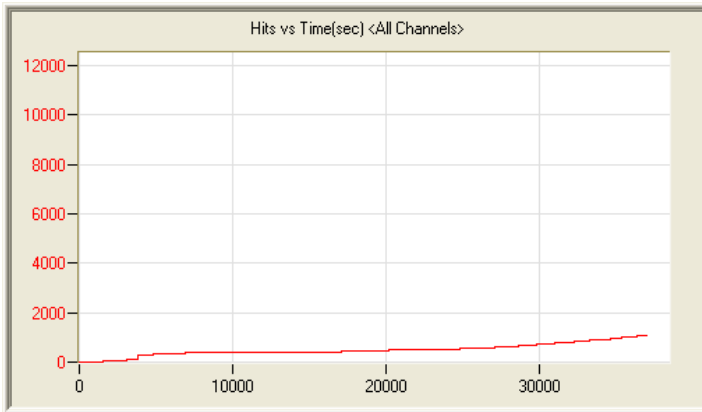
5/11/12 3:12am 3:34:33 59 120511031250_0 584kb



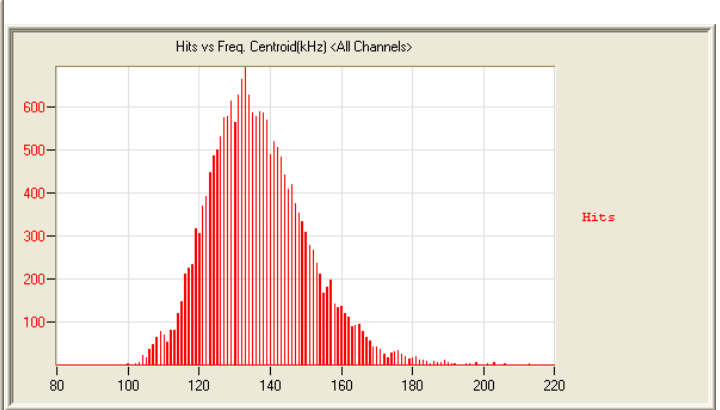
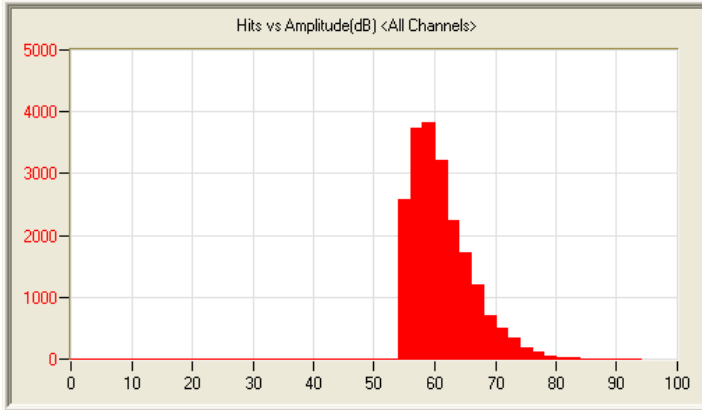
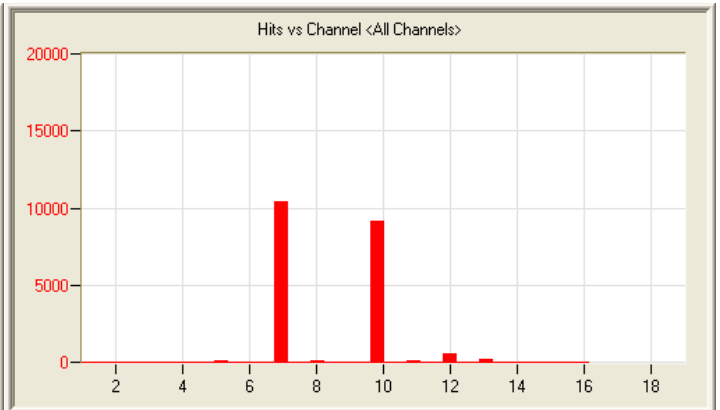
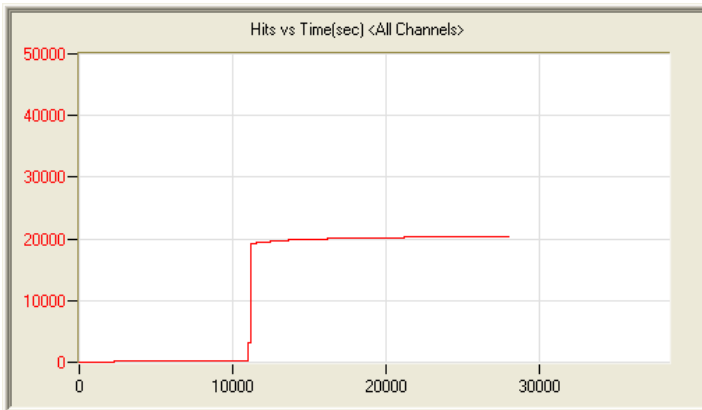
5/11/12 5:08pm 1:20:41 32 120511170851_0 261kb



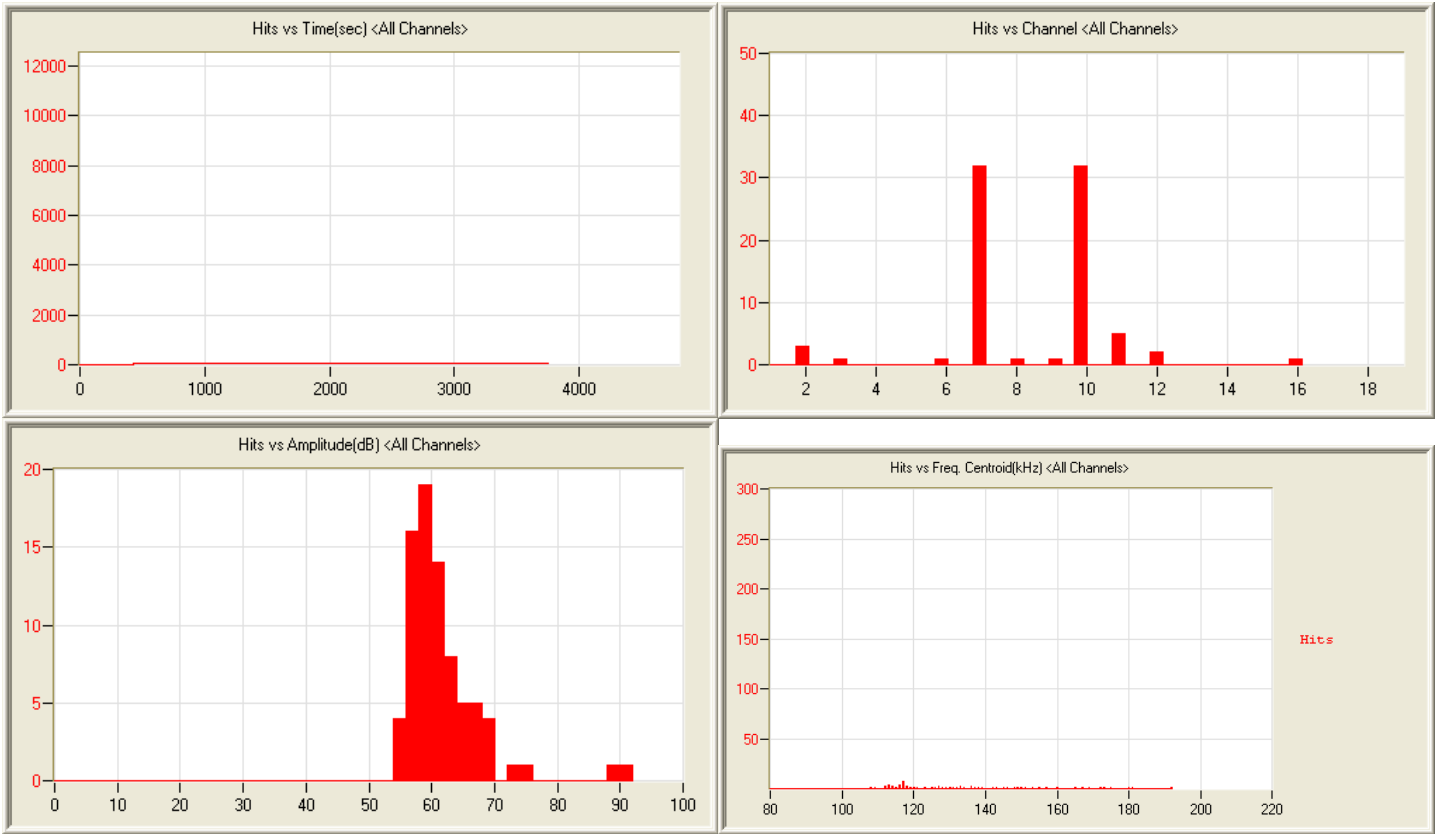
5/13/12 11:55am 8:59:22 323 120513115534_0 1.4mb



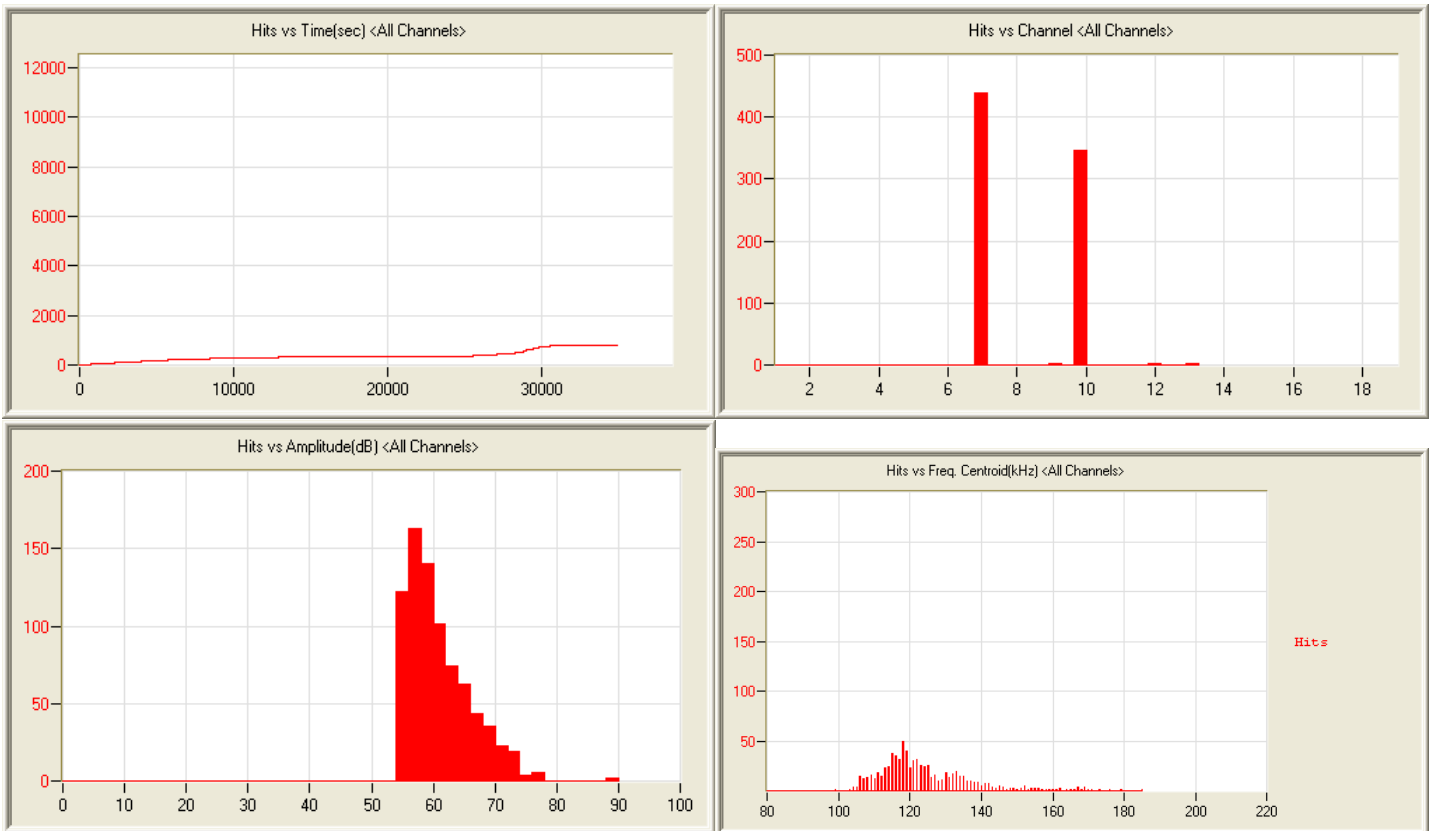
5/14/12 10:43am 10:17:16 1074 120514104348_0 1.6mb



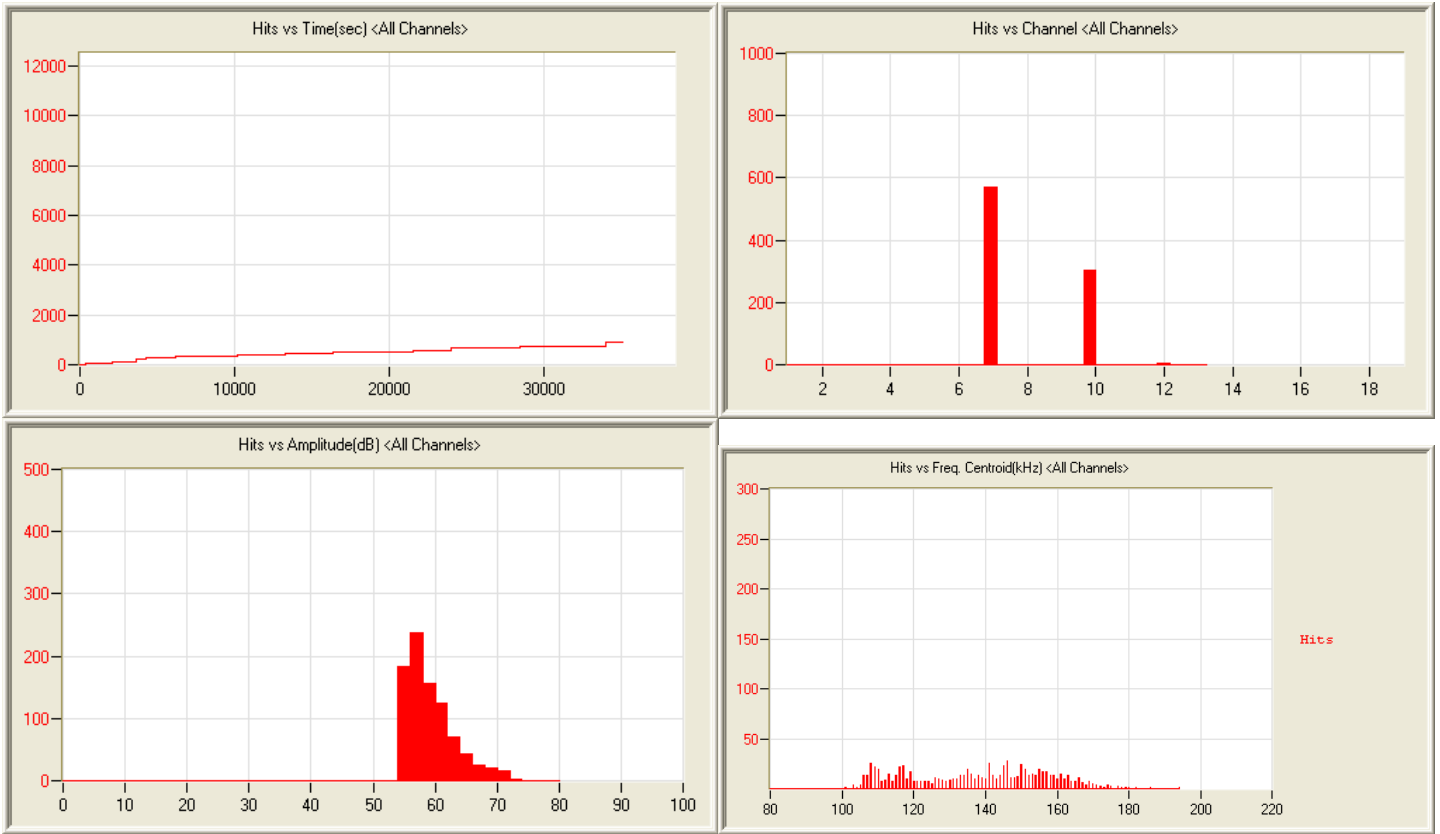
5/16/12 4:26am 7:46:57 20468 120516042603_0 2.0mb



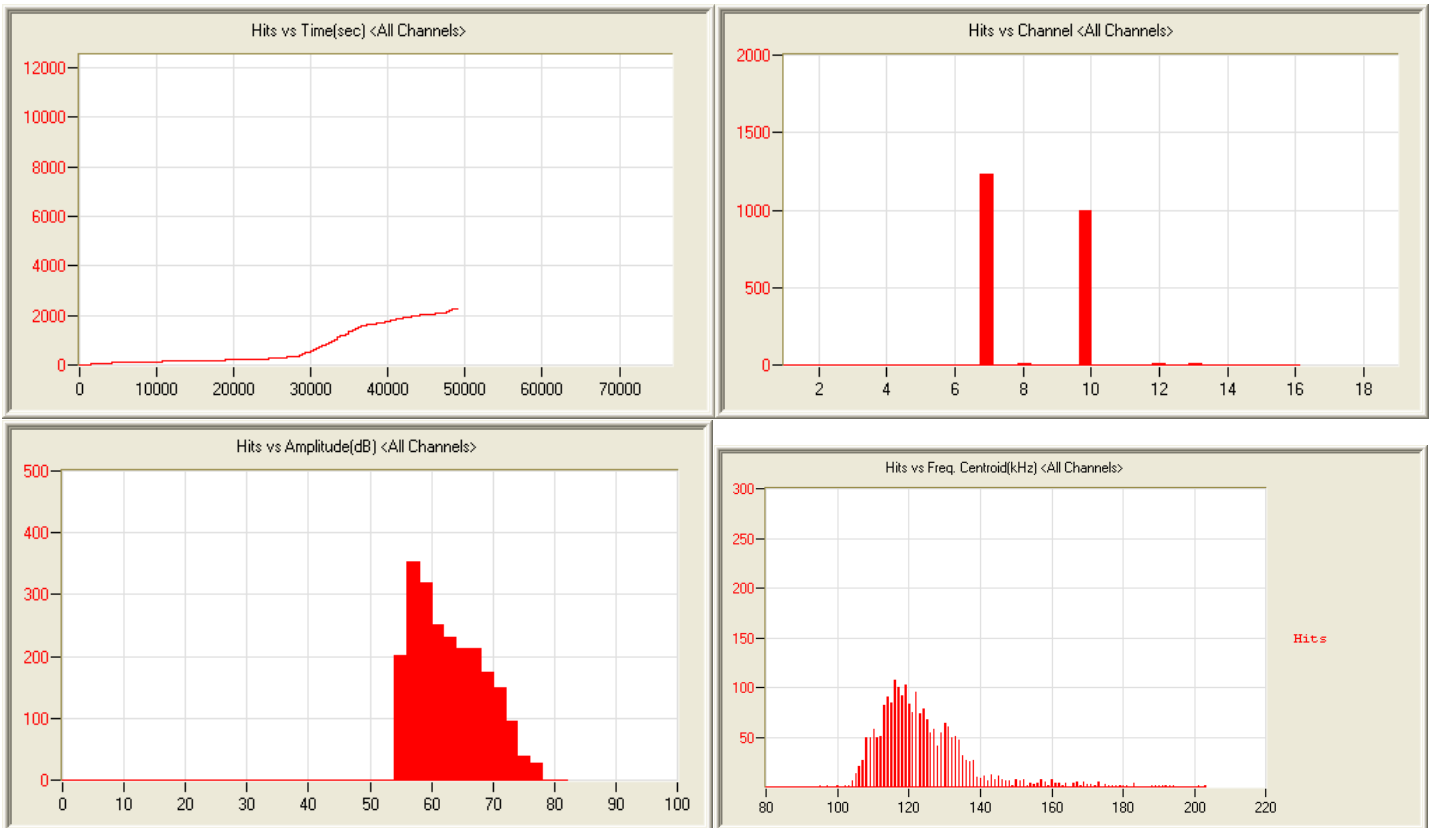
5/16/12 1:40pm 1:10:31 79 120516134051_0 239 120516134051_0 239kb



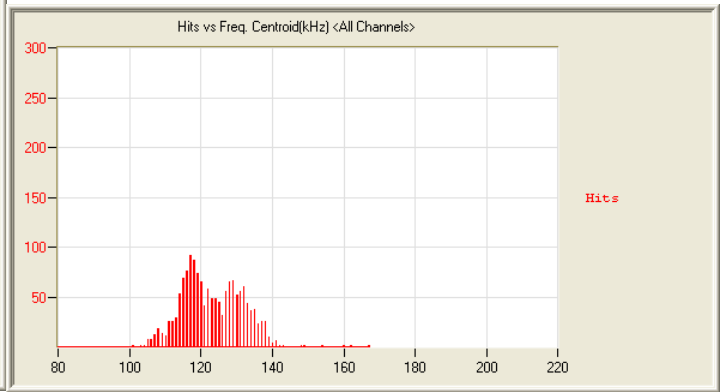
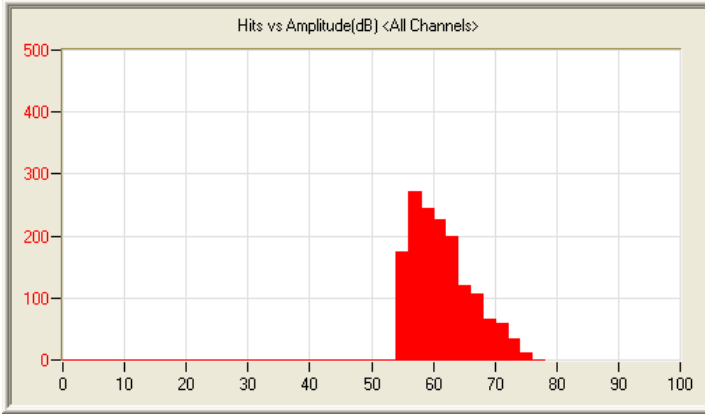
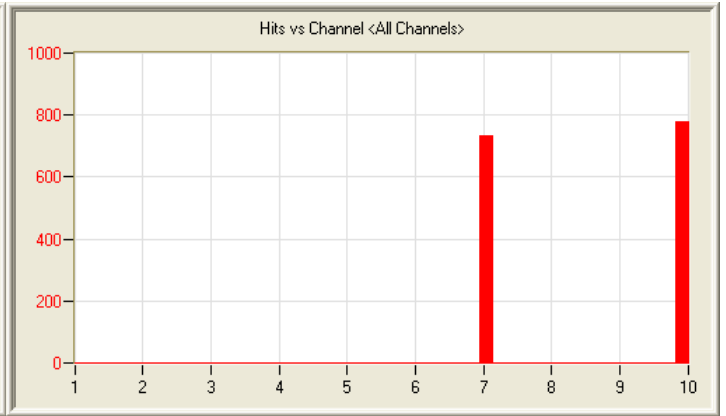
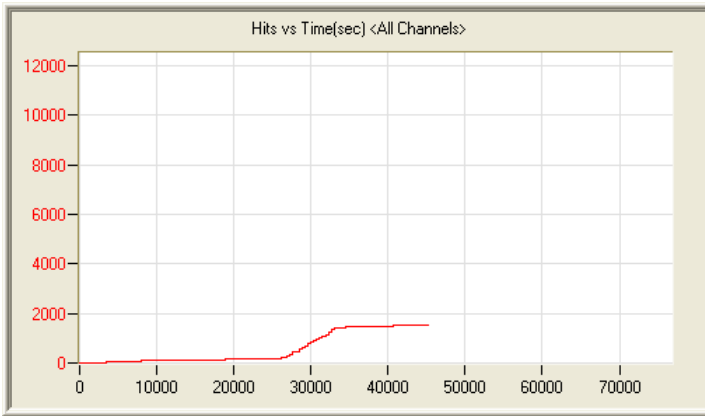
5/17/12 4:27am 10:01:50 793 120517042724_0 1.5mb



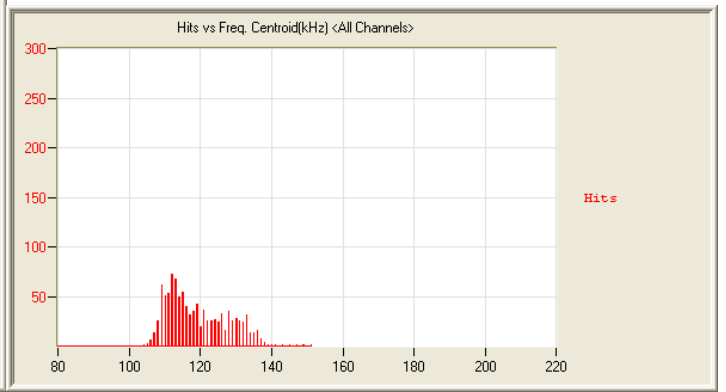
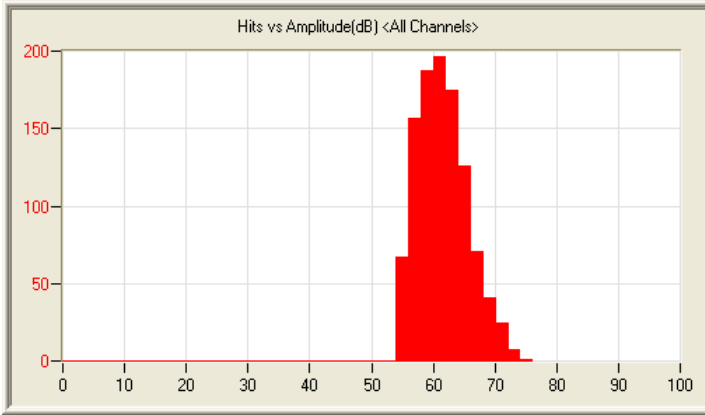
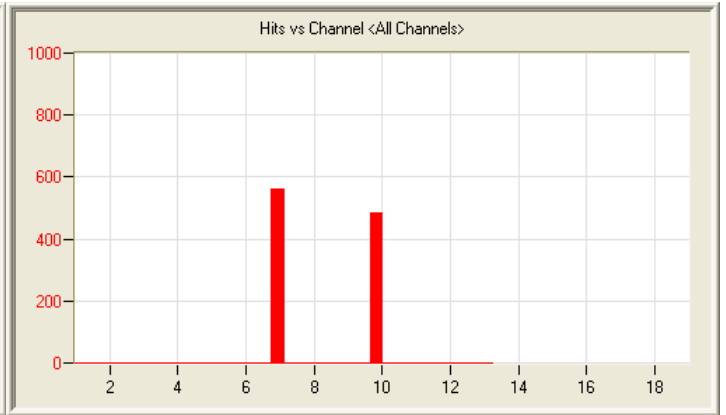
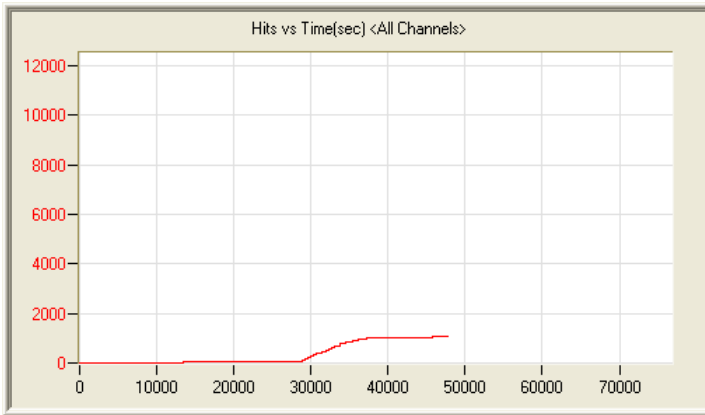
5/18/12 6:27am 9:55:50 880 120518062708_0 1.5mb



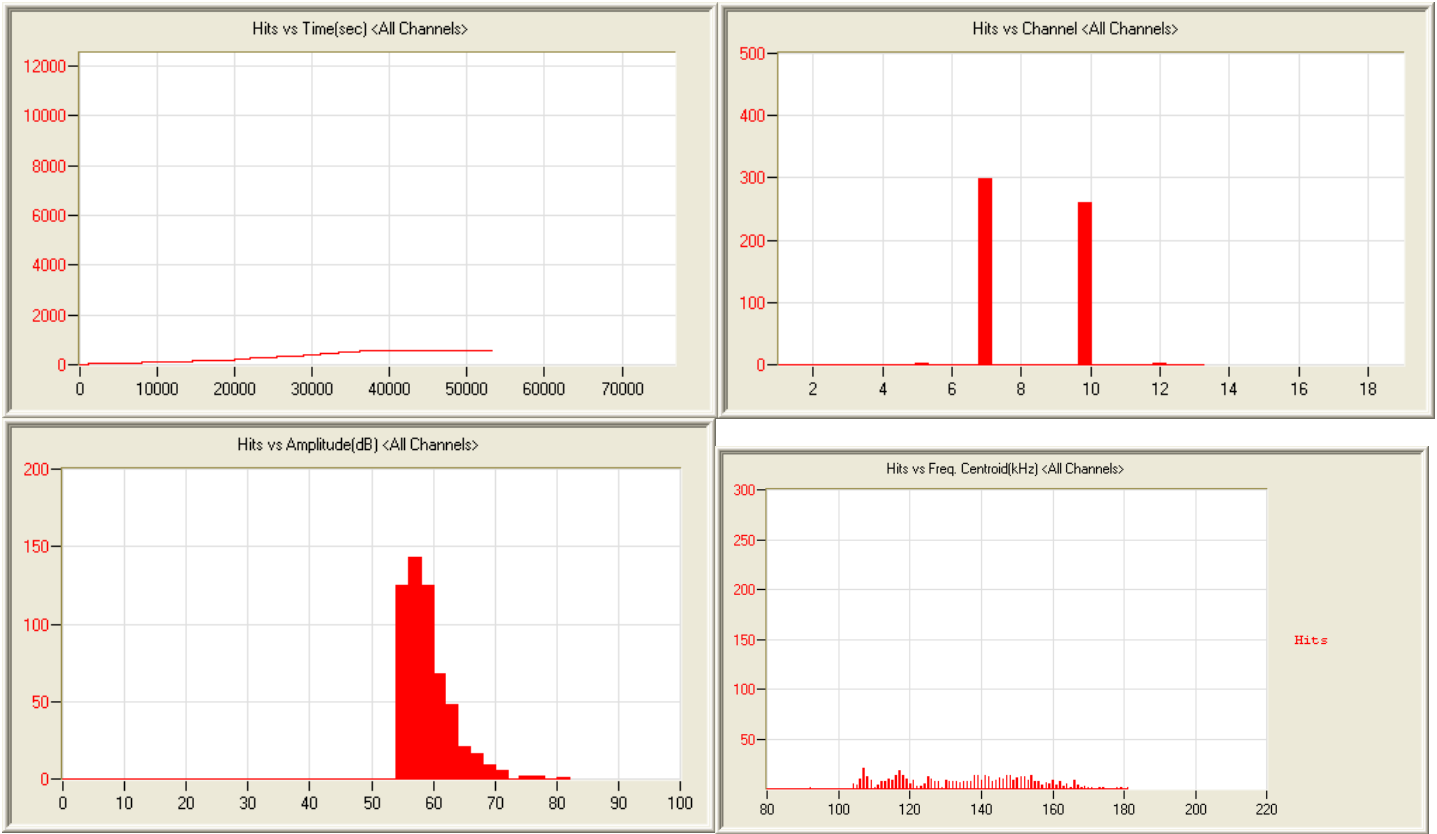
5/19/12 9:36am 13:33:24 2265 120519093616_0 2.1mb



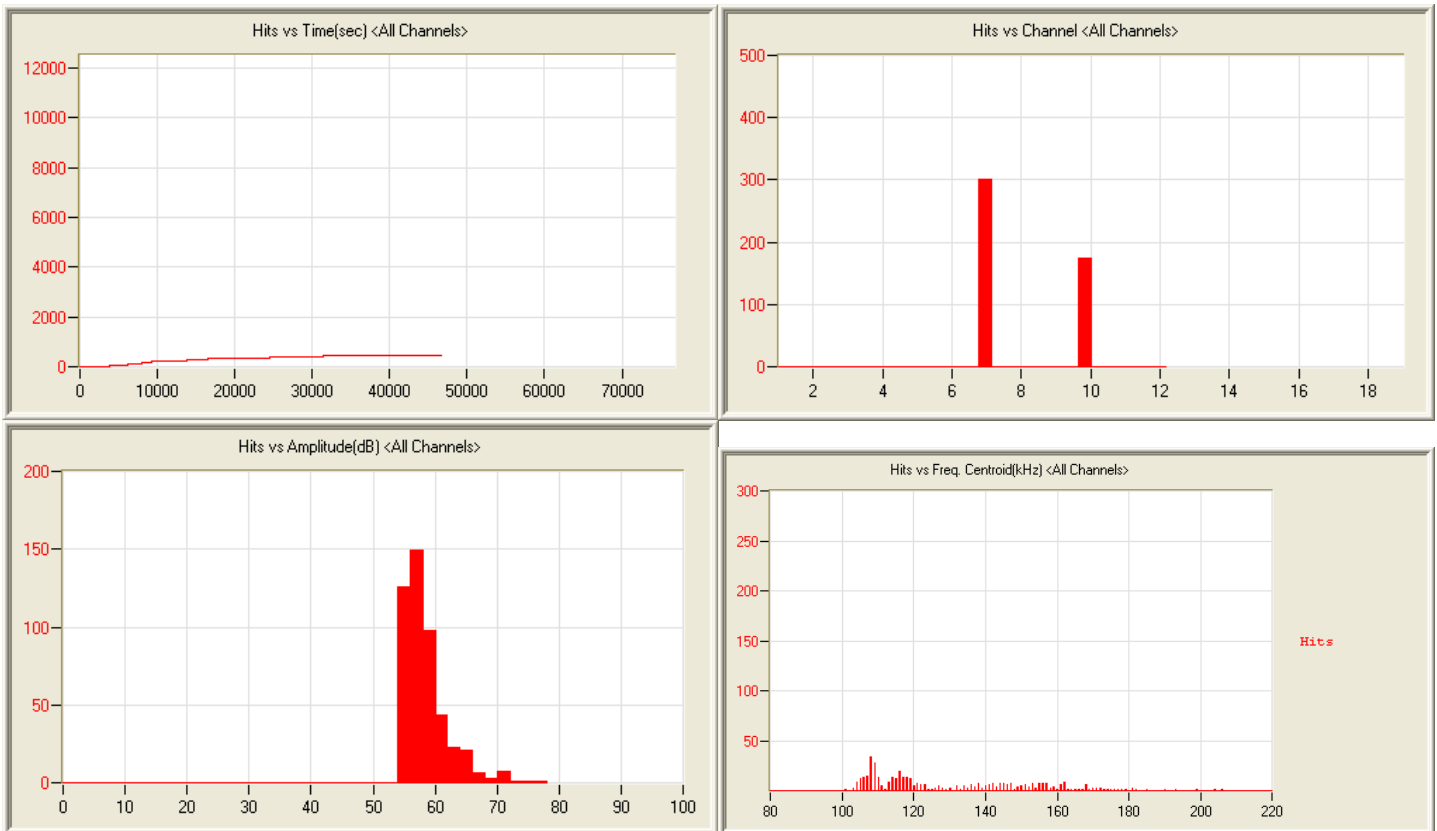
5/20/12 2:15pm 12:38:20 1516 120520141519_0 1.9mb



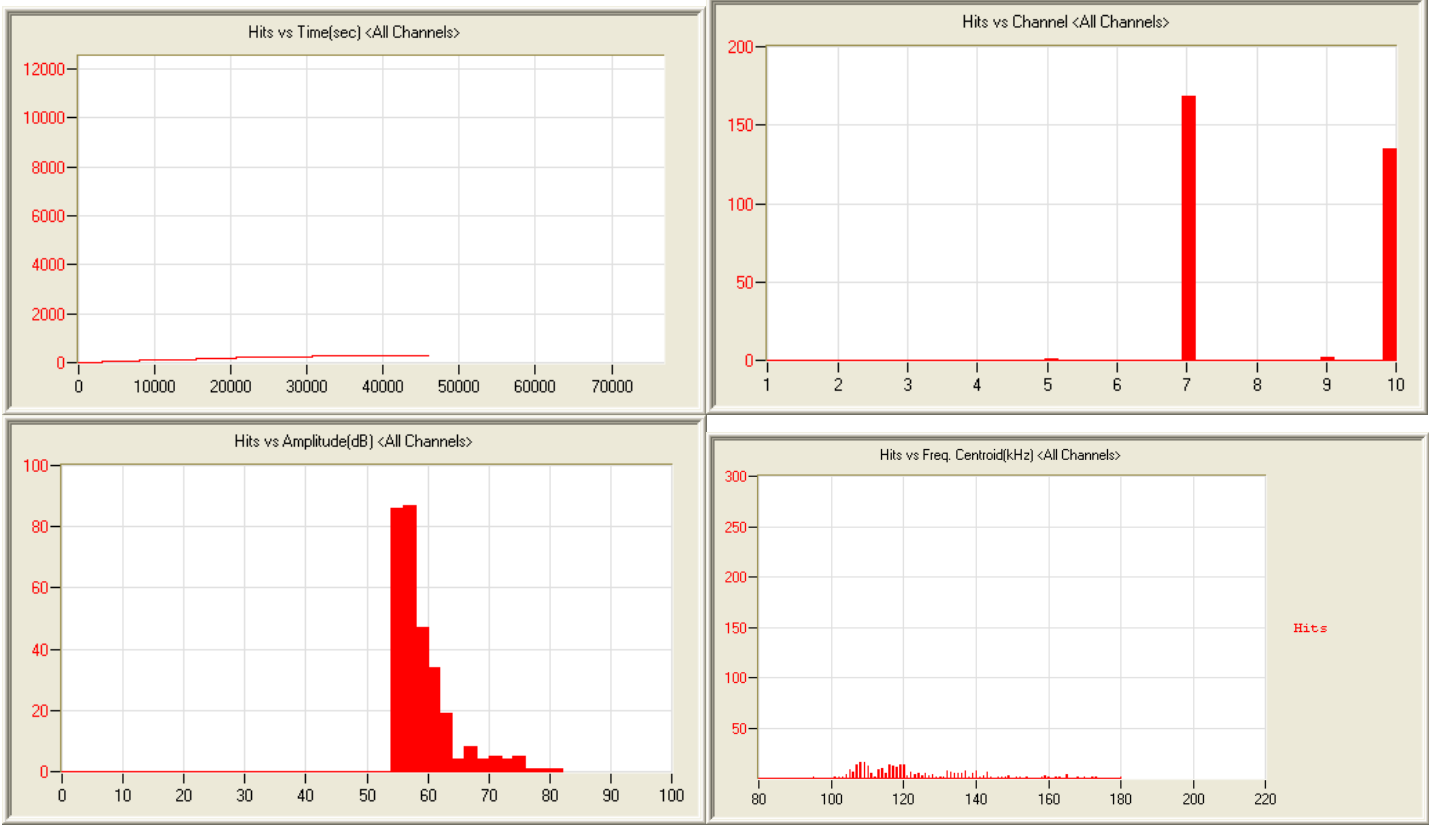
5/21/12 2:25pm 14:23:09 1052 120521142534_0 2.2mb



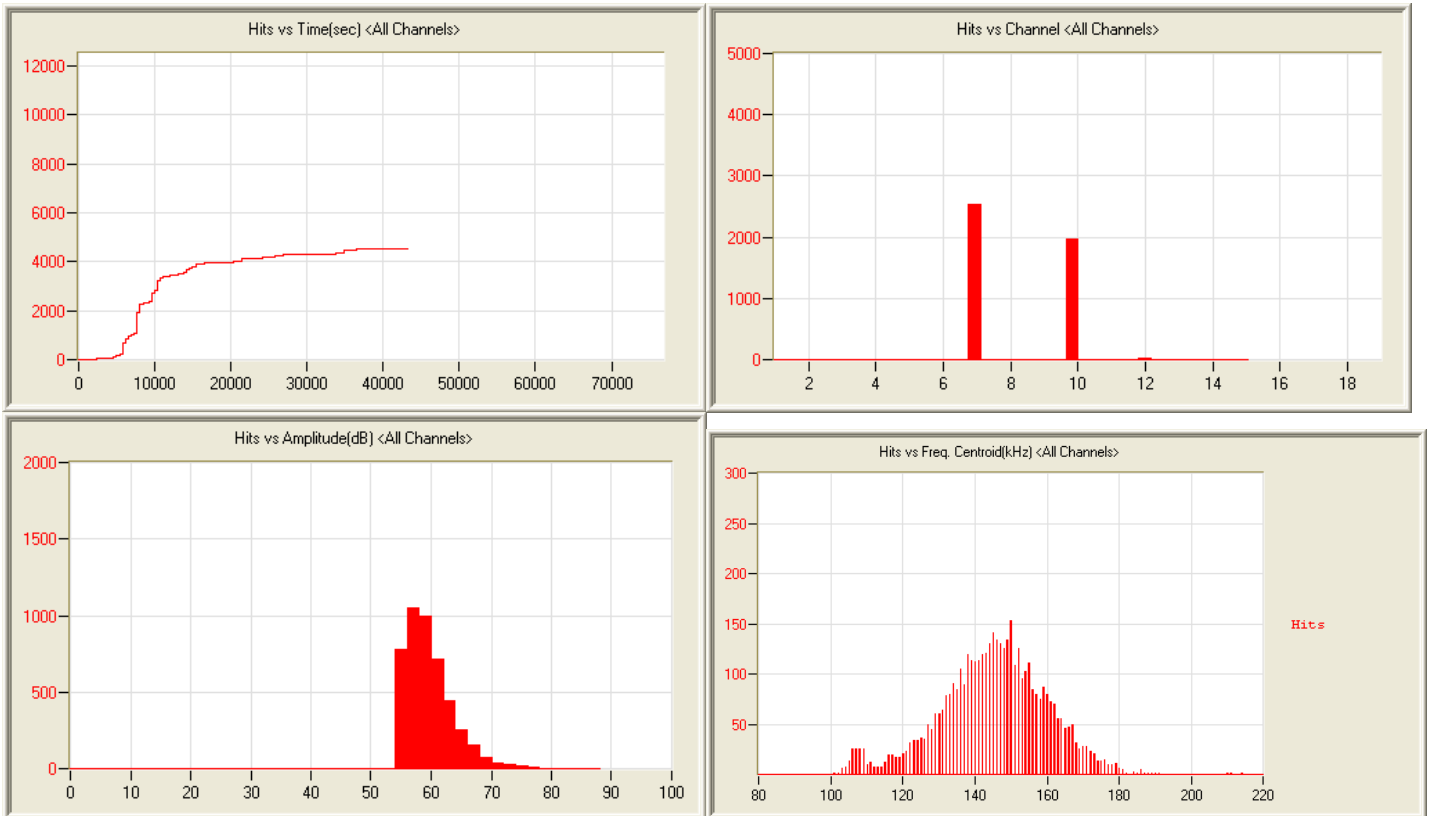
5/22/12 3:23pm 15:11:40 565 120522152332_0 2.3mb



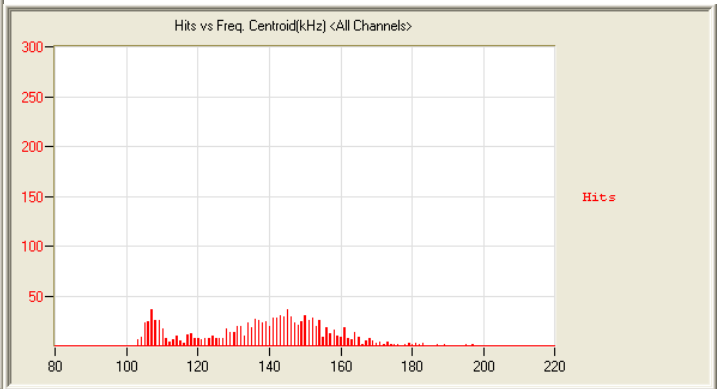
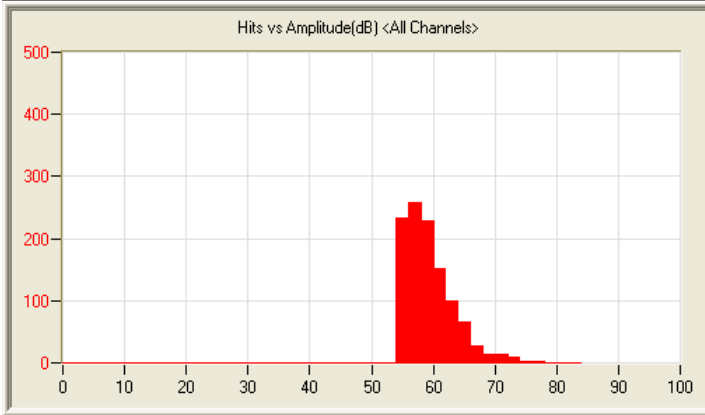
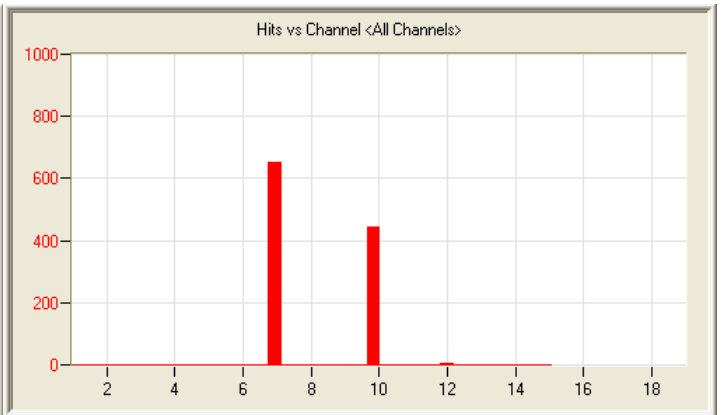
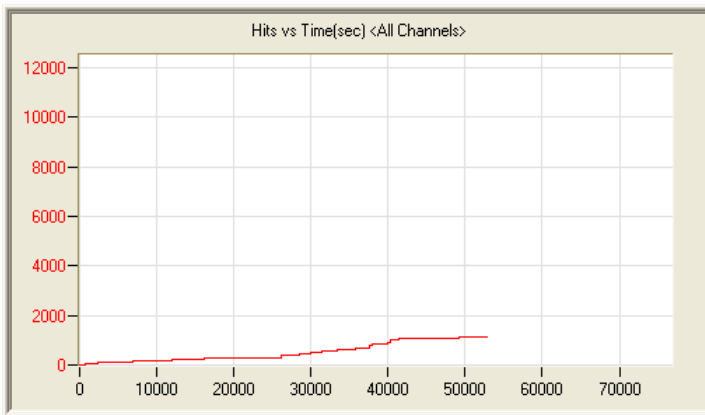
5/23/12 8:18pm 14:07:31 479 120523201851_0 2.1mb



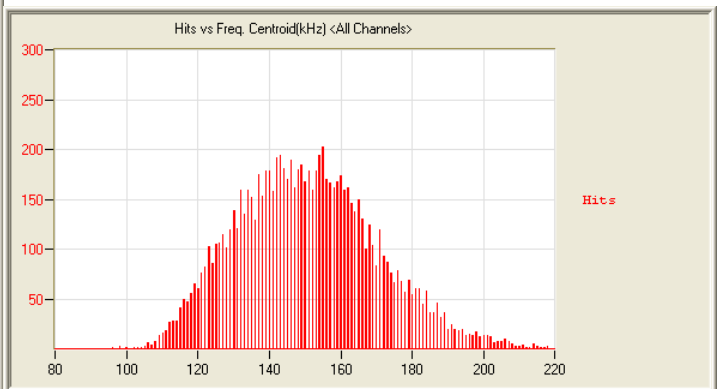
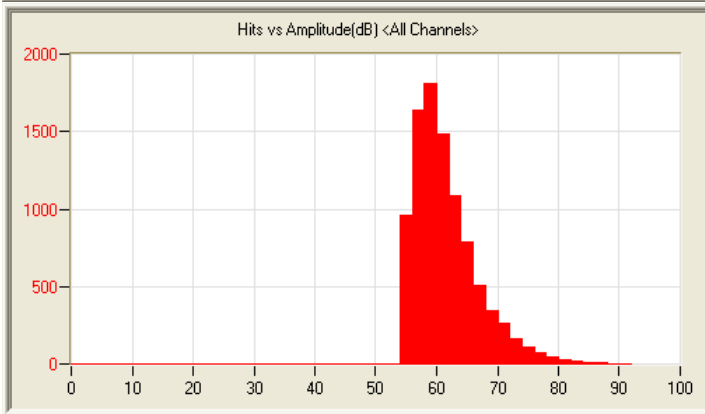
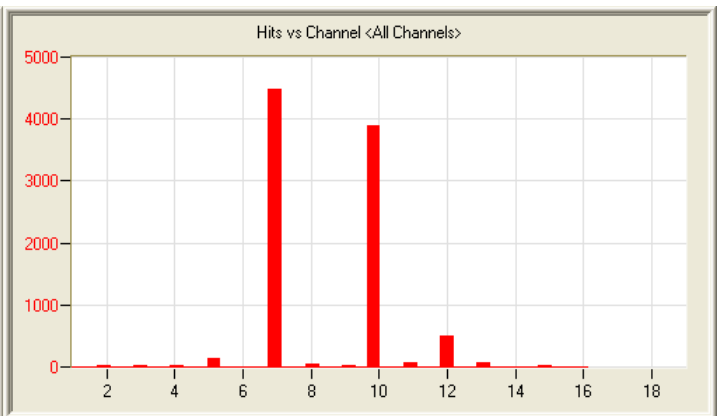
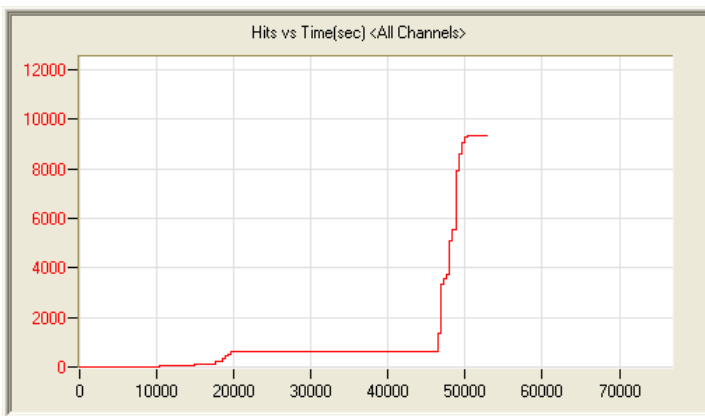
5/24/12 10:24pm 14:15:44 306 120524222417_0 2.1mb



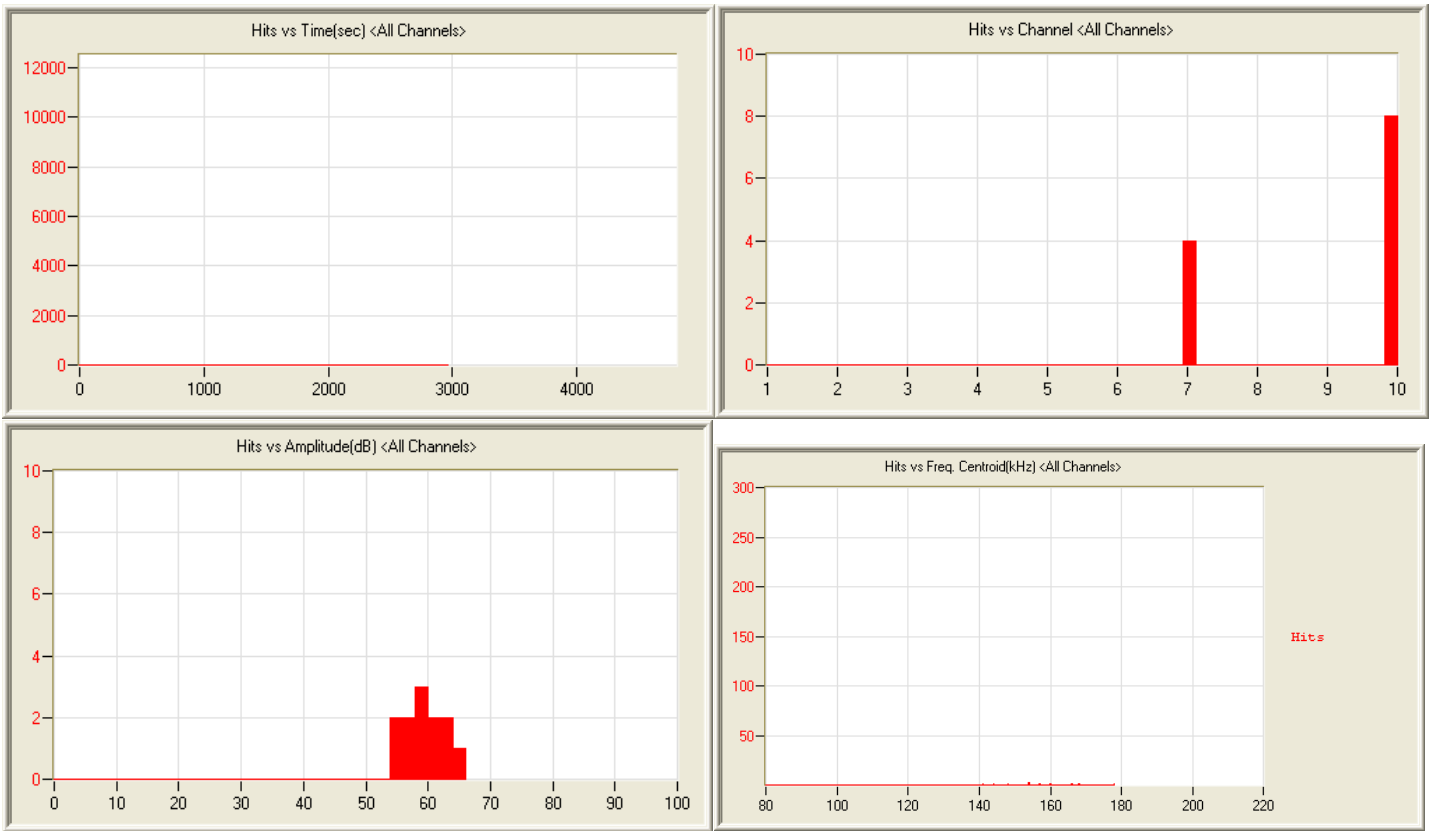
5/26/12 8:51am 12:38:56 4543 120526085123_0 2.1mb



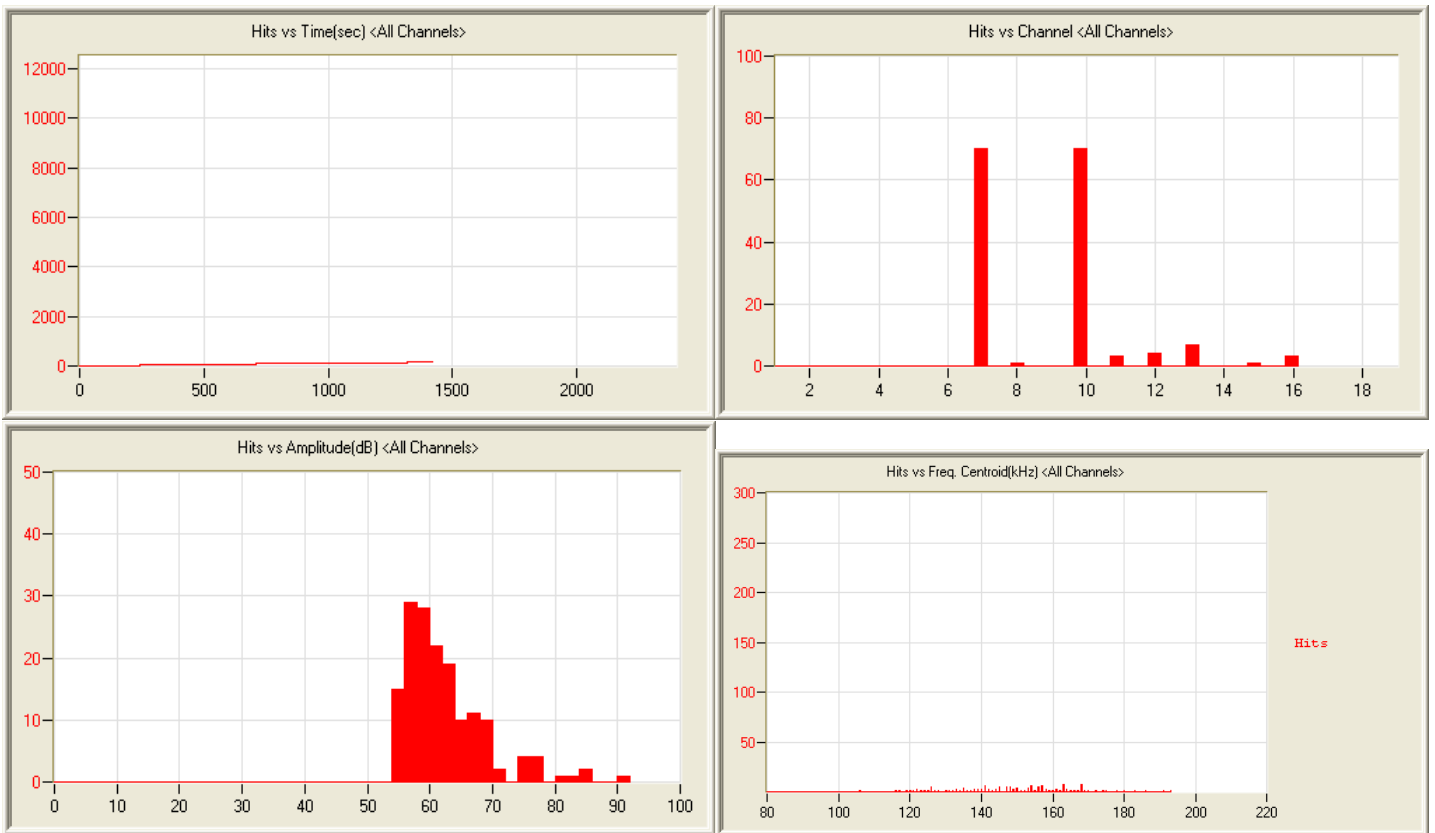
5/27/12 7:28am 14:42:18 1106 120527072815_0 2.2mb



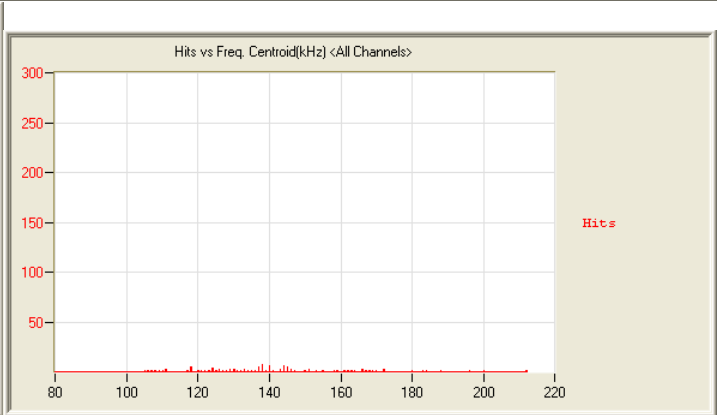
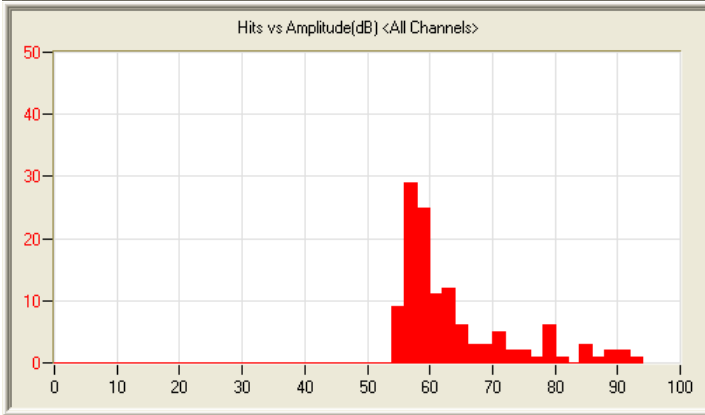
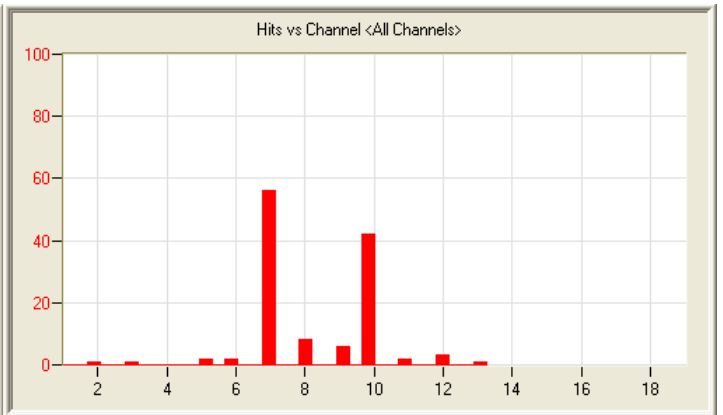
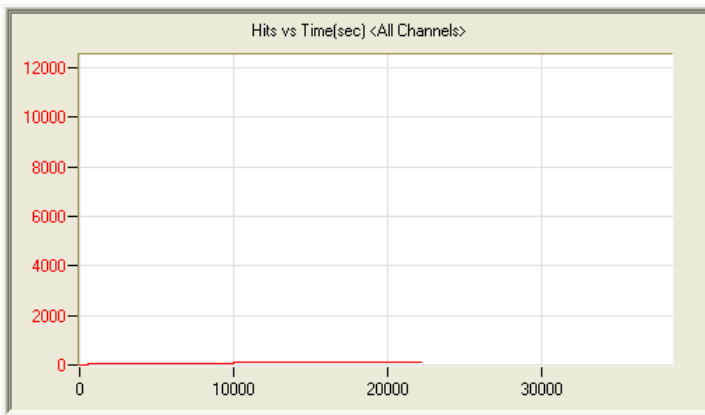
5/28/12 8:27am 15:09:03 9341 120528082732_0 2.6mb



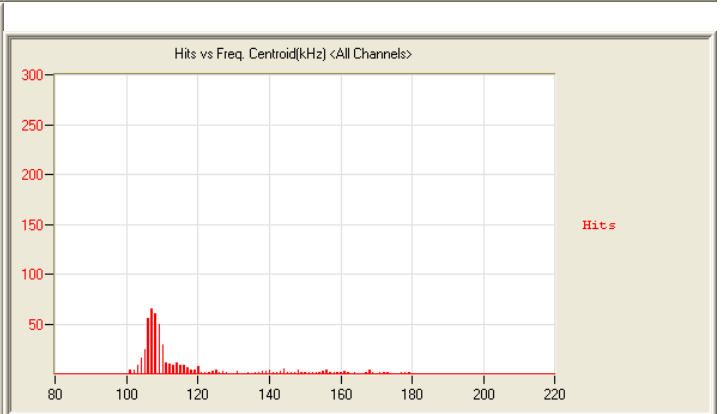
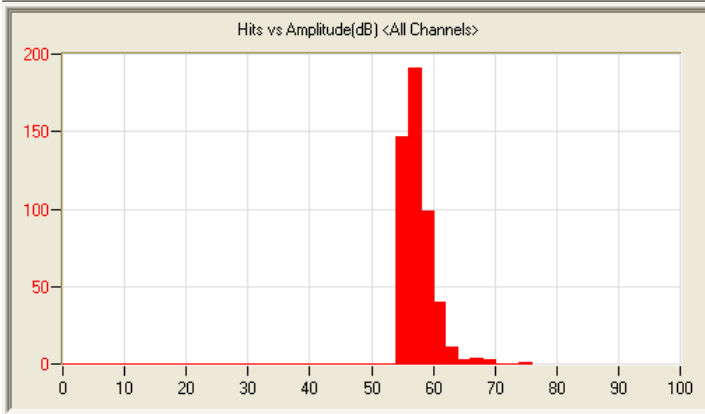
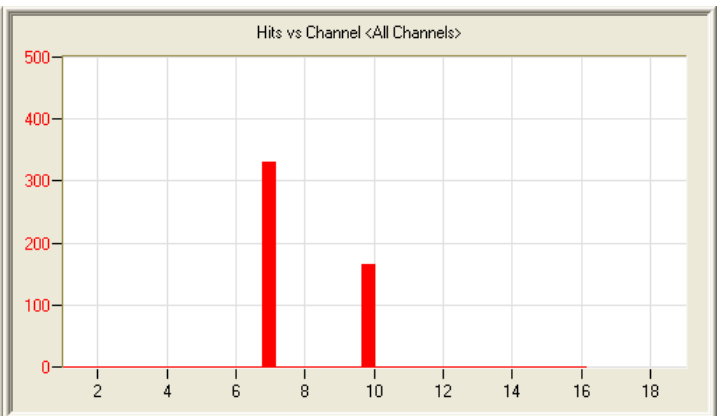
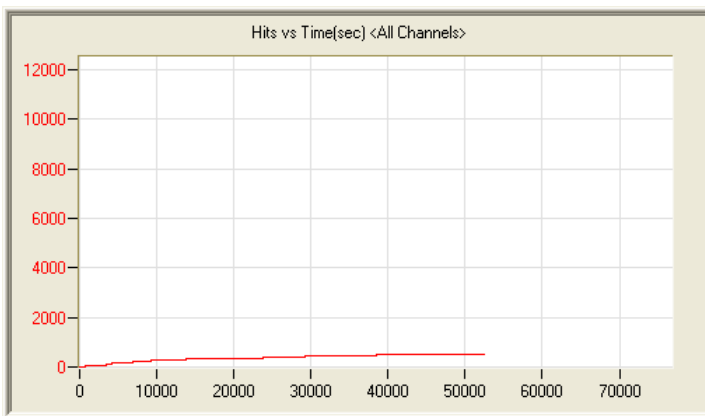
5/29/12 5:49pm 1:20:06 12 120529174859_0 259kb



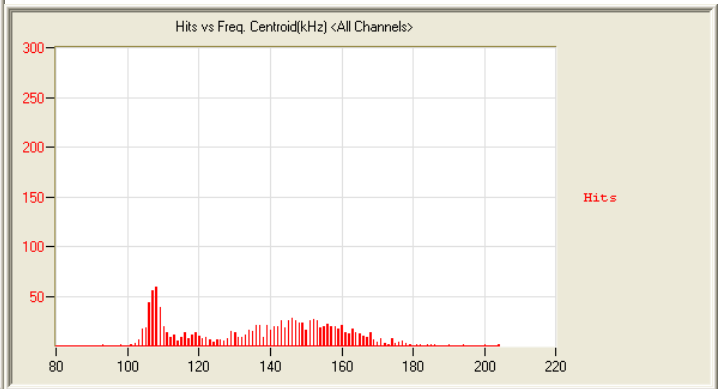
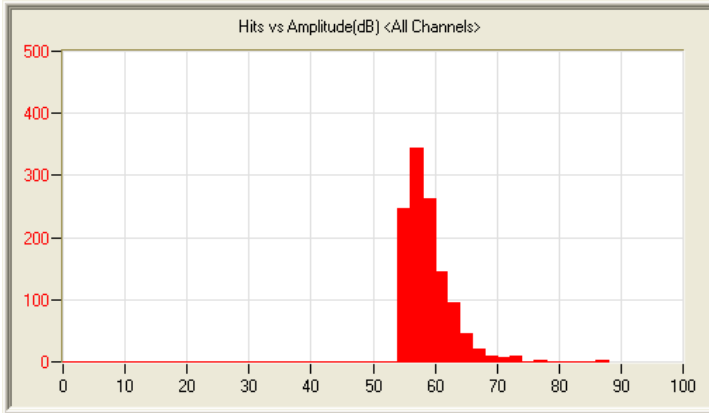
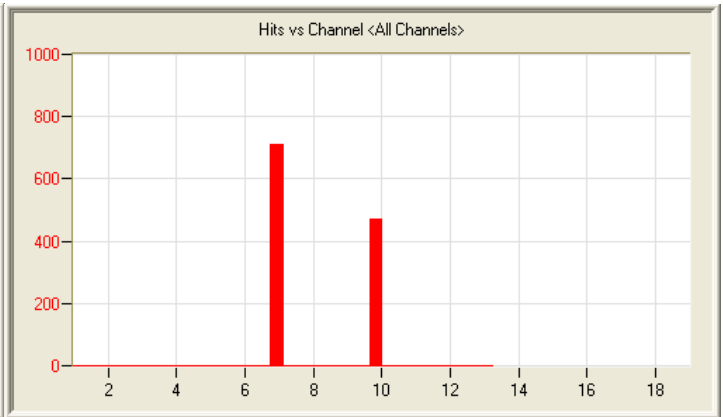
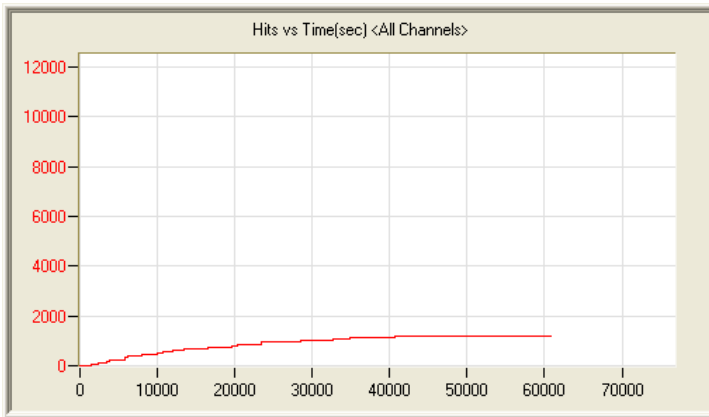
5/30/12 5:19am 0:23:47 159 120530051917_0 130kb



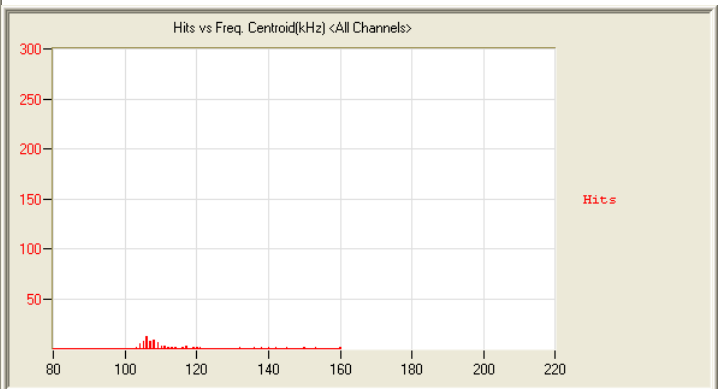
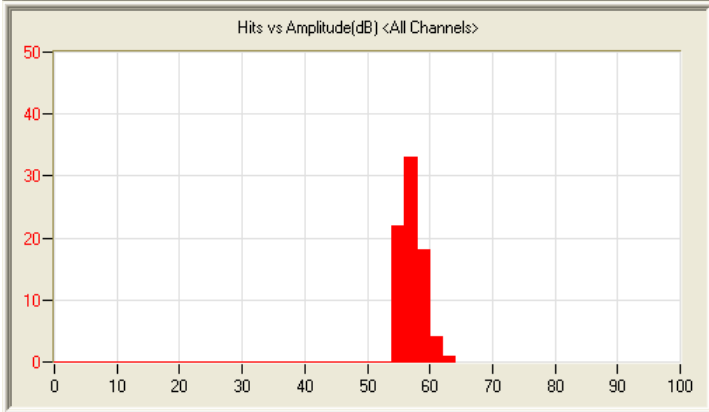
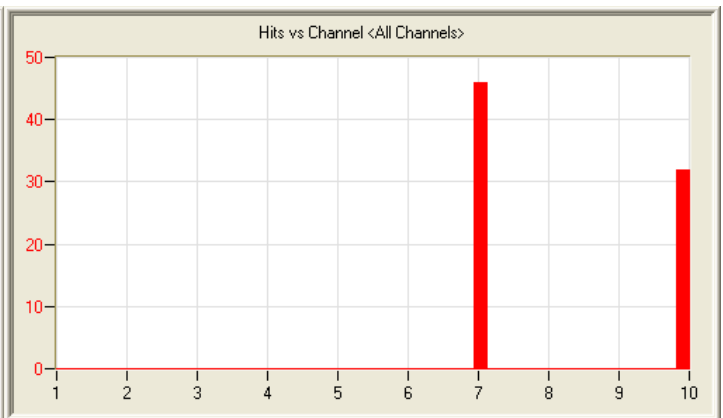
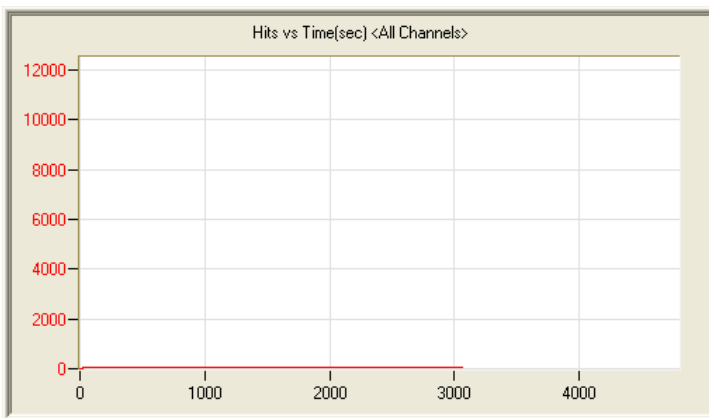
5/30/12 10:20am 6:36:08 124 120530102012_0 1.0mb



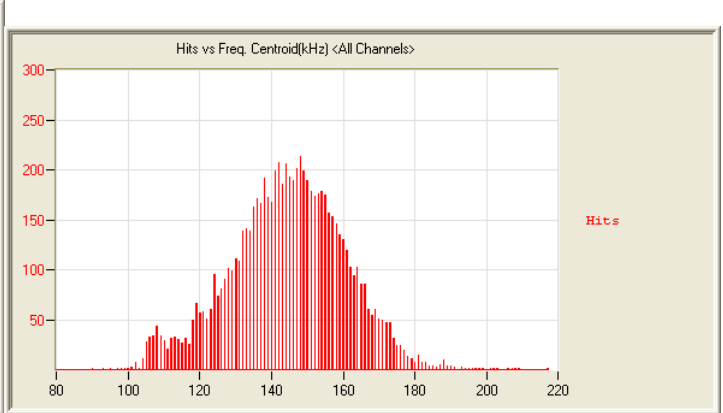
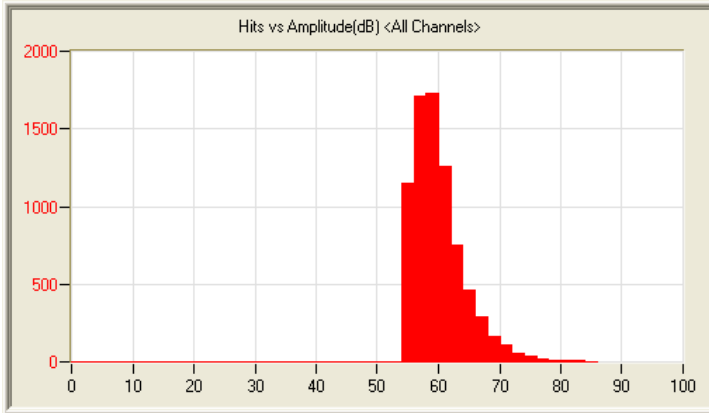
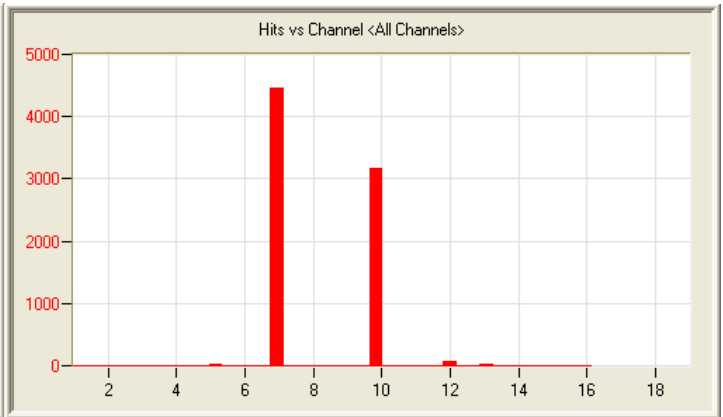
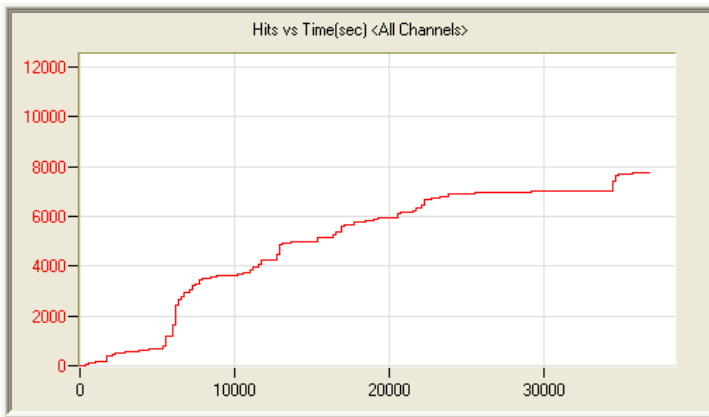
5/31/12 6:18am 15:09:37 499 120531061818_0 2.3mb



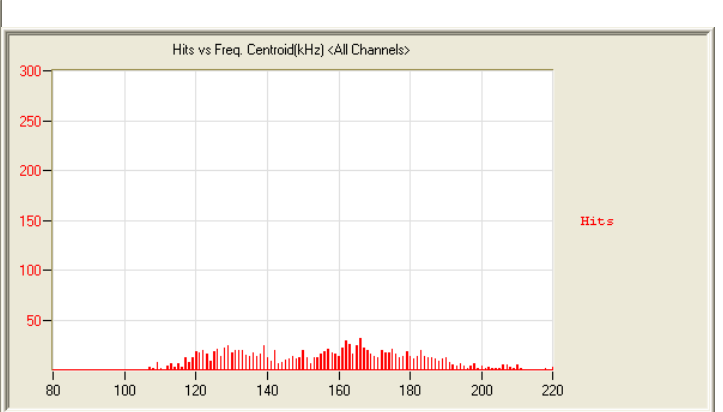
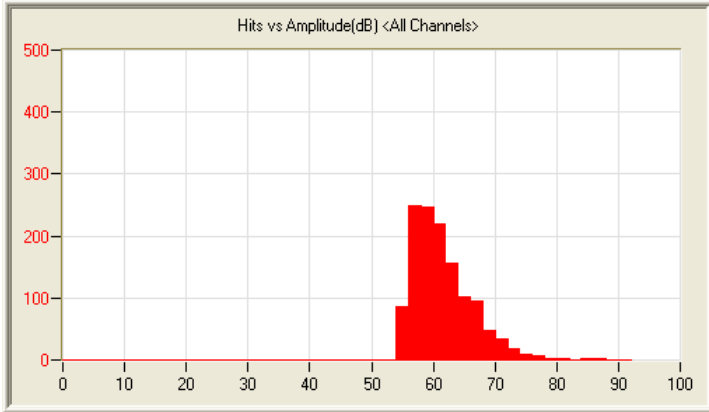
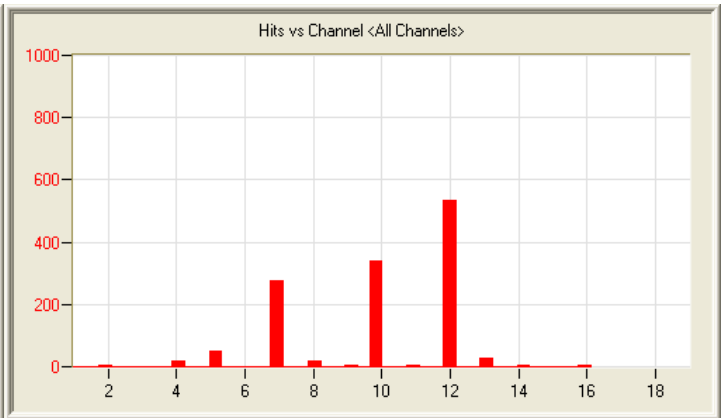
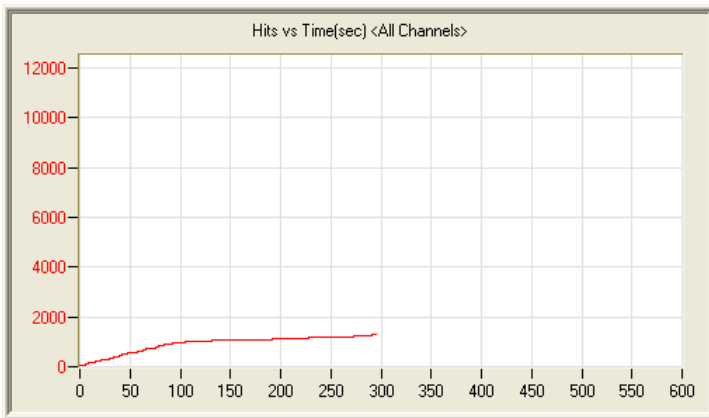
6/1/12 7:19am 16:56:42 1189 120601071941_0 2.6mb



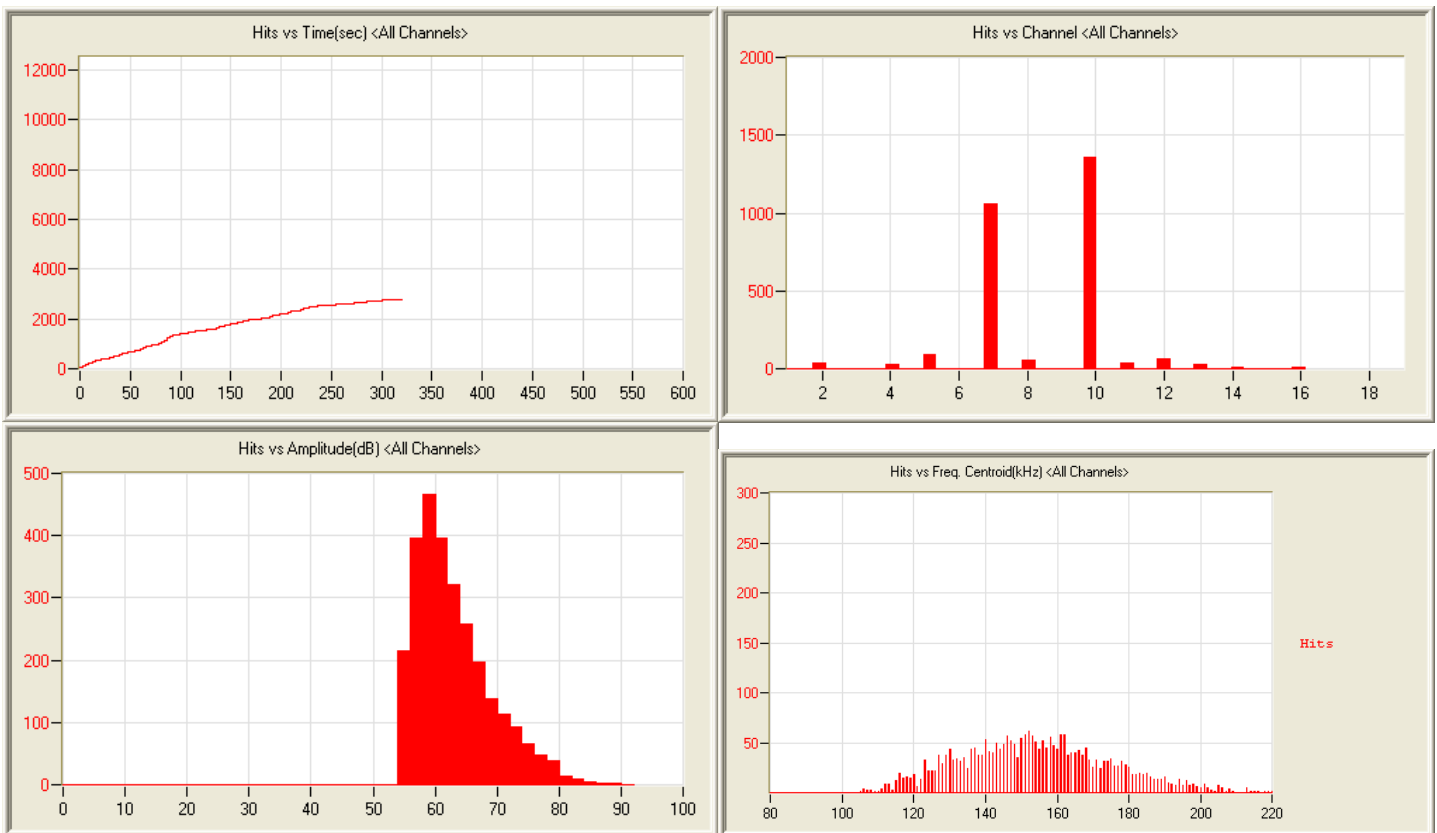
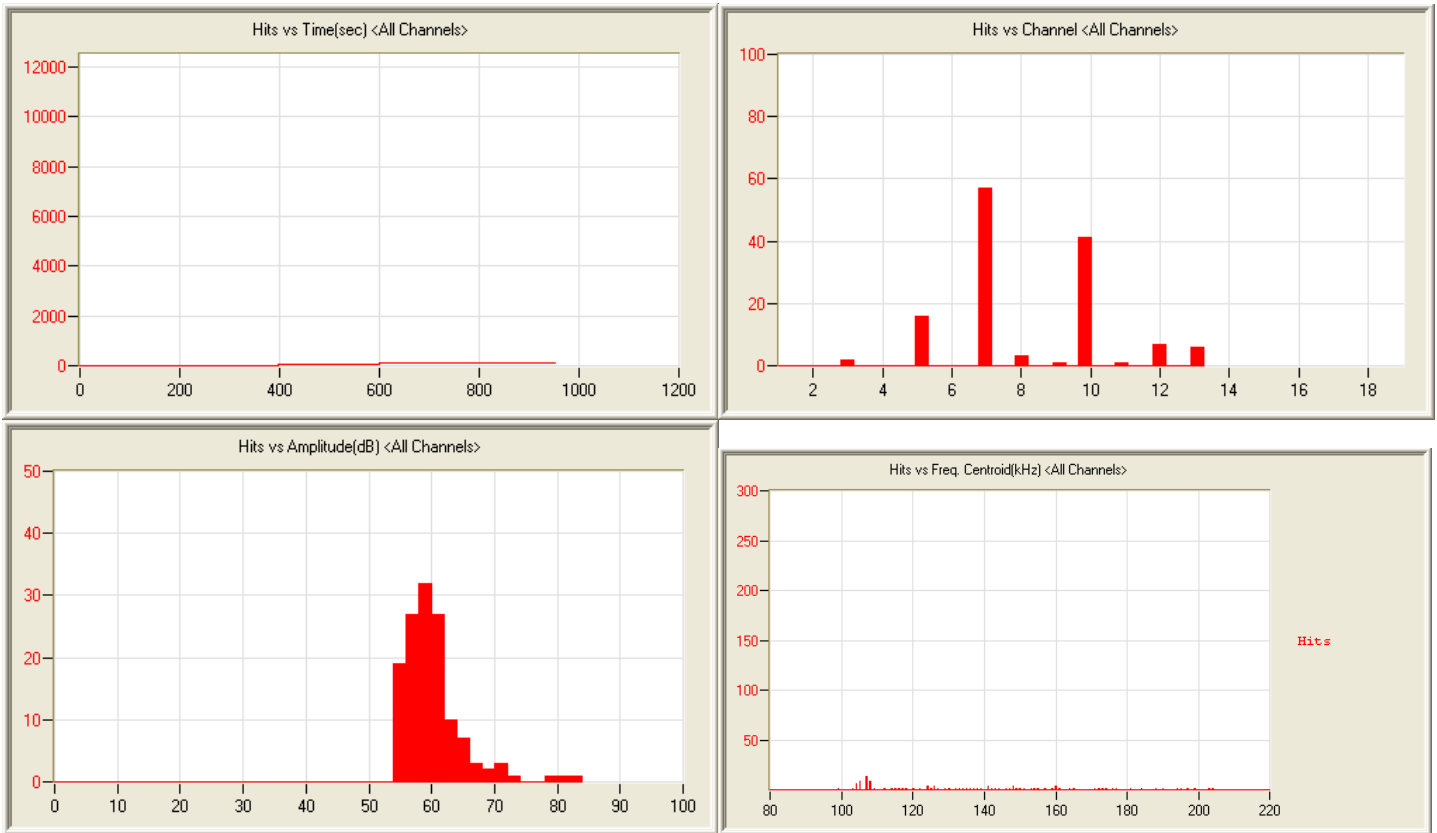
6/2/12 3:11pm 0:55:41 78 120602151107_0 203kb

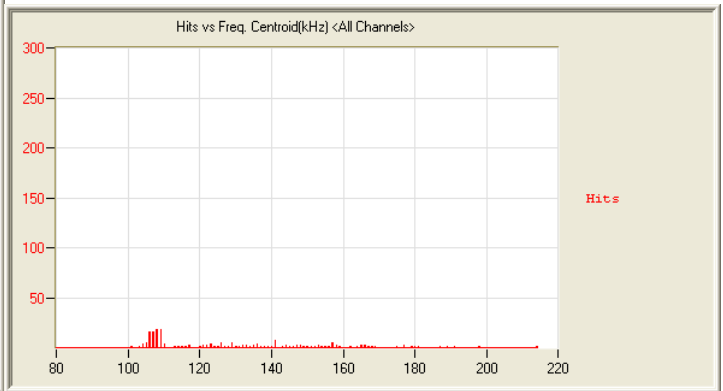
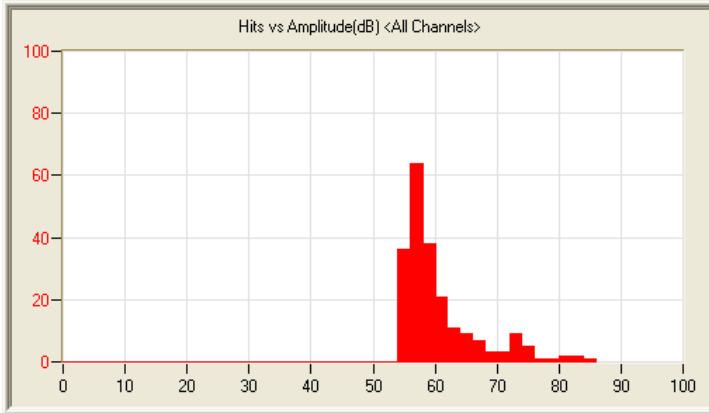
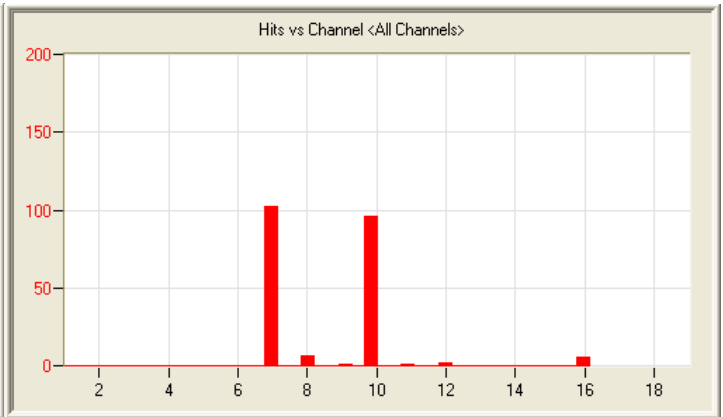
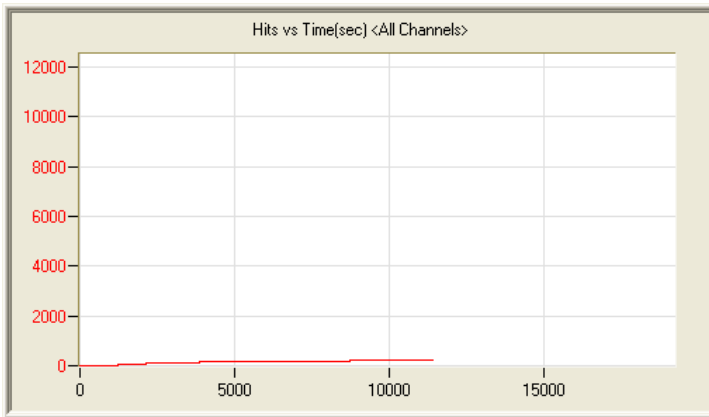


6/2/12 5:11pm 10:26:03 7750 120602171103_0 1.9mb

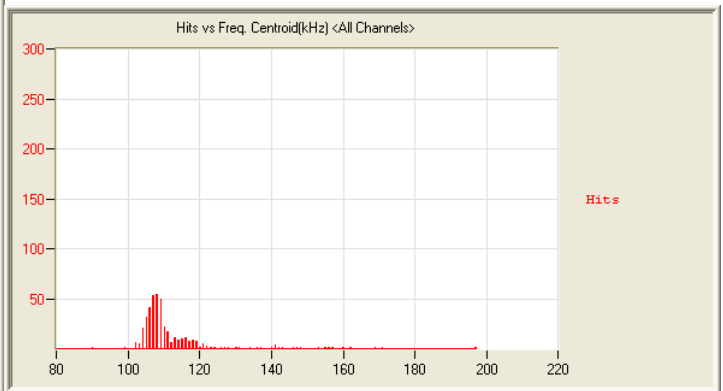
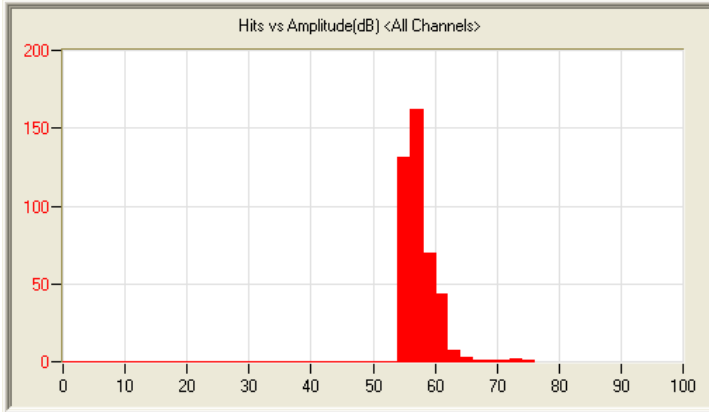
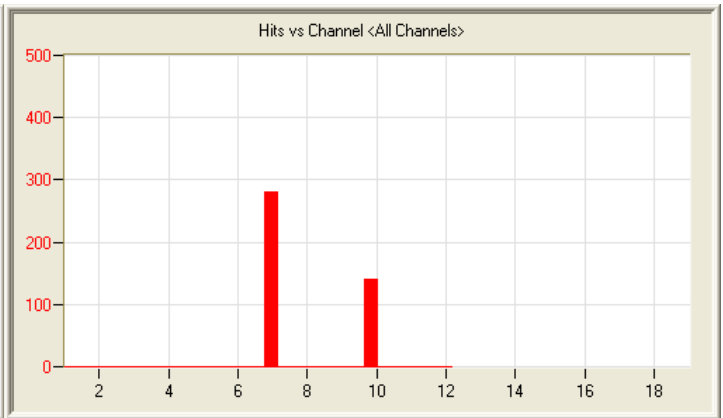
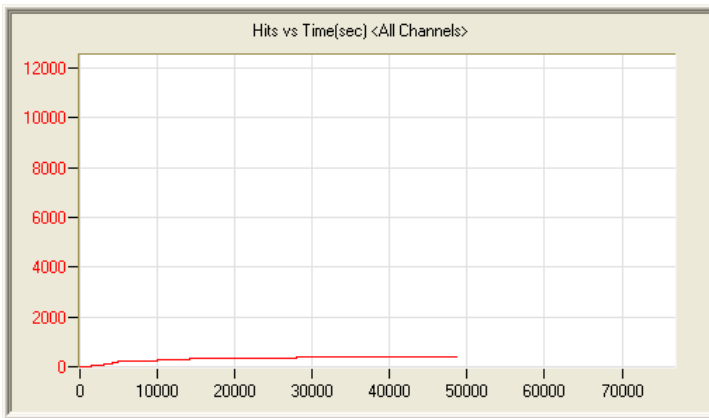


6/3/12 9:02pm 0:04:56 1281 120603210203_0 129kb

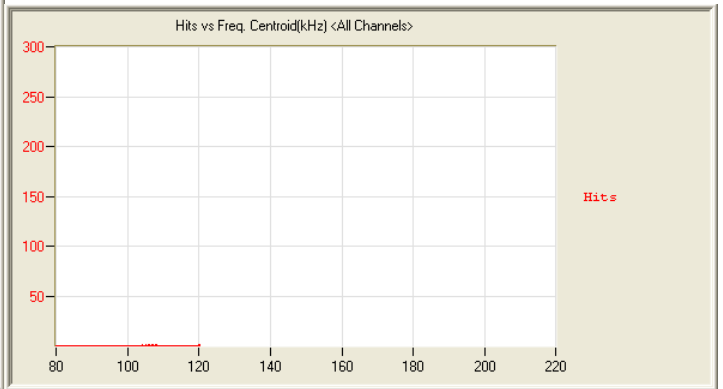
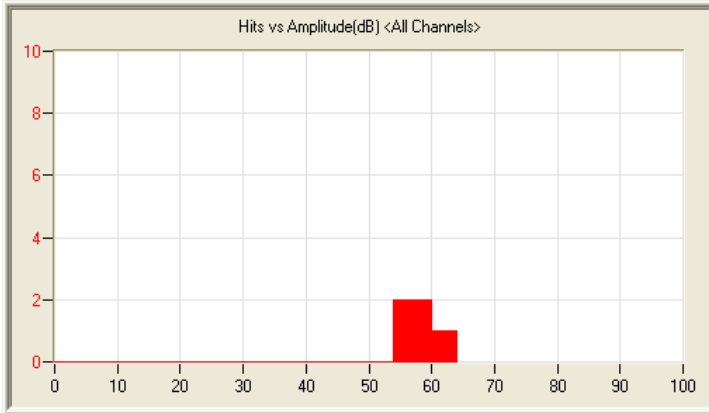
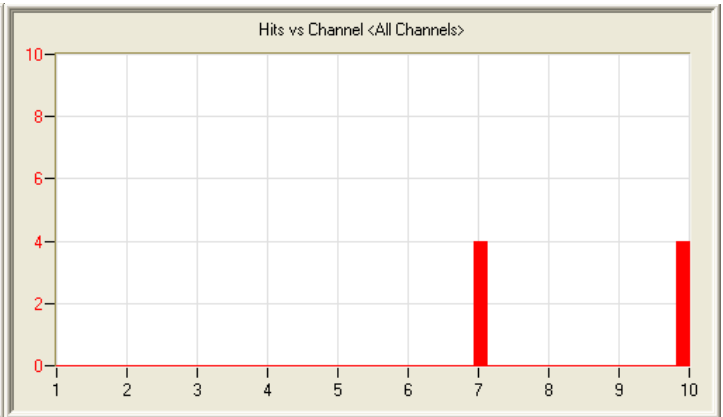
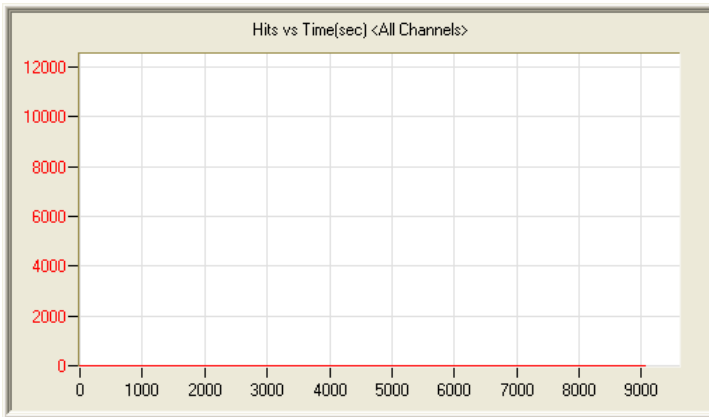




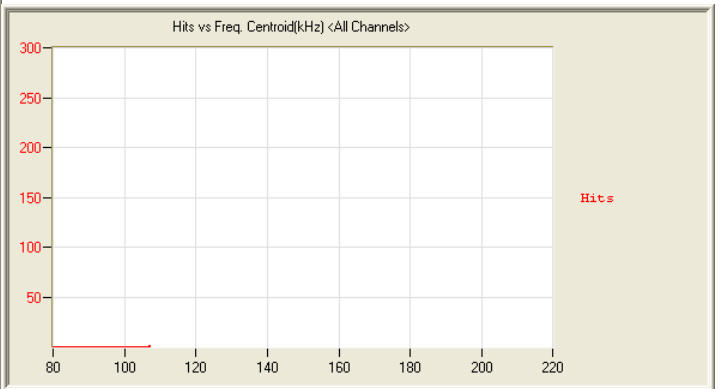
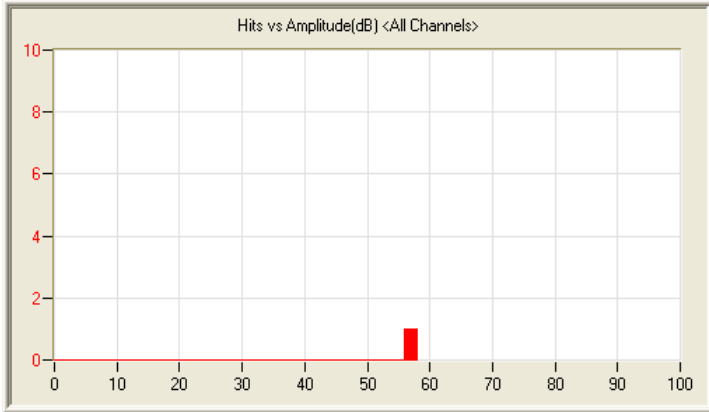
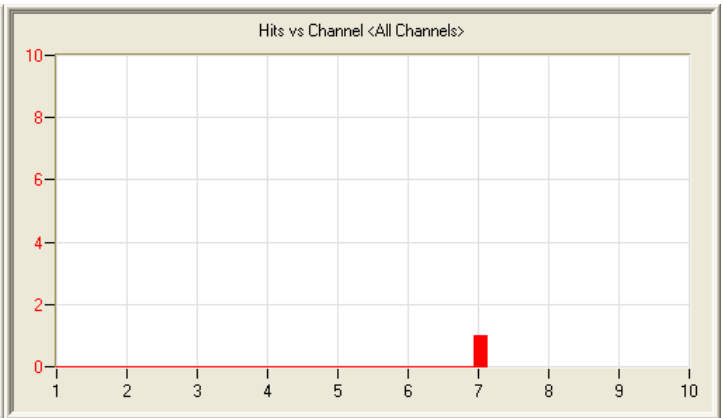
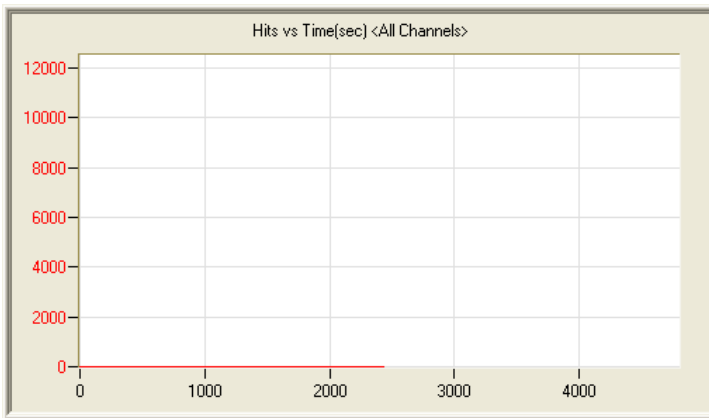
6/5/12 2:24am 3:13:47 213 120605022421_0 540kb



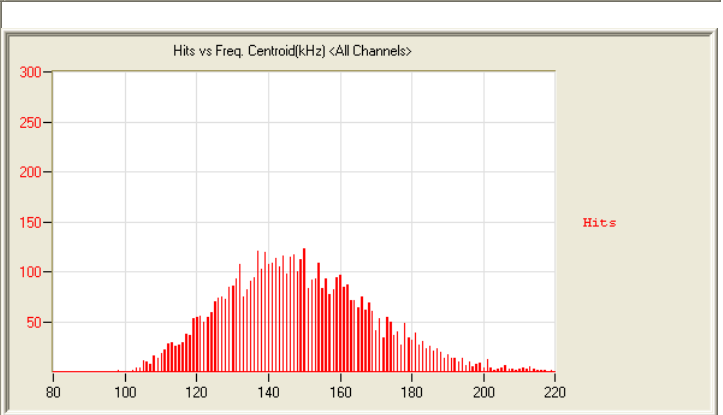
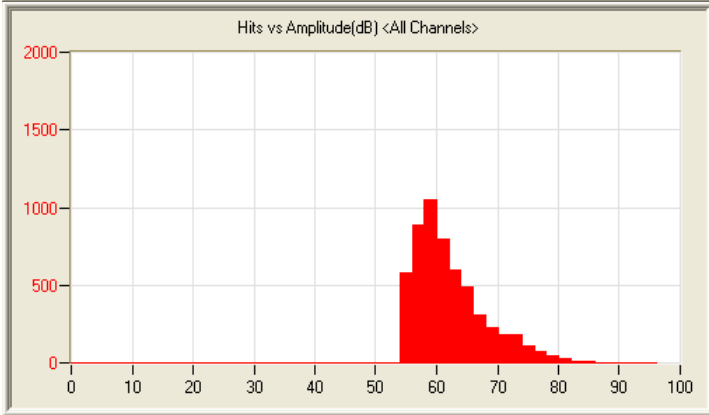
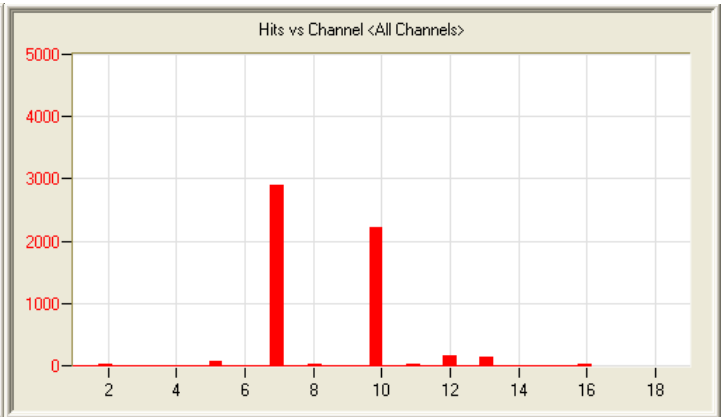
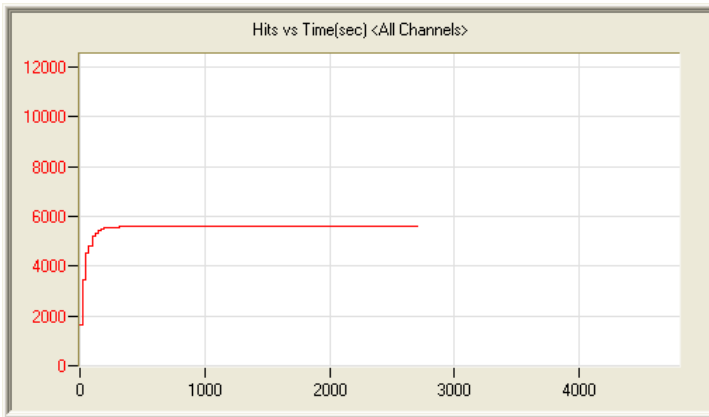
6/6/12 2:18am 14:43:36 422 120606021839_0 2.2mb



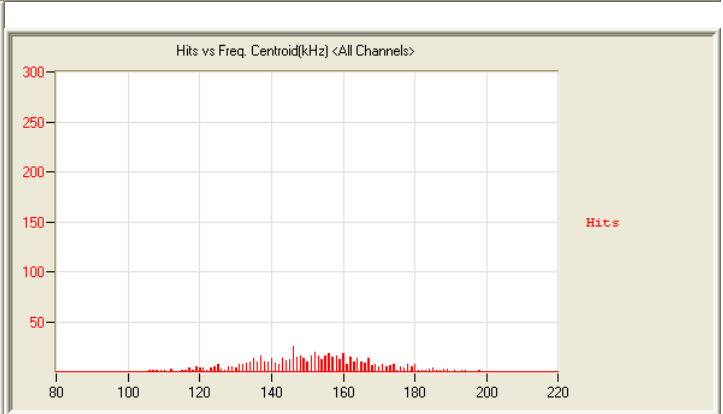
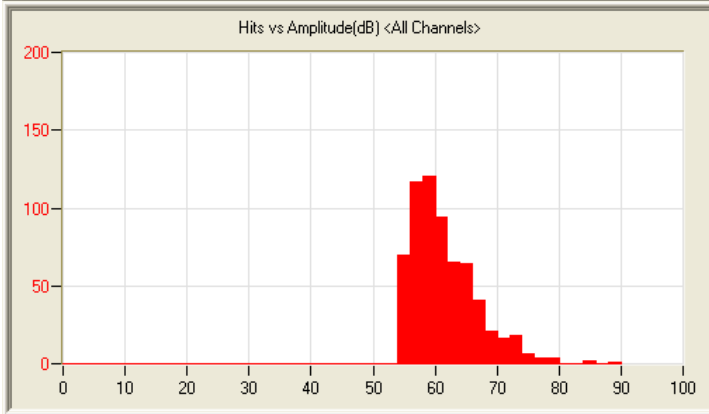
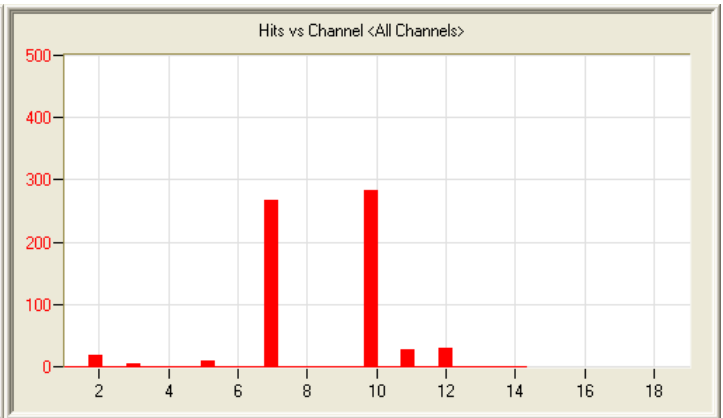
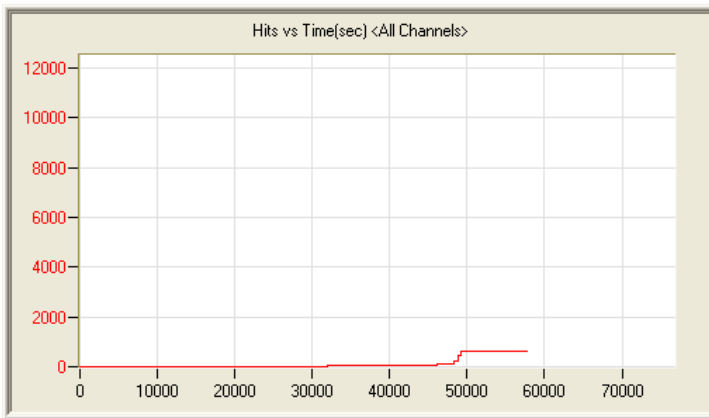
6/7/12 6:13am 2:40:43 8 120607061303_0 543kb



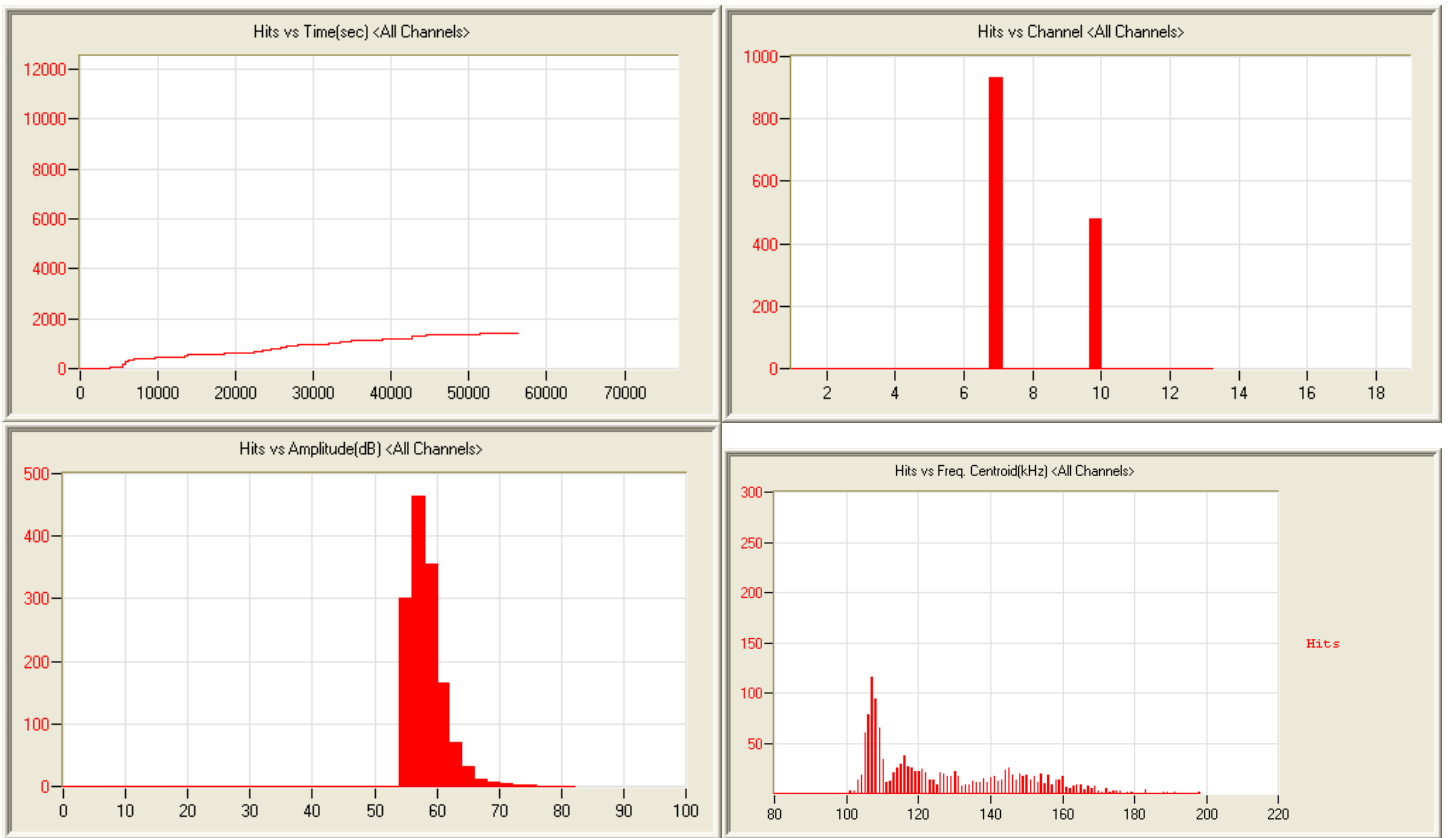
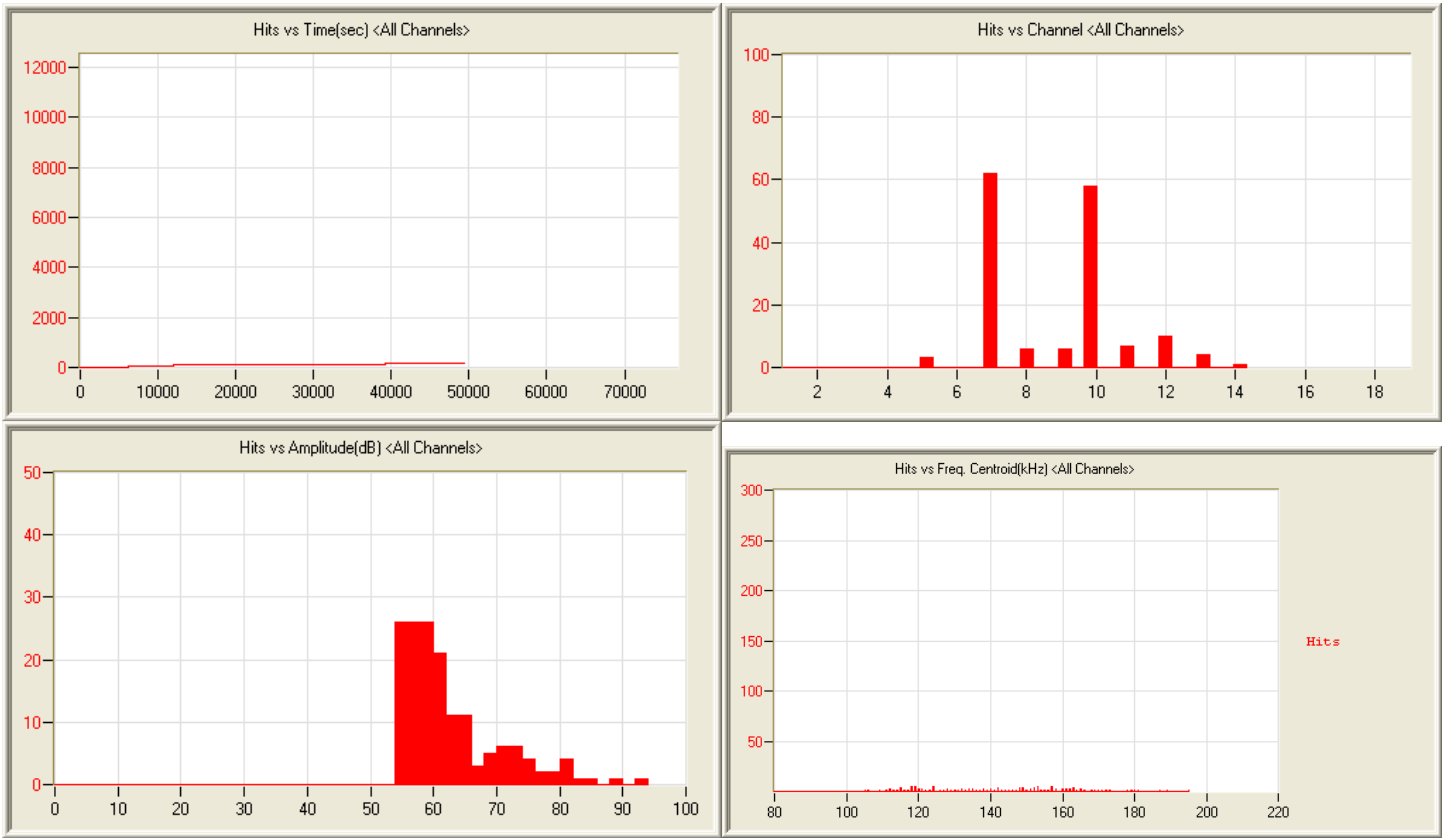
6/7/12 1:06pm 1:01:09 1 120607130639_0 213kb

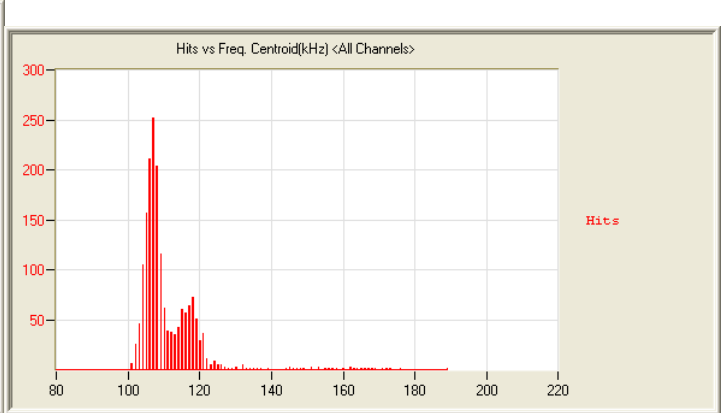
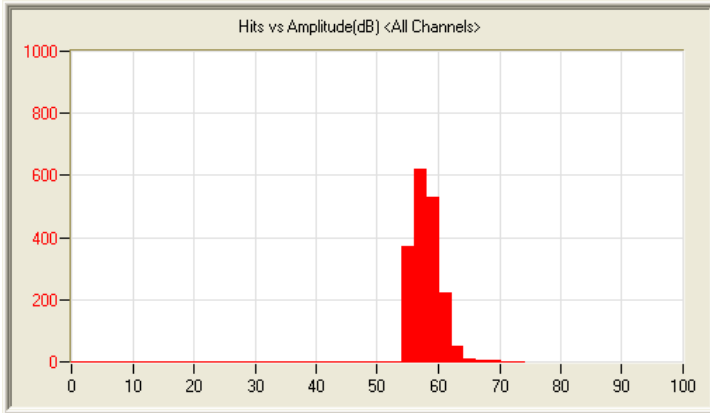
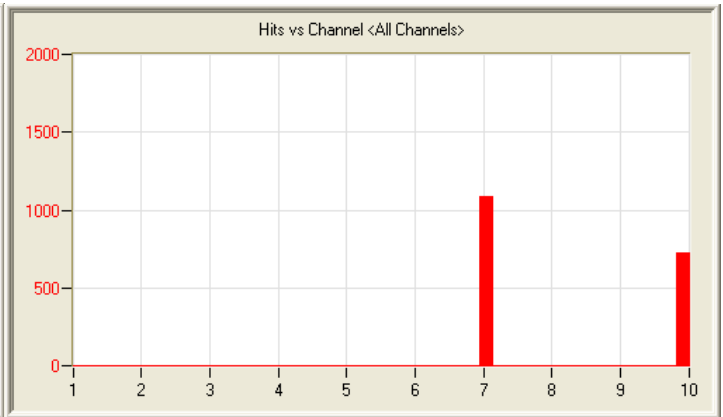
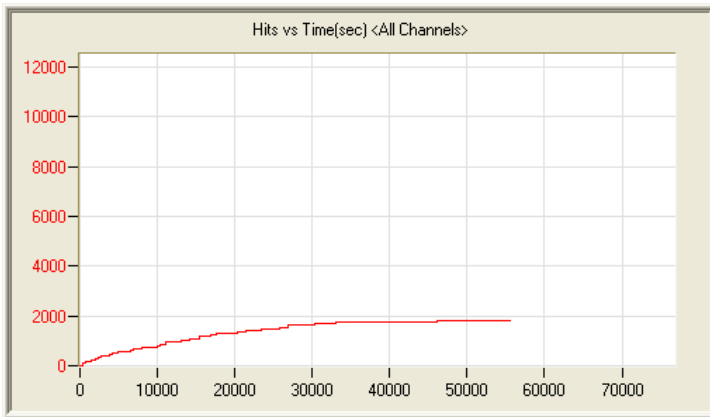


6/7/12 8:26pm 0:50:59 5596 120607202644_0 413kb

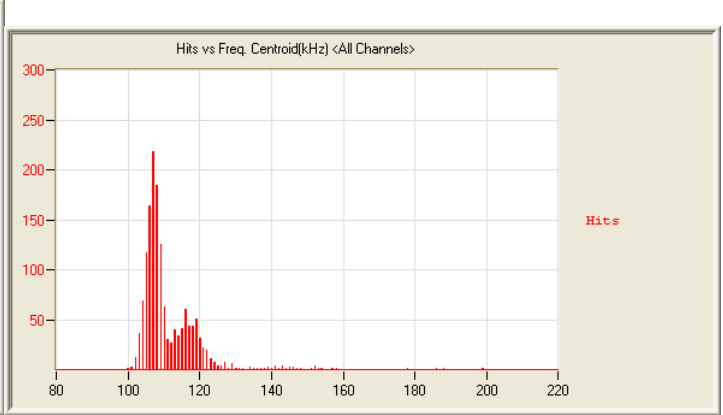
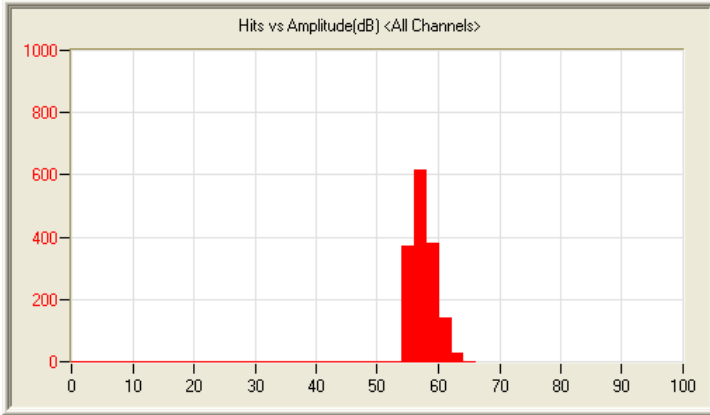
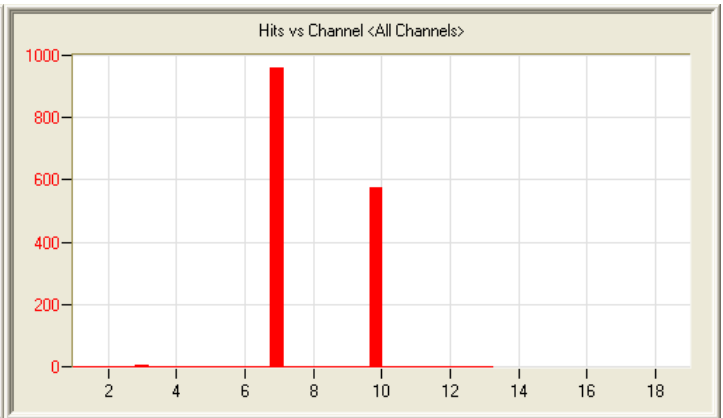
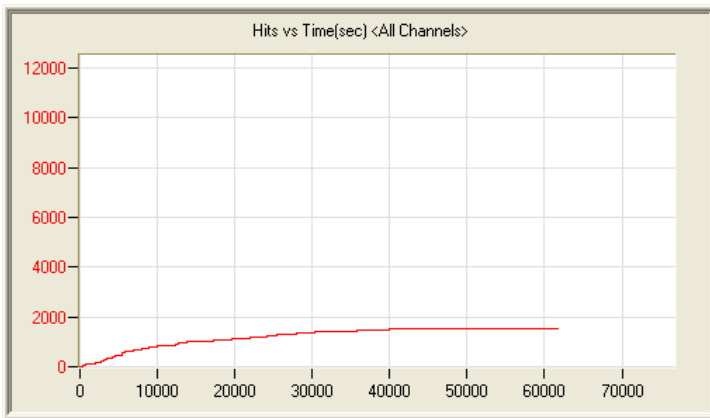


6/9/12 2:35am 16:03:40 643 120609023523_0 2.4mb

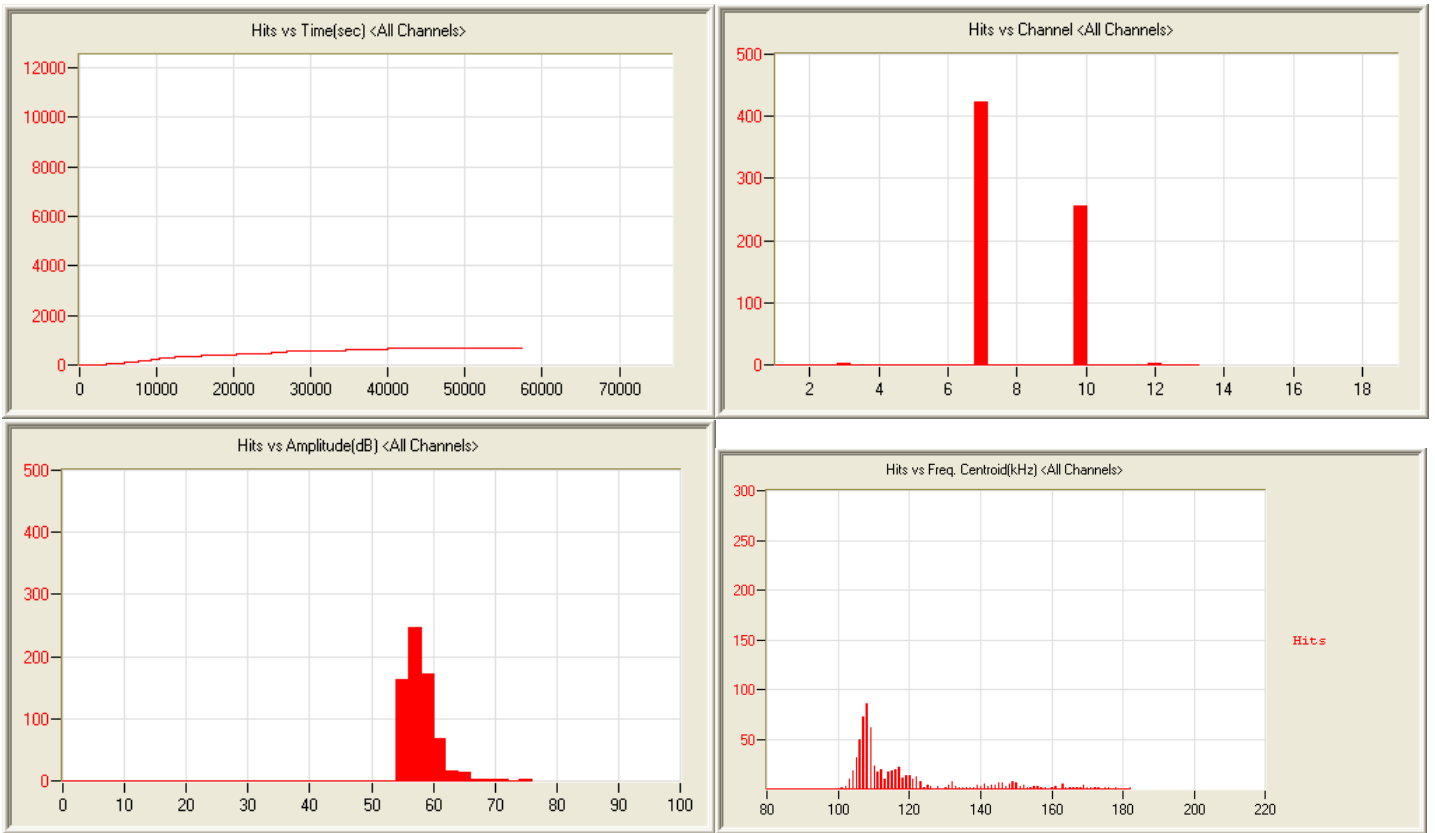




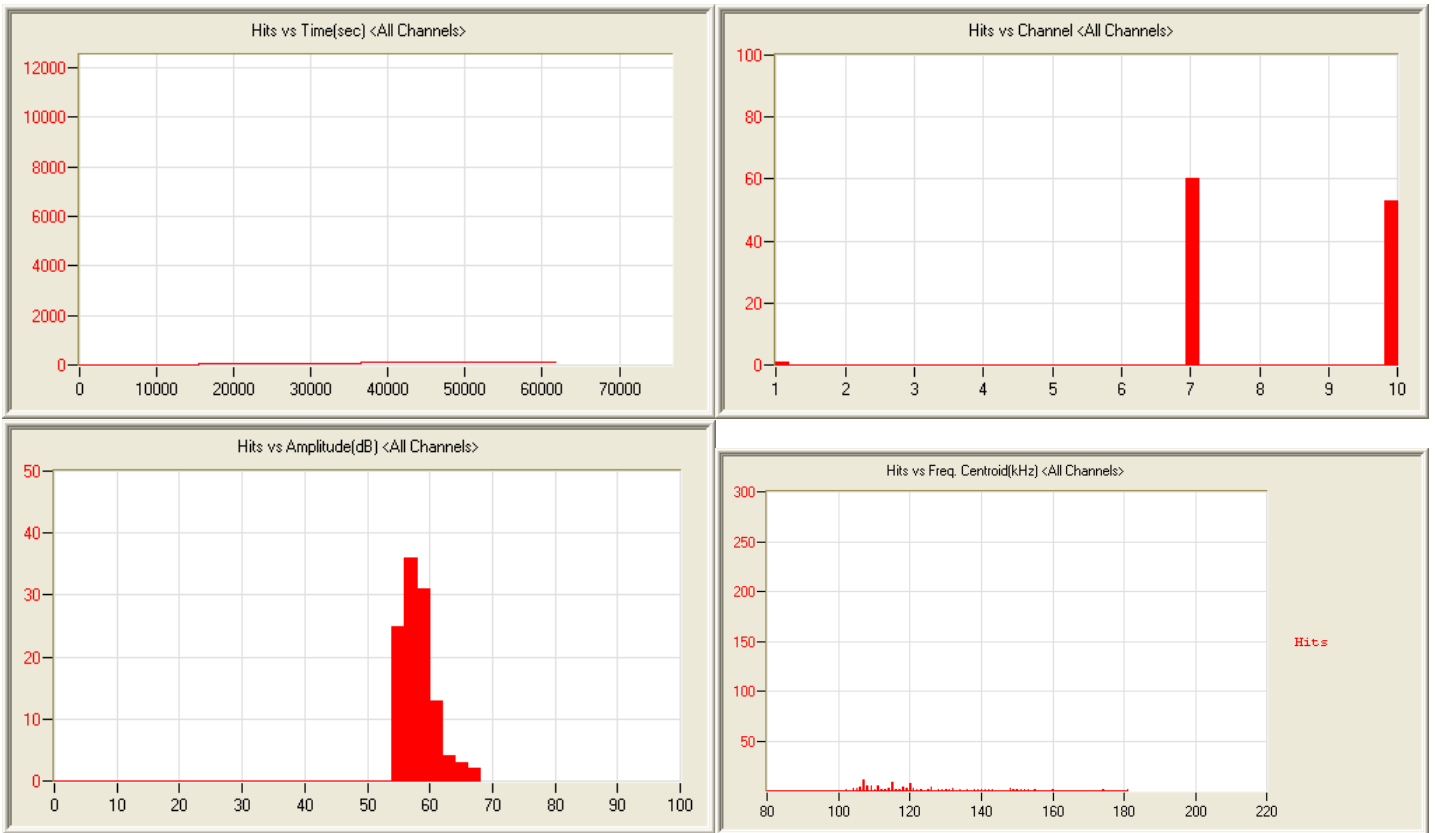
6/12/12 9:53am 15:37:52 1807 120612095334_0 2.4mb



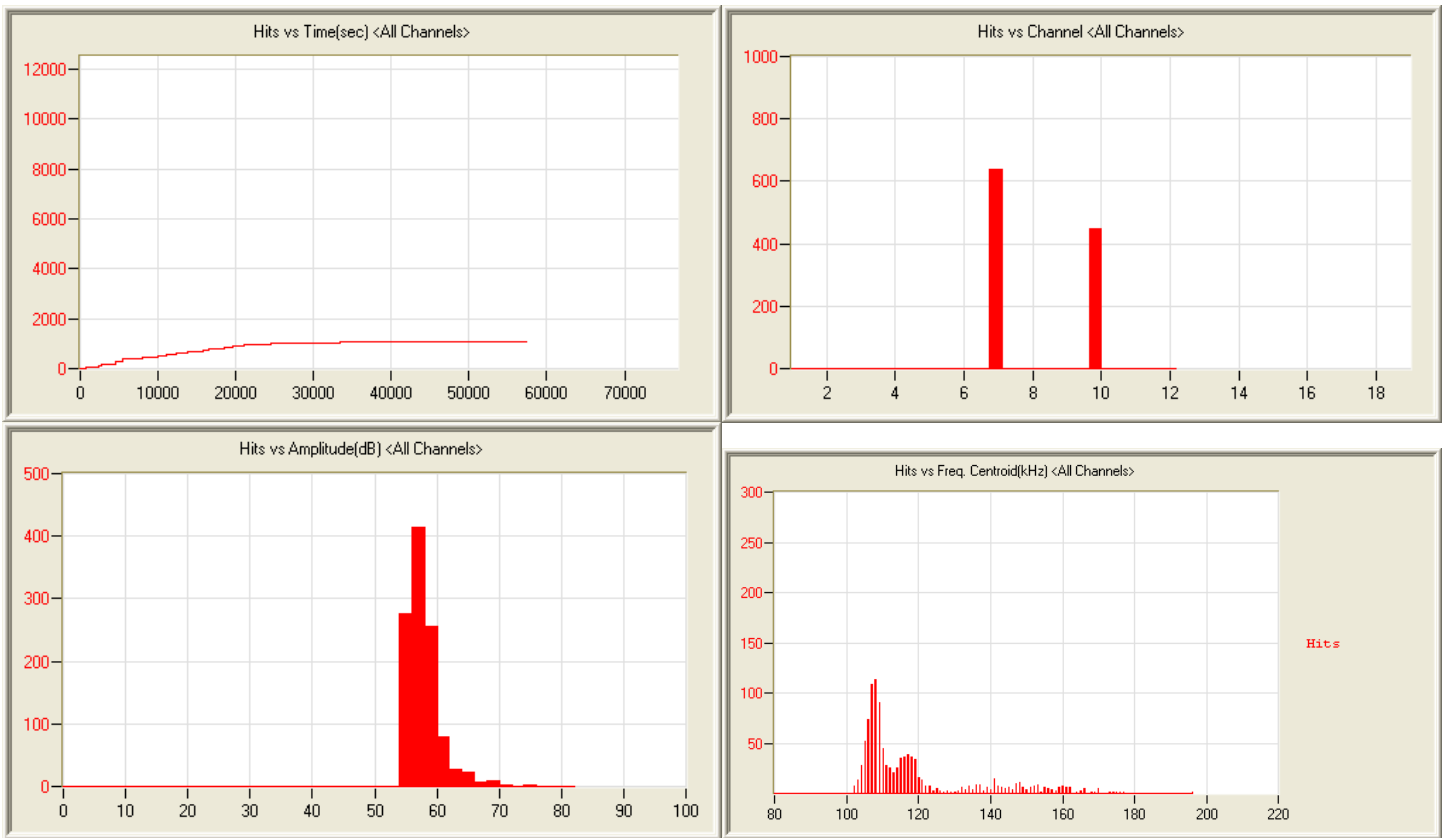
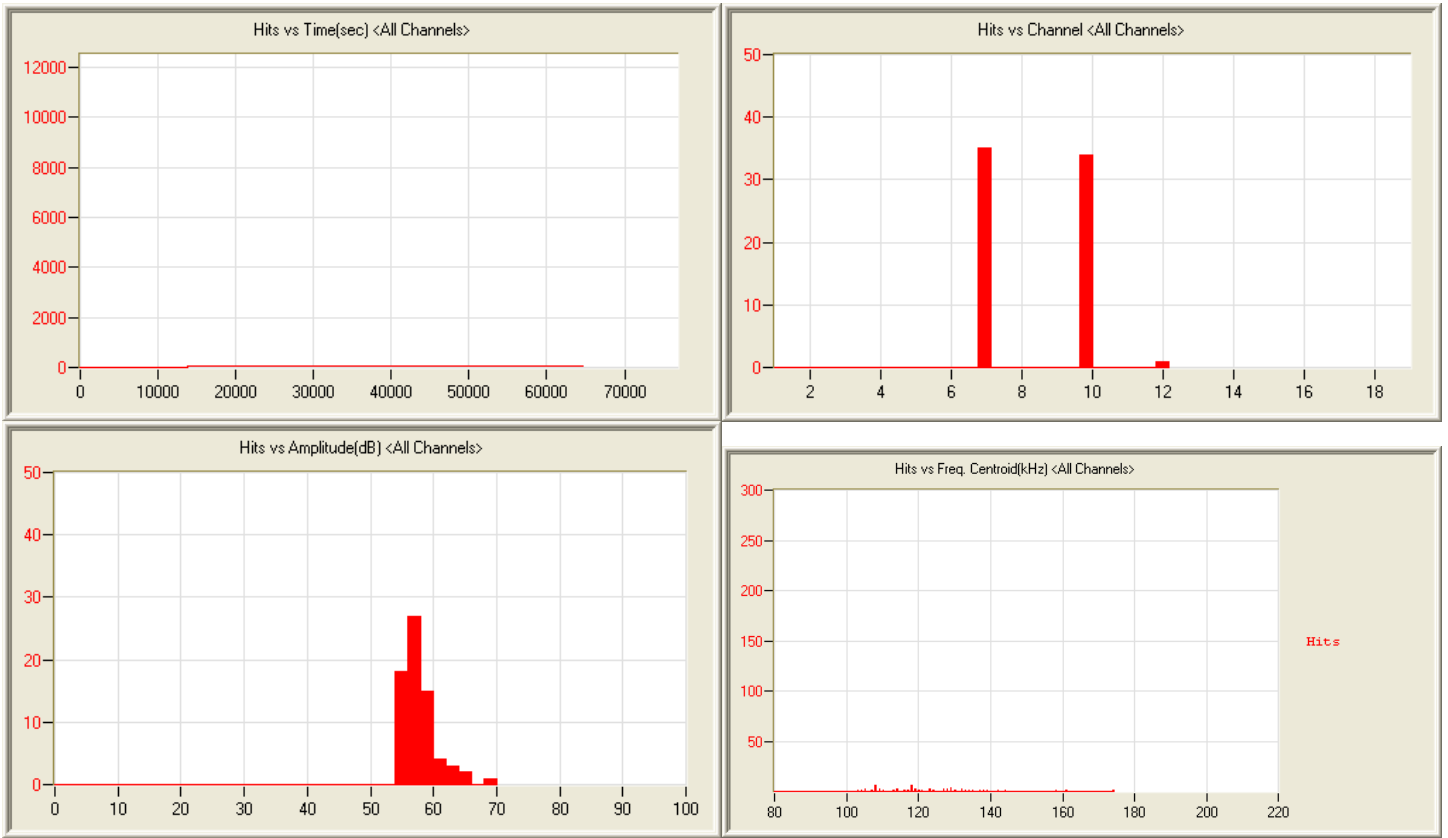
6/13/12 10:22am 17:07:37 1536 120613102257_0 2.6mb

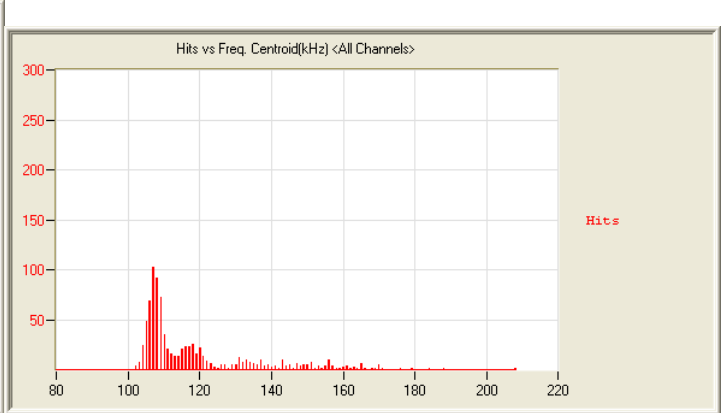
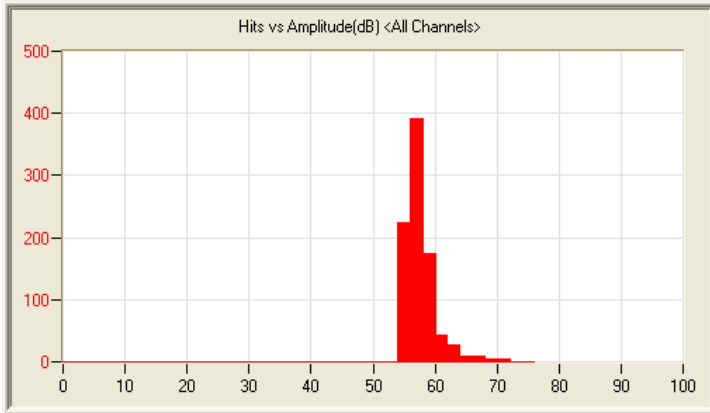
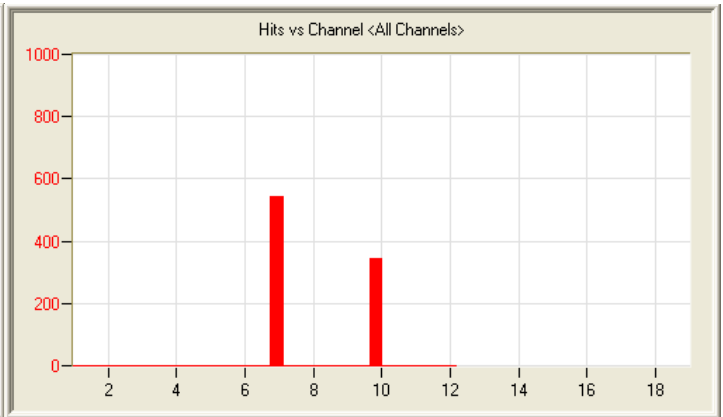
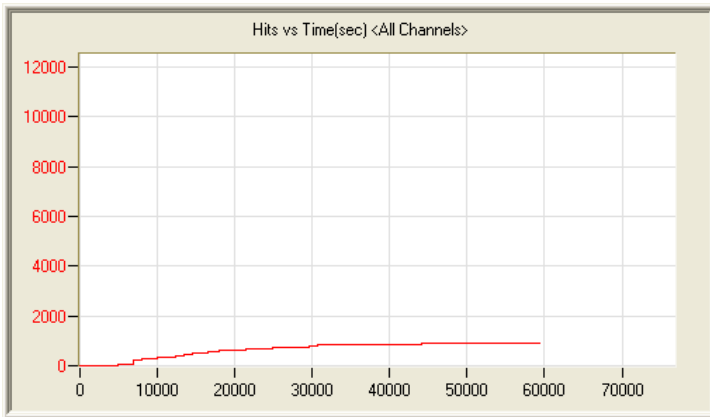


6/14/12 10:44am 17:42:50 688 120614104428_0 2.6mb

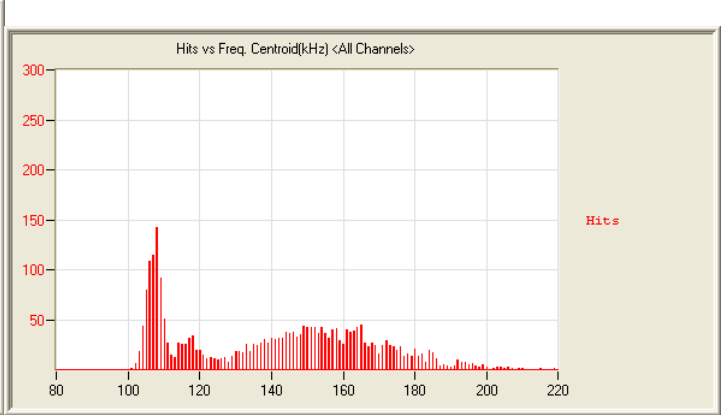
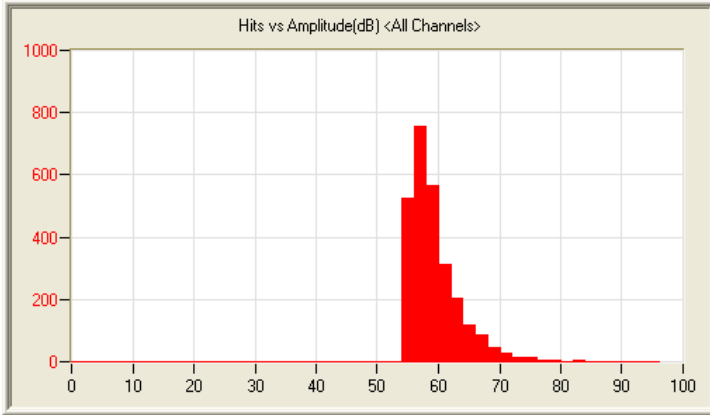
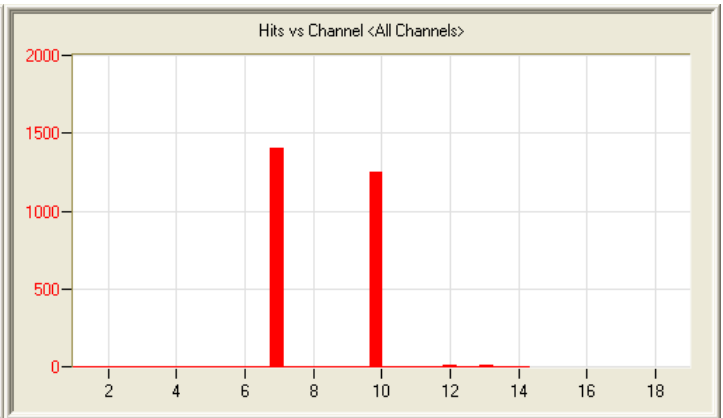
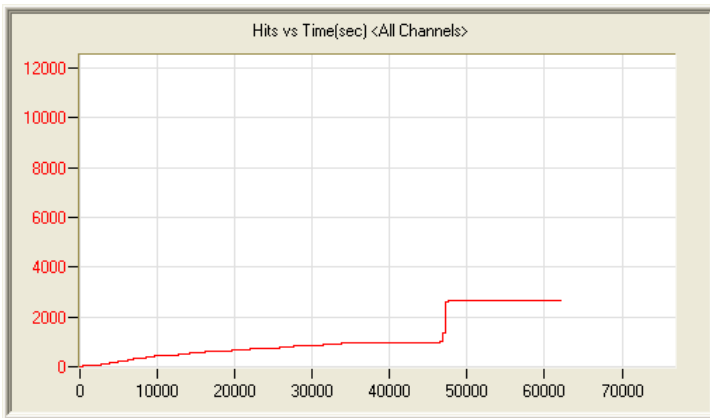


6/15/12 11:45am 18:14:53 114 120615114539_0 2.7mb

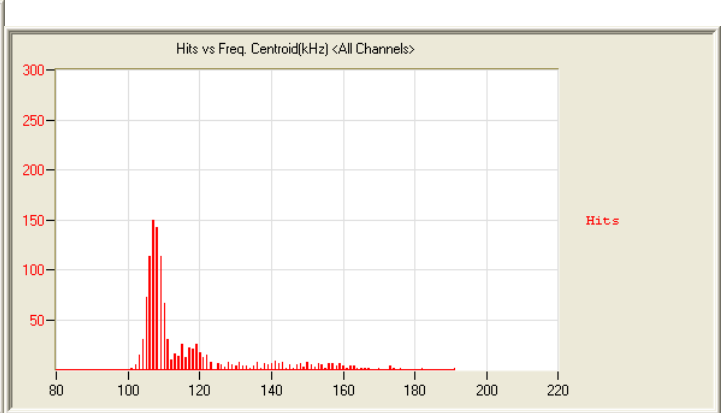
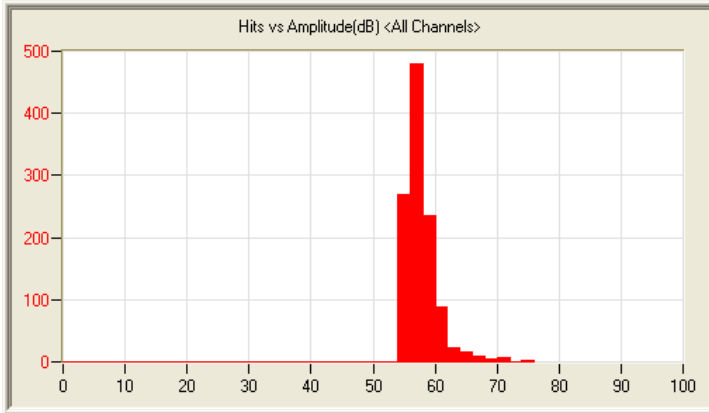
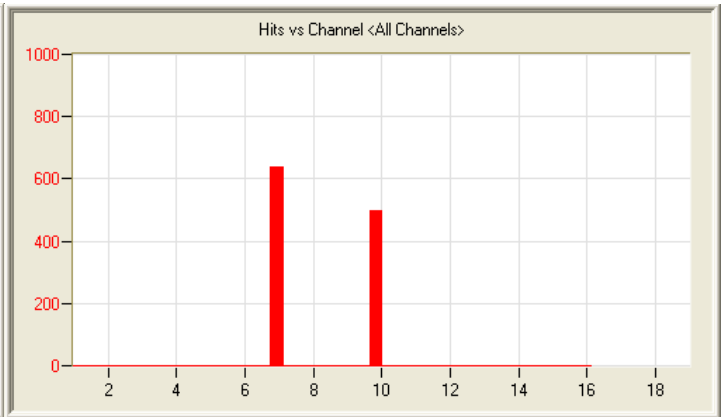
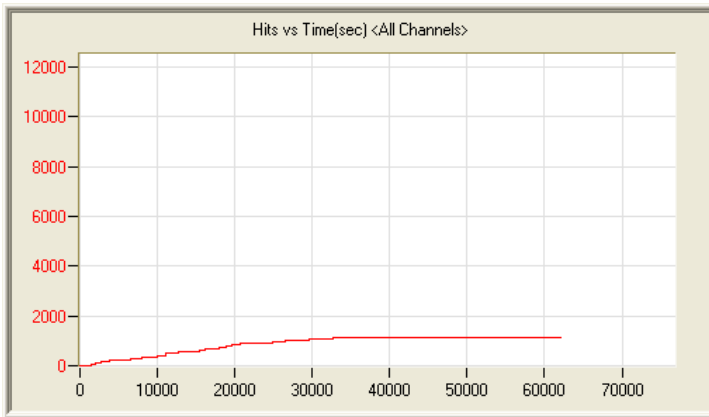




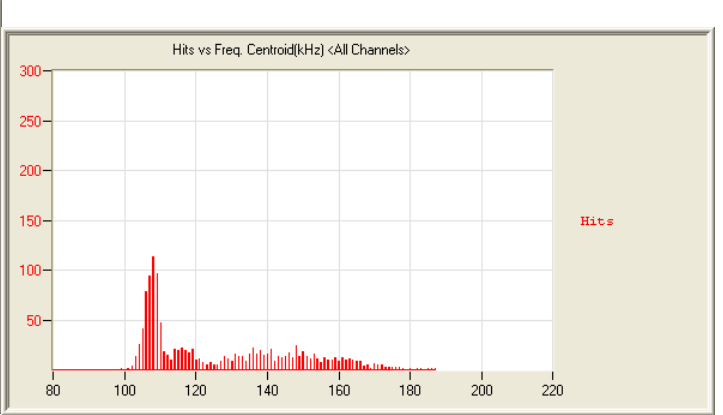
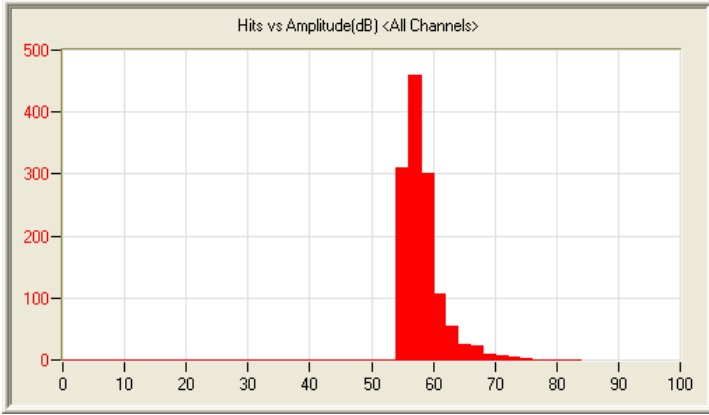
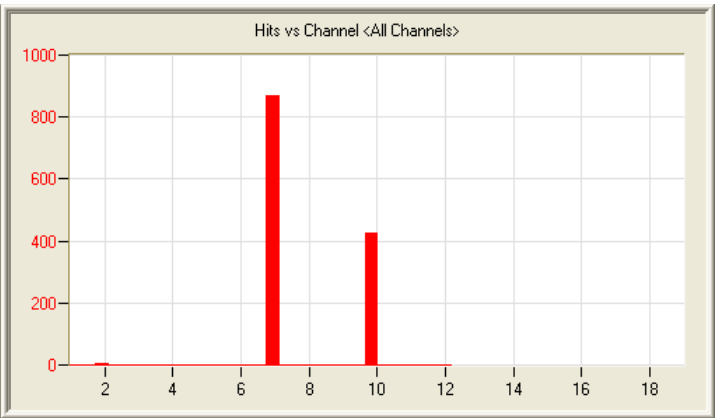
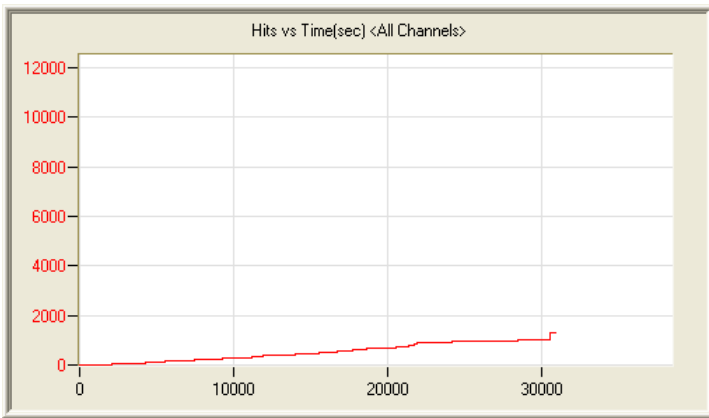
6/18/12 4:59pm 18:11:32 890 120618165906_0 2.7mb



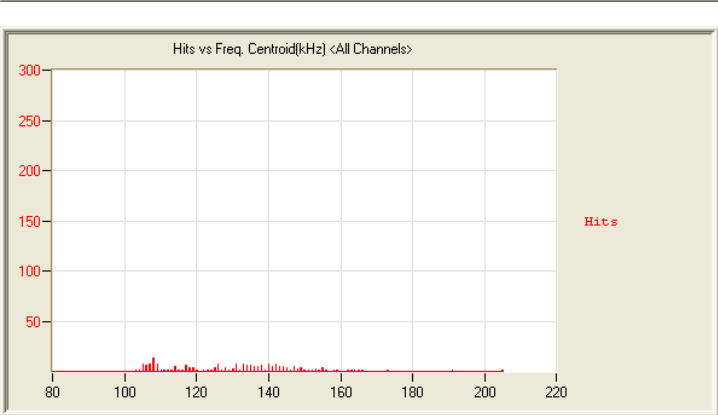
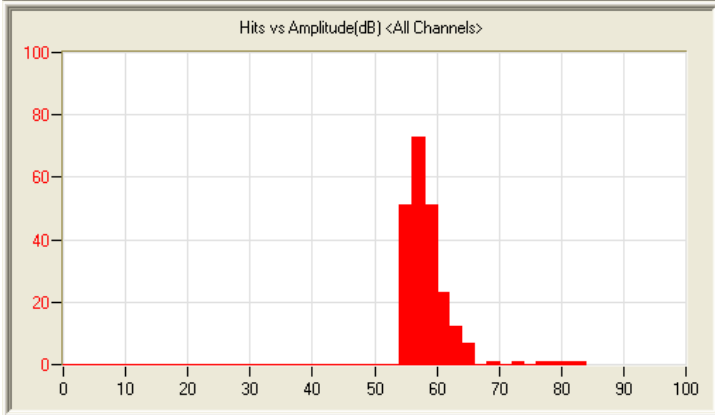
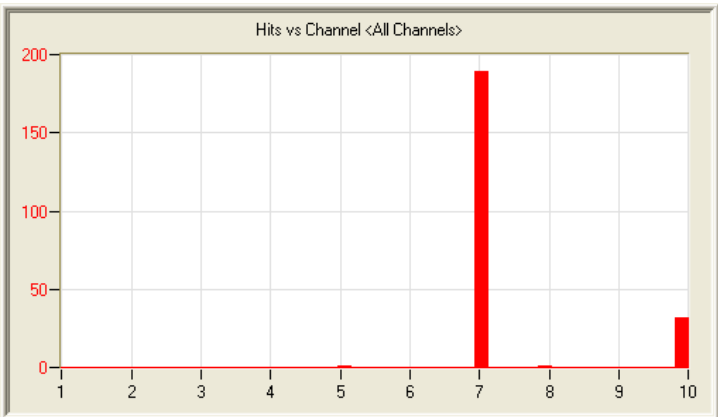
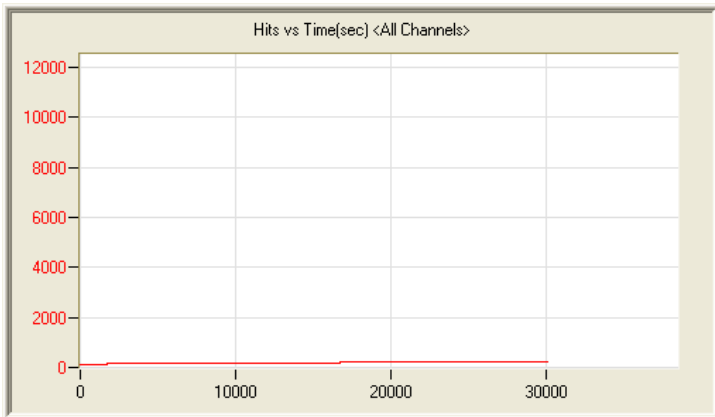
6/19/12 7:31pm 17:27:58 2682 120619193144_0 2.7mb



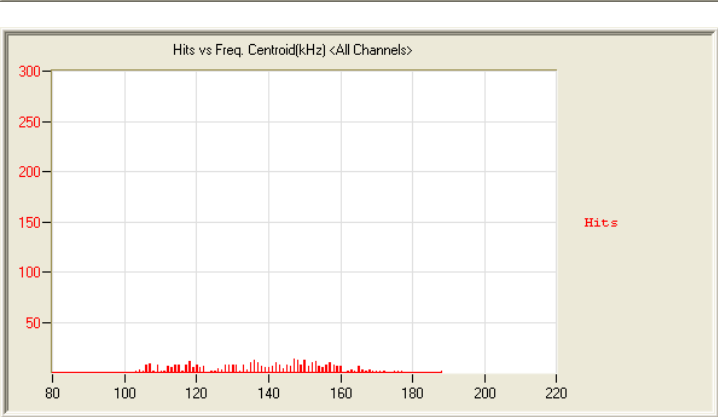
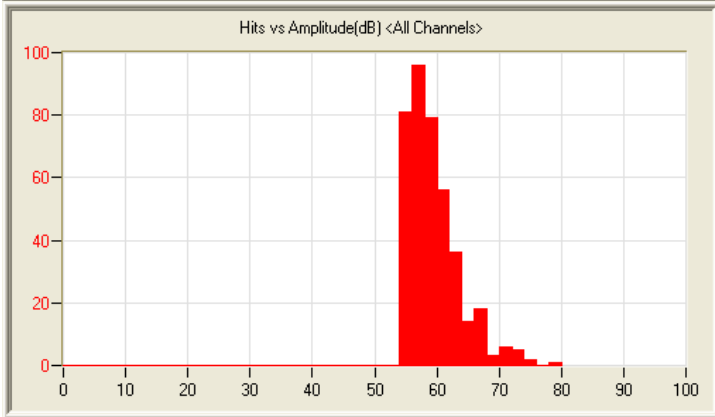
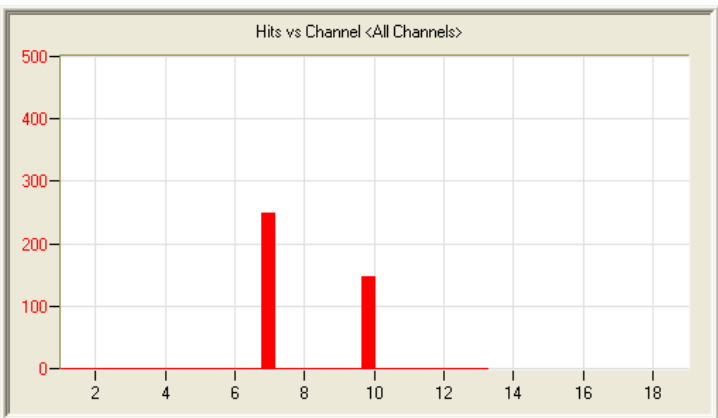
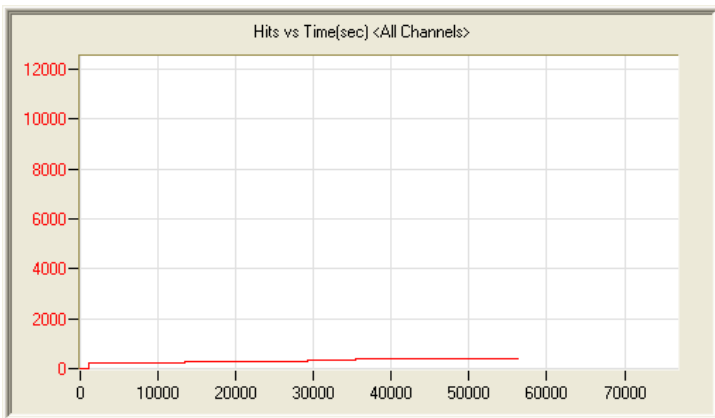
6/20/12 11:05pm 17:27:58 1134 120620230553_0 2.6mb



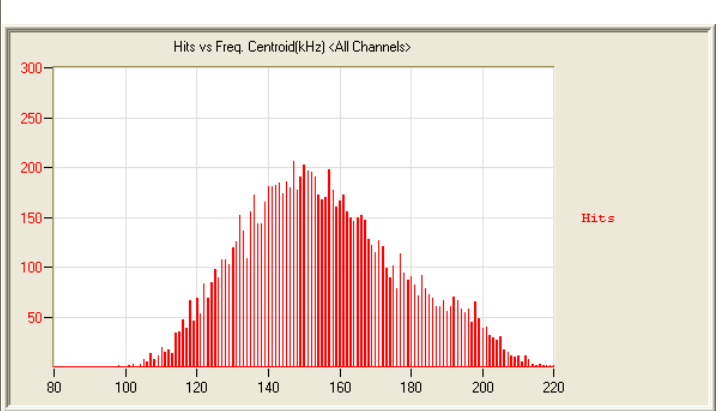
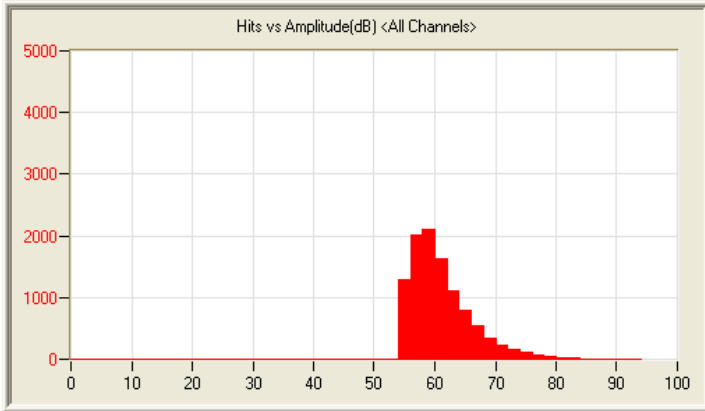
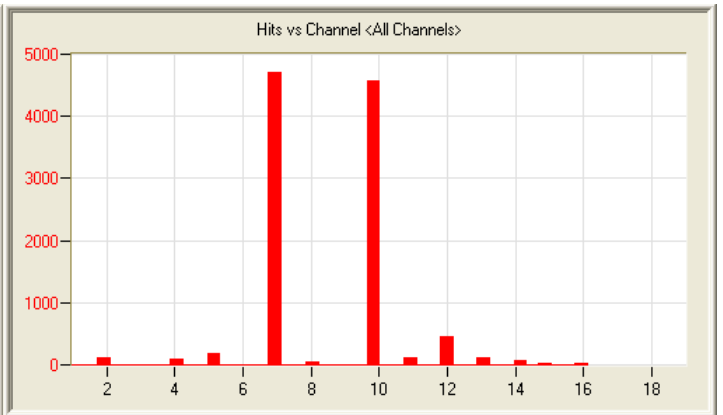
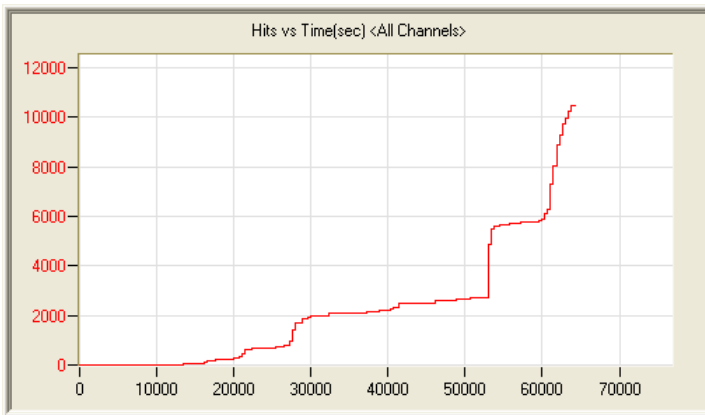
6/21/12 10:57pm 8:33:03 1305 120621225751_0 1.4mb



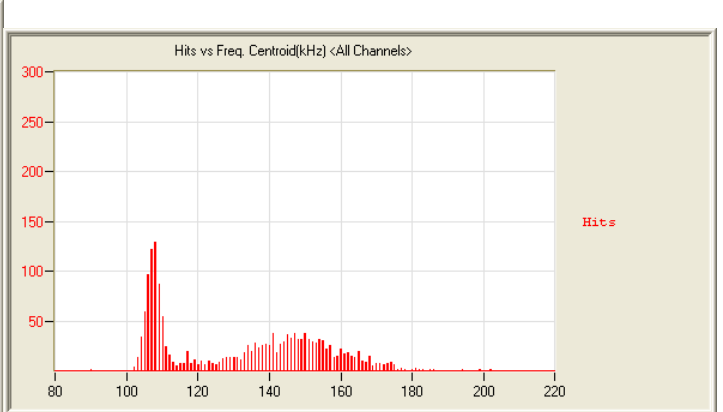
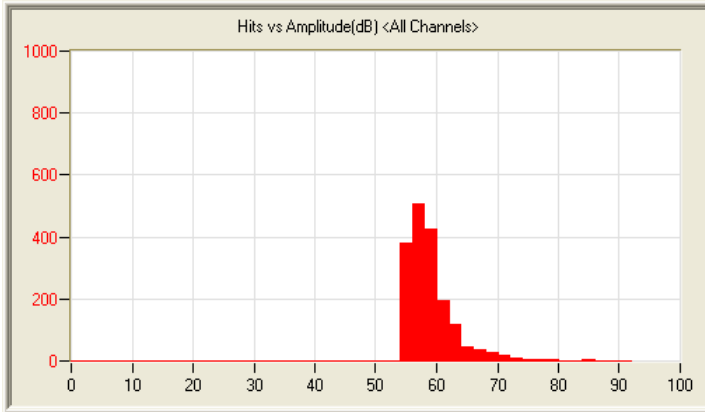
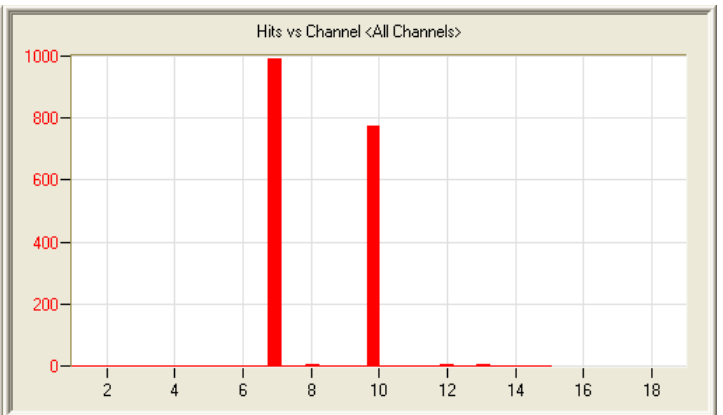
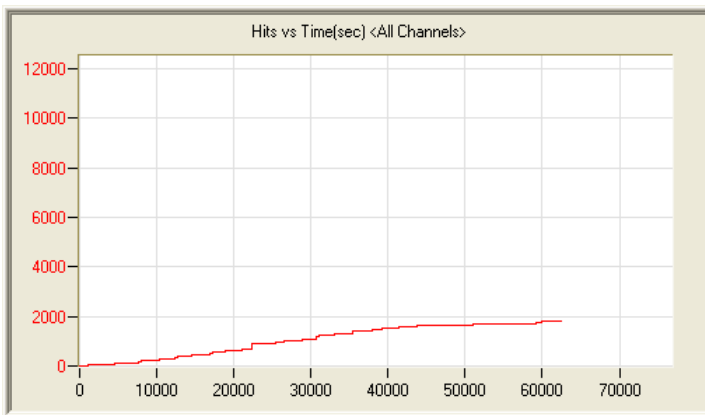
6/22/12 10:59am 8:24:22 223 120622105918_0 1.3mb



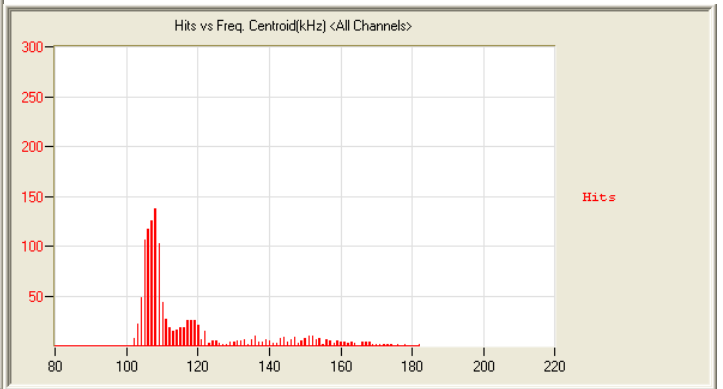
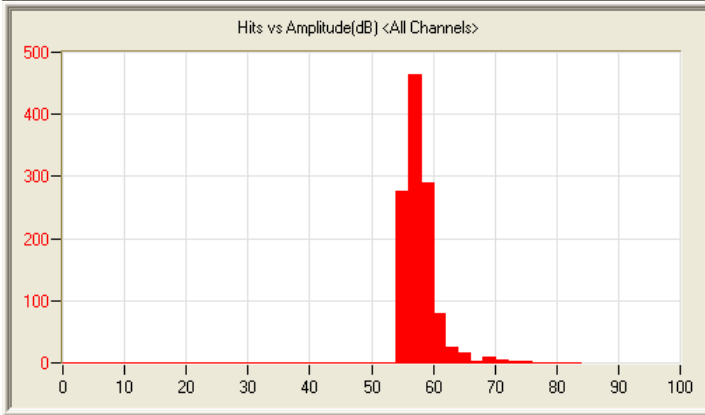
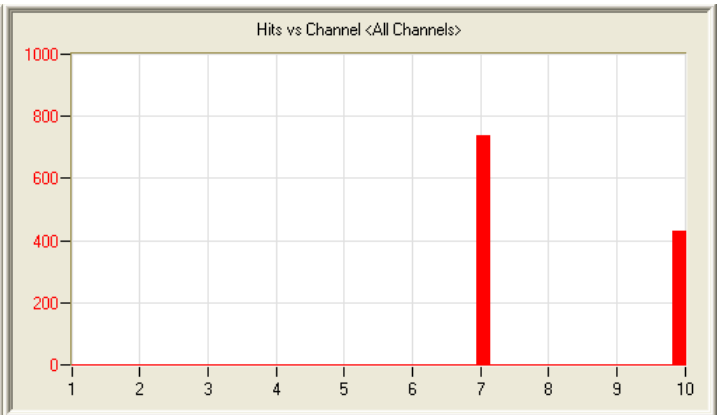
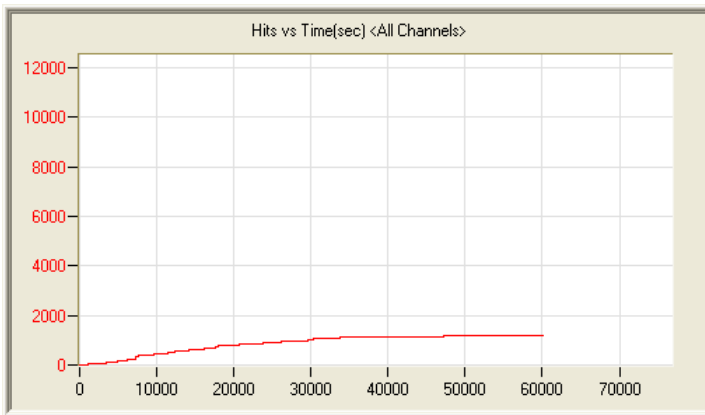
6/23/12 3:08am 17:20:58 397 120623030820_0 2.6mb



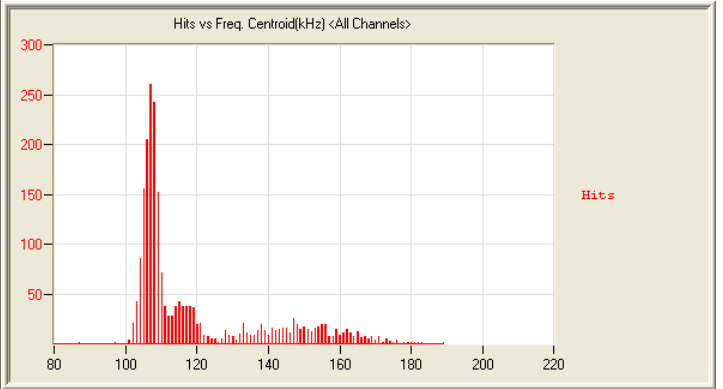
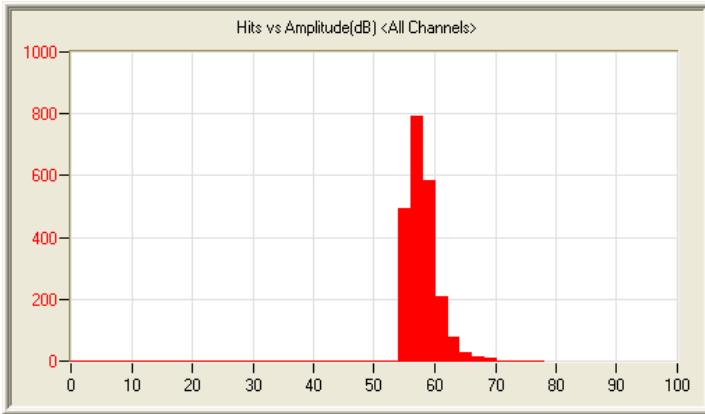
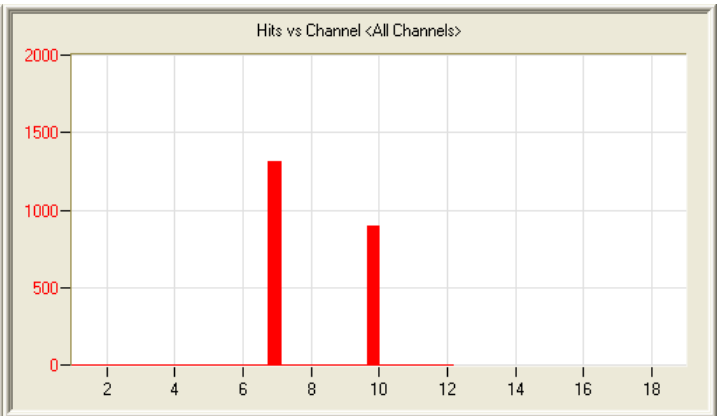
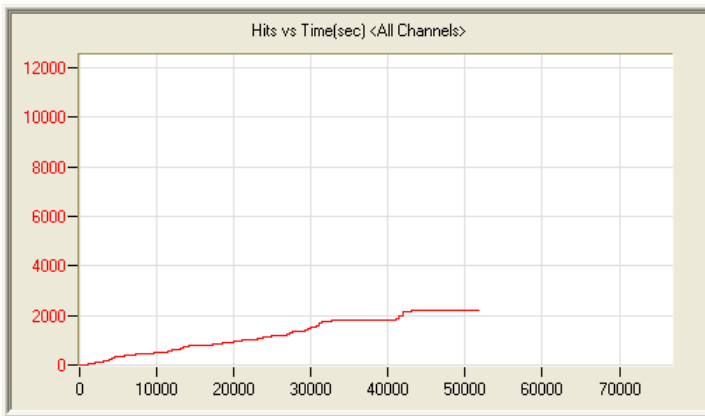
6/24/12 4:05am 17:54:16 10489 120624040541_0 3.1mb



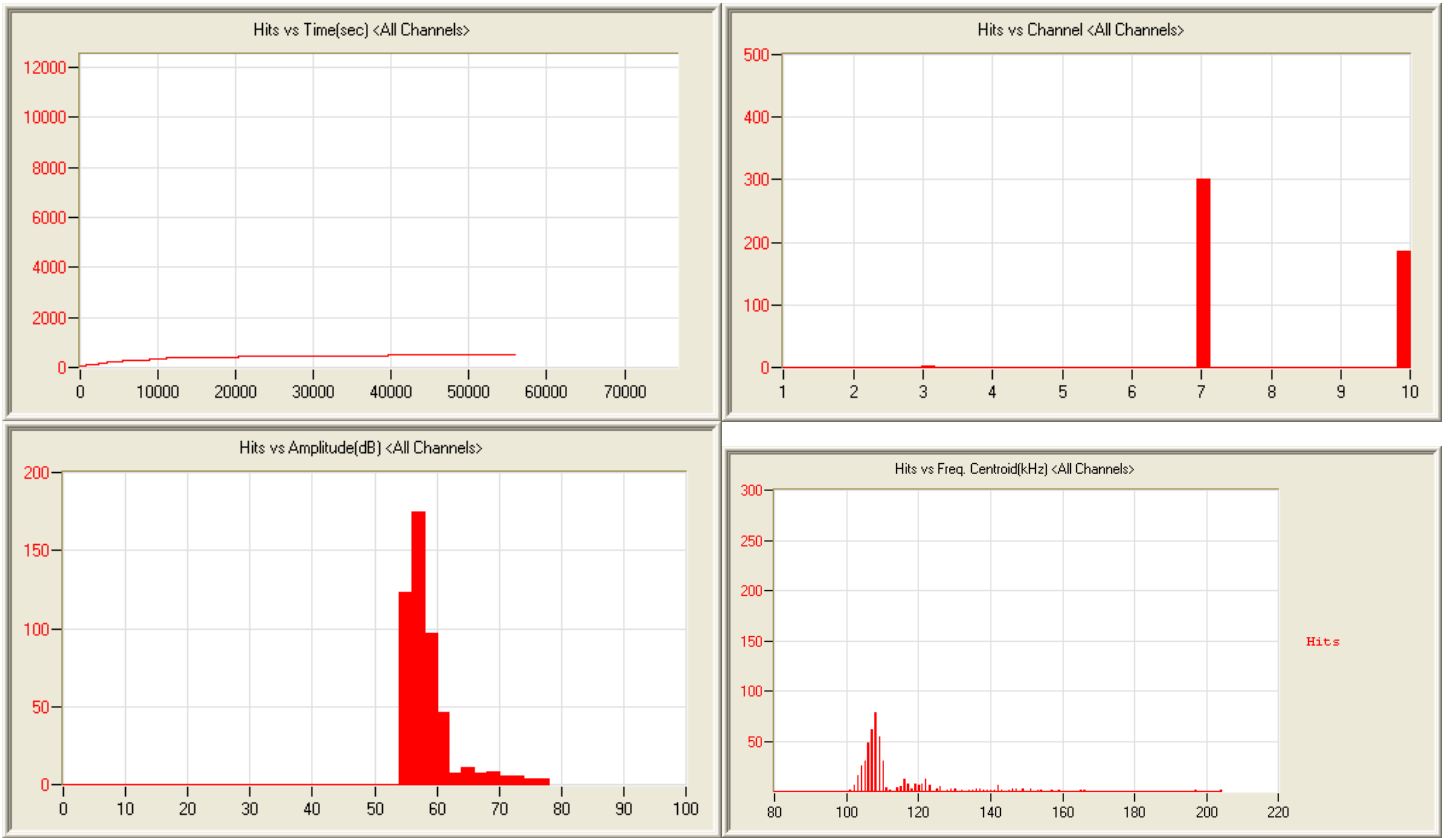
6/25/12 5:17am 17:49:18 1786 120625051737_0 2.7mb



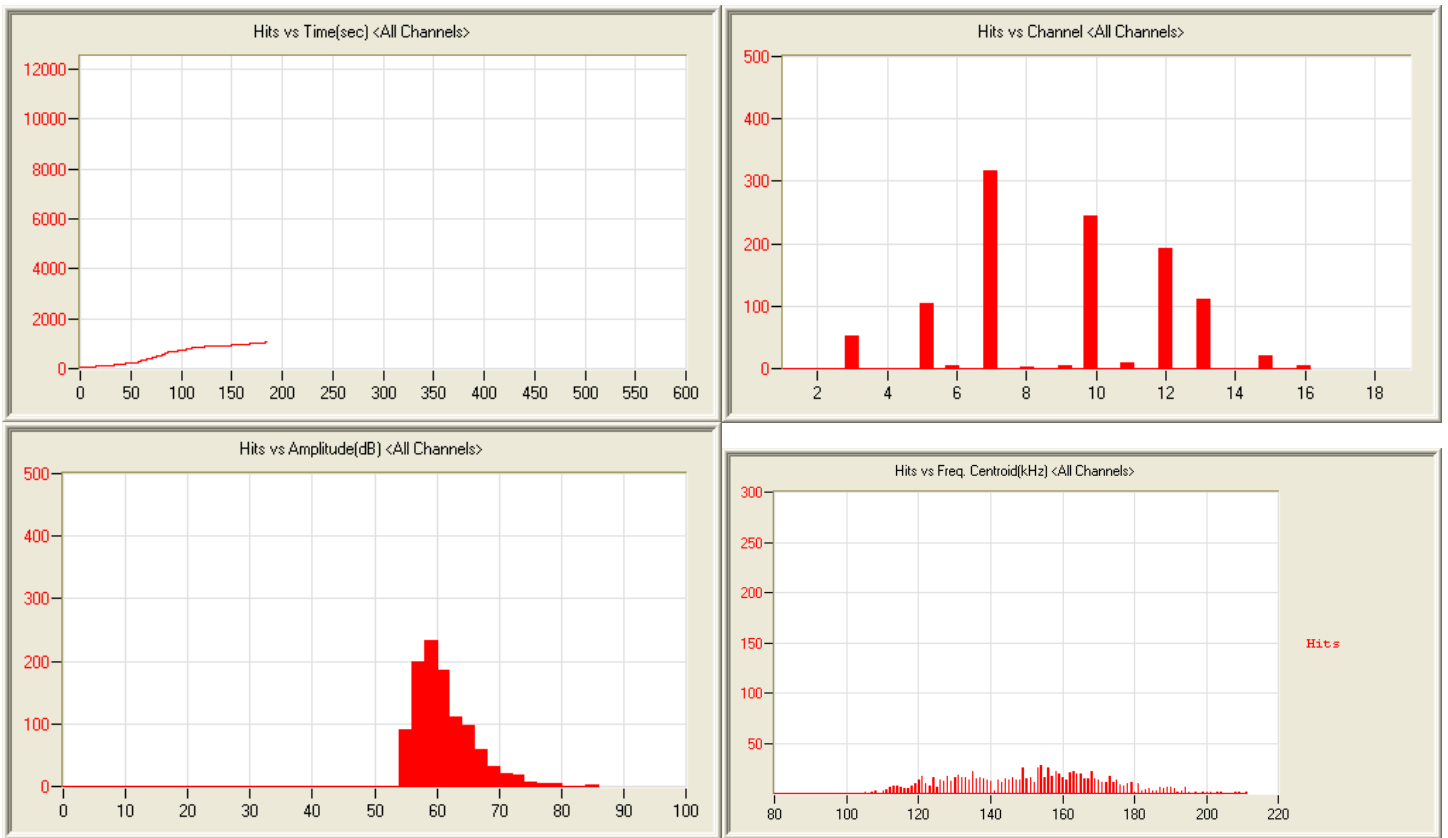
6/26/12 5:59am 17:42:43 1169 120626055949_0 2.7mb



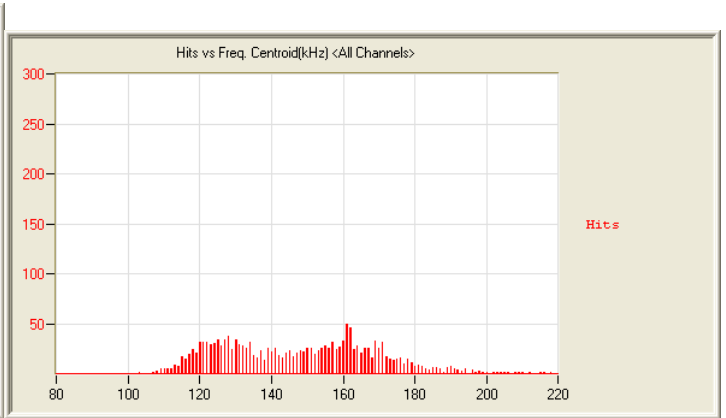
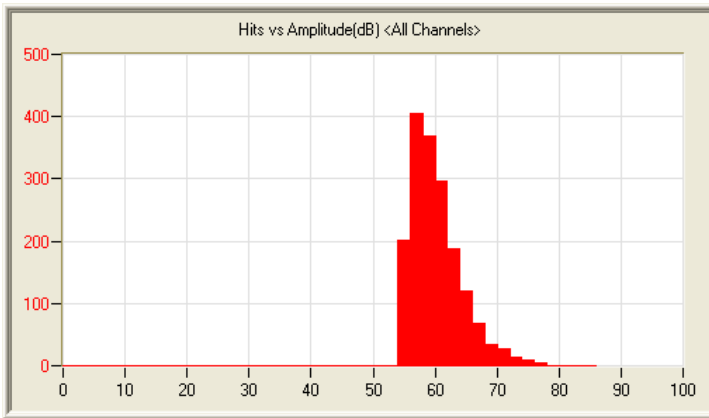
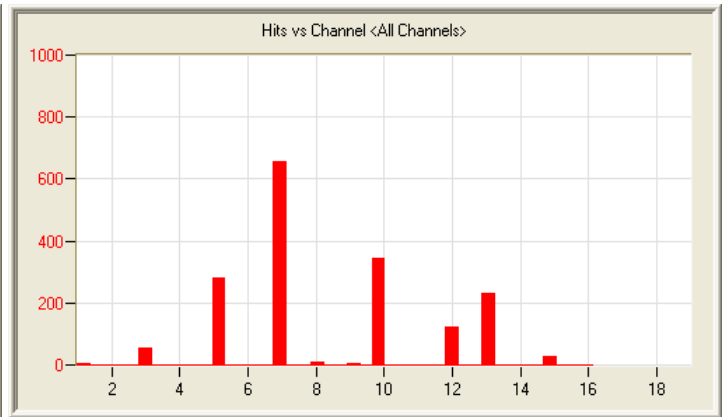
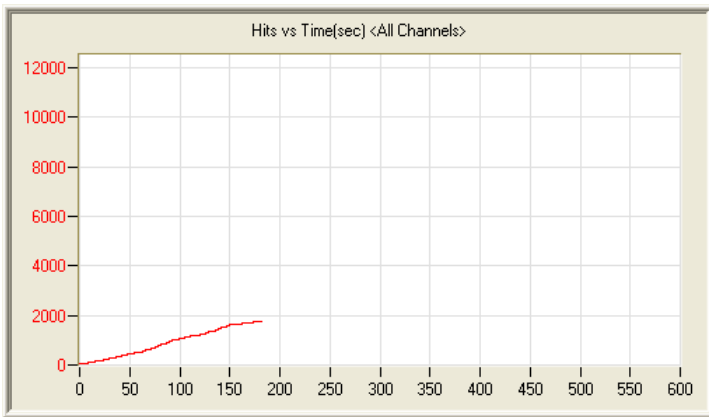
6/27/12 8:30am 15:36:32 2211 120627083008_0 2.4kb



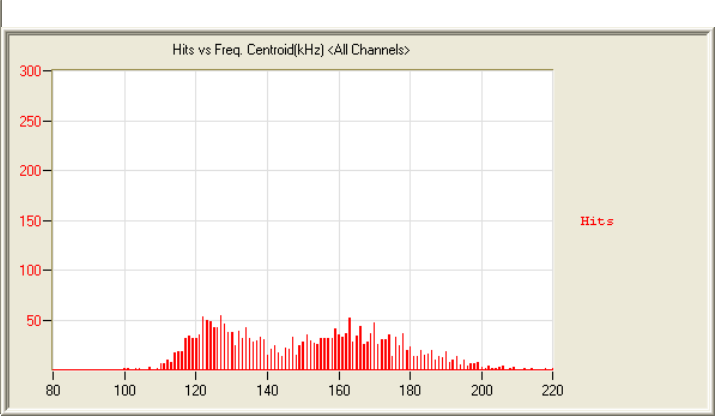
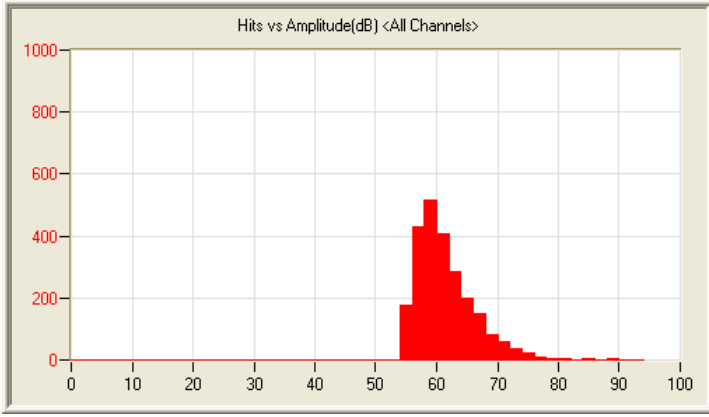
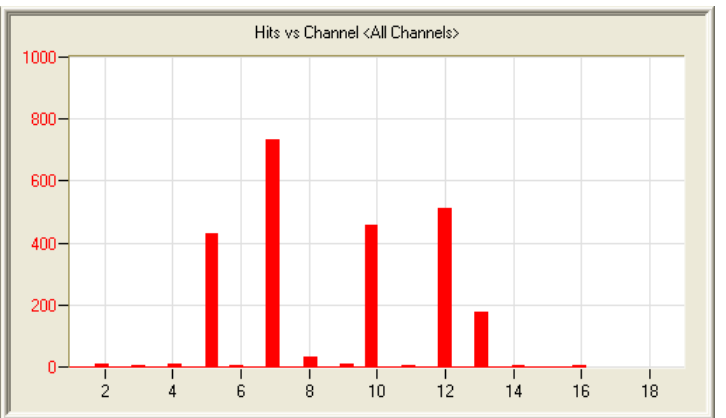
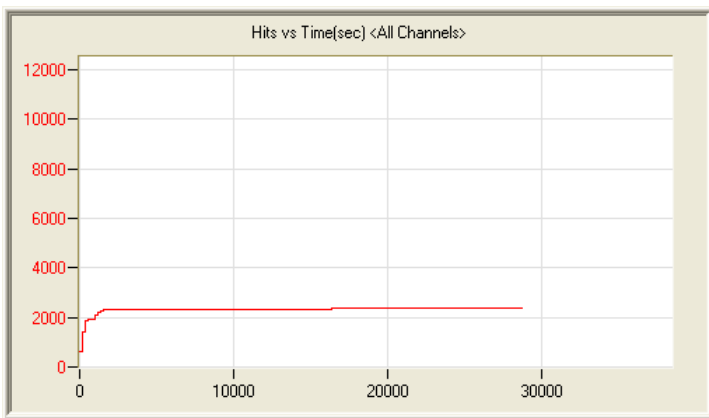
6/30/12 6:13am 15:52:12 492 120630061348_0 2.4mb



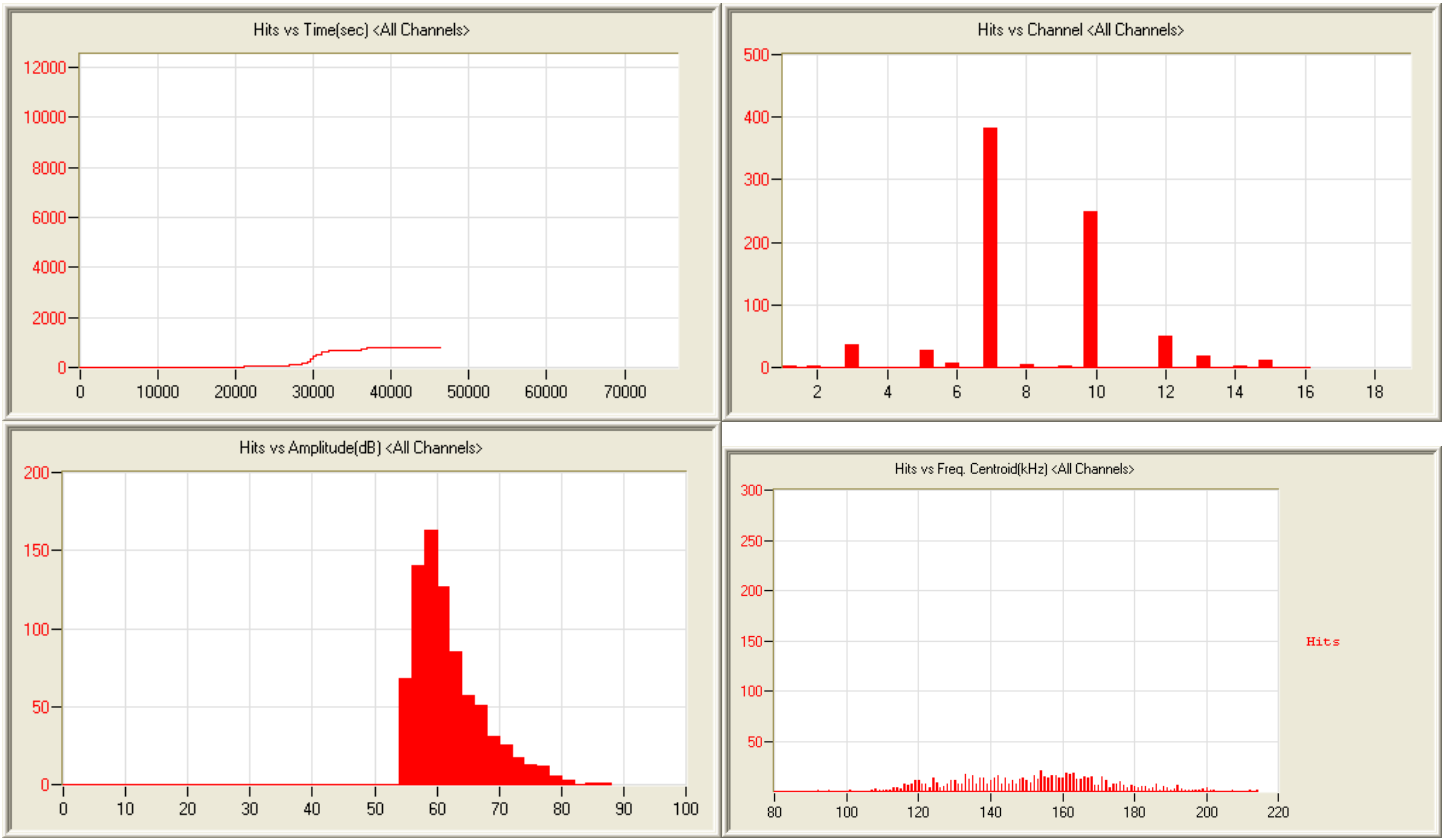
7/1/12 7:40pm 0:03:05 1062 120701194034_0 116kb



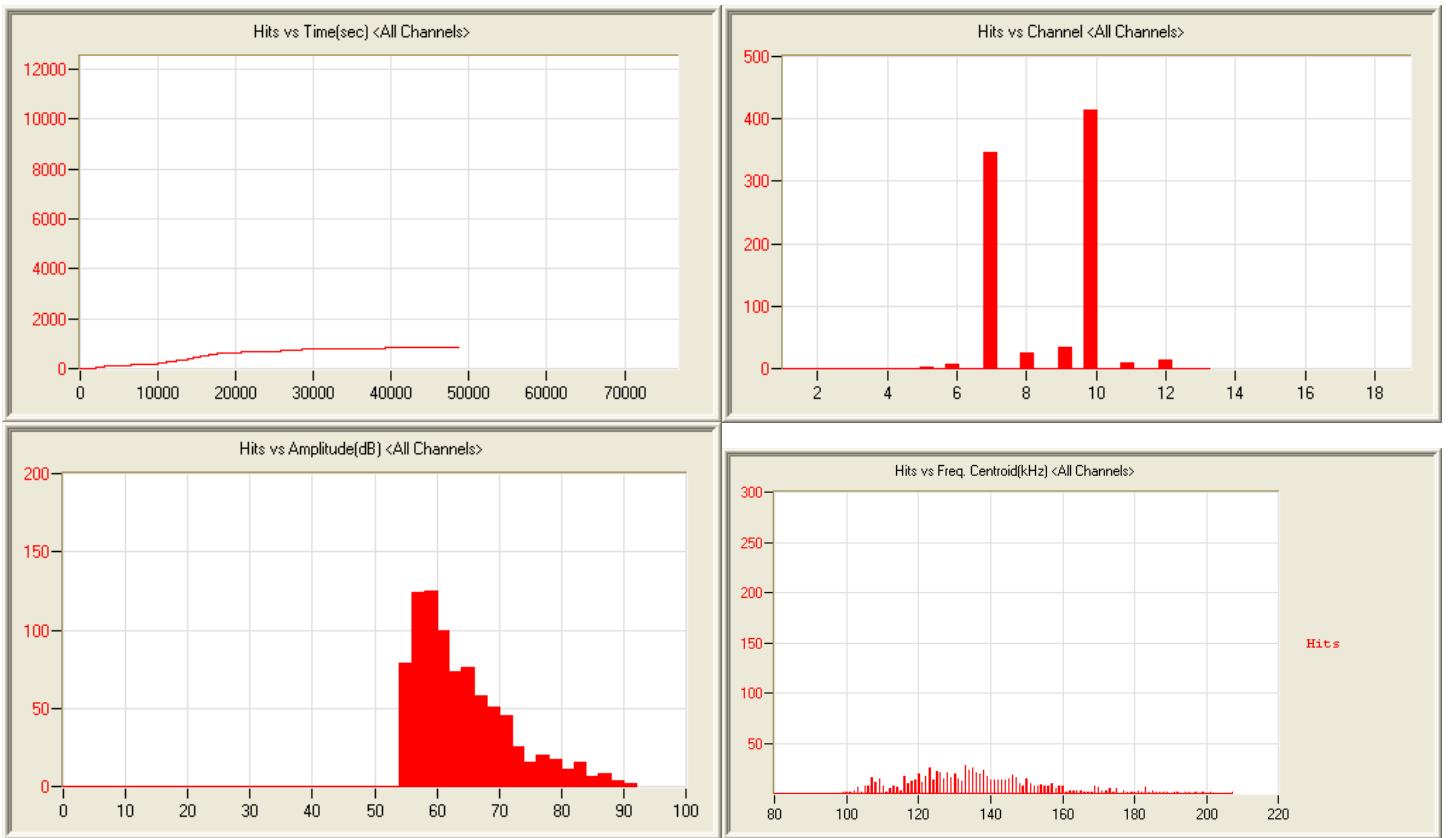
7/1/12 8:49 0:03:00 1741 120701204858_0 143kb



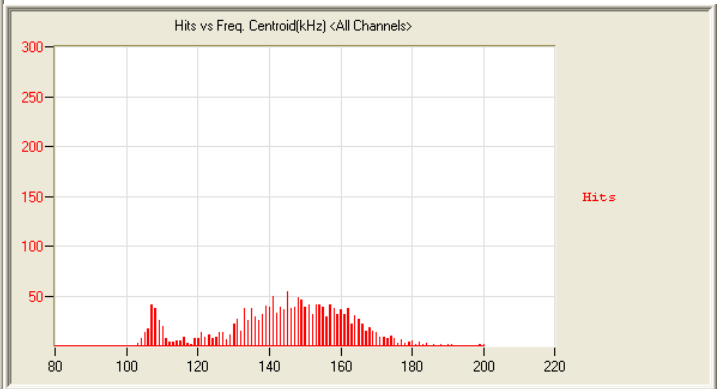
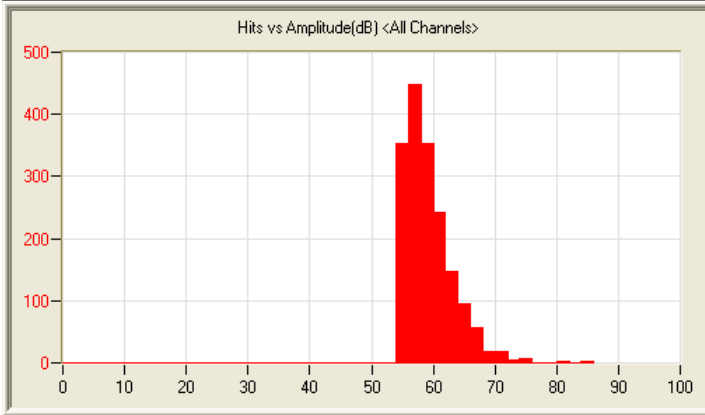
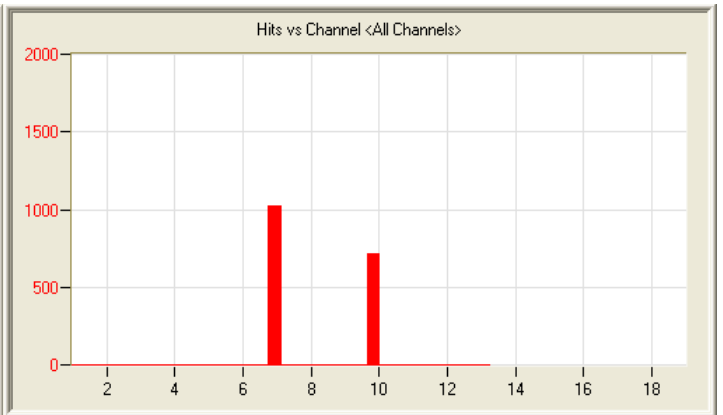
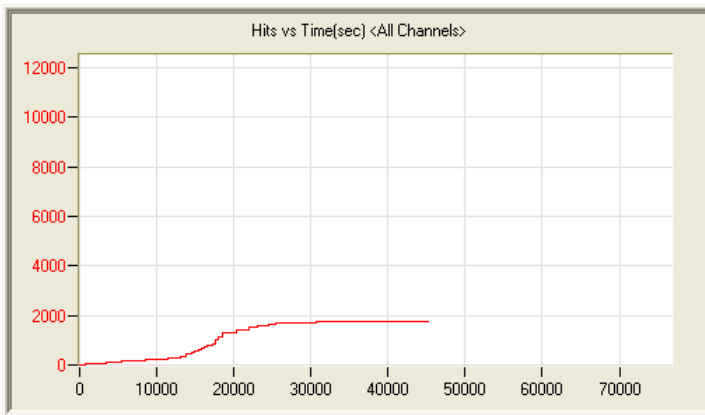
7/2/12 8:20am 9:21:17 2389 120702082029_0 1.5mb



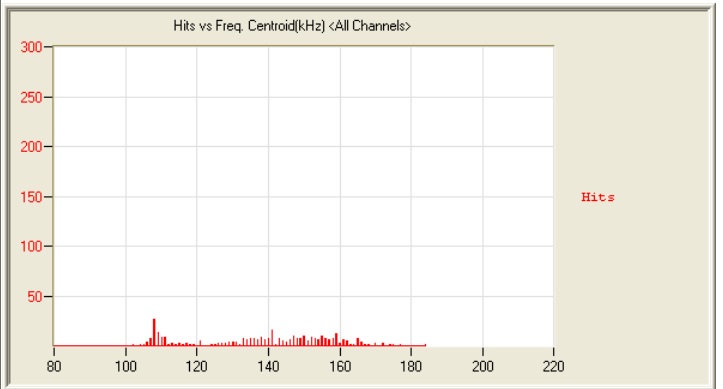
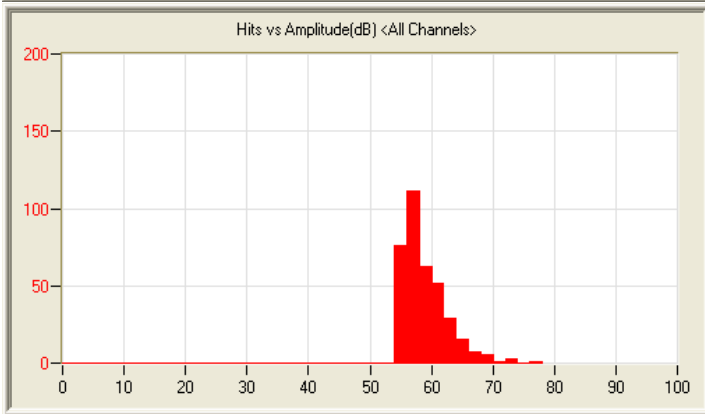
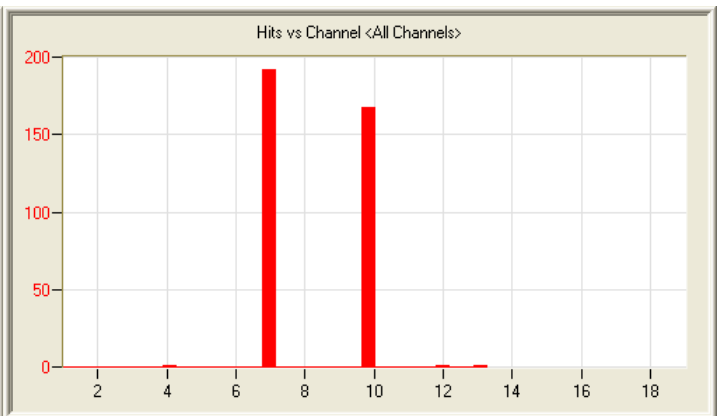
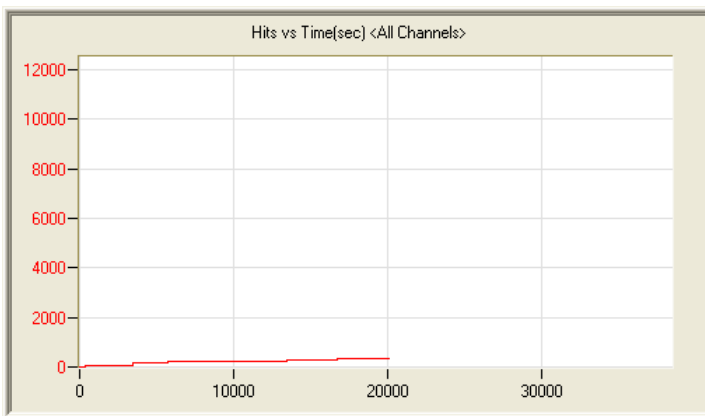
7/3/12 5:25am 13:07:24 799 120703052543_0 2.0mb



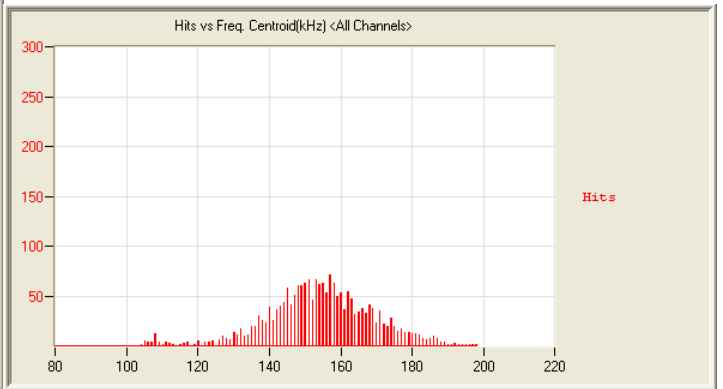
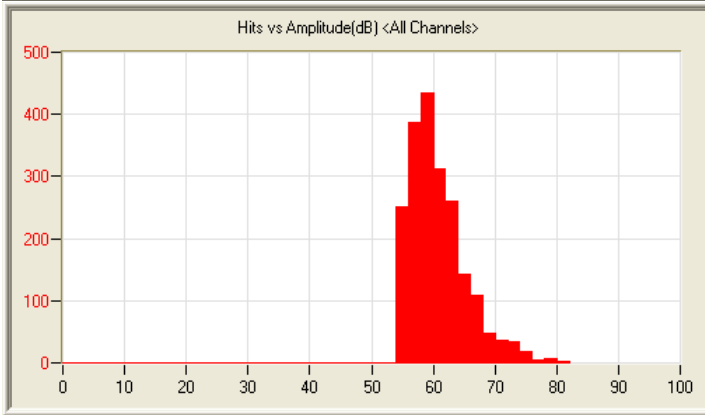
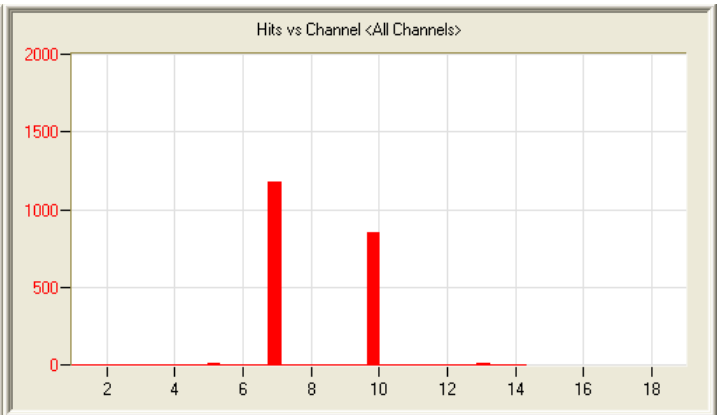
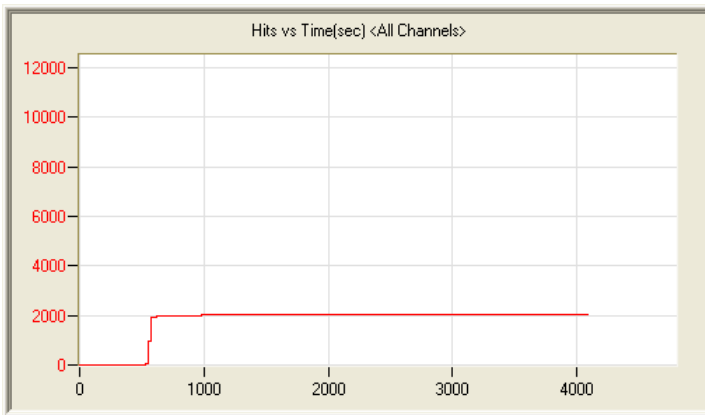
7/4/12 8:51am 14:28:44 854 120704085126_0 2.2mb



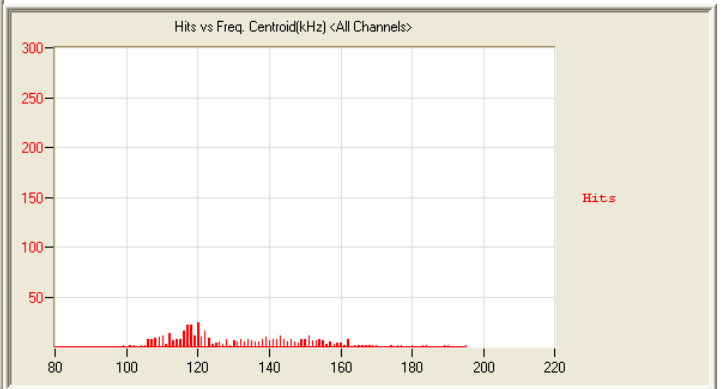
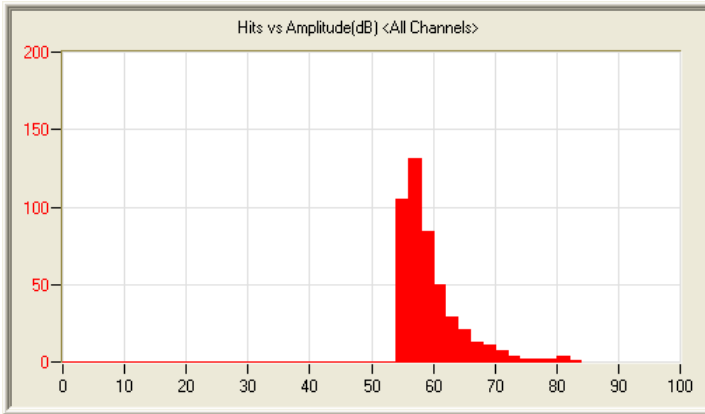
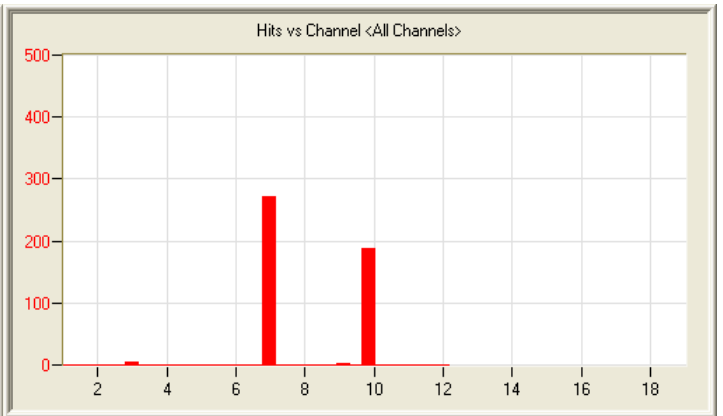
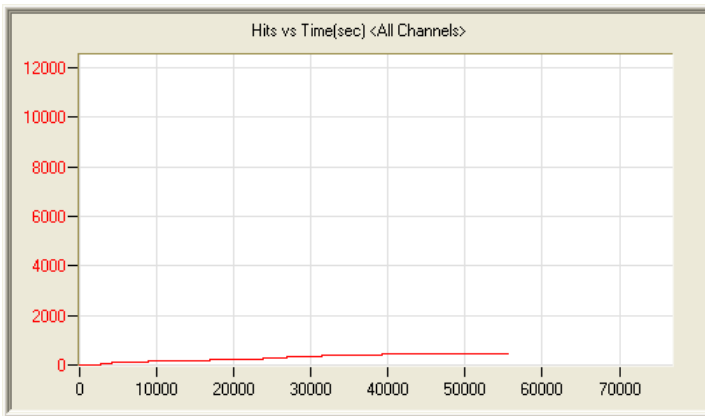
7/5/12 4:10pm 13:38:38 1747 120705161002_0 2.1mb



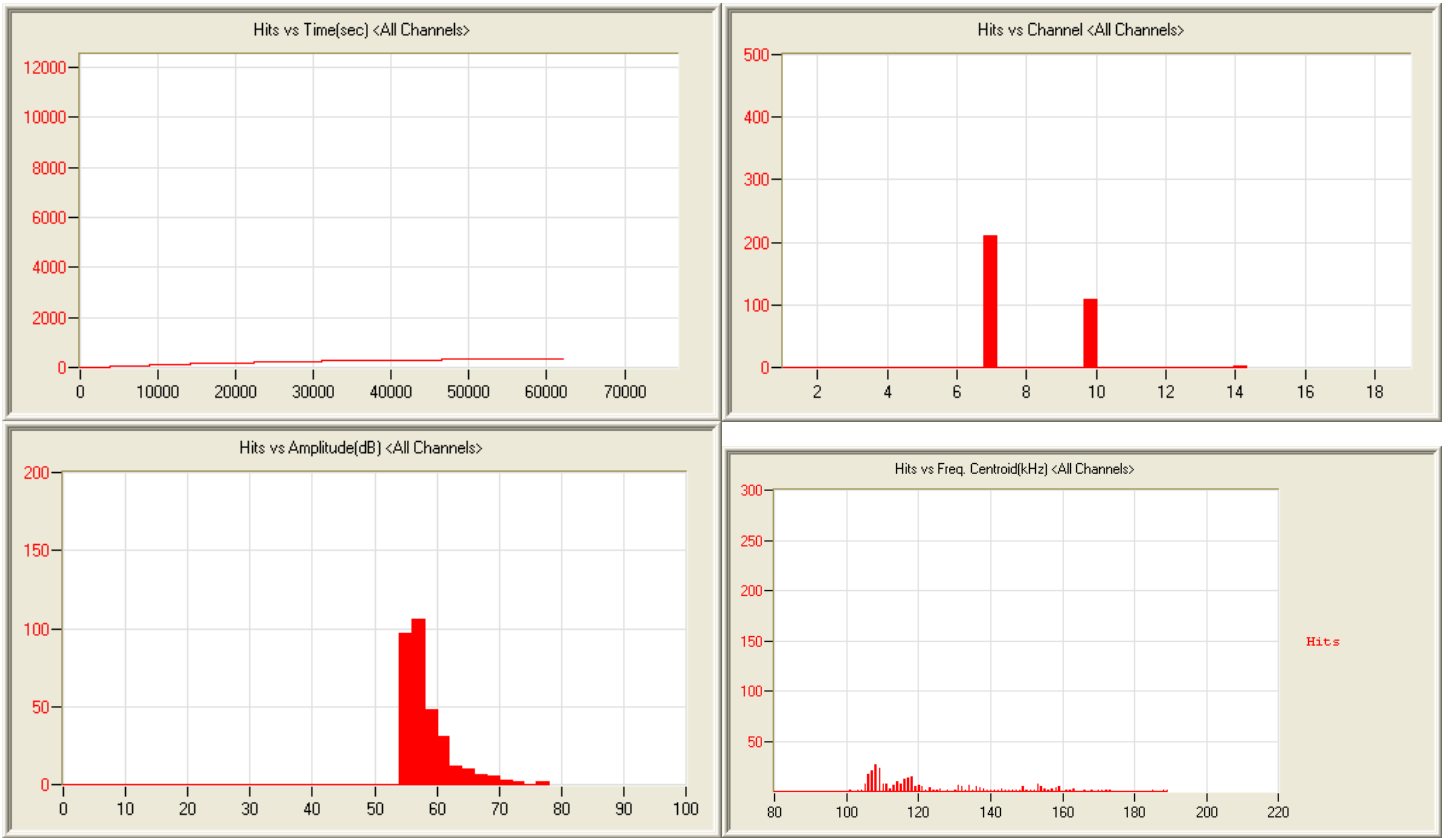
7/6/12 6:02pm 5:36:16 120706180247_0 889kb



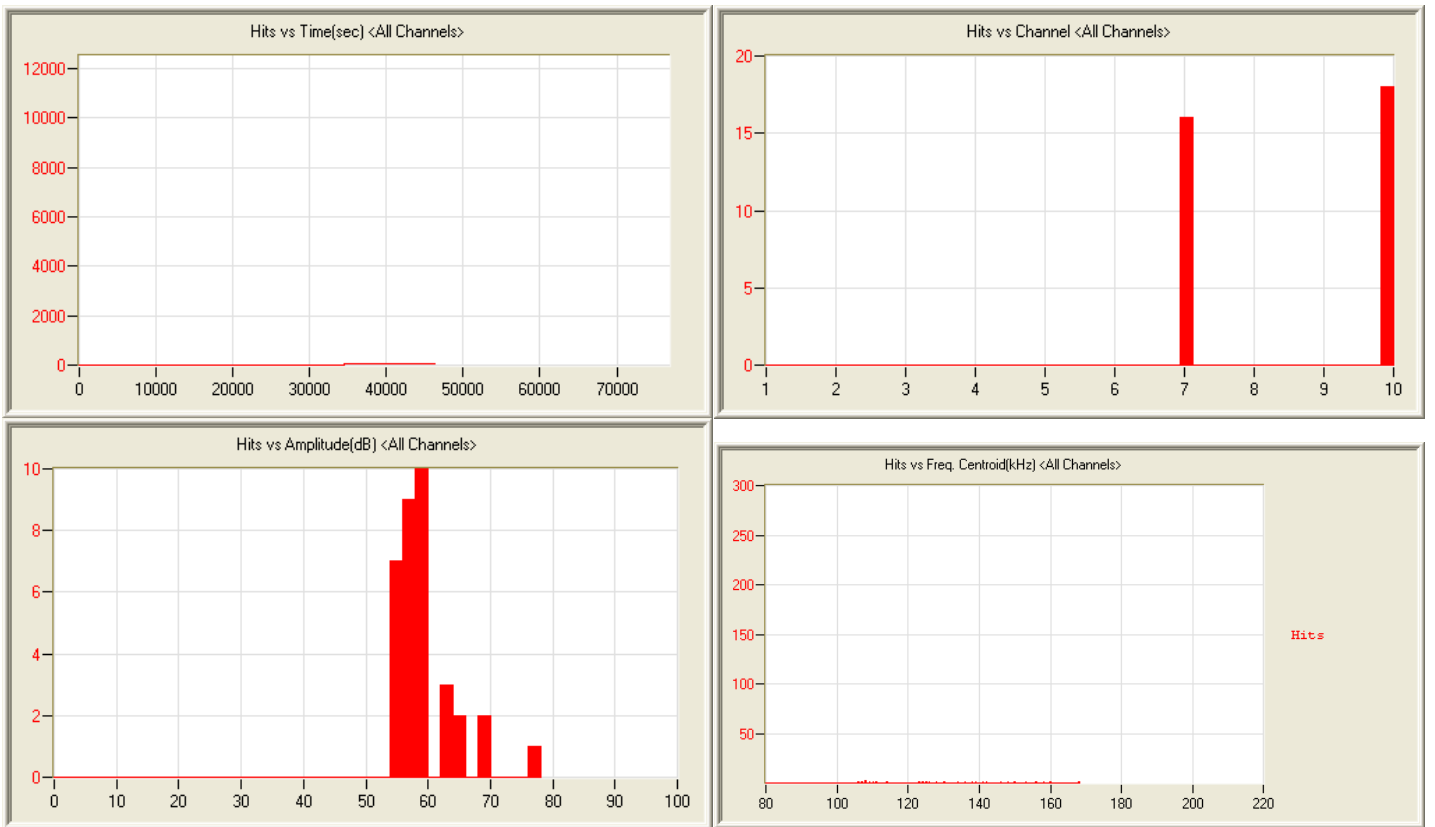
7/7/12 8:26am 1:12:52 2046 120707082650_0 323kb



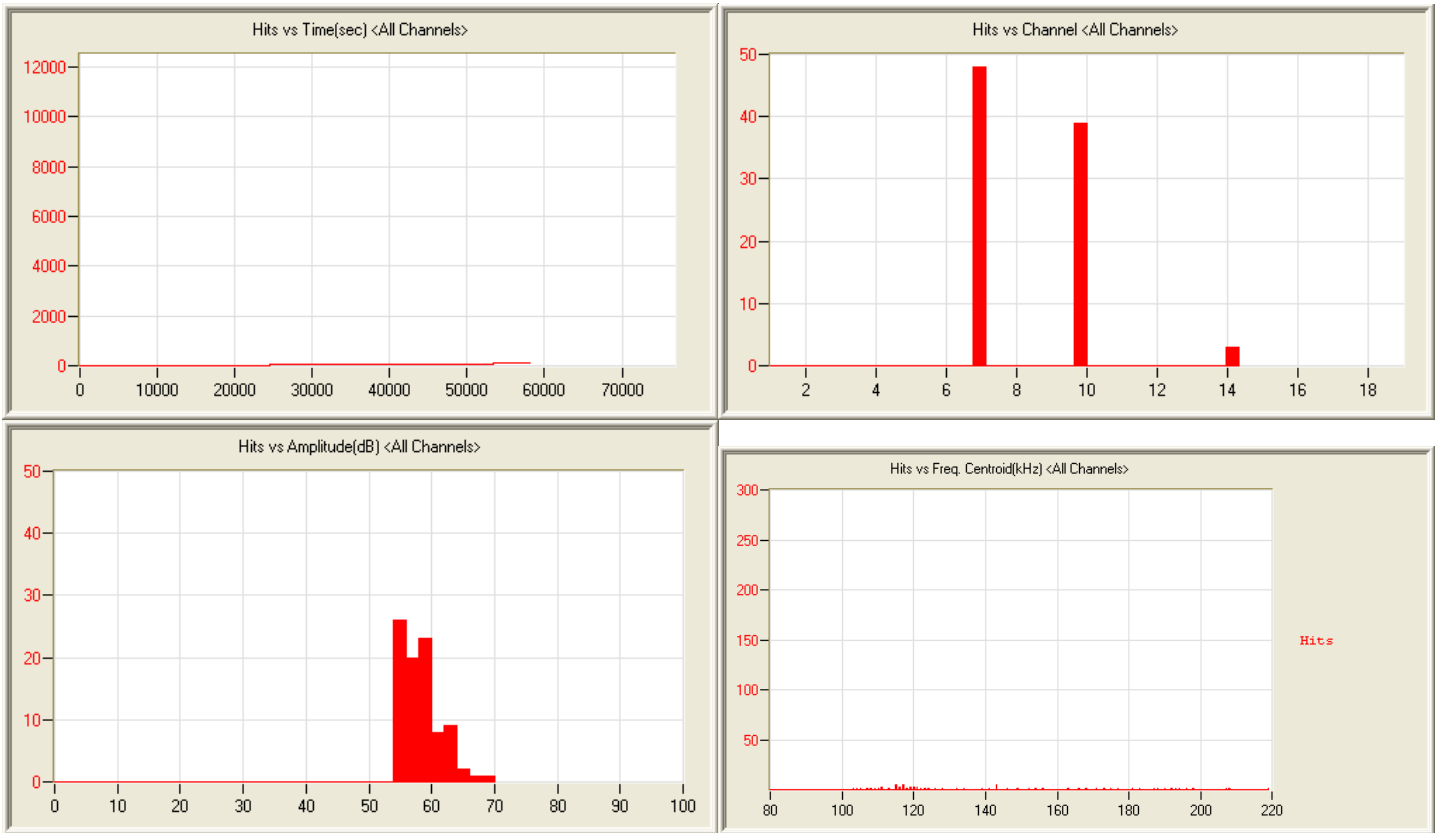
7/8/12 10:26am 16:02:22 466 120708102622_0 2.4mb



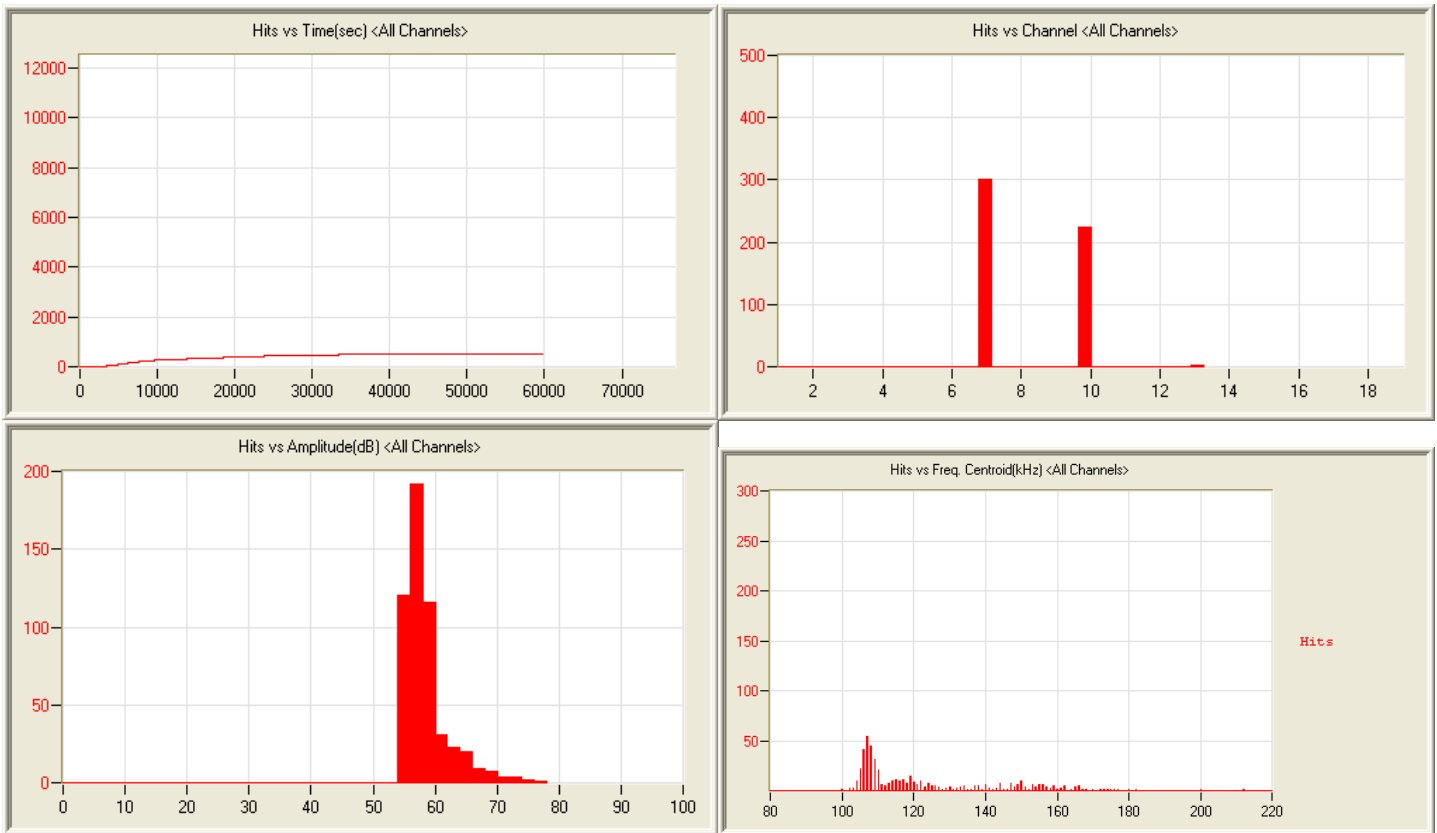
7/9/12 11:06am 17:29:22 322 120709110656_0 2.6mb



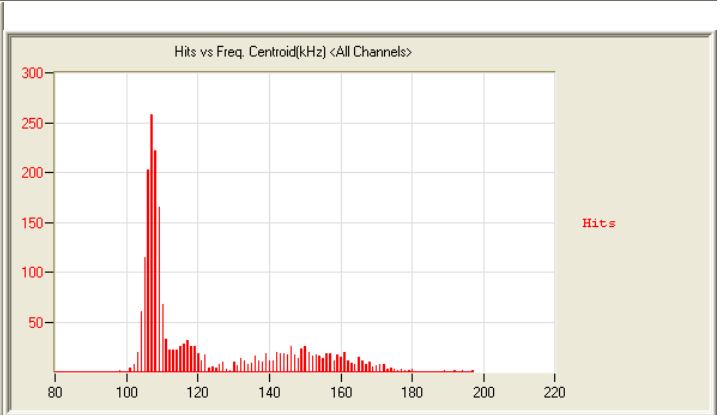
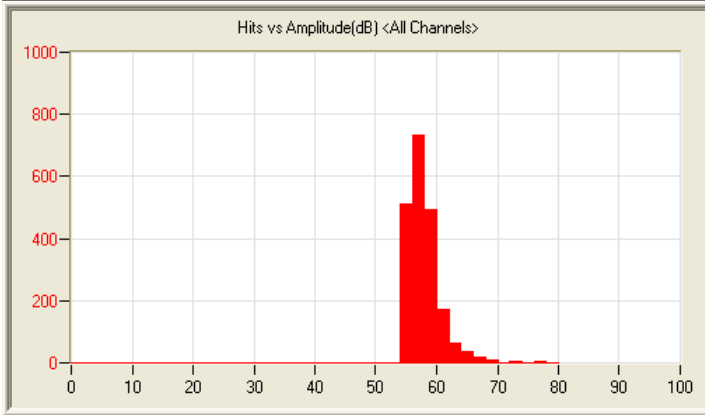
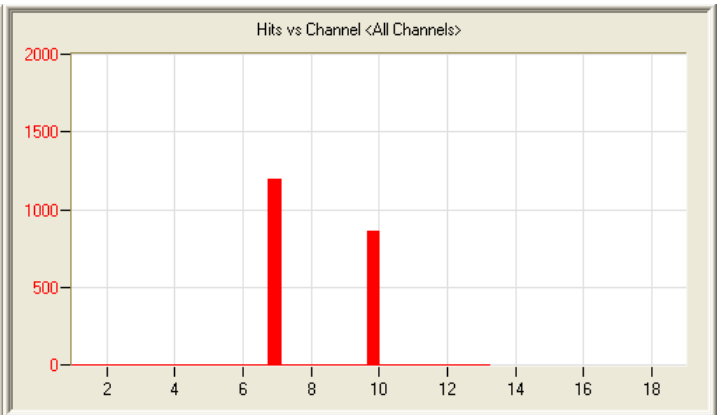
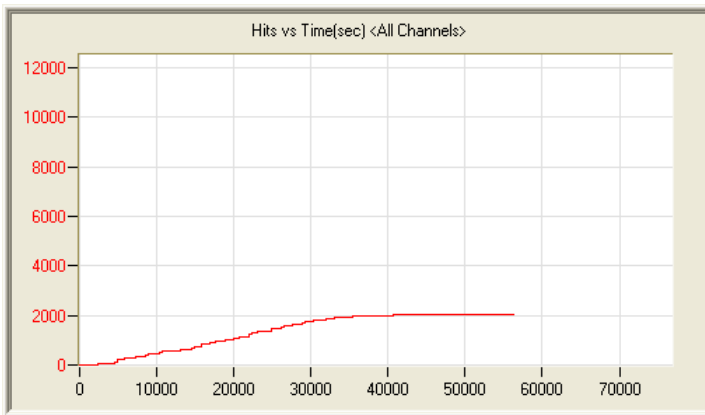
7/10/12 2:32pm 13:27:37 34 120710143202_0 2.0mb



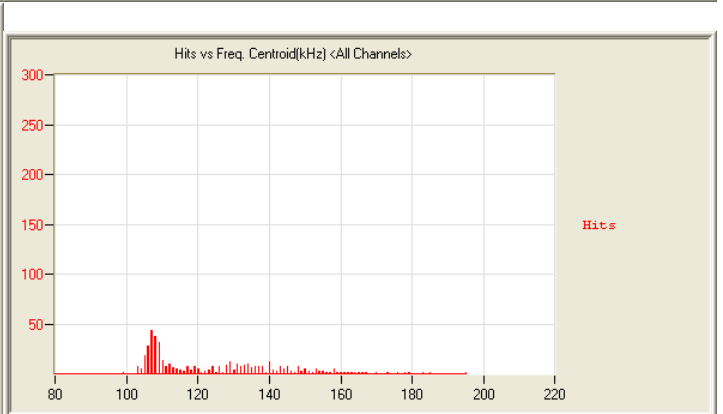
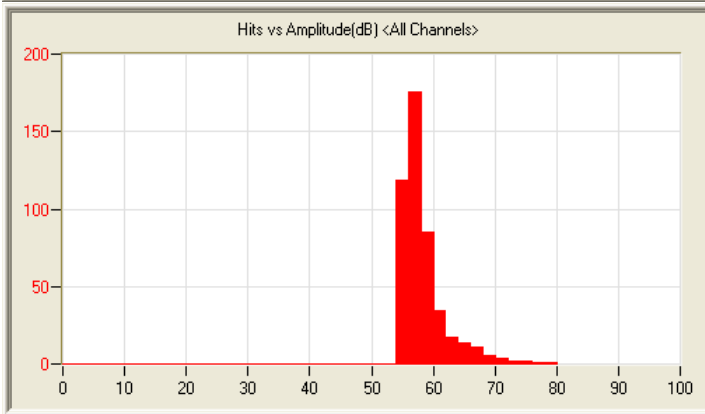
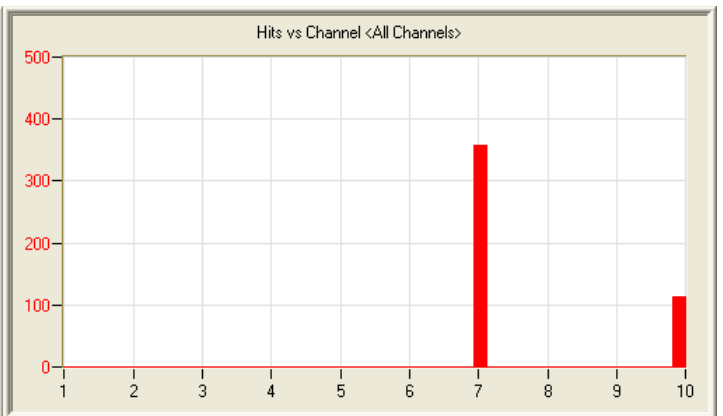
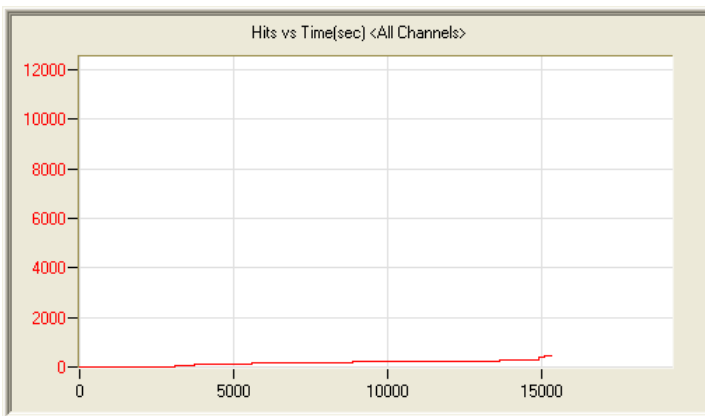
7/11/12 2:32pm 16:21:45 90 120711143237_0 2.4mb



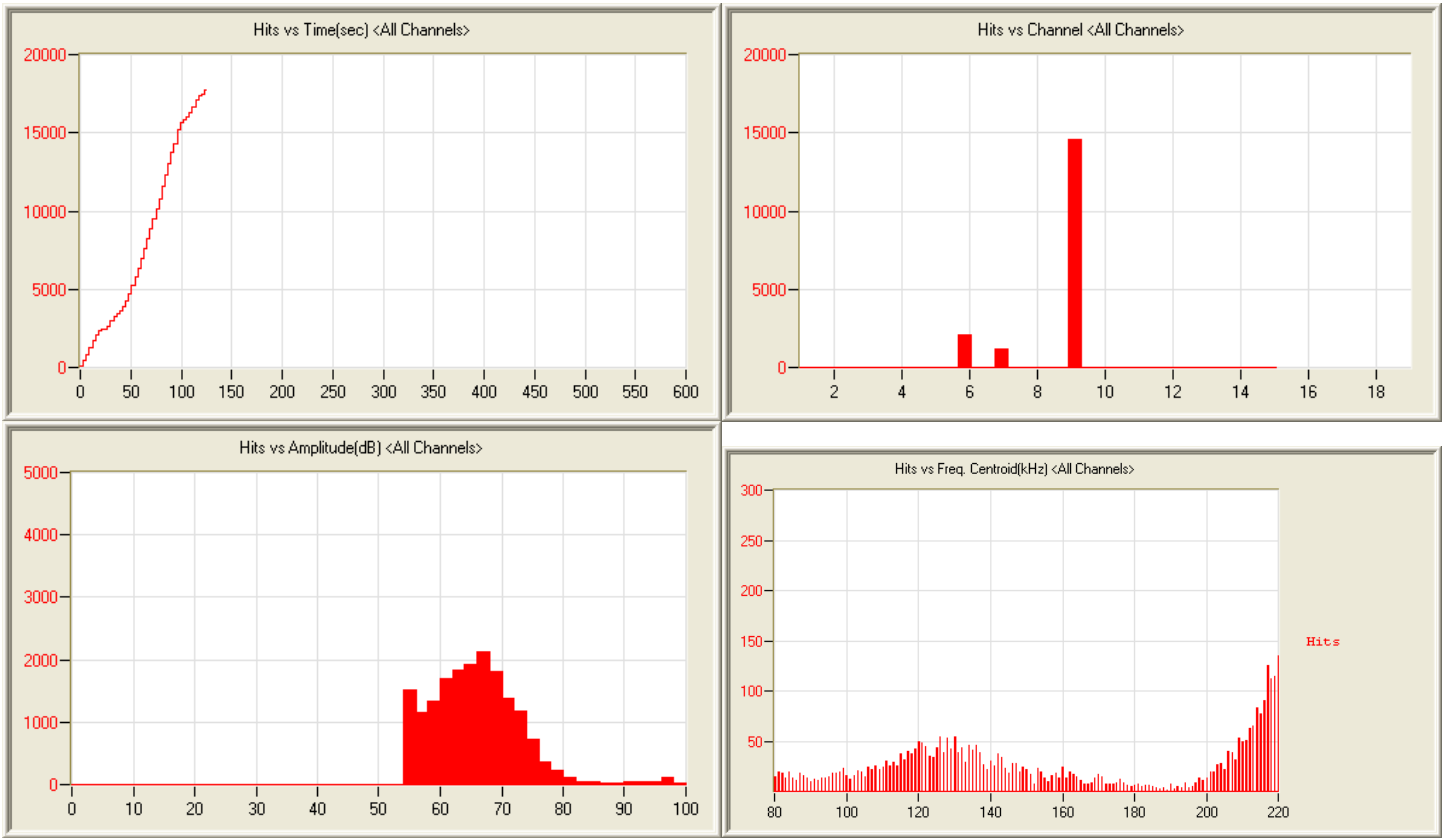
7/12/12 3:02pm 17:21:52 529 120712150228_0 2.6mb



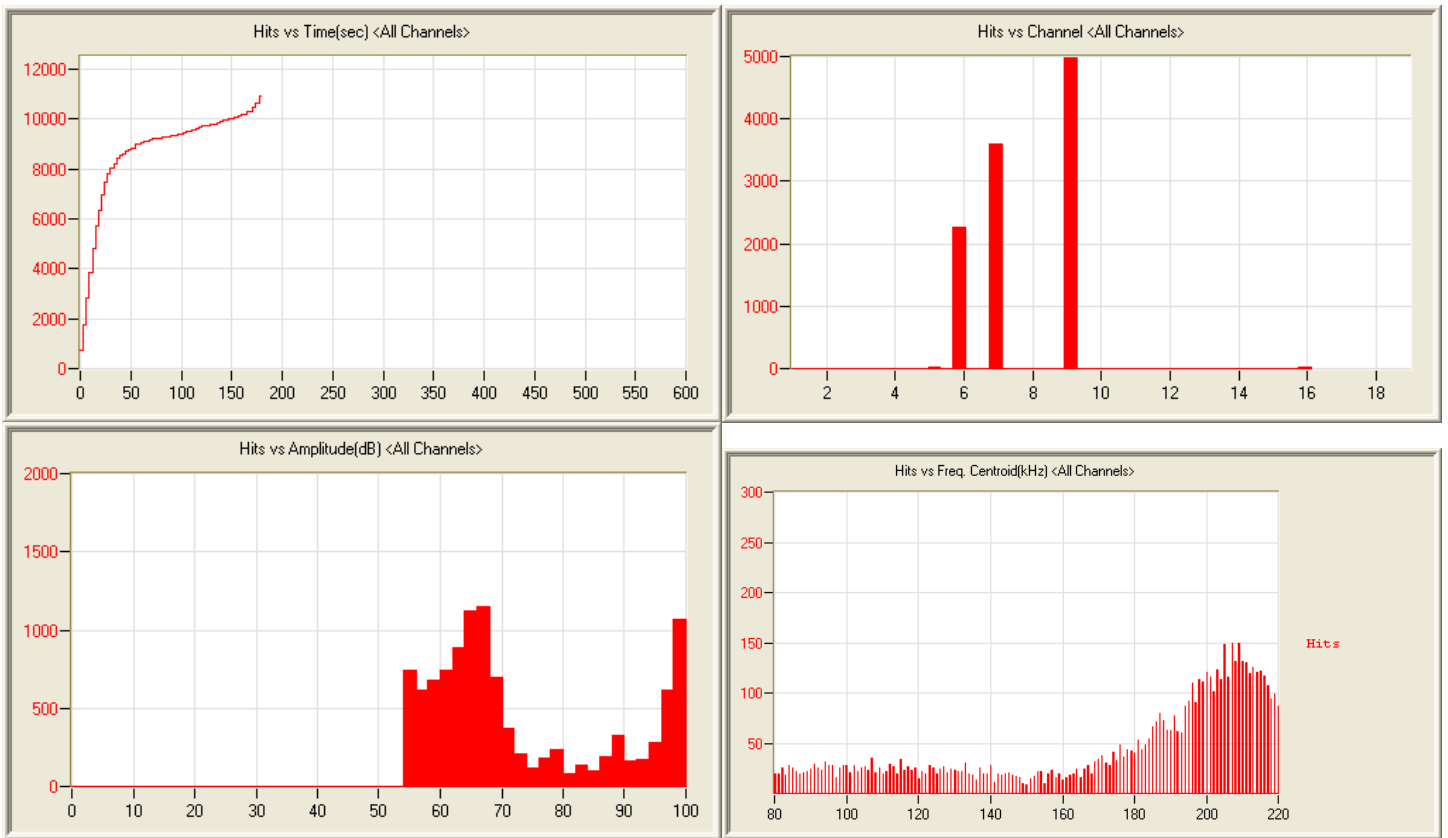
7/13/12 4:00pm 17:23:22 2055 120713160037_0 2.7mb



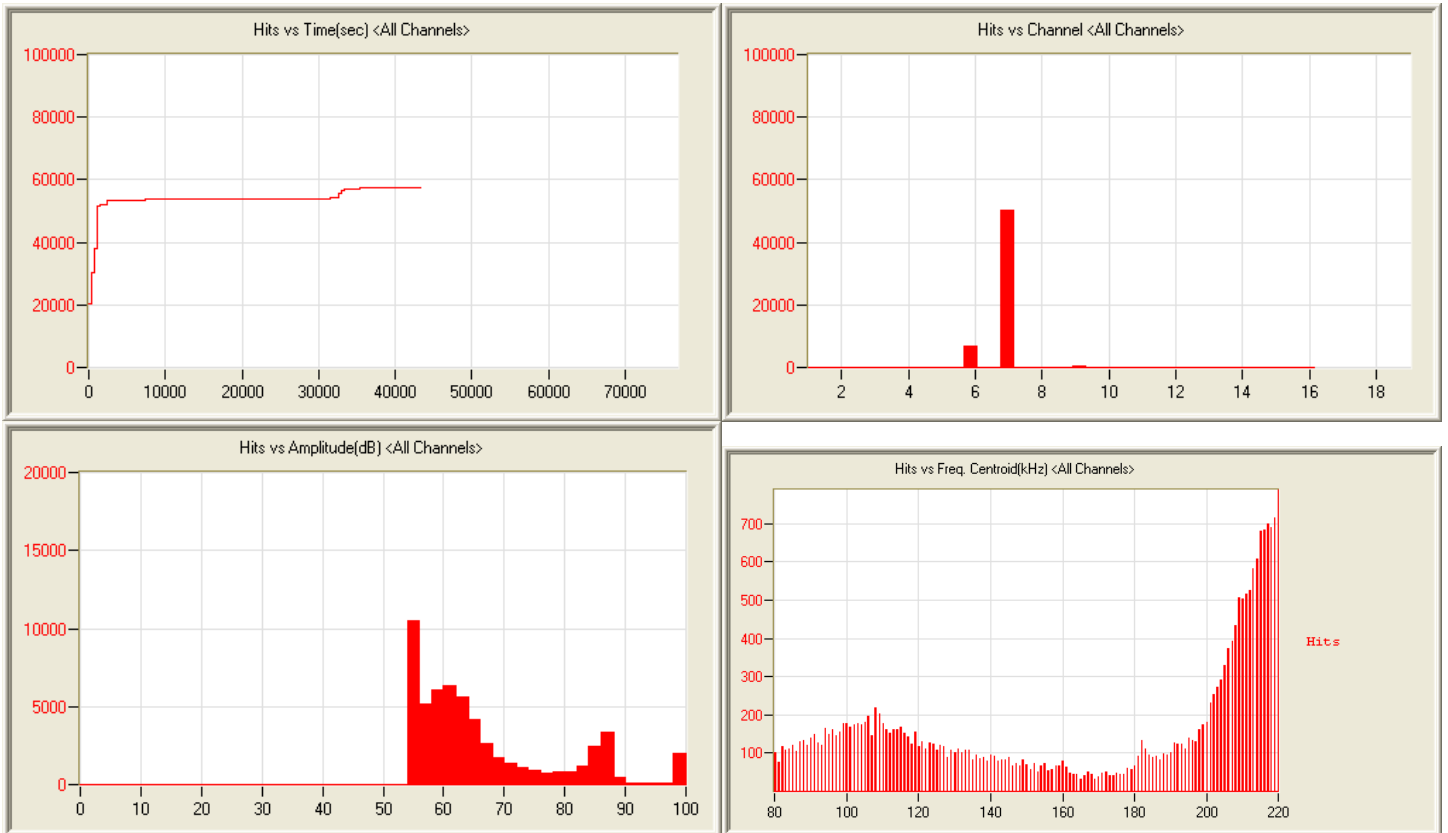
7/14/12 5:14pm 4:14:30 471 120714171407_0 691kb



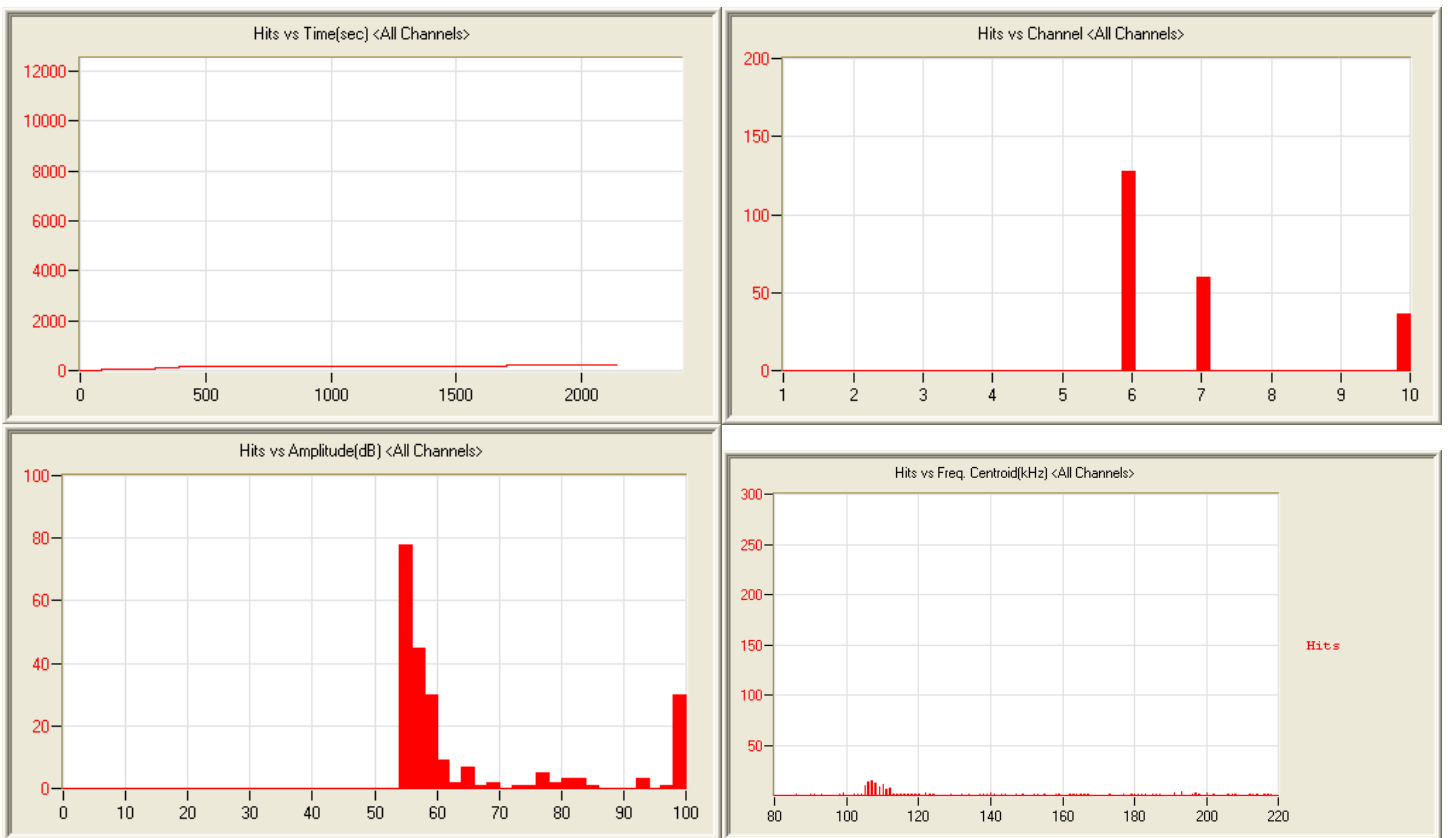
7/15/12 3:56am 0:02:05 17770 120715035602_0 783kb



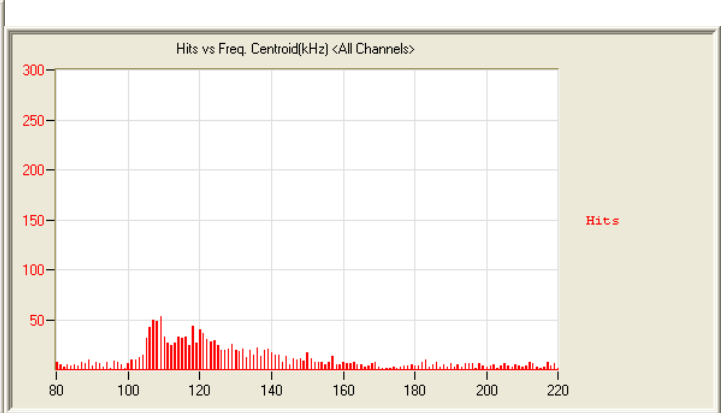
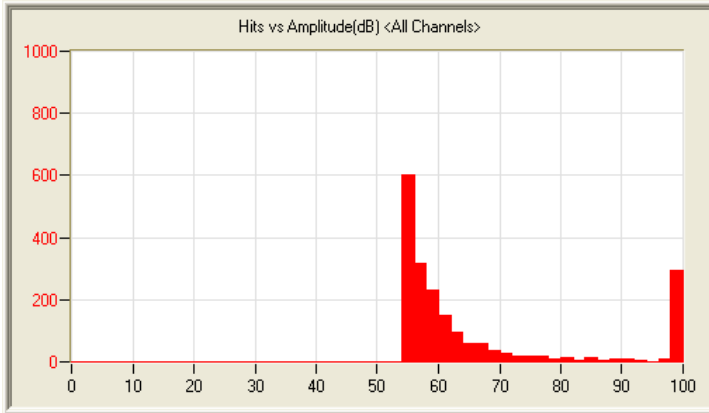
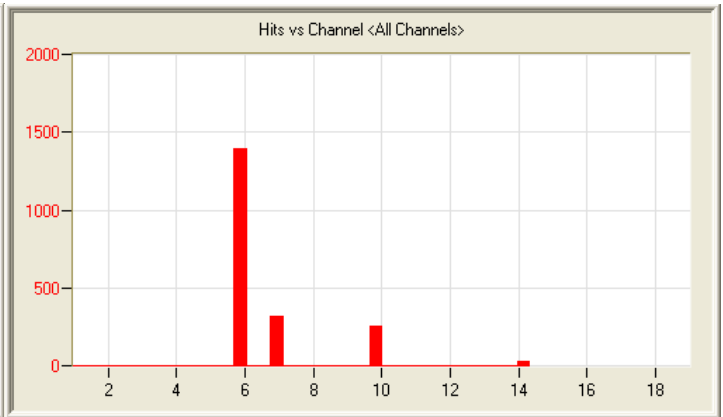
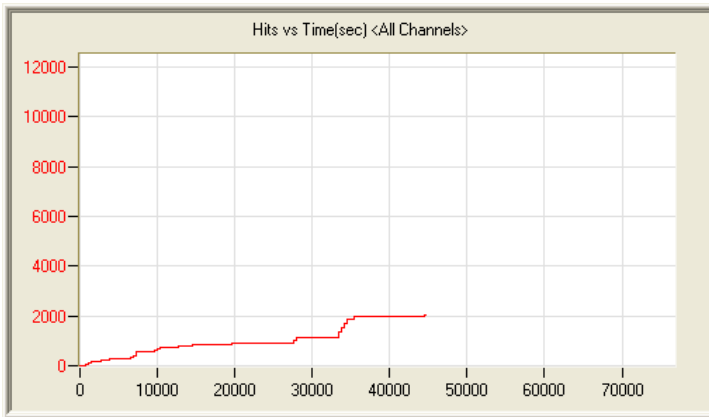
7/15/12 4:59am 0:02:59 10894 120715045935_0 510kb



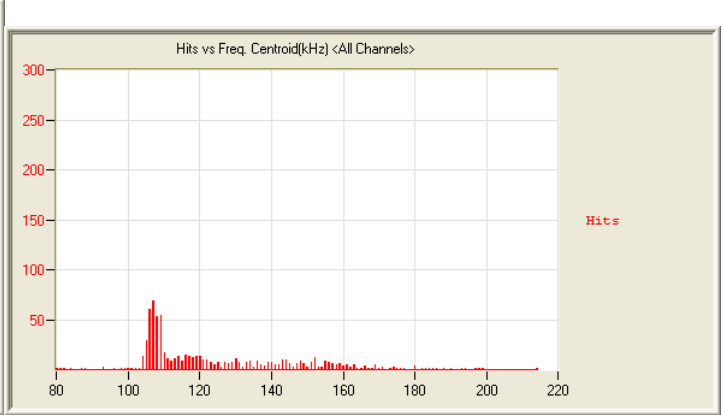
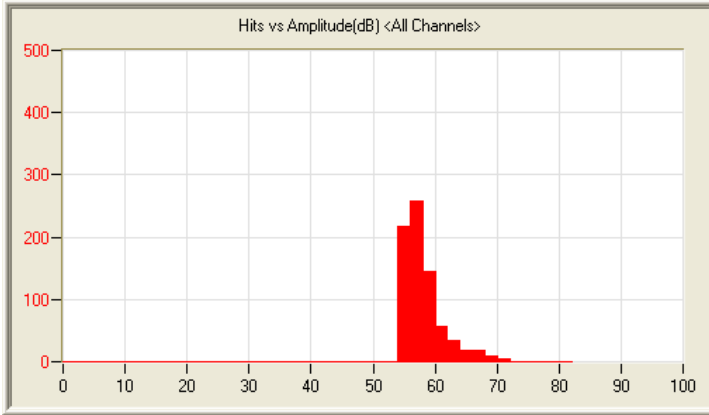
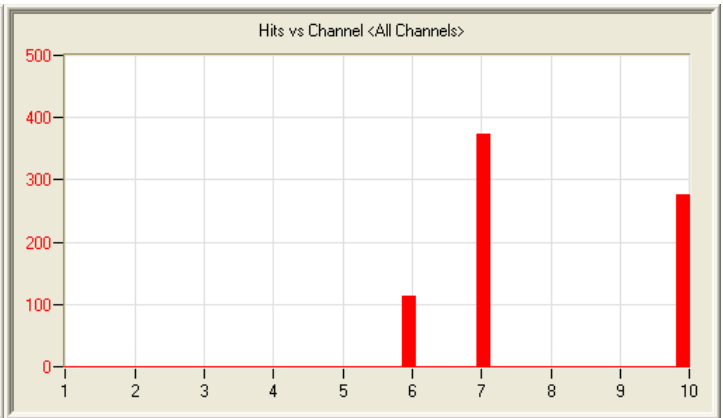
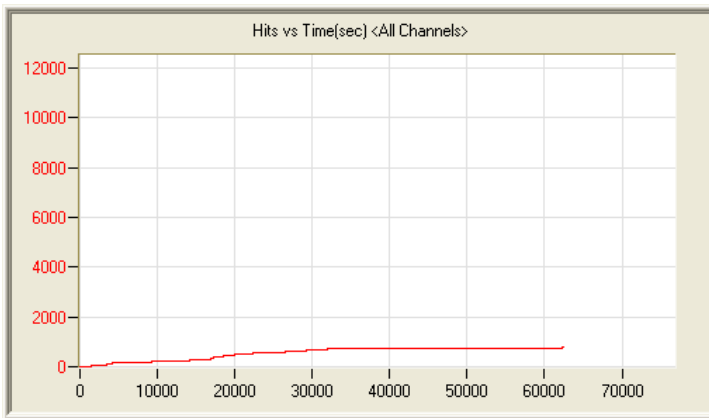
7/15/12 6:08am 12:03:37 57604 120715060848_0 4.1mb



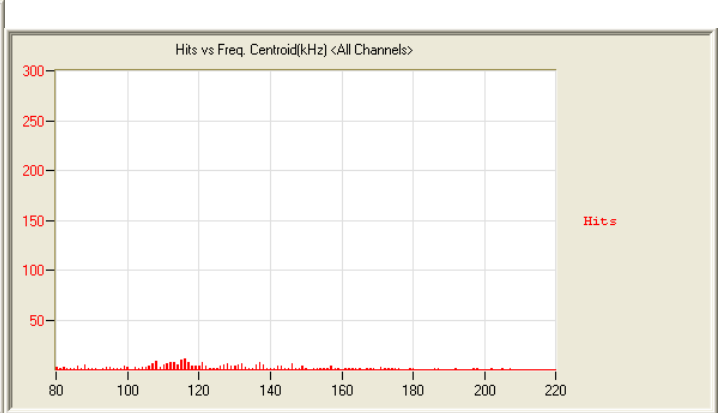
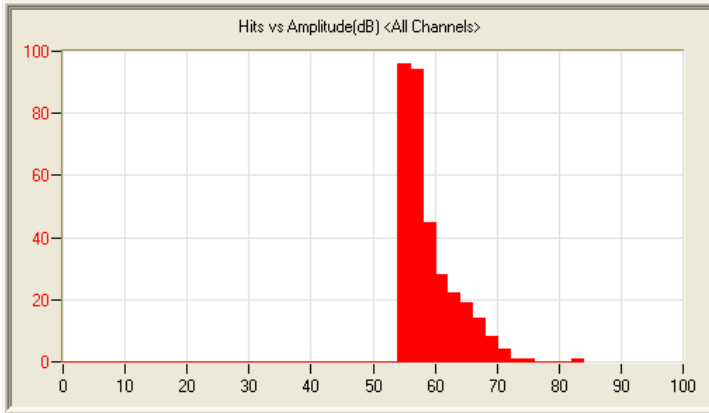
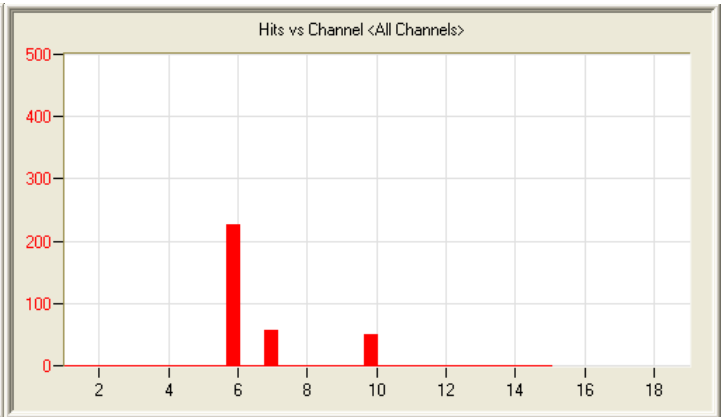
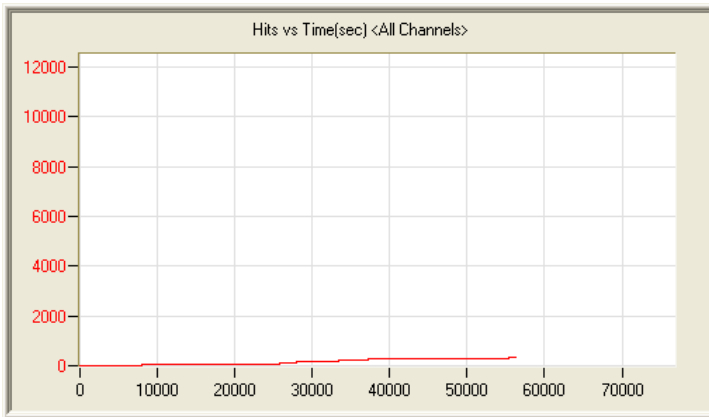
7/16/12 8:37am 0:35:53 224 120716083757_0 161kb



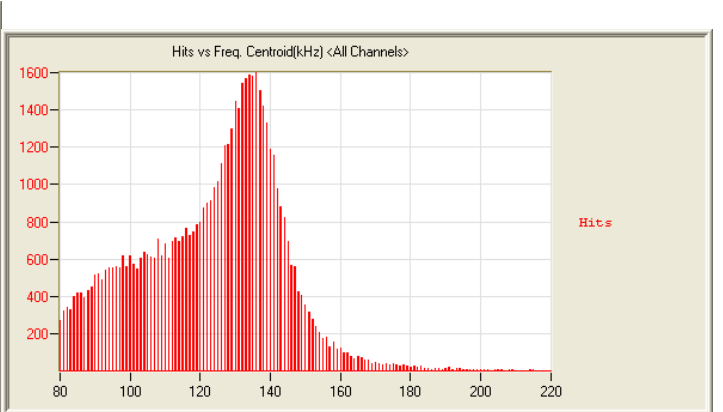
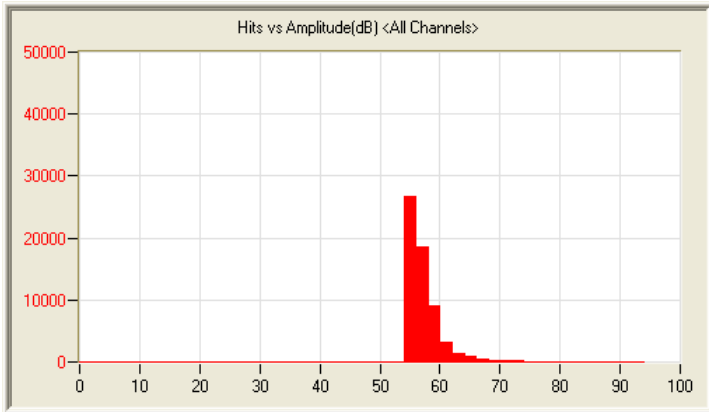
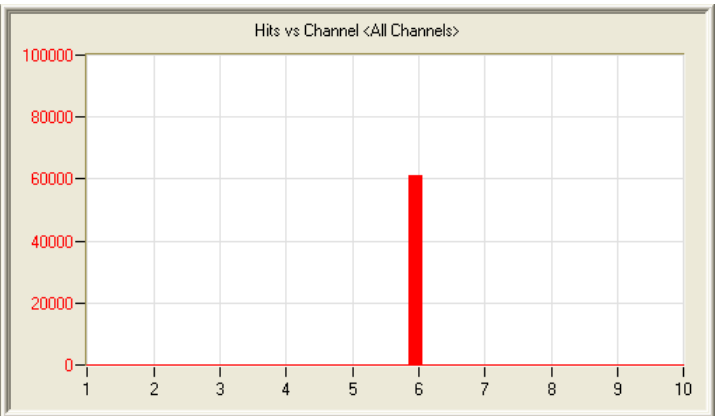
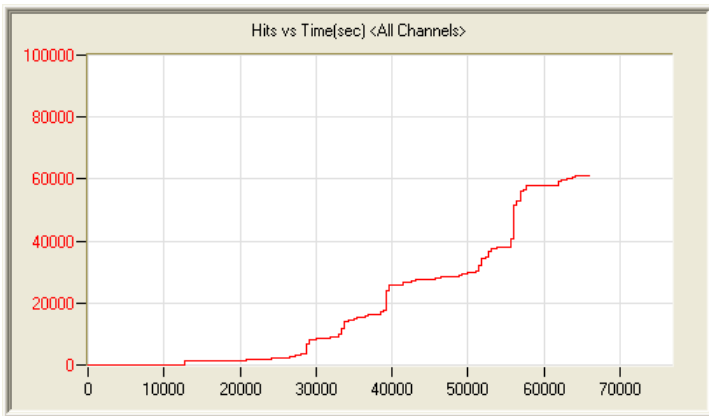
7/16/12 7:53pm 12:27:35 2008 120716195356_0 1.9mb



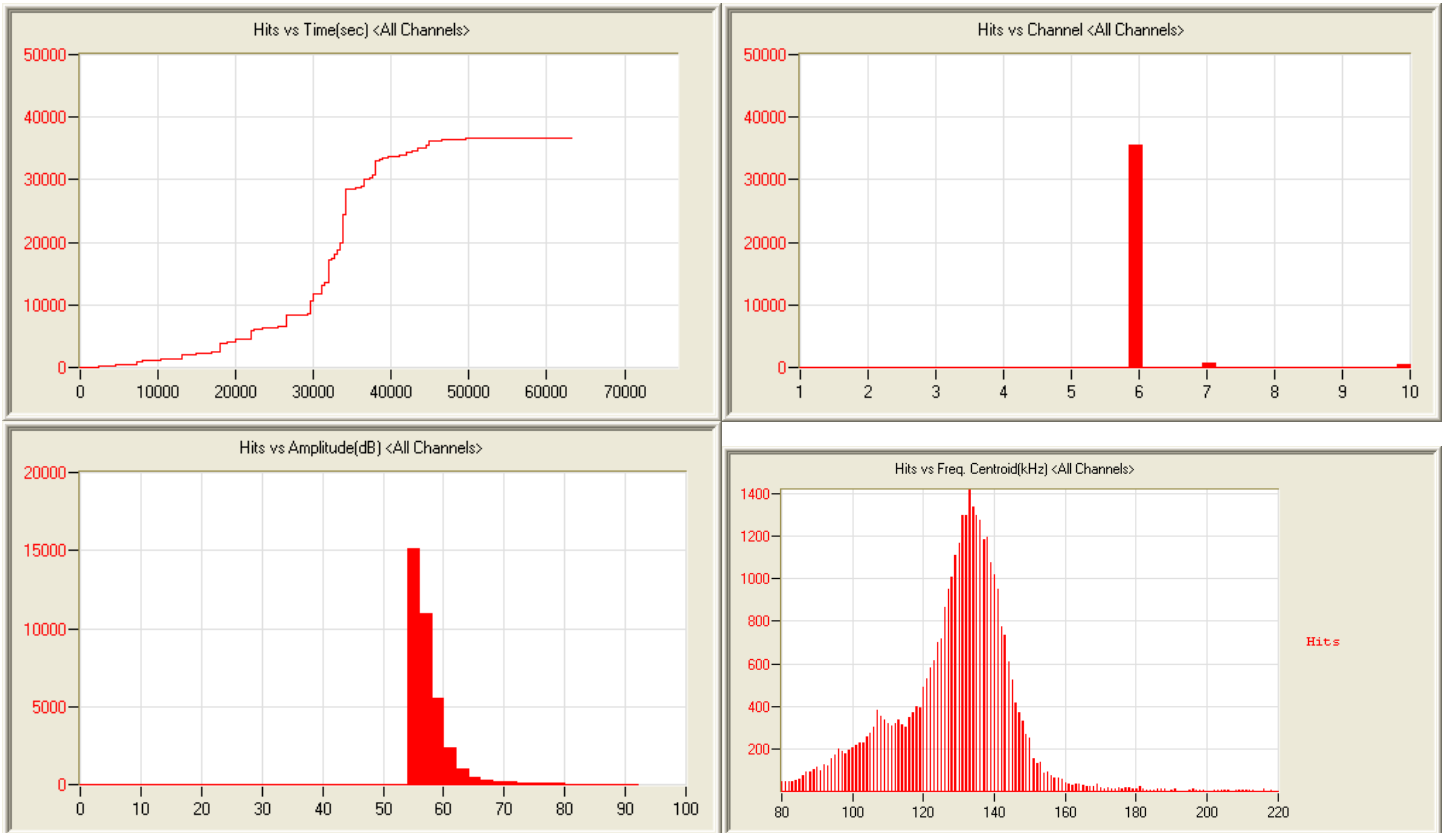
7/17/12 5:10pm 17:28:57 764 120717171049_0 2.6mb



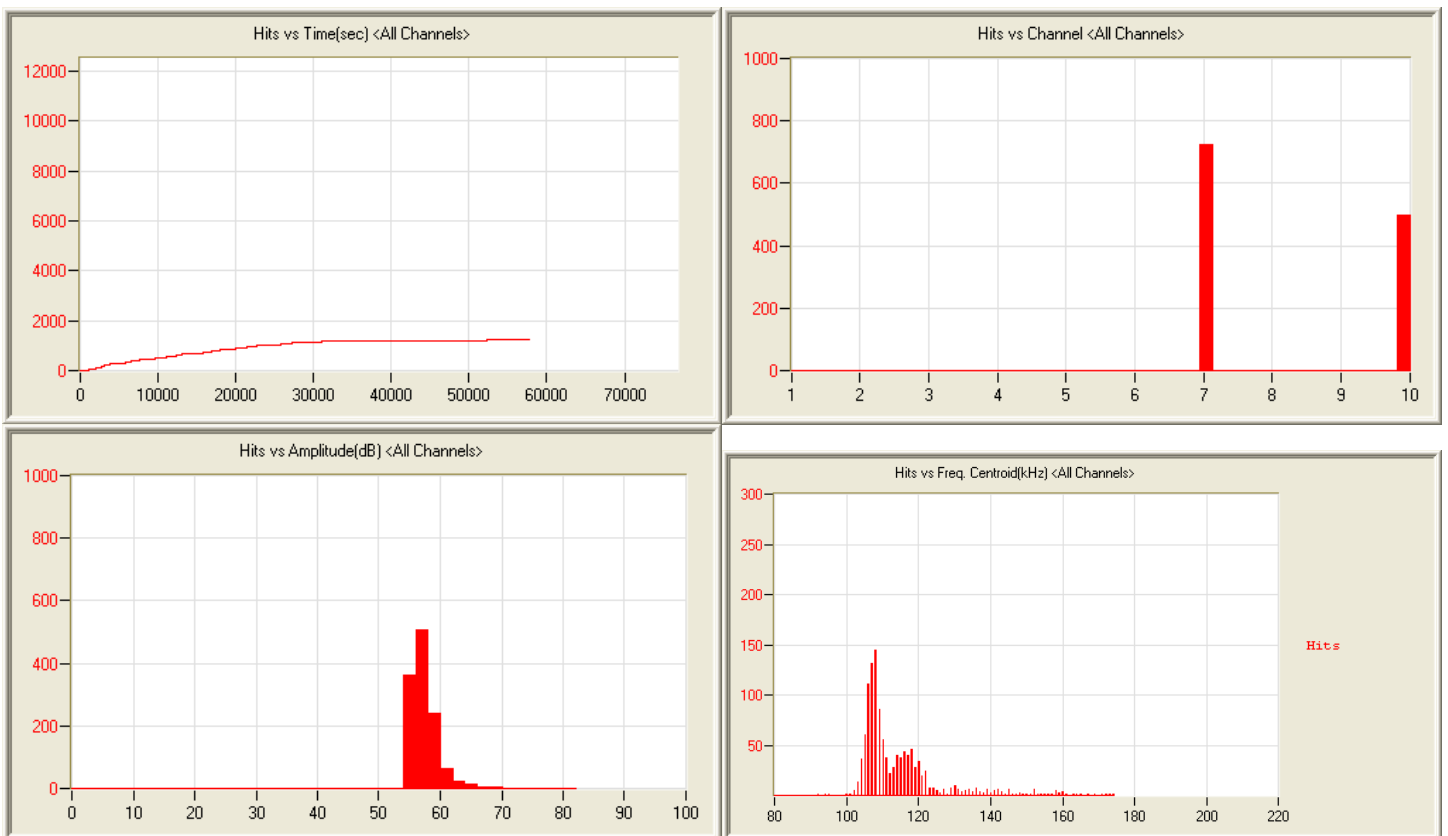
7/18/12 6:02pm 16:33:12 333 120718180219_0 2.5mb



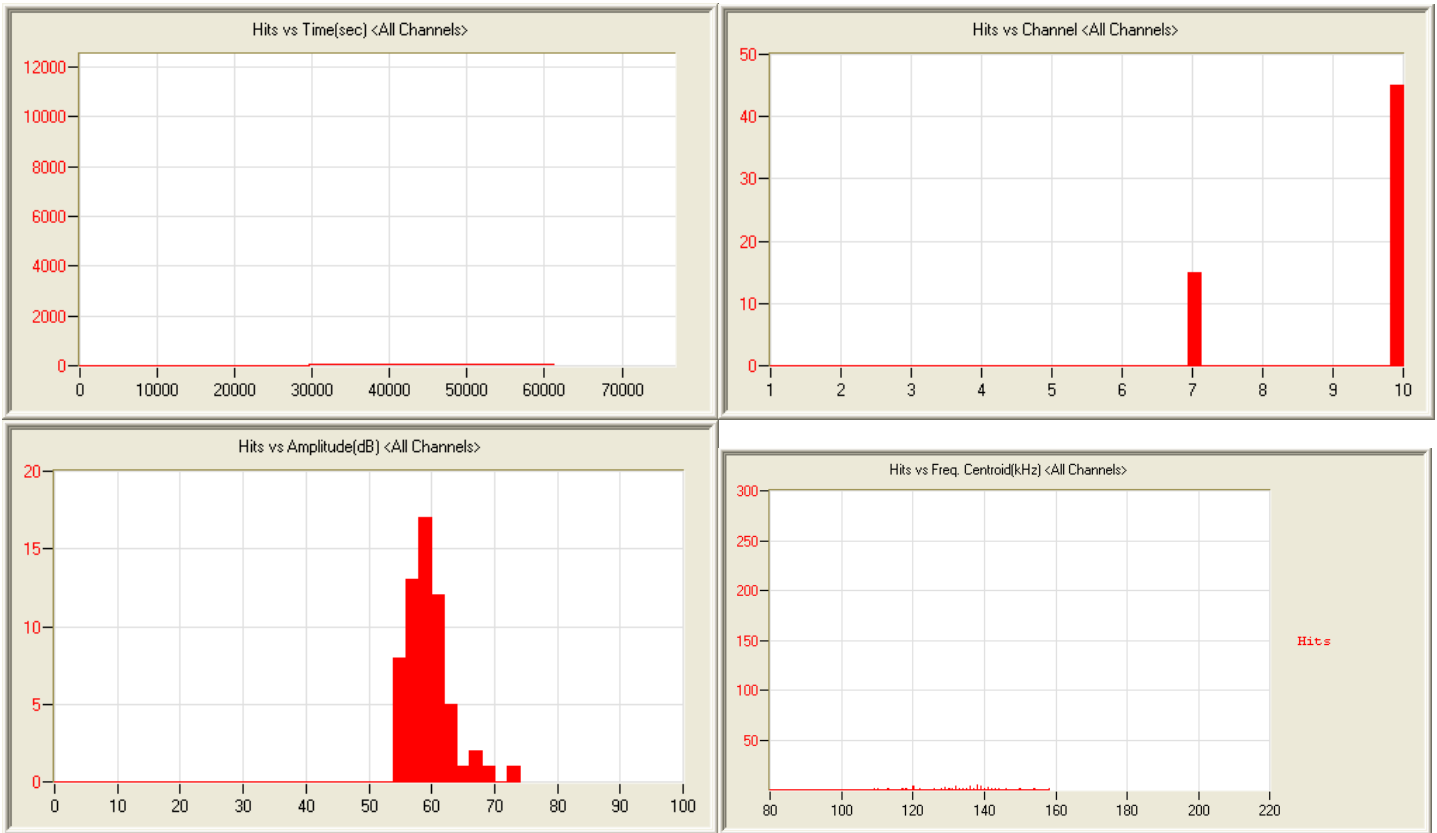
7/17/12 7:14pm 18:18:09 61155 120719191422_0 5.2mb



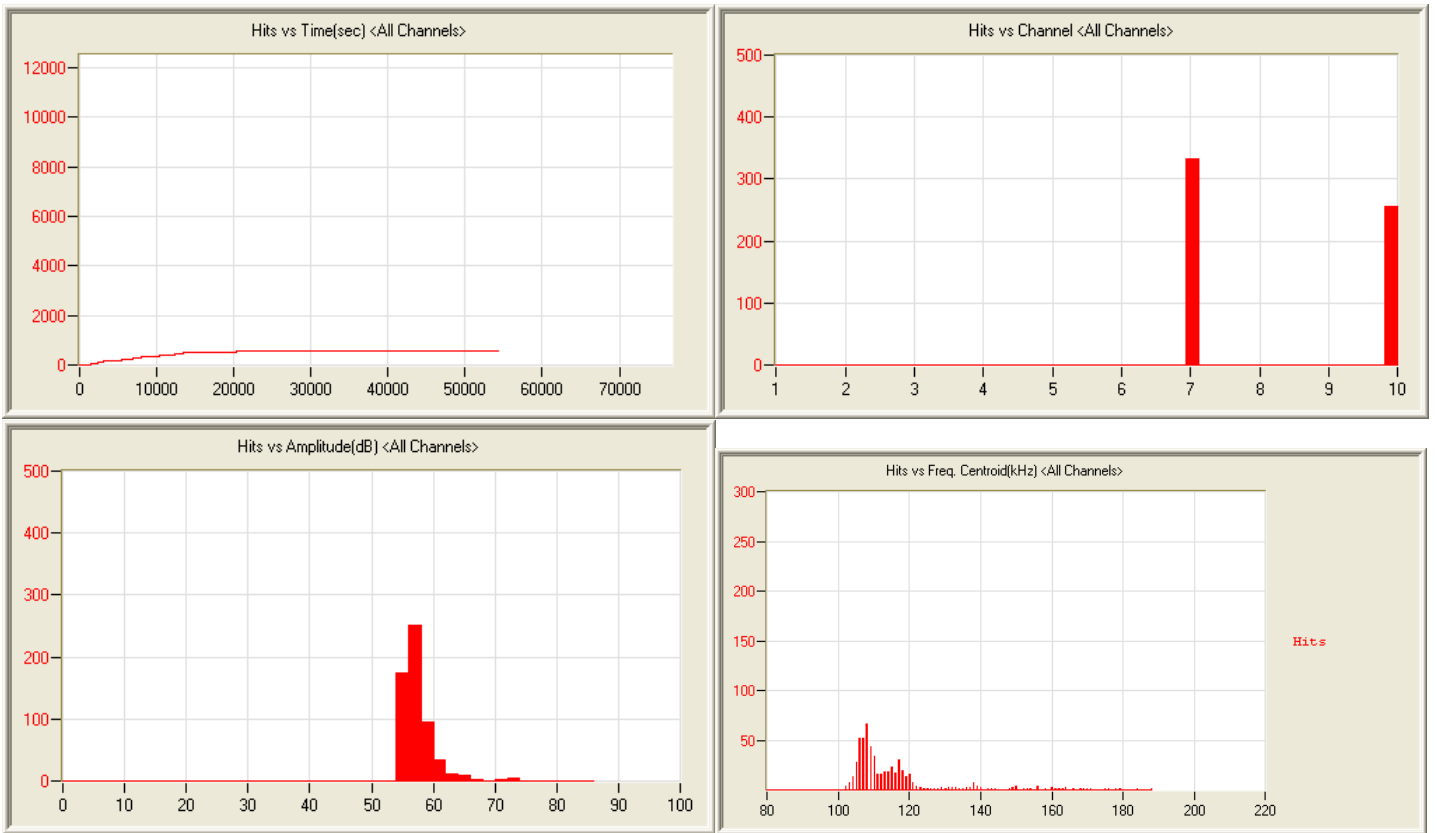
7/20/12 8:16pm 17:39:32 36573 120720201602_0 4.1mb



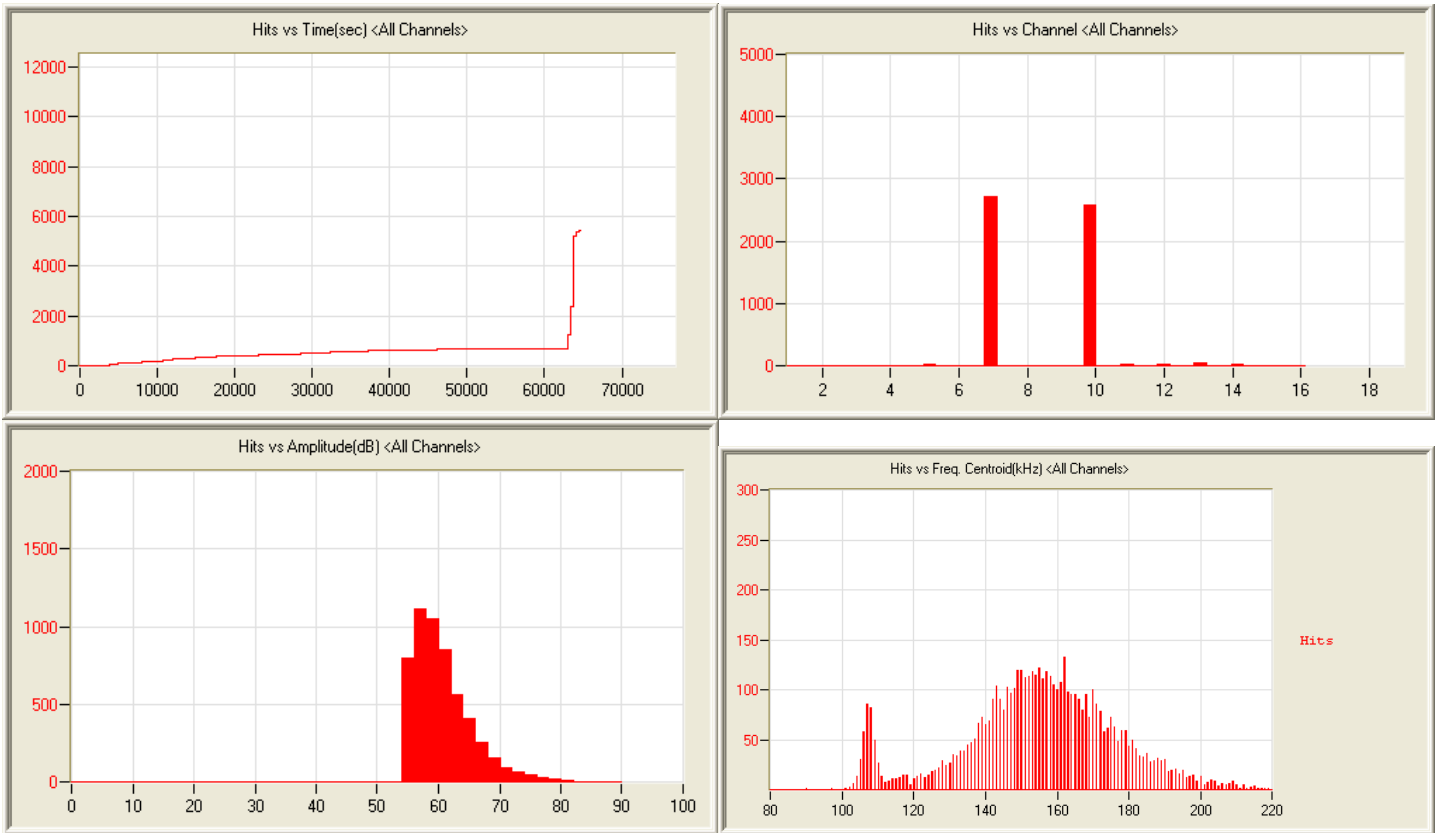
7/21/12 10:40pm 17:28:07 1222 120721224027_0 2.6mb



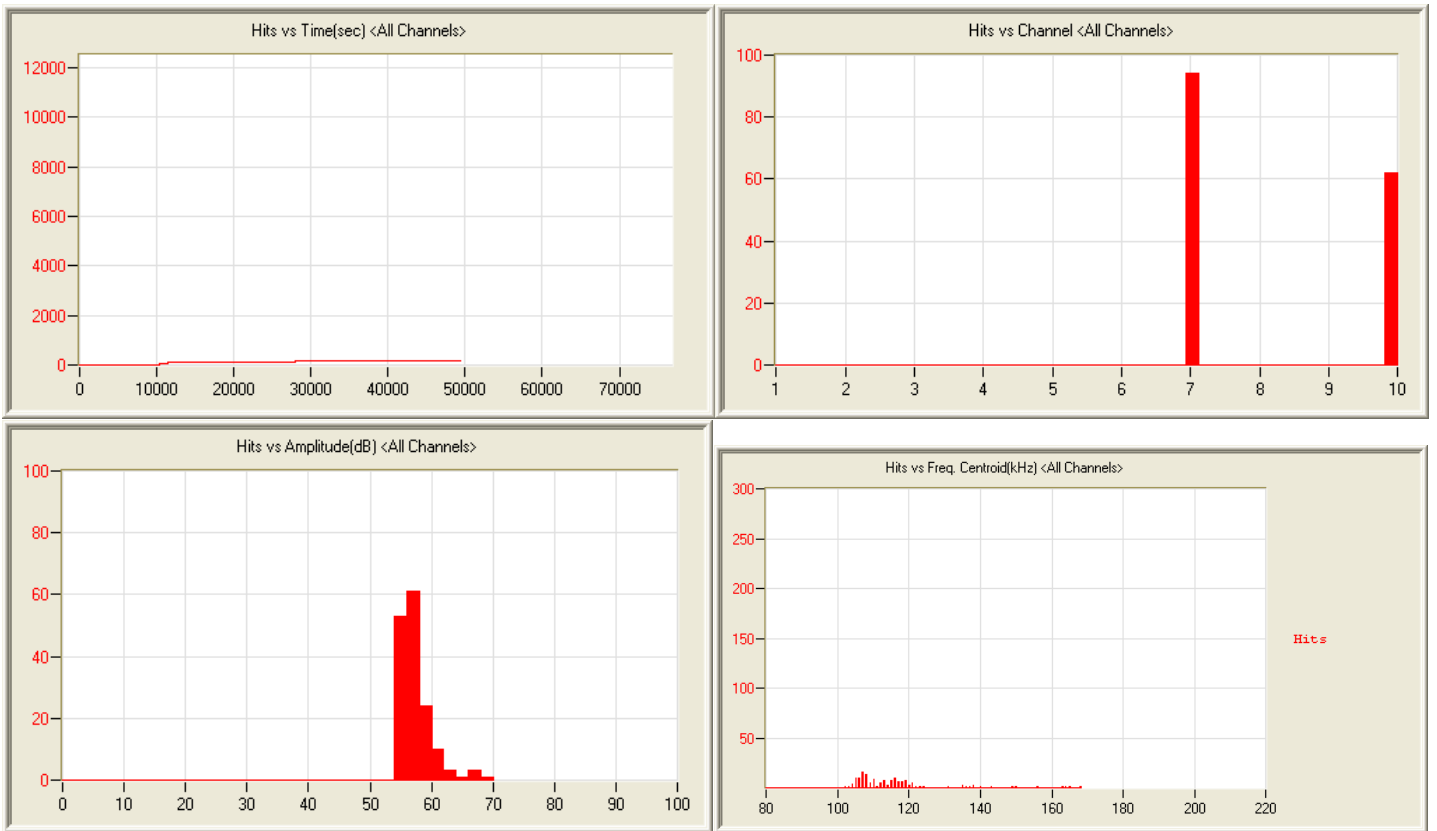
7/23/12 1:32am 17:02:45 60 120723013256_0 2.5mb



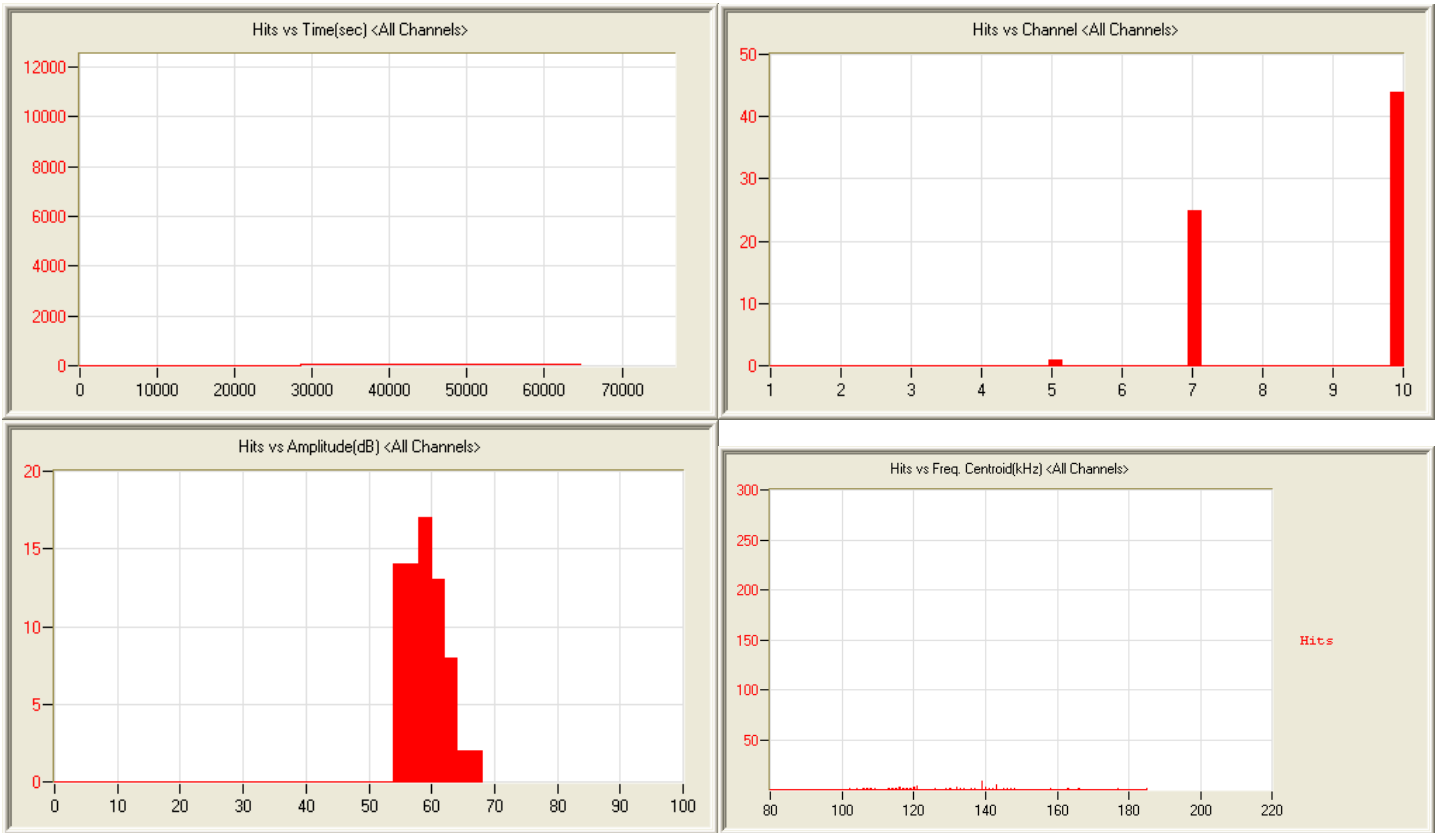
7/24/12 4:03am 16:18:27 120724040338_0 2.4mb



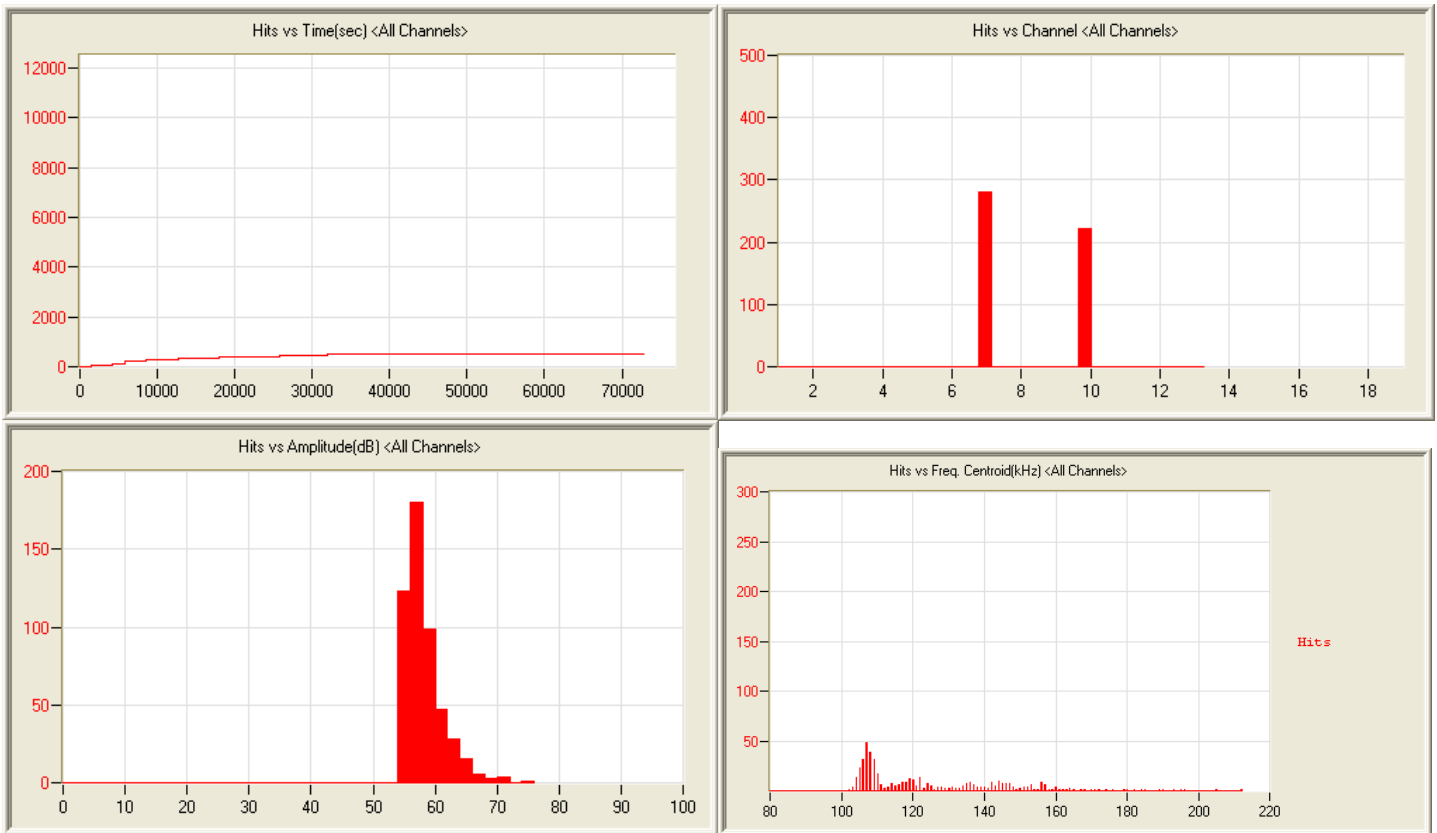
7/25/12 3:07am 18:01:13 5446 120725030742_0 2.9mb



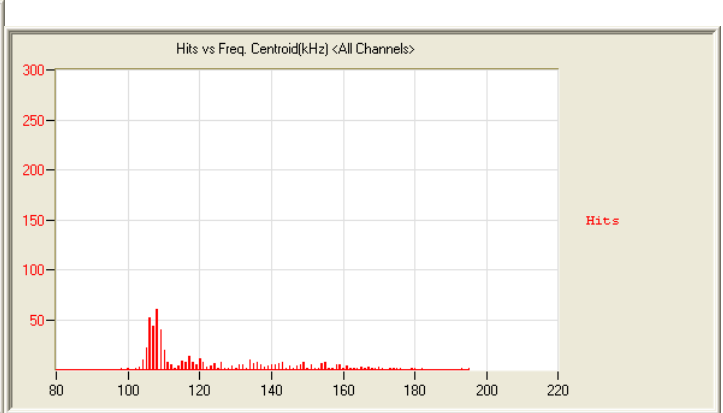
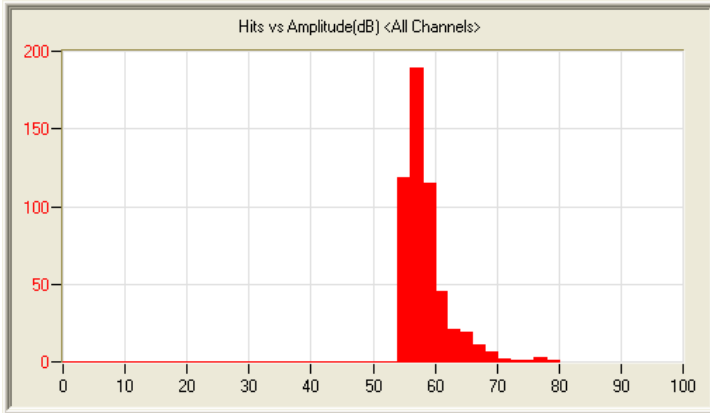
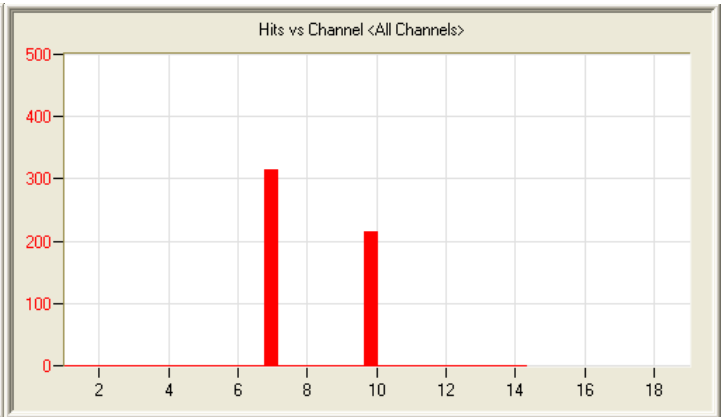
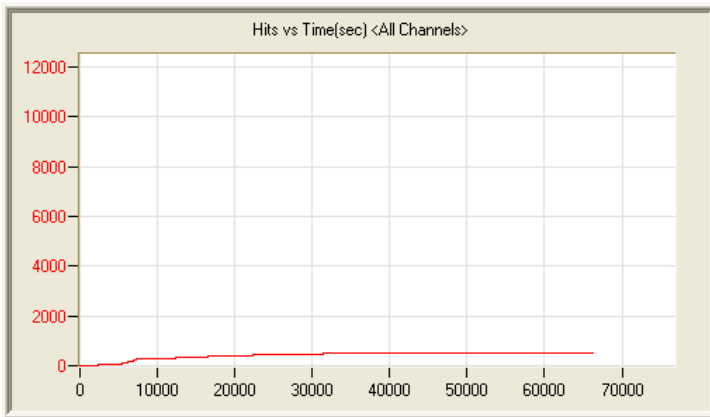
7/26/12 5:46am 16:20:19 156 120726054636_0 2.4mb



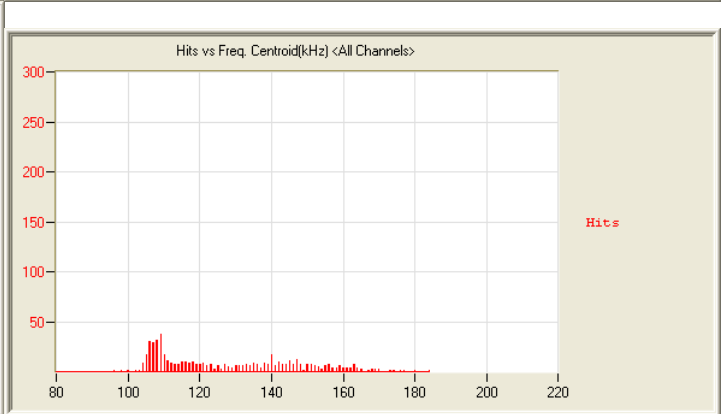
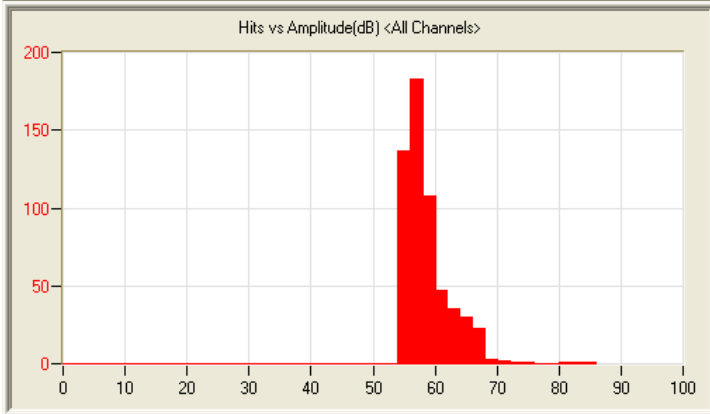
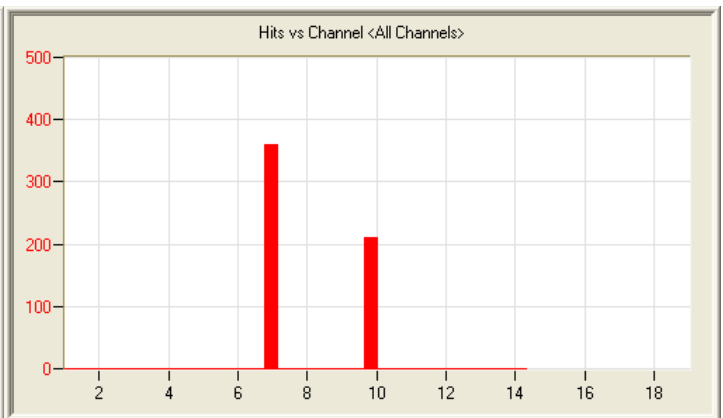
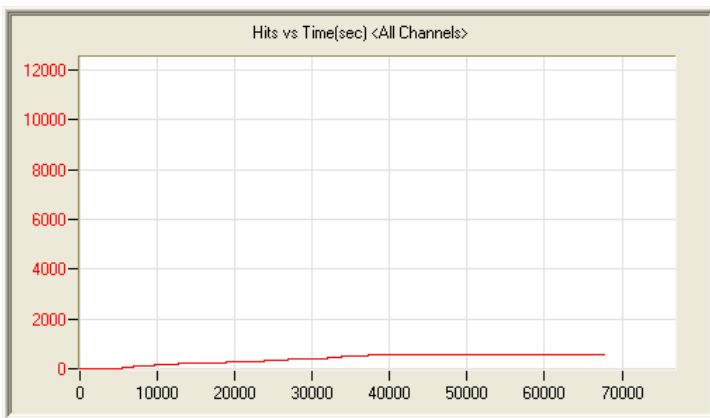
7/27/12 7:50am 18:10:54 70 120727075049_0 2.7mb



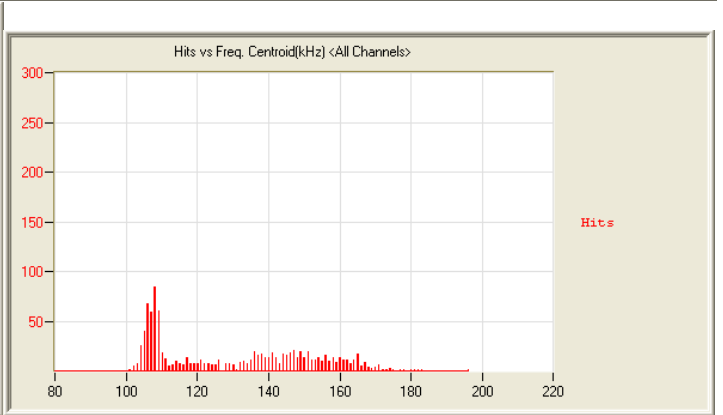
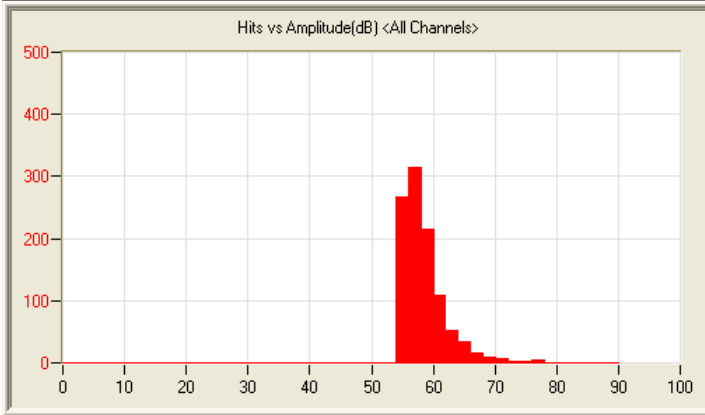
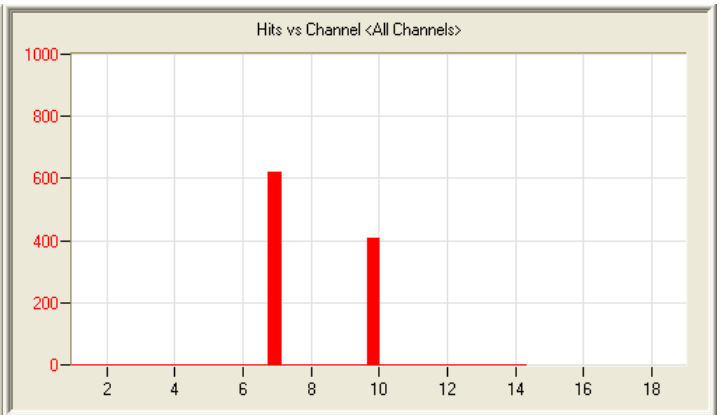
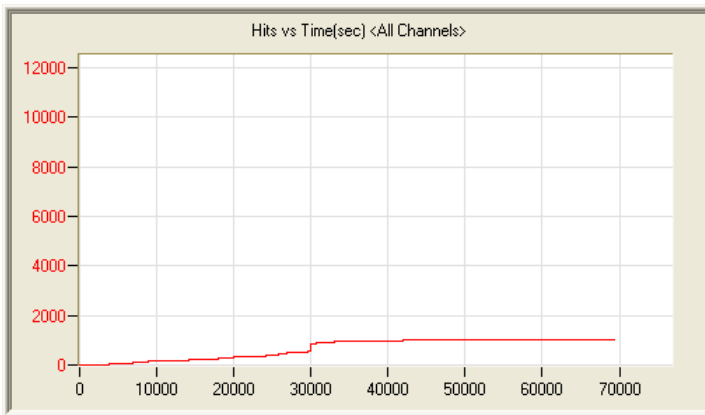
7/28/12 8:17am 21:12:09 505 120728081730_0 3.1mb



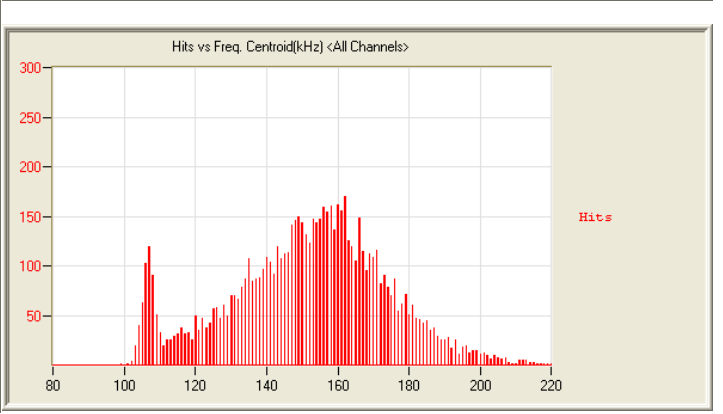
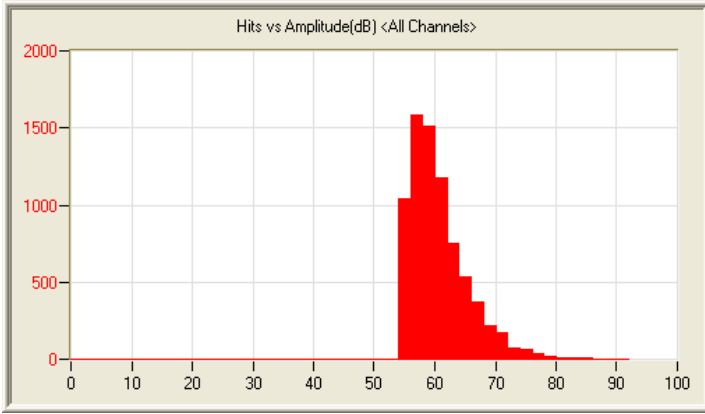
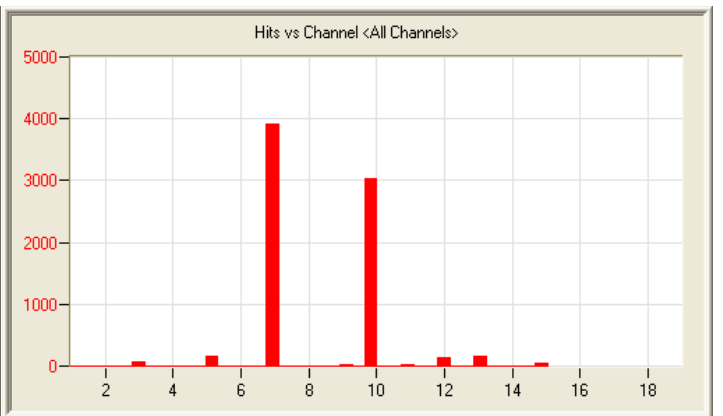
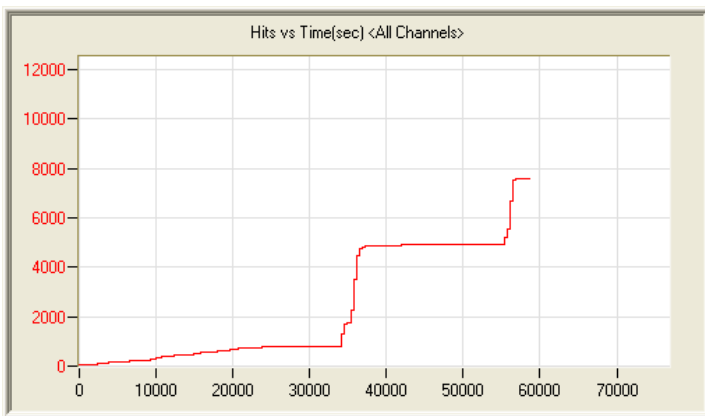
7/29/12 9:15am 18:53:09 533 120729091500_0 2.8mb



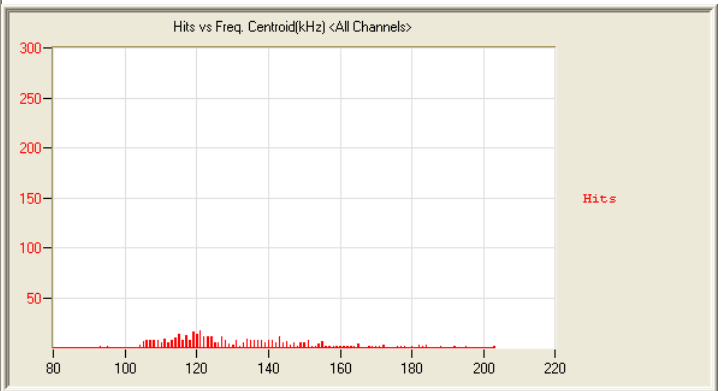
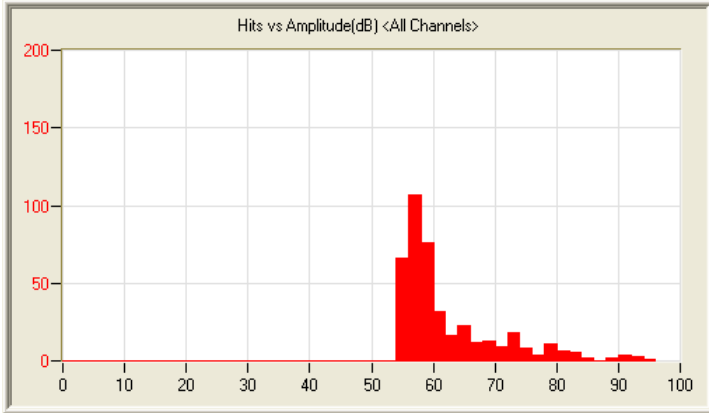
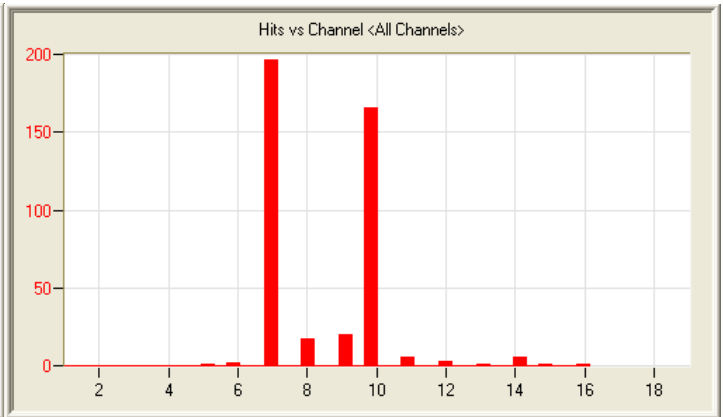
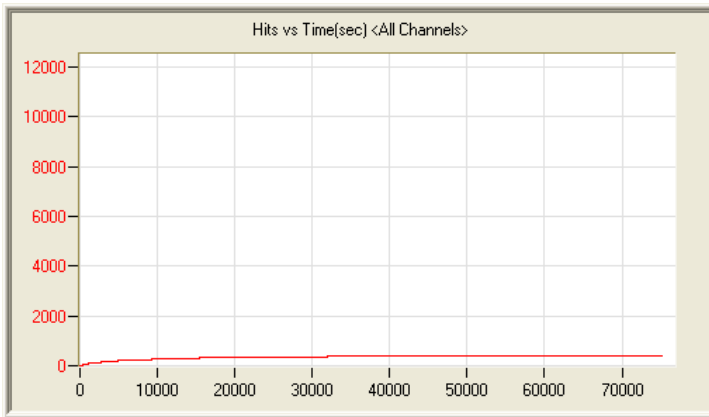
7/30/12 10:11am 20:11:41 573 120730101143_0 3.0mb



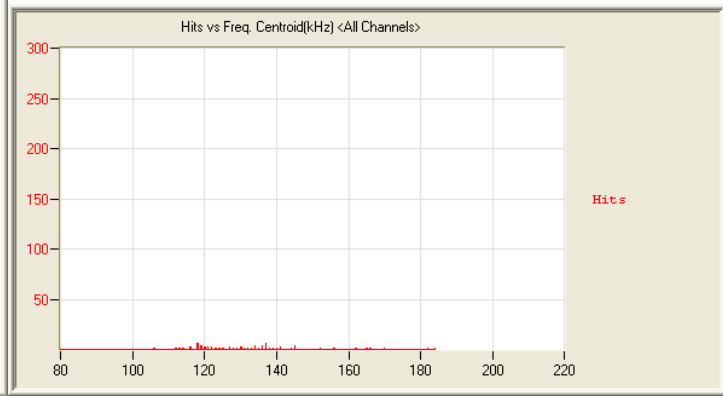
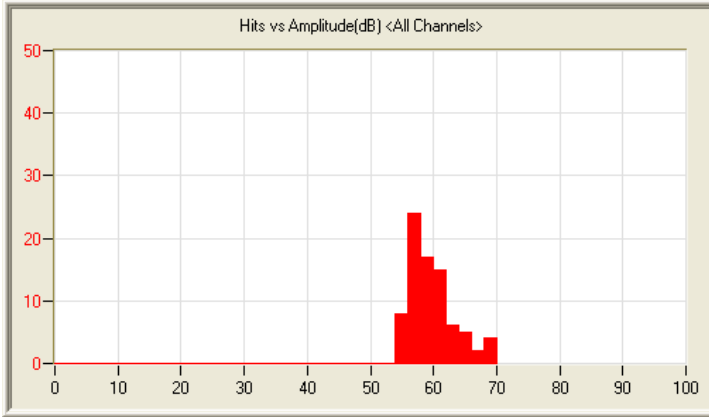
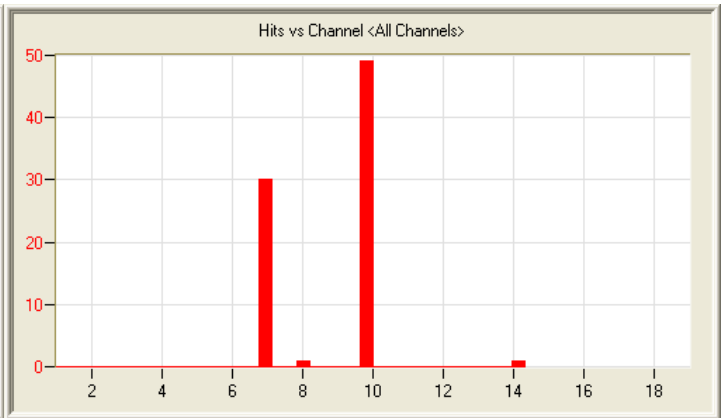
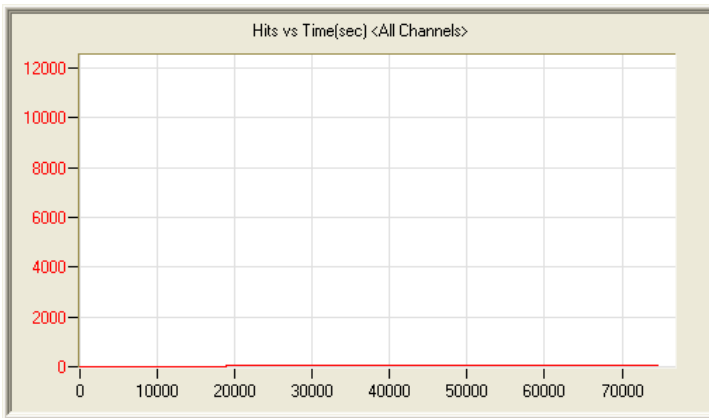
7/31/12 11:13am 19:28:07 1036 120731111354_0 2.9mb



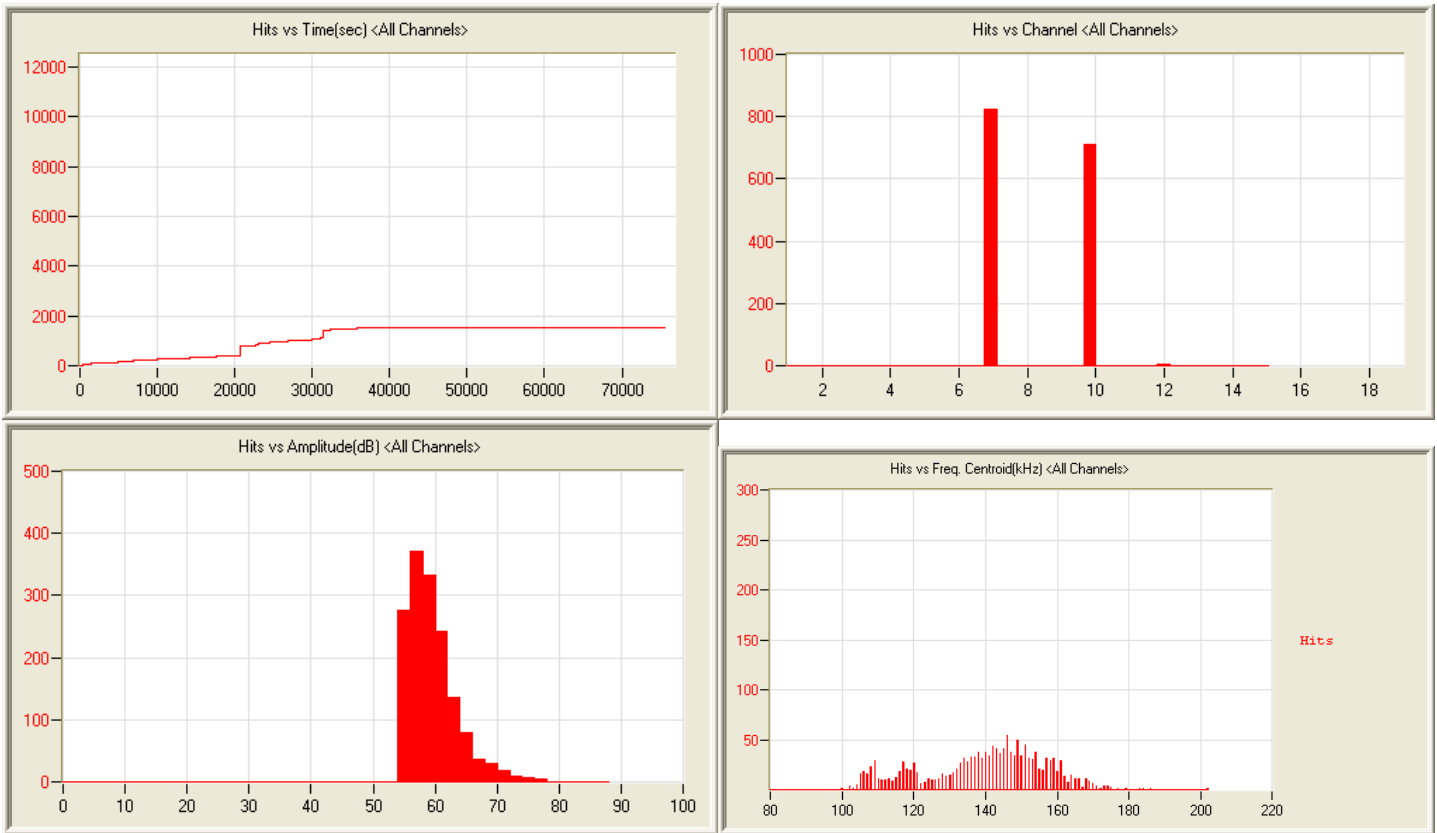
8/1/12 1:53pm 16:18:55 7580 120801135336_0 2.7mb



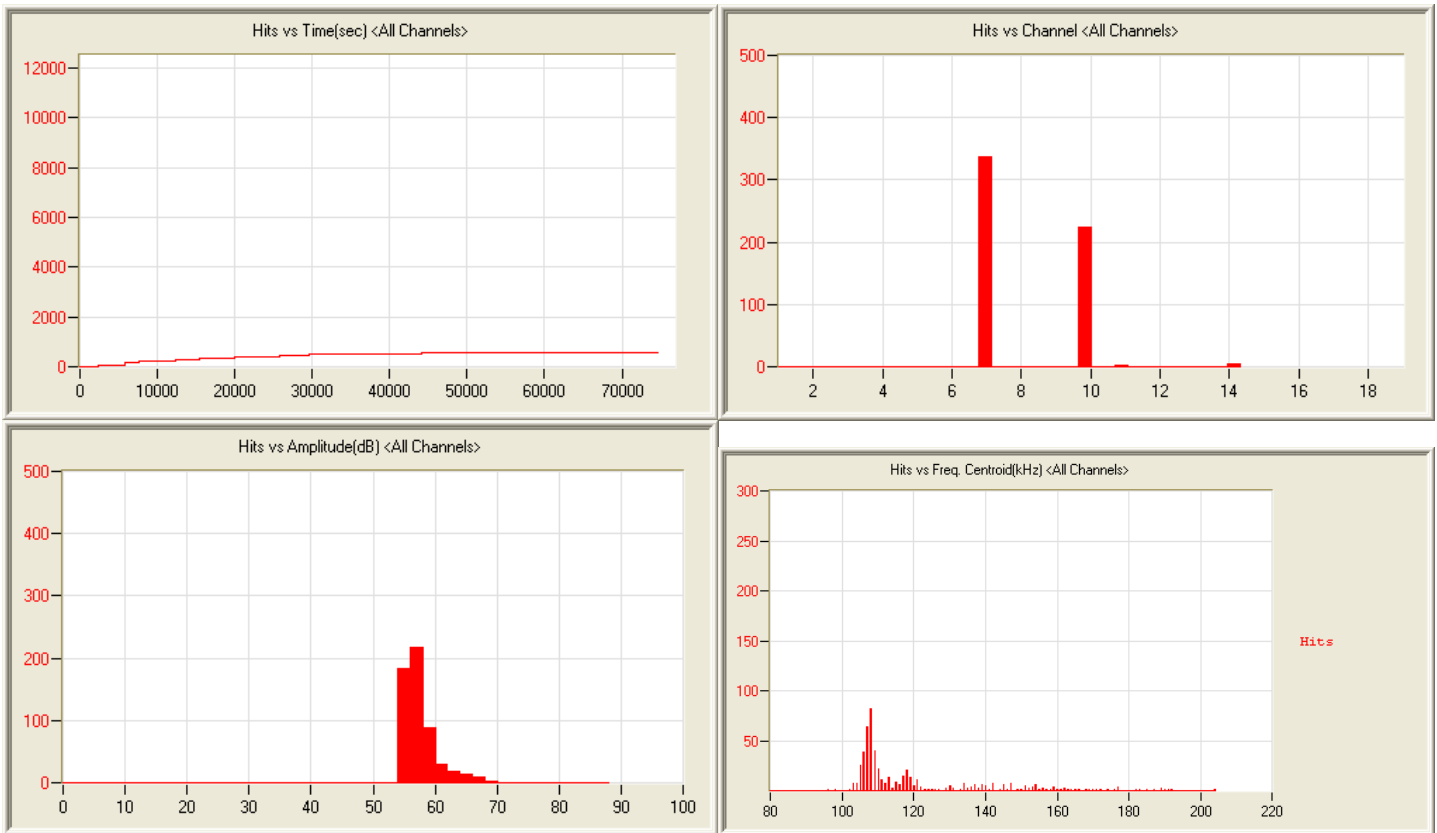
8/2/12 1:34am 21:33:12 418 120802133445_0 3.2mb



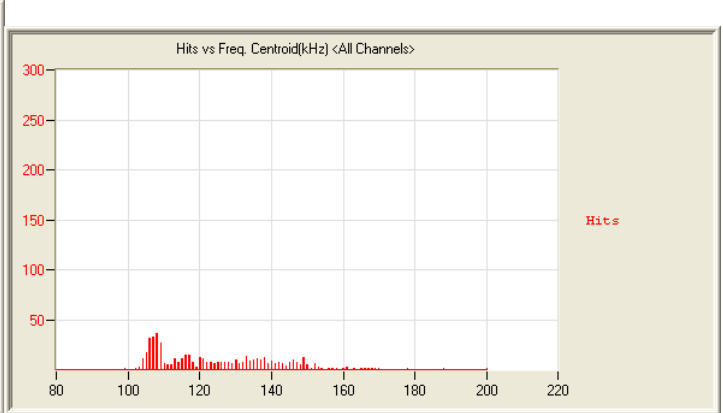
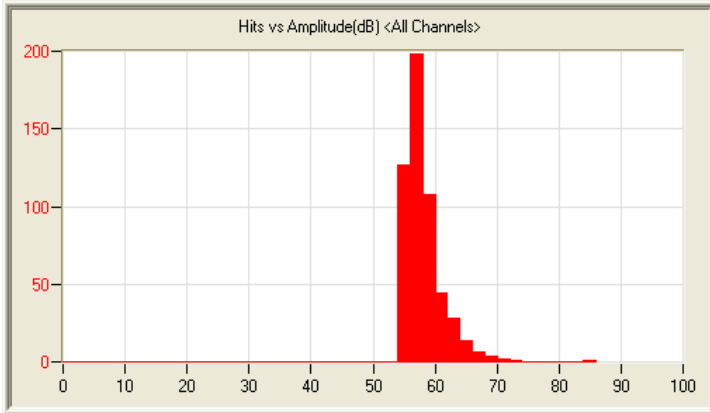
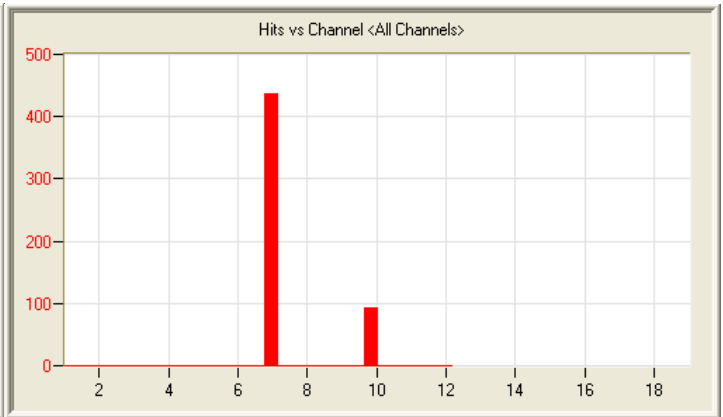
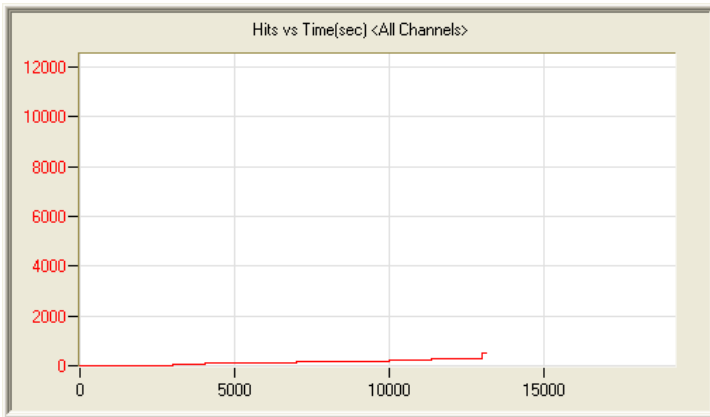
8/3/12 2:19pm 21:41:42 81 120803141907_0 3.2mb



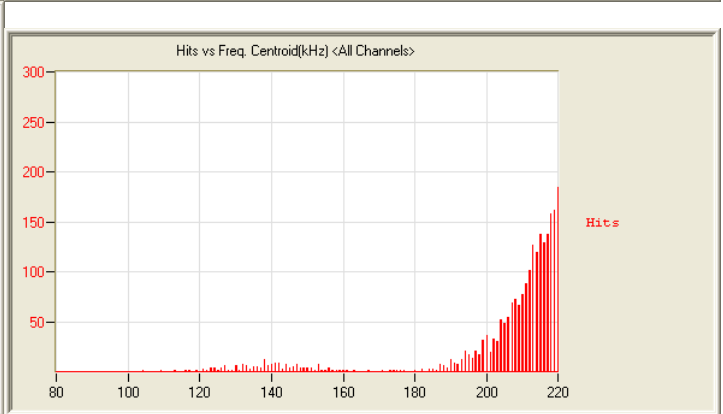
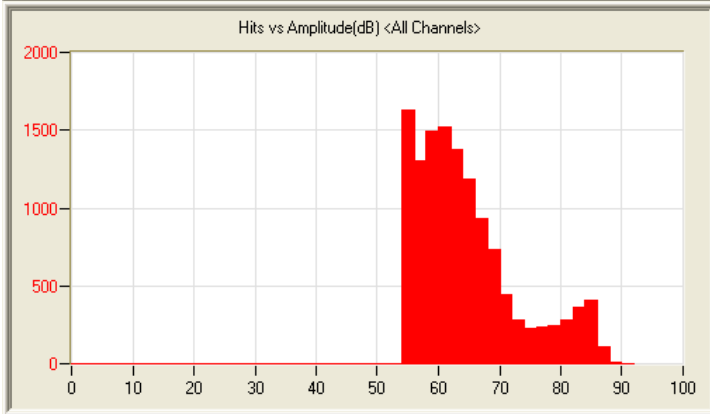
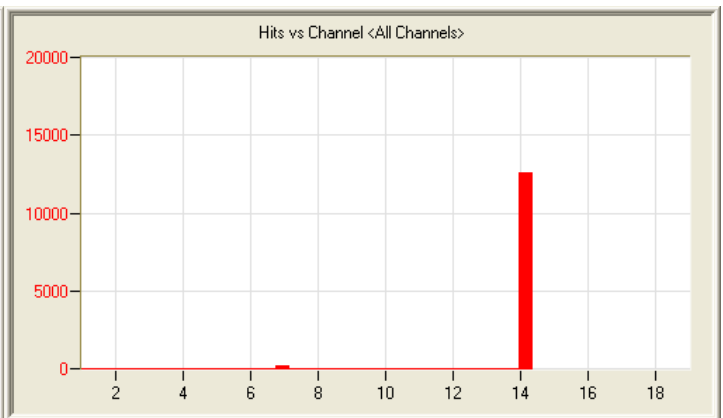
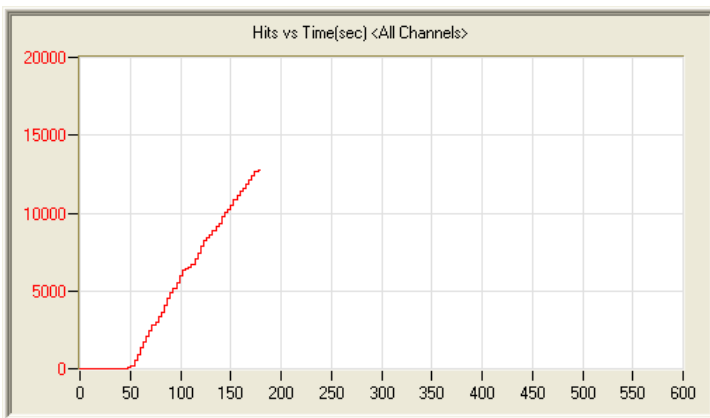
8/4/12 3:20pm 21:23:02 1543 120804152018_0 3.2mb



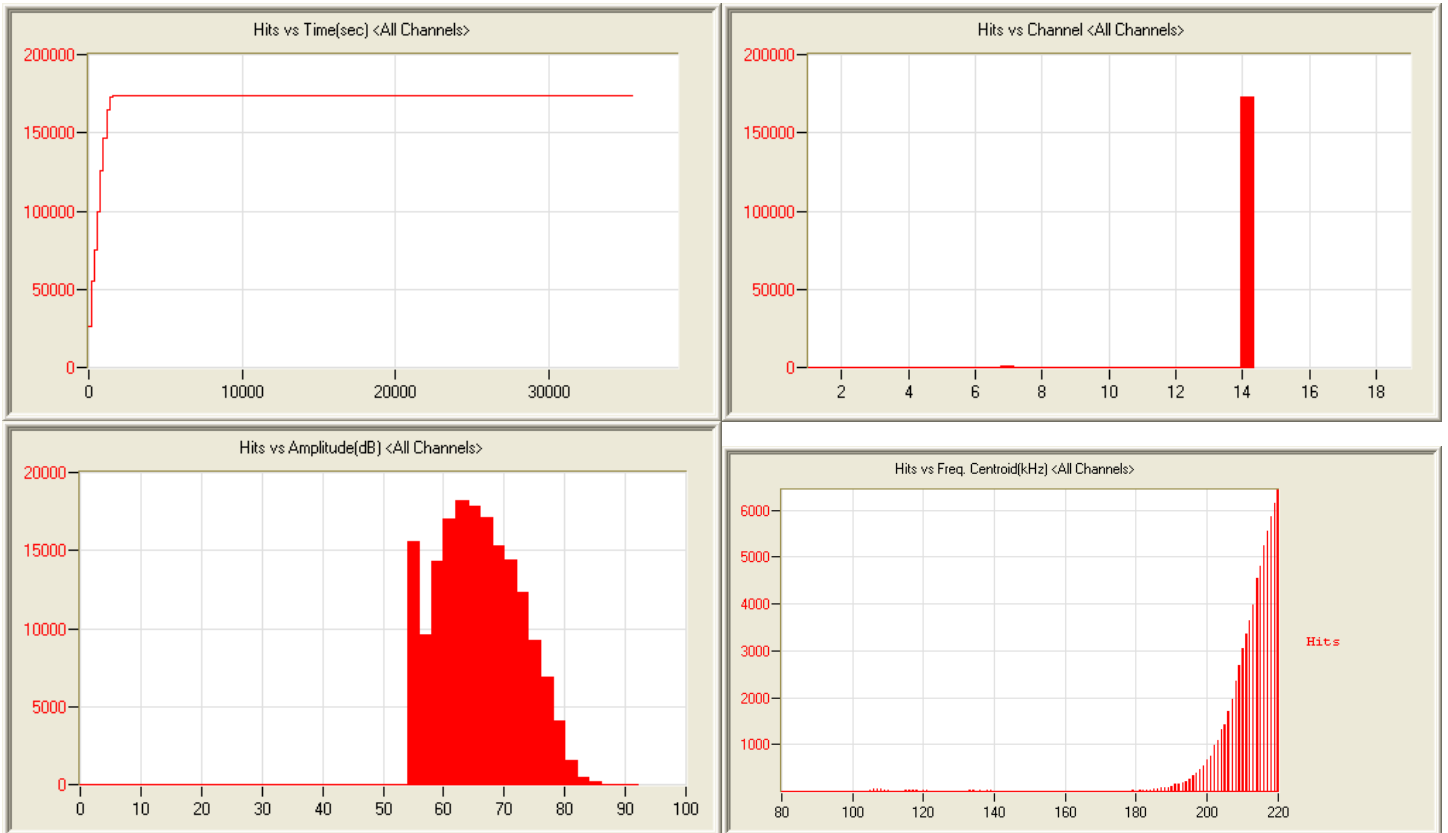
8/5/12 4:23pm 20:54:16 568 120805162320_0 3.1mb



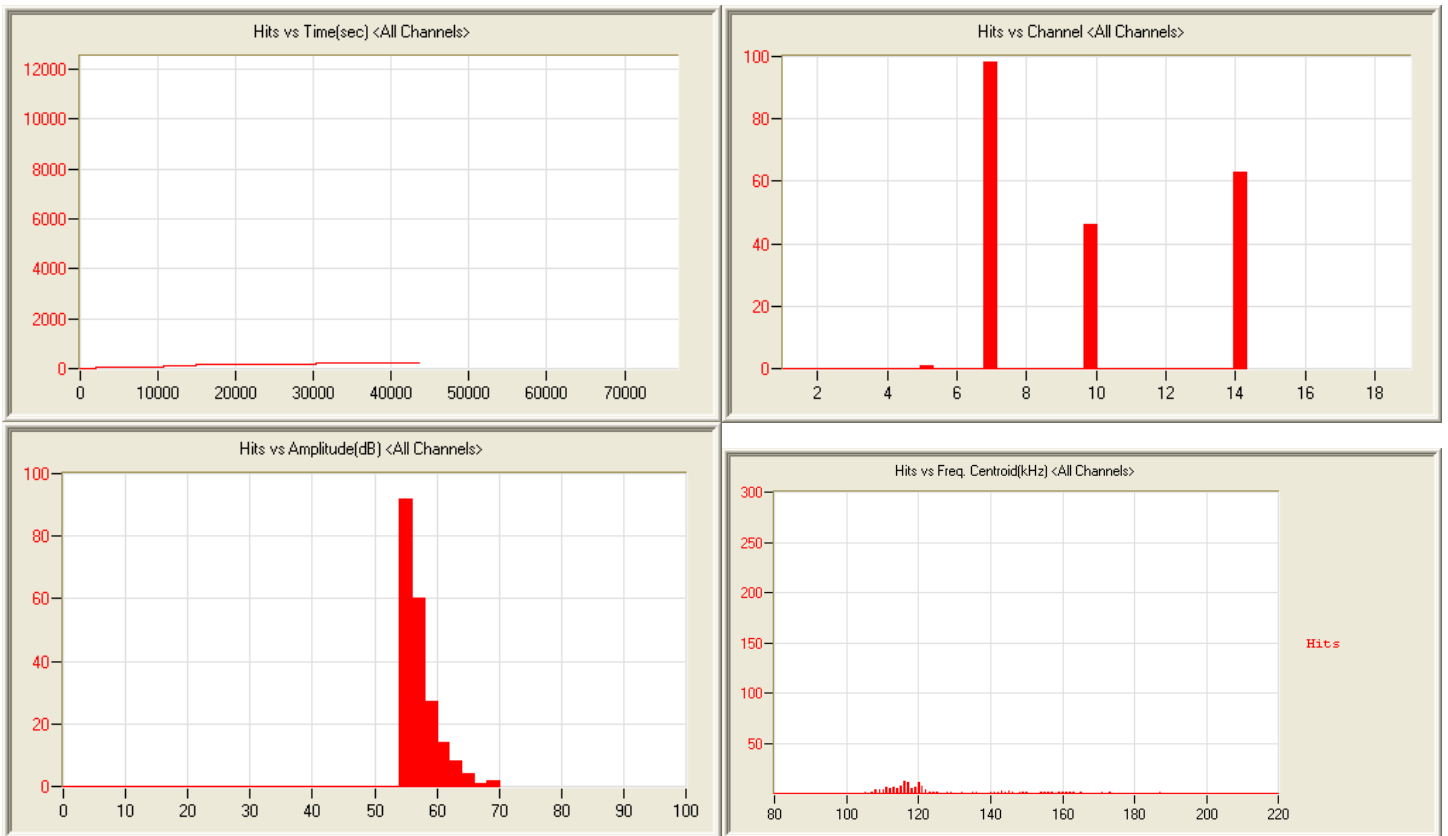
8/6/12 5:28pm 3:38:06 533 120806172801_0 612kb



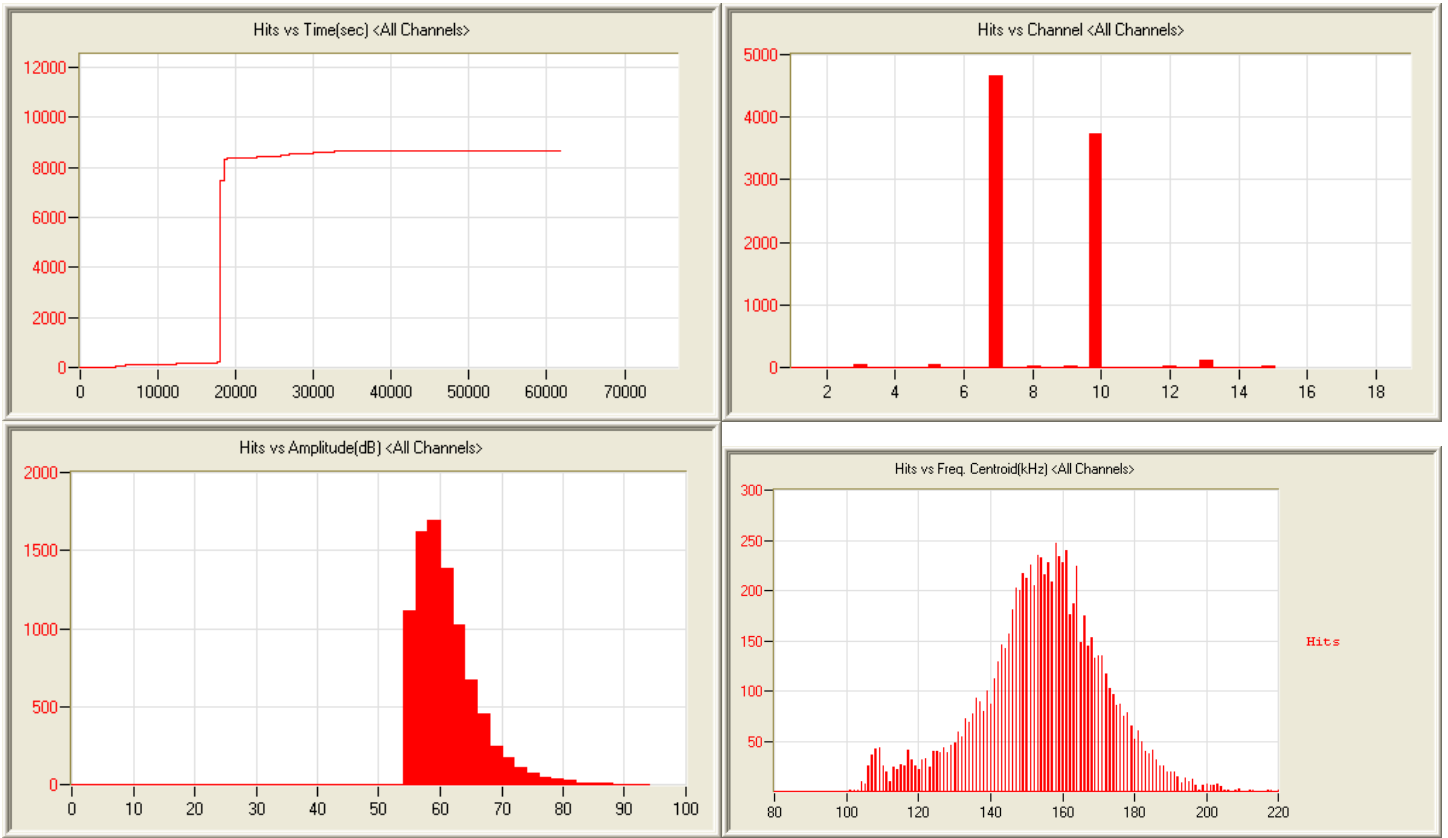
8/6/12 11:31pm 0:02:57 12760 120806233134_0 584kb



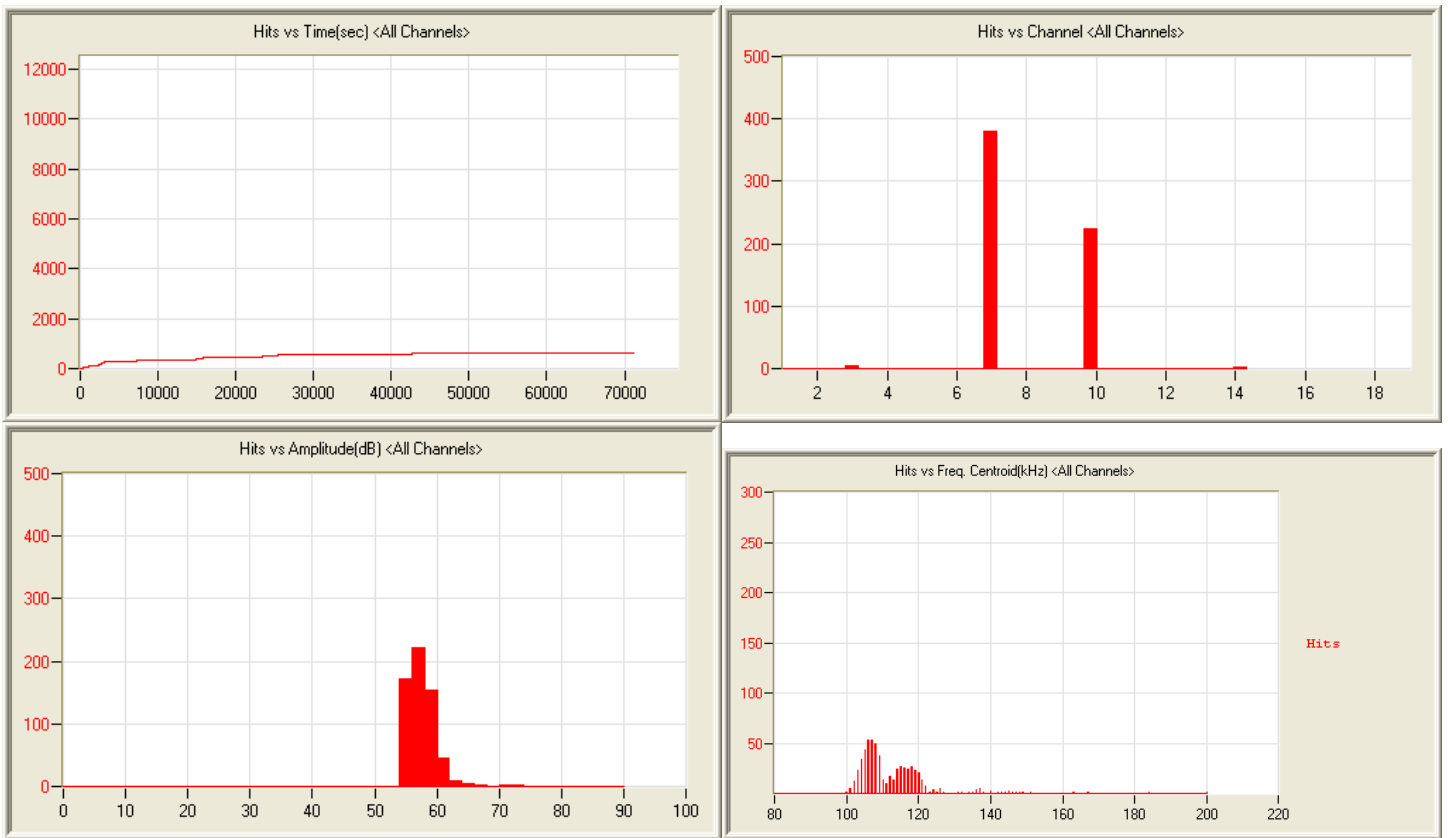
8/7/12 0:38am 10:30:12 173958 120807003828_0 9.5mb



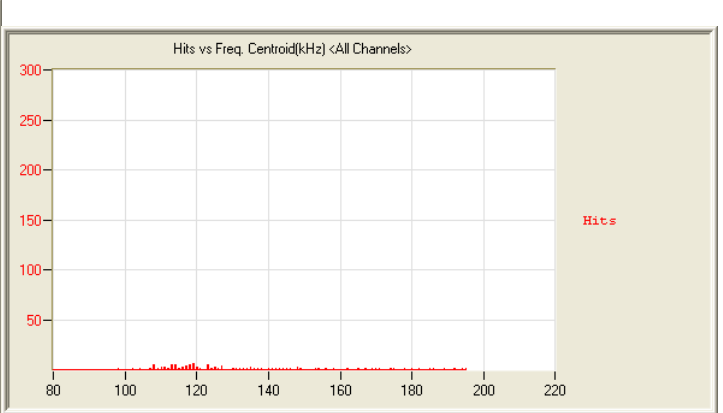
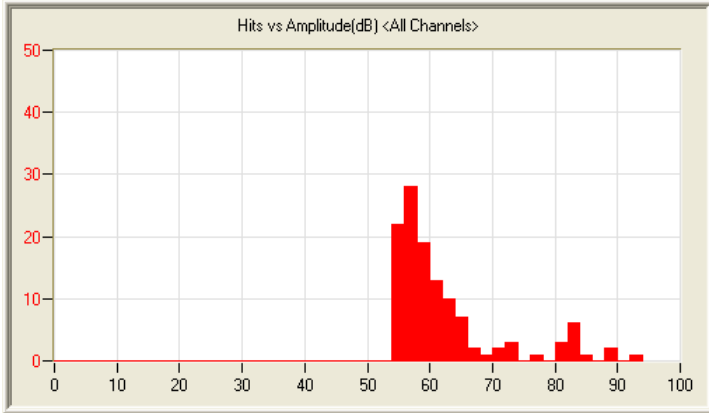
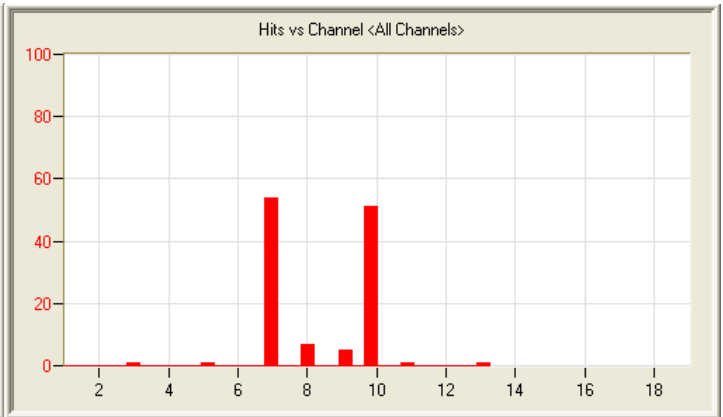
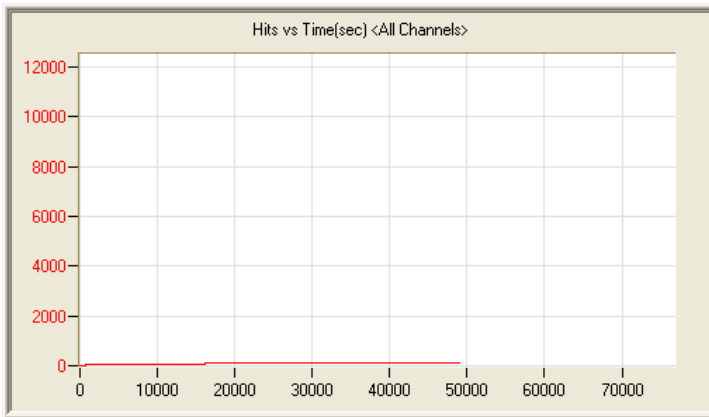
8/8/12 6:03pm 12:10:20 208 120808180356_0 1.8mb



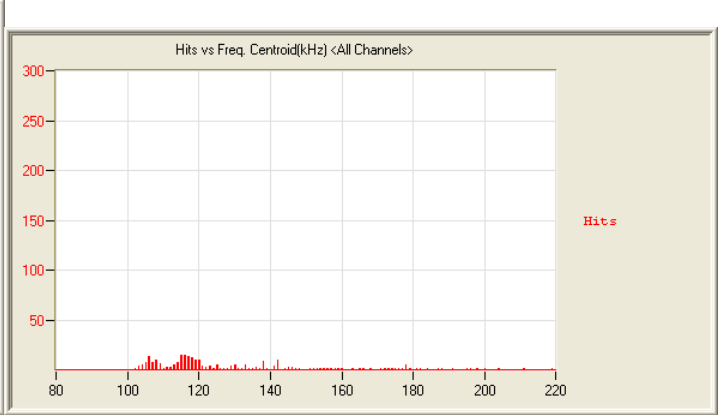
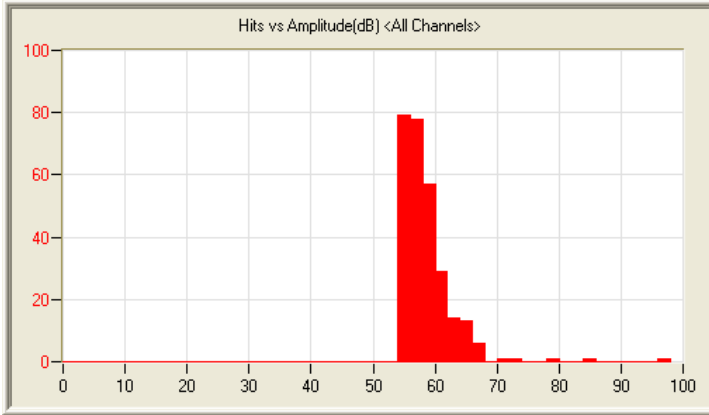
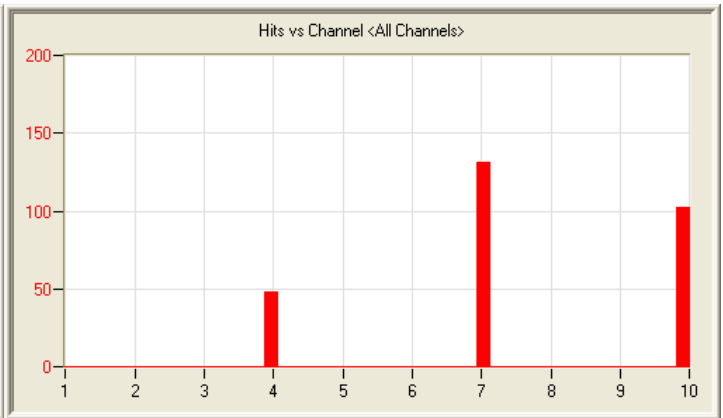
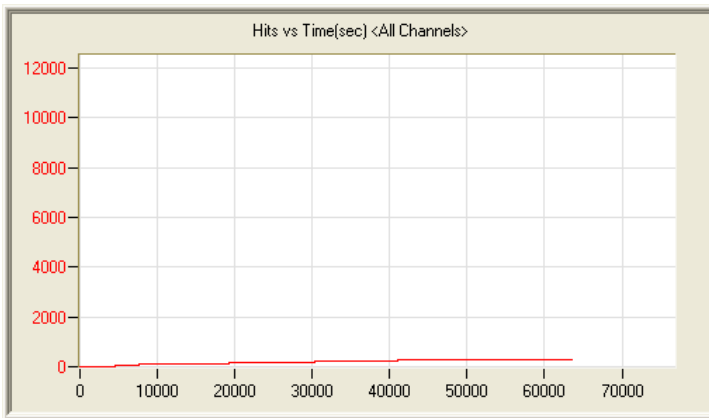
8/9/12 7:53pm 17:16:47 8663 120809195357_0 3.0mb



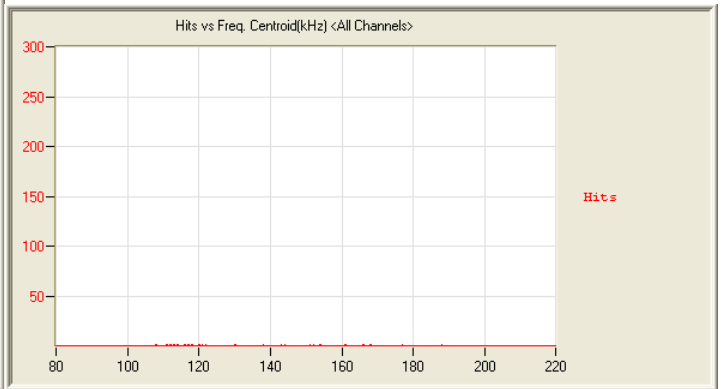
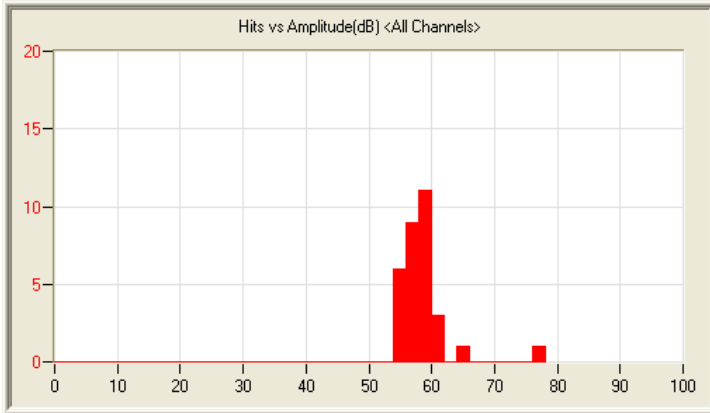
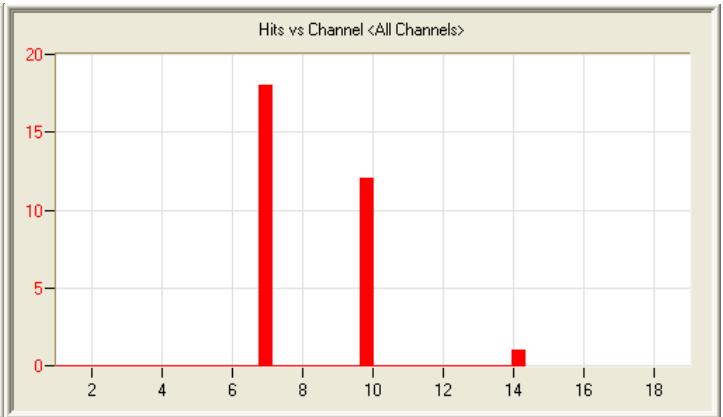
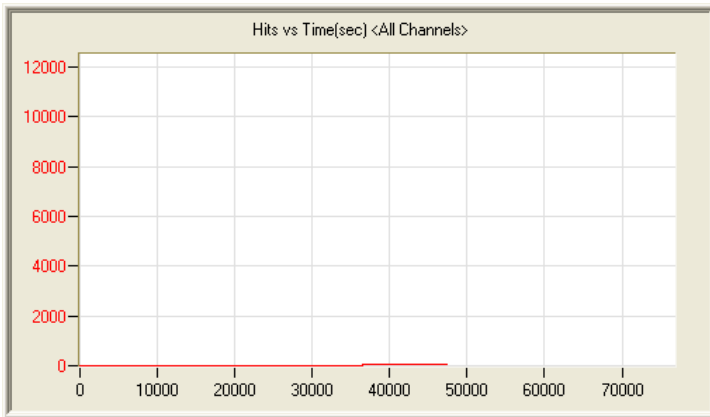
8/10/12 8:51am 21:23:46 615 120810085127_0 3.2mb



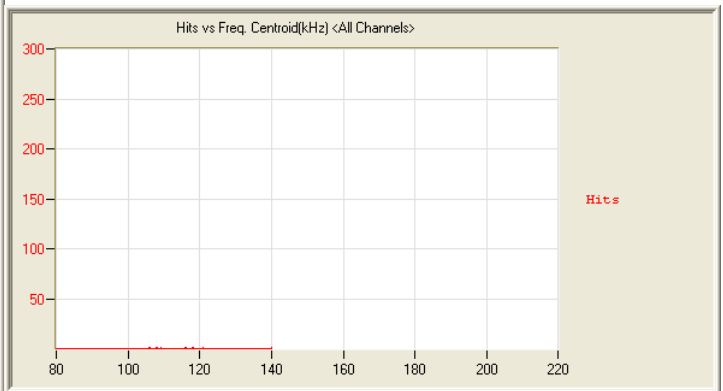
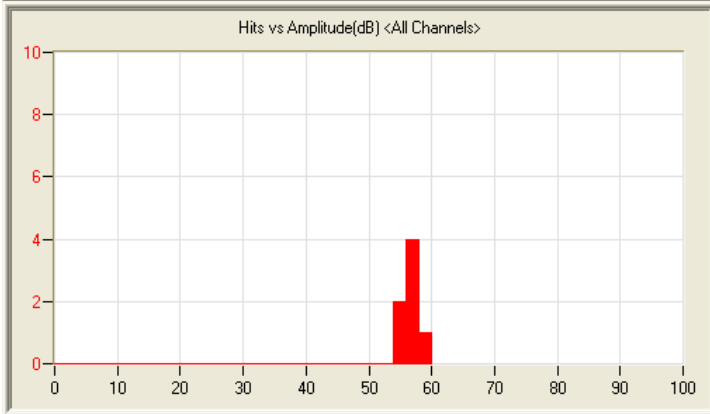
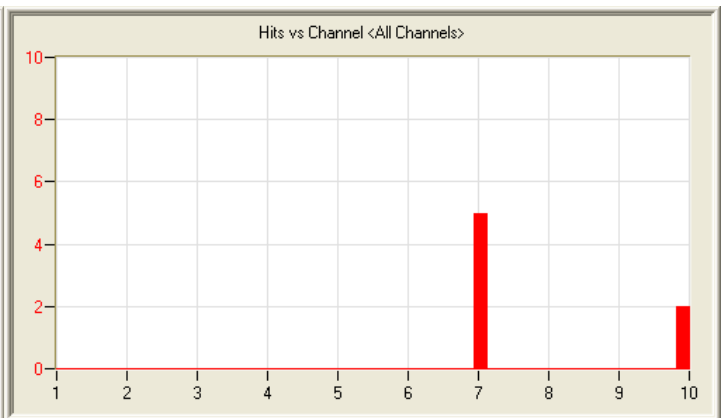
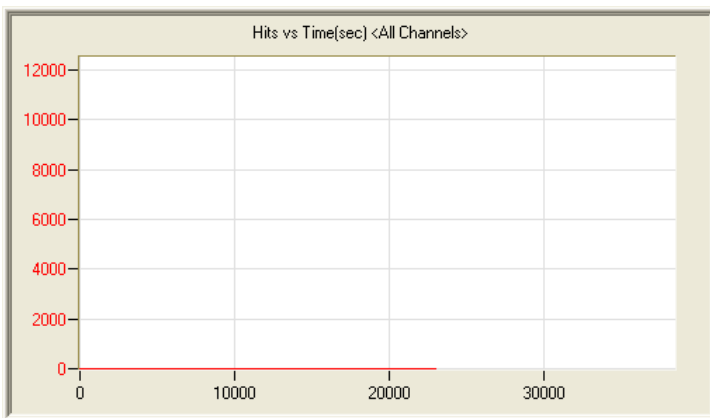
8/11/12 5:18am 13:46:59 121 120811051824_0 2.1mb



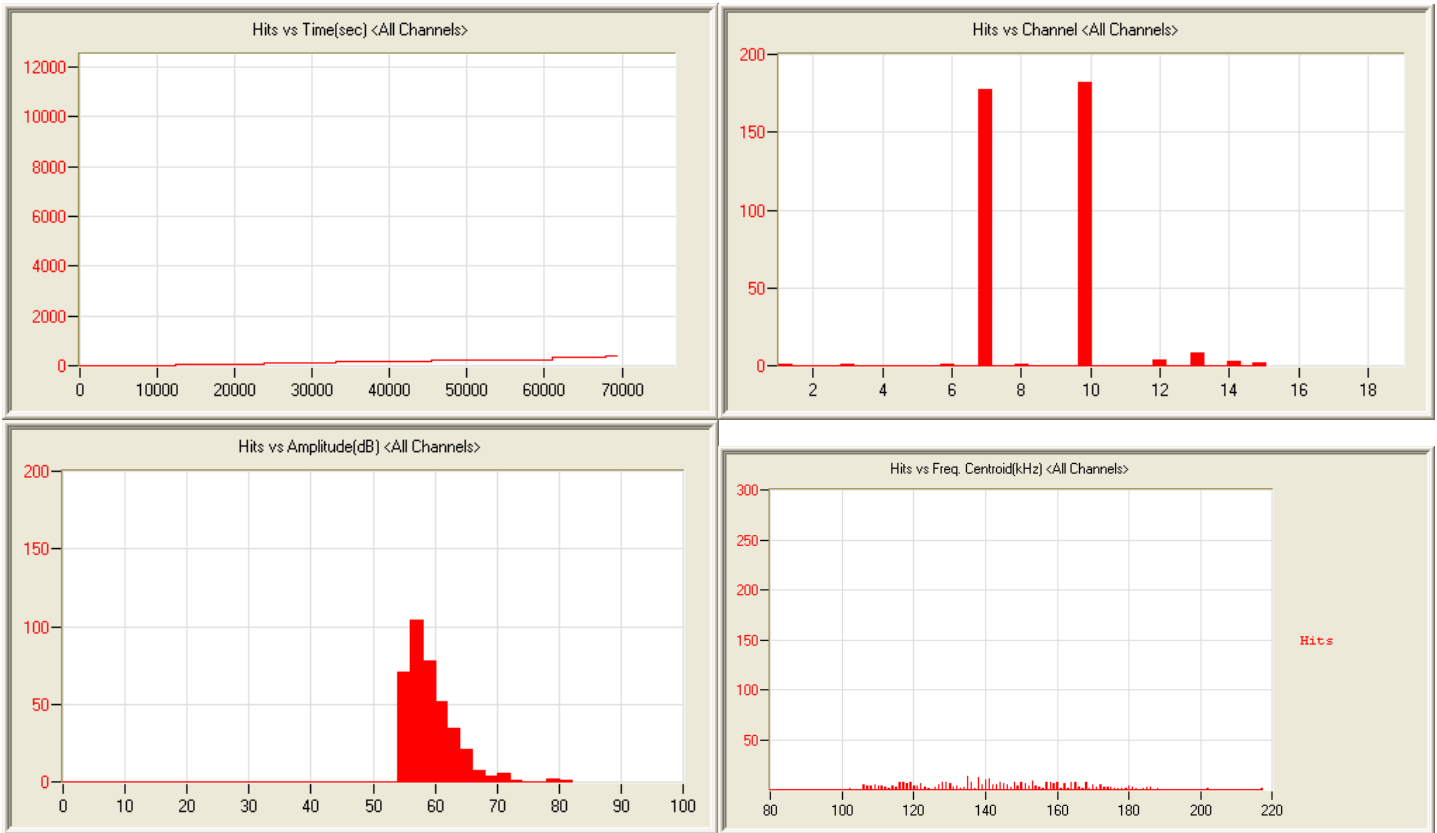
8/11/12 9:50am 20:56:17 281 120811095021_0 3.1mb



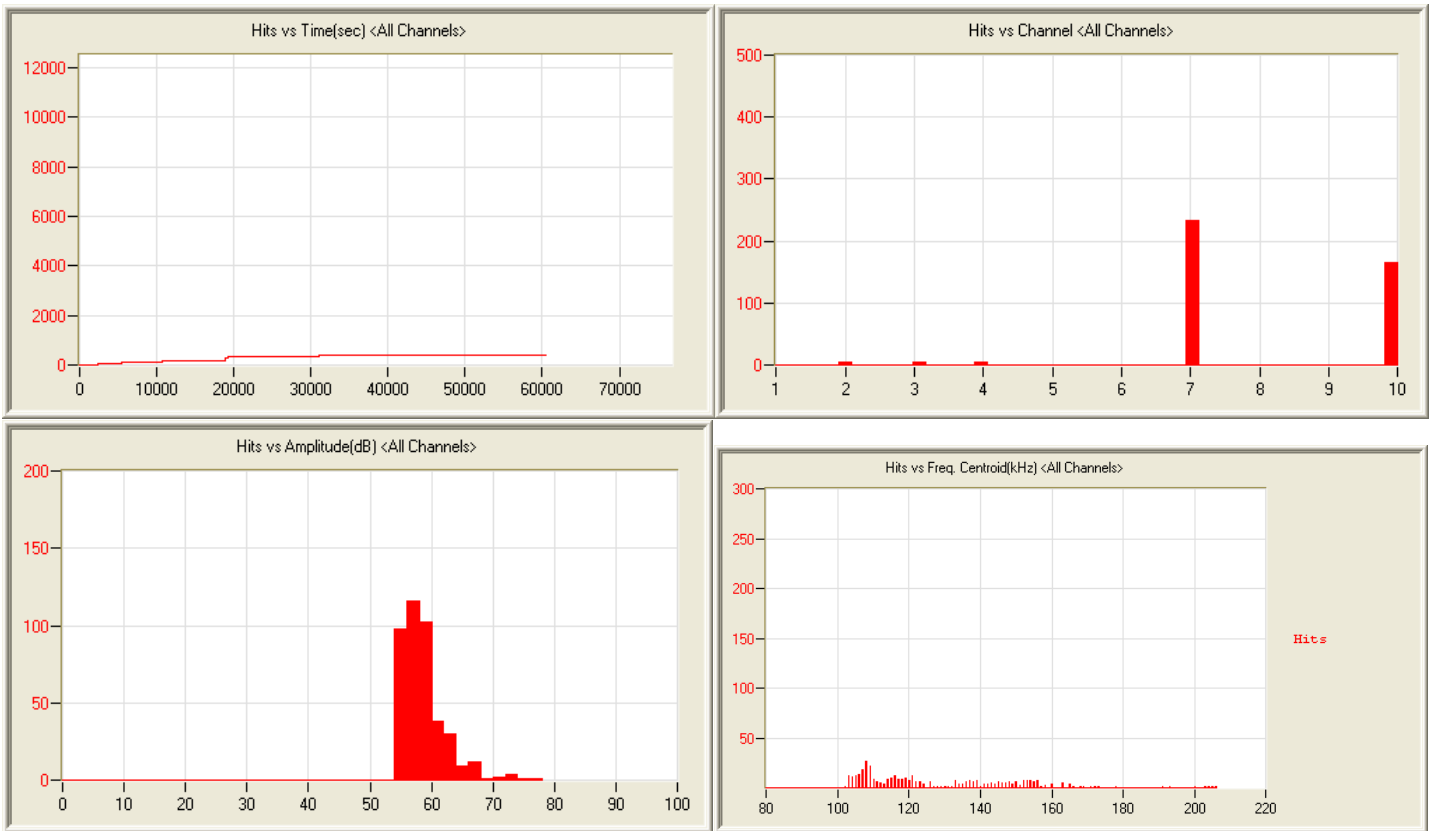
8/12/12 7:49am 13:14:42 31 120812074926_0 2.0mb



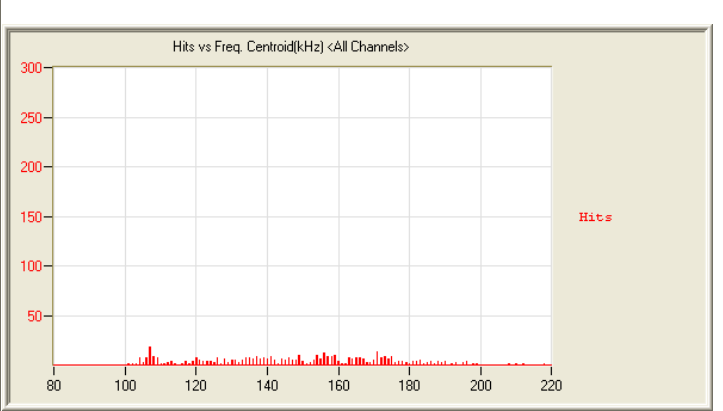
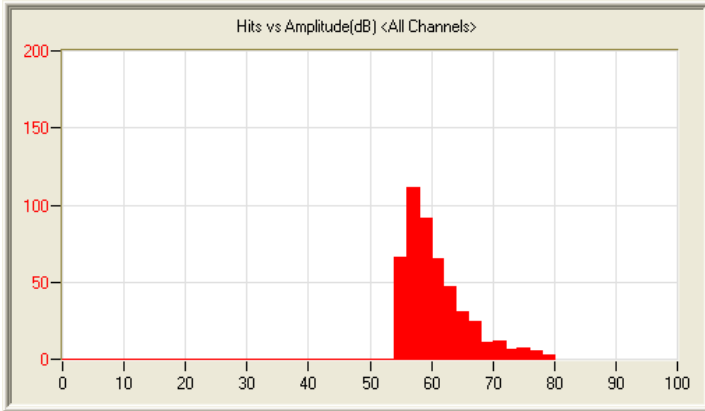
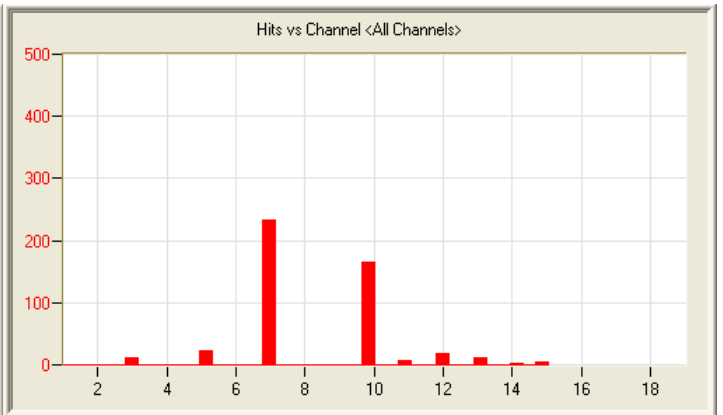
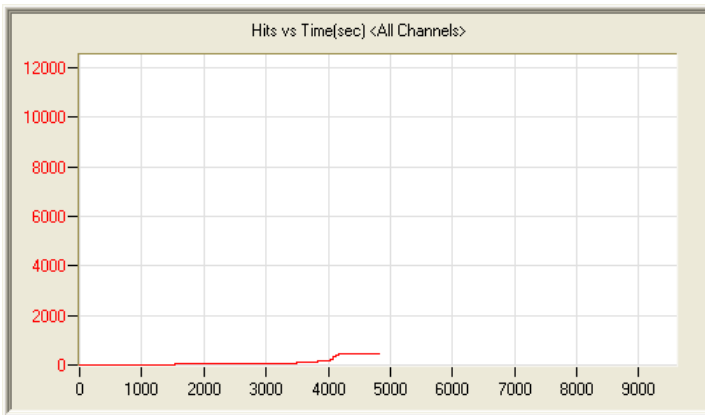
8/13/12 0:20am 8:16:10 7 120813002018_0 1.3mb



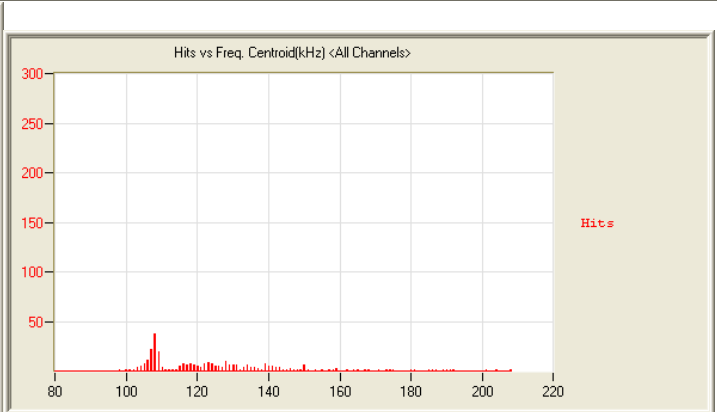
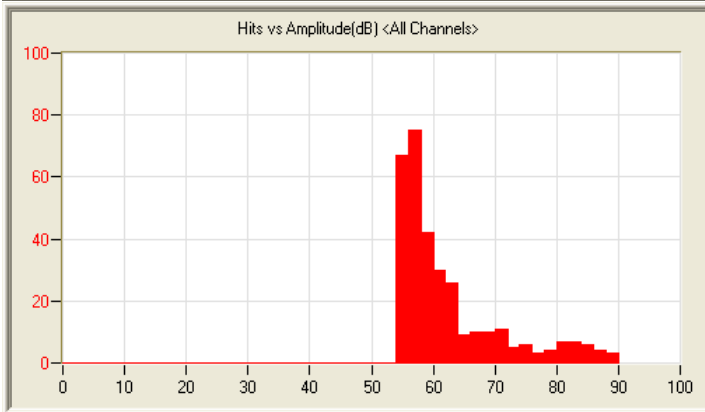
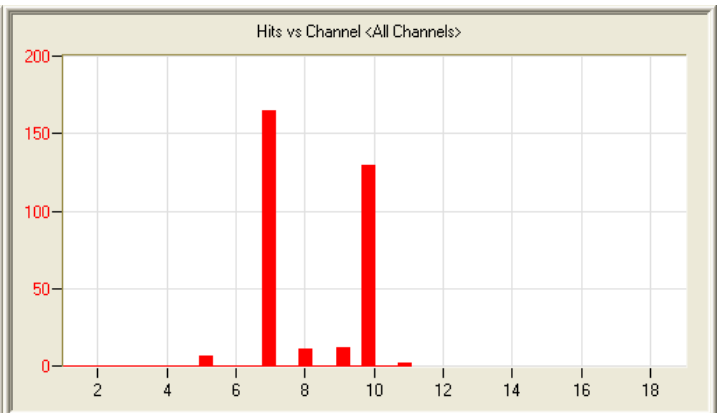
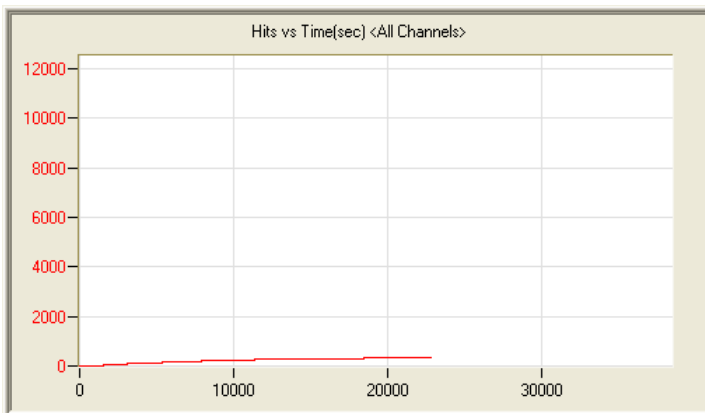
8/13/12 8:32am 19:13:25 380 120813083228_0 2.9mb



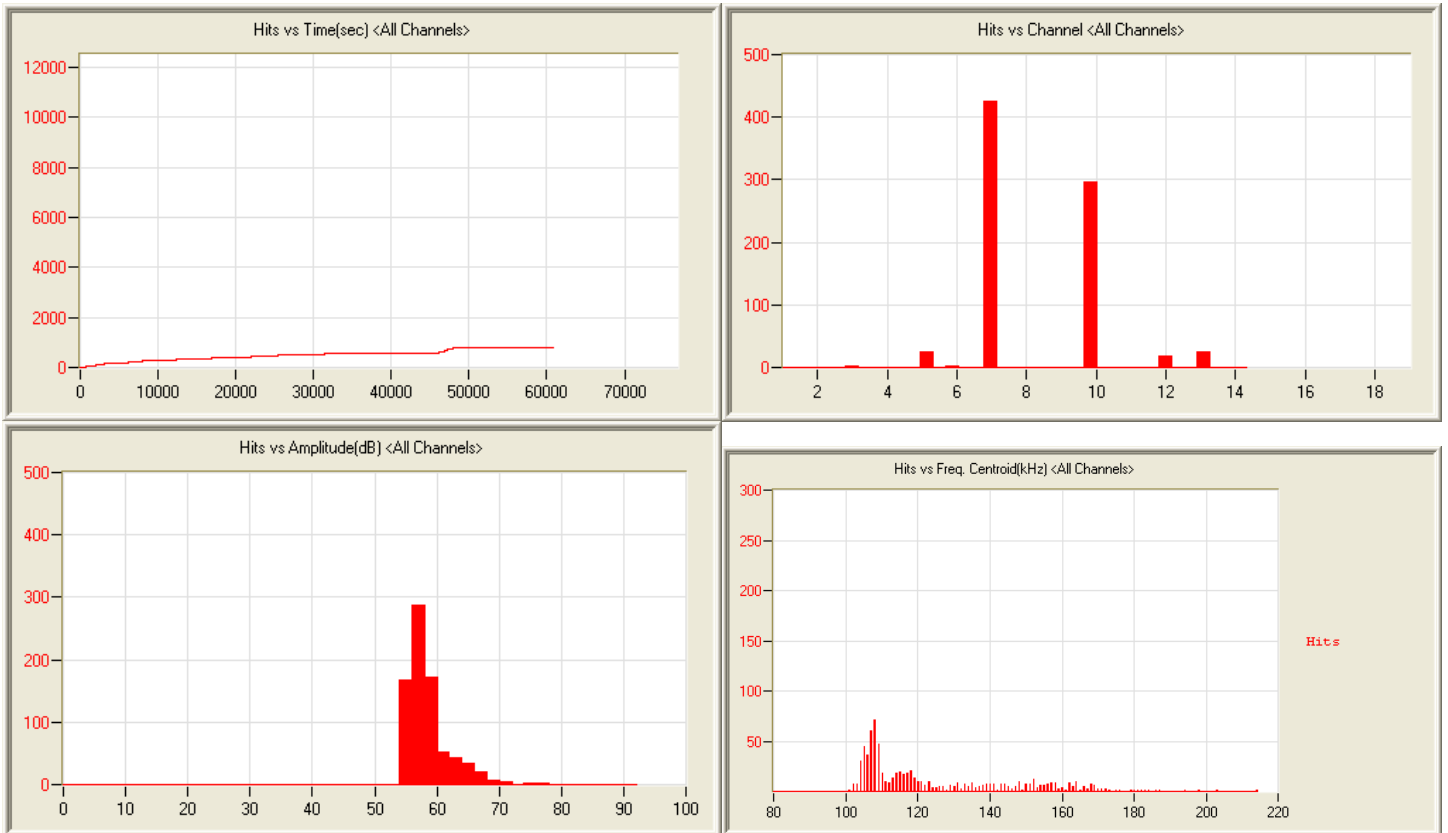
8/14/12 12:00pm 18:03:24 414 120814120003_0 2.7mb



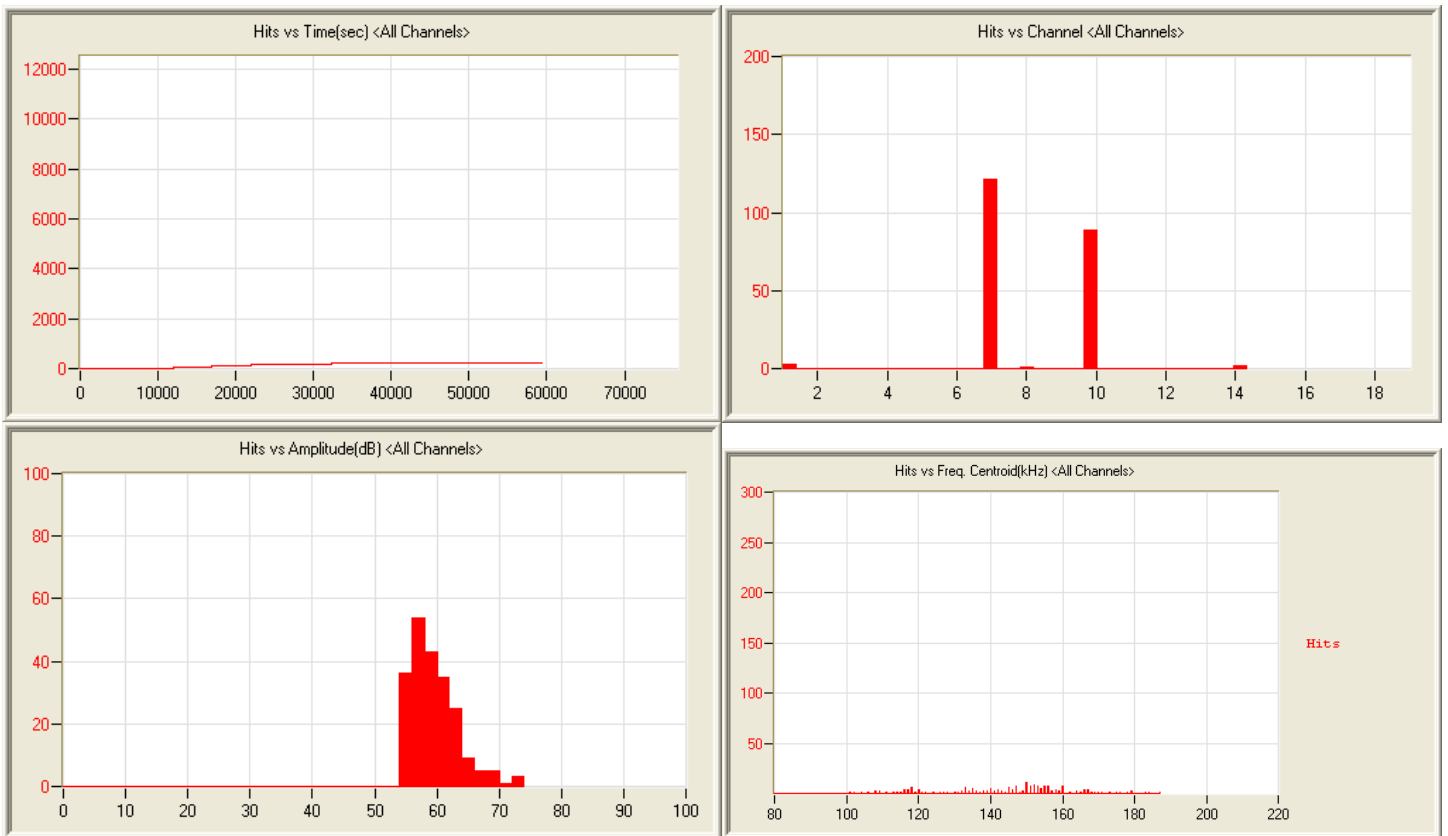
8/15/12 7:58am 1:21:10 479 120815075855_0 280kb



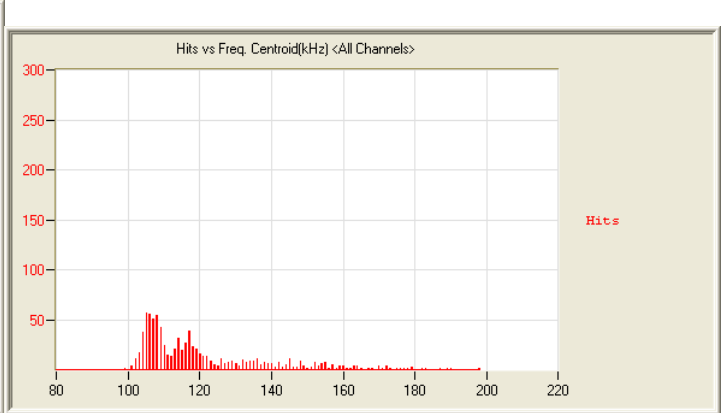
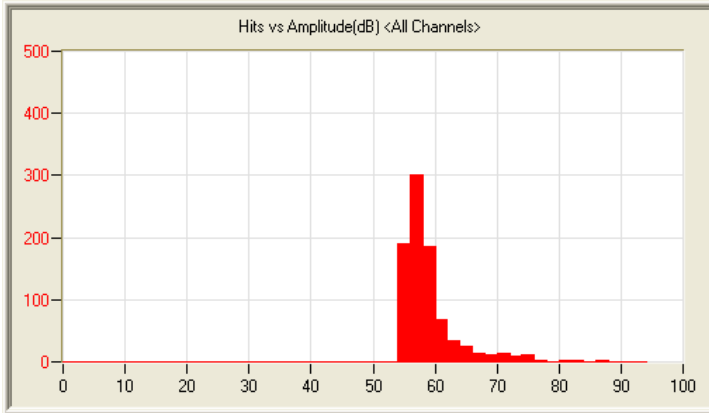
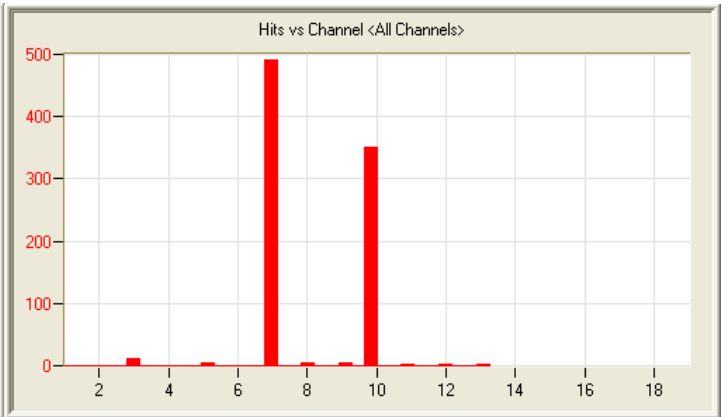
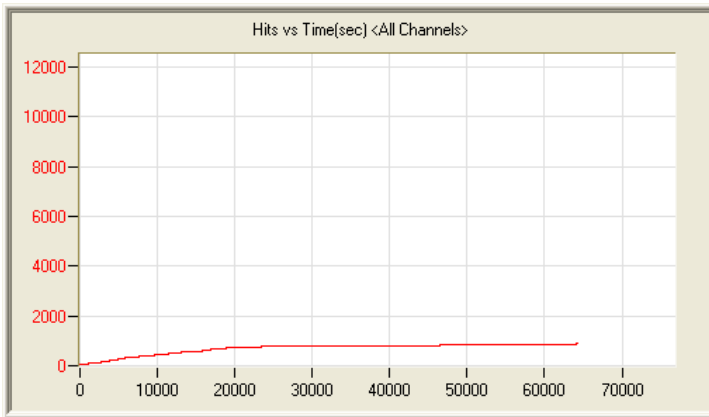
8/15/12 12:42pm 7:20:30 325 120815124256_0 1.1mb



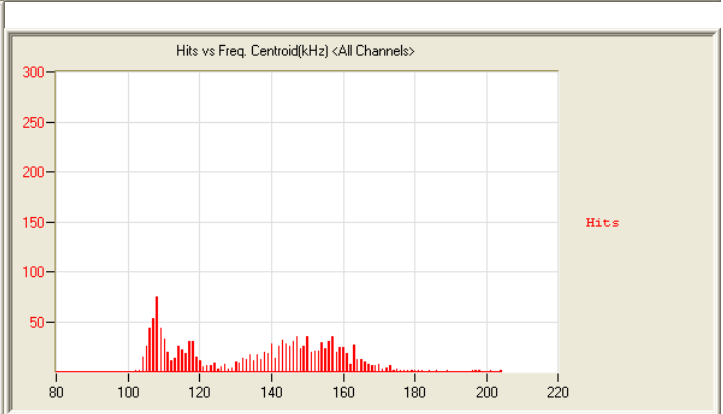
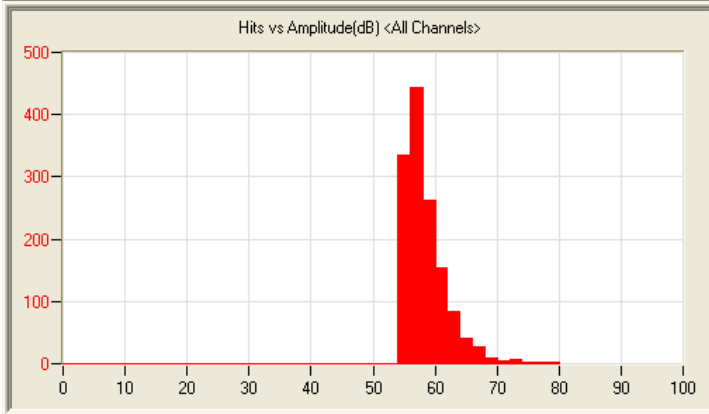
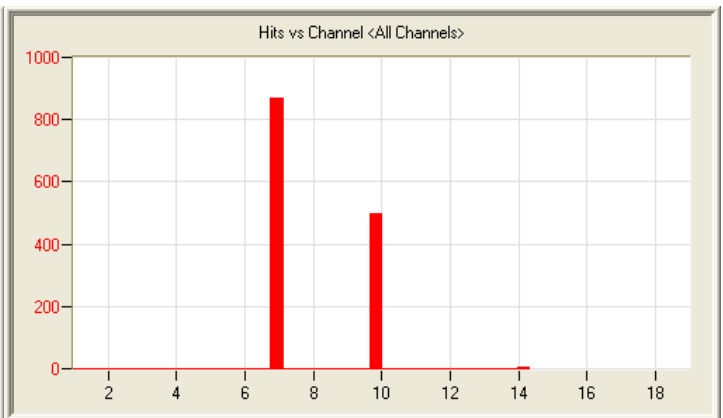
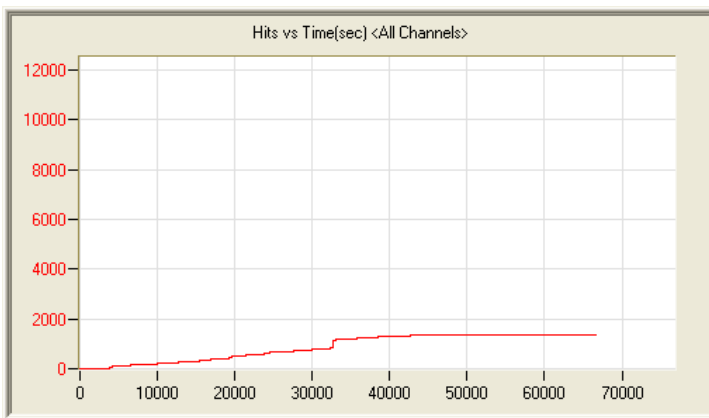
8/15/12 2:11pm 19:14:41 798 120815141100_0 2.9mb



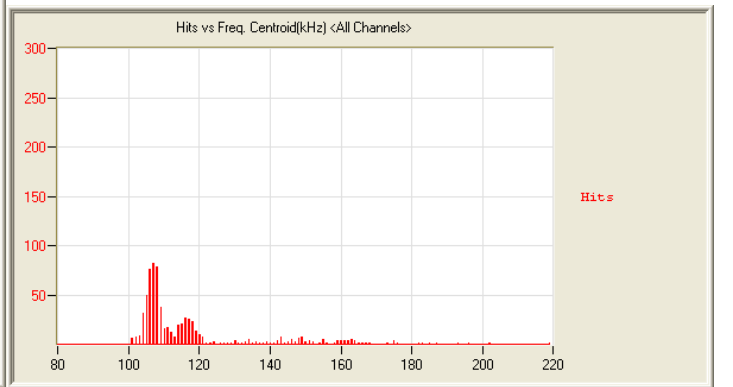
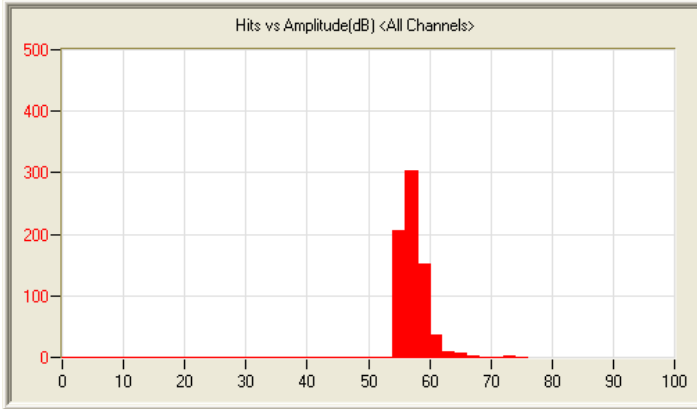
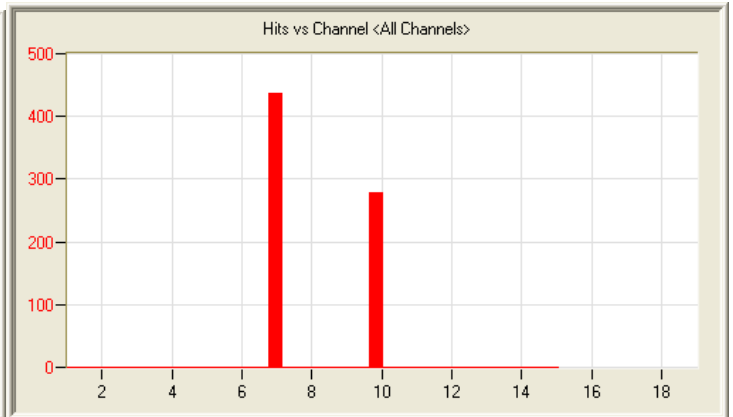
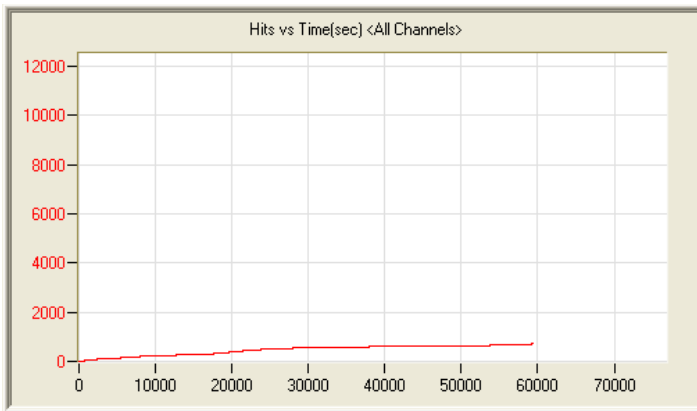
8/16/12 11:42am 18:17:24 216 120816114208_0 2.7mb



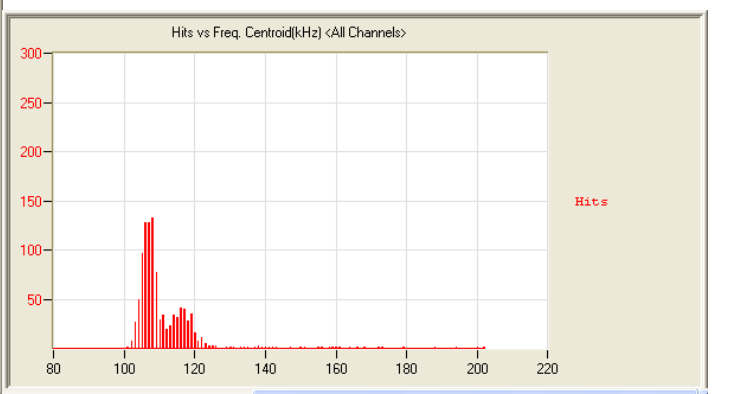
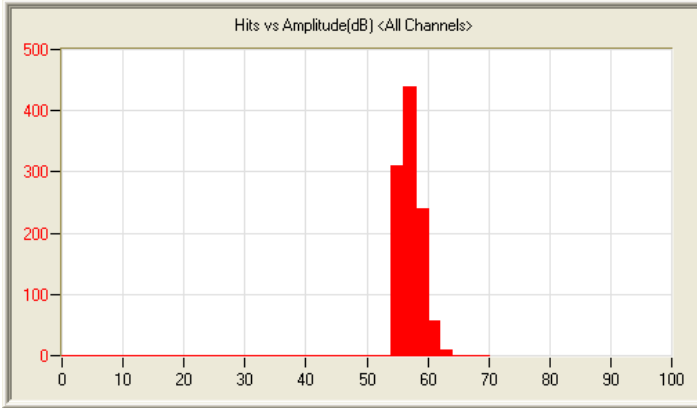
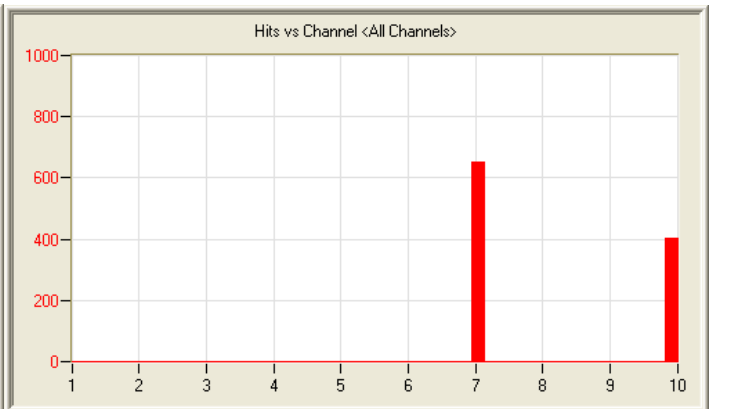
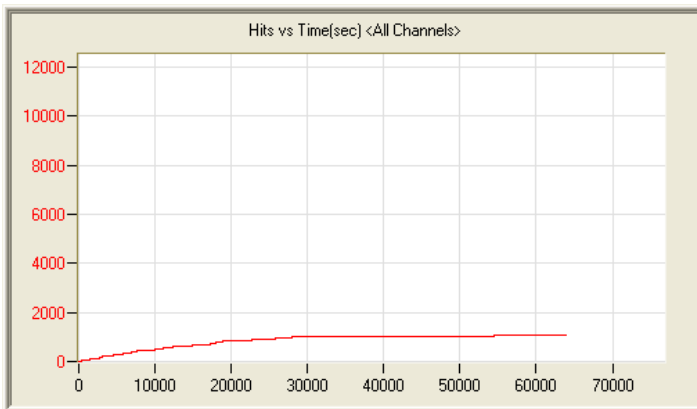
8/16/12 5:53pm 18:23:59 877 120816175337_0 2.8mb



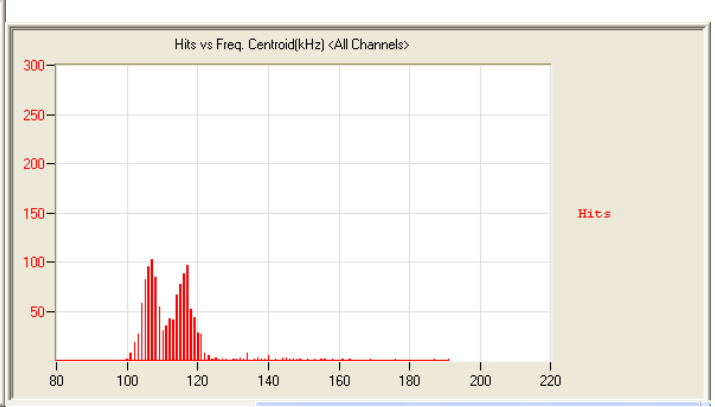
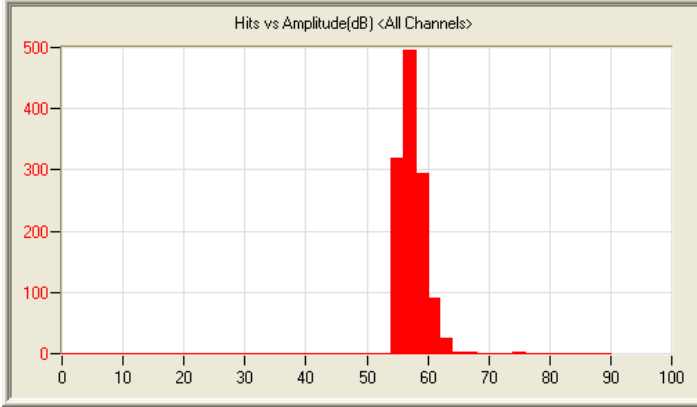
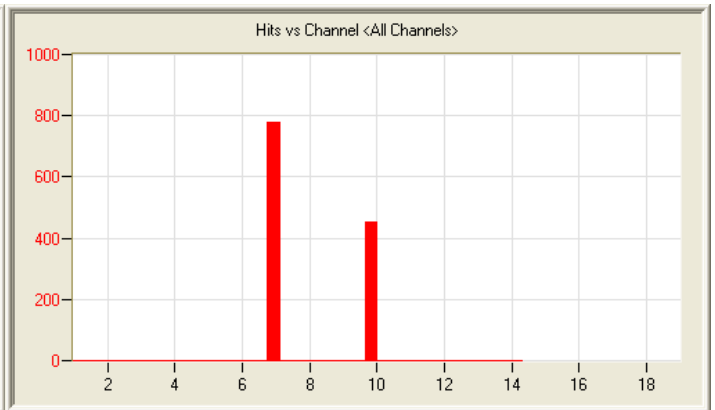
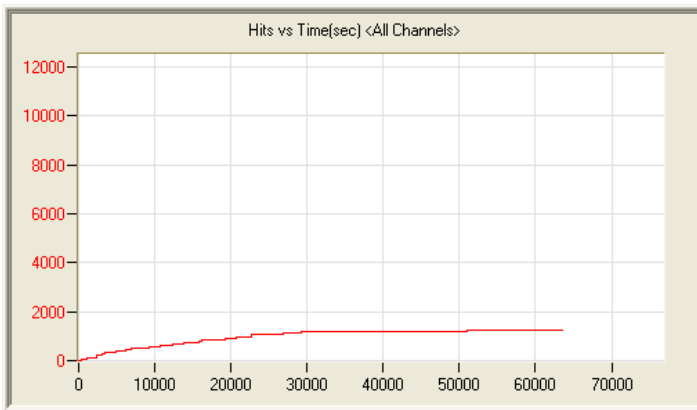
8/17/12 11:19am 19:53:52 1372 120817111937_0 3.0mb



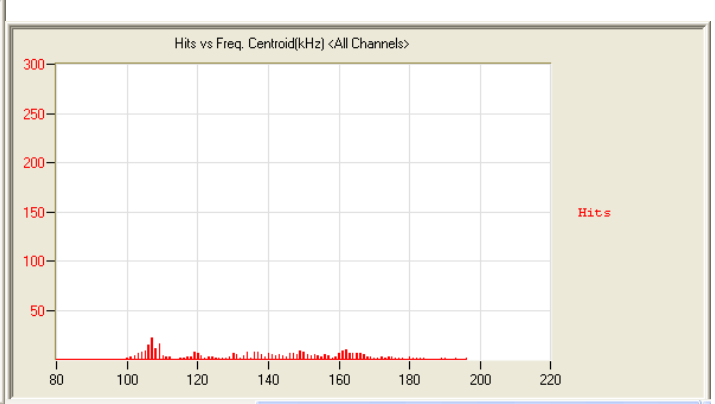
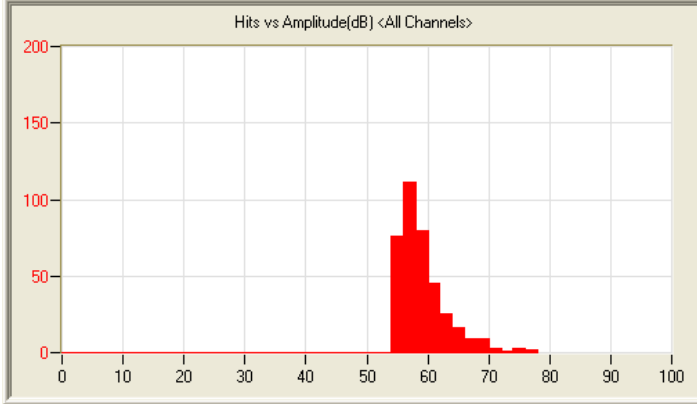
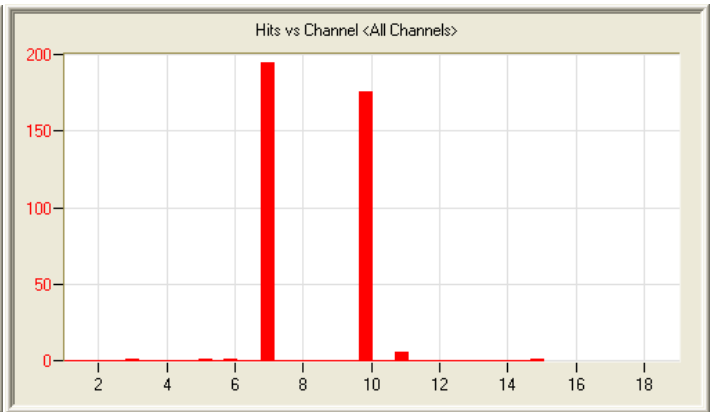
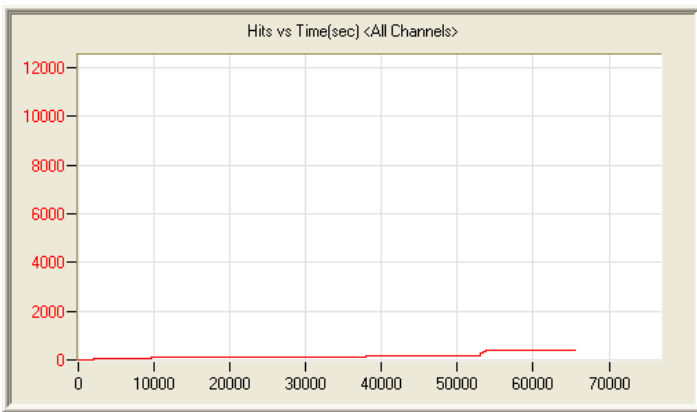
8/17/12 9:23pm 16:55:38 717 120817212355_0 2.5mb



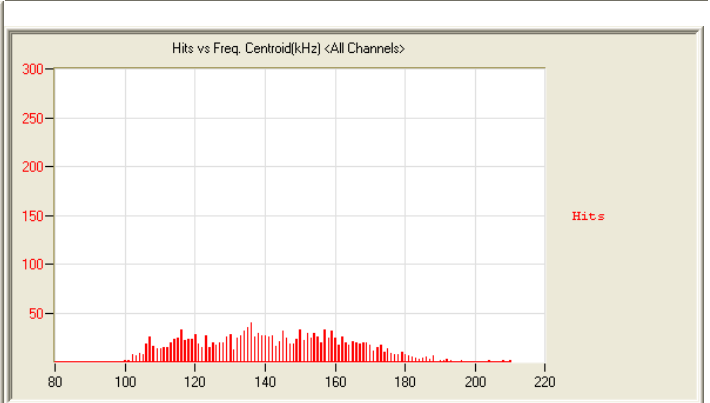
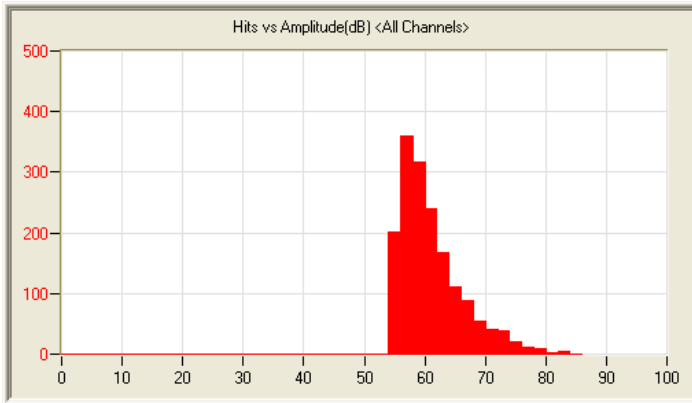
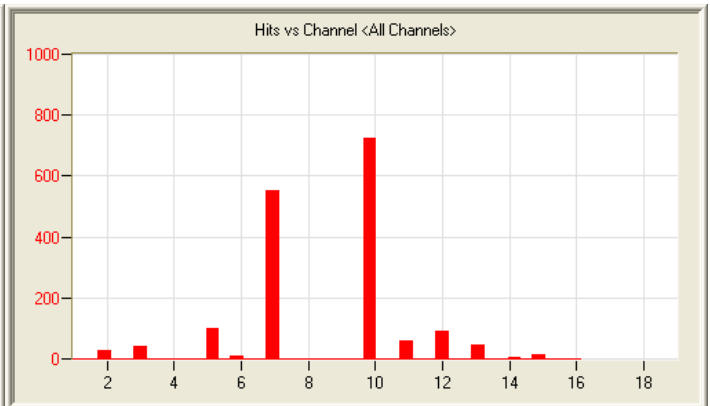
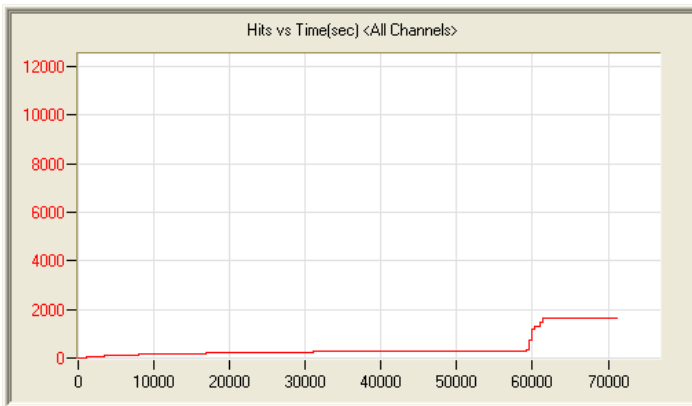
8/18/12 2:36pm 18:19:16 1055 120818143657_0 2.7mb



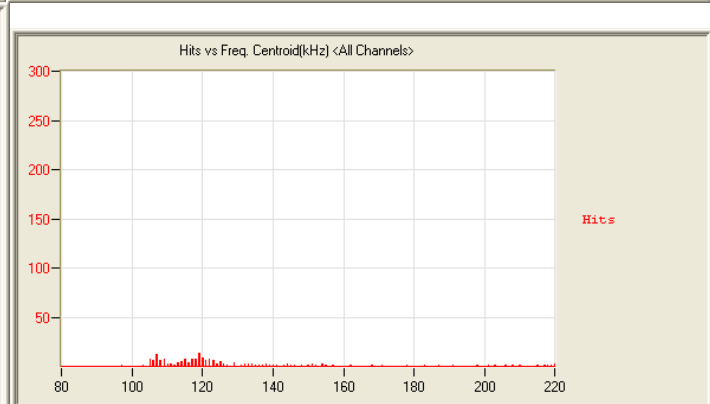
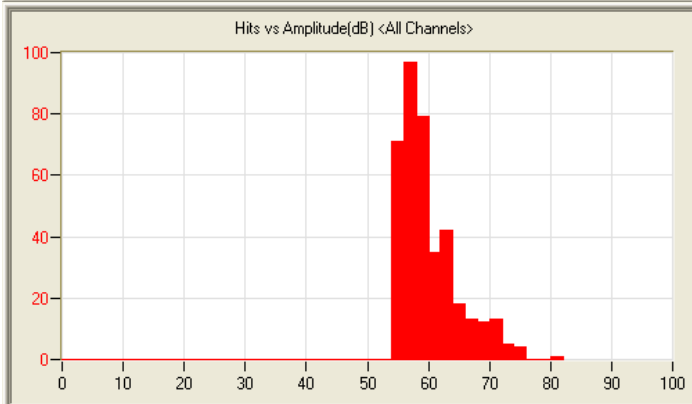
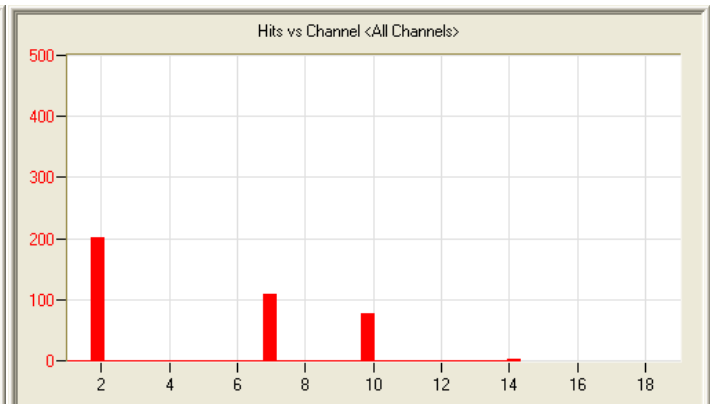
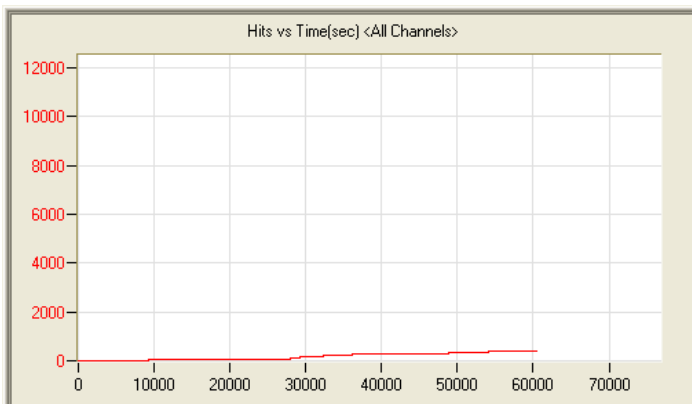
8/18/12 11:58pm 18:18:55 1235 120818235820_0 2.8mb



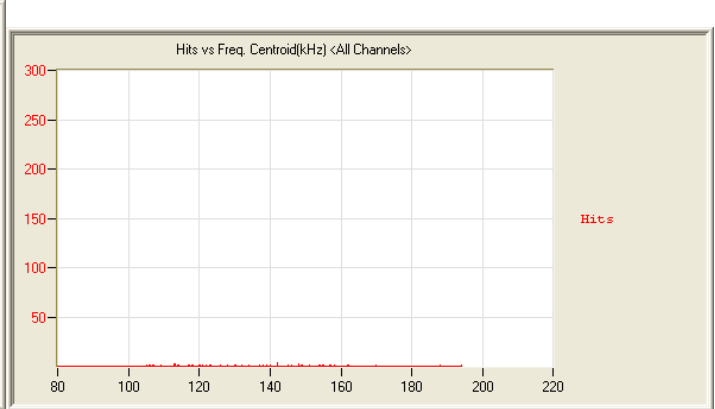
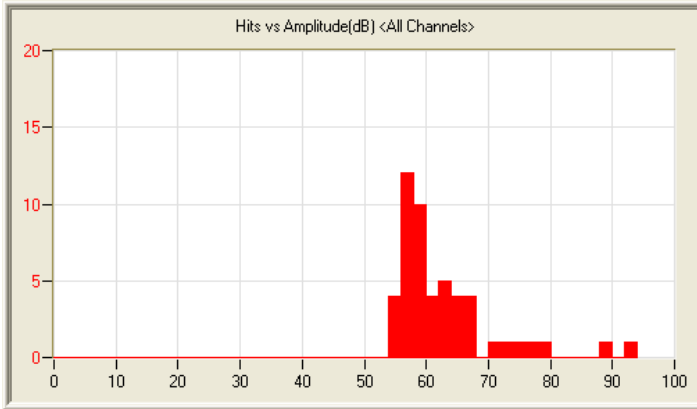
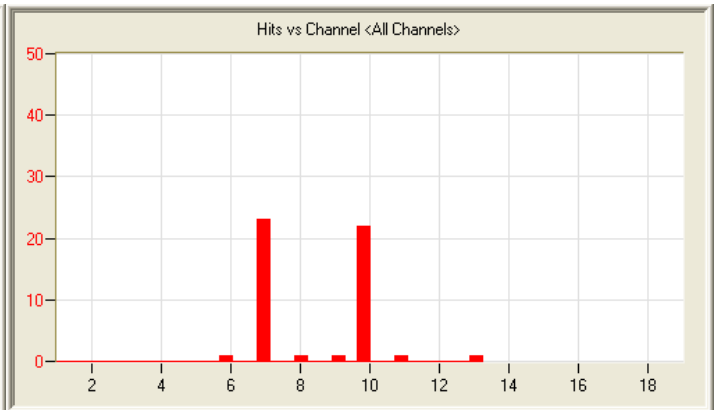
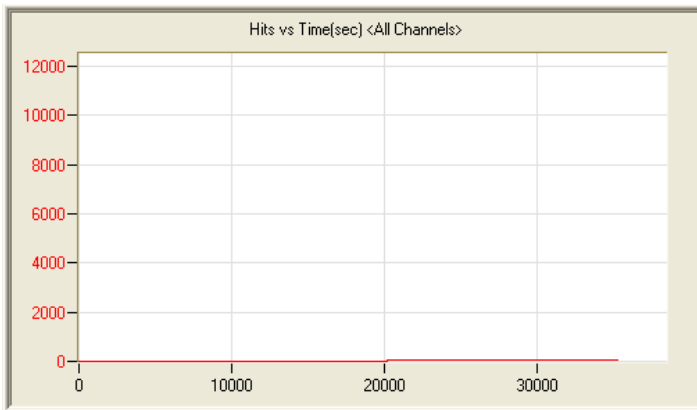
8/19/12 2:37pm 18:12:19 380 120819143746_0 2.7mb



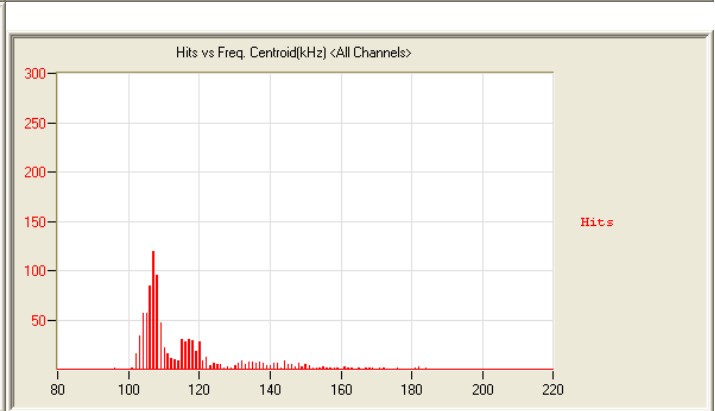
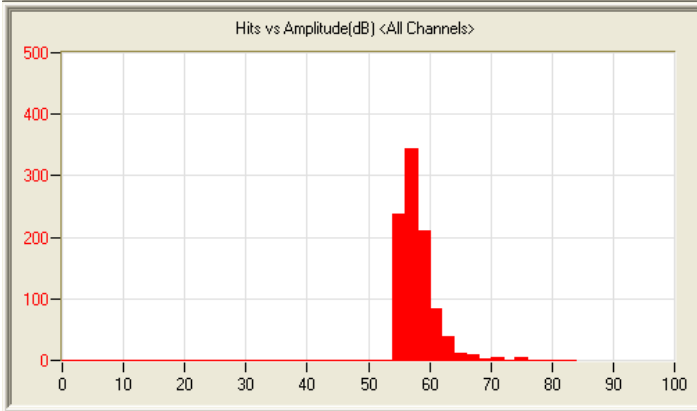
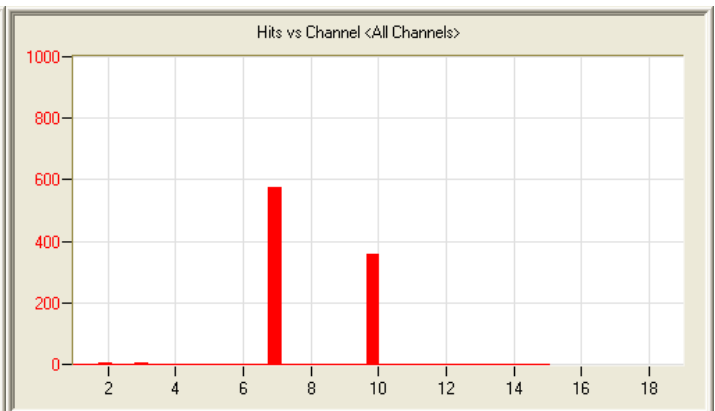
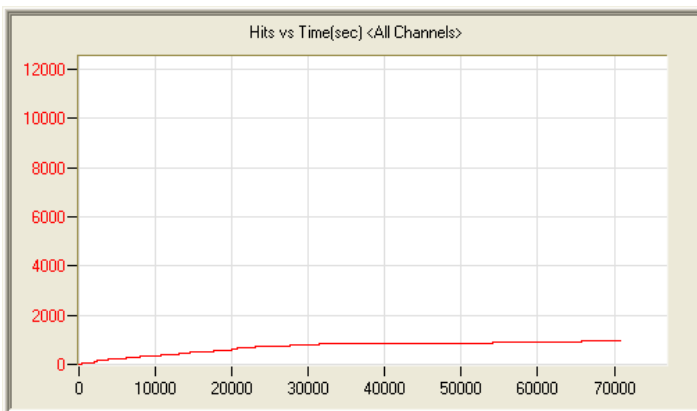
8/20/12 2:01am 20:09:25 1668 120820020117_0 3.0mb



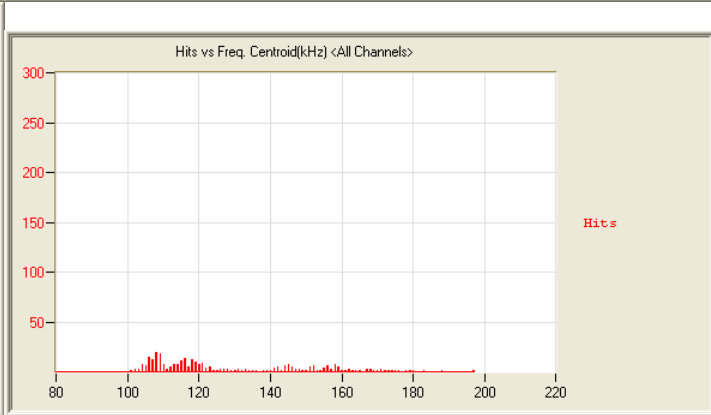
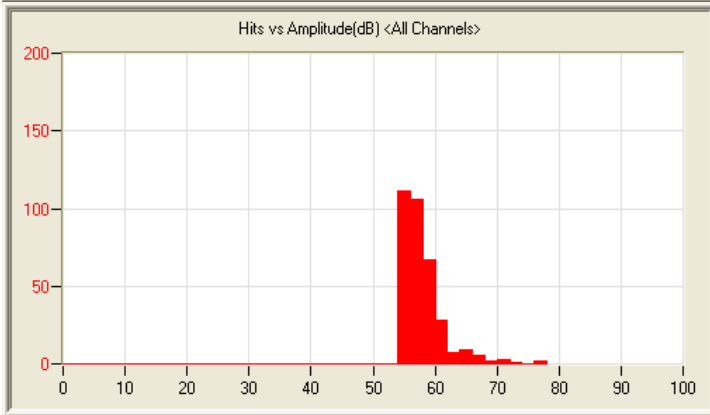
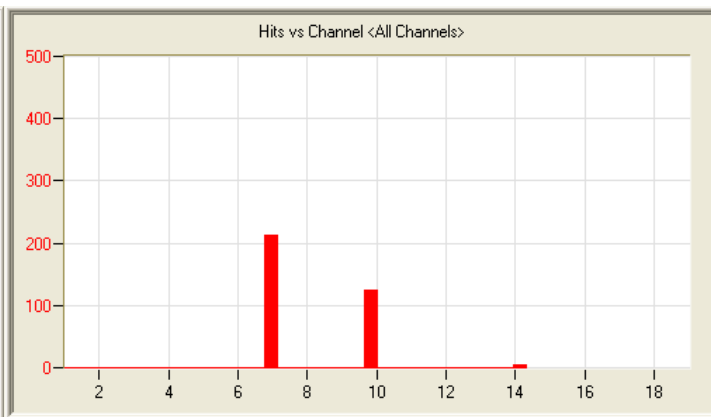
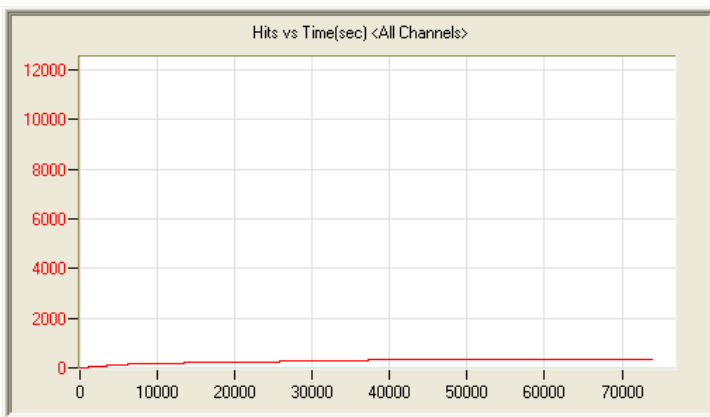
8/21/12 6:41am 16:54:45 390 120821064117_0 2.5mb



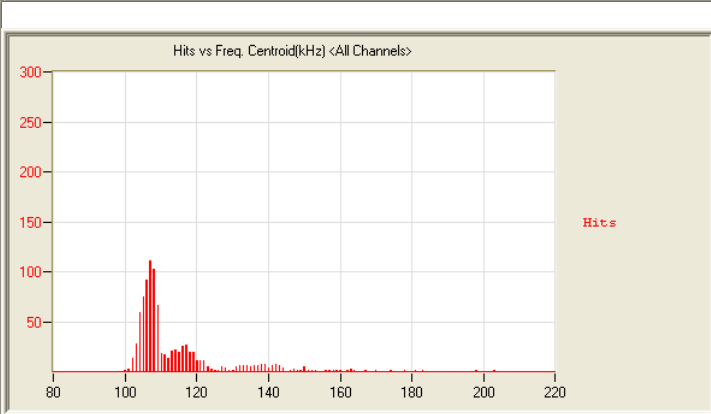
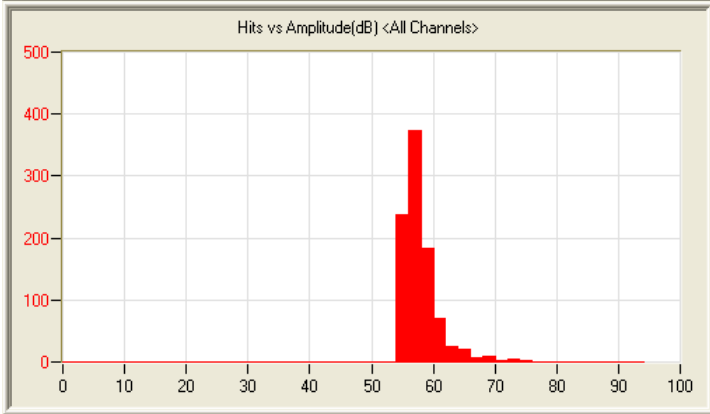
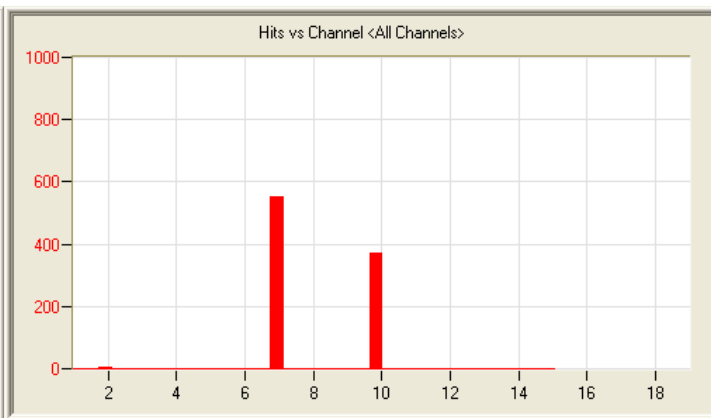
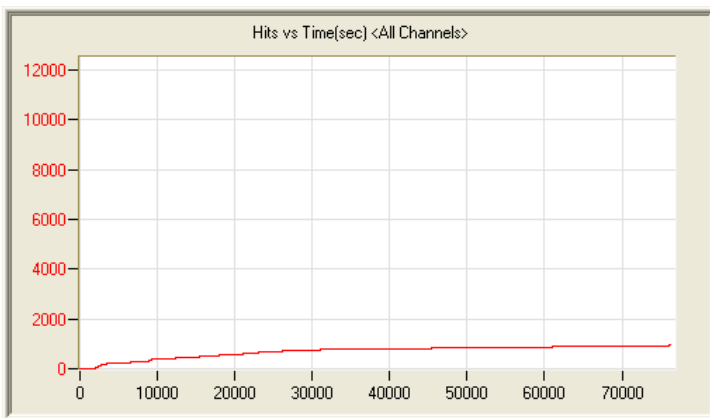
8/21/12 4:06pm 11:03:34 50 120821160653_0 1.7mb



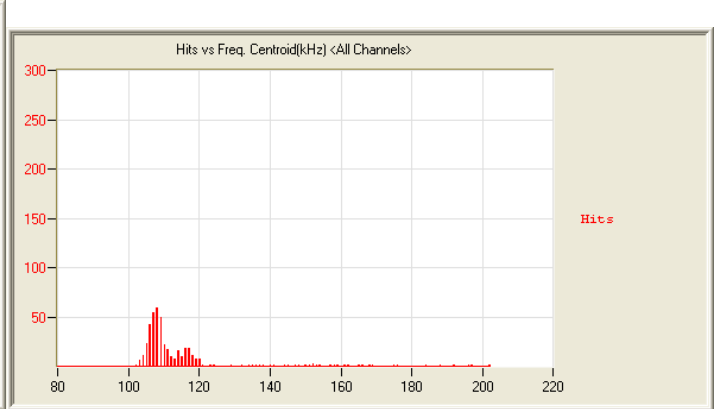
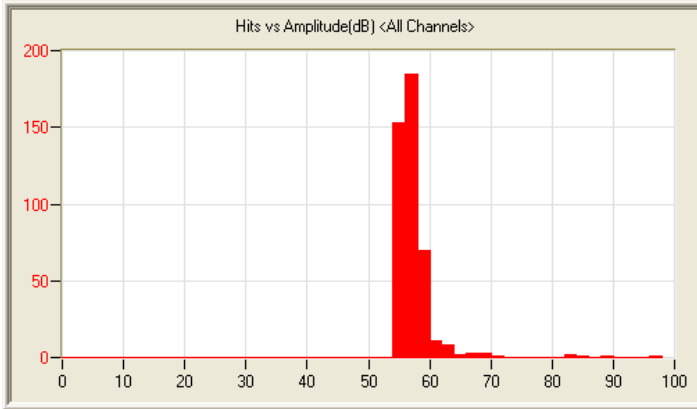
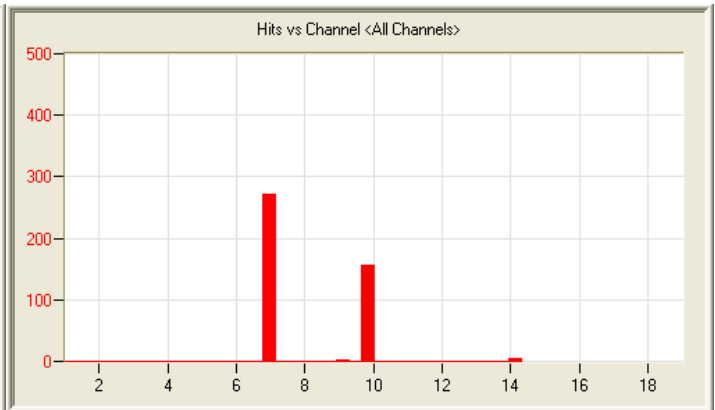
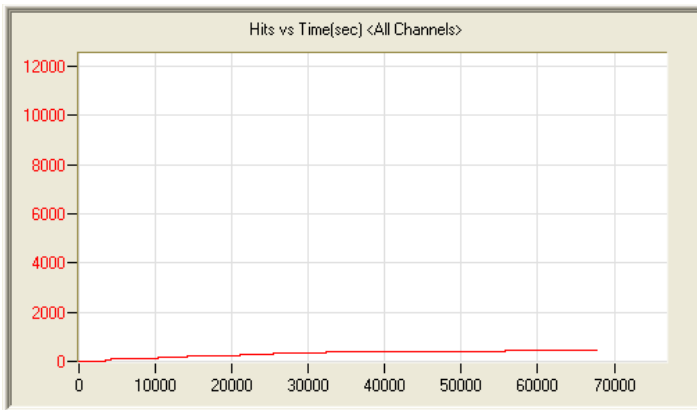
8/22/12 6:58am 19:54:38 947 120822065852_0 3.0mb



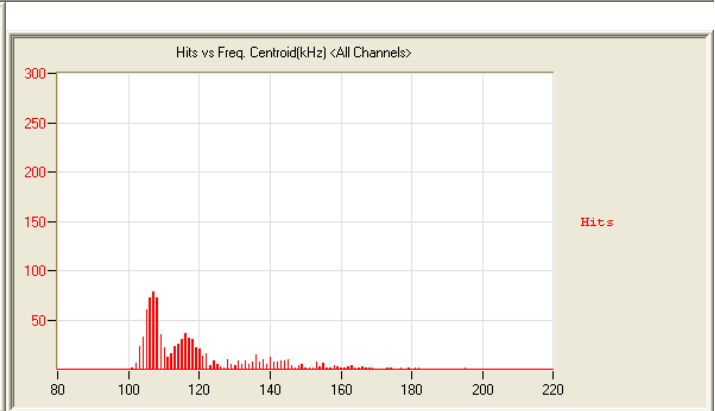
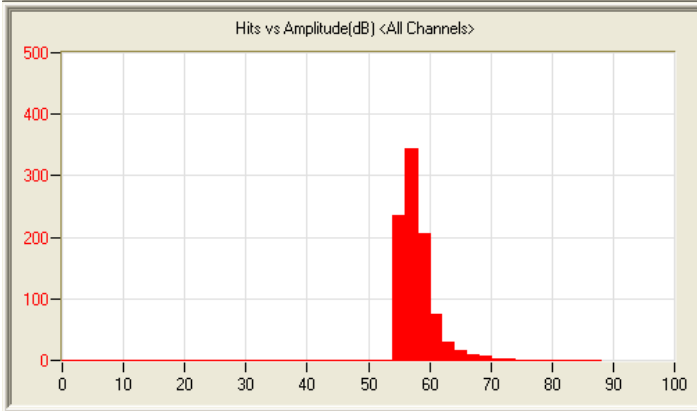
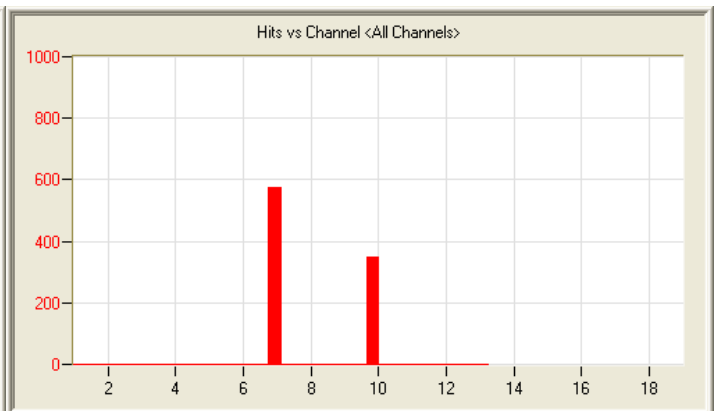
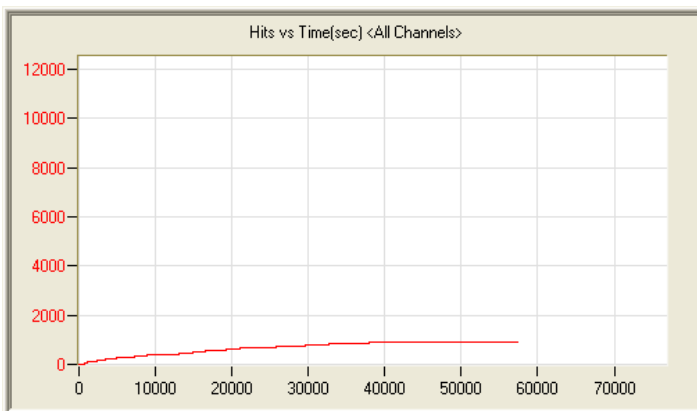
8/22/12 12:34pm 22:08:20 341 120822123429_0 3.3mb



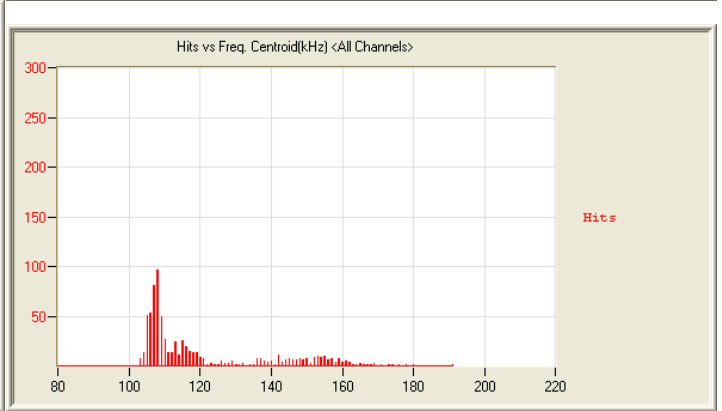
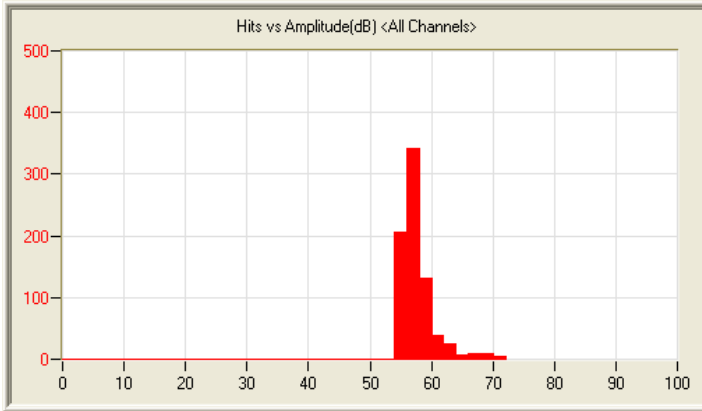
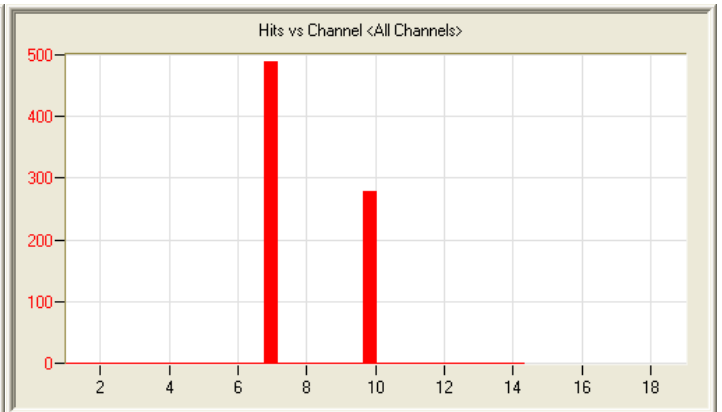
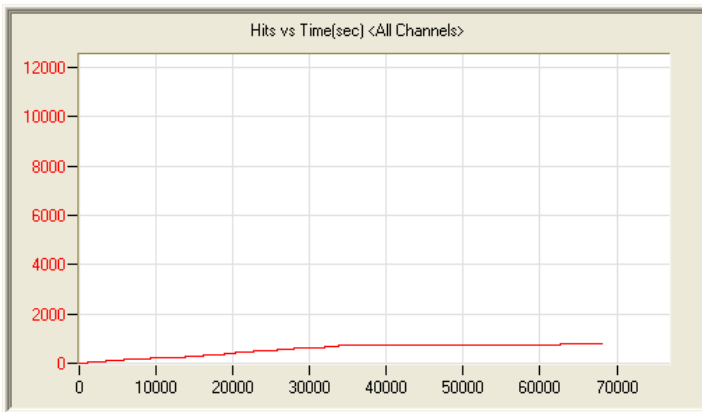
8/23/12 7:56am 21:19:58 938 120823075644_0 3.2mb



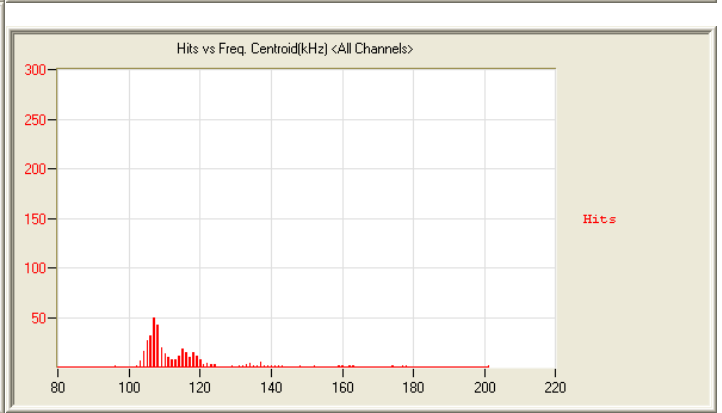
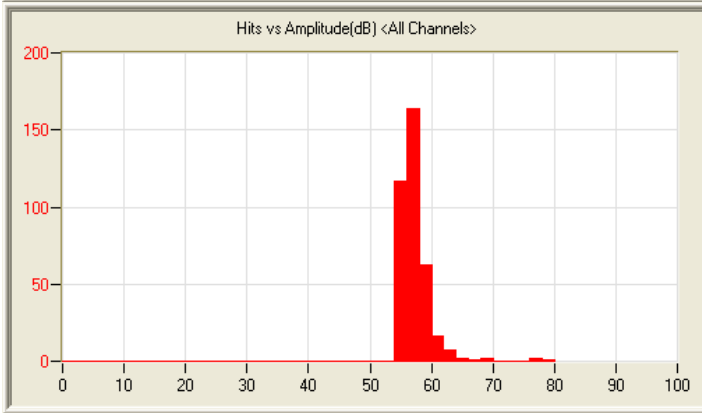
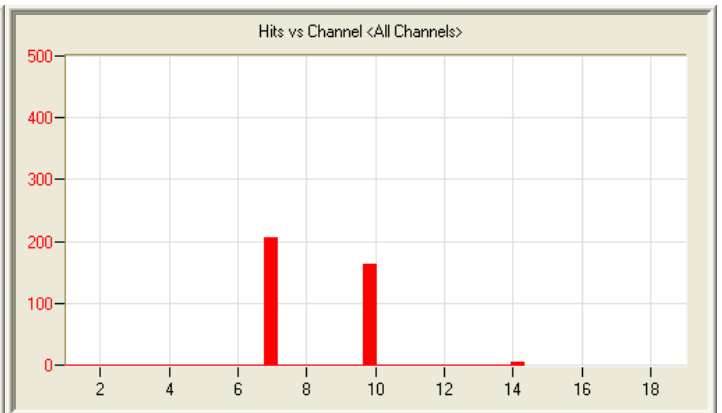
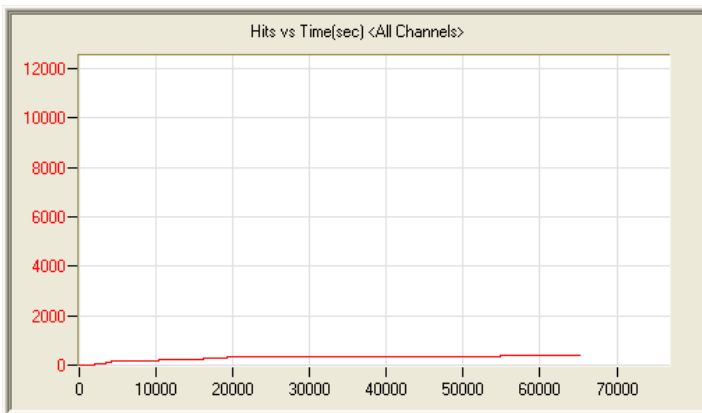
8/23/12 1:33pm 21:04:10 441 120823133330_0 3.1mb



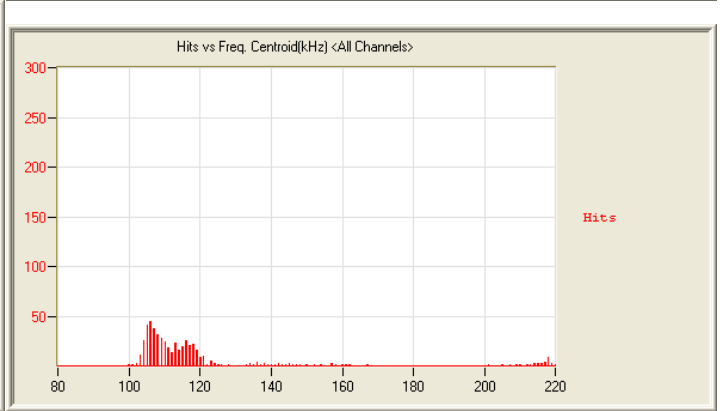
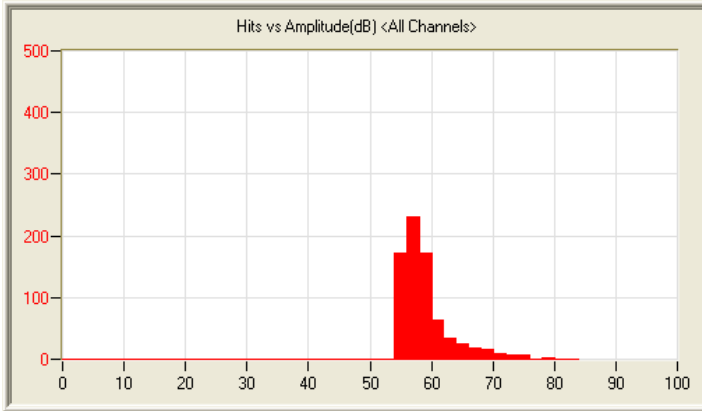
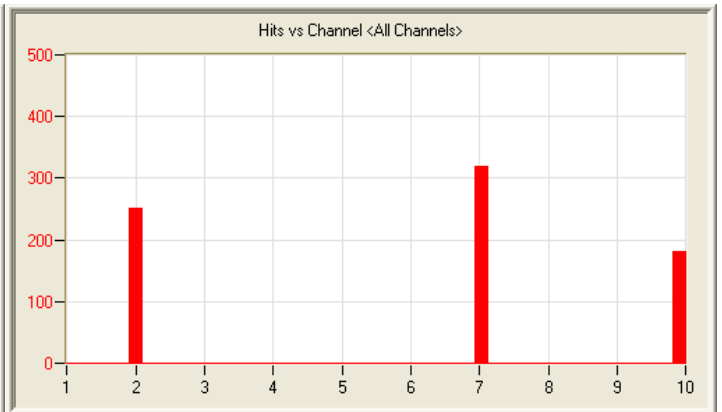
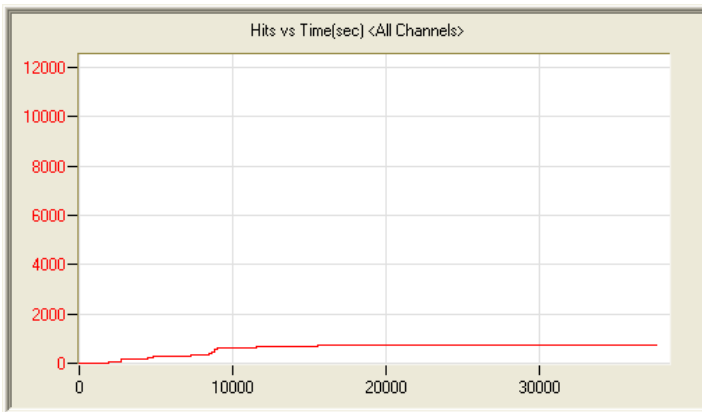
8/24/12 8:53am 16:09:01 929 120824085343_0 2.4mb



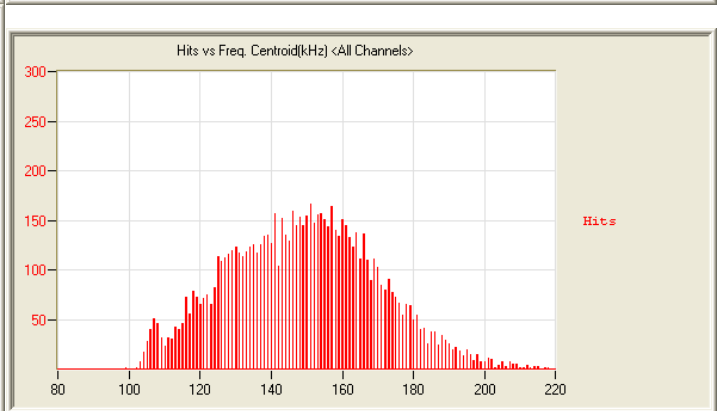
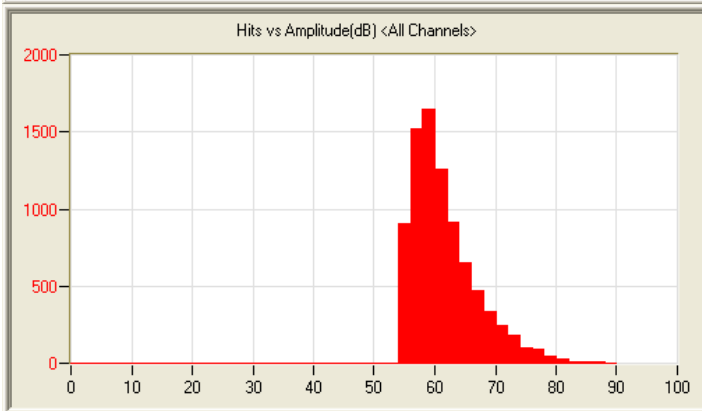
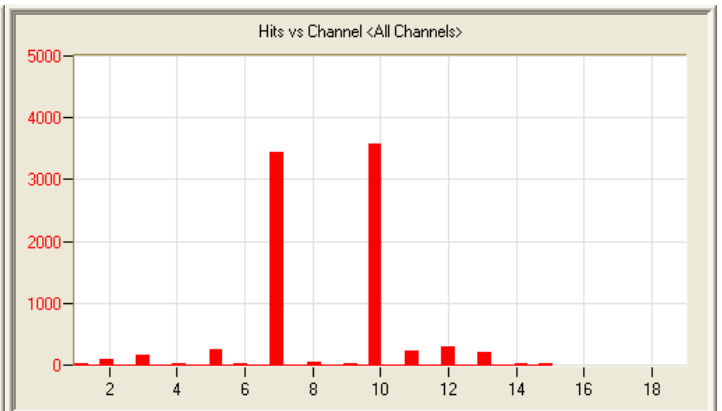
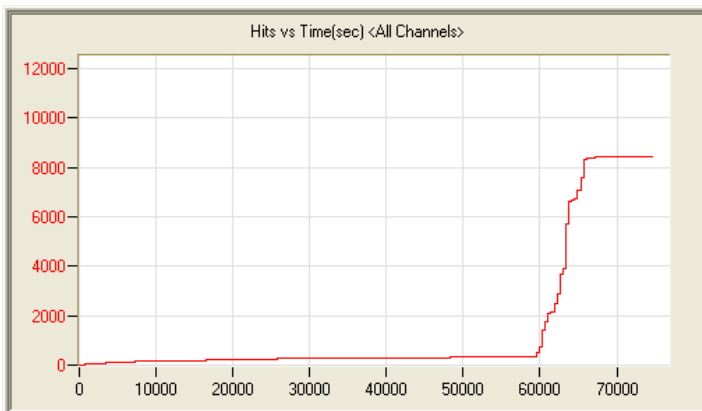
8/24/12 2:34pm 20:36:22 770120824143431_0 3.1mb



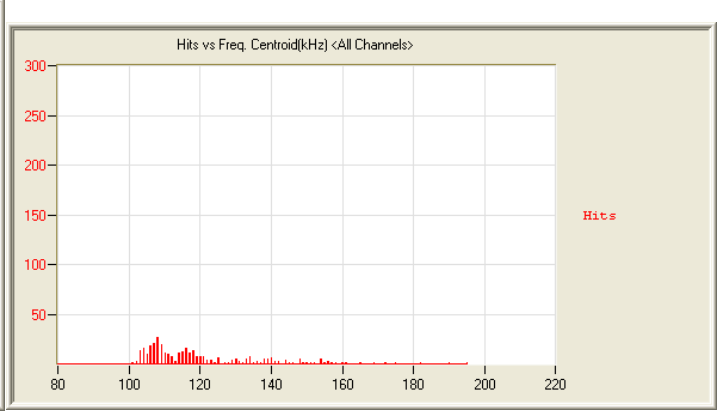
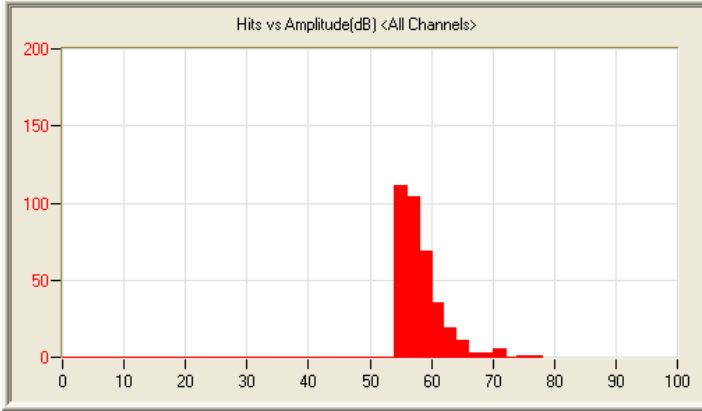
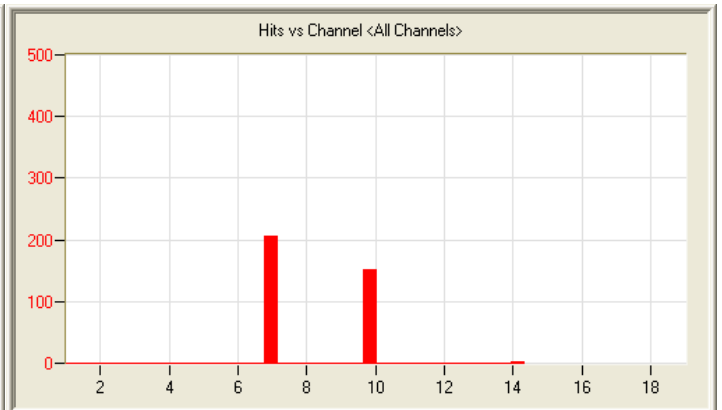
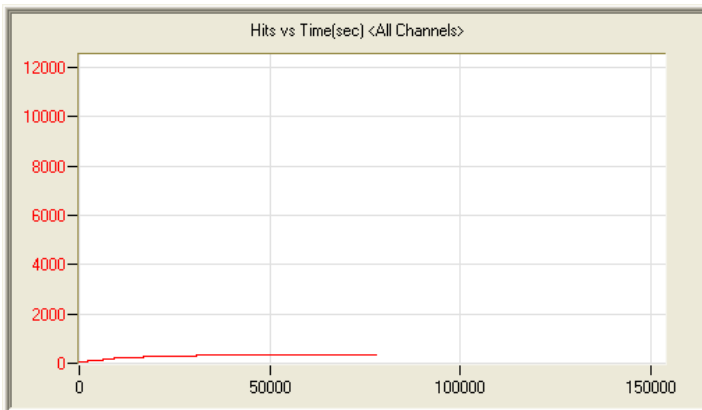
8/25/12 11:05pm 19:53:11 374 120825230550_0 2.9mb



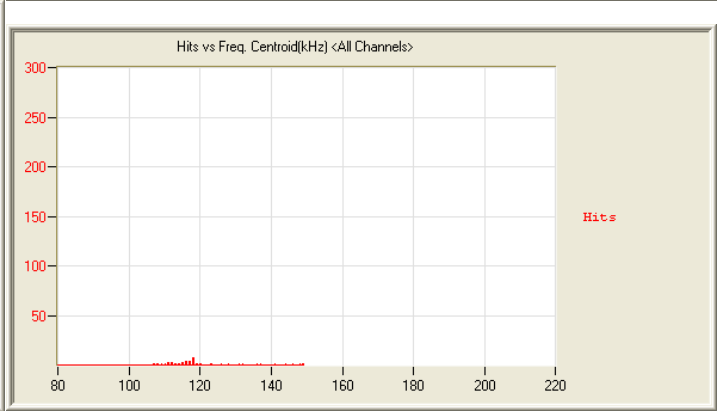
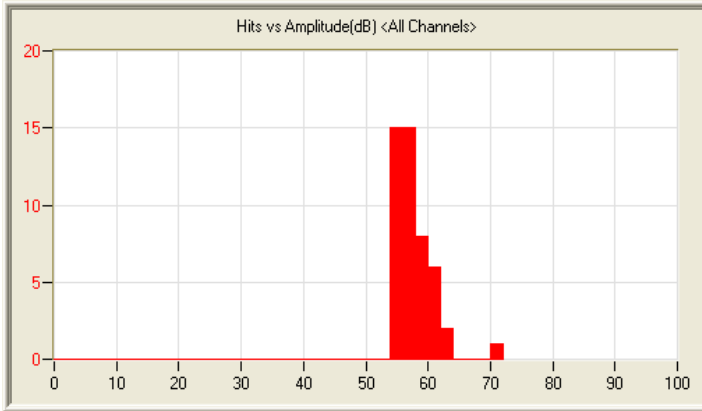
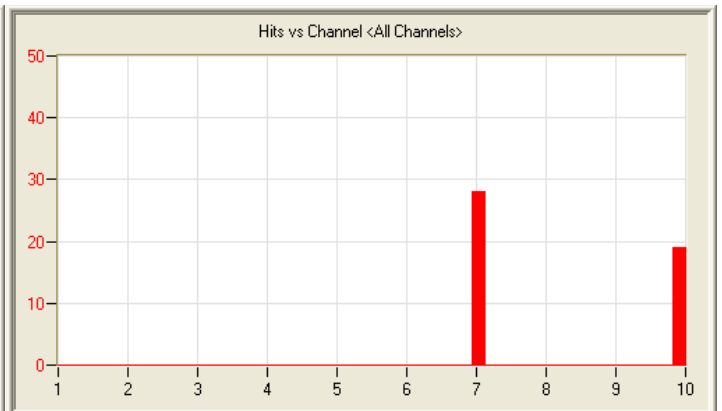
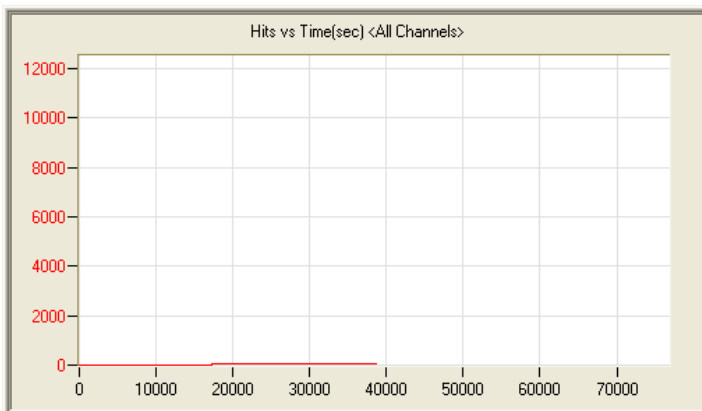
8/26/12 2:22pm 10:56:32 754 120826142254_0 1.7mb



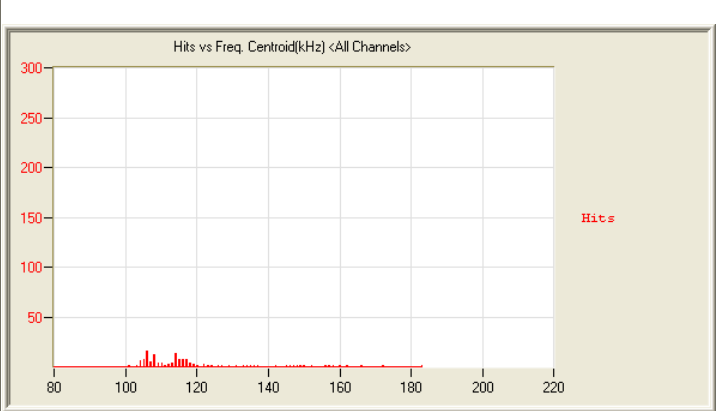
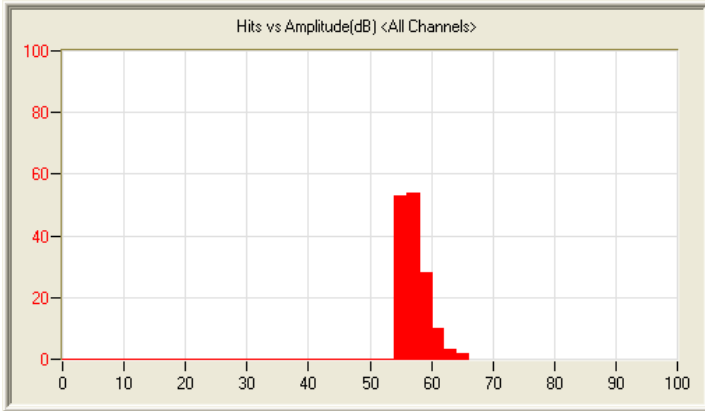
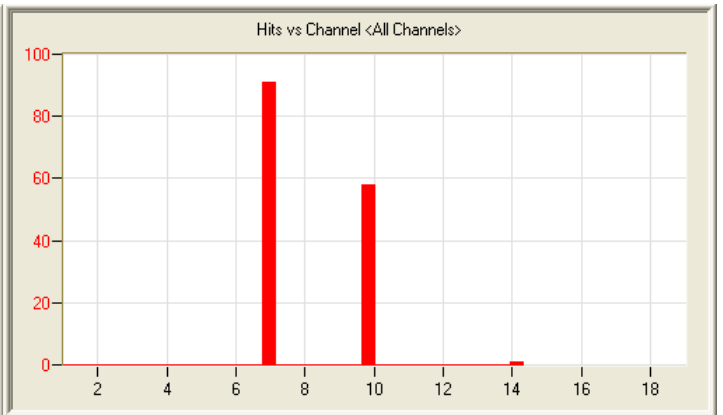
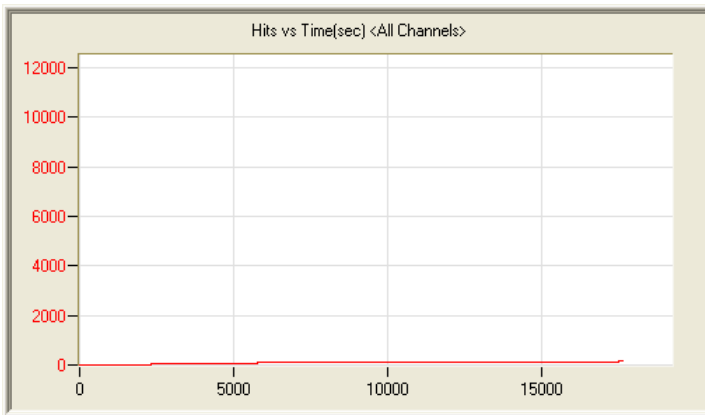
8/26/12 10:44pm 20:49:52 8418 120826224432_0 3.4mb



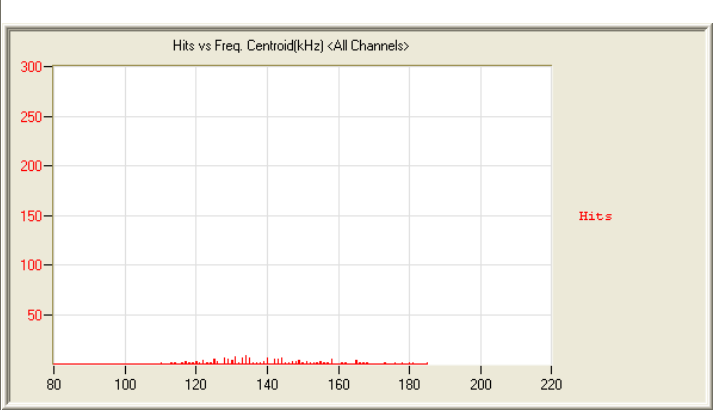
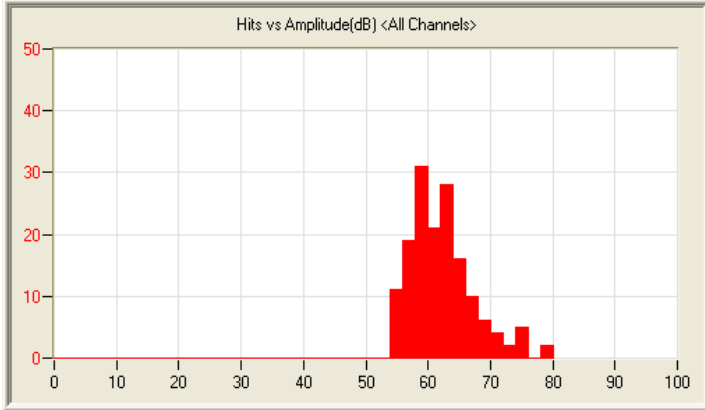
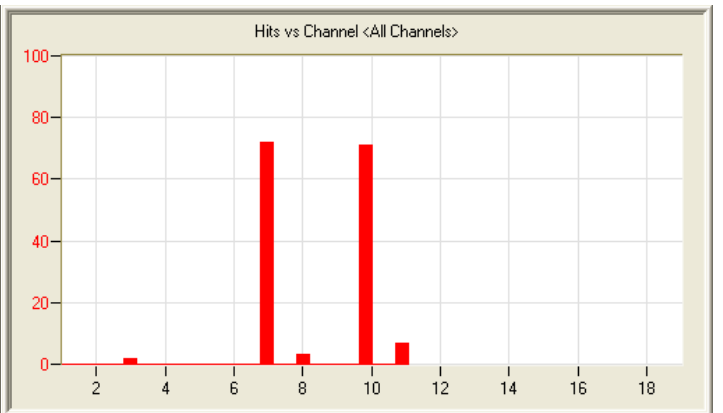
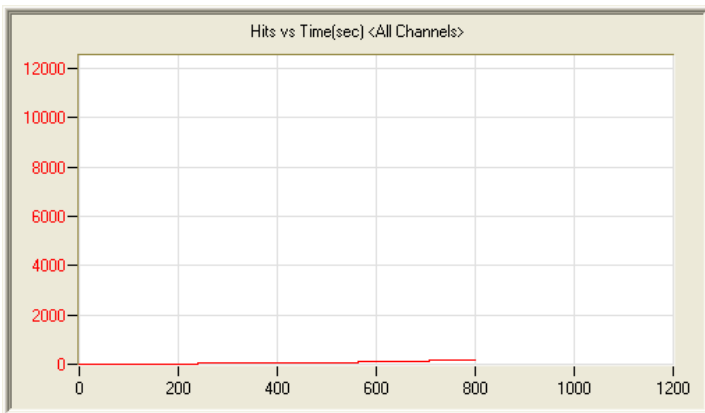
8/27/12 3:10pm 21:46:02 362 120827151053_0 3.2mb



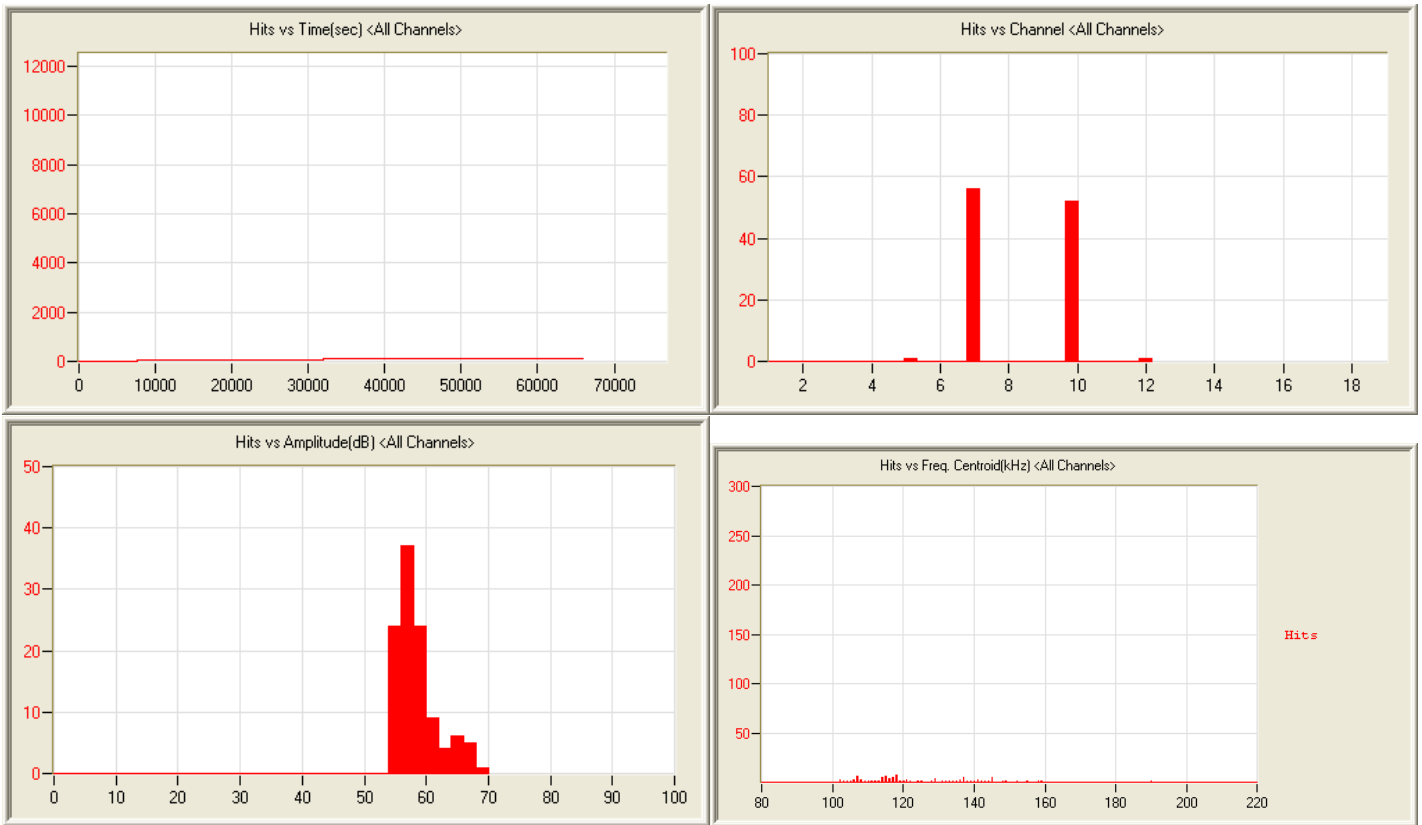
8/28/12 11:43pm 10:47:07 47 120828234319_0 1.6mb



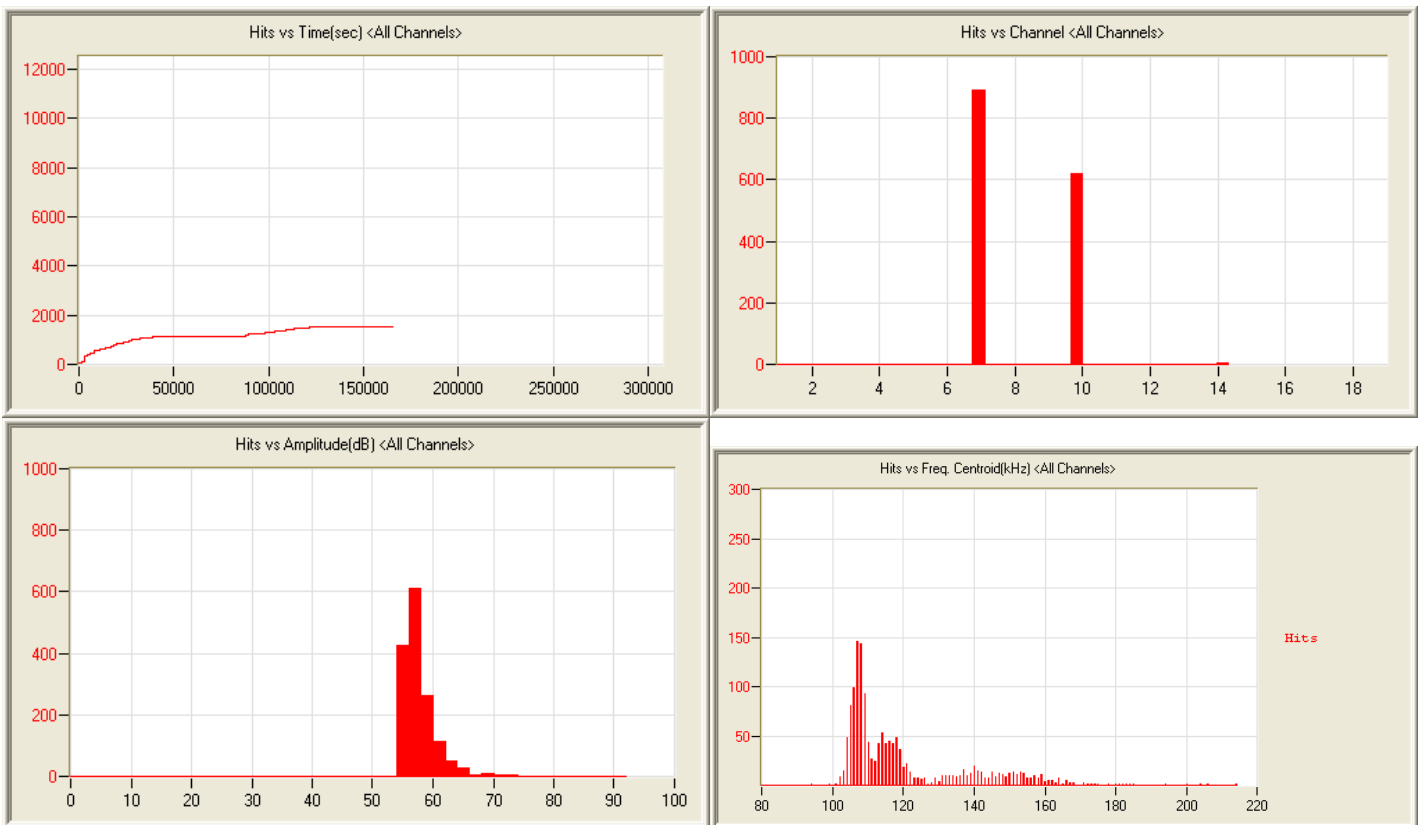
8/29/12 1:52am 4:54:59 150 120829015213_0 781kb



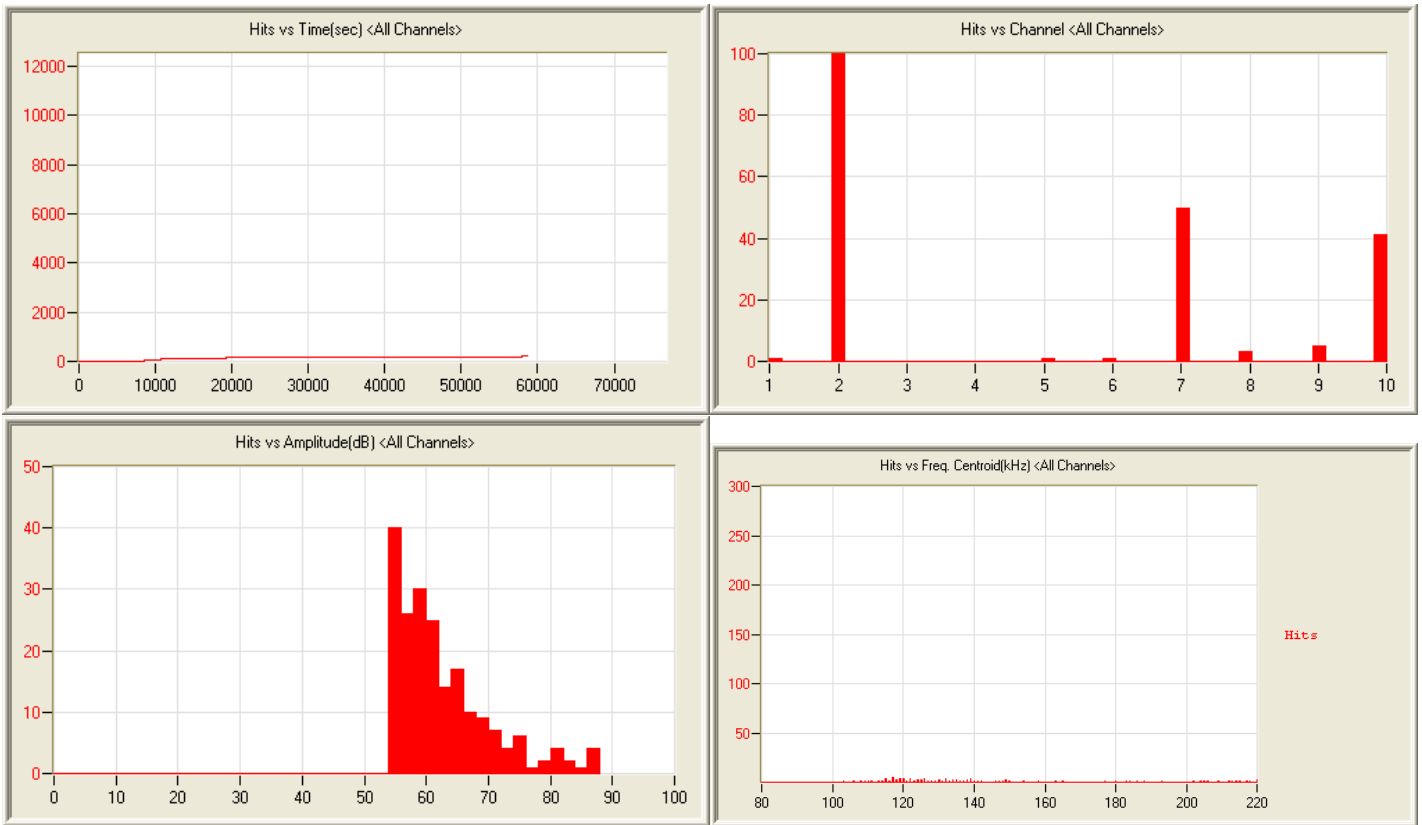
8/29/12 7:51am 0:13:27 155 120829075107_0 105kb



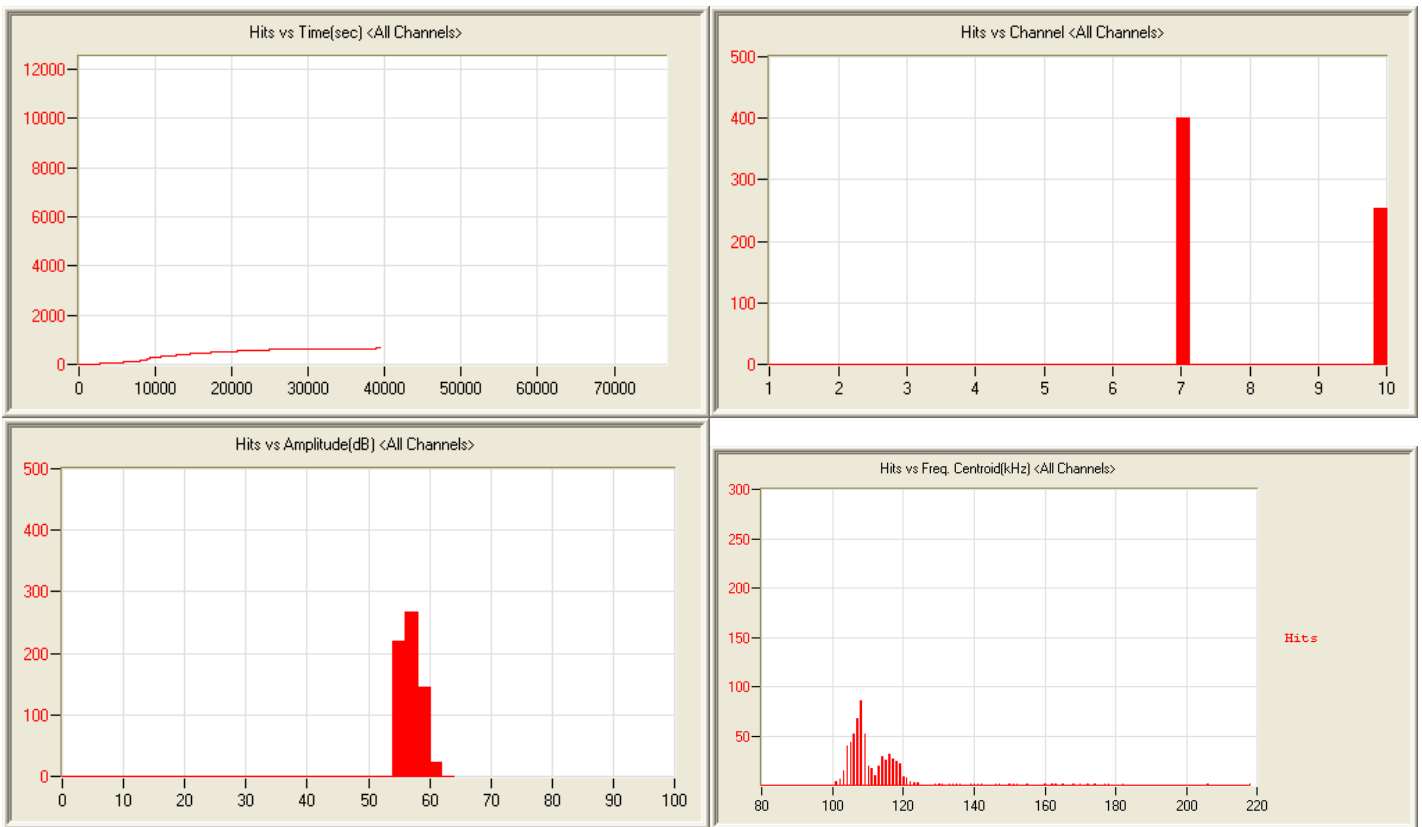
8/29/12 9:49pm 18:17:34 110 120829214932_0 2.7mb



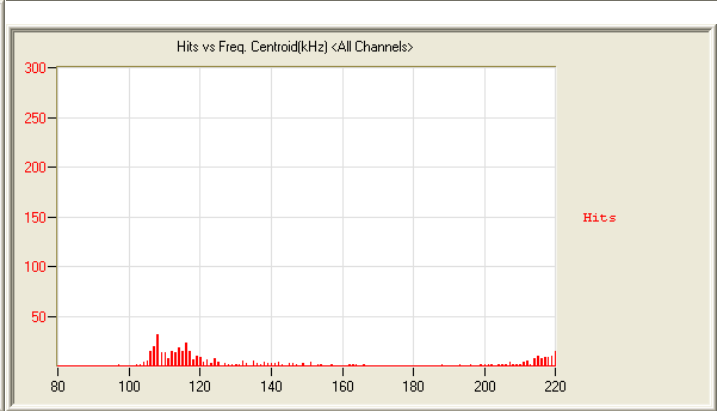
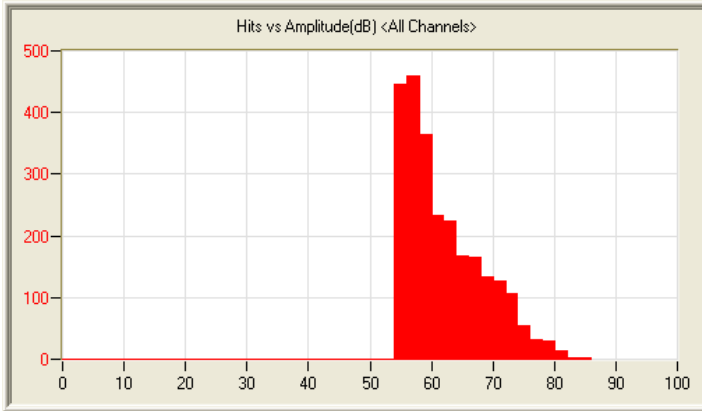
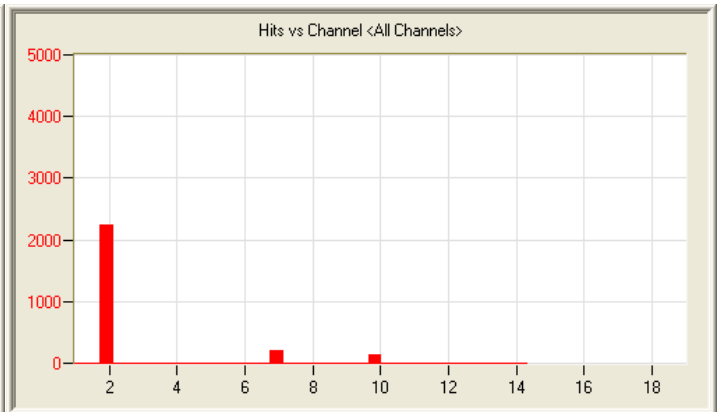
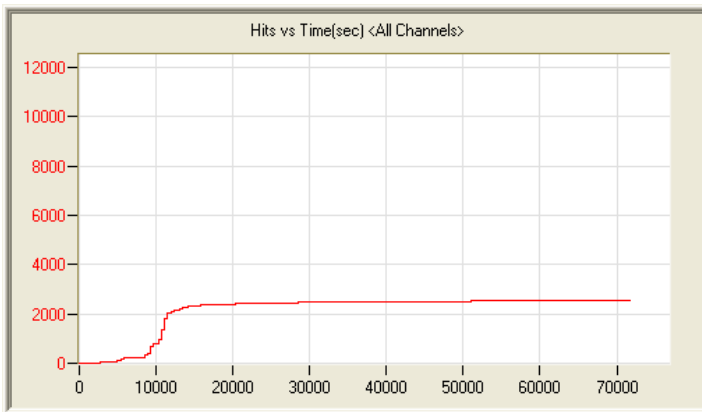
8/30/12 10:43pm 1:21:49:42 1521 120830224355_0 6.8mb



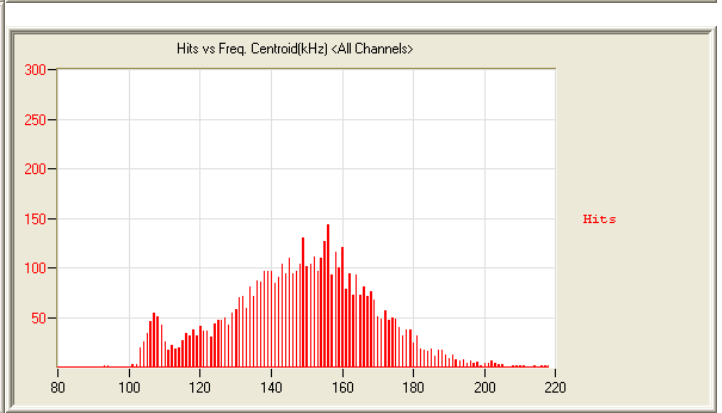
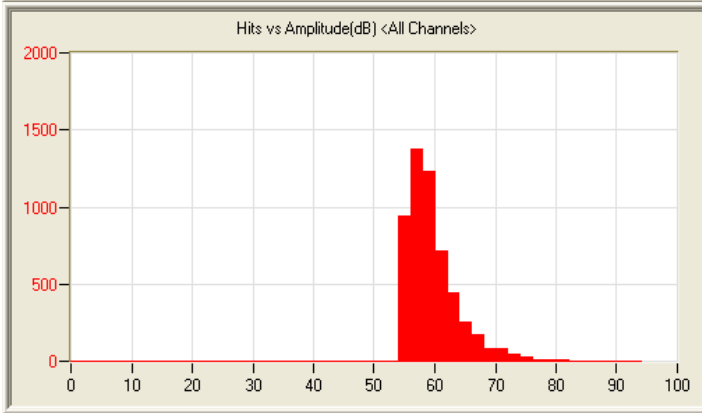
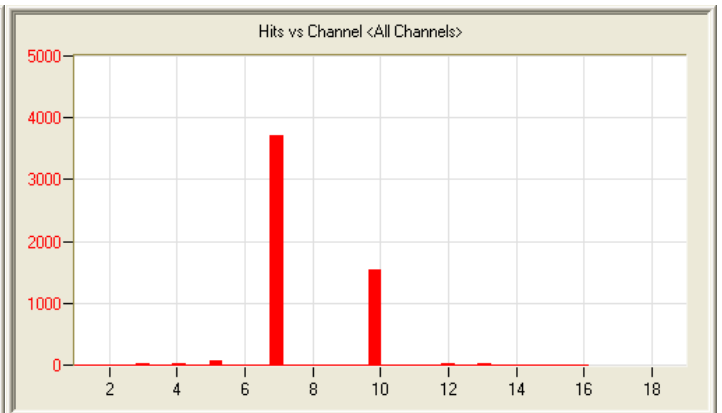
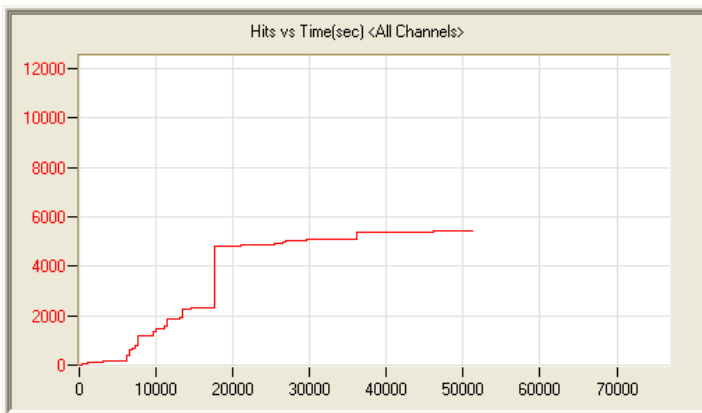
9/1/12 3:39pm 16:20:03 202120901153932_0 2.4mb



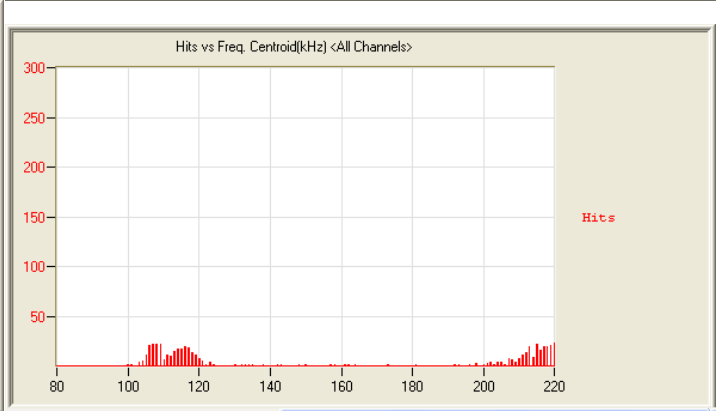
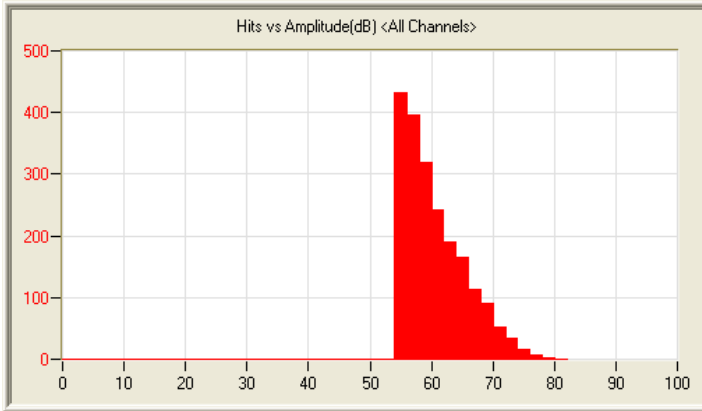
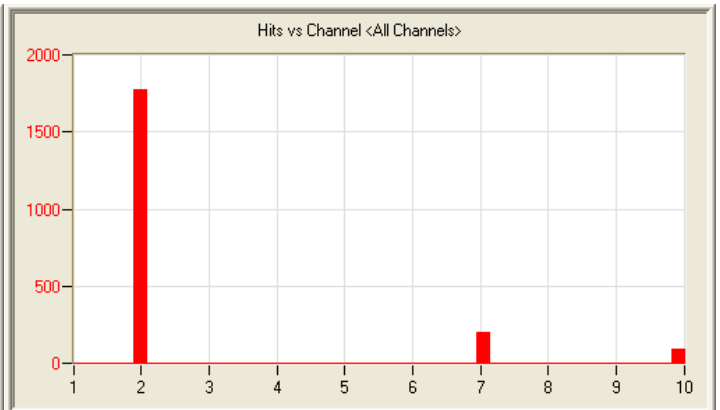
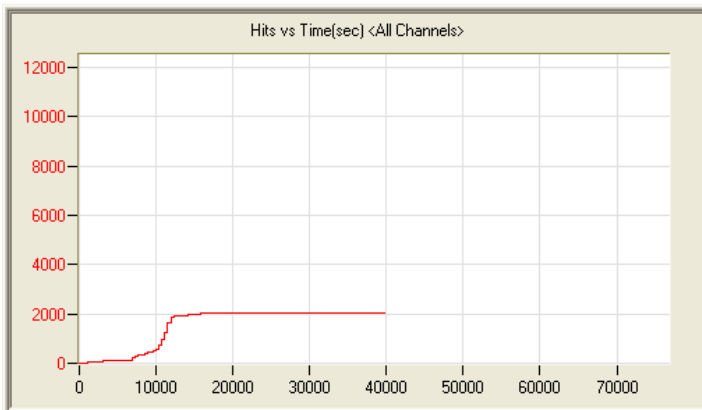
9/2/12 11:24am 12:30:07 656 120902112424_0 1.9mb



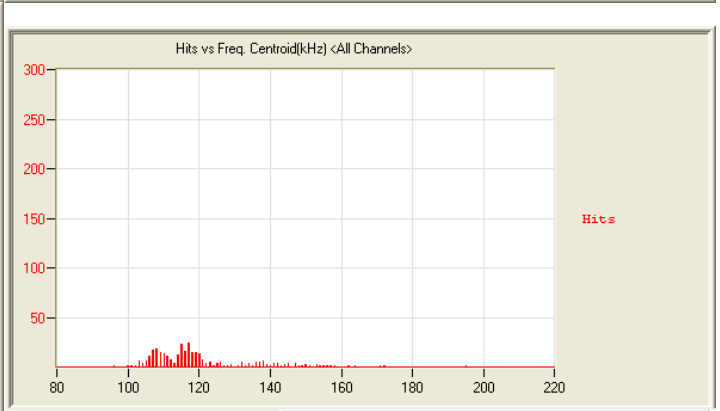
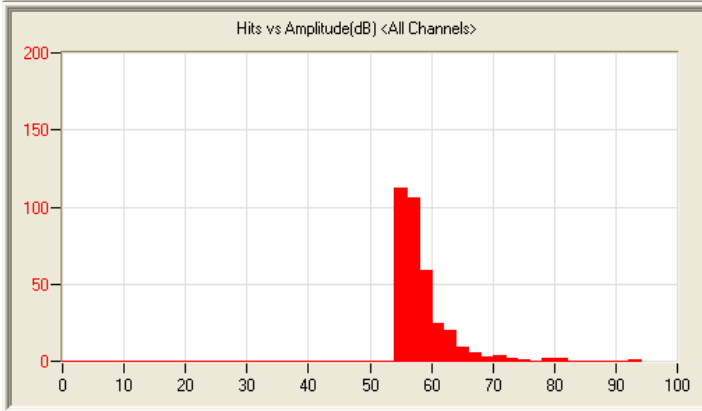
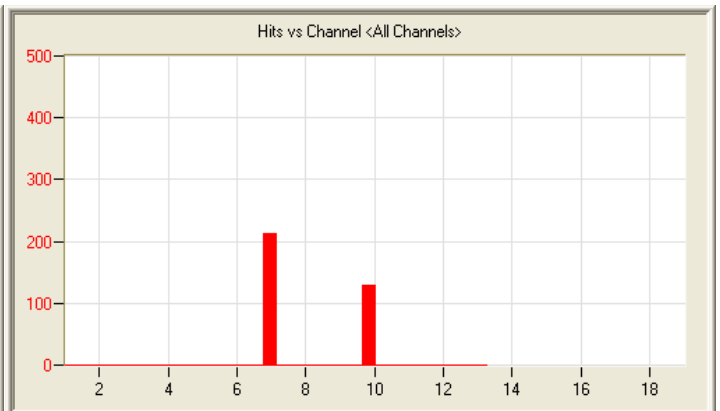
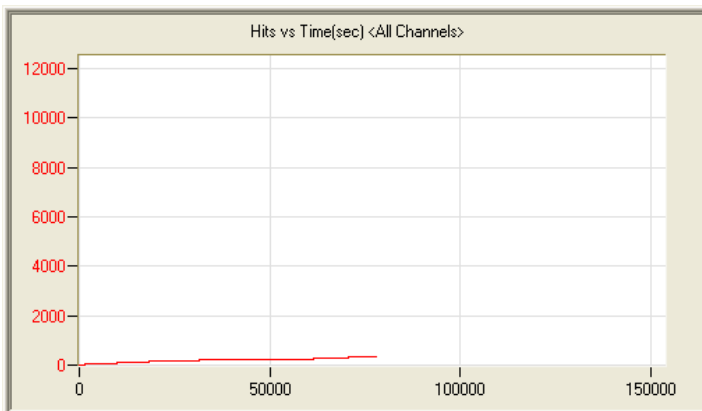
9/2/12 6:08pm 20:13:38 2559 120902180822_0 3.1mb



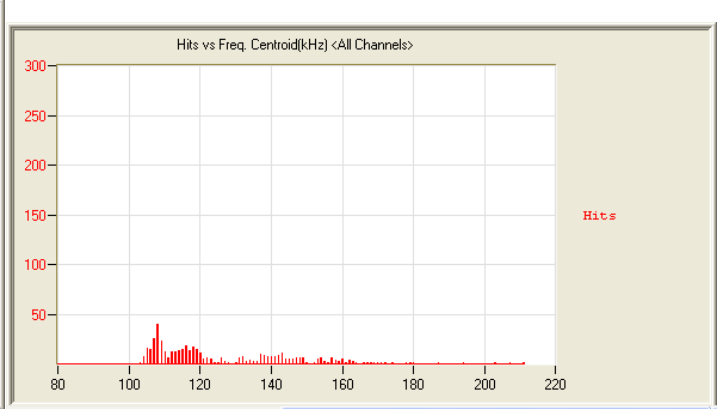
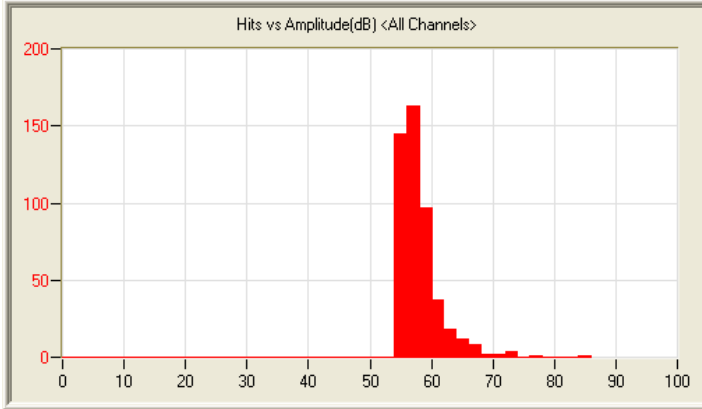
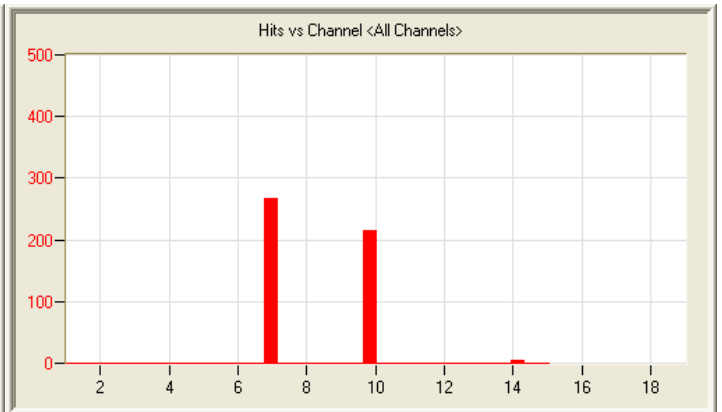
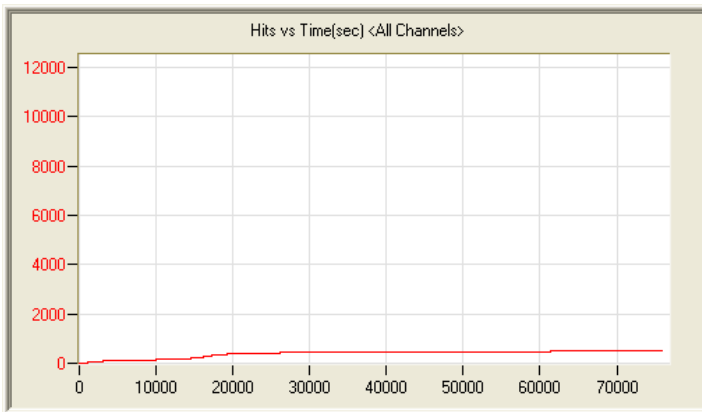
9/3/12 5:38pm 16:06:28 5408 120903173805_0 2.6mb



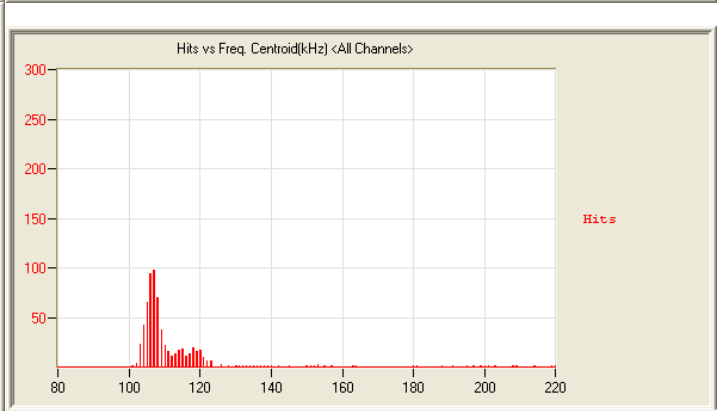
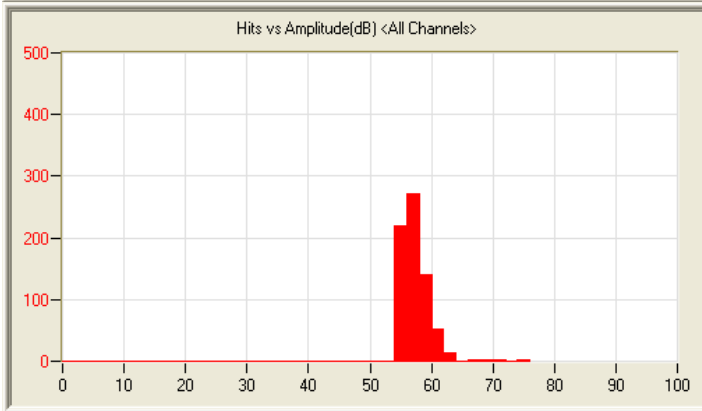
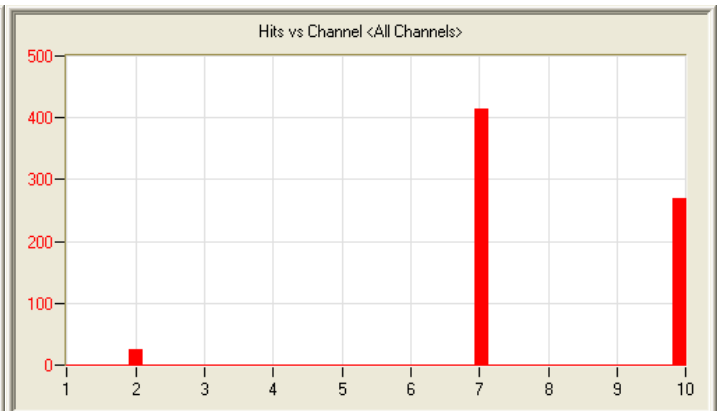
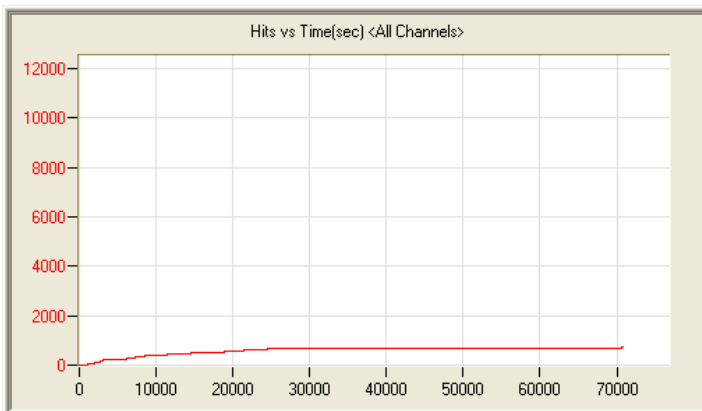
9/4/12 2:05am 12:50:10 2055 120904020526_0 2.0mb



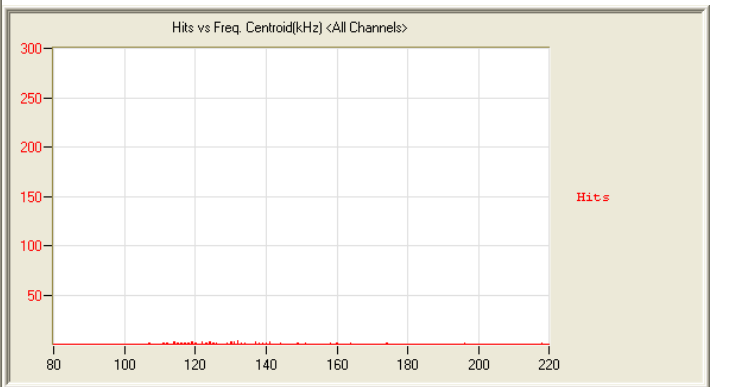
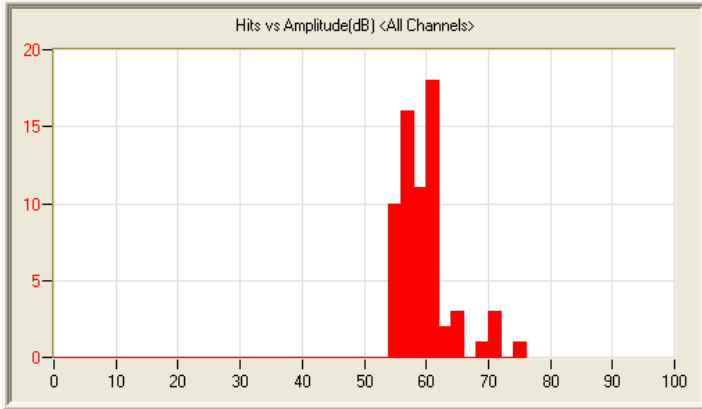
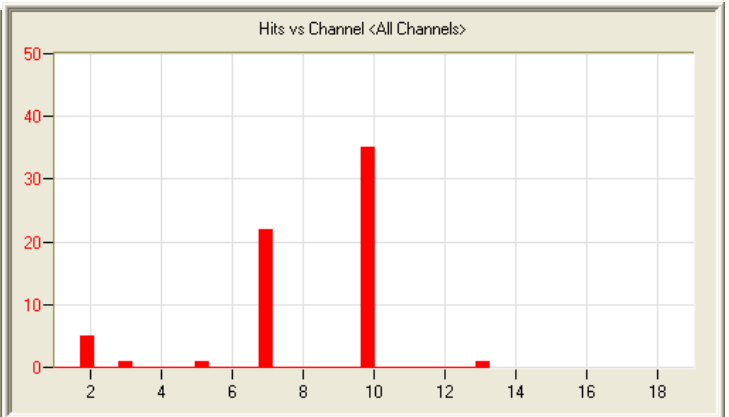
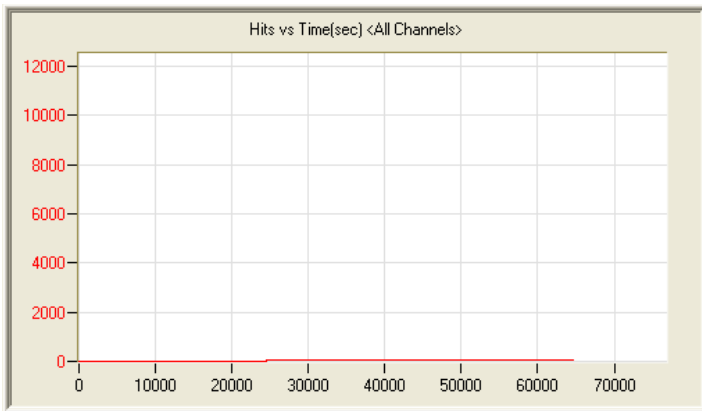
9/5/12 4:09am 21:51:43 350 120905040944_0 3.2mb



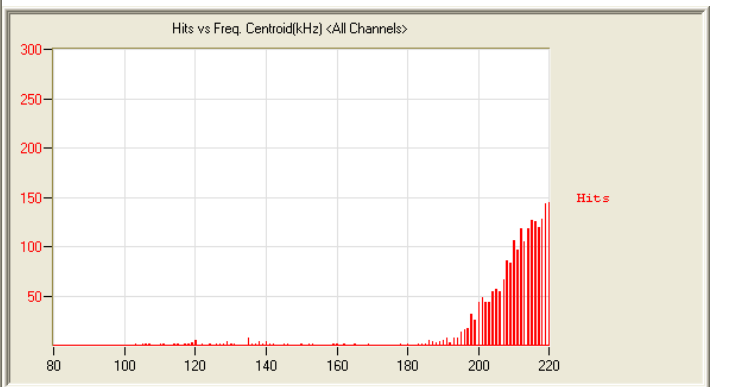
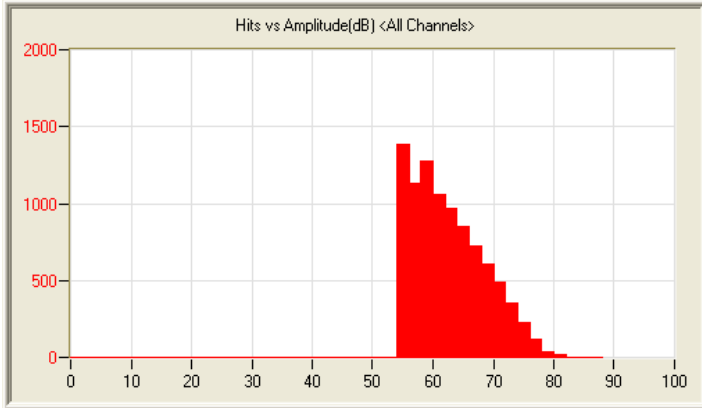
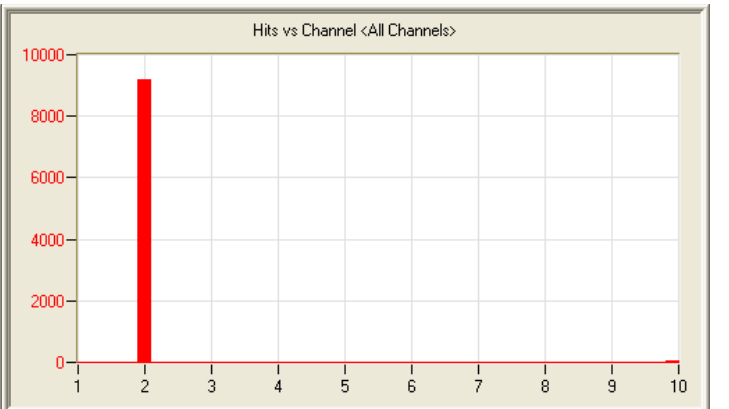
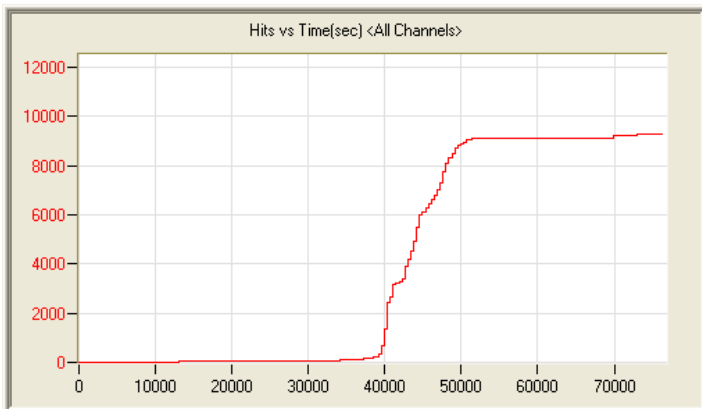
9/6/12 5:11am 21:41:58 490 120906051122_0 3.2mb



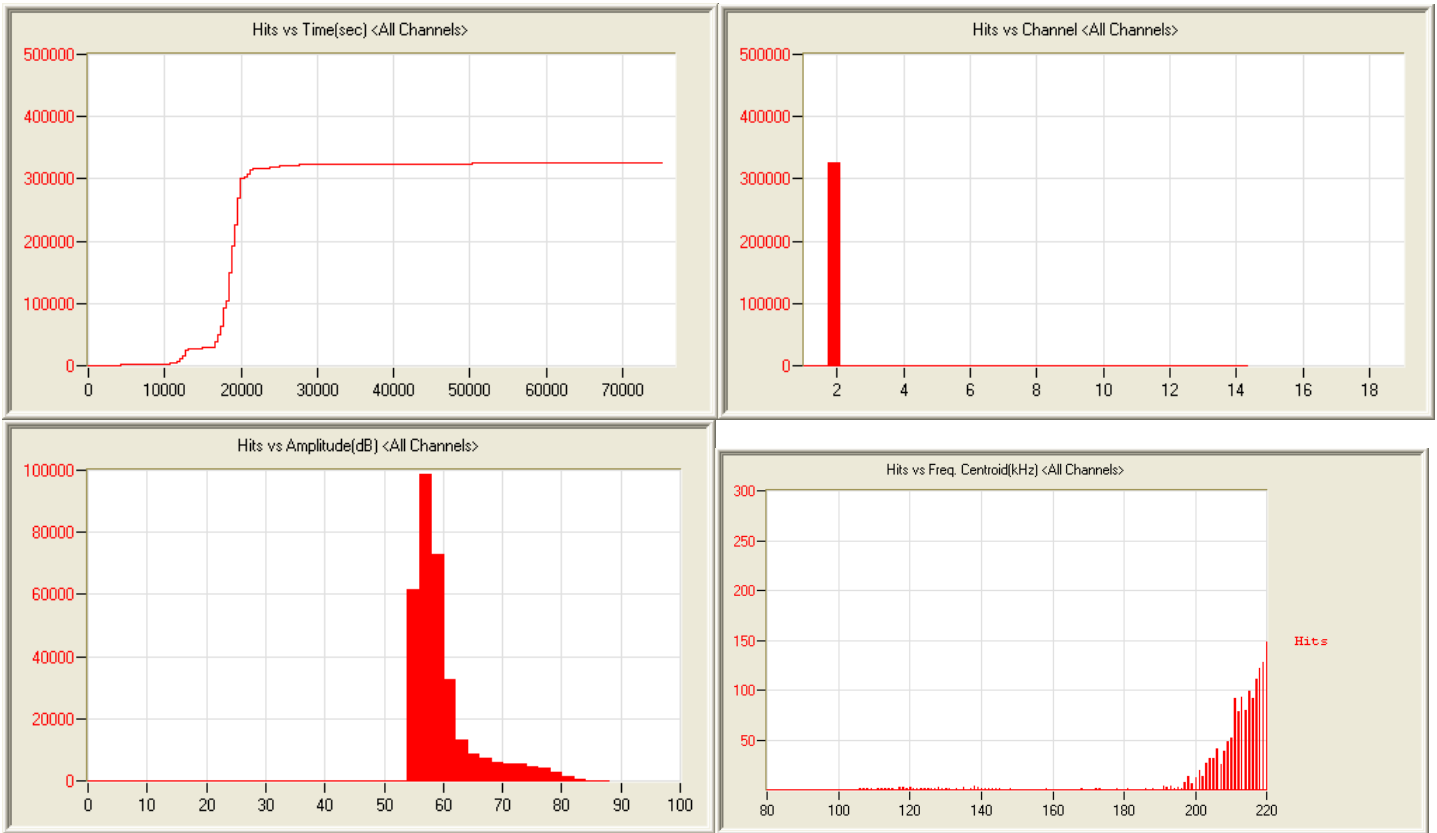
9/7/12 5:55am 20:13:34 708 120907055505_0 3.0mb



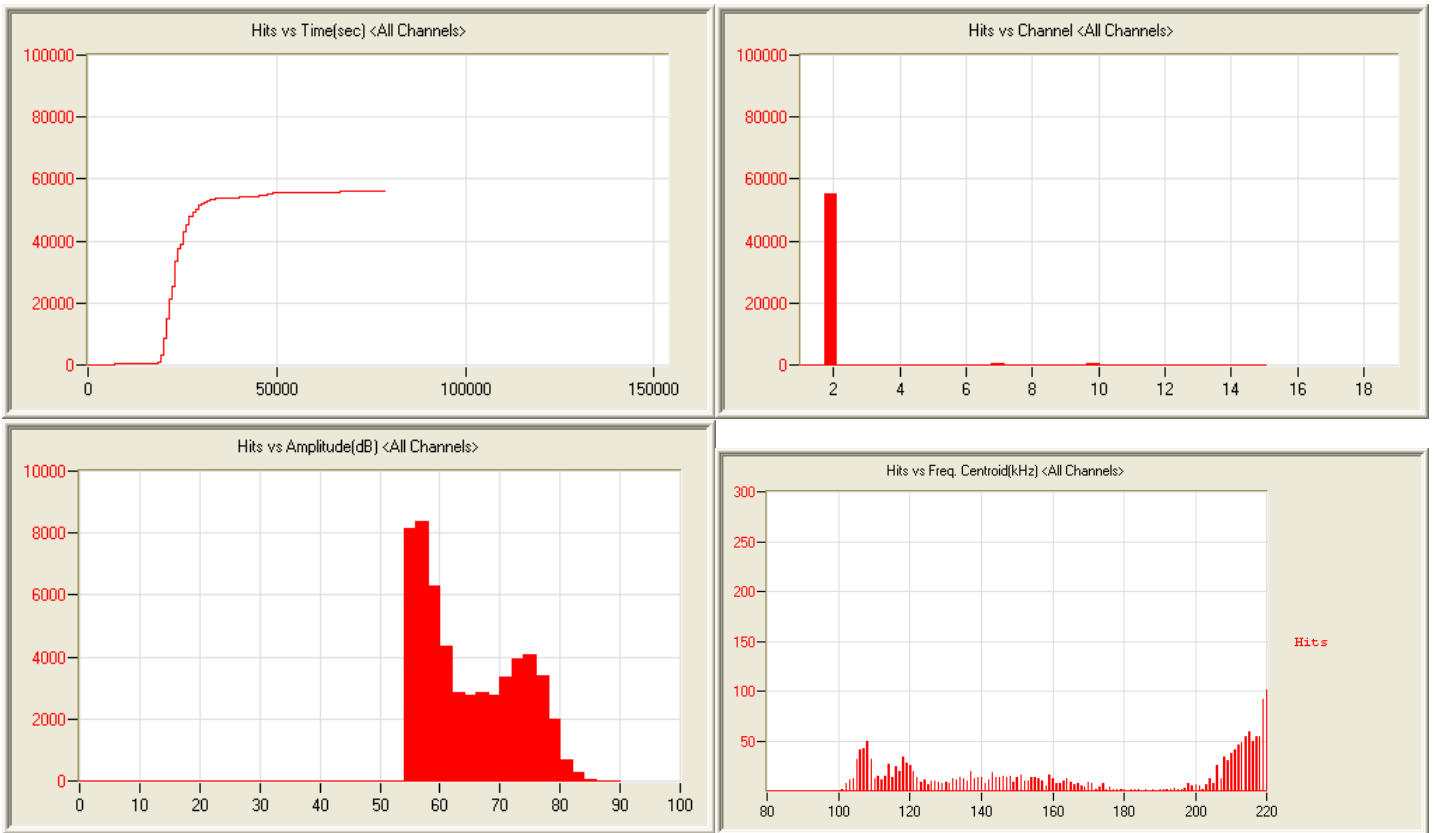
9/8/12 7:02am 19:58:31 65 120908070243_0 2.9mb



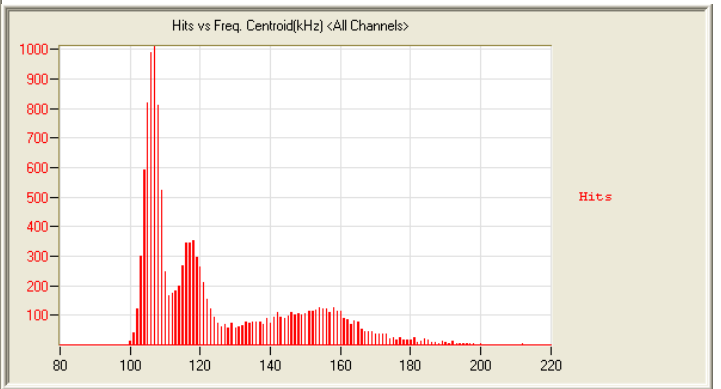
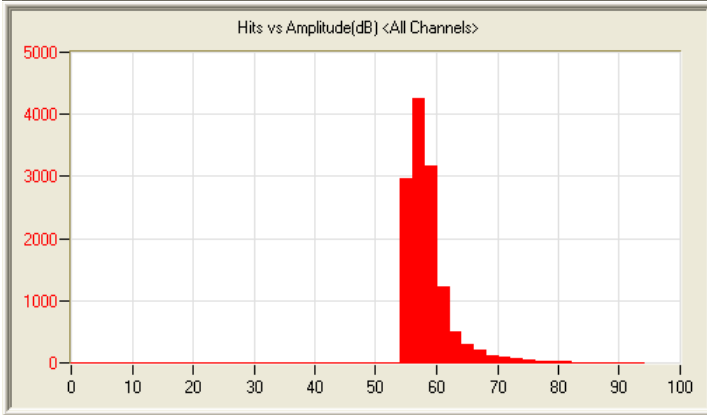
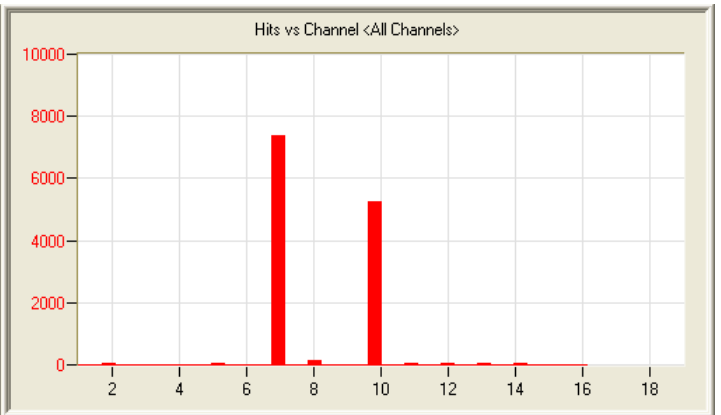
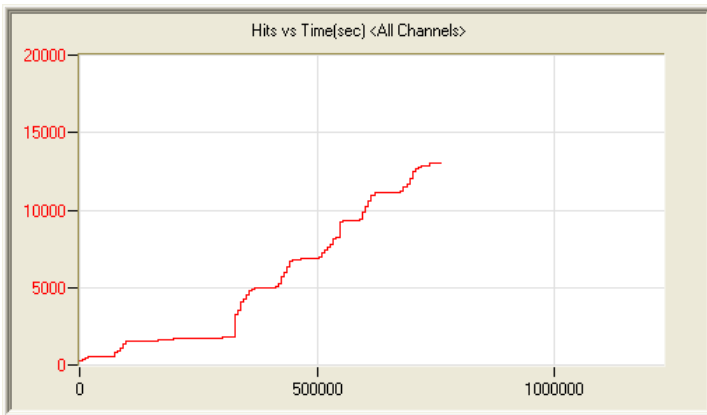
9/9/12 8:07am 21:13:18 9254 120909080710_0 3.5mb



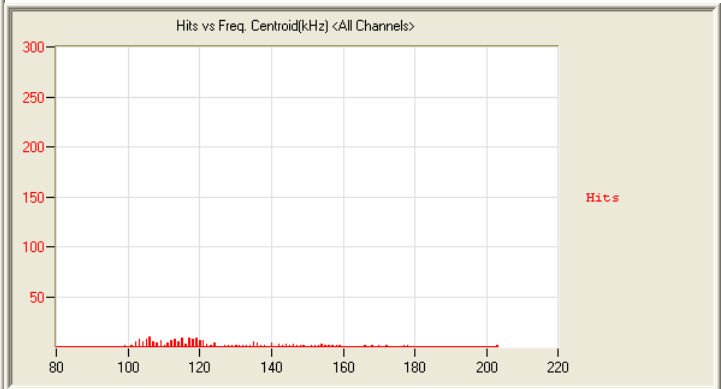
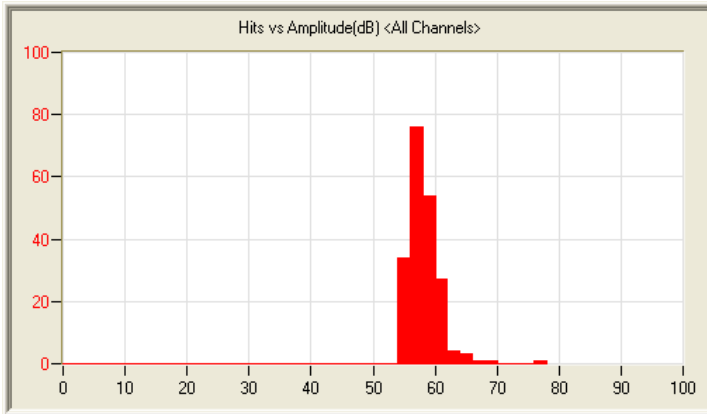
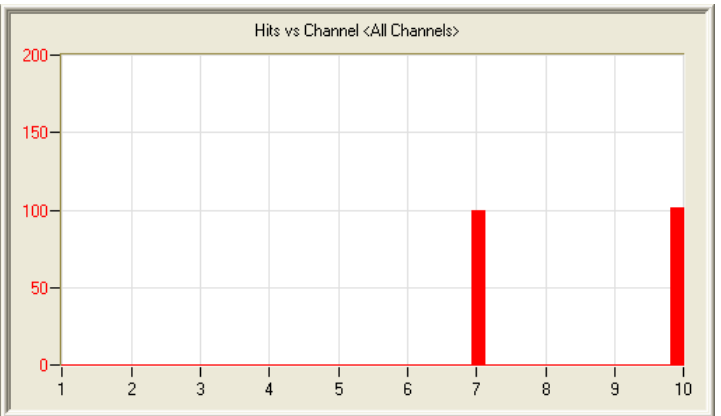
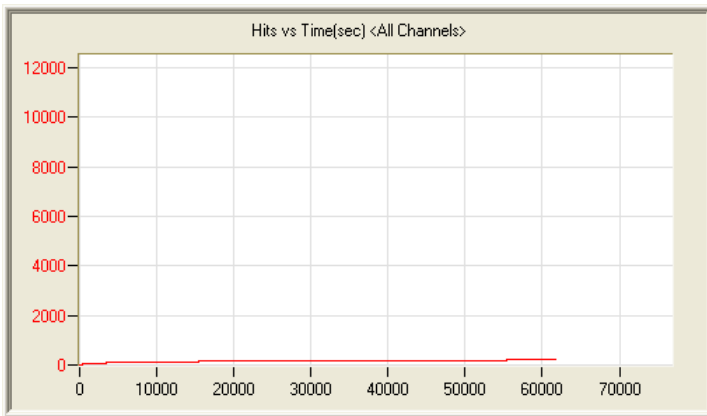
9/10/12 9:26am 20:53:38 325362 120910092631_0 16.2mb



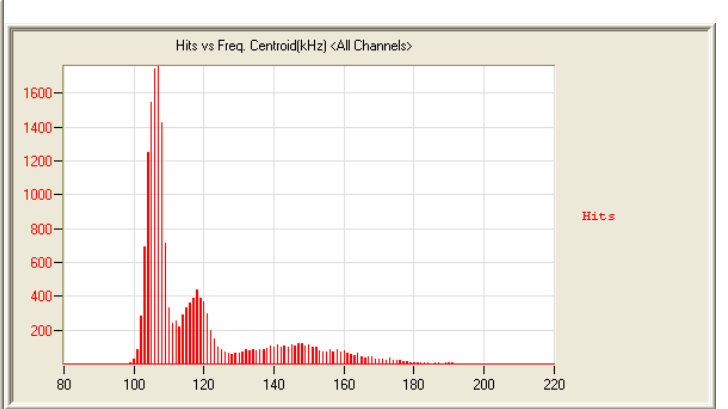
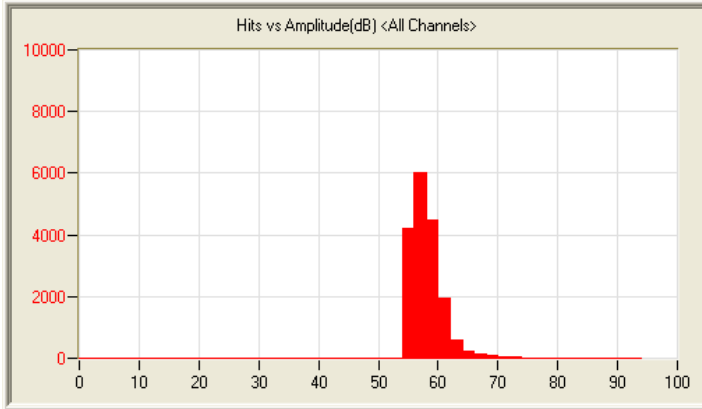
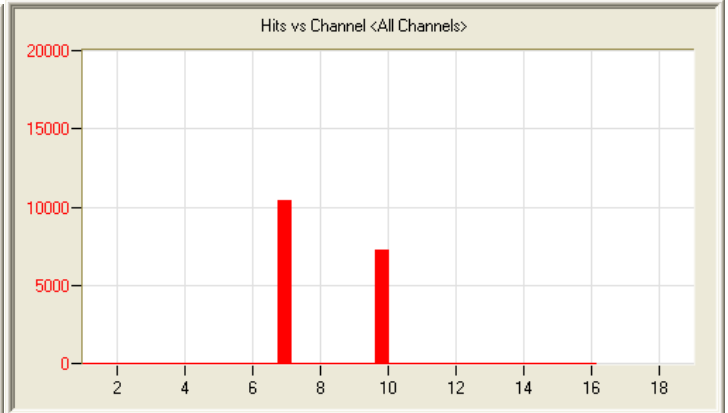
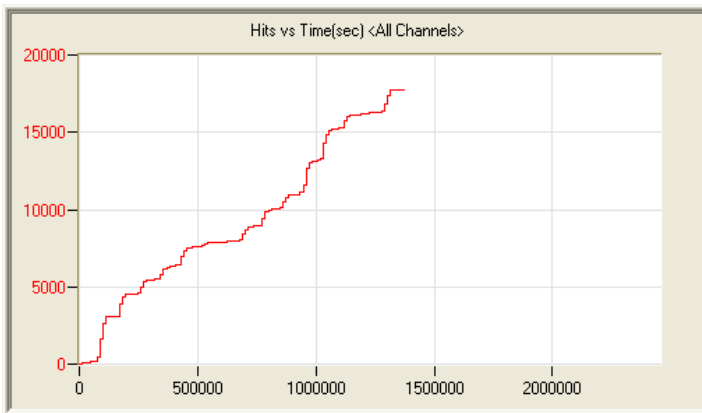
9/11/12 10:08am 22:07:49 56179 120911100854_0 5.5mb



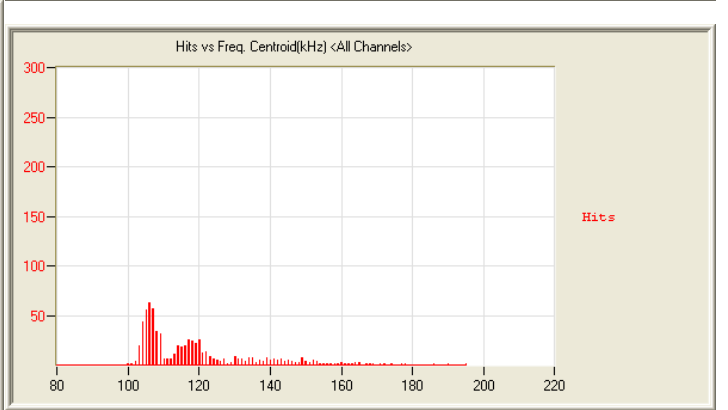
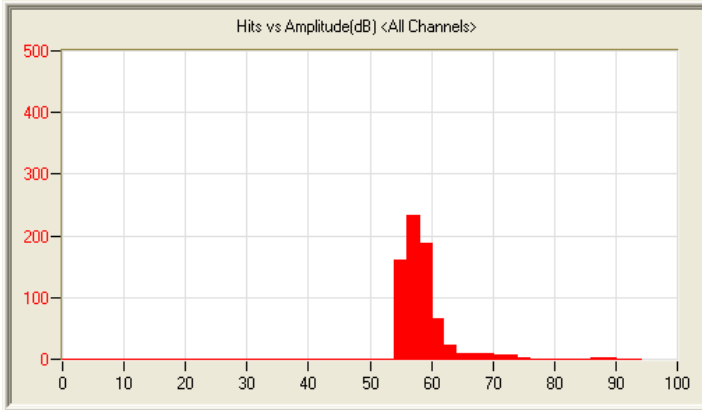
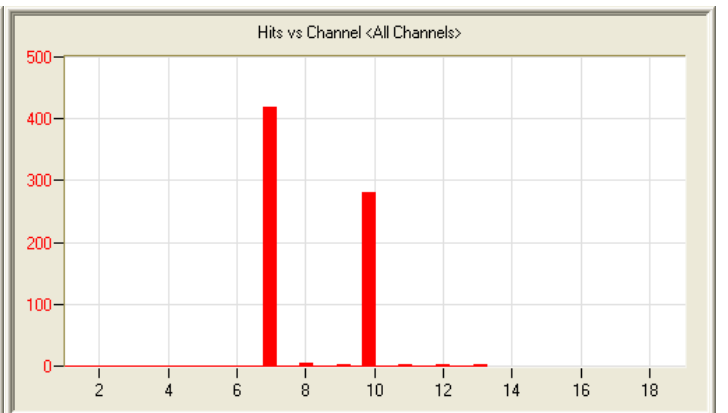
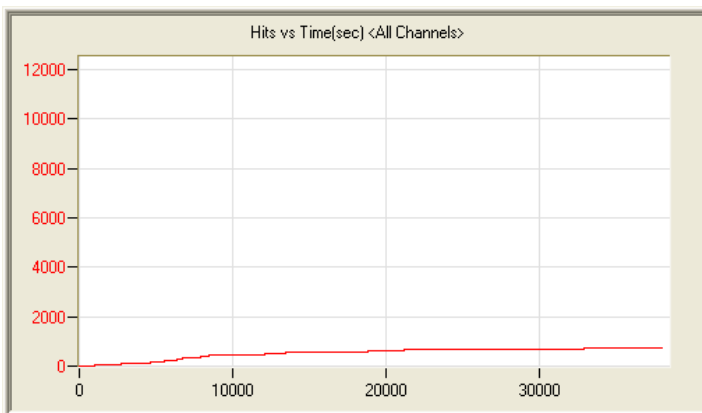
9/13/12 9:29am 8:18:43:09 13030 120913092905_0 30.6mb



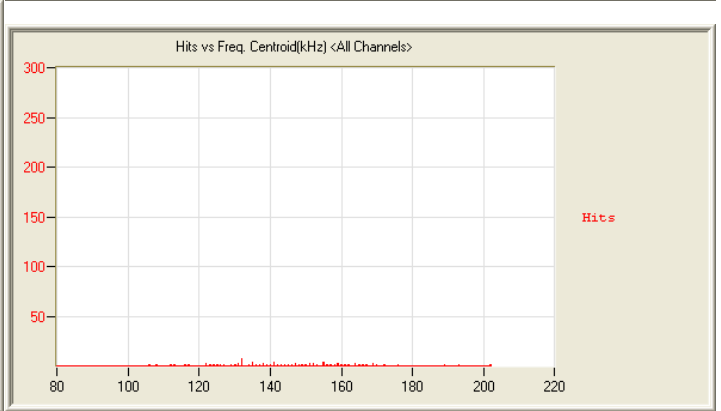
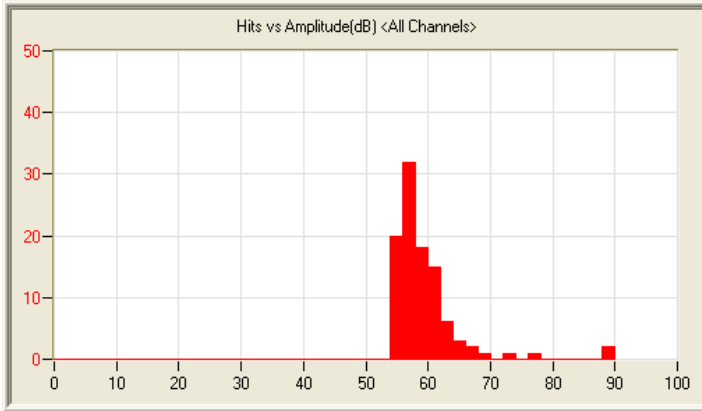
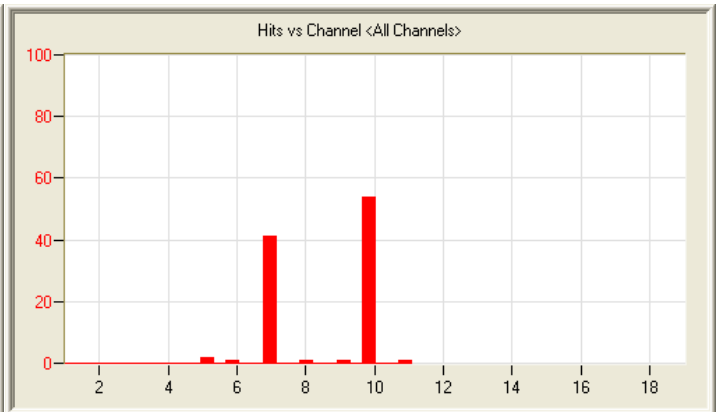
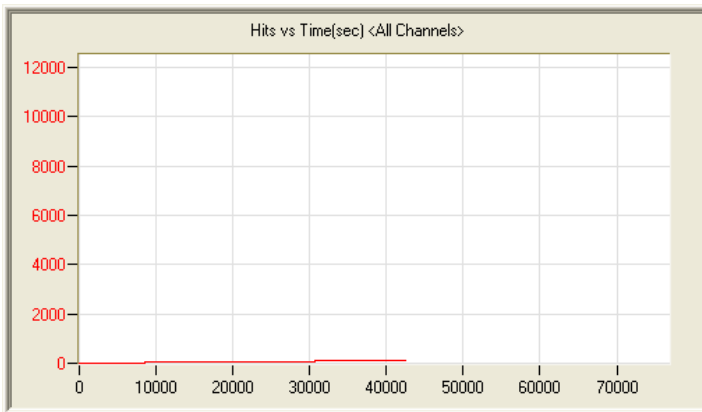
9/22/12 9:54am 18:06:13 201 120922095431_0 2.7mb



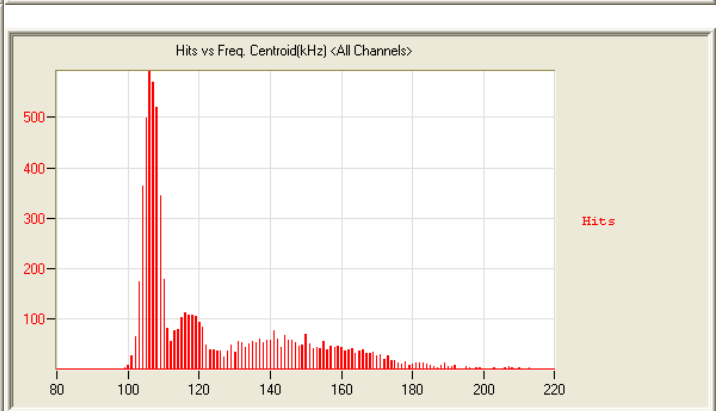
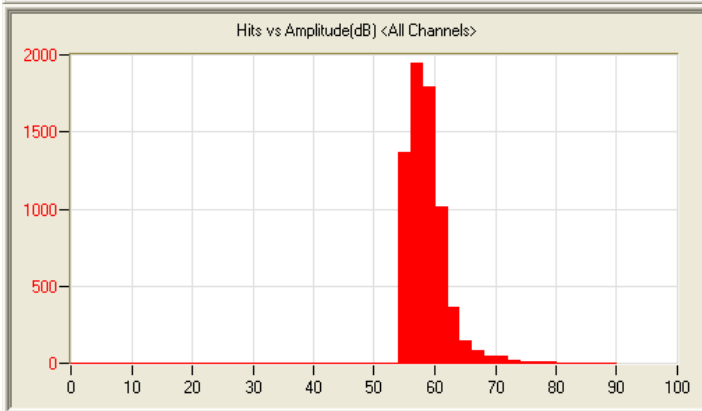
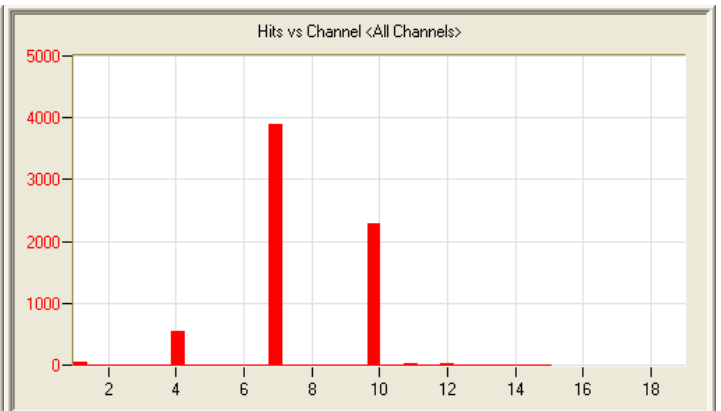
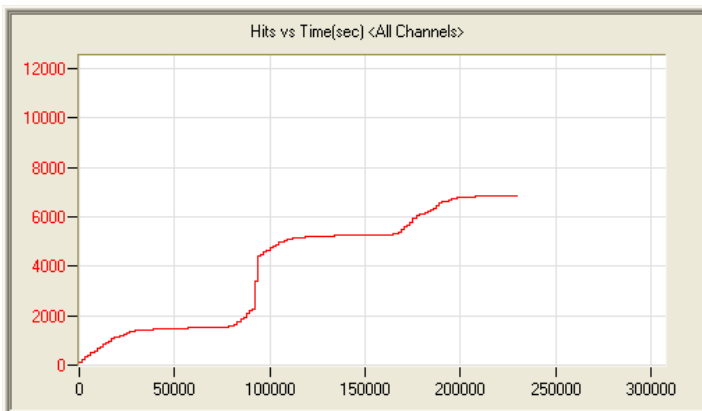
9/23/12 7:36am 15:20:55:01 1776 120923073625_0 56.0mb



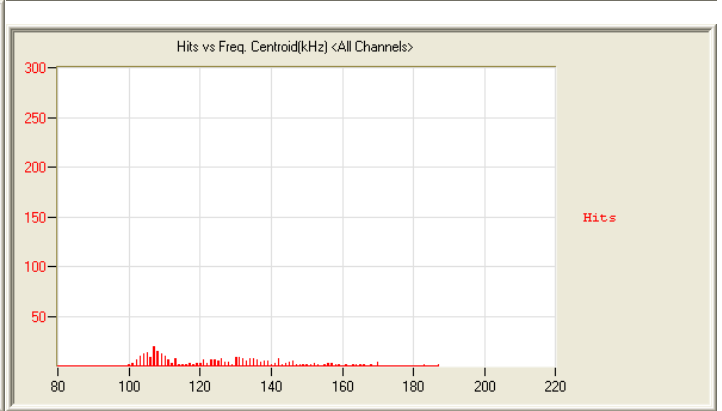
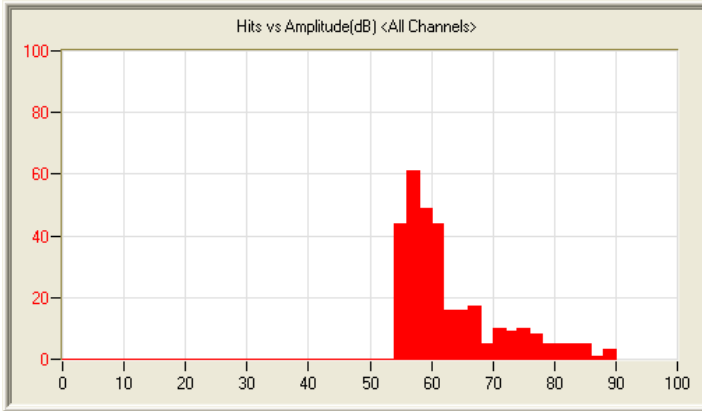
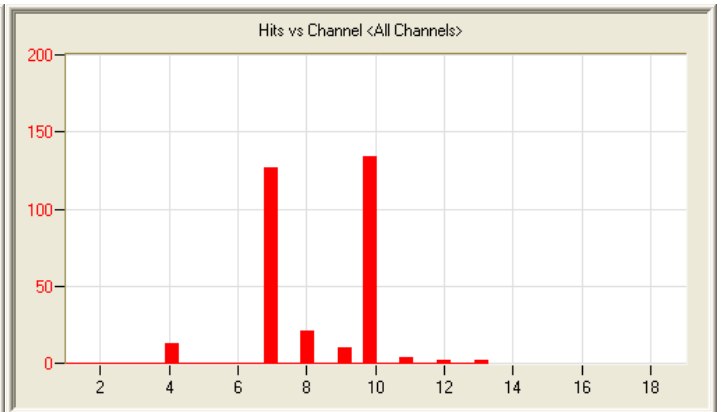
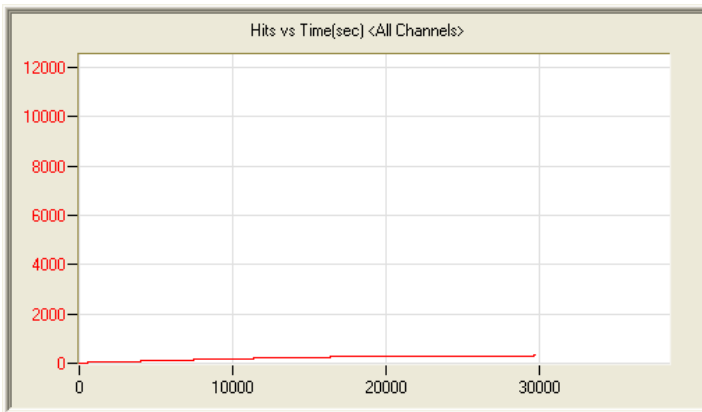
10/9/12 11:28am 10:31:46 717 121009112836_0 1.6mb



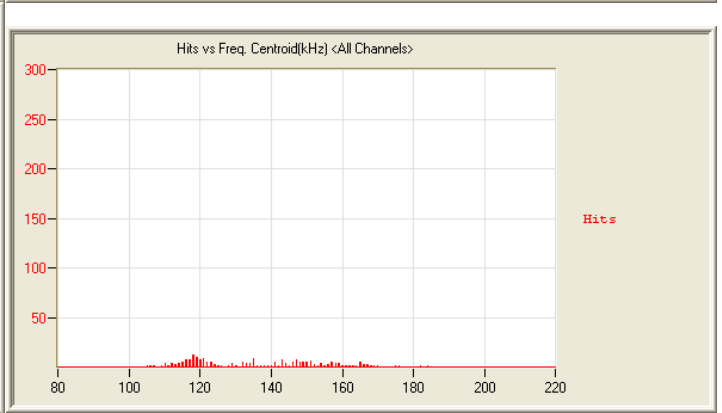
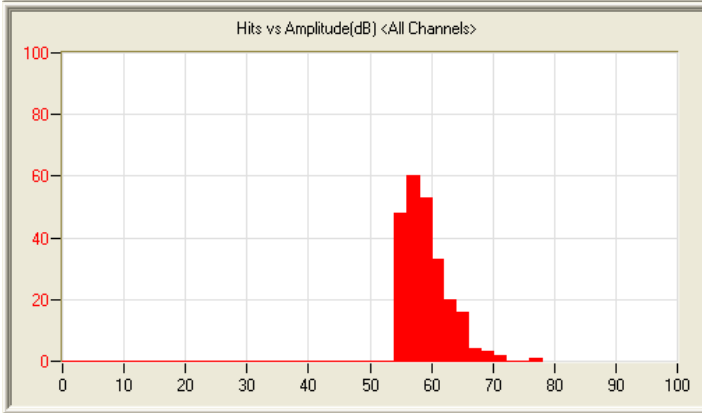
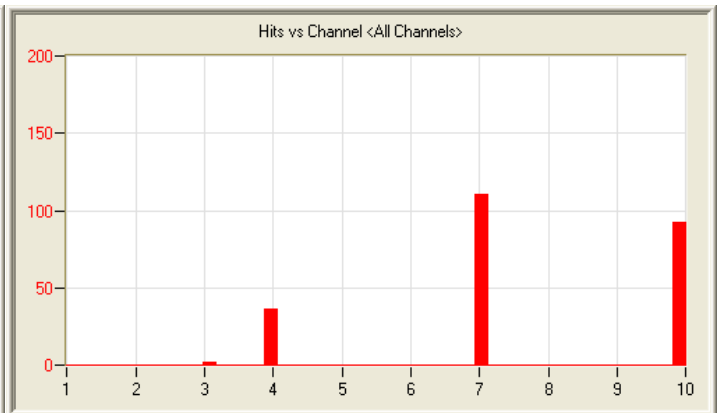
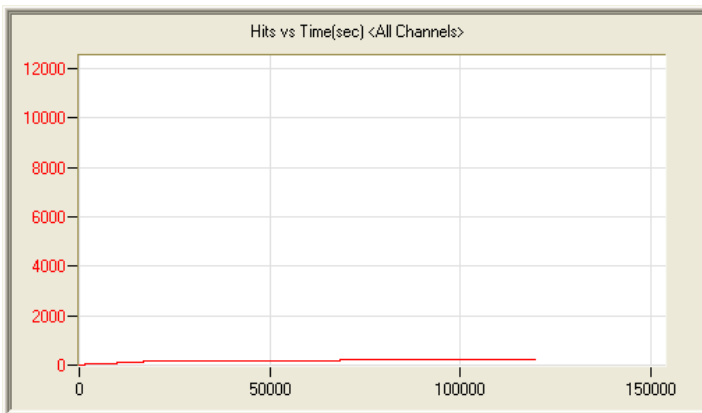
10/14/12 11:38am 11:51:35 101 121014113758_0 1.8mb



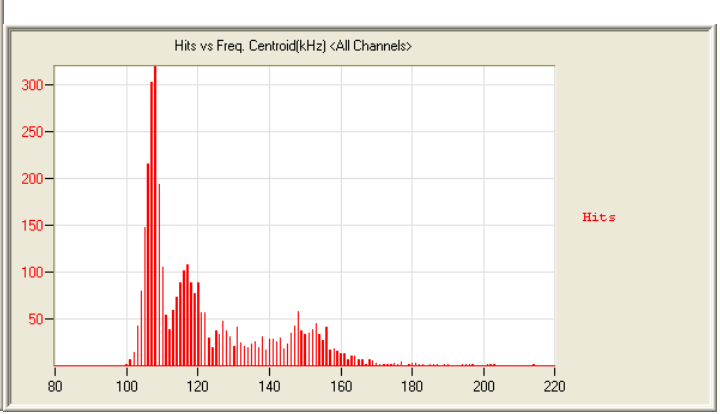
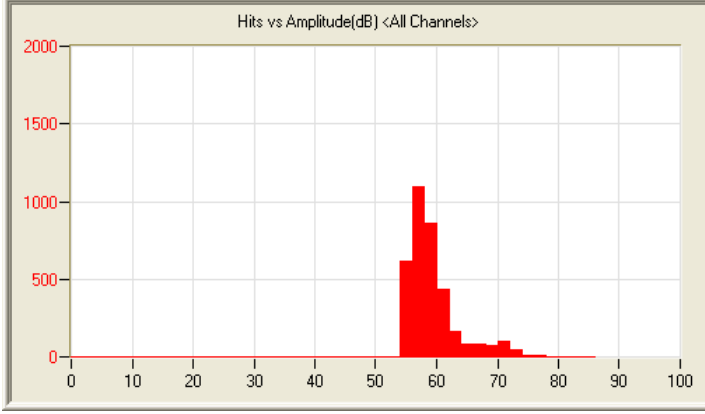
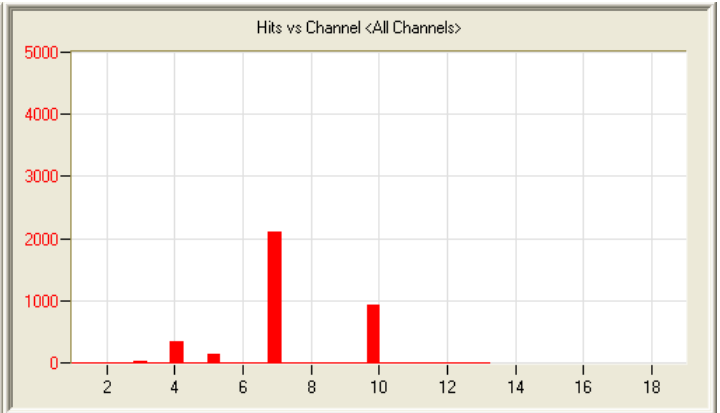
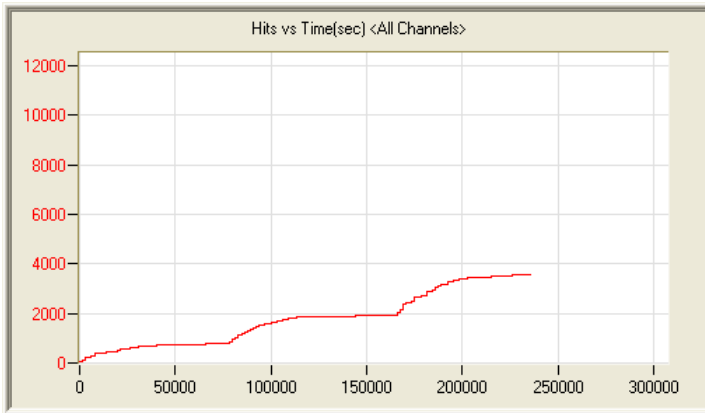
10/15/12 8:00am 2:16:00:32 6864 121015080020_0 9.6mb



10/19/12 12:59pm 8:48:06 313 121019125746_0 1.3mb



10/27/12 8:07am 1:09:21:09 240 121027080711_0 4.9mb



10/30/12 5:19am 2:18:01:02 3557 121030051858_0 9.8mb